

PHOTOMULTIPLIER TUBES

Basics and Applications

FOURTH EDITION



HAMAMATSU

PHOTON IS OUR BUSINESS

Introduction

Light detection technology is a powerful tool that provides deeper understanding of more sophisticated phenomena. Measurement using light offers unique advantages: for example, nondestructive analysis of a substance, high-speed properties and extremely high detectability. Recently, in particular, such advanced fields as scientific measurement, medical diagnosis and treatment, high energy physics, spectroscopy and biotechnology require development of photodetectors that exhibit the ultimate in various performance parameters.

Photodetectors or light sensors can be broadly divided by their operating principle into three major categories: external photoelectric effect, internal photoelectric effect and thermal types. The external photoelectric effect is a phenomenon in which when light strikes a metal or semiconductor placed in a vacuum, electrons are emitted from its surface into the vacuum. Photomultiplier tubes (often abbreviated as PMT) make use of this external photoelectric effect and are superior in response speed and sensitivity (low-light-level detection). They are widely used in medical equipment, analytical instruments and industrial measurement systems.

Light sensors utilizing the internal photoelectric effect are further divided into photoconductive types and photovoltaic types. Photoconductive cells represent the former, and PIN photodiodes the latter. Both types feature high sensitivity and miniature size, making them well suited for use as sensors in camera exposure meters, optical disk pickups and in optical communications. The thermal types, though their sensitivity is low, have no wavelength-dependence and are therefore used as temperature sensors in fire alarms, intrusion alarms, etc.

This handbook has been structured as a technical handbook for photomultiplier tubes in order to provide the reader with comprehensive information on photomultiplier tubes.

This handbook will help the user gain maximum performance from photomultiplier tubes and show how to properly operate them with higher reliability and stability. In particular, we believe that the first-time user will find this handbook beneficial as a guide to photomultiplier tubes. We also hope this handbook will be useful for engineers already experienced in photomultiplier tubes for upgrading performance characteristics.

Information furnished by Hamamatsu Photonics is believed to be reliable. However, no responsibility is assumed for possible inaccuracies or omission. The contents of this manual are subject to change without notice. No patent rights are granted to any of the circuits described herein.

©2017 Hamamatsu Photonics K. K.

CONTENTS

CHAPTER 1 INTRODUCTION

| | | |
|-------|---------------------------------------|----|
| 1.1 | Overview of This Manual | 2 |
| 1.2 | Photometric Units | 4 |
| 1.2.1 | Spectral regions and units | 4 |
| 1.2.2 | Units of light intensity | 5 |
| 1.3 | History | 10 |
| 1.3.1 | History of photocathodes | 10 |
| 1.3.2 | History of photomultiplier tubes..... | 10 |
| | References in Chapter 1 | 12 |

CHAPTER 2 BASIC PRINCIPLES OF PHOTOMULTIPLIER TUBES

| | | |
|-----|---|----|
| 2.1 | Structures and multiplication principles of photomultiplier tubes | 14 |
| 2.2 | Photoelectron Emission | 15 |
| 2.3 | Electron Trajectory | 17 |
| 2.4 | Electron multiplier (dynode)..... | 19 |
| 2.5 | Anode | 20 |
| | References in Chapter 2 | 21 |

CHAPTER 3 BASIC OPERATING METHODS OF PHOTOMULTIPLIER TUBES

| | | |
|-------|---|----|
| 3.1 | Using Photomultiplier Tubes | 24 |
| 3.1.1 | Selection guide | 24 |
| 3.1.2 | Using a photomultiplier tube | 25 |
| 3.1.3 | Precautions | 26 |
| 3.2 | Peripheral devices | 27 |
| 3.2.1 | High voltage power supply | 27 |
| 3.2.2 | Voltage-divider circuit | 27 |
| 3.2.3 | Magnetic shield case and housing..... | 27 |
| 3.2.4 | Amplifier | 27 |
| 3.2.5 | Photomultiplier tube modules..... | 28 |
| 3.2.6 | Signal processing (output connection circuit) | 29 |

CHAPTER 4 CHARACTERISTICS OF PHOTOMULTIPLIER TUBES

| | | |
|-------|---|----|
| 4.1 | Basic Characteristics of Photocathodes | 32 |
| 4.1.1 | Photocathode materials | 32 |
| | (1) Cs-I..... | 32 |
| | (2) Cs-Te..... | 32 |
| | (3) Sb-Cs | 32 |
| | (4) Bialkali (Sb-Rb-Cs, Sb-K-Cs)..... | 32 |
| | (5) Low noise bialkali (Sb-Na-K)..... | 32 |
| | (6) Multialkali (Sb-Na-K-Cs)..... | 33 |
| | (7) Ag-O-Cs | 33 |
| | (8) GaAsP (Cs)..... | 33 |
| | (9) GaAs (Cs) | 33 |
| | (10) InGaAs (Cs) | 33 |
| | (11) InP/InGaAsP(Cs), InP/InGaAs(Cs) | 33 |
| | Reflection mode photocathodes | 36 |
| | Transmission mode photocathodes | 37 |
| 4.1.2 | Window materials..... | 38 |
| | (1) MgF ₂ crystal | 38 |
| | (2) Sapphire..... | 38 |
| | (3) Silica glass | 38 |
| | (4) UV-transmitting glass (UV glass)..... | 38 |
| | (5) Borosilicate glass | 38 |
| 4.1.3 | Spectral response characteristics | 39 |
| | (1) Radiant sensitivity | 39 |
| | (2) Quantum efficiency | 39 |
| | (3) Measurement and calculation of spectral response characteristics..... | 39 |
| | (4) Spectral response range (short and long wavelength limits)..... | 40 |
| 4.1.4 | Luminous sensitivity | 40 |
| | (1) Cathode luminous sensitivity..... | 41 |
| | (2) Anode luminous sensitivity | 42 |
| | (3) Blue sensitivity index and red-to-white ratio..... | 43 |
| 4.1.5 | Luminous sensitivity and spectral response | 44 |
| 4.2 | Basic Characteristics of Dynodes..... | 45 |
| 4.2.1 | Dynode types and features | 45 |
| | (1) Circular-cage type | 46 |
| | (2) Box-and-grid type | 46 |
| | (3) Linear-focused type..... | 46 |
| | (4) Venetian blind type | 46 |
| | (5) Mesh type..... | 46 |
| | (6) MCP (Microchannel plate) type..... | 46 |
| | (7) Metal channel type | 46 |
| | (8) Electron bombardment type | 46 |
| | (9) Box-and-line type | 46 |
| | (10) Circular and linear-focused type | 47 |

| | | |
|-------|--|----|
| 4.2.2 | Collection efficiency and gain (current amplification) | 47 |
| | (1) Collection efficiency | 47 |
| | (2) Gain (current amplification) | 48 |
| 4.3 | Characteristics of Photomultiplier Tubes | 50 |
| 4.3.1 | Time characteristics | 50 |
| | (1) Rise time, fall time, and electron transit time | 51 |
| | (2) T.T.S. (Transit Time Spread) | 52 |
| | (3) C.T.T.D. (Cathode Transit Time Difference) | 54 |
| | (4) C.R.T. (Coincident Resolving Time) | 55 |
| 4.3.2 | Linearity characteristics | 56 |
| | (1) Cathode linearity | 56 |
| | (2) Anode linearity | 56 |
| | (3) Linearity measurement | 58 |
| 4.3.3 | Uniformity | 61 |
| | (1) Spatial uniformity | 62 |
| | (2) Angular response | 64 |
| 4.3.4 | Stability | 65 |
| | (1) Drift (time stability) and life characteristics | 65 |
| | (2) Aging and warm-up | 66 |
| 4.3.5 | Hysteresis | 67 |
| | (1) Light hysteresis | 67 |
| | (2) Voltage hysteresis | 68 |
| | (3) Reducing the hysteresis | 69 |
| 4.3.6 | Dark current | 69 |
| | (1) Causes of dark current | 69 |
| | (2) Expression of dark current | 73 |
| 4.3.7 | Signal-to-noise ratio of photomultiplier tubes | 75 |
| 4.3.8 | Afterpulsing | 79 |
| | Types of afterpulses | 79 |
| 4.3.9 | Polarized-light dependence | 80 |
| | References in Chapter 4 | 82 |

CHAPTER 5 VOLTAGE-DIVIDER CIRCUITS AND ACCESSORIES FOR PHOTOMULTIPLIER TUBES

| | | |
|-------|---|----|
| 5.1 | Voltage-Divider Circuits | 86 |
| 5.1.1 | Basic operation of voltage-divider circuits | 86 |
| 5.1.2 | Anode grounding and cathode grounding | 87 |
| 5.1.3 | Voltage-divider current and output linearity | 88 |
| | (1) Voltage-divider circuit for maintaining the linearity in DC output mode | 91 |
| | (2) Pulse output mode linearity and its countermeasures | 96 |
| 5.1.4 | Voltage distribution in voltage-divider circuits | 99 |

| | | |
|-------|--|-----|
| | (1) Voltage distribution in the anode and latter stages..... | 99 |
| | (2) Voltage distribution for the cathode and earlier stages | 100 |
| 5.1.5 | Countermeasures for fast response circuits..... | 101 |
| 5.1.6 | Practical fast-response voltage-divider circuit example | 103 |
| 5.1.7 | Gate circuit..... | 104 |
| 5.1.8 | Gain adjustment circuits..... | 105 |
| 5.1.9 | Precautions when fabricating a voltage-divider circuit | 107 |
| | (1) Selecting the components used for a voltage-divider circuit | 107 |
| | (2) Precautions for mounting components..... | 111 |
| 5.2 | Selecting the high voltage power supply | 114 |
| 5.3 | Connection to the External Circuit..... | 117 |
| 5.3.1 | Measuring an output signal..... | 117 |
| 5.3.2 | Effects of a coupling capacitor | 119 |
| 5.3.3 | Current-to-voltage conversion of photomultiplier tube output | 120 |
| | (1) Current-to-voltage conversion using load resistance | 120 |
| | (2) Current-to-voltage conversion using an op-amp | 122 |
| | (3) Charge-sensitive amplifier using an op-amp..... | 124 |
| 5.3.4 | Output circuit for fast response photomultiplier tubes | 126 |
| 5.3.5 | Selecting an amplifier for measurement using a photomultiplier tube ... | 128 |
| | (1) Single photon counting (Also refer to Chapter 6, "Photon Counting") ... | 128 |
| | (2) Analog output measurement..... | 129 |
| | (3) Precautions for using an amplifier..... | 129 |
| 5.4 | Housing | 131 |
| 5.4.1 | Light shield..... | 131 |
| 5.4.2 | Electrostatic shield | 131 |
| 5.4.3 | Magnetic shield | 131 |
| | (1) Shielding factor of magnetic shield case and orientation of magnetic field ... | 132 |
| | (2) Saturation characteristics..... | 134 |
| | (3) Frequency characteristics | 136 |
| | (4) Edge effect..... | 136 |
| | (5) Photomultiplier tube magnetic characteristics and shielding effect..... | 137 |
| | (6) Handling the magnetic shield case | 138 |
| 5.5 | Cooling | 139 |
| | References in Chapter 5 | 142 |

CHAPTER 6 PHOTON COUNTING

| | | |
|-----|---|-----|
| 6.1 | Analog and Digital (Photon Counting) Modes | 144 |
| 6.2 | Principle of Photon Counting..... | 145 |
| 6.3 | Operating Method and Characteristics of Photon Counting | 147 |

| | |
|---|-----|
| (1) Circuit configuration | 147 |
| (2) Basic characteristics of photon counting..... | 147 |
| References in Chapter 6 | 154 |

CHAPTER 7 SCINTILLATION COUNTING

| | |
|---|-----|
| 7.1 Scintillators and Photomultiplier Tubes | 156 |
| 7.2 Characteristics | 159 |
| (1) Energy resolution | 159 |
| (2) Relative pulse height..... | 162 |
| (3) Linearity..... | 162 |
| (4) Uniformity | 164 |
| (5) Stability..... | 164 |
| (6) Noise..... | 165 |
| (7) Plateau characteristic..... | 167 |
| References in Chapter 7 | 169 |

CHAPTER 8 PHOTOMULTIPLIER TUBE MODULES

| | |
|--|-----|
| 8.1 What Are Photomultiplier Tube Modules?..... | 172 |
| 8.2 Power Supply Circuits..... | 172 |
| (1) High voltage power supply circuit..... | 172 |
| (2) Input voltage..... | 174 |
| (3) Output current and input current | 174 |
| 8.3 Current Output Type and Voltage Output Type..... | 174 |
| (1) Gain adjustment | 174 |
| (2) Ripple noise | 175 |
| (3) Settling time | 176 |
| 8.3.1 Current output type modules..... | 176 |
| (1) Output linearity (DC output mode) | 177 |
| 8.3.2 Voltage output type modules | 177 |
| (1) Frequency characteristics | 178 |
| (2) Offset voltage | 178 |
| (3) Output signal voltage | 178 |
| 8.4 Photon Counting Heads | 179 |
| (1) Output characteristics | 179 |
| (2) Count sensitivity..... | 180 |
| (3) Dark count..... | 180 |
| (4) Pulse pair resolution..... | 180 |
| (5) Count linearity | 180 |
| (6) Improving the count linearity | 181 |
| (7) Over-light detection | 181 |
| 8.5 Gate Function | 182 |
| 8.5.1 Gate operation | 182 |

| | | |
|-------|--|-----|
| | (1) Operating principle | 182 |
| | (2) Operation mode | 183 |
| | (3) Operation method | 183 |
| 8.5.2 | Gate characteristics | 183 |
| | (1) Time characteristics | 183 |
| | (2) Switching noise | 184 |
| | (3) Extinction ratio..... | 184 |
| 8.6 | Built-in CPU and Interface Type..... | 185 |
| 8.7 | Failure and Malfunction | 185 |
| 8.7.1 | Causes of failure and malfunction..... | 185 |
| 8.7.2 | Troubleshooting..... | 186 |
| | (1) No signal is output..... | 186 |
| | (2) Cannot control the gain..... | 186 |
| | (3) Output signal waveform differs from the actual phenomenon..... | 186 |
| | (4) Number of output pulses from a photon counting head is 0 (zero)..... | 186 |
| | (5) Dark current fluctuates..... | 186 |
| 8.8 | Related optical products | 187 |

CHAPTER 9 MULTIANODE TYPE AND POSITION-SENSITIVE PHOTOMULTIPLIER TUBES

| | | |
|---------|--|-----|
| 9.1 | Multianode Photomultiplier Tubes | 190 |
| 9.1.1 | Matrix multianode photomultiplier tubes | 191 |
| 9.1.2 | Linear multianode photomultiplier tubes | 197 |
| 9.1.2.1 | Linear multianode type for multichannel spectrometry | 199 |
| 9.2 | Center-of-Gravity Position Sensitive Photomultiplier Tubes | 200 |

CHAPTER 10 Micro PMT

| | | |
|------|---|-----|
| 10.1 | Micro PMT overview | 204 |
| 10.2 | Micro PMT operating principle..... | 205 |
| 10.3 | Key features..... | 206 |
| 10.4 | Characteristics..... | 206 |
| | (1) Spectral response characteristics | 206 |
| | (2) Gain characteristics..... | 207 |
| | (3) Dark current characteristics | 207 |
| | (4) Time characteristics | 208 |
| | (5) Uniformity characteristics..... | 209 |
| | (6) Magnetic characteristics..... | 209 |
| | References in Chapter 10 | 210 |

CHAPTER 11 Microchannel Plate-Photomultiplier Tube

| | | |
|------|-----------------|-----|
| 11.1 | Structure | 212 |
|------|-----------------|-----|

| | | |
|--------|---|-----|
| 11.1.1 | Structure of MCP | 212 |
| 11.1.2 | Structure of MCP-PMT..... | 213 |
| 11.1.3 | Voltage-divider circuit and housing structure | 214 |
| 11.2 | Basic Characteristics of MCP-PMT | 215 |
| 11.2.1 | Gain characteristics | 215 |
| 11.2.2 | Time characteristics | 216 |
| | (1) Rise time, fall time | 216 |
| | (2) Transit time | 216 |
| | (3) T.T.S. (Transit Time Spread), I.R.F. (Instrument Response Function) | 216 |
| | (4) Time characteristics of MCP-PMT | 218 |
| 11.2.3 | Temperature characteristics and cooling..... | 219 |
| 11.2.4 | Saturation characteristics..... | 220 |
| | (1) Dead time..... | 220 |
| | (2) Saturation by DC light | 221 |
| | (3) Saturation by pulsed light..... | 222 |
| | (4) Saturation gain characteristics (pulse height distribution) in photon counting mode | 223 |
| | (5) Count rate linearity in photon counting mode..... | 223 |
| 11.2.5 | Magnetic characteristics | 224 |
| 11.3 | Gated MCP-PMT | 226 |
| | References in Chapter 11 | 228 |

CHAPTER 12 HPD (Hybrid Photo-Detector)

| | | |
|--------|---|-----|
| 12.1 | Operating Principle of HPD | 230 |
| 12.2 | Features of HPD | 231 |
| 12.3 | Various Characteristics of HPD | 232 |
| 12.3.1 | Pulse height resolution..... | 232 |
| 12.3.2 | Gain characteristics and electron bombardment gain uniformity ... | 232 |
| 12.3.3 | Time response characteristics | 234 |
| | (1) Rise time, fall time, and electron transit time..... | 234 |
| | (2) T.T.S. (Transit Time Spread) | 236 |
| 12.3.4 | Uniformity..... | 237 |
| 12.3.5 | Temperature characteristics | 238 |
| | (1) Temperature dependence of leak current and breakdown voltage..... | 238 |
| | (2) Temperature dependence of avalanche gain | 239 |
| 12.3.6 | Afterpulsing | 239 |
| 12.3.7 | Effects of X-ray feedback | 240 |
| 12.3.8 | Drift characteristics | 240 |
| 12.3.9 | Life characteristics | 241 |
| 12.4 | Precautions when using an HPD..... | 242 |

| | |
|--------------------------------|-----|
| References in Chapter 12 | 243 |
|--------------------------------|-----|

CHAPTER 13 ENVIRONMENTAL RESISTANCE AND RELIABILITY

| | | |
|--------|--|-----|
| 13.1 | Effects of Ambient Temperature..... | 246 |
| 13.1.1 | Temperature characteristics | 246 |
| (1) | Sensitivity | 246 |
| (2) | Dark current | 247 |
| 13.1.2 | High temperature photomultiplier tubes | 248 |
| 13.1.3 | Storage temperature and cooling precautions | 251 |
| 13.2 | Effects of Humidity..... | 251 |
| 13.2.1 | Operating humidity..... | 251 |
| 13.2.2 | Storage humidity | 251 |
| 13.3 | Effects of External Magnetic Fields | 252 |
| 13.3.1 | Magnetic characteristics | 252 |
| 13.3.2 | Photomultiplier tubes for use in highly magnetic fields | 253 |
| 13.3.3 | Magnetization..... | 254 |
| 13.4 | Vibration and Shock..... | 255 |
| 13.4.1 | Resistance to vibration and shock during non-operation ... | 255 |
| 13.4.2 | Resistance to vibration and shock during operation (resonance) ... | 255 |
| 13.4.3 | Testing methods and conditions..... | 257 |
| 13.4.4 | Ruggedized photomultiplier tubes..... | 258 |
| 13.5 | Effects of Helium Gas..... | 260 |
| 13.6 | Effects of Radiation..... | 261 |
| 13.6.1 | Deterioration of window transmittance | 261 |
| 13.6.2 | Glass scintillation | 265 |
| 13.7 | Effects of Atmosphere | 266 |
| 13.8 | Effects of External Electric Potential..... | 267 |
| 13.8.1 | Experiment..... | 267 |
| 13.8.2 | Taking corrective action..... | 269 |
| 13.9 | Reliability | 270 |
| 13.9.1 | Stability over time (life characteristic)..... | 270 |
| 13.9.2 | Current stress and stability | 271 |
| 13.9.3 | Temperature stress and stability | 272 |
| 13.9.4 | Reliability..... | 273 |
| (1) | Failure mode | 273 |
| (2) | Failure rate | 273 |
| (3) | Mean life..... | 273 |

| | |
|---|-----|
| (4) Reliability..... | 274 |
| 13.9.4 Reliability tests and criteria used by Hamamatsu Photonics ... | 275 |
| References in Chapter 13 | 276 |

CHAPTER 14 APPLICATIONS

| | |
|--|-----|
| 14.1 Spectrophotometry | 278 |
| 14.1.1 Overview | 278 |
| 14.1.2 Application examples | 278 |
| (1) UV-visible spectrophotometers..... | 278 |
| (2) Atomic absorption spectrophotometers..... | 279 |
| (3) Atomic emission spectrophotometers | 279 |
| (4) Fluorescence spectrophotometers | 280 |
| 14.2 Environmental Measurement..... | 281 |
| 14.2.1 Overview | 281 |
| 14.2.2 Application examples | 281 |
| (1) NO _x analyzers | 281 |
| (2) SO _x analyzers | 282 |
| (3) Dust counters | 283 |
| (4) Laser radar (LIDAR) | 284 |
| 14.3 Medical Diagnosis | 285 |
| 14.3.1 PET (Positron Emission Tomography) / CT (Computed Tomography) ... | 285 |
| 14.3.2 Planar imaging devices | 287 |
| 14.3.3 Gamma cameras | 288 |
| 14.3.4 X-ray image diagnostic equipment..... | 290 |
| (1) Computed radiography (CR) | 290 |
| 14.3.5 Laboratory testing | 291 |
| (1) R.I.A. (Radioimmunoassay) | 293 |
| (2) Fluorescence immunoassay | 294 |
| (3) Chemiluminescence immunoassay | 294 |
| 14.4 Microscopy..... | 295 |
| 14.4.1 Overview | 295 |
| 14.4.2 Application examples | 295 |
| (1) Confocal laser scanning microscopy..... | 295 |
| (2) Two-photon microscopy..... | 296 |
| (3) Fluorescence correlation spectroscopy..... | 296 |
| 14.5 Life Science | 297 |
| 14.5.1 Overview | 297 |
| 14.5.2 Application examples | 297 |
| (1) Flow cytometer..... | 297 |
| (2) Real-time PCR / digital PCR | 298 |

| | | |
|---------|---|-----|
| 14.6 | High Energy Experiments..... | 299 |
| 14.6.1 | Overview | 299 |
| 14.6.2 | Collision experiments..... | 299 |
| (1) | Hodoscopes | 299 |
| (2) | TOF counters | 300 |
| (3) | Calorimeters..... | 300 |
| (4) | Cherenkov counters | 301 |
| 14.6.3 | Proton decay and neutrino observation experiments..... | 302 |
| 14.6.4 | Gamma-ray telescopes | 304 |
| 14.6.5 | Dark matter experiments..... | 305 |
| 14.7 | Oil Well Logging..... | 306 |
| 14.8 | Radiation Monitoring..... | 307 |
| 14.8.1 | Overview | 307 |
| 14.8.2 | Application examples | 307 |
| (1) | Handheld radiation monitors (radiation pager)..... | 307 |
| (2) | Radiation monitoring posts..... | 308 |
| (3) | OSL (optically stimulated luminescence) dosimeters..... | 308 |
| 14.9 | Industrial Measurements | 309 |
| 14.9.1 | Overview | 309 |
| 14.9.2 | Application examples | 309 |
| (1) | Semiconductor wafer inspection equipment | 309 |
| (2) | Thickness gauges | 309 |
| (3) | Pinhole inspections | 310 |
| 14.10 | Solid Surface Analysis..... | 311 |
| 14.10.1 | Solid surface analyzers..... | 311 |
| | References in Chapter 14 | 313 |

CHAPTER 1
INTRODUCTION

1.1 Overview of This Manual

The following provides a brief description of each chapter in this technical manual.

Chapter 1 Introduction

Before starting to describe the main subjects, this chapter explains basic photometric units used to measure or express properties of light such as wavelength and intensity. This chapter also describes the history of the development of photocathodes and photomultiplier tubes.

Chapter 2 Basic Principles of Photomultiplier Tubes

This chapter describes the basic operating principles and elements of photomultiplier tubes, including photoelectron emission, electron trajectories, electron multiplication by use of electron multipliers (dynodes), and anodes.

Chapter 3 Basic Operating Methods of Photomultiplier Tubes

This chapter is aimed at first-time photomultiplier tube users. It describes how to select and operate photomultiplier tubes and how to process their signals.

Chapter 4 Characteristics of Photomultiplier Tubes

Chapter 4 explains in detail the basic performance and various characteristics of photomultiplier tubes.

Chapter 5 Photomultiplier Tube Connection Circuits and Their Usage

This chapter describes how to use the basic circuits and accessories needed for correct operation of photomultiplier tubes.

Chapter 6 Photon Counting

Chapter 6 describes the principle, method of use, characteristics and advantages of photon counting used for optical measurement at very low light levels where the absolute amount of light is extremely small.

Chapter 7 Scintillation Counting

Chapter 7 explains scintillation counting with photomultiplier tubes for radiation measurement. It includes descriptions of characteristics, measurement methods, and typical examples of data.

Chapter 8 Photomultiplier Tube Modules

This chapter describes photomultiplier tube modules (often abbreviated PMT modules) developed to make photomultiplier tubes easier to use and also to expand their applications.

Chapter 9 Position Sensitive Photomultiplier Tubes

Chapter 9 describes multianode position-sensitive photomultiplier tubes and center-of-gravity detection type photomultiplier tubes, showing their structure, characteristics and application examples.

Chapter 10 Micro PMT

This chapter describes the world's smallest photomultiplier tubes we developed by reviewing the photomultiplier tube production methods from scratch and utilizing MEMS (micro-electronics-mechanical system) technology.

Chapter 11 Microchannel Plate-Photomultiplier Tube

This chapter explains MCP-PMTs (photomultiplier tubes incorporating microchannel plates) that are high sensitivity and ultra-fast photodetectors.

Chapter 12 HPD (Hybrid Photo-Detectors)

This chapter describes hybrid photo-detectors (HPD) that incorporate a semiconductor detector in an electron tube.

Chapter 13 Environmental Resistance and Reliability

In this chapter, photomultiplier tube performance and usage are discussed in terms of environmental durability and operating reliability. In particular, this chapter describes ambient temperature, humidity, magnetic field effects, mechanical strength, etc. and the countermeasures against these factors.

Chapter 14 Applications

Chapter 14 introduces major applications of photomultiplier tubes, and explains how photomultiplier tubes are used in a variety of fields and applications.

1.2 Photometric Units

Before starting to describe photomultiplier tubes and their characteristics, this section briefly discusses photometric units commonly used to measure the quantity of light. This section also explains the wavelength regions of light (spectral range) and the units to denote them, as well as the unit systems used to express light intensity. Since information included here is just an overview of major photometric units, please refer to specialty books for more details.¹⁾²⁾

1.2.1 Spectral regions and units

Electromagnetic waves cover a very wide range from gamma rays up to millimeter waves. So-called "light" is a very narrow range of these electromagnetic waves.

Table 1-1 shows how spectral regions are designated when light is classified by wavelength, along with the conversion diagram for light units. In general, what we usually refer to as light covers a range from 10^2 to 10^6 nanometers (nm) in wavelength. The spectral region between 350 and 750 nm shown in the table is usually known as the visible region. The region with wavelengths shorter than the visible region is divided into UV (shorter than 350 nm), vacuum UV (shorter than 200 nm) where air is absorbed, and extreme UV (shorter than 100 nm). Even shorter wavelengths span into the region called soft X-rays (shorter than 10 nm) and X-rays.

In contrast, longer wavelengths beyond the visible region extend from near IR (750 nm or up) to the infrared (several micrometers or up) and far IR (several tens of micrometers or up) regions.

| Wavelength (nm) | Spectral Range | Frequency (Hz) | Energy (eV) |
|-----------------|----------------------|----------------|-------------|
| 10 | X-ray Soft X-ray | | |
| 10^2 | Extreme UV region | 10^{16} | 10^2 |
| 200 | Vacuum UV region | | 10 |
| 350 | Ultraviolet region | 10^{15} | |
| 750 | Visible region | | |
| 10^3 | Near infrared region | | 1 |
| 10^4 | Infrared region | 10^{14} | |
| | | 10^{13} | 10^{-1} |
| 10^5 | | | 10^{-2} |
| | Far infrared region | 10^{12} | |
| 10^6 | | | 10^{-3} |

Table 1-1: Spectral regions and unit conversions

Light energy E (J) is given by the following equation (Eq. 1-1).

$$E = h\nu = h \cdot \frac{c}{\lambda} \quad \text{..... (Eq. 1-1)}$$

h : Planck's constant 6.626×10^{-34} (J·s)

ν : Frequency of light (Hz)

c : Velocity of light 3×10^8 m/s

λ : Wavelength (m)

Eq. 1-1 can be rewritten as Eq. 1-2, by substituting E in eV, wavelength in nanometers (nm) and constants h and c in Eq. 1-1. Here, 1 eV equals 1.6×10^{-19} J.

$$E(\text{eV}) = \frac{1240}{\lambda} \quad \text{..... (Eq. 1-2)}$$

From Eq. 1-2, it can be seen that light energy increases in proportion to the reciprocal of wavelength.

1.2.2 Units of light intensity

This section explains the units used to represent light intensity and their definitions.

The radiant quantity of light or radiant flux is a pure physical quantity expressed in units of watts or W (J/s). In contrast, the photometric quantity of light or luminous flux is represented in lumens or lm which correlate to the visual sensation of light.

If the number of photons per second is N and the wavelength is λ , then Eq. 1-1 can be rewritten as Eq. 1-3 from the relation of $W=J/s$.

$$W = NE = \frac{Nhc}{\lambda} \quad \text{..... (Eq. 1-3)}$$

Here, the following equation can be obtained by substituting specific values for the above equation.

$$W = \frac{N \times 2 \times 10^{-16}}{\lambda}$$

The above equation shows the relation between the radiant power (W) of light and the number of photons (N) per second, and will be helpful if you remember it.

Table 1-2 shows comparisons of radiant units with photometric units (in brackets []). Each unit is described in subsequent sections.

| Quantity | Unit Name | Symbol |
|--|--|--|
| Radiant flux [Luminous flux] | watts [lumens] | W [lm] |
| Radiant energy [Quantity of light] | joules [lumen·sec.] | J [lm·s] |
| Irradiance [Illuminance] | watts per square meter [lux] | W/m ² [lx] |
| Radiant emittance [Luminous emittance] | watts per square meter [lumens per square meter] | W/m ² [lm/m ²] |
| Radiant intensity [Luminous intensity] | watts per steradian [candelas] | W/sr [cd] |
| Radiance [Luminance] | watts per steradian·square meter [candelas per square meter] | W/sr/m ² [cd/m ²] |

Table 1-2: Comparisons of radiant units with photometric units (shown in brackets [])

1. Radiant flux [Luminous flux]

Radiant flux is a unit to express radiant quantity, while luminous flux shown in brackets [] in Table 1-2 and the subhead just above is a unit to represent luminous quantity. (Units are shown this way in the rest of this chapter.) Radiant flux (Φ_e) is the flow of radiant energy (Q_e) past a given point in a unit time period, and is defined as follows:

$$\Phi_e = dQ_e/dt \text{ (J/s)} \dots\dots\dots \text{(Eq. 1-4)}$$

On the other hand, luminous flux (Φ) is measured in lumens and defined as follows:

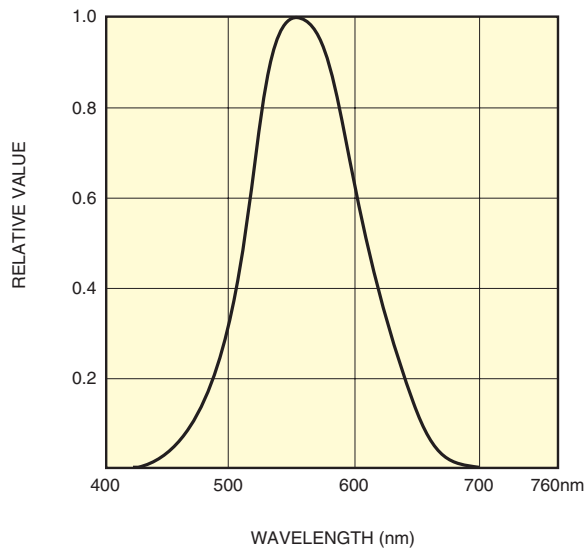
$$\Phi = k_m \int \Phi_e(\lambda) v(\lambda) d\lambda \dots\dots\dots \text{(Eq. 1-5)}$$

where $\Phi_e(\lambda)$: Spectral radiant density of a radiant flux, or spectral radiant flux

k_m : Maximum sensitivity of the human eye (683 lm/W)

$v(\lambda)$: Typical sensitivity of the human eye

The maximum sensitivity of the eye (K_m) is a conversion coefficient used to link the radiant quantity and luminous quantity. Here, $V(\lambda)$ indicates the typical spectral response of the human eye, internationally established as spectral luminous efficiency. A typical plot of spectral luminous efficiency versus wavelength (also called the luminosity curve) and relative spectral luminous efficiency at each wavelength are shown in Figure 1-1 and Table 1-3, respectively.



THBV4_0101EA

Figure 1-1: Spectral luminous efficiency distribution

| Wavelength (nm) | Luminous Efficiency | Wavelength (nm) | Luminous Efficiency |
|-----------------|---------------------|-----------------|---------------------|
| 400 | 0.0004 | 600 | 0.631 |
| 10 | 0.0012 | 10 | 0.503 |
| 20 | 0.0040 | 20 | 0.381 |
| 30 | 0.0116 | 30 | 0.265 |
| 40 | 0.023 | 40 | 0.175 |
| 450 | 0.038 | 650 | 0.107 |
| 60 | 0.060 | 60 | 0.061 |
| 70 | 0.091 | 70 | 0.032 |
| 80 | 0.139 | 80 | 0.017 |
| 90 | 0.208 | 90 | 0.0082 |
| 500 | 0.323 | 700 | 0.0041 |
| 10 | 0.503 | 10 | 0.0021 |
| 20 | 0.710 | 20 | 0.00105 |
| 30 | 0.862 | 30 | 0.00052 |
| 40 | 0.954 | 40 | 0.00025 |
| 550 | 0.995 | 750 | 0.00012 |
| 555 | 1.0 | 60 | 0.00006 |
| 60 | 0.995 | | |
| 70 | 0.952 | | |
| 80 | 0.870 | | |
| 90 | 0.757 | | |

Table 1-3: Relative spectral luminous efficiency at each wavelength

2. Radiant energy [Quantity of light]

Radiant energy (Q_e) is the integral of radiant flux over a duration of time. Similarly, the quantity of light (Q) is defined as the integral of luminous flux over a duration of time. Each term is respectively given by Eq. 1-6 and Eq. 1-7.

$$Q_e = \int \Phi_e dt \text{ (W}\cdot\text{s)} \dots\dots\dots \text{(Eq. 1-6)}$$

$$Q = \int \Phi dt \text{ (lm}\cdot\text{s)} \dots\dots\dots \text{(Eq. 1-7)}$$

3. Irradiance [Illuminance]

Irradiance (E_e) is the radiant flux incident per unit area of a surface, and is also called radiant flux density. (See Figure 1-2.) Likewise, illuminance (E) is the luminous flux incident per unit area of a surface. Each term is respectively given by Eq. 1-8 and Eq. 1-9.

$$\text{Irradiance } E_e = d\Phi_e/ds \text{ (W/m}^2\text{)} \dots\dots\dots \text{(Eq. 1-8)}$$

$$\text{Illuminance } E = d\Phi/ds \text{ (lx)} \dots\dots\dots \text{(Eq. 1-9)}$$

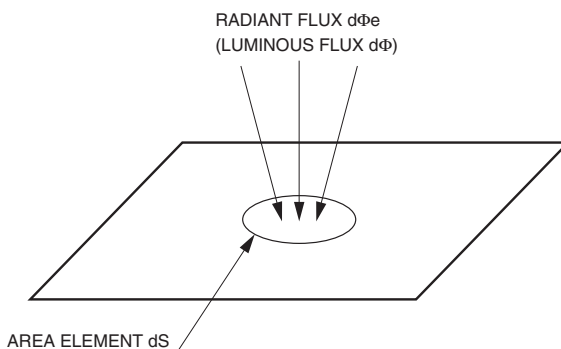


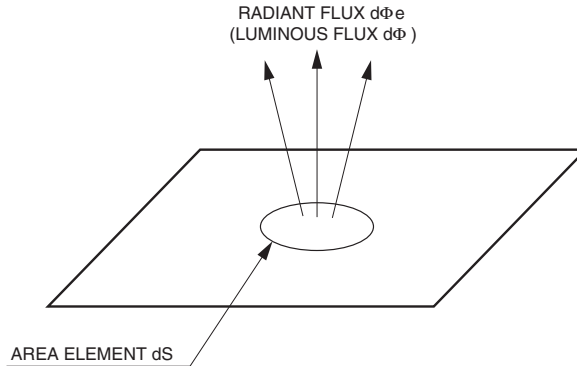
Figure 1-2: Irradiance (Illuminance)

4. Radiant emittance [Luminous emittance]

Radiant emittance (M_e) is the radiant flux emitted per unit area of a surface. (See Figure 1-3.) Likewise, luminous emittance (M) is the luminous flux emitted per unit area of a surface. Each term is respectively expressed by Eq. 1-10 and Eq. 1-11.

Radiant emittance $M_e = d\Phi_e/ds$ (W/m^2) (Eq. 1-10)

Luminous emittance $M = d\Phi/ds$ (lm/m^2) (Eq. 1-11)



THBV4_0103EA

Figure 1-3: Radiant emittance (Luminous emittance)

5. Radiant intensity [Luminous intensity]

Radiant intensity (I_e) is the radiant flux emerging from a point source, divided by the unit solid angle. (See Figure 1-4.) Likewise, luminous intensity (I) is the luminous flux emerging from a point source, divided by the unit solid angle. These terms are respectively expressed by Eq. 1-12 and Eq. 1-13.

Radiant intensity $I_e = d\Phi_e/d\omega$ (W/sr) (Eq. 1-12)

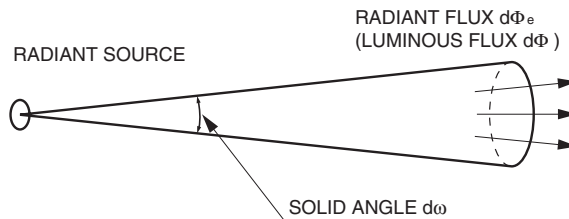
Where

- Φ_e : radiant flux (W)
- ω : solid angle (sr)

Luminous intensity $I = d\Phi/d\omega$ (cd) (Eq. 1-13)

Where

- Φ : luminous flux (lm)
- ω : solid angle (sr)



THBV4_0104EA

Figure 1-4: Radiant intensity (Luminous intensity)

6. Radiance [Luminance]

Radiance (L_e) is the radiant intensity (luminous intensity) emitted in a certain direction from a radiant source, divided by the unit area of an orthographically projected surface of radiant quantity. (See Figure 1-5.) Likewise, luminance (L) is the luminous flux emitted from a light source, divided by the unit area of an orthographically projected surface of radiant quantity. Each term is respectively given by Eq. 1-14 and Eq. 1-15.

Radiance $L_e = dI_e/ds \cdot \cos\theta$ ($W/sr/m^2$) (Eq. 1-14)

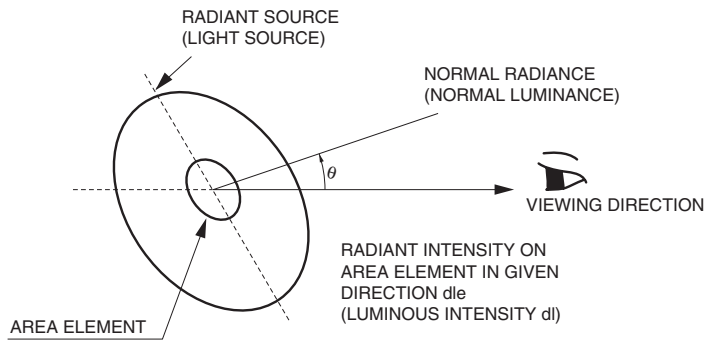
Where

- I_e : radiant intensity
- s : area
- θ : angle between viewing direction and small area surface

Luminance $L = dI/ds \cdot \cos\theta$ (cd/m^2) (Eq. 1-15)

Where

- I : luminous intensity (cd)



THBV4_0105EA

Figure 1-5: Radiant intensity (Luminous intensity)

In the above sections, we discussed basic photometric units which are internationally specified as SI units for quantitative measurements of light. However in some cases, units other than SI units are used. Tables 1-4 and 1-5 show conversion tables for SI units and non-SI units, with respect to luminance and illuminance. Refer to these conversion tables as necessary.

| | Unit Name | Symbol | Conversion Formula |
|-------------|--------------|--------|---|
| SI Unit | nit | nt | $1 \text{ nt} = 1 \text{ cd/m}^2$ |
| | stilb | sb | $1 \text{ sb} = 1 \text{ cd/cm}^2 = 10^4 \text{ cd/m}^2$ |
| | apostilb | asb | $1 \text{ asb} = 1/\pi \text{ cd/m}^2$ |
| | lambert | L | $1 \text{ L} = 1/\pi \text{ cd/cm}^2 = 10^4/\pi \text{ cd/m}^2$ |
| Non SI Unit | foot lambert | fL | $1 \text{ fL} = 1/\pi \text{ cd/ft}^2 = 3.426 \text{ cd/m}^2$ |

Table 1-4: Luminance units

| | Unit Name | Symbol | Conversion Formula |
|-------------|-------------|--------|--|
| SI Unit | photo | ph | $1 \text{ ph} = 1 \text{ lm/cm}^2 = 10^4 \text{ lx}$ |
| Non SI Unit | food candle | fc | $1 \text{ fc} = 1 \text{ lm/ft}^2 = 10.764 \text{ lx}$ |

Table 1-5: Illuminance units

1.3 History

1.3.1 History of photocathodes³⁾

The photoelectric effect was discovered in 1887 by Hertz⁴⁾ through experiments exposing a negative electrode to ultraviolet radiation. In the next year 1888, the photoelectric effect was conclusively confirmed by Hallwachs.⁵⁾ In 1889, Elster and Geitel⁶⁾ reported the photoelectric effect which was induced by visible light striking an alkali metal (sodium-potassium). Since then, a variety of experiments and discussions on photoemission have been made by many scientists. As a result, the concept proposed by Einstein (in the quantum theory in 1905),⁷⁾ “On a Heuristic Viewpoint Concerning the Production and Transformation of Light”, has been proven and accepted.

During this historic period of achievement, Elster and Geitel produced a photoelectric tube in 1913. Then, a compound photoemissive surface (photocathode) made of Ag-O-Cs (silver oxygen cesium, also called S-1) was discovered in 1929 by Koller⁸⁾ and Campbell.⁹⁾ This photocathode showed photoelectric sensitivity about two orders of magnitude higher than previously used photocathode materials, achieving high sensitivity in the visible to near infrared region. In 1930, they succeeded in producing a phototube using this S-1 photocathode. In the same year, a Japanese scientist, Asao reported a method for enhancing the sensitivity of silver in the S-1 photocathode. Since then, various photocathodes have been developed one after another, including bialkali photocathodes for the visible region, multialkali photocathodes with high sensitivity extending to the infrared region, and alkali halide photocathodes intended for ultraviolet detection.¹⁰⁾⁻¹³⁾ In 2007, significant progress was made in enhancing the quantum efficiency of a bialkali photocathode by improving its manufacturing process. This photocathode achieved a quantum efficiency of 43 % at 350 nm and was named “ultra bialkali” or UBA. Besides the ultra bialkali, another bialkali photocathode was developed that offered a quantum efficiency of 35 % and was named “super bialkali” or SBA. Other developments include photocathodes capable of stable operation in harsh environments, for example, at low temperatures below -100 °C or at high temperatures of 200 °C.

In addition, photocathodes using III-V compound semiconductors such as GaAs¹⁴⁾⁻¹⁹⁾ and InGaAs^{20) 21)} have been developed and put into practical use. These semiconductor photocathodes have an NEA (negative electron affinity) structure and offer high sensitivity from the ultraviolet through near infrared region. Currently, a wide variety of photomultiplier tubes utilizing the above photocathodes are available. They are selected and used according to the application required.

1.3.2 History of photomultiplier tubes

Photomultiplier tubes have been making rapid progress since the development of photocathodes, secondary emissive surfaces, and electron multipliers.

The first report on a secondary emissive surface was made by Austin et al.²²⁾ in 1902. Since that time, research into secondary emissive surfaces (secondary electron emission) has been carried out to achieve higher electron multiplication. In 1935, Iams et al.²³⁾ succeeded in producing a triode photomultiplier tube with a photocathode combined with a single-stage electron multiplier, which was used for movie sound pickup. In the next year 1936, Zworykin et al.²⁴⁾ developed a photomultiplier tube having a multi-stage electron multiplier. This tube enabled electrons to travel in the tube by using an electric field and a magnetic field.

Then, in 1939, Zworykin and Rajchman²⁵⁾ developed an electrostatic-focusing type photomultiplier tube (this is the basic structure of photomultiplier tubes currently used). In this photomultiplier tube, an Ag-O-Cs photocathode was first used and later an Sb-Cs photocathode was employed.

An improved photomultiplier tube structure was developed and announced by Morton et al. in 1949²⁶⁾ and in 1956.²⁷⁾ Since then the electron multiplier structure has been intensively studied, leading to the development of a variety of electron multiplier structures including circular-cage, linear-focused, and box-

and-grid types. In addition, photomultiplier tubes using magnetic-focusing type multipliers,²⁸⁾ transmission-mode secondary-emissive surfaces²⁹⁾⁻³¹⁾ and channel type multipliers³²⁾ have been developed.

At Hamamatsu Photonics, the manufacture of various phototubes such as types with an Sb-Cs photocathode was established in 1953. (The company was then called Hamamatsu TV Co., Ltd. until 1983.) In 1959, Hamamatsu Photonics marketed side-on photomultiplier tubes (product names 931A, 1P21 and R106 having an Sb-Cs photocathode) which have been widely used in spectroscopy. Hamamatsu Photonics also developed and marketed side-on photomultiplier tubes (product names R132 and R136) having an Ag-Bi-O-Cs photocathode in 1962. This photocathode had higher sensitivity in the red region of spectrum than that of the Sb-Cs photocathode, making them best suited for spectroscopy in those days. In addition, Hamamatsu Photonics put head-on photomultiplier tubes (product name 6199 with an Sb-Cs photocathode) on the market in 1965. In 1967, Hamamatsu Photonics introduced a 1/2-inch diameter side-on photomultiplier tube (product name R300 with an Sb-Cs photocathode) which was the smallest tube at that time. In 1969, Hamamatsu Photonics developed and marketed photomultiplier tubes having a multialkali (Na-K-Cs-Sb) photocathode (product names R446: side-on and R375: head-on). Then, in 1974 a new side-on photomultiplier tube (product name R928) was developed by Hamamatsu Photonics, which achieved much higher sensitivity in the red to near infrared region. This was an epoch-making event in terms of enhancing photomultiplier tube sensitivity. Since that time, Hamamatsu Photonics has continued to develop and produce a wide variety of state-of-the-art photomultiplier tubes. The product line ranges in size from the world's smallest 3/8-inch diameter photomultiplier tubes (R1635) to the world's largest 20-inch hemispherical tubes (R1449 and R3600). Hamamatsu Photonics also offers ultra-fast photomultiplier tubes using a microchannel plate electron multiplier (R3809) with a time resolution of 30 picoseconds, mesh-electrode type photomultiplier tubes (R5924) that maintain an adequate gain of 10^5 even in high magnetic fields of up to one Tesla, and hybrid photo-detectors (HPD) that multiply photoelectrons from the photocathode with very low multiplication fluctuations by bombarding them directly into the semiconductor. More recently, Hamamatsu Photonics has developed TO-8 metal package type photomultiplier tubes (R7400) using metal channel dynode, various types of position-sensitive photomultiplier tubes capable of position detection, flat panel photomultiplier tubes with a high effective area ratio, and subminiature photomultiplier tubes (micro PMT) that fit on a fingertip. Hamamatsu Photonics is constantly engaged in research and development for manufacturing a wide variety of photomultiplier tubes to meet a wide range of application needs.

References in Chapter 1

- 1) Society of Illumination: Lighting Handbook, Ohm-Sha (1987)
- 2) John W. T. WALSH: Photometry, DOVER Publications, Inc. New York
- 3) T. Hiruma: SAMPE Journal, 24, 35 (1988)
A. H. Sommer: Photoemissive Materials, Robert E. Krieger Publishing Company (1980)
- 4) H. Hertz: Ann. Physik, 31, 983 (1887)
- 5) W. Hallwachs: Ann. Physik, 33, 301 (1888)
- 6) J. Elster and H. Geitel: Ann. Physik, 38, 497 (1889)
- 7) A. Einstein: Ann. Physik, 17, 132 (1905)
- 8) L. Koller: Phys. Rev., 36, 1639 (1930)
- 9) N.R. Campbell: Phil. Mag., 12, 173 (1931)
- 10) P. Gorlich: Z. Physik, 101, 335 (1936)
- 11) A.H. Sommer: U. S. Patent 2,285,062, Brit. Patent 532,259
- 12) A.H. Sommer: Rev. Sci. Instr., 26, 725 (1955)
- 13) A.H. Sommer: Appl. Phys. Letters, 3, 62 (1963)
- 14) A.N. Arsenova-Geil and A. A. Kask: Soviet Phys.- Solid State, 7, 952 (1965)
- 15) A.N. Arsenova-Geil and Wang Pao-Kun: Soviet Phys.- Solid State, 3, 2632 (1962)
- 16) D.J. Haneman: Phys. Chem. Solids, 11, 205 (1959)
- 17) G.W. Gobeli and F.G. Allen: Phys. Rev., 137, 245A (1965)
- 18) D.G. Fisher, R.E. Enstrom, J.S. Escher, H.F. Gossenberger: IEEE Trans. Elect. Devices, Vol ED-21, No.10, 641(1974)
- 19) C.A. Sanford and N.C. Macdonald: J. Vac. Sci. Technol. B8(6), Nov/Dec 1853(1990)
- 20) D.G. Fisher and G.H. Olsen: J. Appl. Phys. 50(4), 2930 (1979)
- 21) J.L. Bradshaw, W.J. Choyke and R.P. Devaty: J. Appl. Phys. 67(3), 1, 1483 (1990)
- 22) H. Bruining: Physics and applications of secondary electron emission, McGraw-Hill Book Co., Inc. (1954)
- 23) H.E. Iams and B. Salzberg: Proc. IRE, 23, 55(1935)
- 24) V.K. Zworykin, G.A. Morton, and L. Malter: Proc. IRE, 24, 351 (1936)
- 25) V.K. Zworykin and J. A. Rajchman: Proc. IRE, 27, 558 (1939)
- 26) G.A. Morton: RCA Rev., 10, 529 (1949)
- 27) G.A. Morton: IRE Trans. Nucl. Sci., 3, 122 (1956)
- 28) Heroux, L. and H.E. Hinteregger: Rev. Sci. Instr., 31, 280 (1960)
- 29) E.J. Sternglass: Rev. Sci. Instr., 26, 1202 (1955)
- 30) J.R. Young: J. Appl. Phys., 28, 512 (1957)
- 31) H. Dormont and P. Saget: J. Phys. Radium (Physique Appliquee), 20, 23A (1959)
- 32) G.W. Goodrich and W.C. Wiley: Rev. Sci. Instr., 33, 761 (1962)

CHAPTER 2

BASIC PRINCIPLES OF PHOTOMULTIPLIER TUBES

This chapter describes the structures and operating principles of photomultiplier tubes, including photoelectron emission, electron trajectories, and electron multipliers.

2.1 Structures and multiplication principles of photomultiplier tubes^{1) - 7)}

A photomultiplier tube is a vacuum tube consisting of an input window, a photocathode, focusing electrodes, an electron multiplier (dynodes), and an anode sealed usually into an evacuated glass tube. Figure 2-1 shows the schematic construction of a photomultiplier tube.

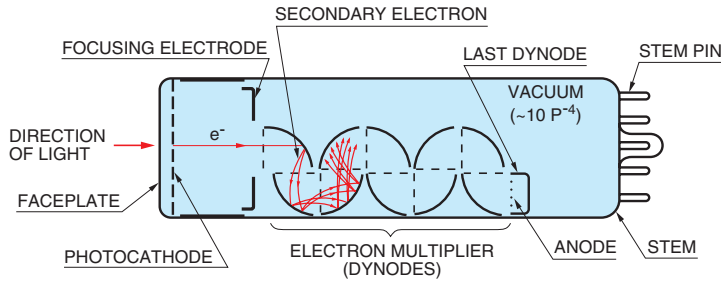


Figure 2-1: Construction of a photomultiplier tube

THBV4_0201EA

Light entering a photomultiplier tube produces an output signal through the following processes:

- (1) Light passes through the input glass window and excites the electrons in the photocathode so that photoelectrons are emitted into the vacuum (external photoelectric effect).
- (2) Photoelectrons are accelerated and focused by the focusing electrode and impinge on the first dynode where they are multiplied by means of secondary electron emission.
- (3) The secondary electron emission is repeated at each dynode in the electron multiplier.
- (4) A cluster of secondary electrons emitted from the last dynode are finally multiplied up to 10^6 to 10^7 times and are extracted from the anode.

2.2 Photoelectron Emission^{6) 7)}

Photoelectric conversion is broadly classified into “external photoelectric effect” by which photoelectrons are emitted into the vacuum from a material and “internal photoelectric effect” by which photoelectrons are excited into the conduction band of a material. The photocathode has the former effect and the latter is represented by the photoconductive or photovoltaic effect.

Since a photocathode is a semiconductor, it can be described using band models as shown in Figure 2-2: (1) alkali photocathode and (2) III-V compound semiconductor photocathode.

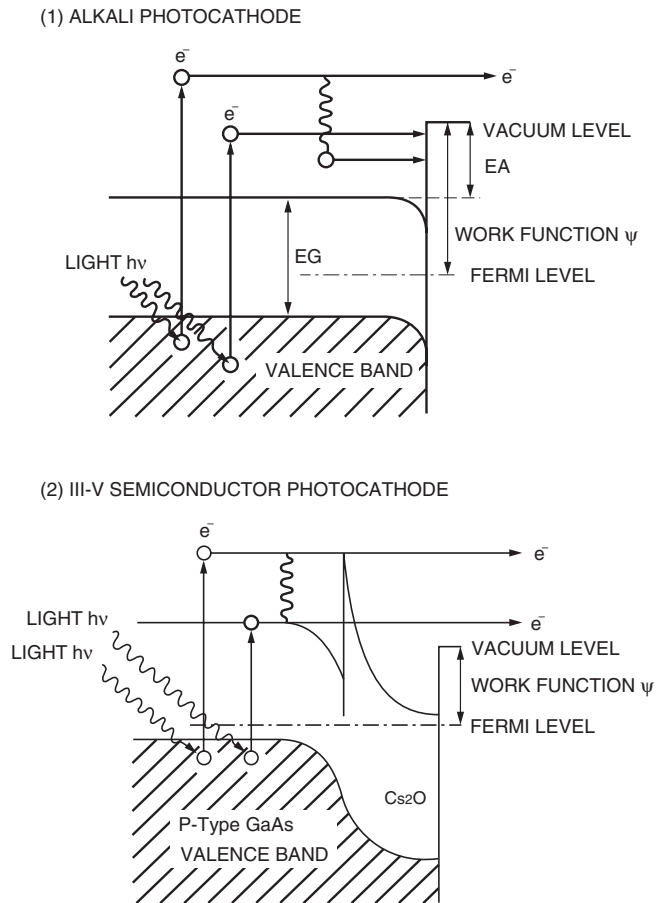


Figure 2-2: Photocathode band models

In a semiconductor band model, there exist a forbidden-band gap or energy gap (EG) that cannot be occupied by electrons, electron affinity (EA) which is an interval between the conduction band and the vacuum level barrier (vacuum level), and work function (ψ) which is an energy difference between the Fermi level and the vacuum level barrier (vacuum level). When photons strike a photocathode, electrons in the valence band absorb photon energy ($h\nu$) and become excited, diffusing toward the photocathode surface. If the diffused electrons have enough energy to overcome the vacuum level barrier, they are emitted into the vacuum as photoelectrons. This can be expressed in a probability process, and the quantum efficiency $\eta(\nu)$, i.e., the ratio of the number of output electrons to the number of incident photons is given by

$$\eta(\nu) = (1-R) \frac{P\nu}{k} \cdot \left(\frac{1}{1+1/kL} \right) \cdot P_s$$

where

- R : reflection coefficient
- k : full absorption coefficient of photons
- P ν : probability that light absorption may excite electrons to a level greater than the vacuum level
- L : mean escape length of excited electrons
- P $_s$: probability that electrons reaching the photocathode surface may be released into the vacuum
- ν : wavenumber of light

In the above equation, if we have chosen an appropriate material which determines parameters R, k and P ν , the factors that dominate the quantum efficiency will be L (mean escape length of excited electrons) and P $_s$ (probability that electrons may be emitted into the vacuum). L becomes longer by use of a better crystal and P $_s$ greatly depends on electron affinity (EA).

Figure 2-2 (2) shows the band model of a photocathode made of III-V compound semiconductors.⁸⁾⁻¹⁰⁾ If the surface layer of this photocathode of III-V compound semiconductors is positively charged by materials such as Cs $_2$ O, a depletion layer is formed, causing the band structure to be bent downward. This bending can make the electron affinity negative. This state is called NEA (negative electron affinity). The NEA effect increases the probability (P $_s$) that the electrons reaching the photocathode surface may be emitted into the vacuum. In particular, it enhances the quantum efficiency at long wavelengths with lower excitation energy. In addition, it lengthens the mean escape distance (L) of excited electrons due to the depletion layer. Photocathodes can be classified by photoelectron emission process into a reflection mode and a transmission mode. The reflection mode photocathode is usually formed on a metal plate, and photoelectrons are emitted in the opposite direction of the incident light. The transmission mode photocathode is usually deposited as a thin film on a glass plate which is optically transparent. Photoelectrons are emitted in the same direction as that of the incident light. (Refer to Figures 2-3, 2-4, 2-5 and 2-6.) The reflection mode photocathode is mainly used for the side-on photomultiplier tubes which receive light through the side of the glass bulb, while the transmission mode photocathode is used for the head-on photomultiplier tubes which detect the input light through the end of a cylindrical bulb.

The wavelength of maximum response and long-wavelength cutoff are determined by the combination of alkali metals used for the photocathode and its fabrication process. As a designation, photocathode sensitivity¹¹⁾ versus wavelength is registered as an "S" number by the JEDEC (Joint Electron Devices Engineering Council), which indicates the combination of a photocathode and window material. At present, however, only some of the registered S numbers (S-1, S-11, S-20 and S-25) are used. Refer to Chapter 4 for the spectral response characteristics of various photocathodes and window materials.

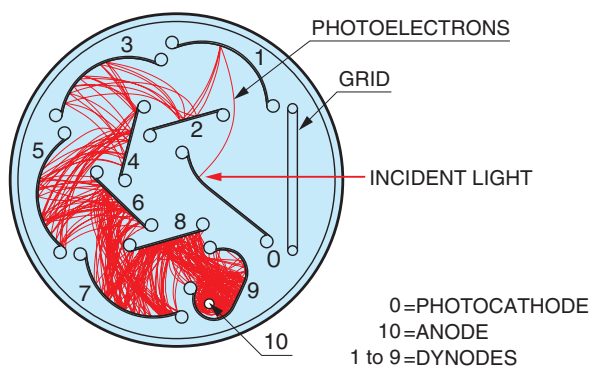
2.3 Electron Trajectory

In order to collect photoelectrons and secondary electrons efficiently on a dynode and also to minimize the electron transit time spread, electrode design must be optimized through an analysis of the electron trajectories.12)-16)

Electron movement in a photomultiplier tube is affected by the electric field which is dominated by the electrode configuration, arrangement, and also the voltage applied to the electrode. The electron trajectories are determined by finding the potential distribution and solving the equation for motion.

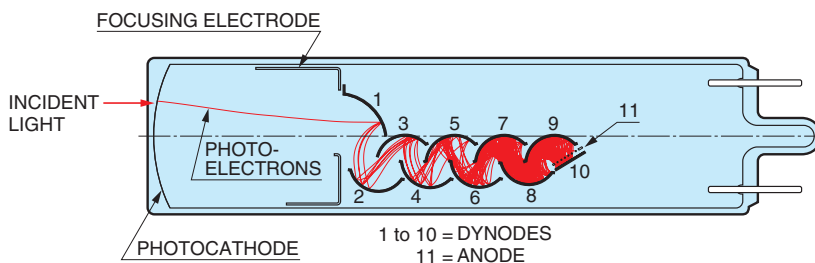
The electron trajectories from the photocathode to the first dynode must be carefully designed in consideration of the photocathode shape (planar or spherical window), the shape and arrangement of the focusing electrode, and the supply voltage, so that the photoelectrons emitted from the photocathode are efficiently focused onto the first dynode. The collection efficiency of the first dynode is the ratio of the number of electrons landing on the effective area of the first dynode to the number of emitted photoelectrons. This is usually from 60 to 90 percent.

The second and subsequent dynodes in the electron multiplier usually consist of several to more than ten stages of secondary-emissive electrodes having a curved surface. Figures 2-3, 2-4 and 2-5 show typical electron trajectories of a circular-cage, linear-focused, and metal channel type of electron multipliers.



THBV4_0203EA

Figure 2-3: Circular-cage type



THBV4_0204EA

Figure 2-4: Linear-focused type

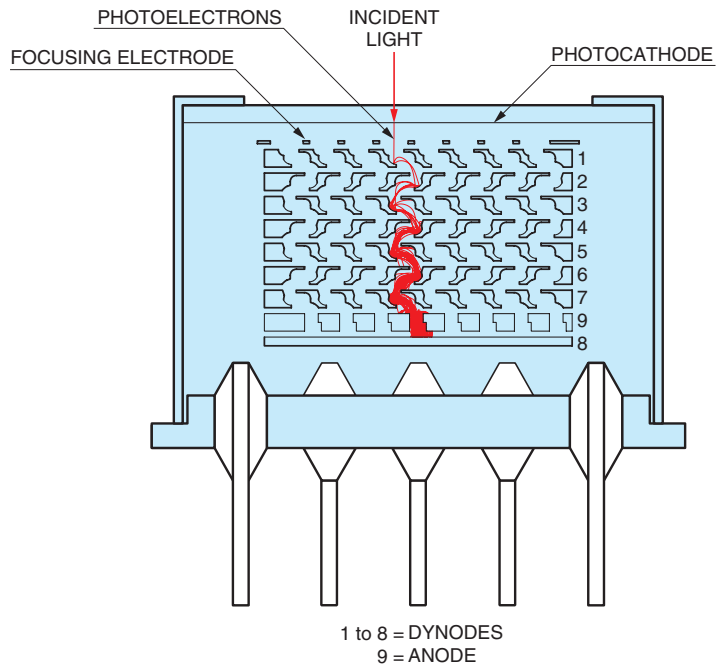


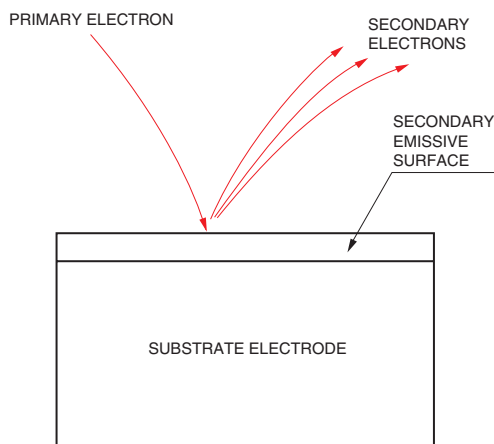
Figure 2-5: Metal channel type

THBV4_0205EA

2.4 Electron multiplier (dynode)

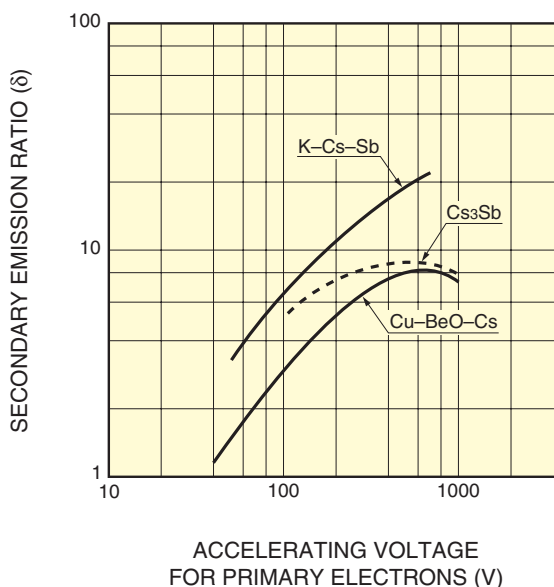
As stated above, the potential distribution and electrode structure of a photomultiplier tube is designed to provide optimum performance. Photoelectrons emitted from the photocathode are multiplied by the first stage through the last stage (up to 19 stages) in the electron multiplier, with current amplification ranging from 10 to as much as 10^8 times, and are finally sent to the anode.

Major secondary emissive materials¹⁷⁾⁻²¹⁾ generally used are alkali antimonide (Sb), beryllium oxide (BeO), and magnesium oxide (MgO). These materials are coated onto a substrate electrode made of nickel, stainless steel, or copper-beryllium alloy. Figure 2-6 shows a model of the secondary emission multiplication of an electron multiplier.



THBV4_0206EA

Figure 2-6: Secondary emission model of electron multiplier



THBV4_0207EA

Figure 2-7: Secondary emission ratio

When a primary electron with initial velocity energy E_p strikes the surface of a dynode, δ secondary electrons are emitted. This δ , the number of secondary electrons per primary electron, is called the secondary emission ratio. Figure 2-7 shows the secondary emission ratio δ for various dynode materials versus the accelerating voltage for the primary electrons. Using the secondary emission ratio, δ , the electron multiplication or gain, μ , is expressed as follows:

$$\mu = \delta^n$$

where

δ : secondary emission ratio at each dynode

n : number of dynode stages

This gain is described in detail in Chapter 4, section 4.2.2.

The gain, time response, and linearity differ depending on the electron multiplier structure, number of dynode stages, and other factors, which must be selected according to the application. These characteristics are described in Chapter 4, section 4.2.1.

2.5 Anode

The anode of a photomultiplier tube is an electrode that collects secondary electrons multiplied in the a multi-stage electron multiplier and outputs the electron current to an external circuit.

Anodes are carefully designed to have a structure optimized for the electron trajectories discussed previously, and are generally fabricated in the form of a rod, plate, or mesh electrode. In order to minimize space charge effects, an anode is arranged so that an adequate potential difference can be established between the last dynode and the anode to obtain as large a current output as possible.

References in Chapter 2

- 1) Hamamatsu Photonics: "Photomultiplier Tubes and Related Products" (revised Feb. 2006)
- 2) Hamamatsu Photonics: "Characteristics and Uses of Photomultiplier Tubes" No.79-57-03 (1982)
- 3) S.K. Poultney: *Advances in Electronics and Electron Physics* 31, 39 (1972)
- 4) D.H. Seib and L.W. Ankerman: *Advances in Electronics and Electron Physics*, 34, 95 (1973)
- 5) J.P. Boutot, et al.: *Advances in Electronics and Electron Physics* 60, 223 (1983)
- 6) T. Hiruma: *SAMPE Journal*, 24, 6, 35-40 (1988)
- 7) T. Hayashi: *Bunkou Kenkyuu*, 22, 233 (1973)
- 8) H. Sonnenberg: *Appl. Phys. Lett.*, 16, 245 (1970)
- 9) W.E. Spicer, et al.: *Pub. Astrom. Soc. Pacific*, 84, 110 (1972)
- 10) M. Hagino, et al.: *Television Journal*, 32, 670 (1978)
- 11) A. Honma: *Bunseki*, 1, 52 (1982)
- 12) K.J. Van Oostrum: *Philips Technical Review*, 42, 3 (1985)
- 13) K. Oba and Ito: *Advances in Electronics and Electron Physics*, 64B, 343
- 14) A.M. Yakobson: *Radiotekh & Electron*, 11, 1813 (1966)
- 15) H. Bruining: *Physics and Applications of Secondary Electron Emission* (1954)
- 16) J. Rodney and M. Vaughan: *IEEE Transaction on Electron Devices*, 36, 9 (1989)
- 17) B. Gross and R. Hessel: *IEEE Transaction on Electrical Insulation*, 26, 1 (1991)
- 18) H.R. Krall, et al.: *IEEE Trans. Nucl. Sci. NS-17*, 71 (1970)
- 19) J.S. Allen: *Rev. Sci. Instr.*, 18 (1947)
- 20) A.M. Tyutikov: *Radio Engineering And Electronic Physics*, 84, 725 (1963)
- 21) A.H. Sommer: *J. Appl. Phys.*, 29, 598 (1958)

MEMO

CHAPTER 3

BASIC OPERATING METHODS OF PHOTOMULTIPLIER TUBES

This chapter provides first-time photomultiplier tube users with a general guide to help select the ideal photomultiplier tube (often abbreviated as PMT), operate it correctly, and use peripheral devices. For more detailed information, refer to the following chapters.

3.1 Using Photomultiplier Tubes

3.1.1 Selection guide

There are many types of photomultiplier tubes that can be classified by shape, sensitivity, structure, etc. Since each type has its own features, it is important to select the type that best matches the application.

| Type | Size (mm) | Effective photocathode area (mm) | Spectral response range (nm) | Photo-cathode material | Light input window | Electrode structure | Number of dynode stages | Number of lead pins | |
|----------|--------------------|----------------------------------|------------------------------|-------------------------|--------------------|---------------------|-------------------------|---------------------|----------|
| Side-on | ϕ 13 (1/2") | 4 × 13 | 185 to 650 | Bialkali Multialkali | Borosilicate glass | Circular-cage | 8 | 10 PIN | |
| | ϕ 28 (1-1/8") | 8 × 24 | 300 to 650 | | | | | | |
| Head-on | ϕ 10 (3/8") | ϕ 8 | 160 to 900 | GaAs | UV glass | Box-and-grid | 9 | 12 PIN | |
| | ϕ 13 (1/2") | ϕ 10 | 185 to 900 | GaAsP | | Linear-focused | 10 | 14 PIN | |
| | ϕ 19 (3/4") | ϕ 15 | 185 to 930 | Cs-Te | | Mesh | 12 | 20 PIN | |
| | ϕ 25 (1") | ϕ 22 | 115 to 320 | Cs-I | | MgF ₂ | Metal channel | ... etc. | ... etc. |
| | ϕ 28 (1-1/8") | ϕ 25 | 115 to 195 | InGaAs(Cs) | | ... etc. | ... etc. | ... etc. | ... etc. |
| | ϕ 38 (1-1/2") | ϕ 34 | 185 to 1010 | InP/InGaAs(Cs) | | ... etc. | ... etc. | ... etc. | ... etc. |
| | ϕ 52 (2") | ϕ 46 | 300 to 900 | ... etc. | | ... etc. | ... etc. | ... etc. | ... etc. |
| | ϕ 76 (3") | ϕ 70 | 300 to 1700 | ... etc. | | ... etc. | ... etc. | ... etc. | ... etc. |
| | ϕ 127 (5") | ϕ 120 | ... etc. | ... etc. | | ... etc. | ... etc. | ... etc. | ... etc. |
| ... etc. | ... etc. | ... etc. | ... etc. | ... etc. | ... etc. | ... etc. | ... etc. | ... etc. | |

Table 3-1: Types of photomultiplier tubes

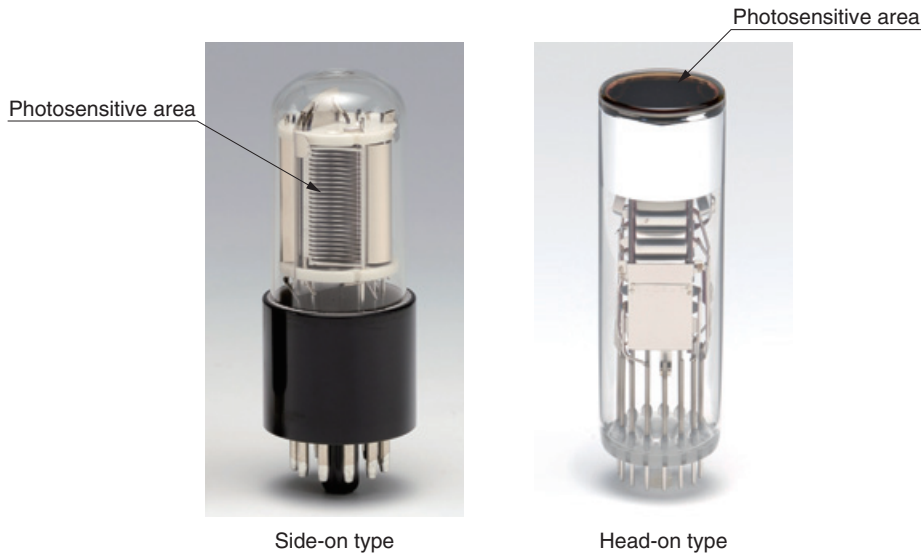


Figure 3-1: Photomultiplier tubes

To select the optimum photomultiplier tube, first narrow down the product selection according to the type, size, photocathode area (photosensitive area) and spectral response range. This means that you should know beforehand the conditions, properties, and wavelengths of the light you need to detect.

Besides the above parameters, our product catalog lists the supply voltage, gain (current amplification), dark current, and time response characteristics, etc. If those parameters are required by the application, select the specifications in order of important parameters to further narrow down the product selection.

The table below shows the selection guide for photomultiplier tubes, using atomic absorption spectrometry as an application example.

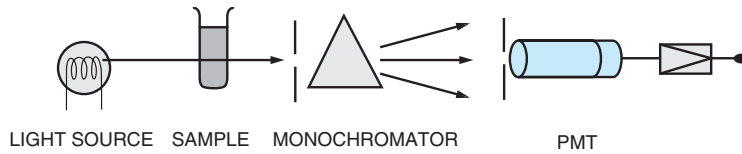


Figure 3-2: Application to atomic absorption spectrometry

THBV4_0302EA

| Light condition to detect | Selection item | |
|-----------------------------|---|--|
| | Photomultiplier tube | Peripheral circuit condition |
| Light wavelength | Light input window material, photocathode type, spectral response range | |
| Light intensity | Gain (supply voltage to electrode), dark current | Signal processing method (analog method, photon counting method) |
| Degree of light spread | Shape, type, and effective photocathode area of photomultiplier tube | |
| Speed of optical phenomenon | Time response characteristics | Frequency bandwidth of connection circuit |

Table 3-2: Selecting a photomultiplier tube

3.1.2 Using a photomultiplier tube

Photomultiplier tubes are photosensitive devices that can be thought of as a current generator that provides a current output in proportion to the incident light. It might help understand the function of photomultiplier tubes if you imagine how a solar cell or photodiode works. A major difference between them is that photomultiplier tubes are capable of outputting a sufficient amount of current even when the incident light is extremely low. The photomultiplier tubes must be operated correctly to provide a measurable output.

Operating a photomultiplier tube requires a high voltage source (normally from 500 to 2000 volts) and a voltage-divider circuit. A proper voltage must be supplied to each electrode to allow the photomultiplier tube to operate with satisfactory performance; however, using independent multiple high voltage power supplies is not practical. Usually, a single high voltage power supply and a voltage-divider circuit are utilized to distribute a suitable voltage to each electrode.

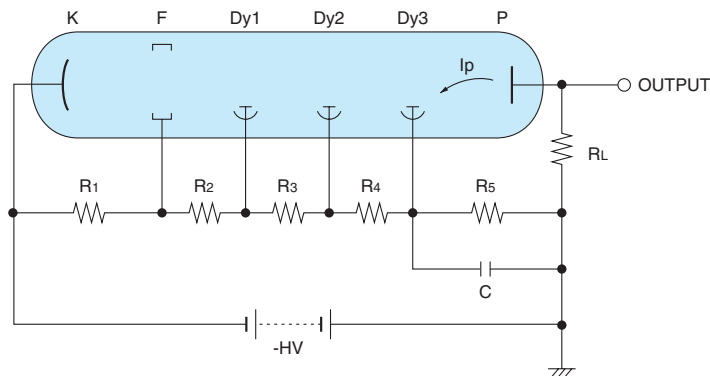


Figure 3-3: Basic photomultiplier tube operation using a voltage-divider circuit

THBV4_0303EA

Since photomultiplier tubes are capable of detecting very-low-level light. This means that extraneous light, even if very weak, will affect the measurement results. Because of this, a shield case or housing for shielding from external factors and a signal amplifier are used according to the particular application. Some applications may require a dark box or light-blocking box in which the entire measuring system can be installed.

For signal processing tasks, an ammeter or oscilloscope is commonly used. An amplifier is also connected when needed.

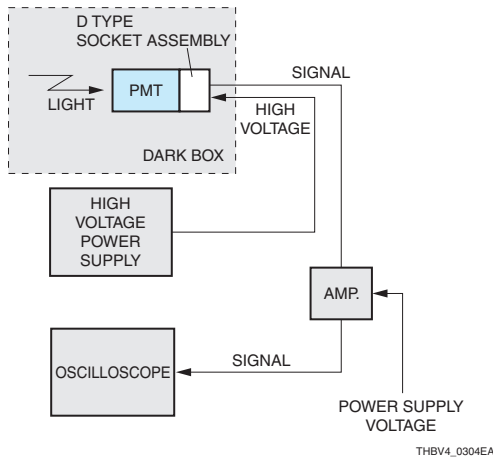


Figure 3-4: Connection block diagram

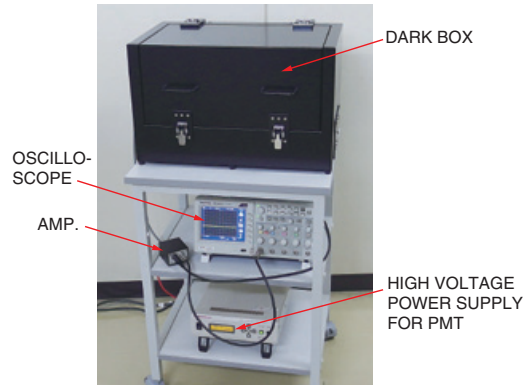


Figure 3-5: Connection example

3.1.3 Precautions

The photomultiplier tube envelope is made of glass, so handle it carefully so as not to apply excessive force, vibrations, or shocks. Since it is a vacuum tube sealed with thin glass, the glass fragments might fly outward if it ruptures or breaks.

Photomultiplier tube performance may degrade if exposed to intense light even when not in operation. Even just room lighting and of course direct sunlight may cause an increase in dark current, and further may lead to a drop in sensitivity after long periods of exposure, so use with caution when selecting storage conditions.

Ambient conditions such as temperature affect photomultiplier tube characteristics. The dark current in particular varies drastically with the ambient conditions. Photomultiplier tubes should therefore be stored at or below room temperature and humidity, and caution should also be taken for magnetic fields and voltage potentials along the periphery.

Also use caution when handling high voltage. Improper use may damage the photomultiplier tube and connected peripheral devices and also create a risk of electrical shock or fire.

3.2 Peripheral devices

3.2.1 High voltage power supply

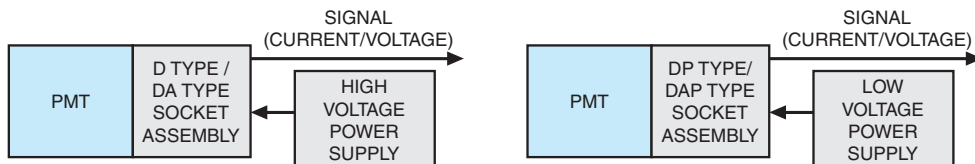
As described above, operating a photomultiplier tube requires a high voltage power supply that provides 500 to 2000 volts at a negative or positive potential. Select a high voltage power supply by considering the voltage supplied to the photomultiplier tube and the current that flows through the voltage-divider circuit. Since the stability of the high voltage power supply affects the photomultiplier tube output, you should preferably select a regulated high voltage power supply with high stability.

3.2.2 Voltage-divider circuit

A voltage-divider circuit is utilized to distribute the output from a high voltage power supply to each electrode. Using a voltage-divider circuit that best meets the application allows the photomultiplier tube to exhibit the required performance. To make it easier to use photomultiplier tubes, Hamamatsu also provides various types of socket assemblies that incorporate a photomultiplier tube socket and a matched divider circuit.

- D-type socket assembly (with built-in voltage-divider circuit)
- DA-type socket assembly (with built-in voltage-divider circuit and amplifier)
- DP-type socket assembly (with built-in voltage-divider circuit and high voltage power supply)
- DAP-type socket assembly (with built-in voltage-divider circuit, amplifier, and high voltage power supply)

When using a DP-type or DAP-type socket assembly there is no need to prepare a high voltage power supply since the socket assembly houses an internal high voltage power supply.



THBV4_0306EA

Figure 3-6: Socket assembly connection examples

3.2.3 Magnetic shield case and housing

Photomultiplier tube characteristics may change due to effects from external magnetic fields and electrical fields. Since photomultiplier tubes have extremely high sensitivity, they might detect extraneous light even if very low, causing a drop in the signal-to-noise ratio. Using a magnetic shield case or housing is effective in reducing or eliminating adverse effects from external factors on photomultiplier tubes.

3.2.4 Amplifier

The output current from photomultiplier tubes changes according to the incident light intensity, and the output voltage also changes depending on the load of the connected device. Since the signal processing unit that connects to a photomultiplier tube usually processes voltage signals, the output current of the photomultiplier tube must be converted into voltage signals by some means, except in cases when using an ammeter.

When an amplifier is used, the anode potential is stabilized and the high-impedance current signal of photomultiplier tubes is converted into a low-impedance voltage signal while being amplified, which is less susceptible to external noise.



Figure 3-7: Peripheral devices and accessories

(From left: high voltage power supplies, socket assemblies, magnetic shield cases and amplifiers)

3.2.5 Photomultiplier tube modules

To make it more convenient to use photomultiplier tubes, Hamamatsu provides photomultiplier tube modules that integrate a photomultiplier tube, voltage-divider circuit, and high voltage power supply into a single compact module case.

Photomultiplier tube modules are easy to handle since they operate just by supplying low voltage. So there is no need to handle high voltages and the module case is effective in blocking light. Moreover, it is easy to install a photomultiplier tube module into equipment and make connections to the peripheral devices. Since only a simple setup is needed to start measurement, photomultiplier tube modules are recommended especially for first time users of photomultiplier tubes.

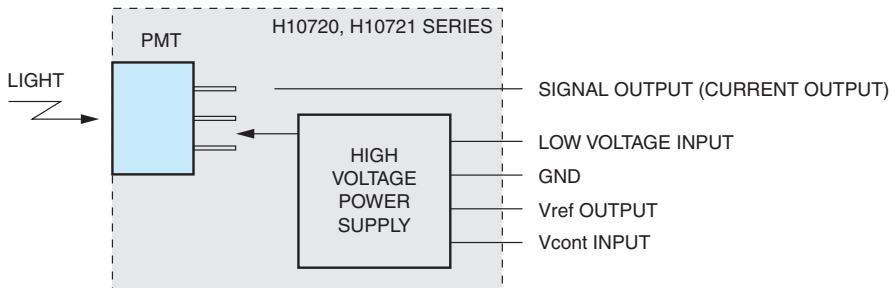


Figure 3-8: Block diagram of a photomultiplier module

THBV4_0308EA

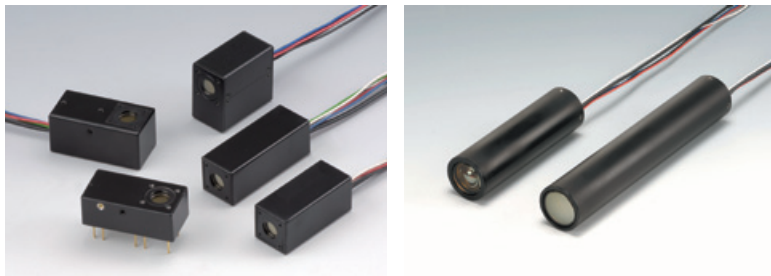


Figure 3-9: External view of photomultiplier modules

In addition to the above example, various types of photomultiplier tube modules are available with a built-in amplifier circuit, gate circuit, photon counting circuit, or USB interface for connection to a PC.

3.2.6 Signal processing (output connection circuit)

Preferably, use a connection circuit for signal processing that matches the incident light intensity and the required time response characteristics.

In regions at relatively high light levels to low light levels, DC or AC mode (analog mode) is usually used for signal processing. In the very-low-light level region, the photon counting mode (digital mode) is often used which is capable of counting individual photons (minimum units of light). In analog mode, the signal is measured with an oscilloscope or is AD-converted (analog-to-digital conversion) for signal processing by PC. Digital mode measures the number of pulses matching the number of photons.

MEMO

CHAPTER 4

CHARACTERISTICS OF PHOTOMULTIPLIER TUBES

This chapter details various characteristics of photomultiplier tubes, including basic characteristics and performance. For example, section 4.1 shows spectral response characteristics of typical photocathodes and also gives the definition of photocathode sensitivity and its measurement procedure.

Section 4.2 explains the types and structures of electron multipliers (dynodes) and their characteristics. Section 4.3 describes various performance characteristics such as time response, operating stability, sensitivity uniformity, and signal-to-noise ratio as well as their definitions, measurement procedures and specific product examples. It also provides precautions and suggestions for use.

4.1 Basic Characteristics of Photocathodes

This section introduces photocathodes and window materials which have been used in practical applications from the past to the present and also explains the terms used to define photocathodes such as quantum efficiency, radiant sensitivity, and luminous sensitivity.

4.1.1 Photocathode materials

Most photocathodes¹⁾⁻¹⁵⁾ are made of compound semiconductors which consist of alkali metals with a low work function. There are approximately ten kinds of photocathodes currently used in practical applications. Each photocathode is available as a transmission (semitransparent) type or a reflection (opaque) type, with different device characteristics. The photocathode materials commonly used in photomultiplier tubes are described below.

(1) Cs-I

Cs-I is insensitive to solar radiation and therefore often called "solar blind". It has almost no sensitivity to wavelengths longer than 200 nanometers and is used for measurement in the vacuum ultraviolet region. As a window material, MgF₂ crystals or silica glass are used to cover a spectral response range from 115 nanometers (160 nanometers) to 200 nanometers.

(2) Cs-Te

Cs-Te is almost insensitive to wavelengths longer than 300 nanometers and is also called "solar blind" just as with Cs-I. With this type of photocathodes, the transmission type and reflection type show the same spectral response range, but the reflection type exhibits higher sensitivity than the transmission type. Silica glass or MgF₂ crystals usually used for the input window.

(3) Sb-Cs

This photocathode has sensitivity in the ultraviolet to visible range. Because the resistance of the Sb-Cs photocathode is lower than that of the bialkali photocathode described next, it is suited for applications where light intensity to be measured is relatively high so that a large current can flow in the cathode. Sb-Cs is also suitable for applications where the photocathode is cooled so its resistance becomes larger and causes problems with the dynamic range. Sb-Cs is chiefly used for reflection type photocathode.

(4) Bialkali (Sb-Rb-Cs, Sb-K-Cs)

Since two kinds of alkali metals are employed, these photocathodes are called "bialkali". The transmission type of bialkali photocathodes has a spectral response range similar to the Sb-Cs photocathode, but has higher sensitivity and lower dark current. It also provides sensitivity that matches the emission of a NaI(Tl) scintillator, making it widely used for scintillation counting in radiation measurements. The reflection type of bialkali photocathodes is fabricated using the same materials, but is processed by a different method to enhance sensitivity on the long wavelength side, so its spectral response ranges from the ultraviolet region to around 700 nanometers.

(5) Low noise bialkali (Sb-Na-K)

As with the bialkali photocathodes describe above, two kinds of alkali metals are used in this photocathode type. The spectral response range is almost identical to that of the above bialkali photocathodes, but this photocathode can withstand operating temperatures up to 175 °C while other normal photocathodes are guaranteed to no higher than 50 °C. For this reason, it is ideally suited for use in oil well logging where photomultiplier tubes are subjected to high temperatures. In addition, when used at room temperatures, this photocathode exhibits very low dark current, which makes it very useful in low level light measurement such as photon counting applications where low noise is a prerequisite.

(6) Multialkali (Sb-Na-K-Cs)

This photocathode uses three or more kinds of alkali metals. Due to high sensitivity over a wide spectral response range from the ultraviolet through near infrared region around 850 nanometers, this photocathode is widely used in broad-band spectrophotometers. Hamamatsu also provides a multialkali photocathode with long wavelength response exceeding 900 nanometers, which is widely used in applications such as for spectrophotometers and gas phase chemiluminescence detectors for NO_x measurement.

(7) Ag-O-Cs

Transmission type photocathodes using this material are sensitive from the visible through near infrared region, from 400 to 1200 nanometers. Compared to other photocathodes, this photocathode has lower sensitivity in the visible region, but it also provides sensitivity at longer wavelengths in the near infrared region and so is chiefly used for near infrared detection.

(8) GaAsP (Cs)

A GaAsP crystal activated with cesium is used as a transmission type photocathode. This photocathode does not have sensitivity in the ultraviolet region but has a very high quantum efficiency (approximately 40 percent) in the visible region. Note that if exposed to incident light with high intensity, sensitivity degradation is more likely to occur when compared with other photocathodes composed of alkali metals.

(9) GaAs (Cs)

A GaAs crystal activated with cesium is used for both reflection type and transmission type photocathodes. The reflection type GaAs(Cs) photocathode has sensitivity across a wide range from the ultraviolet through near infrared region around 900 nanometers. It demonstrates a nearly flat, high-sensitivity spectral response curve from 300 to 850 nanometers. The transmission type has a narrower spectral response range because shorter wavelengths are absorbed. It should be noted that if exposed to incident light with high intensity, these photocathodes tend to suffer sensitivity degradation when compared with other photocathodes primarily composed of alkali metals.

(10) InGaAs (Cs)

This photocathode provides a spectral response extending further into the infrared region than the GaAs(Cs) photocathode. Additionally, it offers higher quantum efficiency in the neighborhood of 900 to 1000 nanometers in comparison with the Ag-O-Cs photocathode. It should be noted that if exposed to incident light with high intensity, these photocathodes tend to suffer sensitivity degradation when compared with other photocathodes primarily composed of alkali metals.

(11) InP/InGaAsP(Cs), InP/InGaAs(Cs)

These are field-assisted photocathodes utilizing a PN junction formed by growing InP/InGaAsP or InP/InGaAs on an InP substrate. These photocathodes were developed by our own in-house semiconductor microprocess technology.^{16) 17)} Applying a bias voltage to this photocathode lowers the conduction band barrier, and allows for higher sensitivity at long wavelengths extending to 1.4 micrometers or even 1.7 micrometers. However, these photocathodes produce large amounts of dark current when used at room temperatures, they must be cooled to between -60 °C to -80 °C during operation. The transmission type of these photocathodes has a narrower spectral response range because shorter wavelengths are absorbed. The band model of these photocathodes is shown in Figure 4-1.

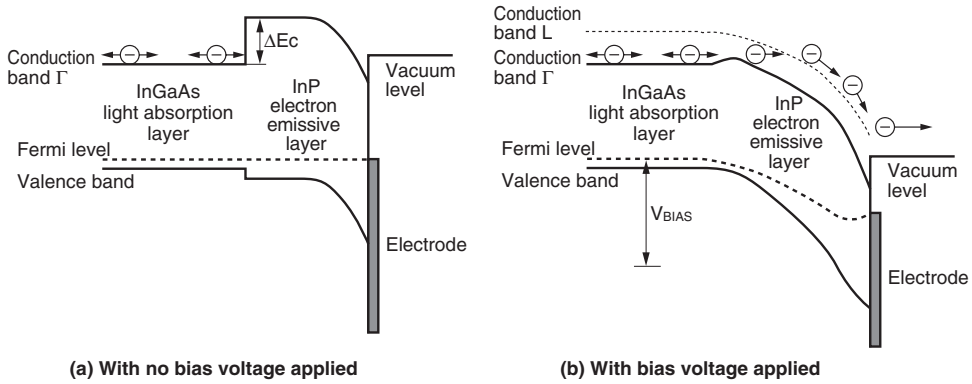


Figure 4-1: Band model

THBV4_0401EA

Typical spectral response characteristics of major photocathodes are shown in Figures 4-2, 4-3 and Table 4-1. The definition of photocathode radiant sensitivity expressed in these figures is explained in section 4.1.3, "Spectral response characteristics". Note that Figures 4-2, 4-3 and Table 4-1 only show typical characteristics and actual data may differ from tube to tube.

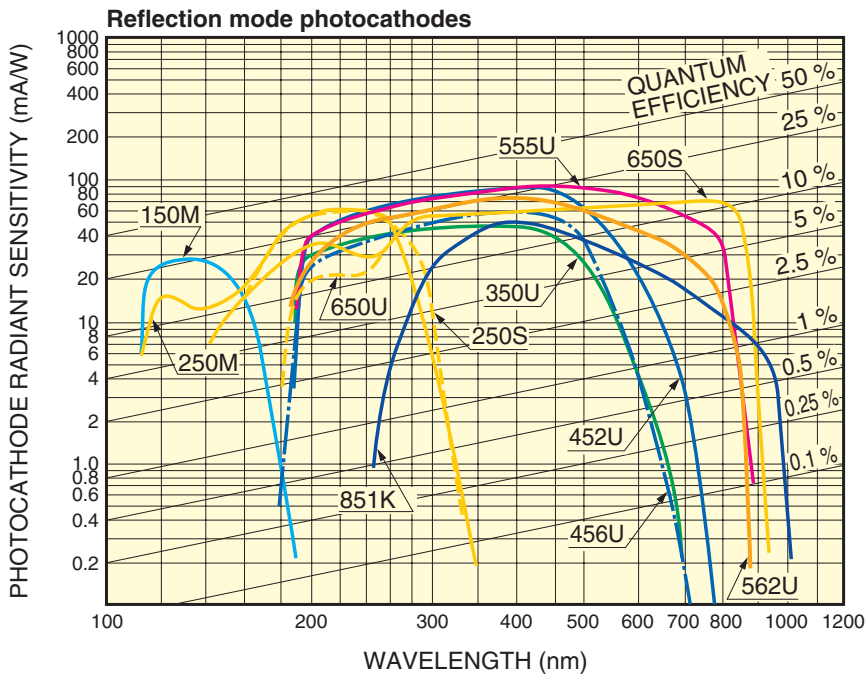
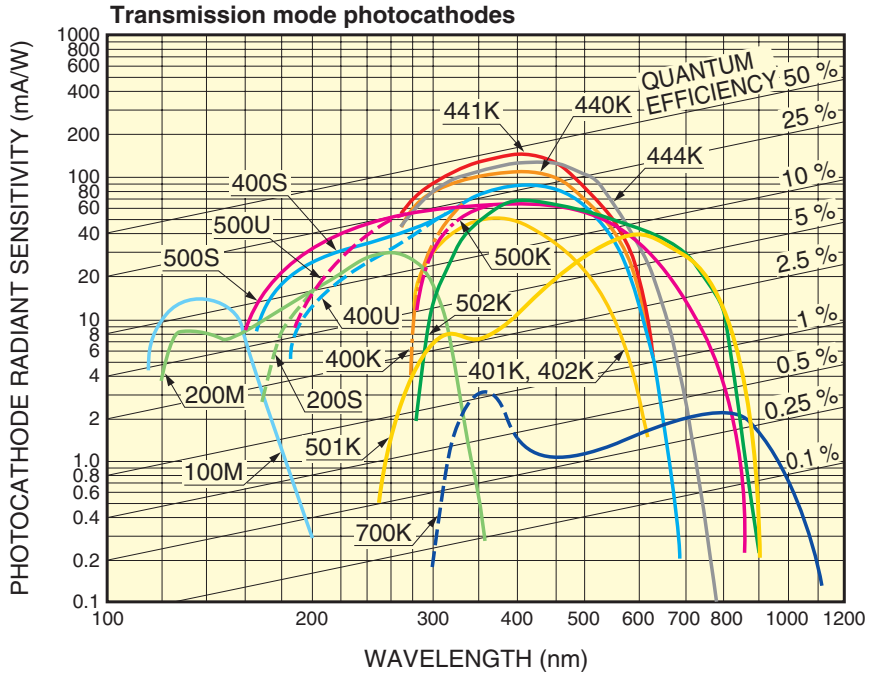


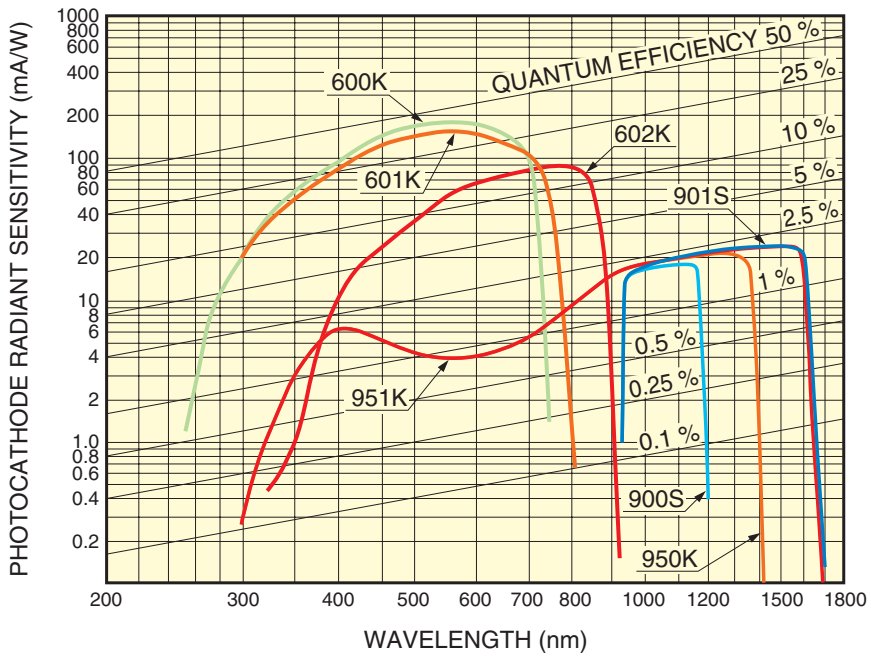
Figure 4-2 (a): Typical spectral response characteristics of reflection type photocathodes

THBV4_0402Ea



THBV4_0402EBb

Figure 4-2 (b): Typical spectral response characteristics of transmission type photocathodes



THBV4_0403EC

Figure 4-3: Typical spectral response characteristics of semiconductor crystal photocathodes

Reflection mode photocathodes

| Curve code | Photocathode material | Window material | Luminous sensitivity (Typ.) ($\mu\text{A}/\text{lm}$) | Spectral response | | | | |
|------------|-----------------------|------------------|---|---------------------|----------------------------|------------|------------------------|--------------|
| | | | | Spectral range (nm) | Peak wavelength | | | |
| | | | | | Radiant sensitivity (mA/W) | | Quantum efficiency (%) | |
| | | | | | (nm) | (nm) | (%) | (nm) |
| 150M | Cs-I | MgF ₂ | — | 115 to 195 | 25.5 | 130 | 26 | 125 |
| 250S | Cs-Te | Silica | — | 160 to 320 | 62 | 230 | 37 | 210 |
| 250M | Cs-Te | MgF ₂ | — | 115 to 320 | 63 | 200 | 35 | 220 |
| 350U | Sb-Cs | UV | 40 | 185 to 650 | 48 | 340 | 20 | 280 |
| 452U | Bialkali | UV | 120 | 185 to 750 | 90 | 420 | 30 | 260 |
| 453K | Bialkali | Borosilicate | 60 | 300 to 650 | 60 | 400 | 20 | 370 |
| 453U | Bialkali | UV | 60 | 185 to 650 | 60 | 400 | 23 | 330 |
| 456U | Low noise bialkali | UV | 60 | 185 to 680 | 60 | 400 | 19 | 300 |
| 550U | Multialkali | UV | 150 | 185 to 850 | 45 | 530 | 15 | 250 |
| 552U | Multialkali | UV | 200 | 185 to 900 | 68 | 400 | 26 | 260 |
| 555U | Multialkali | UV | 525 | 185 to 900 | 90 | 450 | 30 | 260 |
| 556U | Multialkali | UV | 200 | 185 to 850 | 80 | 430 | 27 | 280 |
| 557U | Multialkali | UV | 650 | 185 to 900 | 109 | 450 | 35 | 260 |
| 561U | Multialkali | UV | 200 | 185 to 830 | 70 | 530 | 24 | 250 |
| 562U | Multialkali | UV | 300 | 185 to 900 | 76 | 400 | 26 | 260 |
| 650U | GaAs(Cs) | UV | 550 | 185 to 930 | 62 | 300 to 800 | 23 | 300 |
| 650S | GaAs(Cs) | Silica | 550 | 160 to 930 | 62 | 300 to 800 | 23 | 300 |
| 850U | InGaAs(Cs) | UV | 100 | 185 to 1010 | 40 | 400 | 14 | 330 |
| 851K | InGaAs(Cs) | Borosilicate | 150 | 300 to 1040 | 50 | 400 | 16 | 370 |
| 950K | InP/InGaAsP(Cs) | Borosilicate | — | 300 to 1400 | 21 | 1300 | 2 | 1000 to 1300 |
| 951K | InP/InGaAs(Cs) | Borosilicate | — | 300 to 1700 | 24 | 1500 | 2 | 1000 to 1500 |

Table 4-1: Quick reference for typical spectral response characteristics (1)

Transmission mode photocathodes

| Curve code | Photocathode material | Window material | Luminous sensitivity (Typ.) ($\mu\text{A}/\text{lm}$) | Spectral response | | | | |
|------------|--------------------------|----------------------|--|------------------------|---------------------|------------|--------------------|--------------|
| | | | | Spectral range (nm) | Peak wavelength | | | |
| | | | | | Radiant sensitivity | | Quantum efficiency | |
| | | | | | (mA/W) | (nm) | (%) | (nm) |
| 100M | Cs-I | MgF ₂ | — | 115 to 200 | 14 | 140 | 13 | 130 |
| 200S | Cs-Te | Silica | — | 160 to 320 | 29 | 240 | 16 | 210 |
| 200M | Cs-Te | MgF ₂ | — | 115 to 320 | 29 | 240 | 17 | 200 |
| 201S | Cs-Te | Silica | — | 160 to 320 | 31 | 240 | 17 | 210 |
| 400K | Bialkali | Borosilicate | 95 | 300 to 650 | 88 | 420 | 27 | 390 |
| 400U | Bialkali | UV | 95 | 185 to 650 | 88 | 420 | 27 | 390 |
| 400S | Bialkali | Silica | 95 | 160 to 650 | 88 | 420 | 27 | 390 |
| 401K | High temp. bialkali | Borosilicate | 40 | 300 to 650 | 51 | 375 | 17 | 375 |
| 402K | Low noise bialkali | Borosilicate | 40 | 300 to 650 | 54 | 375 | 18 | 375 |
| 500K | Multialkali | Borosilicate | 150 | 300 to 850 | 64 | 420 | 20 | 375 |
| 500U | Multialkali | UV | 150 | 185 to 850 | 64 | 420 | 25 | 280 |
| 500S | Multialkali | Silica | 150 | 160 to 850 | 64 | 420 | 25 | 280 |
| 501K | Extended red multialkali | Borosilicate | 200 | 300 to 900 | 40 | 600 | 8 | 580 |
| 502K | Multialkali | Borosilicate (prism) | 230 | 300 to 900 | 69 | 420 | 20 | 390 |
| 600K | GaAsP(Cs) | Borosilicate | 700 | 280 to 720 | 180 | 550 to 650 | 40 | 480 to 530 |
| 601K | Extended red GaAsP(Cs) | Borosilicate | 750 | 280 to 820 | 160 | 550 to 650 | 36 | 480 to 530 |
| 602K | GaAs(Cs) | Borosilicate | 700 | 370 to 920 | 85 | 750 to 850 | 12 | 600 to 750 |
| 700K | Ag-O-Cs | Borosilicate | 20 | 400 to 1200 | 2.2 | 800 | 0.36 | 740 |
| 900S | InP/InGaAsP(Cs) | Silica | — | 950 to 1200 | 18 | 1100 | 2 | 1000 to 1100 |
| 901S | InP/InGaAs(Cs) | Silica | — | 950 to 1700 | 24 | 1500 | 2 | 1000 to 1550 |
| 440K | Super bialkali | Borosilicate | 105 | 300 to 650 | 110 | 400 | 35 | 350 |
| 441K | Ultra bialkali | Borosilicate | 135 | 300 to 650 | 130 | 400 | 43 | 350 |
| 442K | Super bialkali | Borosilicate | 105 | 230 to 700 | 110 | 400 | 35 | 350 |
| 443K | Ultra bialkali | Borosilicate | 135 | 230 to 700 | 130 | 400 | 43 | 350 |
| 444K | Extended green bialkali | Borosilicate | 160 | 300 to 700 | 127 | 420 | 40 | 380 |

Table 4-1: Quick reference for typical spectral response characteristics (2)

4.1.2 Window materials

As stated in the previous section, most photocathodes have high sensitivity down to the ultraviolet region. However, because ultraviolet radiation tends to be absorbed by the window material, the short wavelength limit is determined by the ultraviolet transmittance of the window material.¹⁸⁾⁻²²⁾ The window materials commonly used in photomultiplier tubes are as follows:

(1) MgF_2 crystal

The crystals of alkali halide are superior in transmitting ultraviolet radiation, but have the disadvantage of deliquescence. A magnesium fluoride (MgF_2) crystal is used as a practical window material because it offers very low deliquescence and allows transmission of vacuum ultraviolet radiation down to 115 nanometers.

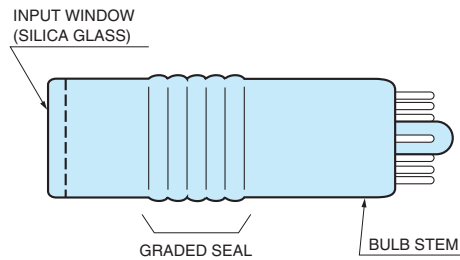
(2) Sapphire

Sapphire is made of Al_2O_3 crystal and shows an intermediate transmittance between the UV-transmitting glass and synthetic silica in the ultraviolet region. Sapphire glass has a short wavelength cutoff in the neighborhood of 150 nanometers, which is slightly shorter than that of synthetic silica.

(3) Silica glass

Silica glass transmits ultraviolet radiation down to 160 nanometers. Since silica glass has a thermal expansion coefficient greatly different from that of the Kovar alloy used for the stem pins (leads) of photomultiplier tubes, it is not suited for use as the bulb stem. Instead, a borosilicate glass is used for the bulb stem and then a so-called graded seal, which uses glasses with gradually changing thermal expansion coefficient, is connected to the silica glass bulb, as shown in Figure 4-4. Because of this structure, the graded seal is very fragile and proper care should be taken when handling the tube. In some tubes, aluminum is used between the silica glass and the Kovar alloy and they are bonded by applying a pressure.

Please note that helium gas is likely to permeate through silica glass and cannot be used in environments where helium is present.



THBV4_0404EA

Figure 4-4: Grated seal

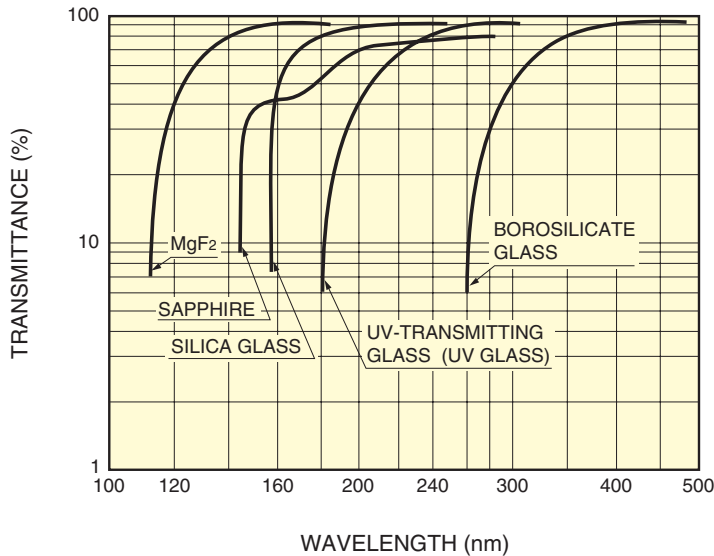
(4) UV-transmitting glass (UV glass)

As the name implies, this glass transmits ultraviolet (UV) radiation well. It transmits ultraviolet radiation down to 185 nanometers.

(5) Borosilicate glass

This is the most commonly used window material. Because the borosilicate glass has a thermal expansion coefficient very close to that of the Kovar alloy used for the leads of photomultiplier tubes, it is often called "Kovar glass". The borosilicate glass does not transmit ultraviolet radiation shorter than 300 nanometers. It is not suited for ultraviolet detection shorter than this wavelength. Some types of head-on photomultiplier tubes using a bialkali photocathode employ a special borosilicate glass (so-called "K-free glass") containing a very small amount of potassium (K^{40}) which may cause unwanted noise. The K-free glass is mainly used for photomultiplier tubes designed for scintillation counting where low background counts are desirable. For more details on background noise caused by K^{40} , refer to section 4.3.6, "Dark current".

Spectral transmittance characteristics of various window materials are shown in Figure 4-5.



THBV4_0405EA

Figure 4-5: Spectral transmittance of window materials

4.1.3 Spectral response characteristics

The photocathode of a photomultiplier converts the energy of incident photons into photoelectrons. The conversion efficiency (photocathode sensitivity) varies with the incident light wavelength. This relationship between the photocathode and the incident light wavelength is referred to as the spectral response characteristics. In general, the spectral response characteristics are expressed in terms of radiant sensitivity and quantum efficiency.

(1) Radiant sensitivity

Radiant sensitivity is defined as the photoelectric current generated by the photocathode divided by the incident radiant flux (W) at a given wavelength, expressed in units of amperes per watts (A/W). Furthermore, relative spectral response characteristics in which the maximum radiant sensitivity is normalized to 100 percent are also conveniently used.

(2) Quantum efficiency

Quantum efficiency is the number of photoelectrons emitted from the photocathode divided by the number of incident photons. Quantum efficiency is symbolized by η and is generally expressed as a percent. Incident photons transfer energy to electrons in the valence band of a photocathode, however not all of these electrons are emitted as photoelectrons. This photoemission takes place according to a certain probability process. Photons at shorter wavelengths carry higher energy per photon compared to photons at longer wavelengths and contribute to an increase in the photoemission probability.

(3) Measurement and calculation of spectral response characteristics

To measure radiant sensitivity and quantum efficiency, a standard phototube or semiconductor detector which is precisely calibrated is used as a secondary standard. At first, the incident radiant flux L_P at the wavelength of interest is measured with the standard phototube or semiconductor detector. Next, the photocurrent I_K of the photomultiplier tube to be evaluated is measured. Then the radiant sensitivity S_K (A/W) of the photomultiplier tube can be calculated from the following equation:

$$S_k = \frac{I_k}{L_p} \text{ (A/W)} \dots\dots\dots \text{(Eq. 4-1)}$$

The quantum efficiency η can be obtained from the radiant sensitivity S_k (A/W) using the following equation:

$$\eta \text{ (%) } = \frac{h \cdot c}{\lambda \cdot e} \cdot S_k = \frac{1240}{\lambda} \cdot S_k \cdot 100 \text{ (%) } \dots\dots\dots \text{(Eq. 4-2)}$$

- h: 6.63×10^{-34} J·s
- c: 3.00×10^8 m·s⁻¹
- e: 1.60×10^{-19} C

where h is Planck's constant, λ is the wavelength of incident light (nanometers), c is the velocity of light in vacuum and e is the electron charge. The quantum efficiency η is expressed in percent.

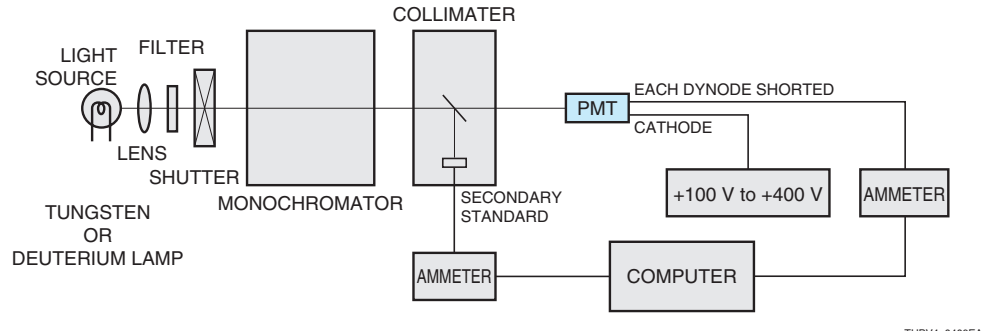


Figure 4-6: Spectral response measurement system

THBV4_0406EA

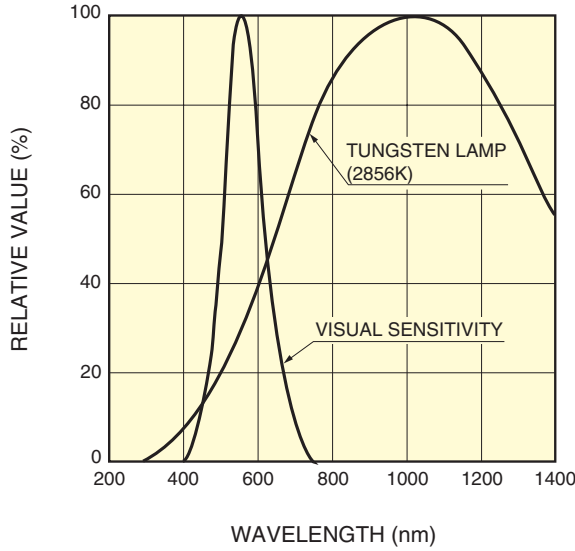
(4) Spectral response range (short and long wavelength limits)

The wavelength at which the spectral response drops on the short wavelength side is called the short wavelength limit or cutoff while the wavelength at which the spectral response drops on the long wavelength side is called the long wavelength limit or cutoff. The short wavelength limit is determined by the window material, while the long wavelength limit depends on the photocathode material. The range between the short wavelength limit and the long wavelength limit is called the spectral response range.

In this handbook, the short wavelength limit is defined as the wavelength at which the incident light is abruptly absorbed by the window material. The long wavelength limit is defined as the wavelength at which the photocathode sensitivity falls to 1 percent of the maximum sensitivity for bialkali and Ag-O-Cs photocathodes and 0.1 percent of the maximum sensitivity for multialkali photocathodes. However, these wavelength limits will depend on the actual operating conditions such as the incident light, photocathode sensitivity, dark current, and signal-to-noise ratio of the measurement system.

4.1.4 Luminous sensitivity

The spectral response measurement of a photomultiplier tube requires an expensive, sophisticated system and also takes much time. It is therefore more practical to evaluate the sensitivity of common photomultiplier tubes in terms of luminous sensitivity. The illuminance on a surface one meter away from a point light source of one candela (cd) is one lux (lx). One lumen equals the luminous flux of one lux passing an area of one square meter. Luminous sensitivity is the output current obtained from the cathode or anode divided by the incident luminous flux (lumen) from a tungsten lamp at a distribution temperature of 2856 K. In some cases, a visual compensation filter is interposed between the photomultiplier tube and the light source, but in most cases it is omitted. Figure 4-7 shows the visual sensitivity and relative spectral distribution of a 2856 K tungsten lamp.



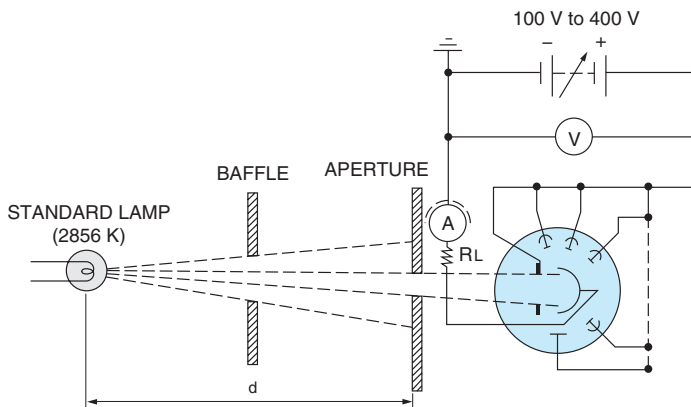
THBV4_0407EA

Figure 4-7: Spectral response of human eye and spectral distribution of 2856 K tungsten lamp

Luminous sensitivity is a convenient parameter when comparing the sensitivity of photomultiplier tubes of the same type. However, it should be noted that "lumen"(lm) is the unit of luminous flux with respect to the standard visual sensitivity and there is no significance for photomultiplier tubes which have a spectral response range beyond the visible region (350 to 750 nanometers). To evaluate photomultiplier tubes using Cs-Te or Cs-I photocathodes which are insensitive to the spectral distribution of a tungsten lamp, radiant sensitivity at a specific wavelength is measured. Luminous sensitivity is divided into two parameters: cathode luminous sensitivity which defines the photocathode performance and anode luminous sensitivity which defines the performance characteristics after multiplication.

(1) Cathode luminous sensitivity

Cathode luminous sensitivity^{(23) (25)} is defined as the photoelectron current generated by the photocathode (cathode current) per luminous flux from a tungsten lamp operated at a distribution temperature of 2856 K. In this measurement, each dynode is shorted to the same potential as shown in Figure 4-8 so that the photomultiplier tube is operated as a bipolar tube. Cathode luminous sensitivity indicates the sensitivity of a photocathode.



THBV4_0408EA

Figure 4-8: Cathode luminous sensitivity measuring diagram

The incident luminous flux used for measurement is in the range of 10^{-5} to 10^{-2} lumens. If the luminous flux is too large, measurement errors may occur due to the surface resistance of the photocathode. The optimum luminous flux must therefore be selected according to the photocathode size and material. A picoammeter is usually used to measure the photocurrent which changes from several nanoamperes to several microamperes. Appropriate countermeasures against leakage current and other possible noise source must be taken. In addition, be careful to avoid contamination on the socket or bulb stem and to keep ambient humidity levels low so that an adequate electrical safeguard is provided. The photomultiplier tube should be operated at a supply voltage at which the cathode current fully saturates. A voltage of 100 to 400 volts is usually applied for this purpose. Cathode saturation characteristics are discussed in section 4.3.2, "Linearity". The ammeter is connected to the cathode via a serial load resistance (R_L) of 100 kilohms to 1 megohm for circuitry protection.

(2) Anode luminous sensitivity

Anode luminous sensitivity^{23) 25)} is defined as the anode output current per luminous flux incident on the photocathode. In this measurement, a proper voltage distribution is given to each electrode as illustrated in Figure 4-9. Although the same tungsten lamp that was used to measure the cathode luminous sensitivity is used again, the light flux is reduced to 10^{-10} to 10^{-5} lumens using a neutral density filter. The ammeter is connected to the anode via the series resistance. Anode luminous sensitivity is equal to the cathode luminous sensitivity multiplied by the gain and indicates the output level in response to light input.

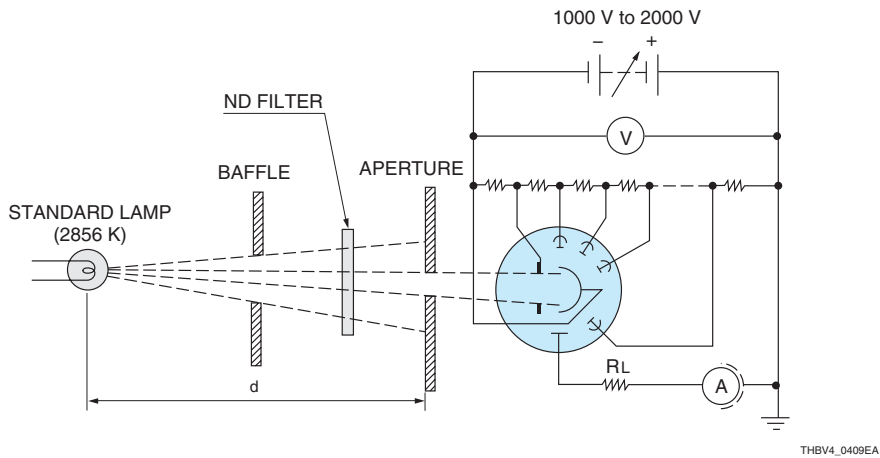
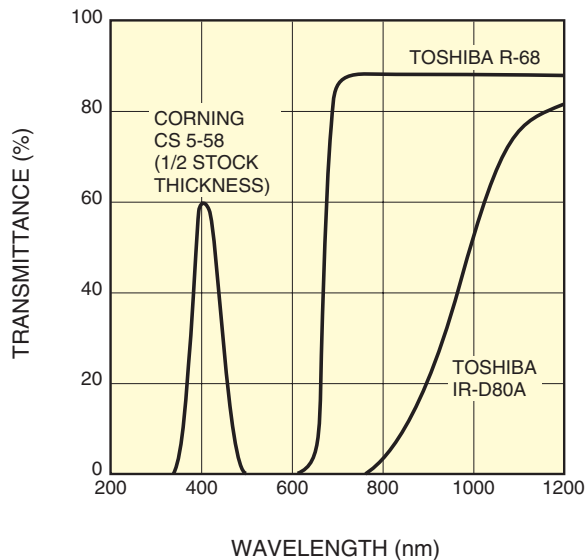


Figure 4-9: Anode luminous sensitivity measuring diagram

(3) Blue sensitivity index and red-to-white ratio

Blue sensitivity index and red-to-white ratio are often used for simple comparison of the spectral response of photomultiplier tubes. Cathode blue sensitivity index is the cathode sensitivity obtained when a blue filter is placed in front of the photomultiplier tube under the same conditions for the cathode luminous sensitivity measurement. The blue filter used is a Corning CS 5-58 polished to half stock thickness. Since the light flux entering the photomultiplier tube has been transmitted through the blue filter once, it cannot be directly represented in lumens. Therefore at Hamamatsu Photonics, it is expressed as a blue sensitivity index without using units. The spectral transmittance of this blue filter matches well the emission spectrum of a NaI(Tl) scintillator (peak wavelength 420 nanometers) which is widely used for scintillation counting. Photomultiplier tube sensitivity to the scintillation flash correlates well with the sensitivity using this blue filter. The blue sensitivity index is an important factor that affects energy resolution in scintillation measurement. For detailed information, refer to Chapter 7, "Scintillation counting".

The red-to-white ratio is used to evaluate photomultiplier tubes with a spectral response extending to the near infrared region. This parameter is defined as the quotient of the cathode sensitivity measured with a long-wavelength transmitting filter interposed under the same conditions for cathode luminous sensitivity divided by the cathode luminous sensitivity without a filter. The filter used is a Toshiba IR-D80A for Ag-O-Cs photocathodes or a Toshiba R-68 for other photocathodes. If other types of filters are used, the red-to-white ratio will vary. Figure 4-10 shows the spectral transmittance of the filters used for measurements of blue sensitivity index and red-to-white ratio.



THBV4_0410EA

Figure 4-10: Typical spectral transmittance of optical filters

4.1.5 Luminous sensitivity and spectral response

To some extent, there is a correlation between luminous sensitivity and spectral response in a specific wavelength region. Figure 4-11 shows the correlation between the photocathode radiant sensitivity and the luminous sensitivity, blue sensitivity index (CS 5-58) and red-to-white ratio (R-68, IR-D80A) as a function of wavelength.

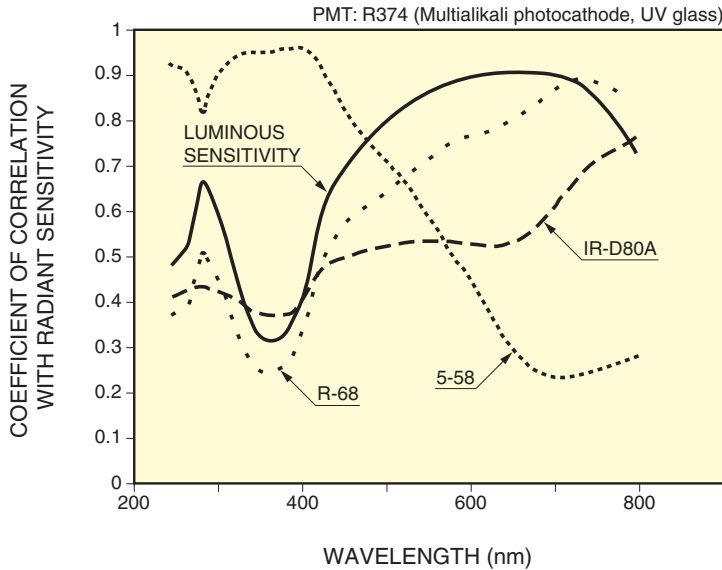


Figure 4-11: Correlation between luminous sensitivities and radiant sensitivity

It can be seen from the figure that the radiant sensitivity of a photomultiplier tube correlates well with the blue sensitivity index at wavelengths shorter than 450 nanometers, with the luminous sensitivity at 500 to 700 nanometers, with the red-to-white ratio using the Toshiba R-68 filter at 700 to 800 nanometers, and with the red-to-white ratio using the Toshiba IR-D80A filter at 800 nanometers or longer. From these correlation values, a photomultiplier tube with optimum sensitivity at a certain wavelength can be selected by simply measuring the sensitivity using a filter which has the best correlation value at that wavelength rather than measuring the spectral response.

4.2 Basic Characteristics of Dynodes

This section introduces typical dynode types currently in use and describes their basic characteristics: collection efficiency and gain (current amplification).

4.2.1 Dynode types and features

There are a variety of dynode types available and each type exhibits different gain, time response and linearity depending upon the structure and the number of stages. The optimum dynode type must be selected according to application. Figure 4-12 illustrates the cross sectional views of typical dynodes and their features are briefly discussed in the following sections. The mesh type is explained in detail in chapter 9. The microchannel plate type is explained in detail in chapter 11. The electron bombardment type is explained in detail in Chapter 12.

There are also combination dynodes such as a box-and-line type and a circular and linear-focused type that utilize the advantage of each dynode.

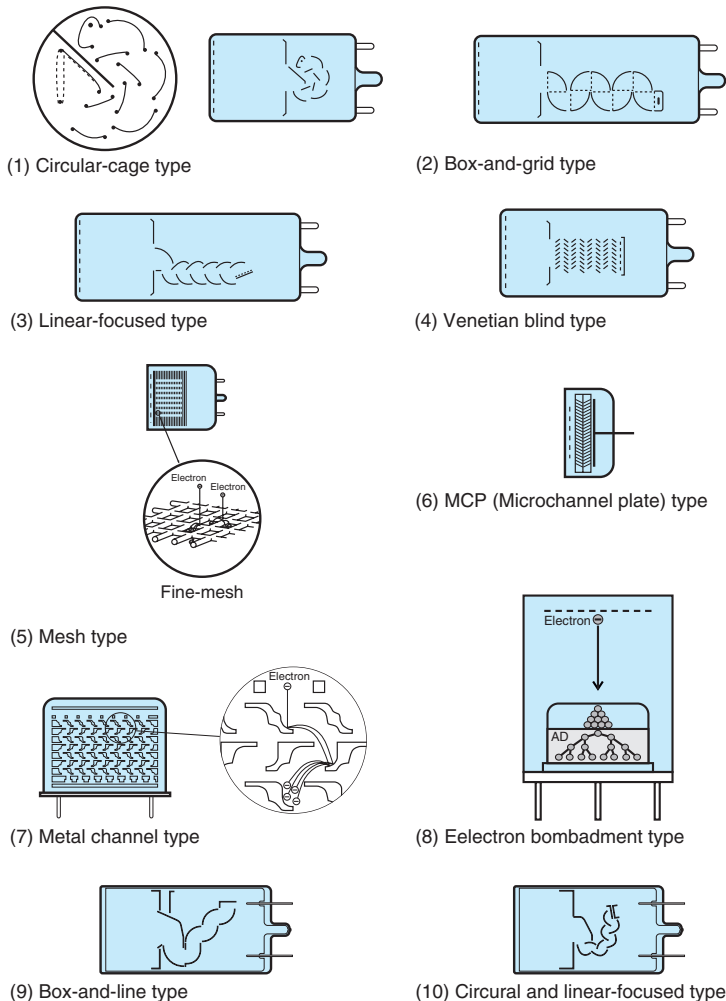


Figure 4-12: Types of electron multipliers

(1) Circular-cage type

The circular-cage type has an advantage of compactness and is used in all side-on photomultiplier tubes and in some head-on photomultiplier tubes. The circular-cage type also features fast time response and a high gain that is obtained at a relatively low supply voltage.

(2) Box-and-grid type

This type is used in head-on photomultiplier tubes and has superior photoelectron collection efficiency.

(3) Linear-focused type

The linear-focused type is also used in head-on photomultiplier tubes. Its prime features include fast time response, good time resolution, and excellent pulse linearity.

(4) Venetian blind type

The venetian blind type creates an electric field that easily collects electrons, and is mainly used for head-on photomultiplier tubes with a large photocathode diameter.

(5) Mesh type

This type of dynode uses mesh electrodes stacked in close proximity to each other. There are two types: coarse mesh type and fine-mesh type. Both are excellent in output linearity and have high immunity to magnetic fields. When used with a cross wire anode (cross plate) or multianode, the position of incident light can be detected. Fine-mesh types are developed primarily for photomultiplier tubes which are used in high magnetic fields. (Refer to Chapter 9 for detailed information.)

(6) MCP (Microchannel plate) type

A microchannel plate (MCP) with 1 millimeter thickness is used as a dynode that exhibits dramatically improved time resolution. This dynode structure ensures stable gain in magnetic fields and, like the mesh type dynode, provides position-sensitive capabilities when combined with a multianode. (Refer to Chapter 10 for detailed information.)

(7) Metal channel type

This dynode structure consists of extremely thin electrodes fabricated by our advanced microfabrication technology and precisely stacked according to computer simulation of electron trajectories. Since each dynode is in close proximity to one another, the electron path length is very short ensuring excellent time characteristics and stable gain even in magnetic fields. When combined with a multianode, multichannel data or position information can be obtained. (Refer to Chapter 9 for detailed information.)

(8) Electron bombardment type

In this type, photoelectrons are accelerated by a high voltage and strike a semiconductor so that the photoelectron energy is transferred to the semiconductor to produce a gain. This simple structure features a small noise figure, excellent uniformity, and high linearity.

(9) Box-and-line type

This type has a structure that combines a box-and-grid type with a linear-focused type. This type offers faster time response, higher time resolution, and better pulse linearity compared to the box-and-grid type, and higher electron collection efficiency compared to the linear-focused type.

(10) Circular and linear-focused type

This type has a structure that combines a circular-cage type with a linear-focused type. This type provides better pulse linearity while maintaining the compactness of the circular-cage type.

The electrical characteristics of a photomultiplier tube depend not only on the dynode type but also on the photocathode size and focusing system. As a general guide, Table 4-2 summarizes typical performance characteristics of head-on photomultiplier tubes (up to 127 millimeter (5 inch) diameter) classified by the dynode type. Magnetic characteristics listed are measured in a magnetic field in the direction of the tube axis which less affects the characteristics.

| Characteristics Dynode type | Time characteristics Rise time [ns] | Pulse linearity at 2% [mA] | Magnetic immunity [mT] | Uniformity | Collection efficiency | Features |
|--------------------------------|--|-------------------------------|---------------------------|------------|-----------------------|--|
| Circular-cage | 0.9 to 3.0 | 1 to 10 | 0.1 | Poor | Good | Compact, high-speed |
| Box-and-grid | 6 to 20 | | | Good | Very good | High collection efficiency |
| Linear-focused | 0.7 to 3 | 10 to 250 | | Poor | Good | High-speed, high linearity |
| Venetian blind | 6 to 18 | 10 to 40 | | Good | Poor | Suited for large diameter |
| Mesh | 1.5 to 5.5 | 300 to 1000 | 500 to 1500* | Good | Poor | High magnetic immunity, high linearity |
| MCP | 0.1 to 0.3 | 700 | 1500* | Good | Poor | High-speed |
| Metal channel | 0.65 to 1.5 | 30 | 5** | Good | Good | Compact, high-speed |
| Bombardment type | Depends on internal semiconductor | | — | Very good | Very good | High photoelectron resolution |

* In magnetic field parallel to tube axis

** Metal package PMT

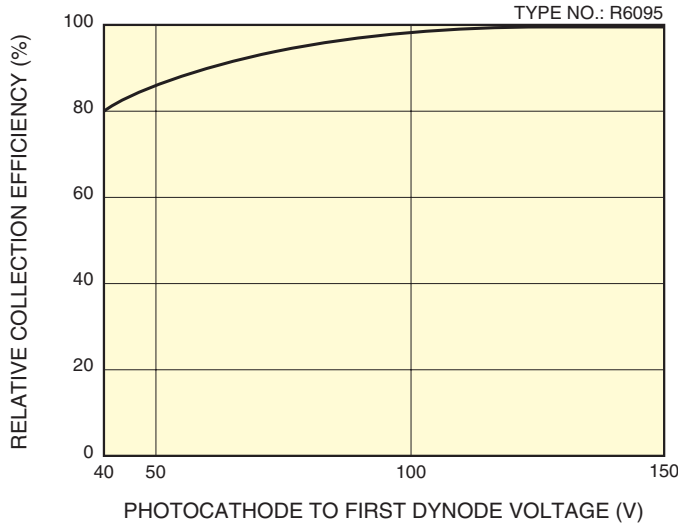
Table 4-2: Typical characteristics for dynode types

4.2.2 Collection efficiency and gain (current amplification)

(1) Collection efficiency

The electron multiplier mechanism of a photomultiplier tube is designed with consideration of the electron trajectories so that electrons are efficiently multiplied at each dynode stage. However, some electrons may deviate from their favorable trajectories, not contributing to multiplication. In photomultiplier tube operation, the ratio of the number of pulses output from the anode to the number of photoelectrons emitted from the photocathode is termed the collection efficiency. Generally it is important that the photoelectrons enter the effective area of the first dynode. This effective area is the area of the first dynode where photoelectrons can be multiplied effectively at the successive dynode stages without deviating from their favorable trajectories. Although there exist secondary electrons which do not contribute to multiplication at the second dynode or latter dynodes, they will tend to have less of an effect on the total collection efficiency as the number of secondary electrons emitted increases greatly.

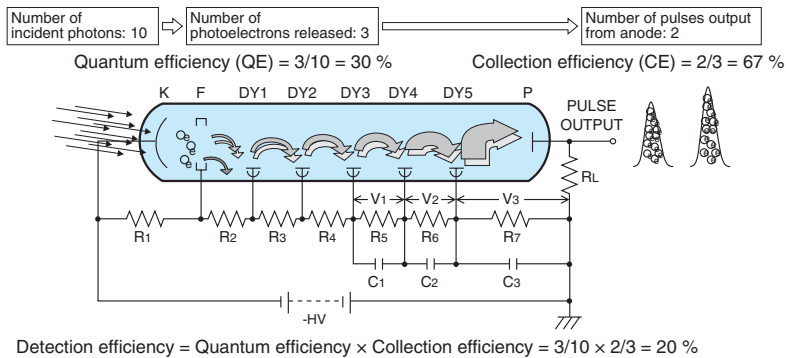
Figure 4-13 shows an example of relative collection efficiency of a 28-mm diameter head-on photomultiplier tube as a function of cathode to first dynode voltage. The photoelectrons do not enter the effective area of the first dynode unless the cathode to first dynode voltage is appropriate. In particular, if the cathode-to-first dynode voltage is low, the number of photoelectrons reaching the effective area of the first dynode becomes low, resulting in a decrease in the collection efficiency.



THBV4_0413EA

Figure 4-13: Relative collection efficiency vs. photocathode to first dynode voltage

Figure 4-13 shows that about 100 volts should be applied between the cathode and the first dynode. The collection efficiency affects energy resolution, detection efficiency, and signal-to-noise ratio in scintillation counting. The detection efficiency is the ratio of the detected signal to the input signal of a photomultiplier tube. In photon counting this is expressed as the product of the photocathode quantum efficiency and the collection efficiency.



THBV4_0414EA

Figure 4-14: Example of detection efficiency

(2) Gain (current amplification)

Secondary emission ratio δ is a function of the interstage voltage of dynodes E, and is given by the following equation:

$$\delta = a \cdot E^k \dots\dots\dots (Eq. 4-3)$$

Where a is a constant and k is determined by the structure and material of the dynode and has a value from 0.7 to 0.8.

The photoelectron current I_k emitted from the photocathode strikes the first dynode where secondary electrons I_{d1} are released. At this point, the secondary emission ratio δ_1 at the first dynode is given by

$$\delta_1 = \frac{I_{d1}}{I_k} \dots\dots\dots (Eq. 4-4)$$

These electrons are multiplied in a cascade process from the first dynode → second dynode → the n-th dynode. The secondary emission ratio δ_n of n-th stage is given by

$$\delta_n = \frac{I_{dn}}{I_{d(n-1)}} \dots\dots\dots (Eq. 4-5)$$

The anode current I_p is given by the following equation:

$$I_p = I_k \cdot \alpha \cdot \delta_1 \cdot \delta_2 \cdot \dots \cdot \delta_n \dots\dots\dots (Eq. 4-6)$$

Then

$$\frac{I_p}{I_k} = \alpha \cdot \delta_1 \cdot \delta_2 \cdot \dots \cdot \delta_n \dots\dots\dots (Eq. 4-7)$$

where α is the collection efficiency.

The product of $\alpha \cdot \delta_1 \cdot \delta_2 \cdot \dots \cdot \delta_n$ is called the gain μ (current amplification), and is given by the following equation:

$$\mu = \alpha \cdot \delta_1 \cdot \delta_2 \cdot \dots \cdot \delta_n \dots\dots\dots (Eq. 4-8)$$

Accordingly, in the case of a photomultiplier tube with $\alpha=1$ and the number of dynode stages = n, which is operated using an equally-distributed divider, the gain μ changes in relation to the supply voltage V, as follows:

$$\mu = (a \cdot E^k)^n = a^n \left(\frac{V}{n+1}\right)^{kn} = A \cdot V^{kn} \dots\dots\dots (Eq. 4-9)$$

where A should be equal to $a^n/(n+1)^{kn}$. From this equation, it is clear that the gain μ is proportional to the kn exponential power of the supply voltage. Figure 4-15 shows typical gain vs. supply voltage. Since Figure 4-15 is expressed in logarithmic scale for both the abscissa and ordinate, the slope of the straight line becomes kn and the current multiplication increases with the increasing supply voltage. This means that the gain of a photomultiplier tube is susceptible to variations in the high voltage power supply, such as drift, ripple, temperature stability, input regulation, and load regulation.

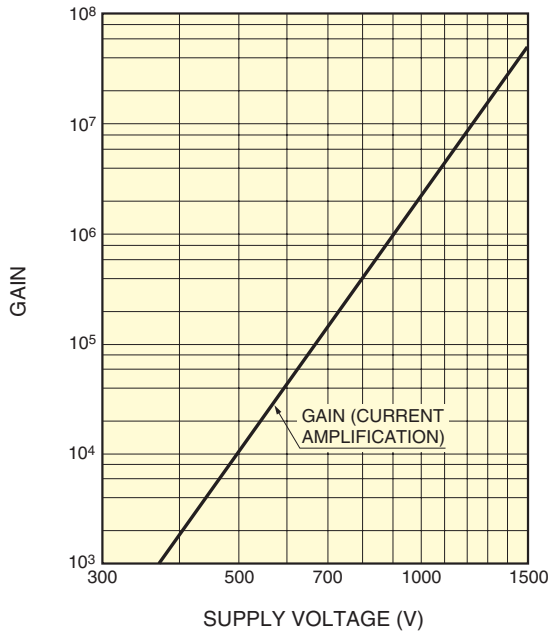


Figure 4-15: Gain vs. supply voltage

4.3 Characteristics of Photomultiplier Tubes

This section describes important characteristics for photomultiplier tube operation and their evaluation methods, and photomultiplier tube usage.

4.3.1 Time characteristics

The photomultiplier tube is a photodetector that has an exceptionally fast time response.^{1) 23)-27)} The time response is determined primarily by the transit time required for the photoelectrons emitted from the photocathode to reach the anode after being multiplied as well as the transit time difference between each photoelectron. Accordingly, fast response photomultiplier tubes are designed to have a spherical inner window and carefully engineered electrodes so that the transit time difference can be minimized.

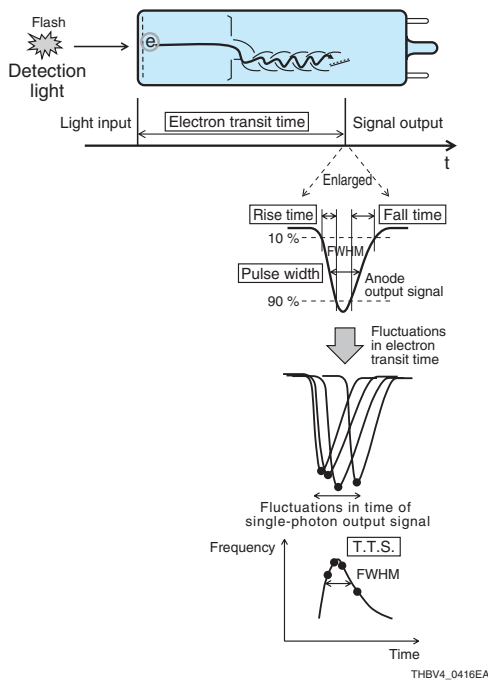
Table 4-3 lists the timing characteristics of 52-millimeter diameter head-on photomultiplier tubes categorized by their dynode type. As can be seen from the table, the linear-focused type and metal channel type exhibit the best time characteristics, while the box-and-grid and venetian blind types show rather poor properties.

Unit: ns

| Dynode type | Rise time | Fall time | Pulse width (FWHM) | Electron transit time | T.T.S. |
|----------------|-------------|-----------|--------------------|-----------------------|----------------|
| Linear-focused | 0.7 to 3 | 1 to 10 | 1.3 to 5 | 16 to 50 | 0.37 to 1.1 |
| Circular-cage | 3.4 | 10 | 7 | 31 | 3.6 |
| Box-and-grid | to 7 | 25 | 13 to 20 | 57 to 70 | Less than 10 |
| Venetian blind | to 7 | 25 | 25 | 60 | Less than 10 |
| Mesh | 2.5 to 2.7 | 4 to 6 | 5 | 15 | Less than 0.45 |
| Metal channel | 0.65 to 1.5 | 1 to 3 | 1.5 to 3 | 4.7 to 8.8 | 0.4 |

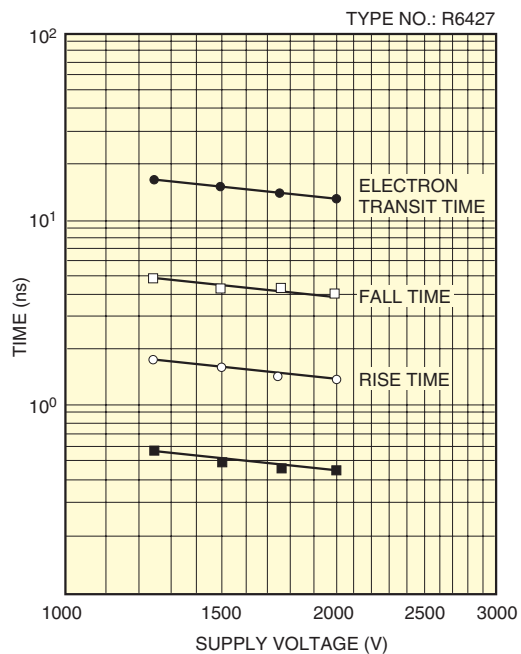
T.T.S.: Transit Time Spread

Table 4-3: Time characteristics (52-mm diameter head-on photomultiplier tubes)



THBV4_0416EA

Figure 4-16: Concept of time characteristics



THBV4_0417EA

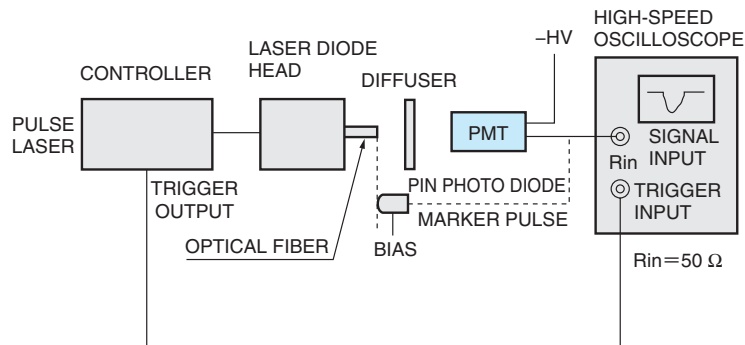
Figure 4-17: Time characteristics vs. supply voltage

The time response is mainly determined by the dynode type, but also depends on the supply voltage. Increasing the electric field intensity or supply voltage improves the electron transit speed and thus shortens the transit time. In general, the time response improves in inverse proportion to the square root of the supply voltage. Figure 4-17 shows typical time characteristics vs. supply voltage.

The following section explains the definitions of photomultiplier tube time characteristics and their measurement methods.

(1) Rise time, fall time, and electron transit time

Figure 4-18 shows a block diagram for time response measurements and Figure 4-19 illustrates the definitions of the rise time, fall time, and electron transit time of a photomultiplier tube output.

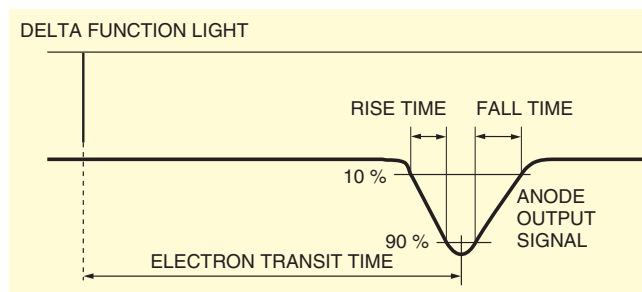


THBV4_0418EA

Figure 4-18: Measurement block diagram for rise/fall times and electron transit time

As the light source, a laser diode is used that emits a sufficiently short pulse of light relative to the time characteristics of the photomultiplier tube and so can be regarded as a delta-function light source. A high-speed oscilloscope is used to acquire an output waveform of the photomultiplier tube in real-time or sampling mode. This output waveform is composed of waveforms which are produced by electrons emitted from every position of the photocathode. Therefore, the rise and fall times are mainly determined by the electron transit time difference that depends on the incident light position and also by the electric field distribution and intensity (supply voltage) between the electrodes.

As indicated in Figure 4-19, the rise time is defined as the time for the output pulse to increase from 10 to 90 percent of the peak pulse height. Conversely, the fall time is defined as the time required to decrease from 90 to 10 percent of the peak output pulse height. In time response measurements where the rise and fall times are critical, a waveform distortion tends to occur and so proper impedance matching must be provided. In some cases, a voltage-divider circuit with damping resistors is used. (See section 5.1.5 of Chapter 5.)

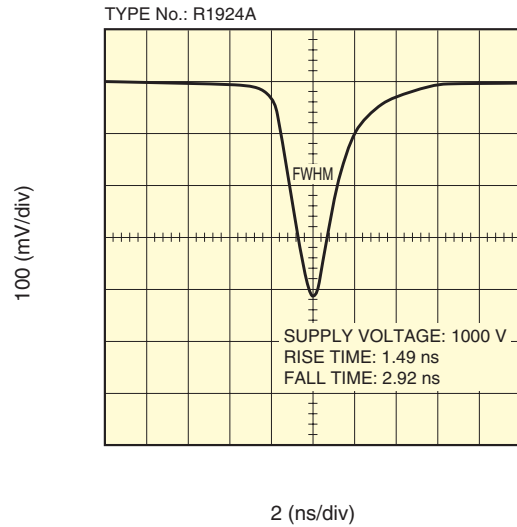


THBV4_0419EA

Figure 4-19: Definitions of rise/fall times and electron transit time

Figure 4-20 shows an actual output waveform obtained from a photomultiplier tube. In general, the fall time is two to three times longer than the rise time. This means that when measuring repetitive pulses, care must be taken so that each output pulse does not overlap. The FWHM (full width at half maximum) of the output pulse will usually be about 1.5 to 2 times the rise time.

The electron transit time is the time interval between the arrival of a light pulse at the photocathode and the appearance of the output pulse. To measure the electron transit time, a PIN photodiode is placed as reference (0 seconds) at the same position as the photomultiplier tube photocathode. The time interval between the instant the PIN photodiode detects a light pulse and the instant the output pulse of the photomultiplier tube reaches its peak amplitude is measured. This transit time is a useful parameter in determining the delay time of a measurement system in such applications as fluorescence lifetime measurement using repetitive light pulses.

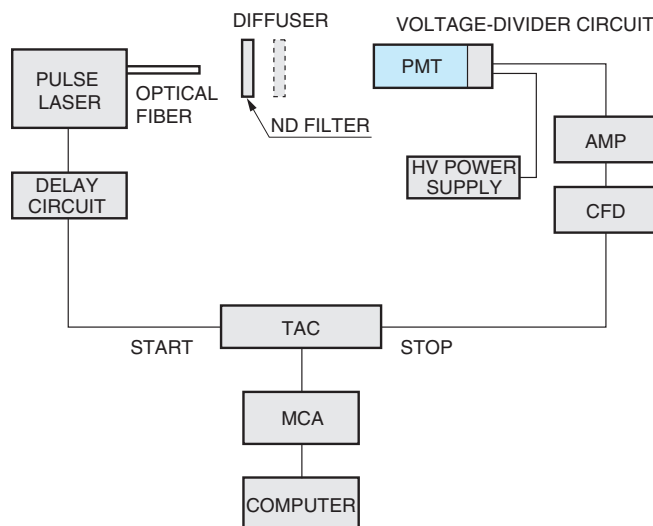


THBV4_0420EA

Figure 4-20: Output waveform

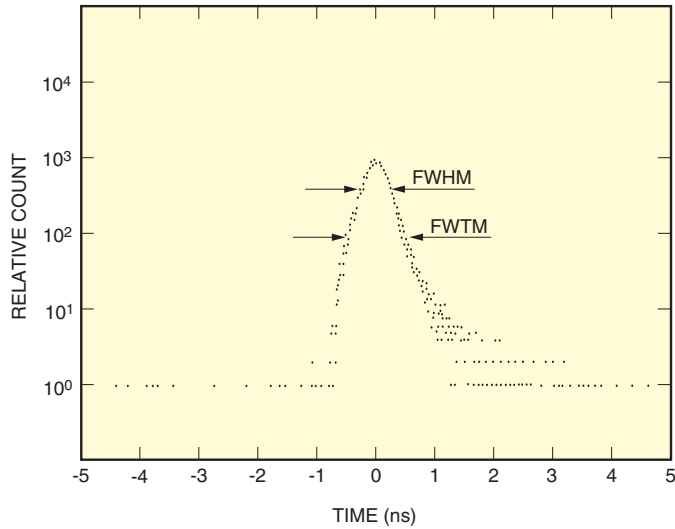
(2) T.T.S. (Transit Time Spread)

When a photocathode is fully illuminated with single photons, the transit time of each photoelectron pulse has a fluctuation. This fluctuation is called T.T.S. (Transit Time Spread). A block diagram for T.T.S. measurement is shown in Figure 4-21 and typical measured data is shown in Figure 4-22.



THBV4_0421EA

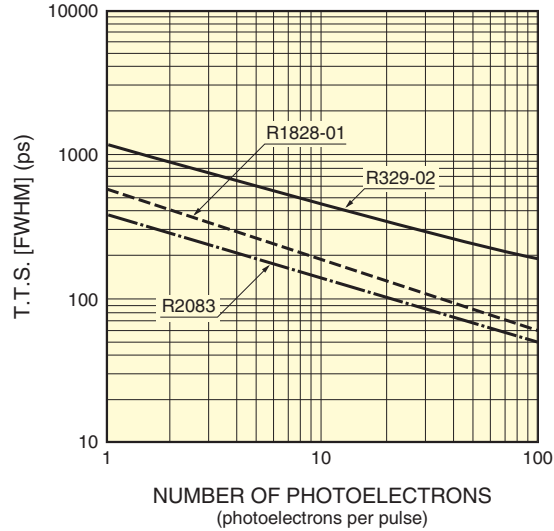
Figure 4-21: Block diagram for T.T.S. measurement



THBV4_0422EA

Figure 4-22: T.T.S. (Transit Time Spread)

In this measurement, a trigger signal from the pulsed laser is passed through the delay circuit and then fed as the start to the T.A.C. (Time-to-Amplitude Converter) which converts the time difference into pulse height. Meanwhile, the output from the photomultiplier tube is fed as the stop signal to the T.A.C. via the C.F.D. (Constant Fraction Discriminator) which reduces the time jitter resulting from fluctuation of the pulse height. The T.A.C. generates a pulse height proportional to the time interval between the "start" and "stop" signals. This pulse is fed to the M.C.A. (Multichannel Analyzer) for pulse height analysis. Since the time interval between the "start" and "stop" signals corresponds to the electron transit time, a histogram displayed on the M.C.A., by integrating individual pulse height values many times in the memory, indicates the statistical spread of the electron transit time. At Hamamatsu Photonics, the T.T.S. is usually expressed in the FWHM of this histogram, but it may also be expressed in standard deviation. When the histogram shows a Gaussian distribution, the FWHM is equal to a value which is 2.35 times the standard deviation. The T.T.S. improves as the number of photoelectrons per pulse increases, in inverse proportion to the square root of the number of photoelectrons. This relation is shown in Figure 4-23.

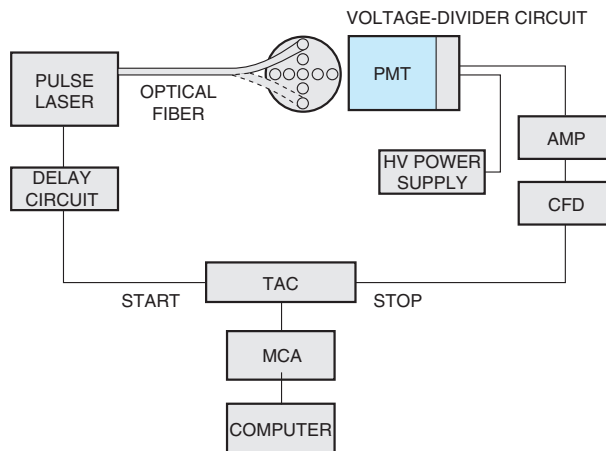


THBV4_0423EA

Figure 4-23: T.T.S. vs. number of photoelectrons

(3) C.T.T.D. (Cathode Transit Time Difference)

The C.T.T.D. (Cathode Transit Time Difference) is the difference in transit time when the incident light position on the photocathode is shifted. In most time response measurements the entire photocathode is illuminated. However, as illustrated in Figure 4-21, the C.T.T.D. measurement employs an aperture plate to shift the position of a light spot entering the photocathode, and the transit time difference between each incident position is measured.



THBV4_0424EA

Figure 4-24: Block diagram for C.T.T.D. measurement

Basically, the same measurement system as for T.T.S. measurement is employed, and the T.T.S. histogram for each of the different incident light positions is obtained. Then the change in the peak pulse height of each histogram, which corresponds to the C.T.T.D., is measured. The C.T.T.D. data of each position is represented as the electron transit time difference with respect to the electron transit time measured when the light spot enters the center of the photocathode. In actual applications, the C.T.T.D. data is not usually needed but rather primarily used for evaluation in the photomultiplier tube manufacturing process. However, the C.T.T.D. is an important factor that affects the rise time, fall time and T.T.S. described previously and also C.R.T. (Coincident Resolving Time) discussed next.

(4) C.R.T. (Coincident Resolving Time)

As with the T.T.S., this is a measure of fluctuations in the transit time. The C.R.T. measurement system resembles that used for positron CT or T.O.F. (time of flight) measurement. The C.R.T. is therefore a very practical parameter for evaluating the performance of photomultiplier tubes used in the above fields or similar applications. Figure 4-25 shows a block diagram of the C.R.T. measurement.

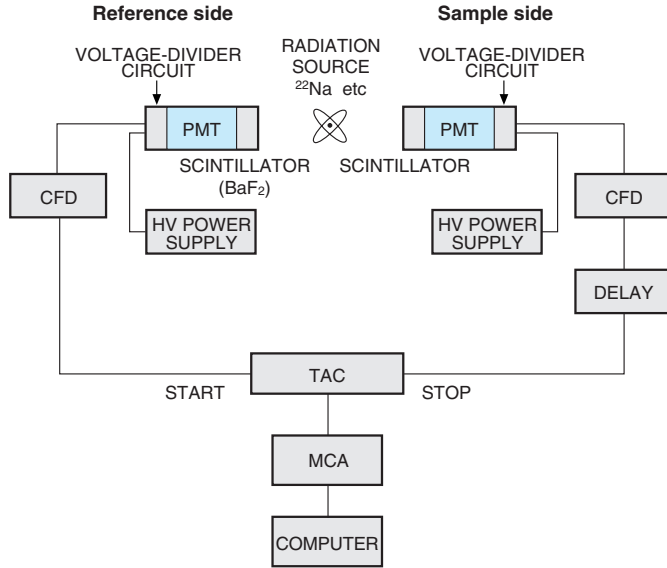


Figure 4-25: Block diagram for C.R.T. measurement

THBV4_0425EA

As a radiation source ²²Na or ⁶⁸Ge-Ga is commonly used. As a scintillator, a BaF₂ is used on the reference side, while an LSO:Ce, BaF₂, LaBr3:Ce, or plastic scintillator is used on the sample side. A proper combination of radiation source and scintillator should be selected according to the application. The radiation source is placed in the middle of a pair of photomultiplier tubes and emits gamma-rays in opposing directions at the same time. A coincident flash occurs from each of the two scintillators coupled to the photomultiplier tube. The signal detected by one photomultiplier tube is fed as the start signal to the T.A.C., while the signal from the other photomultiplier tube is fed as the stop signal to the T.A.C. via the delay circuit used to obtain proper trigger timing. Then, as in the case of the T.T.S. measurement, this event is repeatedly measured many times and the pulse height (time distribution) is analyzed by the M.C.A. to create a C.R.T. spectrum. This spectrum statistically displays the time fluctuation of the signals that enter the T.A.C.. This fluctuation mainly results from the T.T.S. of the two photomultiplier tubes. As can be inferred from Figures 4-17 and 4-23, the T.T.S. is inversely proportional to the square root of the number of photoelectrons per pulse and also to the square root of the supply voltage. In general, therefore, the higher the radiation energy and the supply voltage, the better the C.R.T. will be. If the fluctuation in the T.T.S. of each photomultiplier tube is τ_1 and τ_2 , the C.R.T. is given by

$$\text{C.R.T.} = (\tau_1^2 + \tau_2^2)^{1/2} \dots\dots\dots (\text{Eq. 4-10})$$

4.3.2 Linearity characteristics

The photomultiplier tube exhibits good linearity^{1) 24) 27) 28)} in anode output current over a wide range of low light levels including the photon counting region. In other words, it offers a wide dynamic range. However, if the incident light level is too high, the output begins to deviate from the ideal linearity. This is primarily caused by linearity characteristics near the anode, but it may also be affected by cathode linearity characteristics when a photomultiplier tube with a transmission type photocathode is operated at a low supply voltage and large current. Both cathode and anode linearity characteristics are dependent only on the current value if the supply voltage is constant, while being independent of the incident light wavelength.

(1) Cathode linearity

| Photocathode Materials | Parameters | Spectral response (Peak wavelength) (nm) | Upper limit of linearity (Average current) |
|------------------------|------------|---|--|
| Ag-O-Cs | | 300 to 1200 (800) | 1 μ A |
| Sb-Cs | | up to 650 (440) | 1 μ A |
| Sb-Rb-Cs | | up to 650 (420) | 0.1 μ A |
| Sb-K-Cs | | up to 650 (420) | 0.01 μ A |
| Sb-Na-K | | up to 650 (375) | 10 μ A |
| Sb-Na-K-Cs | | up to 850 (420), up to 900 (600) extended red | 1 μ A |
| Ga-As (Cs) | | up to 930 (300 to 700) | (*) 1 μ A |
| Ga-As-P (Cs) | | up to 720 (580) | (*) 1 μ A |
| Cs-Te | | up to 320 (210) | 0.1 μ A |
| Cs-I | | up to 200 (140) | 0.1 μ A |

(*) Cathode sensitivity considerably degrades if this current is high.

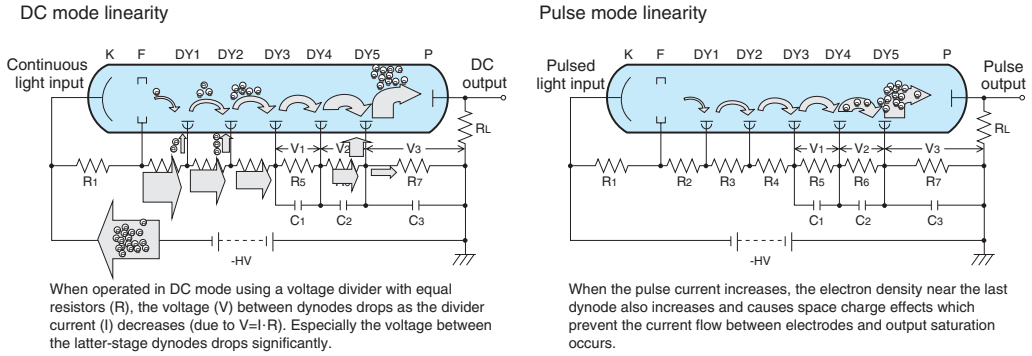
Table 4-4: Photocathode materials and cathode linearity limits

The photocathode is a semiconductor and its electrical resistance depends on the photocathode materials. Therefore, the cathode linearity differs depending on the photocathode materials as listed in Table 4-4. The upper limit of current flow also depends on the area of the photocathode. It should be noted that Table 4-4 shows characteristics only for transmission type photocathodes. In the case of reflection type photocathodes which are formed on a metal plate and thus have a sufficiently low resistivity, the linearity will not be a significant problem. To reduce the effects of photocathode resistivity on the device linearity without degrading the collection efficiency, it is recommended to apply a voltage of 50 to 300 volts between the photocathode and the first dynode, depending on the structure. For semiconductors, the photocathode surface resistivity increases as the temperature decreases. Thus, consideration must be given to the temperature characteristics of the photocathode resistivity when the photomultiplier tube is cooled to a very low temperature.

(2) Anode linearity

The anode linearity is limited by two factors: the voltage-divider circuit and space charge effects due to a large current flowing in the electron multiplier. As shown below, the linearity in DC mode operation is mainly limited by the voltage-divider circuit, while the pulse mode operation is limited by space charge effects.

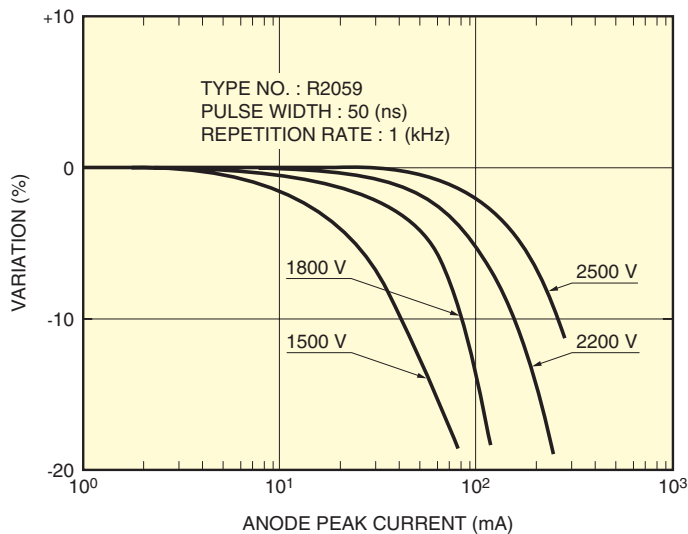
Linearity — DC mode — Limited by a change in the voltage-divider voltage due to the magnitude of signal current.
 — Pulse mode — Limited by the space charge effects.



THBV4_0426EA

Figure 4-26: Factors that affect linearity

The linearity limit defined by the voltage-divider circuit is described in section 1-3 of Chapter 5. The pulse linearity in pulse mode is chiefly dependent on the peak signal current. When an intense light pulse enters a photomultiplier tube a large current flows in the latter-stage dynodes, increasing the space charge density, and causing current saturation. The extent of these effects depends on the dynode structure, as indicated in Table 4-2. The space charge effects depend on the electric field distribution and intensity between each dynode. The mesh type dynodes offer superior linearity because they have a structure resistant to the space charge effects. Each dynode is arranged in close proximity providing a higher electric field strength and the dynode area is large so that the signal density per unit area is lower. In general, any dynode type provides better pulse linearity when the supply voltage is increased, or in other words, when the electric field strength between each dynode is enhanced. Figure 4-27 shows the relationship between the pulse linearity and the supply voltage of a Hamamatsu photomultiplier tube R2059. The linearity can be improved by use of a special voltage-divider (called "a tapered voltage-divider") designed to increase the voltages at the latter-stage dynodes. This is described in section 5.1.4 of Chapter 5. Because such a tapered voltage-divider must have an optimum electric field distribution and intensity that match the structure and characteristics of each dynode, it is rather complicated to determine the proper voltage distribution ratio.



THBV4_0427EA

Figure 4-27: Voltage dependence of linearity

(3) Linearity measurement

The linearity measurement method mainly includes the DC mode and the pulse mode. Each mode is described below.

(a) DC mode

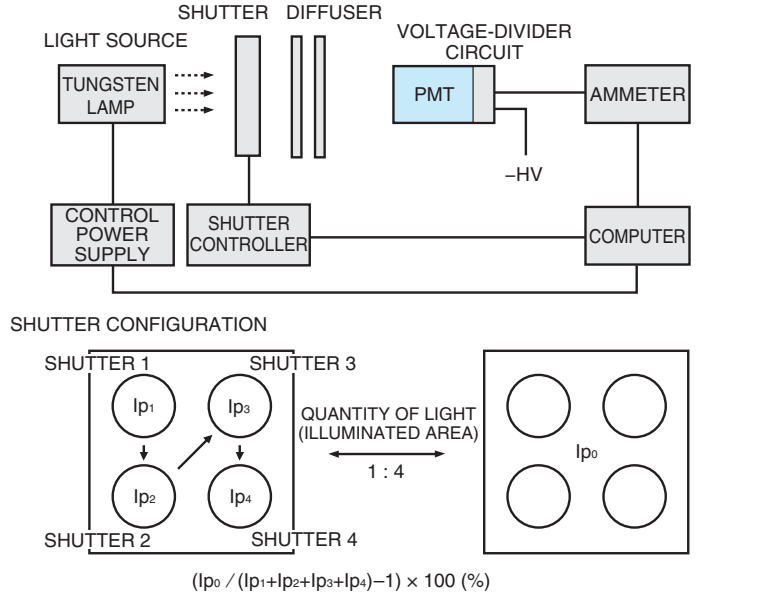


Figure 4-28: Block diagram for DC mode linearity measurement

This section introduces the DC linearity measurement method used by Hamamatsu Photonics. As Figure 4-28 shows, a 4-aperture plate equipped with shutters is installed between the light source and the photomultiplier tube. Each aperture is opened in the order of 1, 2, 3 and 4, finally all four apertures are opened, and the photomultiplier tube outputs are measured (as I_{p1} , I_{p2} , I_{p3} , I_{p4} and I_{p0} , respectively). Then the ratio of I_{p0} to $(I_{p1}+I_{p2}+I_{p3}+I_{p4})$ is calculated as follows:

$$(I_{p0} / (I_{p1}+I_{p2}+I_{p3}+I_{p4})-1) \times 100 (\%) \dots\dots\dots (\text{Eq. 4-11})$$

This value represents a deviation from linearity and if the output is within the linearity range, I_{p0} becomes

$$I_{p0} = I_{p1}+I_{p2}+I_{p3}+I_{p4} \dots\dots\dots (\text{Eq. 4-12})$$

Under these conditions, Eq. 4-11 becomes zero.

Repeating this measurement by changing the intensity of the light source, in other words, changing the photomultiplier tube output current, gives a plot as shown in Figure 4-29. This indicates an output deviation from linearity. This linearity measurement greatly depends on the magnitude of the current flowing through the voltage-divider circuit and its structure.

As a simple method, linearity can also be measured using neutral density filters which are calibrated in advance for changes in the incident light level.

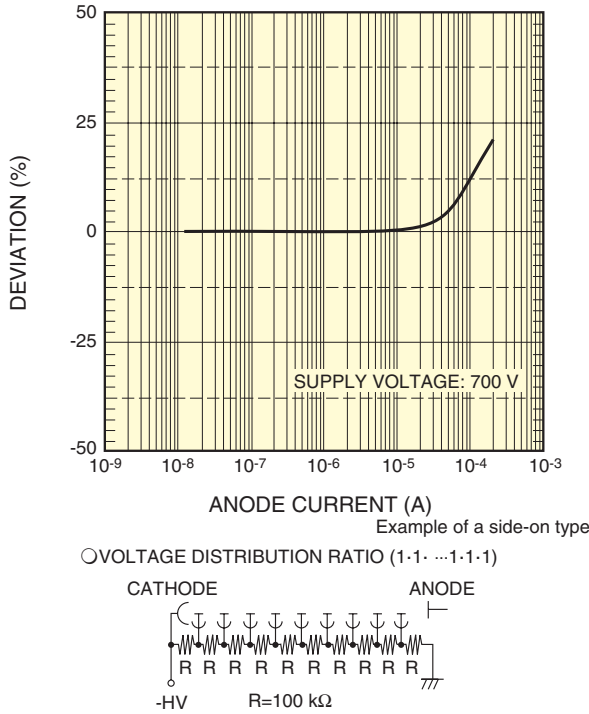


Figure 4-29: DC linearity

(b) Pulse mode

A simplified block diagram for the pulse mode linearity measurement is shown in Figure 4-30. In this measurement, an LED operated in a double-pulsed mode is used to provide higher and lower pulse amplitudes alternately. The higher and lower pulse amplitudes are fixed at a ratio of approximately 4:1. If the photomultiplier tube outputs in response to the higher and lower pulsed light at sufficiently low light levels, the peak currents are I_{p01} and I_{p02} respectively, then the ratio of I_{p02}/I_{p01} is proportional to the pulse amplitude; thus

$$I_{p02}/I_{p01} = 4 \quad \text{..... (Eq. 4-13)}$$

When the LED light sources are brought close to the photomultiplier tube (see Figure 4-30) and the subsequent output current increases, the photomultiplier tube output begins to deviate from linearity. If the output for the lower pulsed light (A_1) is I_{p1} and the output for the higher pulsed light (A_2) is I_{p2} , the ratio between the two output pulses has the following relation:

$$I_{p2}/I_{p1} \neq I_{p02}/I_{p01} \quad \text{..... (Eq. 4-14)}$$

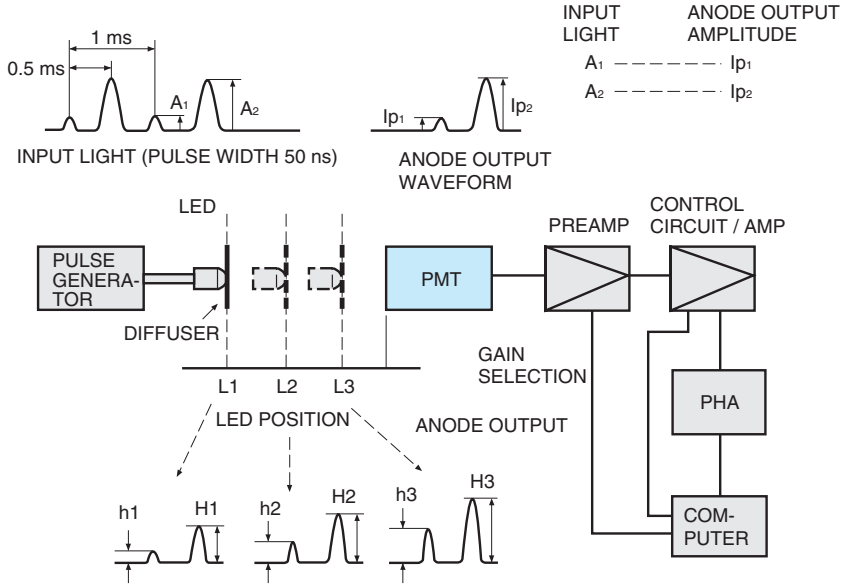
Linearity can be measured by measuring the ratio between the two outputs of the photomultiplier tube, produced by the two different intensities of pulsed light, I_{p2}/I_{p1} . Linearity is then calculated as follows:

$$\frac{(I_{p2}/I_{p1}) - (I_{p02}/I_{p01})}{(I_{p02}/I_{p01})} \times 100(\%) \quad \text{..... (Eq. 4-15)}$$

This indicates the extent of deviation from linearity at the anode output I_{p2} . If the anode output is in the linearity range, the following relation is always established:

$$(I_{p2}/I_{p1}) = (I_{p02}/I_{p01}) \quad \text{..... (Eq. 4-16)}$$

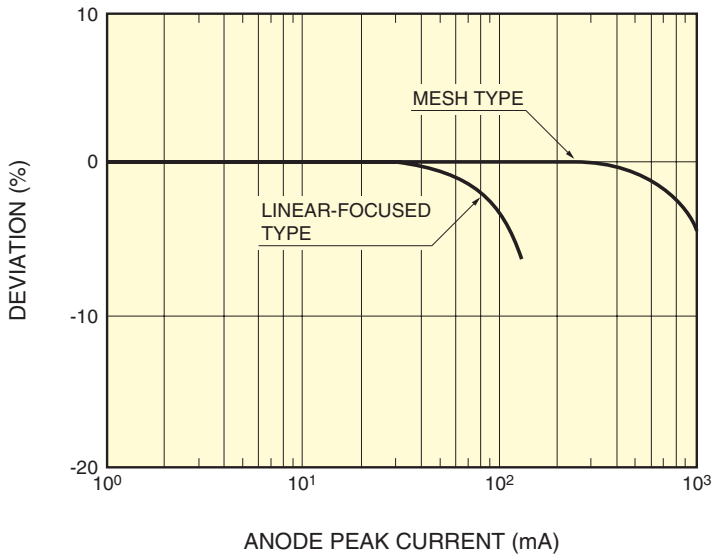
Under these conditions, Eq. 4-15 becomes zero.



THBV4_0430EA

Figure 4-30: Block diagram for pulse mode linearity measurement

By repeating this measurement while varying the distance between the LED light source and the photomultiplier tube so as to change the output current of the photomultiplier tube, linearity curves like those shown in Figure 4-31 can be obtained.



THBV4_0431EA

Figure 4-31: Pulse linearity

4.3.3 Uniformity

Uniformity is the variation of the output signal with respect to the incident light position. Anode uniformity is thought to be the product of the photocathode uniformity and the electron multiplier (dynode section) uniformity. Figure 4-32 shows an example of anode uniformity measured at a wavelength of 400 nanometers. This data is obtained with a light spot of 1 mm diameter scanned over the photocathode surface.

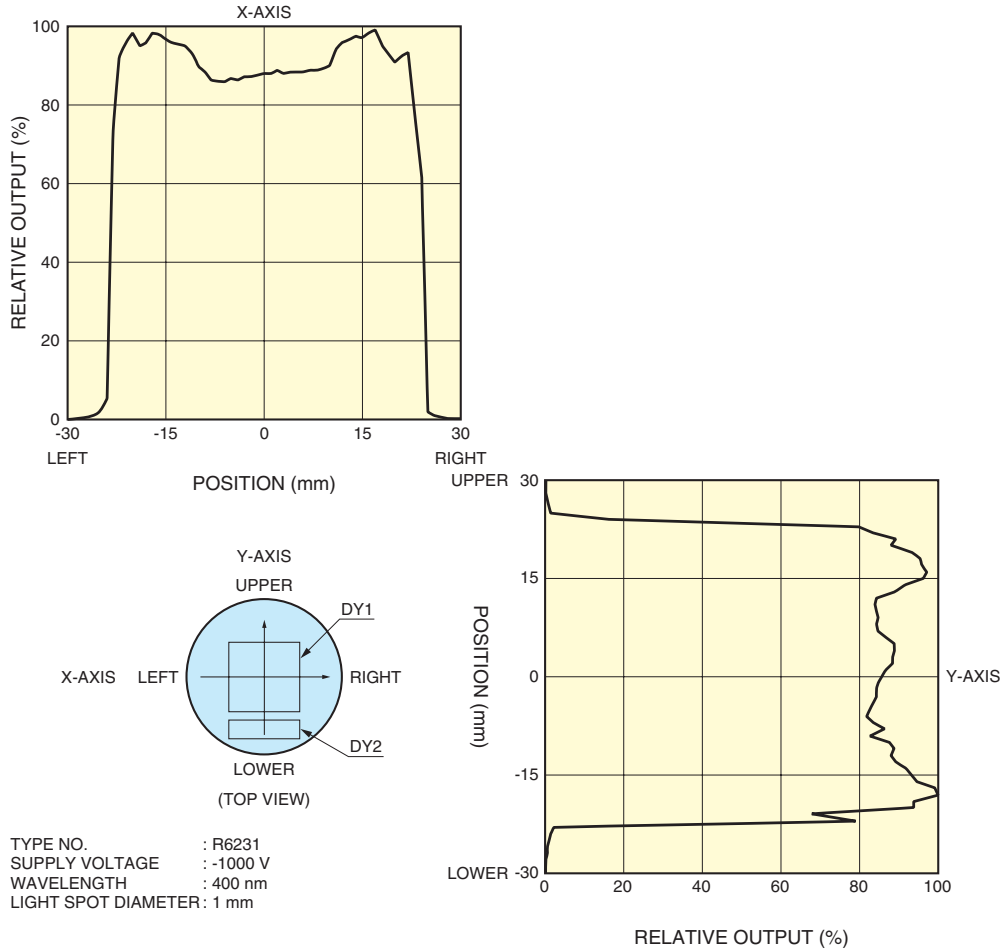
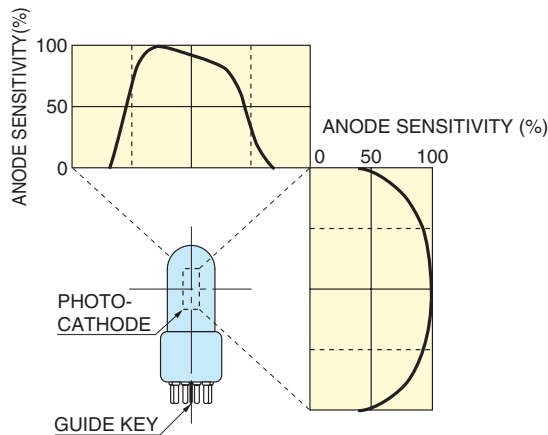


Figure 4-32: Uniformity

THBV4_0432EA

In general, both photocathode uniformity and anode uniformity deteriorate as the incident light shifts to a longer wavelength, and especially as it approaches the long-wavelength limit. This is because the cathode sensitivity near the long-wavelength limit greatly depends on the surface conditions of the photocathode and thus fluctuations increase. Moreover, if the supply voltage is too low, the electron collection efficiency between dynodes may degrade and adversely affect uniformity.

Head-on photomultiplier tubes provide better uniformity in comparison with side-on types. In such applications as gamma cameras used for medical diagnosis where good position detecting ability is demanded, uniformity is an important parameter in determining equipment performance. Photomultiplier tubes used in this field are specially designed and selected for better uniformity. Figure 4-33 shows typical uniformity data for a side-on tube. The same measurement procedure as for head-on tubes is used. Uniformity is also affected by the dynode structure. As can be seen from Table 4-2, the box-and-grid type, venetian blind type, and mesh type offer better uniformity.



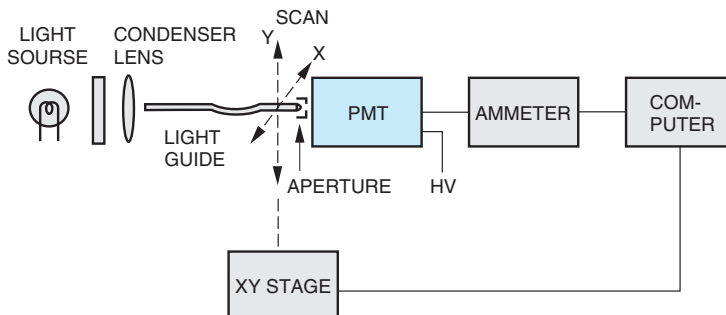
THBV4_0433EA

Figure 4-33: Uniformity of a side-on photomultiplier tube

Considering actual photomultiplier tube usage, uniformity is evaluated by two methods: one measured with respect to the position of incident light (spatial uniformity) and one with respect to the angle of incident light (angular response). The following sections explain their measurement procedures and typical characteristics.

(1) Spatial uniformity

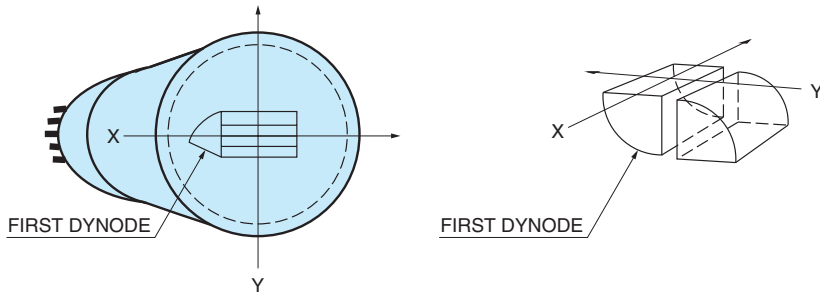
To measure spatial uniformity, a light spot is scanned in two-dimensions over the photocathode of a photomultiplier tube and the variation in output current is graphically displayed. Figure 4-34 shows a schematic diagram for the spatial uniformity measurement.



THBV4_0434EA

Figure 4-34: Schematic diagram for spatial uniformity measurement

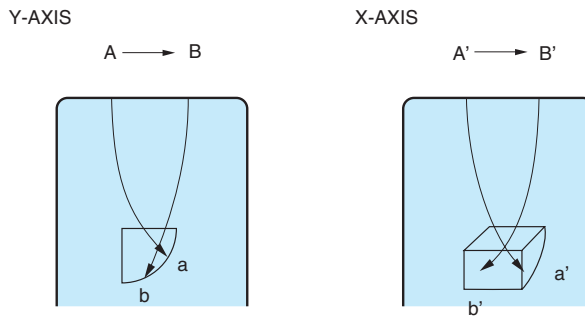
For convenience, the photocathode is scanned along the X-axis and Y-axis. The direction of the X-axis or Y-axis is determined with respect to the orientation of the first dynode as shown in Figure 4-35. Figure 4-35 also shows the position relation between the XY axes and the first dynode. The degree of loss of electrons in the dynode section significantly depends on the position of the first dynode on which the photoelectrons strike. Refer to Figure 4-32 for specific uniformity data.



THBV4_0435EA

Figure 4-35: Spatial uniformity measurement for head-on types

While the photocathode is scanned by the light spot along the X-axis or the Y-axis, it is thought that the emitted photoelectrons travel along the X-axis or Y-axis of the first dynode as shown in Figure 4-36.



THBV4_0436EA

Figure 4-36: Position of photoemission and the related position on the first dynode

The X-axis uniformity is usually better than the Y-axis uniformity, since the dynode structure in the X-axis direction is symmetrical along the tube axis. In some cases, spatial uniformity is evaluated by dividing the photocathode into a grid pattern, so that sensitivity distribution is displayed in two or three dimensions.

Anode output non-uniformity ranges from 20 to 40 percent for head-on tubes, and may exceed those values for side-on tubes. The adverse effects of spatial uniformity can be minimized by placing a diffuser in front of the input window of a photomultiplier tube or by using a photomultiplier tube with a frosted glass window.

(2) Angular response

Photomultiplier tube sensitivity somewhat depends on the angle of incident light on the photocathode. This dependence on the incident angle is called the angular response.²⁸⁾⁻³⁰⁾ To measure the angular response, the entire photocathode is illuminated with collimated light, and the output current is measured while rotating the photomultiplier tube. A block diagram for the angular response measurement is shown in Figure 4-37 and specific data is plotted in Figure 4-38. As the rotary table is rotated, the projected area of the photocathode is reduced. This means that the output current of a photomultiplier tube is plotted as a cosine curve of the incident angle even if the output has no dependence on the incident angle. Normally, the photocathode sensitivity improves at larger angles of incidence and so the output is plotted along a curve showing higher sensitivity than the cosine ($\cos \theta$) curve. This is because the incident light transmits across a longer distance at large angles of incidence. In addition, this increase in sensitivity usually becomes larger at longer wavelengths.

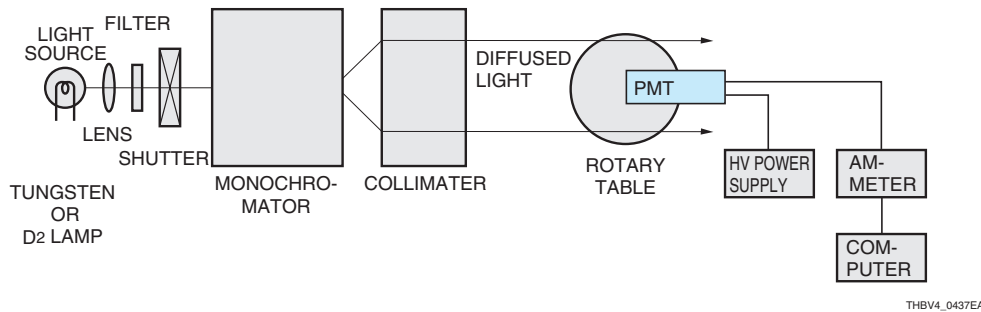


Figure 4-37: Schematic diagram for angular response measurement

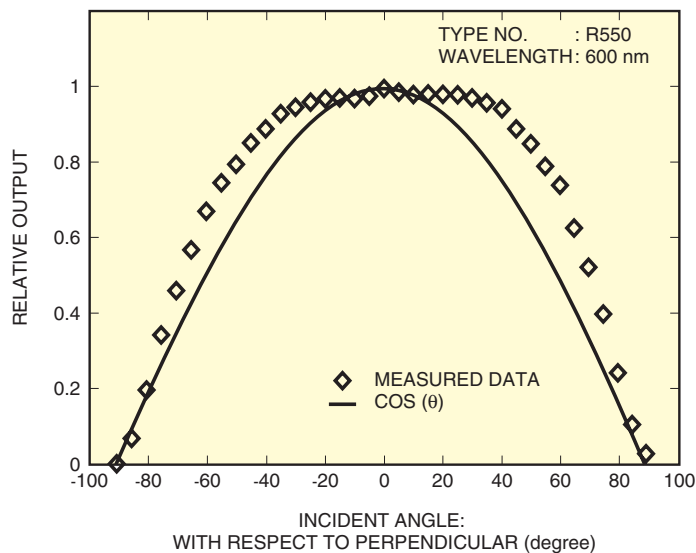


Figure 4-38: Typical angular response

4.3.4 Stability

The output variation of a photomultiplier tube with operating time is commonly termed as "drift" or "life" characteristics. On the other hand, the performance deterioration resulting from the stress imposed by the supply voltage, current, and ambient temperature is called "fatigue".

(1) Drift (time stability) and life characteristics

Variations (instability) over short time periods are mainly referred to as drift¹⁾³¹⁾, while variations (instability) over spans of time longer than 1000 to 10 000 hours are referred to as the life characteristics (Refer to 13.8.2 in Chapter 13.). Since the cathode sensitivity of a photomultiplier tube exhibits good stability even after long periods of operating time, the drift and life characteristics primarily depend on variations in the secondary emission ratio. In other words, these characteristics indicate the extent of gain variation with operating time. Drift per unit time generally improves with longer operating time and this tendency continues even if the photomultiplier tube is left unused for a short time after operation. Aging or applying the power supply voltage to the photomultiplier tube prior to use ensures more stable operation.

Since drift and life characteristics greatly depend on the magnitude of signal output current, keeping the average output current within a few microamperes is recommended. At Hamamatsu Photonics, drift is usually measured in the DC mode by illuminating a photomultiplier tube with a continuous light and recording the output current with the operating time. Figure 4-39 shows specific drift data for typical Hamamatsu photomultiplier tubes. In most cases, the drift of a photomultiplier tube tends to vary largely during initial operation and stabilizes as operating time elapses. In pulsed or intermittent operation (cyclic on/off operation), the pattern and magnitude of the drift are nearly the same as those obtained in the DC mode if the average output current is of the same level.

In addition, there are other methods for evaluating the drift and life characteristics, which are chiefly used for photomultiplier tubes designed for scintillation counting. For more details refer to Chapter 7, "Scintillation counting".

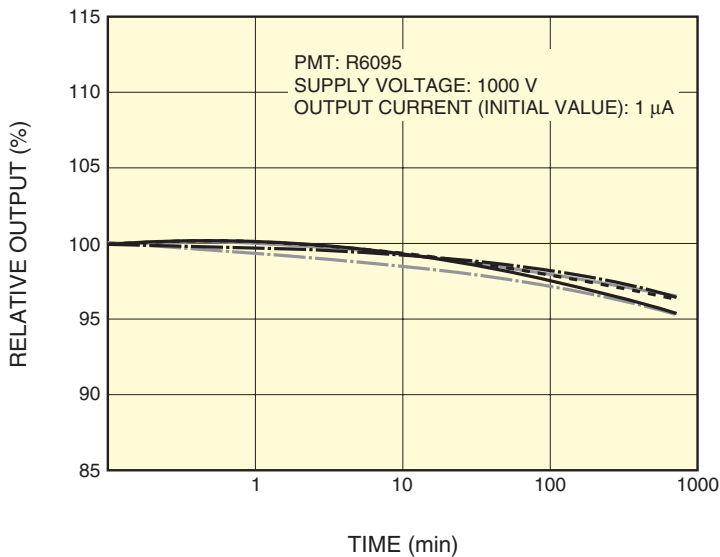


Figure 4-39: Examples of drift characteristics

(2) Aging and warm-up

In applications where output stability within a few percent is required, aging or warm-up is recommended as explained below.

(a) Aging

Aging is a technique in which a photomultiplier tube is continuously operated for a period ranging from several hours to several tens of hours while being illuminated with a constant level of light that does not cause the anode output current to exceed its maximum rating. Through this aging, drift can be effectively stabilized. In addition, if the photomultiplier tube is warmed up (see the next item) just before actual use, the drift will be further stabilized.

(b) Warm-up

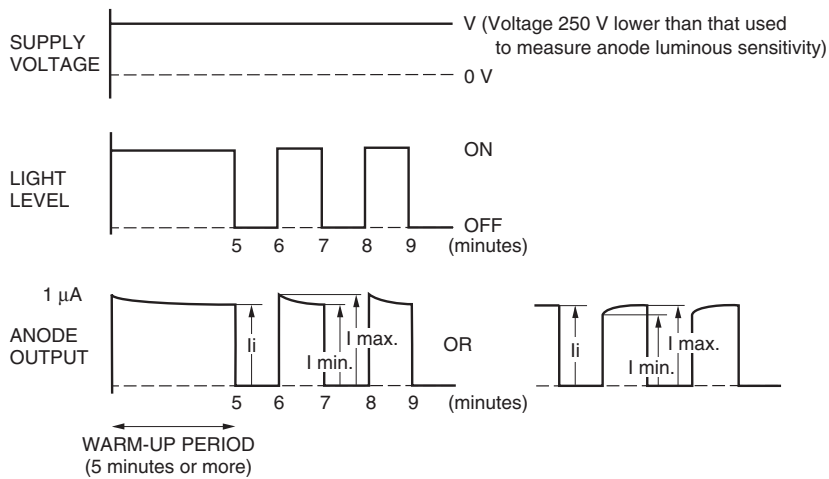
Before using a photomultiplier tube, a warm-up for about 30 to 60 minutes is recommended to ensure stable operation. The warm-up period should be longer at the initial phase of photomultiplier tube operation, particularly in intermittent operation. After a long period of operation warm-up can be shortened. At a higher anode current the warm-up period can be shortened and at a lower anode current the warm-up should be longer to obtain the same effect. In most cases, a warm-up is performed for several ten minutes at a supply voltage near the actual operating voltage and an anode current of several microamperes. However, in low current operation (average output current from less than one hundred up to several hundred nanoamperes), just applying a voltage to the photomultiplier tube for about one hour in the dark state will be effective to some extent as a warm-up.

4.3.5 Hysteresis

When the incident light or the supply voltage is changed in a step function, a photomultiplier tube may not produce an output comparable with the same step function. This phenomenon is known as "hysteresis"^{(1) (32)} and also depends on the immediately preceding operation. Hysteresis is observed as two behaviors: "overshoot" in which the output current first increases greatly and then settles and "undershoot" in which the output current first decreases and then returns to a steady level. Hysteresis is further classified into "light hysteresis" and "voltage hysteresis" depending on the measurement conditions.

(1) Light hysteresis

When a photomultiplier tube is operated at a constant voltage, it may exhibit a temporary variation in the anode output after the incident light is changed in a step function. This variation is called light hysteresis. Figure 4-40 shows the Hamamatsu test method for light hysteresis.



THBV4_0440EA

Figure 4-40: Light hysteresis

In light hysteresis test, the photomultiplier tube is operated at a voltage, which is 250 volts lower than the voltage used to measure the anode luminous sensitivity, and is warmed up for five minutes or more at a light level producing an anode current of approximately 1 microampere. Then the incident light is shut off for one minute and then input again for one minute. This procedure is repeated twice to confirm the reproducibility. By measuring the variations of the anode outputs, the extent of light hysteresis can be expressed in percent, as follows:

$$\text{Light hysteresis } H_L = ((I_{MAX} - I_{MIN}) / I_i) \times 100 \text{ (\%)} \dots\dots\dots \text{(Eq. 4-17)}$$

where I_{MAX} is the maximum output value, I_{MIN} is the minimum output value, and I_i is the average output value.

Table 4-5 shows typical light hysteresis data for major Hamamatsu photomultiplier tubes. Most photomultiplier tubes display a slight hysteresis within ± 1 percent, except for some special types. It should be noted that light hysteresis behaves in different patterns or values, depending on the magnitude of the output current.

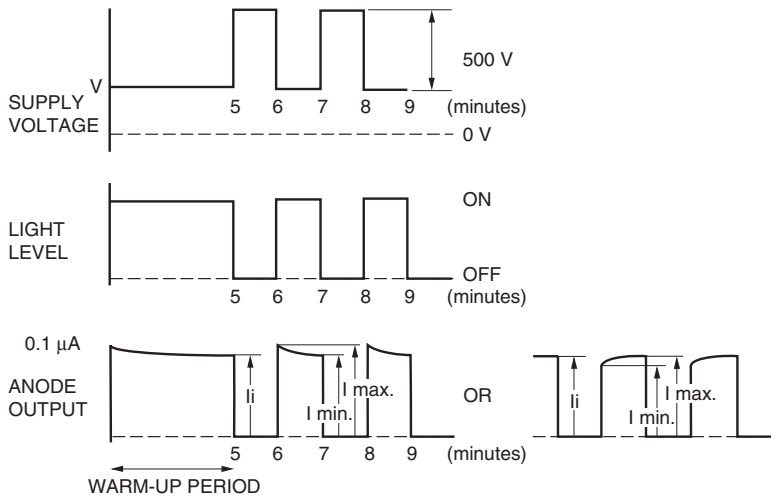
(2) Voltage hysteresis

When the incident light level changes in a step function, the photomultiplier tube is sometimes operated with a feedback circuit that changes the supply voltage in a complementary step function so that the photomultiplier tube output is kept constant. In this case, the output signal may overshoot or undershoot immediately after the supply voltage is changed. It is important to minimize this phenomenon. Generally, this voltage hysteresis is larger than light hysteresis and even tubes with small light hysteresis.

| PMT | Light hysteresis H _L (%) | Voltage hysteresis H _V (%) | Tube diameter (mm) |
|--------|-------------------------------------|---------------------------------------|--------------------|
| R6350 | 0.8 | 3.0 | 13mm side-on |
| R11568 | 0.5 | 1.0 | 28mm side-on |
| R928 | 0.5 | 1.0 | 28mm side-on |
| R12421 | 0.3 | 1.0 | 13mm head-on |
| R6095 | 0.4 | 2.0 | 28mm head-on |
| R1306 | 0.07 | 0.06 | 52mm head-on |

Table 4-5: Typical hysteresis data for major Hamamatsu photomultiplier tubes

Figure 4-41 shows a procedure for measuring voltage hysteresis. A photomultiplier tube is operated at a voltage V, which is 700 volts lower than the voltage used to measure the anode luminous sensitivity. The tube is warmed up for five minutes or more at a light level producing an anode current of approximately 0.1 microamperes.



THBV4_0441EA

Figure 4-41: Voltage hysteresis

Then the incident light is shut off for one minute while the supply voltage is increased in 500 volt step. Then the light level and supply voltage are returned to the original conditions. This procedure is repeated to confirm the reproducibility. By measuring the variations in the anode outputs, the extent of voltage hysteresis is expressed in percent, as shown in Eq. 4-18 below. In general, the higher the change in the supply voltage, the larger the voltage hysteresis will be. Other characteristics are the same as those for light hysteresis.

$$\text{Voltage hysteresis } H_V = ((I_{MAX} - I_{MIN}) / I_i) \times 100 \text{ (\%)} \dots\dots\dots (\text{Eq. 4-18})$$

where I_{MAX} is the maximum output value, I_{MIN} is the minimum output value and I_i is the average output value.

(3) Reducing the hysteresis

When a signal light is blocked for a long period of time, applying a dummy light to the photomultiplier tube to minimize the change in the anode output current is effective in reducing the possible light hysteresis. Voltage hysteresis may be improved by use of HA treatment. (Refer to 13.8.2 in Chapter 13.)

For some products such as side-on photomultiplier tubes, voltage hysteresis can be improved by making the irradiation area of incident light smaller.

4.3.6 Dark current

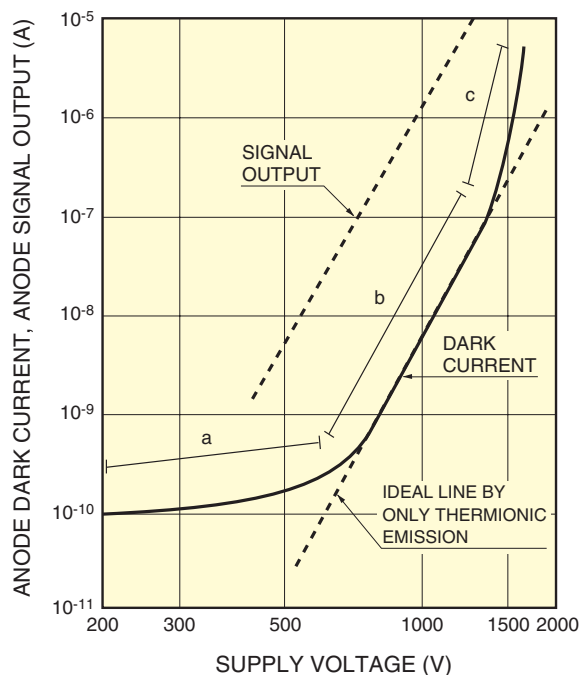
A small amount of current flows in a photomultiplier tube even when operated in a completely dark state. This output current is called the dark current^{1) 23) 25) 33)} and ideally it should be kept as small as possible because photomultiplier tubes are used for handling minute amounts of light and current.

(1) Causes of dark current

Dark current may be categorized by cause as follows:

- (a) Thermionic emission from the photocathode and dynode surface
- (b) Leakage current (ohmic leakage) between the anode and other electrodes inside the tube and/or between the anode pin and other pins on the bulb stem
- (c) Scintillation from glass envelope or electrode supports
- (d) Field emission
- (e) Ionization of residual gases (ion feedback)
- (f) Scintillation from glass caused by cosmic rays, radiation from radioisotopes contained in the glass envelope, and environmental gamma rays

Dark current increases with an increasing supply voltage, but the rate of increase is not constant. Figure 4-42 shows a typical dark current vs. supply voltage characteristic.



THBV4_0442EA

Figure 4-42: Typical dark current vs. supply voltage characteristic

This characteristic is related to three regions of the supply voltage: a low voltage region (a in Figure 4-42), a medium voltage region (b in Figure 4-42), and a high voltage region (c in Figure 4-42). Region a is dominated by the leakage current, region b by the thermionic emission, and region c by the field emission and glass or electrode support scintillation. In general, region b provides the best signal-to-noise ratio, so operating the photomultiplier tube in this region would prove ideal. Ion feedback³⁴⁾ and noise^{34) 35) 36)} originating from cosmic rays and radioisotopes will sometimes be a problem in pulse operation.

When a photocathode is exposed to room illumination, the dark current will return to the original level by storing the photomultiplier tube in a dark state for one to two hours. However, if exposed to sunlight or extremely intense light (10 000 lux or higher), this may cause unrecoverable damage and must therefore be avoided. It is recommended to store the photomultiplier tube in a dark state before use.

The dark current data furnished with Hamamatsu photomultiplier tubes is measured after the tube has been stored in a dark state for 30 minutes. This "30-minute storage in a dark state" condition allows most photomultiplier tubes to approach the average dark current level attained after being stored for a long period in a dark state. This is also selected in consideration of the work efficiency associated with measuring the dark current. If the tube is stored for a greater length of time in a dark state, the dark current will decrease further. The following sections explain each of the six causes of dark current listed above.

a) Thermionic emission

Since the photocathode and dynode surfaces are composed of materials with a very low work function, they emit thermionic electrons even at room temperatures. This effect has been studied by W. Richardson, and is stated by the following equation.³⁷⁾

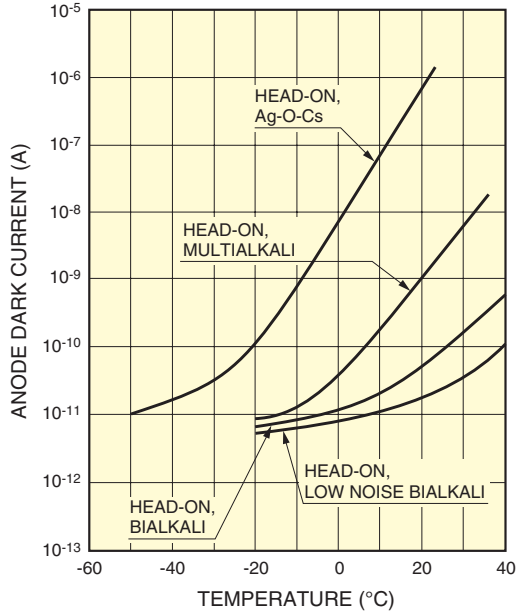
$$i_s = AT^{5/4}e^{(-e\psi/KT)} \dots\dots\dots \text{(Eq. 4-19)}$$

where

| | |
|------------------------|--------------------------|
| ψ : work function | T : absolute temperature |
| e : electron charge | A : constant |
| K : Boltzmann constant | |

This equation indicates that thermionic emission is a function of the photocathode work function and absolute temperature. So the magnitude of the work function or the photocathode material governs the amount of thermionic emission. When the photocathode work function is low, the spectral response extends to the light with lower energy or longer wavelengths, but with an increase in the thermionic emission. Among generally used photocathodes composed of alkali metals, the Ag-O-Cs photocathode with sensitivity in a longer wavelength range (see Figure 4-2) has high dark current. In contrast, photocathodes (Cs-Te, Cs-I) for ultraviolet light detection have the long wavelength limit at shorter wavelengths and so exhibit low dark current.

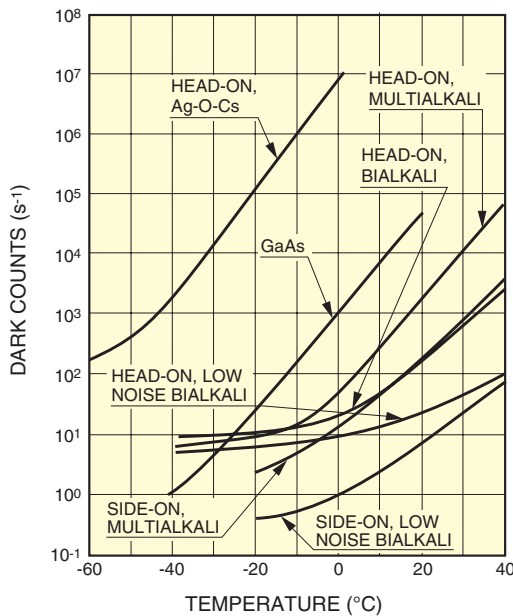
The above equation shows that the dark current decreases with decreasing temperature. In other words, cooling a photomultiplier tube is very effective in reducing the dark current, as shown in Figure 4-43.



THBV4_0443EA

Figure 4-43: Temperature characteristics of anode dark current

However, when the dark current is reduced by cooling to a level where the leakage current predominates, this effect becomes limited. Although thermionic emission occurs both from the photocathode and the dynodes, the thermionic emission from the photocathode has a much larger effect on the dark current. This is because the photocathode is larger than each dynode in size and also because the dynodes, especially at the latter stages, contribute less to the output current. Consequently, the dark current caused by the thermionic emission vs. the supply voltage characteristic will be nearly identical with the slope of gain vs. supply voltage. Figure 4-44 shows temperature characteristics for dark pulses measured in the photon counting method. In this case as well, the number of dark pulses is decreased by cooling the photocathode.



THBV4_0444EA

Figure 4-44: Temperature characteristics for dark counts

b) Leakage current (ohmic leakage)

Photomultiplier tubes are operated at high voltages from 500 up to 3000 volts, but they handle very low currents from several nanoamperes to less than 100 microamperes. Therefore, the quality of the insulating materials used in the tubes is very important. For instance, if the insulation resistance is around 10^{12} ohms, the leakage current may reach the nanoampere level. The relationship between the leakage current from the insulating materials and the supply voltage is determined by Ohm's law, i.e., current value (I) = supply voltage (V)/insulation resistance (R), regardless of the gain of the photomultiplier tube as seen in Figure 4-42. On the other hand, the dark current resulting from thermionic emission varies exponentially with the supply voltage. Thus, as mentioned in the previous section, the leakage current has relatively more effect on the dark current as the supply voltage is lowered.

A leakage current may be generated between the anode and the last dynode inside a tube. It may also be caused by imperfect insulation of the glass stem and base, and between the socket anode pin and other pins. Since contamination from dirt and moisture on the surface of the glass stem, base, or socket increases the leakage current, care should be taken to keep these parts clean and at low humidity.

If contaminated, they can be cleaned with alcohol in most cases. This is effective in reducing the leakage current.

c) Scintillation from the glass envelope or electrode support materials

Some electrons emitted from the photocathode or dynodes may deviate from their normal trajectories and do not contribute to the output signal. If these stray electrons impinge on the glass envelope, scintillations may occur and result in dark pulses. In general, a photomultiplier tube is operated with a negative high voltage applied to the photocathode and is housed in a metal case at ground potential. This arrangement tends to cause stray electrons to impinge on the glass envelope. However, this problem can be minimized by using a technique called "HA treatment". Refer to section 13.8.2 of Chapter 13 for detailed information on HA treatment.

d) Field emission

If a photomultiplier tube is operated at an excessive voltage, electrons may be emitted from the dynodes by the strong electric field, causing the dark current to increase abruptly. This phenomenon occurs in region c in Figure 4-42. Since this considerably shortens the life of the photomultiplier tube considerably, the maximum supply voltage is specified for each tube type. In most cases, there will be no problem when operated within this maximum rating. But for safety, operating the photomultiplier tube at a voltage 20 to 30 percent lower than the maximum rating is recommended.

e) Ionization of residual gases (ion feedback)

The interior of a photomultiplier tube is kept at a vacuum as high as 10^{-6} to 10^{-5} Pa. Even so, there exist residual gases that cannot be ignored. The molecules of these residual gases may be ionized by collisions with electrons, and the resulting positive ions strike the front stage dynodes or the photocathode and produce many secondary electrons, resulting in a large noise pulse output. This noise pulse is output with a slight time delay after the signal current output. This noise pulse is therefore called an afterpulse^{38) 39) 40)} and may cause a measurement error during pulsed operation.

f) Scintillation from glass caused by cosmic rays, radiation from radioisotopes contained in the glass envelope, and environmental gamma rays

Many types of cosmic rays are always falling on the earth. Among them, muons (μ) can be a major source of photomultiplier tube noise. When muons pass through the glass envelope, Cherenkov radiation may occur, releasing a large number of photons. In addition, most glasses contain potassium oxide (K_2O) which also contains a minute amount of the radioactive element ^{40}K . ^{40}K emits beta and gamma rays which may cause noise. Furthermore, environmental gamma rays emitted from radioisotopes contained in buildings may be another noise source. However, because these dark noises occur much less frequently, they are negligible except for applications such as liquid scintillation counting where the number of signal counts is exceptionally small.

(2) Expression of dark current

Dark current is a critical factor that governs the lower detection limit in low light level measurements. There are various methods and terms used to express dark current. The following introduces some of them.

a) DC expression

In general, most Hamamatsu photomultiplier tubes are supplied with dark current data measured at a constant voltage. The dark current may be measured at a voltage at which a particular value of anode sensitivity is obtained. In this case, the dark current is expressed in terms of equivalent dark current or EADCI (equivalent anode dark current input). The equivalent dark current is simply the dark current measured at the voltage producing a specific anode luminous sensitivity, and is a convenient parameter when the tube is operated with the anode sensitivity maintained at a constant value. The EADCI is the value of the incident light flux required to produce an anode current equal to the dark current and is represented in units of lumens or watts as follows:

$$\text{EADCI (lm)} = \text{Dark current (A)} / \text{Anode luminous sensitivity (A/lm)} \dots \text{(Eq. 4-20)}$$

When representing the EADCI in watts (W), a specified wavelength is selected and the dark current is divided by the anode radiant sensitivity (A/W) at that wavelength. Figure 4-45 shows an example of EADCI data along with the anode dark current and anode luminous sensitivity. A better signal-to-noise ratio can be obtained when operated in the supply voltage region with a small EADCI. As seen from the figure, the supply voltage region in the vicinity of 1000 volts displays a small, flat EADCI curve, yet offers an adequate anode sensitivity of three orders of magnitude.

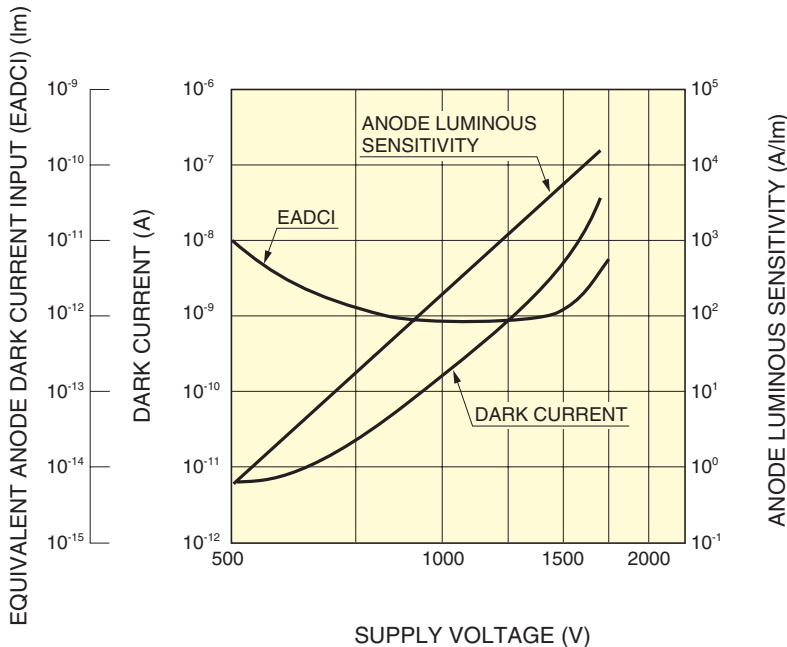


Figure 4-45: Example of EADCI

THBV4_0445EA

b) AC expression

In low-level-light measurements, the DC components of dark current can be subtracted. The lower limit of light detection is determined rather by the fluctuating components or noise. In this case, the noise is commonly expressed in terms of ENI (equivalent noise input). The ENI is the value of incident light flux required to produce an output current equal to the noise current, i.e., the incident light level that provides a signal-to-noise ratio of unity. When the ENI is expressed in units of watts (W) at the peak wavelength or at a specific wavelength, it is also referred to as the NEP (noise equivalent power).

Because the noise is proportional to the square root of the frequency bandwidth of the circuit, the ENI²³⁾ is defined as follows:

$$\text{ENI} = (2e \cdot I_d \cdot \mu \cdot B)^{1/2} / S \text{ (W)} \quad \dots\dots\dots \text{(Eq. 4-21)}$$

where

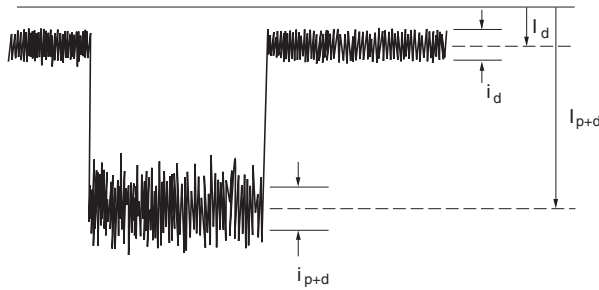
- e: electron charge (1.6×10^{-19} C)
- I_d : anode dark current (A)
- μ : gain
- B: frequency bandwidth of circuit (Hz)
- S: anode radiant sensitivity (A/W)

Generally, $B = 1$ Hz is used and the ENI value ranges from 10^{-15} to 10^{-16} (W) at the peak wavelength.

4.3.7 Signal-to-noise ratio of photomultiplier tubes

When observing the output waveform of a photomultiplier tube, two types of noise components can be seen: one is present even without light input, and the other is generated by the input of signal light. Normally, these noise components are governed by the dark current generated by the photocathode thermionic emission and the shot noise resulting from the signal current. Both of these noise sources are discussed here.

The signal-to-noise ratio referred to in the following description is expressed in r.m.s. (root mean square). When signal and noise waveforms like those shown in Figure 4-46 are observed, they can be analyzed as follows:



THBV4_0446EA

Figure 4-46: Example of signal-to-noise ratio

- Mean value of noise component : I_d
- AC component of noise : i_d (r.m.s.)
- Mean value of signal (noise component included) : I_{p+d}
- AC component of signal (noise component included) : i_{p+d} (r.m.s.)

Using these factors, the signal-to-noise ratio⁽²⁵⁾⁽⁴¹⁾⁽⁴²⁾ is given by

$$\text{SN ratio} = I_p / i_{p+d} \dots\dots\dots (\text{Eq. 4-22})$$

where I_p is the mean value of the signal component only, which is obtained by subtracting I_d from I_{p+d} . If the dark current I_d is low enough to be ignored ($I_p \gg I_d$), the signal-to-noise ratio will be

$$\text{SN ratio} \approx I_p / i_p \dots\dots\dots (\text{Eq. 4-23})$$

where I_p is the mean value of the signal component and i_p is the AC component (r.m.s.) of the signal. i_p consists of a component associated with the statistical fluctuation of photons and the photoemission process and a component created in the multiplication process. The noise component produced in the multiplication process is generally expressed in terms of the noise figure $F^{(42)}$ which indicates how much the signal-to-noise ratio will degrade between the input and output, and is defined as follows:

$$F = (S/N)_{in}^2 / (S/N)_{out}^2 \dots\dots\dots (\text{Eq. 4-24})$$

where $(S/N)_{in}$ is the signal-to-noise ratio on the photomultiplier tube input side and $(S/N)_{out}$ is the signal-to-noise ratio on the photomultiplier tube output side. With a photomultiplier tube having n dynode stages, the noise figure from the cascade multiplication process is given by the following equation:

$$F = 1 + 1/\delta_1 + 1/\delta_1\delta_2 + \dots + 1/\delta_1\delta_2 \dots \delta_n \dots \dots \dots \text{(Eq. 4-25)}$$

where $\delta_1, \delta_2, \dots, \delta_n$ are the secondary emission ratios at each stage.

With $\delta_1, \delta_2, \dots, \delta_n = \delta$, Eq. 4-25 is simplified as follows:

$$F \approx \delta / (\delta - 1) \dots \dots \dots \text{(Eq. 4-26)}$$

Thus by adding the noise figure to the AC component i_p , i_p is expressed by the following equation:

$$i_p = \mu(2 \cdot e \cdot I_k \cdot \alpha \cdot B \cdot F)^{1/2} \dots \dots \dots \text{(Eq. 4-27)}$$

where α is the collection efficiency, μ is the gain, e is the electron charge, I_k is the cathode current, and B is the frequency bandwidth of the measurement system. From this equation and Eq. 4-25, i_p becomes

$$i_p = \mu\{2 \cdot e \cdot I_k \cdot \alpha \cdot B(1 + 1/\delta_1 + 1/\delta_1\delta_2 + \dots + 1/\delta_1\delta_2 \dots \delta_n)\}^{1/2} \dots \dots \dots \text{(Eq. 4-28)}$$

On the other hand, the average anode current I_p is expressed in the following equation:

$$I_p = I_k \cdot \alpha \cdot \mu \dots \dots \dots \text{(Eq. 4-29)}$$

From Eq. 4-28 and Eq. 4-29, the signal-to-noise ratio becomes

$$\begin{aligned} \text{SN ratio} &= I_p / i_p \\ &= \left(\frac{I_k \alpha}{2eB} \cdot \frac{1}{1 + 1/\delta_1 + 1/\delta_1\delta_2 + \dots + 1/\delta_1\delta_2 \dots \delta_n} \right)^{1/2} \end{aligned}$$

With $\alpha = 1$ the above equation can be simplified using Eq. 4-26, as follows:

$$\text{SN ratio} \approx \left(\frac{I_k}{2eB} \cdot \frac{1}{\delta / (\delta - 1)} \right)^{1/2} \dots \dots \dots \text{(Eq. 4-30)}$$

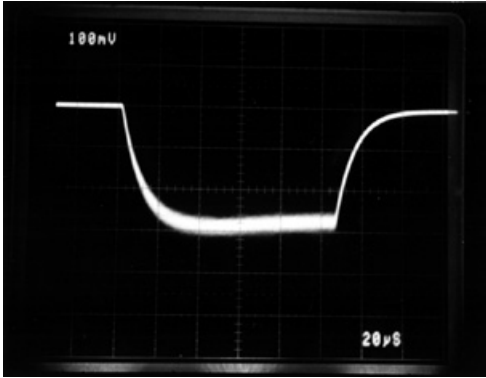
From this relationship, it is clear that the signal-to-noise ratio is proportional to the square root of the cathode current I_k and is inversely proportional to the square root of the frequency bandwidth B .

By substituting $\delta = 6$ into Eq. 4-30, which is the typical secondary emission ratio of a normal photomultiplier tube, the value $\delta / (\delta - 1)$ will be 1.2, a value very close to 1. If the noise in the multiplication process is disregarded, the signal-to-noise ratio can be rearranged as follows:

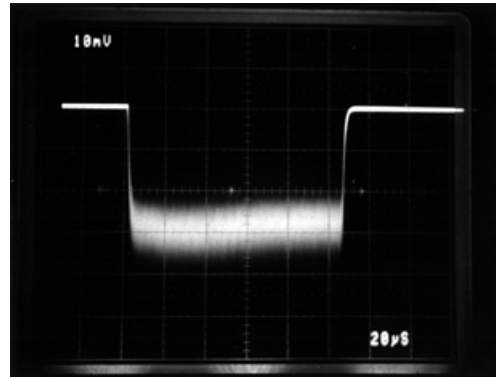
$$\text{SN ratio} = (I_k / 2eB)^{1/2} \approx 1.75 \times 10^3 \sqrt{\frac{I_k (\mu\text{A})}{B (\text{MHz})}} \dots \dots \dots \text{(Eq. 4-31)}$$

Figure 4-47 shows the output voltage waveforms obtained while the light level and load resistance are changed under certain conditions. These prove that the relation in Eq. 4-31 is correct.

(a) $R_L=20\text{ k}\Omega$



(b) $R_L=2\text{ k}\Omega$ (Bandwidth is 10 times wider than (a))



(c) Light level is 10 times higher than (b)

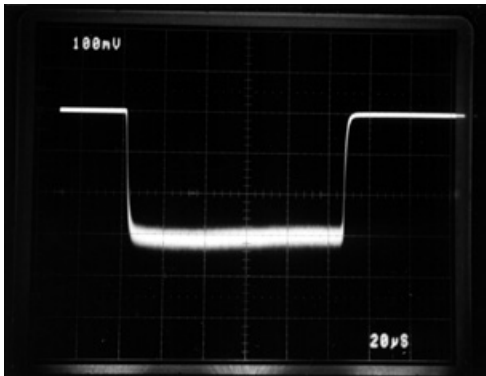


Figure 4-47: Change in signal-to-noise ratio for R329 when light level and load resistance are changed

The above description ignores the dark current. Taking into account the contribution of the cathode equivalent dark current (I_d) and the noise current (N_A) of the amplifier circuit, Eq. 4-30 can be rewritten as follows:

$$\text{SN ratio} = \frac{I_k}{(2eB \cdot \delta / (\delta - 1) \cdot (I_k + 2I_d) + N_A^2)^{1/2}} \dots\dots\dots (\text{Eq. 4-32})$$

In cases where the noise of the amplifier circuit is negligible ($N_A=0$), the signal-to-noise ratio becomes

$$\text{SN ratio} = \frac{I_k}{(2eB \cdot \delta / (\delta - 1) \cdot (I_k + 2I_d))^{1/2}} \dots\dots\dots (\text{Eq. 4-33})$$

where $I_k = \eta \cdot e \cdot P \cdot \lambda / hc$, and each symbol stands for the following:

- | | |
|---|--|
| I_k : cathode current (A) | e : electron charge (C) |
| λ : wavelength (m) | h : Planck's constant (J·s) |
| c : velocity of light (m/s) | η : quantum efficiency |
| P : input light amount (W) | B : frequency bandwidth (Hz) |
| δ : secondary emission ratio | N_A : noise of amplifier circuit (A) |
| I_d : cathode equivalent dark current (A) | |

If $F=(\delta/(\delta-1))$ is inserted in Eq. 4-33, then

$$\begin{aligned} \text{SN ratio} &= \frac{I_k}{(2 \cdot e \cdot (I_k + 2 \cdot I_{da}) \cdot F \cdot B)^{1/2}} = \frac{I_k \cdot \mu}{(2e(I_{ph} + 2I_{da})FB \cdot \mu^2)^{1/2}} \\ &= \frac{I_p}{\sqrt{2e(I_p + 2I_{da})\mu FB}} = \frac{S_p P_i}{\sqrt{2e(S_p P_i + 2I_{da})\mu FB}} \end{aligned}$$

where I_p is the anode signal current and I_{da} is the anode dark current.

I_p is given by: $I_p = I_h \cdot \mu = S_p \cdot P_i$

where S_p is the anode radiant sensitivity and P_i is the incident light power.

If the signal-to-noise ratio is 1, then

$$S_p P_i = \sqrt{2e(S_p P_i + 2I_{da})\mu FB}$$

This relation is expressed as follows to find the variable P_i that gives

$$\begin{aligned} (S_p P_i)^2 - 2e(S_p P_i + 2I_{da})\mu FB &= 0 \\ S_p P_i &= \frac{-(-2eS_p \mu FB) \pm \sqrt{(-2eS_p \mu FB)^2 - 4S_p^2(-4eI_{da}\mu FB)}}{2S_p^2} \end{aligned}$$

Therefore, P_i becomes

$$P_i = \frac{e\mu FB}{S_p} + \frac{\sqrt{(e\mu FB)^2 + 4eI_{da}\mu FB}}{S_p}$$

This is the detection limit.

Detection limits at different bandwidths are plotted in Figure 4-48. When compared to ENI (obtained from Eq. 4-21) that takes into account only the dark current, the difference is especially significant at higher bandwidths. The detection limit can be approximated as ENI when the frequency bandwidth B of the circuit is low (up to about a few kilohertz), but it is dominated by the shot noise component originating from signal light at higher bandwidths. (Refer to Chapter 6, "Photon Counting".)

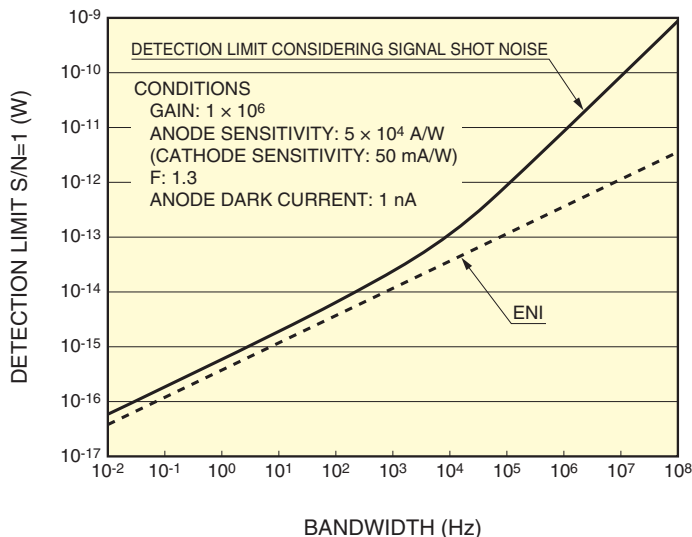


Figure 4-48: Detection limit considering signal shot noise component

To minimize the shot noise to obtain a better signal-to-noise ratio, the following points should be observed:

- (1) Use a photomultiplier tube that has as high a quantum efficiency as possible in the wavelength range to be measured.
- (2) Design the optical system for better light collection efficiency so that the incident light is guided to the photomultiplier tube with minimum loss.
- (3) Use a photomultiplier tube that has an optimum configuration for light collection.
- (4) Narrow the bandwidth as much as possible, as long as no problems occur in the measurement system.

4.3.8 Afterpulsing

When a photomultiplier tube is operated in a pulse detection mode as in scintillation counting or in laser pulse detection, spurious pulses with small amplitudes may be observed. Since these pulses appear after the signal output pulse, they are called afterpulses. Afterpulses often disturb accurate measurement of low level signals following a large amplitude pulse, degrade energy resolution in scintillation counting (See Chapter 7.), and cause errors in pulse counting applications.

Types of afterpulses

There are two types of afterpulses: one is output with a very short delay (several nanoseconds to several tens of nanoseconds) after the signal pulse and the other appears with a longer delay ranging from several hundreds of nanoseconds to several microseconds, each being generated by different mechanisms. In general, the latter pulses appearing with a long delay are commonly referred to as afterpulses.

Most afterpulses with a short delay are caused by elastic scattering electrons on the first dynode. The probability that these electrons are produced can be reduced to about one-tenth in some types of photomultiplier tubes by placing a special electrode near the first dynode. Usually, the time delay of this type of afterpulse is small and hidden by the time constant of the subsequent signal processing circuit, so it does not create significant problems in most cases. However, this should be eliminated in time-correlated photon counting for measuring very short fluorescence lifetime, laser radar (LIDAR), and fluorescence or particle measurement using an auto correlation technique.

In contrast, afterpulses with a longer delay are caused by the positive ions which are generated by the ionization of residual gases in the photomultiplier tube. These positive ions return to the photocathode (ion feedback) and produce many photoelectrons which result in afterpulses. The amplitude of this type of afterpulse depends on the type of ions and the position where they are generated. The time delay with respect to the signal output pulse ranges from several hundred nanoseconds to over a few microseconds, and depends on the supply voltage for the photomultiplier tube. Helium gas is known to produce afterpulses because it easily penetrates through a silica glass bulb, so use caution with operating environments. Afterpulses can be reduced temporarily by aging (see section 4.3.4 in this chapter), but this is not a permanent measure. Afterpulse components resulting from inert gases such as helium will not be reduced by aging.

In actual measurements, the frequency of afterpulses and the amount of charge may sometimes be a problem. The amount of output charge tends to increase when the photomultiplier tube is operated at a higher supply voltage or at a high gain, even though the number of generated ions is the same. In pulse counting applications such as photon counting, the frequency of only afterpulses with an amplitude higher than a certain threshold level will be a problem.

Depending on the electrode structure, another spurious pulse (prepulse) may be observed just before the signal pulse output. But, this pulse is very close to the signal pulse and has a low amplitude, causing almost no problems.

4.3.9 Polarized-light dependence

Photomultiplier tube sensitivity may be affected by polarized light.^{43) 44)} This must be taken into account when measuring polarized light. Also it should be noted that light may be polarized at optical devices such as monochromators. When polarized light obliquely enters the photocathode of a photomultiplier tube, the photocathode reflectance varies depending on the polarization components, which causes apparent sensitivity changes. Figure 4-49 shows the reflectance measured by changing the incident angle of the polarization component R_p parallel to the photocathode surface (P component) and the polarization component R_s perpendicular to the photocathode surface (S component). Because this figure shows the calculated examples with the assumption that the absorption coefficient at the photocathode is zero, the actual data will be slightly more complicated.

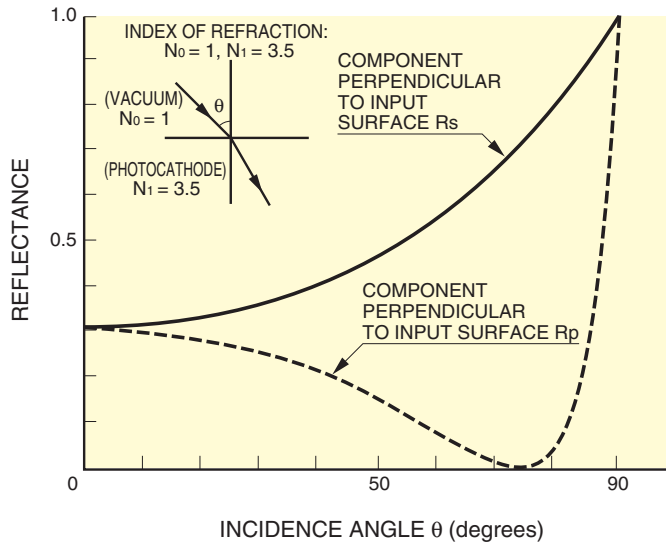


Figure 4-49: Angle dependence of reflectance

If the polarization plane of the incident light has an angle θ with respect to the perpendicular of the photocathode surface, the photocurrent I_θ is given by the following expression:

$$I_\theta = I_s \cos^2 \theta + I_p \sin^2 \theta = \frac{1}{2} (I_p + I_s) \left(1 - \frac{I_p - I_s}{I_p + I_s} \cdot \cos^2 \theta \right) \quad \text{..... (Eq. 4-34)}$$

where

I_s : Photocurrent produced by polarized component perpendicular to the photocathode

I_p : Photocurrent produced by polarized component parallel to the photocathode

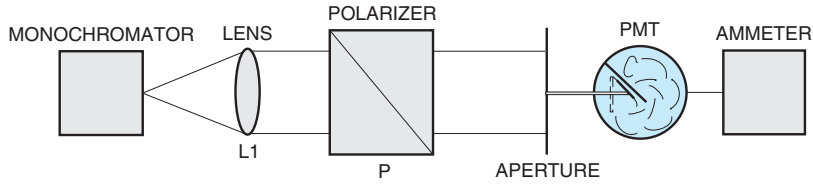
while

$$I_0 = \frac{I_p + I_s}{2}, P = \frac{I_p - I_s}{I_p + I_s} \quad \text{..... (Eq. 4-35)}$$

then substituting Eq. 4-35 into Eq. 4-34 gives the following relationship

$$I_\theta = I_0 (1 - P \cdot \cos^2 \theta) \quad \text{..... (Eq. 4-36)}$$

P is called the polarization factor and indicates the polarized-light dependence of a photomultiplier tube, and is usually measured using the optical system like that shown in Figure 4-50.



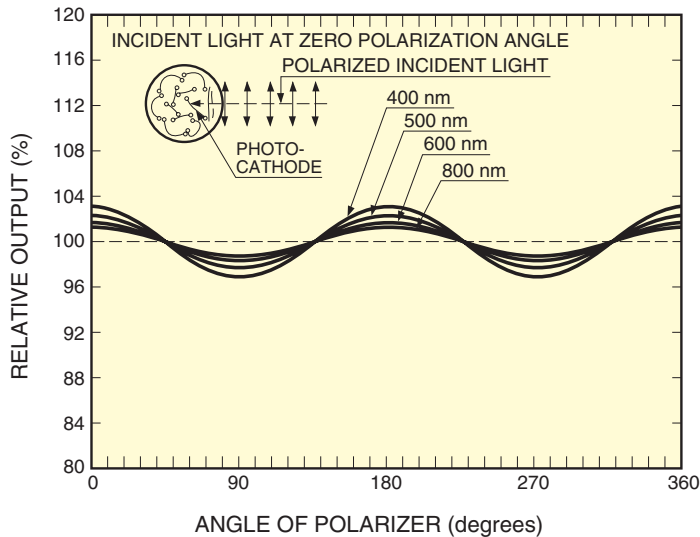
THBV4_0450EA

Figure 4-50: Optical system used for measuring polarized-light dependence

In the above measurement, monochromatic light from the monochromator is collimated by L_1 (collimator lens) and is linearly polarized by the polarizer (P). The polarized light is then focused onto the photomultiplier tube through L_2 (condenser lens). The dependence on the polarized light is measured by recording the photomultiplier tube output in accordance with the rotating angle of the polarizer.

In this case, the polarization component of the light source must be removed. This is done by interposing a diffuser plate such as frosted glass or by compensating for the photomultiplier tube output values measured when the tube is at 0 degree and is then rotated to 90 degrees with respect to the light axis.

Figure 4-51 shows the polarized-light dependence of a photomultiplier tube with a reflection type photocathode, measured with the above method. In principle, this dependence exists when the light obliquely enters the photocathode surface. When the light enters perpendicular to the transmission type photocathode surface, the polarization factor is almost zero.



THBV4_0451EA

Figure 4-51: Typical polarization-light dependence of a photomultiplier tube with reflection type photocathode

In the case of photomultiplier tubes with a reflection-type photocathode, the photocathode is arranged at a certain angle with respect to the light input window, so the sensitivity is affected by the polarization components if the light enters without any countermeasure. Figure 4-51 indicates that the polarization factor becomes smaller as the direction of the incident light nears the perpendicular of the photocathode surface. Photomultiplier tubes with a reflection-type alkali antimonide photocathode usually exhibit a small polarization factor of 3 percent or less. A single crystal photocathode such as gallium arsenide (GaAs) has high reflectance and show a polarization factor of around 20 percent.

In applications where the polarized-light dependence of a photomultiplier tube cannot be ignored, it will prove effective to place a diffuser such as frosted glass or tracing paper in front of the input window of the photomultiplier tube or to use a photomultiplier tube with a frosted window.

References in Chapter 4

- 1) Hamamatsu Photonics Catalog: Photomultiplier Tubes
- 2) T. Hiruma, SAMPE Journal. 24, 35 (1988)
- 3) A. H. Sommer: Photoemissive Materials, Robert E. Krieger Publishing Company (1980)
- 4) T. Hirohata and Y. Mizushima: Japanese Journal of Applied Physics. 29, 8, 1527 (1990)
- 5) T. Hirohata, T. Ihara, M. Miyazaki, T. Suzuki and Y. Mizushima: Japanese Journal of Applied Physics. 28, 11, 2272 (1989)
- 6) W.A. Parkhurst, S. Dallek and B.F. Larrick: J. Electrochem. Soc, 131, 1739 (1984)
- 7) S. Dallek, W.A. Parkhurst and B.F. Larrick: J. Electrochem. Soc, 133, 2451 (1986)
- 8) R.J. Cook: Phys. Rev. A25, 2164; 26,2754 (1982)
- 9) H.J. Kimble and L. Mandel: Phys. Rev. A30, 844 (1984)
- 10) M. Miyao, T. Wada, T. Nitta and M. Hagino: Appl. Surf. Sci. 33/34, 364 (1988)
- 11) Tailing Guo: J. Vac. Sci. Technol. A7, 1563 (1989)
- 12) Huairong Gao: J. Vac. Sci. Technol. A5, 1295 (1987)
- 13) C.A. Sanford and N.C. MacDonald: J. Vac. Sci. Technol. B 6. 2005 (1988)
- 14) C.A. Sanford and N.C. MacDonald: J. Vac. Sci. Technol. B 7. 1903 (1989)
- 15) M. Domke, T. Mandle, C. Laubschat, M. Prietsch and G.Kaindl: Surf. Sci. 189/190, 268 (1987)
- 16) M. Niigaki, T. Hirohata, T. Suzuki, H. Kan and T. Hiruma: Appl. Phys. Lett. 71 (17) 27, Oct. 1997
- 17) K. Nakamura, H. Kyushima: Japanese Journal of Applied Physics, 67, 5, (1998)
- 18) D. Rodway: Surf. Sci. 147, 103 (1984)
- 19) "Handbook of Optics": McGraw-Hill (1978)
- 20) James A. R. Samson: "Techniques of Vacuum Ultraviolet Spectroscopy" John Wiley & Sons, Inc. (1967)
- 21) C.R. Bamford: Phys. Chem. Glasses, 3, 189 (1962)
- 22) Corning Glass Works Catalog
- 23) IEEE ET-61A 1969.5.8
- 24) IEEE STD 398-1972
- 25) IEC PUBLICATION 306-4, 1971
- 26) H. Kume, K. Koyama, K. Nakatsugawa, S. Suzuki and D. Fatlowitz: Appl. Opt, 27, 1170 (1988)
- 27) T. Hayashi: "PHOTOMULTIPLIER TUBES FOR USE IN HIGH ENERGY PHYSICS"
Hamamatsu Photonics Technical Publication (APPLICATION RES-0791-02)
- 28) Hamamatsu Photonics Technical Publication "USE OF PHOTOMULTIPLIER TUBES IN SCINTILLATION APPLICATIONS" (RES-0790)
- 29) T.H. Chiba and L. Mmandel: J. Opt. Soc. Am. B,5, 1305 (1988)
- 30) D.P. Jones: Appl. Opt. 15,14 (1976)
- 31) D.E. Persyk: IEEE Trans. Nucl. Sci. 38, 128 (1991)
- 32) Mikio Yamashita: Rev. Sci. Instrum., 49, 9 (1978)
- 33) "Time-Related Single-Photon Counting": Academic Press, Inc (1985)
- 34) G.F. Knoll: "RADIATION DETECTION and MEASUREMENT", John Wiley & Sons, Inc. (1979)
- 35) C.E. Miller, et al.: IEEE Trans. Nucl. Sci. NS-3, 91 (1956)

-
- 36) A.T. Young: Appl. Opt., 8, 12, (1969)
 - 37) R.L. Bell: "Negative Electron Affinity Devices", Clarendon Press. Oxford (1973)
 - 38) G.A. Morton et al.: IEEE Trans. Nucl. Sci. NS-14 No.1, 443 (1967)
 - 39) R. Staubert et al.: Nucl. Instrum. & Methods 84, 297 (1970)
 - 40) S.J. Hall et al.: Nucl. Instrum. & Methods 112, 545 (1973)
 - 41) Illes P. Csorba "Image Tubes" Howard W, Sams & Co (1985)
 - 42) F. Robber: Appl. Opt., 10, 4 (1971)
 - 43) S.A. Hoenig and A. Cutler: Appl. Opt. 5,6, 1091 (1966)
 - 44) H. Hora: Phys. Stat. Soli Vol (a), 159 (1971)

MEMO

CHAPTER 5

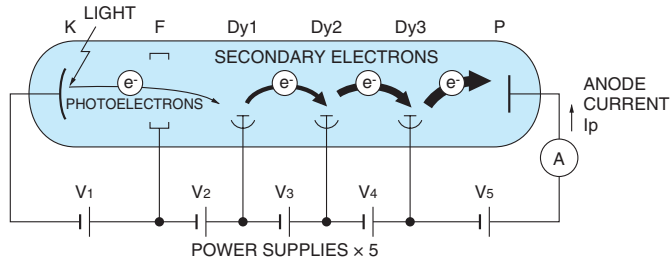
VOLTAGE-DIVIDER CIRCUITS AND ACCESSORIES FOR PHOTOMULTIPLIER TUBES

This chapter describes how to use the basic circuits and accessories necessary to operate a photomultiplier tube correctly.¹⁾

5.1 Voltage-Divider Circuits

5.1.1 Basic operation of voltage-divider circuits

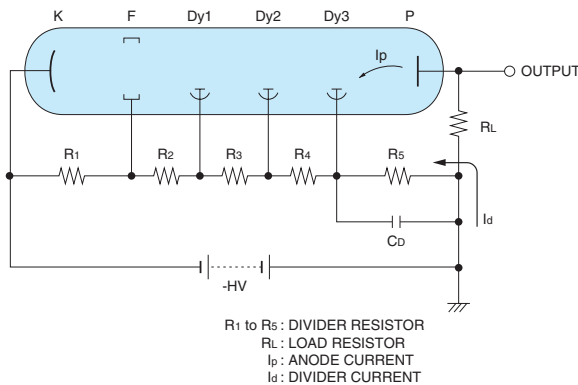
To operate a photomultiplier tube, a high voltage of 500 to 3000 volts is usually supplied between the cathode (K) and the anode or plate (P), with a proper voltage gradient set up along the photoelectron focusing electrode (F) or grid (G), secondary electron multiplier consisting of about 10 stages of electrodes or dynodes (Dy) and depending on the photomultiplier tube type, an accelerating electrode or accelerator (Acc). Figure 5-1 shows a schematic representation of photomultiplier tube operation using independent multiple power supplies but is not actually a practical method. Instead, a voltage-divider circuit is commonly used that divides the output of a single high voltage power supply by using resistors.



THBV4_0501EA

Figure 5-1: Schematic representation of photomultiplier tube operation

In practice, as shown in Figure 5-2, the interstage voltage for each electrode is supplied by using voltage-divider resistors (100 kilohms to 1 megohms) connected between the cathode and the anode. In some cases, transistors or Zener diodes are used with voltage-divider resistors. These circuits are known as voltage-divider circuits. Voltage-divider circuits for typical photomultiplier tubes are designed to have a voltage division ratio suitable for each type of photomultiplier tubes.



THBV4_0502EA

Figure 5-2: Voltage-divider circuit example (anode grounded)

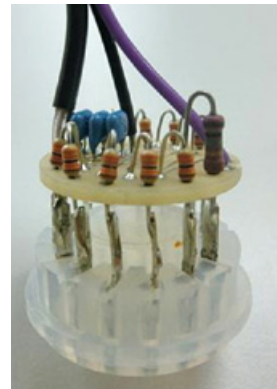


Figure 5-3: Voltage-divider circuit example for photomultiplier tube

The current I_d flowing through the voltage-divider circuit shown in Figures 5-2 is called the voltage-divider current, and is closely related to the output linearity described later. The divider current I_d is approximately the supply voltage V ($= -HV$) divided by the sum of the resistor values as given by the following equation (Eq. 5-1).

$$I_d = \frac{V}{(R_1 + R_2 + R_3 + R_4 + R_5)} \quad \text{..... (Eq. 5-1)}$$

5.1.2 Anode grounding and cathode grounding

As shown in Figure 5-2, the general technique used for voltage-divider circuits is to ground the anode and apply a large negative voltage ($-HV$) to the cathode. This scheme eliminates the potential voltage difference between the photomultiplier tube anode and the external circuit, making it easier to connect to an ammeter or current-to-voltage conversion amplifier (operational amplifier). This scheme provides a signal output in both DC and pulse modes and so is used in many applications.

In this anode grounding scheme however, if a grounded metal holder, housing or magnetic shield case is brought near the glass bulb of the photomultiplier tube or makes contact with the glass bulb, electrons in the photomultiplier tube are attracted toward the ground potential near the bulb and strike the inner wall of the bulb. This may produce a glass scintillation resulting in a significant increase in noise. Also, in the case of head-on photomultiplier tubes, if the bulb or faceplate near the cathode is grounded, the slight conductivity of the glass material causes a small current to flow between the cathode and the ground. This may cause electrical damage to the photocathode and possibly lead to drastic deterioration. For this reason, extreme care must be taken when designing a housing for photomultiplier tubes or using an electromagnetic shield case. It is also very important to ensure that the materials have sufficiently good insulation properties when wrapping the bulb of a photomultiplier tube with foam rubber or similar shock-absorbing materials before mounting the tube within its electromagnetic shield case at ground potential.

The above problems with the anode grounding scheme can be solved by “HA treatment” in which the bulb surface is coated with black conductive paint and connected to a point at cathode potential, and the conductive coating further covered with an insulating material for safety. However, in photon counting and scintillation counting where a grounded scintillator is usually coupled directly to the faceplate of a photomultiplier tube, the cathode is grounded with a high positive voltage applied to the anode as shown in Figure 5-4. This grounded cathode scheme uses a coupling capacitor (C_c) to separate the positive high voltage ($+HV$) applied to the anode from the signal and cannot extract a DC signal and so is only used for pulse output. In scintillation counting using this voltage-divider circuit, a problem concerning baseline shift may occur if the count rate increases to a very high level, or noise may be generated if a leakage current is present in the coupling capacitor, so care should be taken regarding these points.

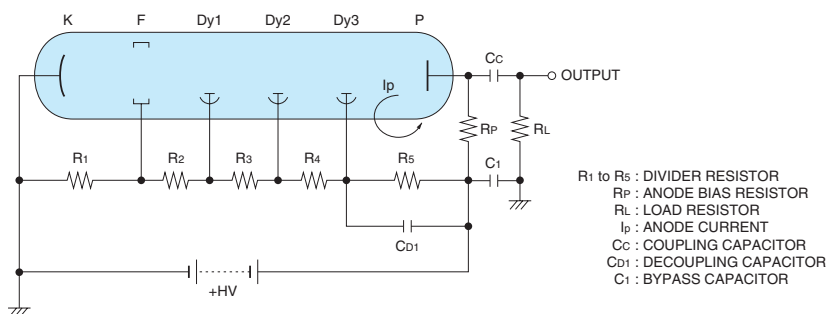


Figure 5-4: Voltage-divider circuit with grounded cathode

In Figure 5-4 (voltage-divider circuit with grounded cathode), R_p is the resistor that applies a potential for collecting the secondary electrons emitted from Dy3 to the anode, and R_L is the load resistor. The actual load resistance seen from the anode is the combined value of R_p and R_L .

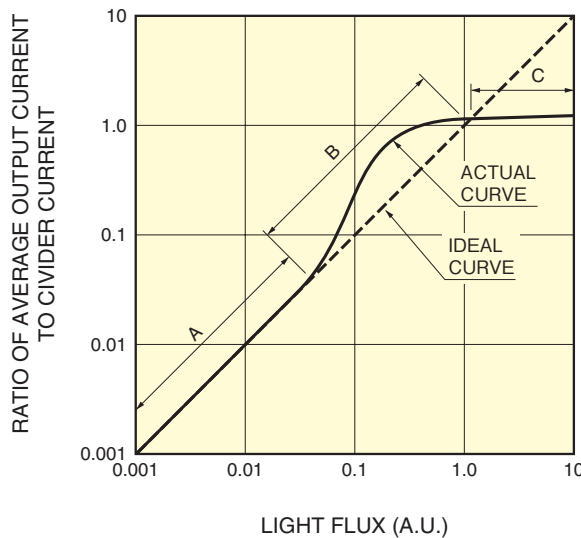
$$\text{Actual load resistance} = \frac{R_p \times R_L}{(R_p + R_L)}$$

(The signal frequency, coupling capacitor and the impedance in the circuit such as wiring inductance should also be considered for even greater accuracy, but these can be ignored to simplify the calculation.)

5.1.3 Voltage-divider current and output linearity

In the anode grounding and cathode grounding schemes for photomultiplier tubes and in both DC and pulse output modes, the proportional relationship (linearity) between the incident light level and the output begins to deviate from ideal linearity at a certain level of incident light.

In Figure 5-5, the output maintains a good linearity in region A, but becomes larger than the ideal level in region B which is called over-linearity, and finally becomes saturated and smaller than the ideal level in region C. In precision photometry, the maximum output current is limited within region A, while the lower limit is determined by the dark current and noise of the photomultiplier, as well as by the leak current and noise of the external circuit.



THBV4_0505EA

Figure 5-5: Relation between linearity and voltage-divider current of a photomultiplier tube

The following describes the basic operation of a photomultiplier tube in DC output mode. To make it easier to understand, we use a simplified photomultiplier tube model having 3 dynodes and 4 voltage-divider resistors R_n of equivalent resistance.

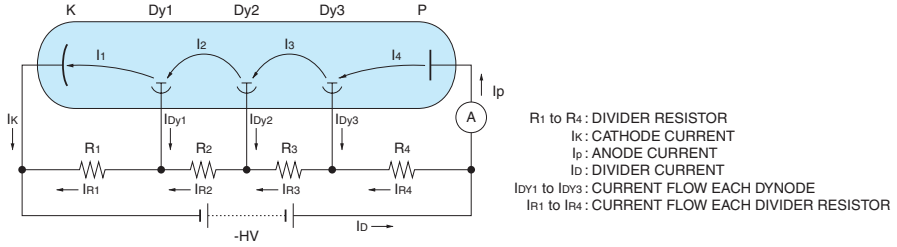


Figure 5-6: Current flow in a photomultiplier tube and voltage-divider circuit

First, let's discuss the case where no light is incident on the photomultiplier tube.

When a high voltage is supplied to the photomultiplier tube with no incident light, the photomultiplier tube starts operating but outputs no signal except for negligible dark current from the photomultiplier tube. In this condition, the only current flowing through the voltage-divider circuit of Figure 5-6 is illustrated by the thick lines in Figure 5-7, along with the current and voltage supplied to each part.

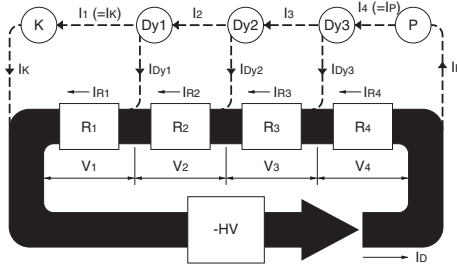


Figure 5-7: Operation with no incident light

The current flowing between each electrode in the photomultiplier tube is as follows:

$$I_1 = I_2 = I_3 = I_4 (= 0 \text{ A})$$

The current flowing in each electrode of the photomultiplier tube is as follows:

$$I_K = I_{Dy1} = I_{Dy2} = I_{Dy3} = I_P (= 0 \text{ A})$$

The current flowing in each part of the voltage-divider circuit is as follows:

$$I_{R1} = I_{R2} = I_{R3} = I_{R4} = I_D = (HV / \sum_{n=1}^4 R_n)$$

The voltage applied across each part of the voltage-divider circuit is as follows:

$$V_1 = V_2 = V_3 = V_4 = I_D \cdot R_n (= HV/4)$$

Next, let's discuss the case where light is incident on the photomultiplier tube.

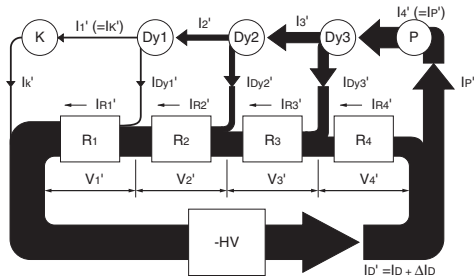


Figure 5-8: Operation with incident light

When light enters the photomultiplier tube that is operated as in Figure 5-7, the resulting photocurrent flows and this operation can be schematically illustrated as in Figure 5-8. Here, all symbols used to represent the currents and voltages have a prime (') to tell them apart from those during operation with no signal. For example, the voltage-divider circuit current, which was I_D during operation with no signal, is expressed as I_D' during operation with incident light. This I_D' is the sum of I_D and ΔI_D that is equal to the average inter-electrode current flowing in the photomultiplier tube. However, because ΔI_D is very low compared to I_D , the voltage-divider current may simply be considered to branch into the photomultiplier tube current when operated in a good linearity range (region A in Figure 5-5). The current IR_n' flowing in each divider resistor R_n placed between each electrode becomes as follows:

$$IR_n' = I_D' - I_n'$$

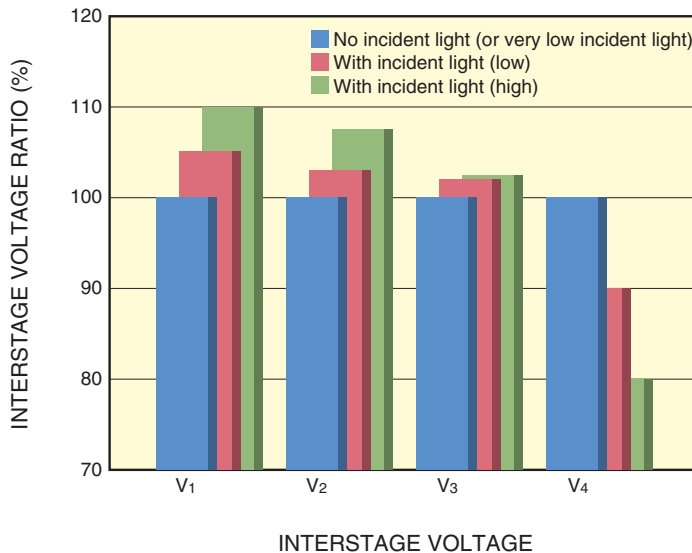
Where I_n' is the inter-electrode current flowing in the photomultiplier tube and has the following relation:

$$I_1' < I_2' < I_3' < I_4'$$

Thus, the inter-electrode voltage V_n' ($= IR_n' \cdot R_n$) becomes smaller from the first stage to the last stage, as follows:

$$V_1' > V_2' > V_3' > V_4'$$

A graph of these changes in inter-electrode voltages (also called interstage voltage) is shown in Figure 5-9. The interstage voltage V_4' during operation with incident light will drop compared to V_4 during operation with no incident light. This voltage drop in V_4' is redistributed to the other electrodes, resulting in an increase in V_1' , V_2' and V_3' which are higher than those (V_1 , V_2 and V_3) with no incident light. Because V_4' is required only for collecting the secondary electrons released from the last dynode to the anode, it has little effect on the anode current even there is a drop of 20 or 30 volts. On the other hand, the increases in V_1' , V_2' and V_3' directly raise the secondary emission ratios (δ_1 , δ_2 and δ_3) at Dy1, Dy2 and Dy3, and so boost the overall gain μ ($=\delta_1 \cdot \delta_2 \cdot \delta_3$). This is the cause of over-linearity that occurs in region B of Figure 5-5. As the incident light further increases to a level where V_4' approaches 0 volts, the secondary electron collection efficiency at the anode drops significantly, resulting in saturation in region C.



(The inter-stage voltage V_1 with no incident light is viewed as 100 %.)

THBV4_0509EA

Figure 5-9: Changes in interstage voltage as a function of light input

(1) Voltage-divider circuit for maintaining the linearity in DC output mode

To maintain the linearity of the photomultiplier tube operating in DC output mode, it is essential to minimize fluctuations in the interstage voltage that may occur when the photocurrent flows in the photomultiplier tube. While there are differences depending on the type of photomultiplier tube and voltage-divider circuit, the maximum practical value of DC output is usually 1/20th to 1/50th of the voltage-divider current. If a linearity better than ± 1 percent is required, the maximum output must be held to less than 1/100th of the voltage-divider current.

There are also several techniques other than the above method for maintaining linearity.

① Increasing the voltage-divider current

Figure 5-10 shows the linearity of a 28-millimeter diameter side-on photomultiplier tube, by plotting the relation between the linearity error and the anode current to voltage-divider current ratio. For example, it can be seen that if an output with a linearity error of 1 percent is required, the upper limit of the anode current must be held to about 1.4 percent of the voltage-divider current. This relation is plotted by calculation, so the actual characteristics will vary depending on individual differences such as in the supply voltage and dynode gain, even among the photomultiplier tubes of the same type. To ensure high photometric accuracy, the voltage-divider current should be maintained at least at twice the values obtained from this figure.

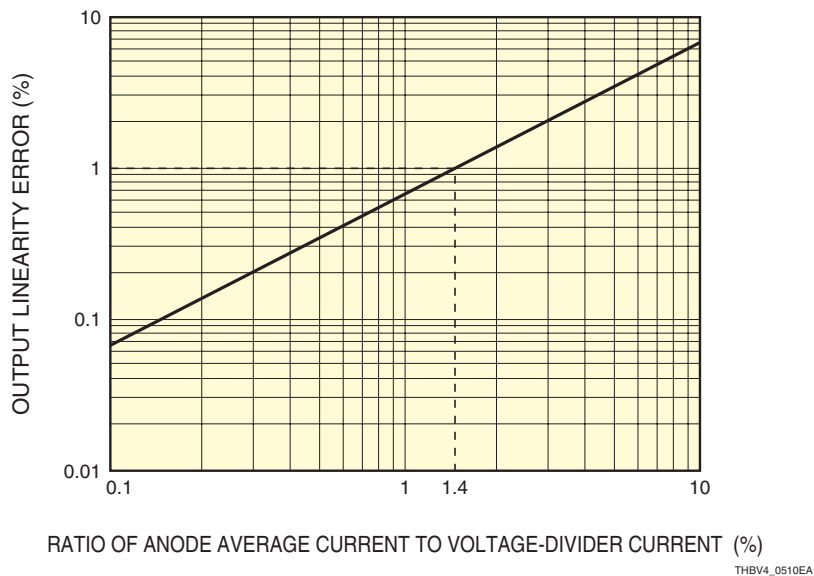


Figure 5-10: Linearity error vs. anode average current to voltage-divider current ratio

A good linearity can be obtained simply by increasing the voltage-divider current. However, this also increases the power consumption and leads to insufficient output current from the high voltage power supply. An increase of the power consumption is also accompanied by the heat generated in the voltage-divider circuit. This heat, if conducted to the photomultiplier tube, may increase the dark current or lower the output stability so caution is needed.

② Using an active voltage-divider circuit

An active voltage-divider circuit uses transistors in place of a few divider resistors near the last stage or anode. By utilizing the transistor characteristics, this circuit ensures a good linearity up to about 60 to 70 percent of the voltage-divider current, because the inter-electrode voltage is not affected by the inter-electrode current in the photomultiplier tube. A typical active voltage-divider circuit is shown in Figure 5-11.

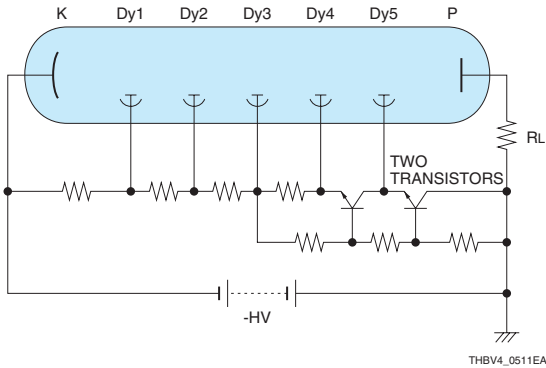


Figure 5-11: Active voltage-divider circuit

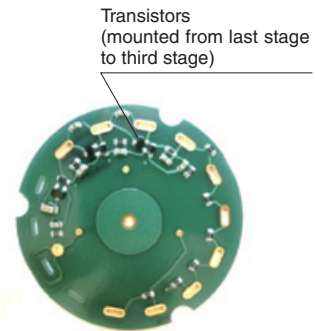


Figure 5-12: Voltage-divider circuit example for photomultiplier tube

In Figure 5-11, the emitter of each transistor is connected to a dynode. A characteristic of the transistor emitter is that its voltage potential drops slightly lower (approximately 0.6 volts) than the base, so the dynode potential connected to the emitter is determined by the base voltage. This means that the potential of each dynode connected to the transistor can be determined by setting the base potential of each transistor by means of the resistor provided on the base side. In this case, even if the transistor's collector-emitter current changes, or in other words, the current flowing in the photomultiplier tube changes, the transistor's base potential or dynode potential is not affected by that change but is kept stable. This helps maintain the linearity of the photomultiplier tube.

To fabricate an active voltage-divider circuit for actual applications, an effective technique is to provide transistors in the last few stages (2 to 4 stages) where there are large changes in the photomultiplier tube current.

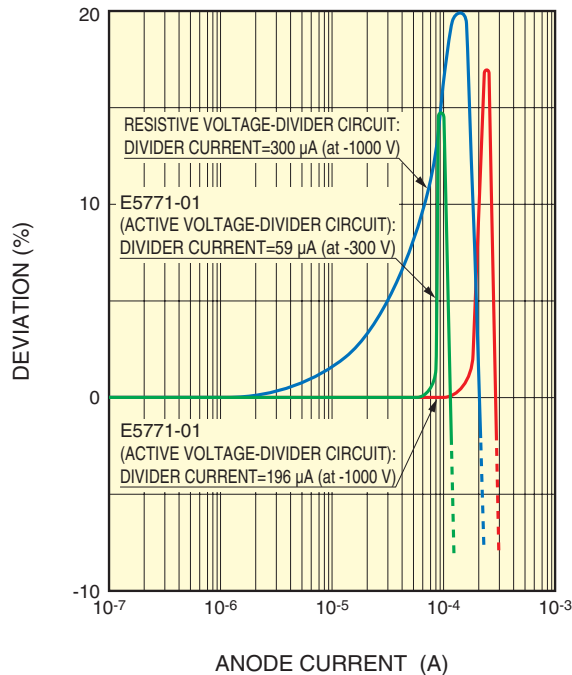
Note the following points when selecting the transistors for this circuit.

- Select a transistor having high current amplification and sufficient derating for the rated collector-emitter voltage relative to the interstage voltage in the photomultiplier tube.
- Select a transistor having a high DC current amplification factor, h_{fe} , and capable of sufficient current flow to the collector.
- Select a transistor with good frequency characteristics.
- Determine the number of stages in which to use transistors by taking account of the operating conditions of the photomultiplier tube.
- Use a diode as needed for reverse bias protection between the base and emitter of the transistor.

Figure 5-13 shows typical linearity data for active voltage-divider circuits. Compared to an ordinary resistive voltage-divider circuit, the active voltage-divider circuits exhibit efficient operation with higher anode output linearity when the same electrical power is supplied or in other words when the same voltage-divider current flows.

Note, however, that when the anode output current reaches the voltage-divider current, the voltage-divider circuit becomes saturated, causing a sharp change in output (jump in gain) which is larger than that in an ordinary resistive voltage-divider circuit. Therefore be aware that an increase in the anode output current may cause this change to appear.

Hamamatsu Photonics provides active voltage-divider circuit products. When used with a general photomultiplier tube operated at the rated voltage, these ensure a stable output up to 100 microamperes which is the maximum rating of the average anode current.

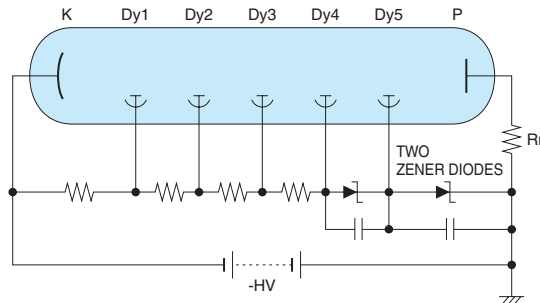


THBV4_0513EA

Figure 5-13: Linearity of active voltage-divider circuit

③ Using Zener diodes

Using Zener diodes (constant voltage diodes) in place of the few divider resistors near the anode helps stabilize the inter-electrode voltage and improves the linearity. Note, however, that if there is a large change in the supply voltage this may cause an imbalance in the voltage distribution ratio relative to other inter-electrode voltages, limiting the supply voltage range that can actually be adjusted. Moreover, when the supply voltage is reduced or the current flowing through the Zener diodes becomes insufficient due to an increase in the anode current, noise may be generated from the Zener diodes. To avoid this, keep the voltage-divider current sufficiently high or connect noise-absorbing capacitors in parallel with the Zener diodes. Take other measures as needed to reduce the bandwidth of the subsequent signal processing circuit to a minimum necessary level. Figure 5-14 shows a voltage-divider circuit using Zener diodes.



THBV4_0514EA

Figure 5-14: Voltage-divider circuit using Zener diodes

④Using a Cockcroft-Walton circuit

Good linearity can also be obtained by using a Cockcroft-Walton circuit (also called Cockcroft-Walton voltage multiplier circuit or simply a CW circuit) like that shown in Figure 5-15.

The Cockcroft-Walton circuit uses an array of diodes connected in series, and capacitors are stacked and connected in series as illustrated along each side of the alternate connection points. If the reference voltage V is applied, this circuit provides voltage potentials of $V, 2V, 3V$ and so on at each connection point, serving as a voltage boosting circuit (voltage multiplier circuit). In addition to functioning just like a resistive voltage-divider circuit, this circuit ensures very low power consumption making it ideal for battery operation because the components used for this circuit have less waste heat than resistors. Since a high voltage is generated by supplying a low voltage to the oscillator circuit, there is no need to prepare an additional high voltage power supply so using this circuit is effective in reducing the photomultiplier tube module size.

A point to be noted is that this circuit boosts the voltage by an integer multiple, and so it is difficult to provide a voltage distribution ratio (voltage divider ratio) which is not an integer ratio. Also, since this circuit contains an oscillator circuit, care should be taken so that the oscillator circuit noise is induced to the anode output.

Applications of the Cockcroft-Walton circuit are described in detail in section 8.2 of Chapter 8.

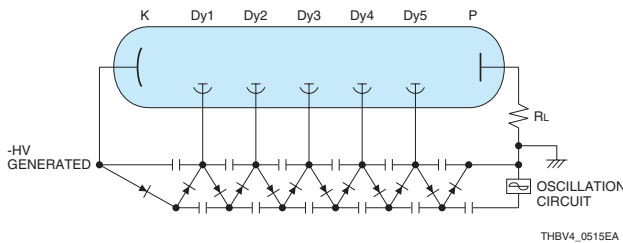


Figure 5-15: Cockcroft-Walton circuit

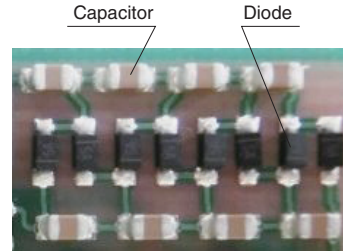


Figure 5-16: Example of components mounted on a CW circuit

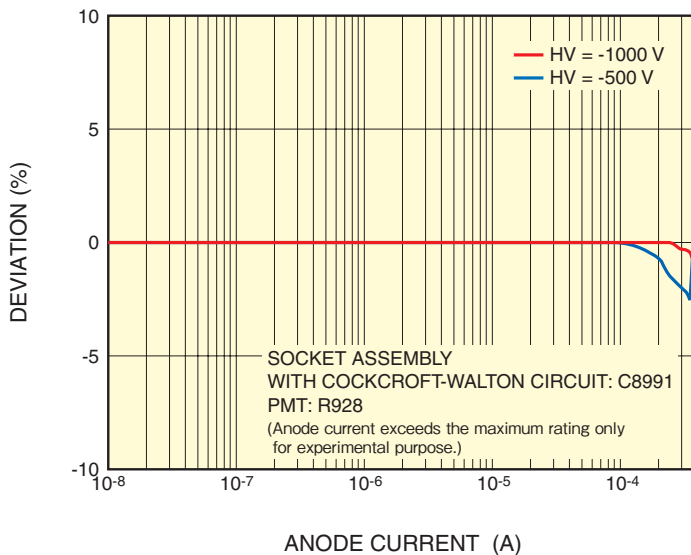


Figure 5-17: Linearity obtained with a Cockcroft-Walton circuit

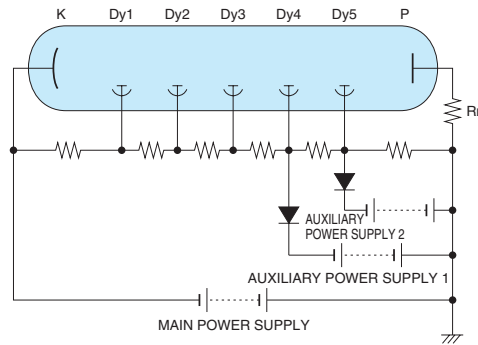
THBV4_0517EA

⑤ Using multiple high-voltage power supplies

As shown in Figure 5-18, this technique uses external power supplies (auxiliary high-voltage power supplies) to directly supply a voltage to the few dynodes near the anode. This is also called the booster method and is mainly used for high pulse and high count rate applications such as in high energy physics experiments.

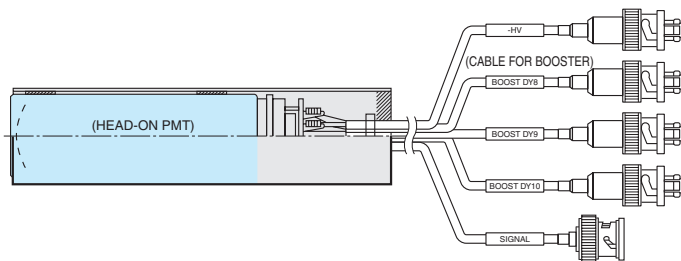
Since this circuit directly supplies voltage to the dynodes that require a large current in the photomultiplier tube, it maintains the desired voltage distribution ratio without causing changes in the interstage voltage that occur in ordinary resistive voltage-divider circuits even when the anode output current increased. In this way, sufficient current is constantly supplied to the dynodes where a power supply is directly connected, and so allows obtaining a good linearity.

On the other hand, since multiple power supplies are used, when changing the overall high-voltage supply to adjust the gain of the photomultiplier tube, it is necessary to adjust all power supplies, not only the main high voltage power supply but also auxiliary high-voltage power supplies for boosting the voltage. Care should also be taken to prevent unwanted current from flowing into the auxiliary high-voltage power supplies for boosting voltage. Figure 5-19 shows an assembly example where auxiliary high-voltage power supplies are connectable to the last 3 stages of dynode.



THBV4_0518EA

Figure 5-18: Voltage-divider circuit using multiple high-voltage power supplies (booster method)



THBV4_0519EA

Figure 5-19: Photomultiplier tube assembly with a booster method voltage-divider circuit

⑥ Using a high-linearity active voltage-divider circuit

A high-linearity active voltage-divider circuit is a high-performance version of the active voltage-divider circuit described earlier in ②, which uses transistors. This voltage-divider circuit uses semiconductor devices to stabilize the potential of all dynodes so that the output current of the photomultiplier tube will not be limited by the voltage-divider current. This allows the photomultiplier tube to exhibit its fullest performance. Besides excellent linearity characteristics, this voltage-divider circuit offers low power consumption. Even when the incident light level and resulting anode current increase, there is almost no fluctuation in the potential of each dynode and none of the overlinearity which occurs in an ordinary resistive voltage-divider circuits (see Figure 5-21). Furthermore, the constant current flow in the voltage-divider circuit reaches nearly zero and only a current corresponding to the anode output flows in the voltage-divider circuit. This minimizes generation of heat in the voltage-divider circuit, eliminating a major cause of higher dark current.

Since the voltage-divider current fluctuates according to the anode output, the high voltage power supply used with this voltage-divider circuit must have high stability. Hamamatsu Photonics offers the E12788 socket assembly that uses a high-linearity active voltage-divider circuit and also provides the C12789 as the recommended high voltage power supply.

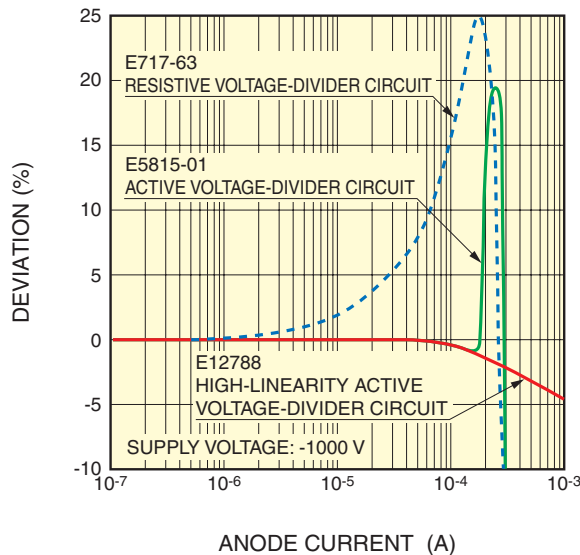


High-linearity active D type socket assembly
E12788



High voltage power supply for high-linearity
active voltage-divider circuit C12789

Figure 5-20: E12788 socket assembly using a high-linearity active voltage-divider circuit



THBV4_0521EA

Figure 5-21: Linearity characteristics with the high-linearity active voltage-divider circuit

(2) Pulse output mode linearity and its countermeasures

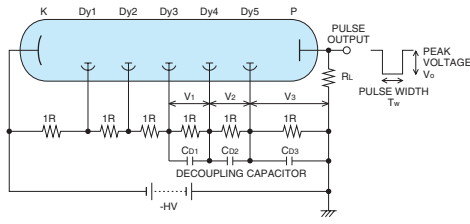
In applications such as scintillation counting where the light input to the photomultiplier tube is in the form of pulses, individual pulses may range from a few to several dozen milliamperes even though the average anode current is small at low count rates. In this pulsed output mode, the peak current in extreme cases may reach a level hundreds of times higher than the voltage-divider current. In such cases, it is not possible for the voltage-divider circuit to supply sufficient inter-electrode current to dynodes near the anode in the photomultiplier tube and this state leads to degradation in the output linearity.

When measuring such large pulse signals, there are countermeasures that will help maintain the output linearity as described next.

Using decoupling capacitors for improving the pulse linearity

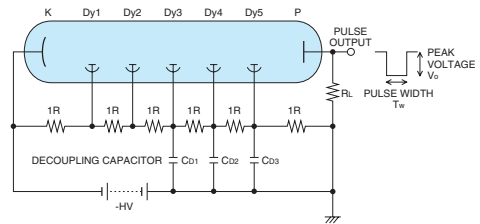
In pulse signal measurement, applying the previously described booster method can supply sufficient current to the dynodes and maintain the pulse signal output linearity. However, it is not easy to use in view of the size and cost of the circuit. In most cases, decoupling capacitors are added and connected to the few dynodes near the anode in order to supply the inter-electrode current to the photomultiplier tube during shaping of a signal pulse and to curb the voltage drop between the dynodes near the anode and also between the last dynode and the anode.

There are two methods for connecting the decoupling capacitors: the serial method (Figure 5-22) and the parallel method (Figure 5-23). The serial method is more widely used because of the withstand voltage (or breakdown voltage) of the capacitors.



THBV4_0522EA

Figure 5-22: Voltage-divider circuit with decoupling capacitors added in series



THBV4_0523EA

Figure 5-23: Voltage-divider circuit with decoupling capacitors added in parallel

The following explains the procedure for calculating the capacitor values, using the circuit shown in Figure 5-22 as an example.

First of all, if the peak voltage of the required pulse output is V_0 , the pulse width is T_w , and the load resistance is R_L , then the output pulse charge Q_0 per pulse is expressed by Eq. 5-22) as follows:

$$Q_0 = T_w \frac{V_0}{R_L} \dots\dots\dots (Eq. 5-2)$$

Here, let's find the capacitance values (F or farads) of the decoupling capacitors C_{D1} to C_{D3} , using Q_0 . If the charge stored in capacitor C_{D3} is Q_3 , then to achieve a good output linearity of better than ± 3 percent, the following relation should generally be established:

$$Q_3 \geq 100 Q_0 \dots\dots\dots (Eq. 5-3)$$

If the voltage across C_{D3} is V_3 , then C_{D3} is given by Eq. 5-4 from the common relation of $Q=CV$.

$$C_{D3} \geq 100 \frac{Q_0}{V_3} \dots\dots\dots (Eq. 5-4)$$

Next, let's calculate the capacitance values of C_{D1} and C_{D2} . Normally, the secondary emission ratio δ (delta) per stage of a photomultiplier tube is 3 to 5 at the interstage voltage of 100 volts. However, assuming that δ (delta) between each dynode is 2 in consideration of cases where the interstage voltage drops to about 70 or 80 volts, the charges Q_2 and Q_1 stored respectively in C_{D2} and C_{D1} are calculated as follows:

$$Q_2 = \frac{Q_3}{2} \quad Q_1 = \frac{Q_2}{2} = \frac{Q_3}{4}$$

Then, the capacitance values of C_{D2} and C_{D1} can be obtained in the same way as in C_{D3} .

$$C_{D2} \geq 50 \frac{Q_0}{V_2} \quad C_{D1} \geq 25 \frac{Q_0}{V_1}$$

(V_2 and V_1 are the voltage across C_{D2} and C_{D1} , respectively.)

If decoupling capacitors need to be placed in the dynode stages earlier than Dy3 in order to derive an even larger current output, the same calculation can also be used.

Here, as an example, with an output pulse peak voltage $V_0=50$ mV, pulse width $T_w=1$ μ s, load resistance $R_L=50$ Ω , and interstage voltages $V_3=V_2=V_1=100$ V, each capacitor value can be calculated in the following steps:

First, the amount of charge per output pulse is obtained as follows:

$$Q_0 \geq \frac{50 \text{ mV}}{50 \Omega} \times 1 \mu\text{s} = 1 \text{ nC}$$

The capacitance values required of the decoupling capacitors C_{D3} , C_{D2} and C_{D1} are respectively calculated as follows:

$$C_{D3} \geq 100 \frac{1 \text{ nC}}{100 \text{ V}} = 1 \text{ nF}$$

$$C_{D2} \geq 50 \frac{1 \text{ nC}}{100 \text{ V}} = 0.5 \text{ nF}$$

$$C_{D1} \geq 25 \frac{1 \text{ nC}}{100 \text{ V}} = 0.25 \text{ nF}$$

The above capacitance values are minimum values required for proper operation. It is therefore suggested that the voltage-divider circuit be designed with a safety margin in the capacitance value that is about 10 times larger than the calculated values. If the output current increases further, additional decoupling capacitors should be connected as necessary to the earlier stages, as well as increasing the capacitance values of C_{D1} to C_{D3} .

Even with the above countermeasures provided, when the duty ratio increases at high count rates and the average anode current becomes too high to ignore, the voltage-divider current, as in the case of DC output mode, should be maintained at a level at least several dozen times higher than the average anode current. To cope with this current, use of an active voltage-divider circuit or booster method will prove effective in maintaining a good pulse linearity even at a high duty ratio.

Figure 5-24 shows an example of a photomultiplier tube assembly designed to ensure high pulse linearity. This assembly includes ceramic capacitors connected to the middle to last stages of the voltage-divider circuit relative to ground as shown in Figure 5-23.

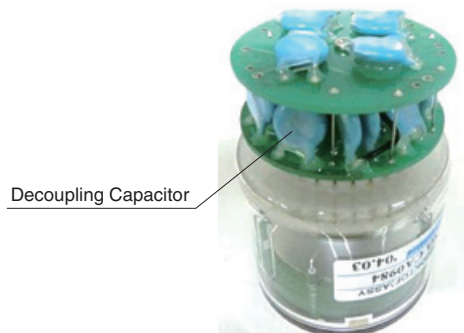


Figure 5-24: Photomultiplier tube assembly with pulse linearity countermeasures taken

Please note that when output saturation occurs due to space charge effects from the dynodes in the photomultiplier tube, which are described in Chapter 4, a deterioration in pulse linearity is unavoidable even if decoupling capacitors are added.

The countermeasures for this are described in the next section 5.1.4, “Voltage distribution in voltage-divider circuits.”

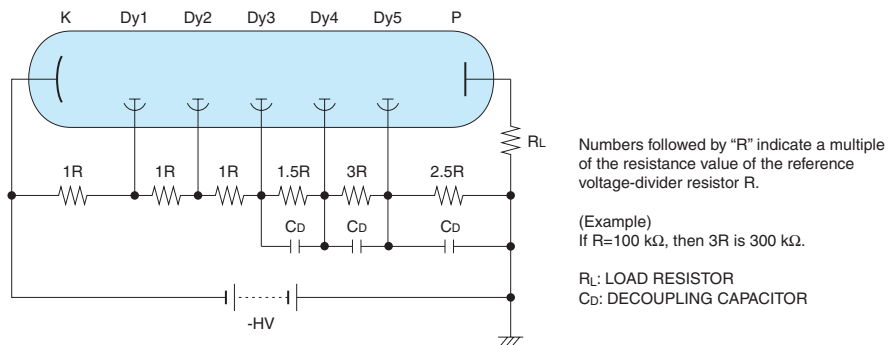
5.1.4 Voltage distribution in voltage-divider circuits

(1) Voltage distribution in the anode and latter stages

Even under conditions where adequate countermeasures for pulse output linearity have been taken by using decoupling capacitors, output saturation will occur at a certain level as the incident pulse light level is increased while the interstage voltage in the electron multiplier section is kept fixed. This is due to an increase in electron density between the electrodes, causing space charge effects which disturb the electron current. This saturated current level varies, depending on the electrode structures of the anode and last few dynodes of the photomultiplier tube and also on the voltage applied between each electrode. As a corrective action to overcome space charge effects, the voltage applied to the last few dynodes (2 to 4 stages) near the anode, where the electron density becomes high, should be set higher than the standard voltage distribution so that the voltage gradient between those electrodes is enhanced to handle a larger amount of charge. For this purpose, a so-called “tapered voltage-divider circuit” is commonly employed, in which the interstage voltage is increased from the cathode side toward the latter dynode stages.

Although the tapered voltage-divider circuit allows higher pulse current output, be aware of the withstand voltage (breakdown voltage) between electrodes, as well as a decrease in the gain and a change in the collection efficiency, which may occur due to the changed voltage dividing ratio.

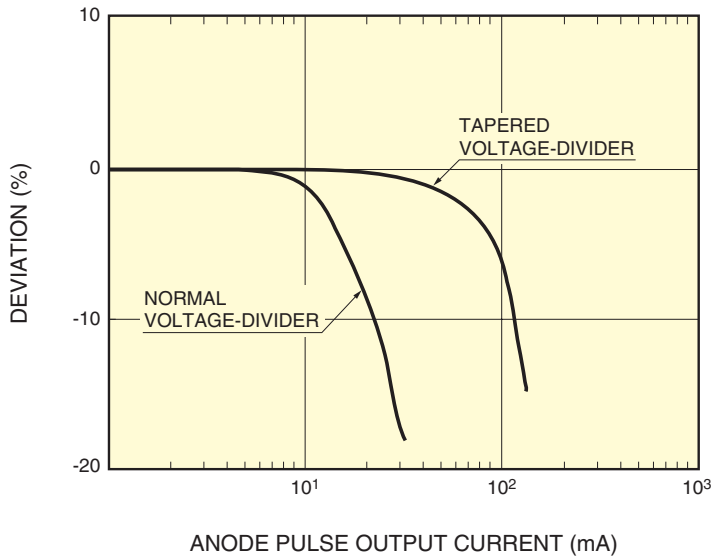
As an example, Figure 5-25 shows a tapered voltage-divider circuit for a 5-stage photomultiplier tube. The voltage dividing ratio for this circuit is designed so that the interstage voltages at the latter dynode stages are larger than those at the earlier dynode stages, but the Dy5-to-P (anode) voltage is set slightly lower than the Dy4-to-Dy5 voltage. This is because the electrode distance between the last dynode and the anode, where the electrons are finally collected, is usually short so that a voltage gradient sufficient for the anode to collect the released secondary electrons can be obtained at a relatively low voltage.



THBV4_0525EA

Figure 5-25: Pulse output linearity countermeasures using decoupling capacitors and tapered voltage-divider circuit

The voltage dividing ratio that provides optimum pulse linearity depends on the type of photomultiplier tube. In high energy physics applications, a higher pulse output is usually required. Our catalog “Photomultiplier Tubes and Assemblies for Scintillation Counting and High Energy Physics” lists the recommended voltage dividing ratios (for tapered voltage-dividers) and their maximum output current values. Using a tapered voltage-divider based on these improves pulse linearity 5 to 10 times more than that obtained with normal voltage-divider circuits (equally divided ratio). Figure 5-26 shows a comparison of pulse linearity characteristics measured with a tapered voltage-divider circuit versus that of a normal voltage-divider circuit. The figure clearly shows that pulse linearity is improved about 10 times by using the tapered voltage-divider circuit. Note that when a tapered voltage-divider circuit is used, the gain is reduced to about 1/3rd to 1/5th compared to a normal voltage-divider circuit. Adjustment to increase the supply voltage for the photomultiplier tube is therefore needed.



THBV4_0526EA

Figure 5-26: Linearity characteristic using a tapered voltage-divider circuit

The above methods for improving pulse output linearity by decoupling capacitors and tapered voltage-divider circuits can also be applied to cathode grounding voltage-divider circuits.

(2) Voltage distribution for the cathode and earlier stages

As mentioned above, the voltage dividing ratio for the latter stages near the anode is an important factor that determines the output linearity. In contrast, the voltage distribution between the cathode, focusing electrode and first dynode affects the photoelectron collection efficiency and the secondary emission ratio of the first dynode. These parameters are major factors in determining the output signal-to-noise ratio, pulse height dispersion in the single and multiple photon regions, and also electron transit time spread (T.T.S.).

Furthermore, the voltage distribution at the earlier stages affects the cathode linearity, energy resolution in scintillation counting, and magnetic characteristics, so its setting requires care just as in the case of the latter stages. Except for special types, the voltage dividing ratios for the earlier dynode stages listed in our catalog are determined in consideration of the electron collection efficiency, time properties, and signal-to-noise ratio. Since these are based on the rated supply voltage, proper corrective action may be required in cases where the supply voltage is less than one half that of the rated voltage. For example, it may be necessary to increase the voltage dividing ratio at the earlier stages or place Zener diodes to hold the dynode voltage constant. For more information on the electron collection efficiency, output signal-to-noise ratio and other characteristics refer to Chapter 4.

Figure 5-27 is a tapered voltage-divider circuit modified based on the circuit shown in Figure 5-25. It provides the above measures for the cathode to the first dynode.

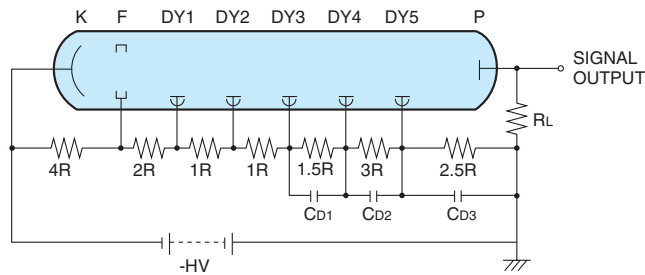


Figure 5-27: Voltage-divider circuit with the earlier and latter stages tapered

The recommended voltage dividing ratios listed in our photomultiplier tube catalogs are selected to meet a wide range of applications with consideration primarily given to the gain.

In pulse operation mode where the output current reaches a high peak value or in cases where the supply voltage has to be set lower than the standard values, selecting a proper voltage dividing ratio that matches the measurement conditions is necessary.

For example, in single photon counting or very low-light-level measurement where shot noise may create a problem, increasing the voltage distribution ratio at the earlier stages of the voltage-divider circuit helps enhance the electron collection efficiency of the photomultiplier tube and reduce the shot noise.

In applications such as TOF (time-of-flight) measurement and fluorescence lifetime measurement requiring a fast time response, it is important to supply the correct voltage to the cathode, focusing electrode and the precision-designed electron lens system near the first dynode.

5.1.5 Countermeasures for fast response circuits

Due to their operation principle, photomultiplier tubes exhibit very fast time response. To utilize this advantage, care must be taken when handling high-speed signals including the voltage-divider circuits.

In the measurement of high-speed signals, external noise is a major factor that degrades the signal-to-noise ratio, so it is necessary to take measures to minimize noise on the high voltage supply line. In the voltage-divider circuit shown in Figure 5-28, a low-pass filter comprised of a resistor R_1 and capacitor C_1 is formed to reduce the noise pickup from the high voltage supply line. Usually, a metal film resistor of several dozen kilohms is used as R_1 and a ceramic capacitor of 0.001 to 0.05 microfarads which withstands high voltage is used as C_1 .

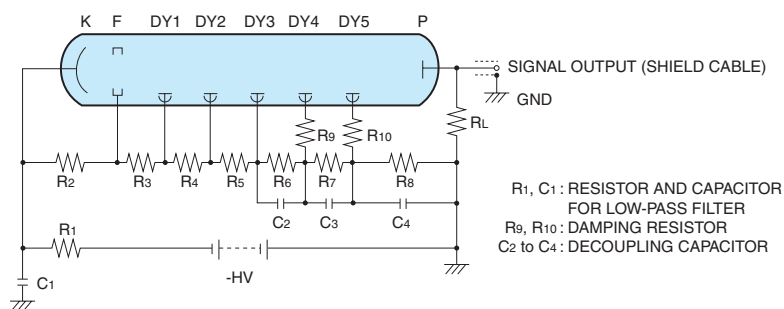


Figure 5-28: Voltage-divider circuit with countermeasure for noise from high voltage power supply and countermeasure for ringing in signal output

The cutoff frequency (f_c : at 3 dB loss) of the low-pass filter is given by the following equation:

$$f_c = \frac{1}{2\pi \cdot R_1 \cdot C_1} \text{ (Hz)} \dots\dots\dots \text{(Eq. 5-5)}$$

Here, R_1 is the resistance (in ohms) and C_1 is the capacitance (in farads).

The loss becomes larger at frequencies higher than the calculated cutoff frequency, so a low-pass filter less of several dozen kilohertz can be configured by applying the above mentioned constants.

If the R_1 value is excessively increased to lower the cutoff frequency, the voltage drop across R_1 becomes larger and lowers the voltage that is actually supplied to the photomultiplier tube, so care should be taken when designing the circuit.

When the rise in connected high voltage power supply is fast or a transient voltage such as an overshoot occurs, this may exceed the rated power of R_1 causing damage to R_1 , so use caution.

When handling high-speed output pulses with a rise time of 10 nanoseconds or less, the output signal waveform may become distorted. This is caused by resonance resulting from the electrode structure of the photomultiplier tube and the reactance of the signal output system including the voltage-divider circuit. The distortion of the output waveform can be improved by inserting a resistor into the last dynode like R_{10} in Figure 5-28, and if necessary into the next to the last dynode like R_9 in Figure 5-28. These resistors are commonly called the damping resistors. Here, the reactance on the signal current flowing in the connected dynode is adjusted by the capacitance component accompanying the resistor so that resonance noise is suppressed. This effect helps smooth the waveforms. Resistors of about 10 to 200 ohms are used as damping resistors. If these values are too large, the time response will deteriorate, so the minimum possible values should be selected in the necessary range while observing the actual output waveforms. Also, be aware that induced noise may occur unless non-inductive resistors are used.

Figure 5-29 shows typical waveforms as observed in an ordinary resistive voltage-divider circuit with or without damping resistors. The figure clearly shows that damping resistors effectively reduce ringing.

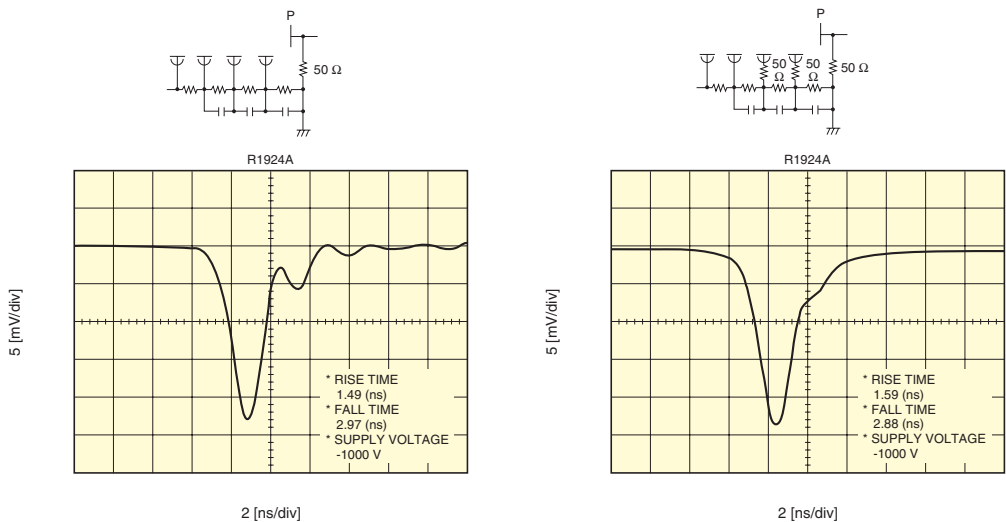
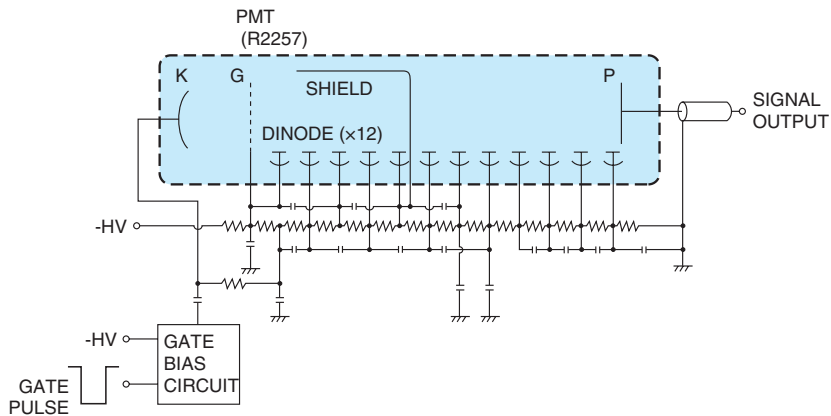


Figure 5-29: Effect of damping resistors on ringing

5.1.7 Gate circuit

Next, we introduce gate circuits as a variant of voltage-divider circuits. Generally, in applications such as time-resolved fluorescence measurement and LIDAR (laser radar), the signal light to be measured is extremely weak in comparison with the primary light levels such as excitation light. For this reason, the detector system is set up to have extremely high sensitivity. If even part of the primary light enters the detector system as stray light, it may cause saturation in the photomultiplier tube output and the subsequent circuits, causing their characteristics to deteriorate. To block the stray light, mechanical shutters might be used, but they cannot work at high-speed in the sub-microsecond range and have other problems such as limited mechanical life span. One effective technique is to use a “gate circuit” that electronically switches the photomultiplier tube on and off to eliminate output during unnecessary periods.



THBV4_0532EA

Figure 5-32: Gated voltage-divider circuit example

Figure 5-32 shows a diagram of a gated voltage-divider circuit. This circuit works in a “normally OFF” mode that normally sets the photomultiplier tube output to OFF and switches it to ON by gate signal input. This gate operation can be reversed to work in a “normally ON” mode that switches the photomultiplier tube output to OFF by gate signal input.

When this circuit is operated in a “normally OFF” mode, the photomultiplier tube output is OFF while the gate pulse input is 0 volts. In this condition, a reverse bias of about 10 volts relative to the focusing electrode and first dynode is supplied to the cathode so that photoelectrons, if emitted from the cathode, will not reach the electron multiplier section (dynode section) and no signal is output. Here, when a negative-going pulse is applied to the gate input terminal, a bias in the direction opposite the bias that has been applied to the cathode via a capacitor is then applied to the cathode, switching the photomultiplier tube output to ON during the period determined by the gate pulse width and the time constant of the capacitance-coupled circuit. This circuit provides a switching ratio (or extinction ratio) of 10^4 or more. A number of capacitors connected from the first dynode to the middle-stage dynode absorb the switching noise often encountered in this type of gate circuit. The gate circuit functions are described in detail in section 8.5 of Chapter 8.

5.1.8 Gain adjustment circuits

The gain of a photomultiplier tube is mostly adjusted by changing the supply voltage. However, if a single power supply is used to operate two or more photomultiplier tubes or the variable range of the high voltage power supply is limited, then a gain adjustment circuit is often added to the voltage-divider circuit. There are three typical methods for adjusting the gain as described below.

The first is the cathode voltage adjustment method shown in Figure 5-33 (1).

In anode grounded voltage-divider circuits, this method uses a variable resistor VR (potentiometer or trimmer) connected in series between the cathode (K) and the high voltage power supply (-HV) to generate a voltage drop. Adjusting this trimpot changes the supply voltage actually applied to the photomultiplier tube. This method allows adjusting the photomultiplier tube gain by about one order of magnitude. Note, however, that the higher the resistance of the voltage-divider resistors, the higher the resistance needed from the trimpot, and it might be difficult to procure a trimpot with such high resistance and high rated voltage. On the other hand, if the resistance of the voltage-divider resistors is small, the current flowing through the trimpot becomes large, requiring a high-wattage trimpot to avoid burnout.

Moreover, in the circuit with a negative high voltage applied to the cathode, the trimpot is floating at a high potential (floating potential), so take this point fully into account in designing the housing which is usually at ground potential. When adjusting the gain while power is supplied to the circuit, always use an insulated screwdriver and tool to avoid electrical shocks and of course do not touch any components with bare hands. This also holds true when adjusting the gain by the middle-dynode potential adjustment method described next.

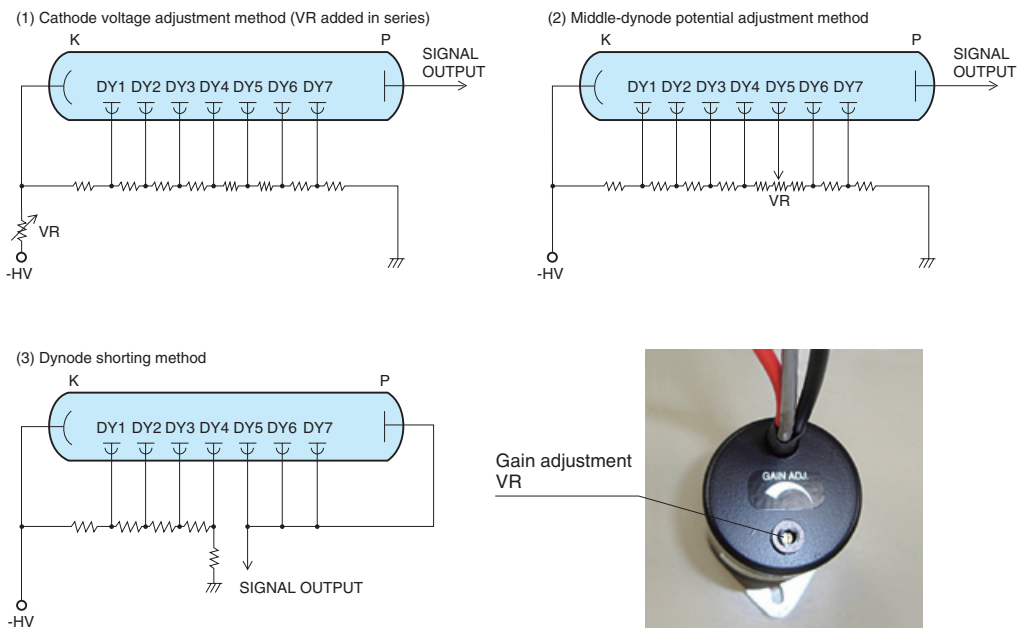


Figure 5-33: Gain adjustment circuits

THBV4_0533EA

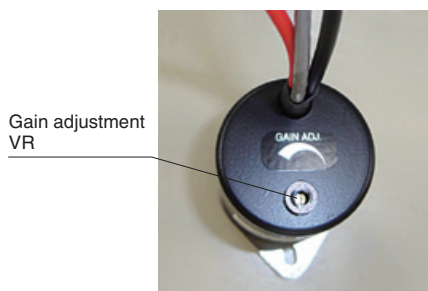


Figure 5-34: DA-type socket assembly with a VR for gain adjustment

The second is the middle-dynode potential adjustment method shown in Figure 5-33 (2).

This method makes use of the fact that the number of secondary electrons decreases and the collection efficiency between dynodes drops by varying the potential of a middle dynode. To vary the potential of the middle dynode, a trimpot is used between the two dynodes adjacent to the middle dynode as shown. Although this method is relatively easy to implement, there is the disadvantage that the signal-to-noise ratio may deteriorate if the dynode potential is varied too much. Figure 5-35 shows changes in the gain and energy resolution of a photomultiplier tube when the dynode potential is varied continuously. Here it can be seen that the energy resolution begins to deteriorate near the point at which the relative gain drops by more than 50 percent. This differs depending on individual photomultiplier tubes and the actual adjustable gain range is not very wide.

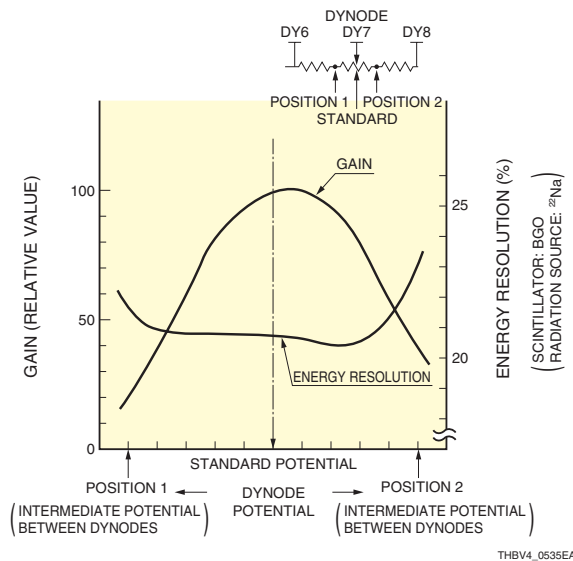


Figure 5-35: Changes in gain and energy resolution as a function of dynode potential

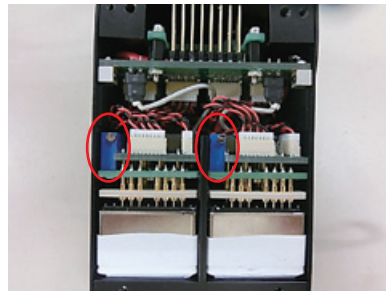


Figure 5-36: PMT module using middle-dynode potential adjustment (VR for gain adjustment is circled in red)

The third is the dynode shorting method shown in Figure 5-33 (3).

This method is used only when the incident light level is so high that the supply voltage must be drastically decreased to prevent the photomultiplier tube output from being saturated. The decrease in the supply voltage lowers the voltage between the dynodes, degrading the electron collection efficiency and secondary emission ratio. In this dynode shorting method, the latter-stage dynodes are shorted to the anode, and the signal is derived from a middle-stage dynode.

Shorting the latter-stage dynodes as shown substantially reduces the number of dynode stages and assures a higher interstage voltage which results in improvement of the signal-to-noise ratio. However, this is accompanied by a sacrifice in linearity characteristics because the output is derived from an earlier-stage dynode. Furthermore, since the total number of dynode stages that are actually used is changed, the gain versus supply voltage characteristics also vary accordingly. The degree of this variation differs from tube to tube, so caution is needed.

5.1.9 Precautions when fabricating a voltage-divider circuit

This section describes the precautions to take when fabricating a voltage-divider circuit.

(1) Selecting the components used for a voltage-divider circuit

Since the voltage-divider circuit directly affects the photomultiplier tube operation, careful selection of components is necessary.

Voltage-divider resistors

Since the photomultiplier tube gain is very susceptible to changes in the supply voltage and interstage voltage, the voltage-divider circuit utilizes resistors with a minimum temperature coefficient (TCR) such as metal-film resistors. When selecting high-resistance resistors for suppressing power consumption or resistors with a high dielectric strength voltage (rated voltage) for use in a tapered voltage-divider, metal glaze resistors are suitable. The same type of resistor should preferably be used in all stages, but if not available, select resistors with similar temperature coefficients. The resistance accuracy, however, is not so critical. There will be no problems even if the resistance variation is about $\pm 5\%$. This is because the photomultiplier tube gain varies from tube to tube and also because a voltage difference of a few volts does not significantly change the electron trajectories. A power rating of at least 1.7 times higher than actually required is ideal for preventing dielectric strength failure and damage, and the voltage rating must at least 1.5 times higher than the required value. Considering the power consumption and self-heating of the resistors, the practical resistance per stage is 100 kilohms to 1 megohm as a rough guide.

Use of surface-mount resistors (chip resistors) is increasing due to productivity benefits. When using these resistors, the above points should also be taken into account. Chip resistors can be broadly classified into two types: thick film resistors and thin film resistors. Thin film resistors offer better resistance accuracy and temperature coefficients, but most of them do not have an adequate power rating for voltage dividers, so use of thick film resistors is appropriate here.

When selecting a variable resistor for use in gain adjustment, the dielectric strength, power rating, and temperature characteristics should also be taken into account. There is a variable resistor called the cermet type which is manufactured by firing metal on a ceramic substrate. Cermet resistors are superior in reliability and temperature characteristics and are widely used.

In the variable resistor or trimpot used in Figure 5-33 (1), increasing its resistance value increases the voltage applied across it and decreasing the resistance increases the current flowing through it. Adjusting the resistance of the trimpot therefore varies the range of the dielectric strength and power capacity, so carefully check the usage conditions and then select the component with an adequate margin of the ratings.

When precise adjustment is needed, it is preferable to use a multi-turn VR capable of fine-adjustment as well as having sufficient accuracy and stability. VR have a sliding contact (wiper) where the amount of current flow is limited. Also, be aware of contact noise that may occur depending on the component.

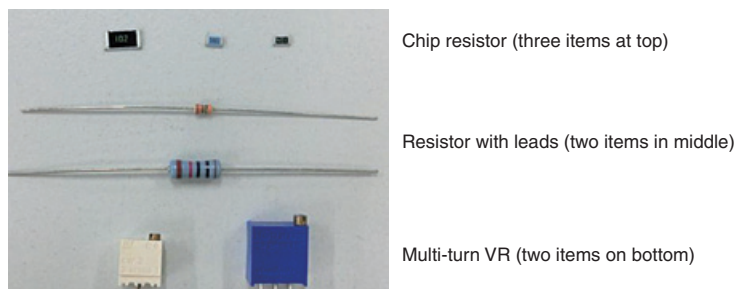


Figure 5-37: Resistors and trim pots

Load resistors and damping resistors

Use non-inductive resistors suitable for high frequencies. In the case of using a winding resistor, be aware that it may function as a coil (inductance or L) according to the applied pulse signals and become a source of noise.

When selecting a chip resistor to use as a load resistor, thin film resistors are appropriate because of their resistance accuracy. However, it is also important to select one with an adequate power rating margin in view of the signal peak current and pulse width. If a thin film resistor with sufficient power rating is not available, select and use a thick film resistor with a better resistance accuracy that matches the required measurement accuracy.

Decoupling capacitors and coupling capacitors

In pulsed light applications where a fast response photomultiplier tube handles the output with a rise time of less than 10 nanoseconds, decoupling capacitors are connected between dynodes. In this case, using ceramic capacitors with sufficiently low impedance in a high frequency range and an adequate voltage rating at least 1.5 times higher than the maximum voltage applied between dynodes is recommended. If decoupling capacitors with a larger electrostatic capacity are needed, then film capacitors are sometimes used.

If a bypass capacitor (low-pass filter) is needed for eliminating noise from the power supply connected to the high voltage input terminal, use ceramic capacitors with low impedance at high frequencies and an adequate voltage rating.

Coupling capacitors are needed for isolating the signal from the positive high voltage applied to the anode in a cathode grounded voltage-divider circuits. Ceramic capacitors with minimum leakage current (which may be a source of noise), superior frequency characteristics, and sufficiently high voltage endurance are frequently used to perform this task.

Ceramic capacitors are classified by their characteristics into two types: a low dielectric constant type and a high dielectric constant type. The low dielectric constant type has relatively good temperature stability, but cannot provide large capacitance since its dielectric constant is low. In contrast, the high dielectric constant type provides large capacitance since its dielectric constant is high, but the capacitance tends to vary with temperature. In general, decoupling capacitors require a few nanofarads or more, and so are selected from among the high dielectric constant type capacitors in most cases. Note, however, that the high dielectric constant type ceramic capacitors have DC bias characteristics that significantly reduce their capacitance when a DC voltage is applied. This makes it important to select the capacitance value by anticipating this drop in capacitance beforehand. Film capacitors, on the other hand, do not usually exhibit such a drop in capacitance due to DC bias and work stably, but the size of these capacitors is relatively large, making it difficult to downsize the voltage-divider circuit.

Use of surface-mount capacitors (chip capacitors) is also increasing the same as for the resistors mentioned above. When selecting electrical characteristics of chip capacitors, use the same criteria as capacitors with leads.

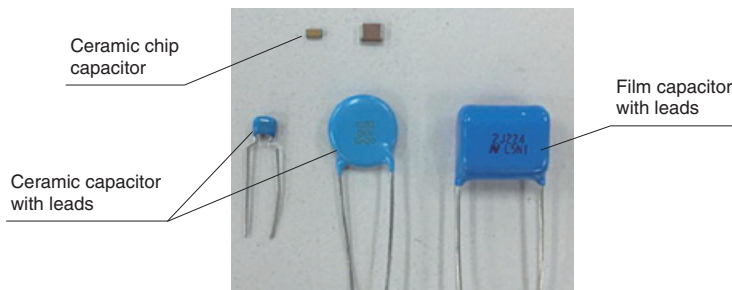


Figure 5-38: Ceramic capacitors and film capacitors

Printed circuit boards (PCB)

When assembling a voltage-divider circuit on a PCB and not on a photomultiplier tube socket, use a high-quality PCB made of glass-epoxy or similar materials which exhibit high insulation, low leakage current, and high frequency characteristics. If both sides of the PCB are used for assembly, select a board with adequate thickness by taking the insulation and mechanical strength into account. Generally, glass-epoxy boards called FR-4 (frame resistant 4: a type of flame retardant glass-epoxy-based material used for making PCB) with a thickness of about 1.6 millimeters are widely used.

Besides glass-epoxy boards, high-quality boards made of polyimide or teflon are available and used in special applications where even a small leakage current affects measurement or there are strict environmental conditions such as for temperature. These boards are expensive and so are selected only when needed.

When needed, resist is coated on the board surface to protect the wiring pattern, improve the soldering workability and to protect the pattern insulation. In this case, however, if moisture is absorbed at locations with different voltage potentials such as the anode wiring section and high voltage supply section, the resulting leakage current may increase noise so use caution.

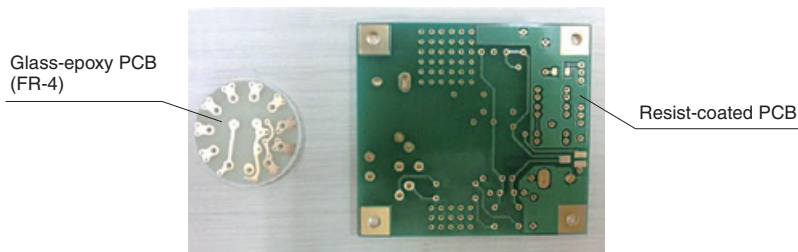


Figure 5-39: Printed circuit board examples

Leads and connectors

In high voltage circuits, use teflon or silicone insulated wires with a high voltage rating, or use coaxial cables with the required voltage rating (example: RG-59B/U with a voltage rating of 2.3 kV). In either case, take sufficient care to ensure proper insulation of conductor wires.

As signal lines, coaxial cables such as RG-174/U and 3D-2V are recommended since they are easy to handle and procure. For high-speed circuits, in particular, a 50-ohm coaxial cable must be used to match the input impedance with a measuring device. However, if the signal current to be derived is higher than a few microamperes and the lead wire length is no longer than 20 centimeters, then using single wire lead will not cause any problems in actual operation as long as there is no noise source near the photomultiplier tube.

Lead wires used for low voltage circuits can also be used for grounding. However, if there is a possibility that the ground wire might make contact with components or socket pins which are at a high potential, then the lead wire must have a high voltage rating. So, use a lead wire that is used for high voltage lines or use cross-linked polyethylene insulated wire that meets the required voltage rating.

Specifications for coaxial cables RG/174/U and 3D-2V respectively comply with MIL standards and JIS standards.

When using a coaxial cable as the signal line, a coaxial connector is also used in most cases for noise measures and impedance matching. In addition, a coaxial connector may also be used for the high voltage line for noise measures and protection from high voltage.

The most common coaxial connector is the 50-ohm BNC connector which is widely used with various signal processing devices such as oscilloscopes. This connector has good frequency characteristics and is compact and easy to plug/unplug. Another BNC connector with the same shape, but with 75-ohm impedance, is also available on the market, so select a connector that is a good match for the measurement system being used.

In high-speed signal processing applications requiring more compact and lightweight components, SMA connectors are used that are smaller than BNC connectors yet have high frequency characteristics. Besides SMA connectors, there are other small connectors for high frequency applications such as SMB and MCX connectors. Select one that matches the device to be connected.

As high voltage connectors suitable for coaxial cables, SHV connectors are used mainly for safety reasons. Since SHV connectors are designed for high voltage applications, they are relatively large but easy to plug/unplug like BNC connectors.

Regardless of the type of connector, check the required characteristic impedance and polarity (plug or receptacle) and select the correct one. When installing the connector, do it carefully to avoid making a poor connection. Improper connector mating with the cable or a poor connection may cause an impedance mismatch and/or dielectric strength failure.

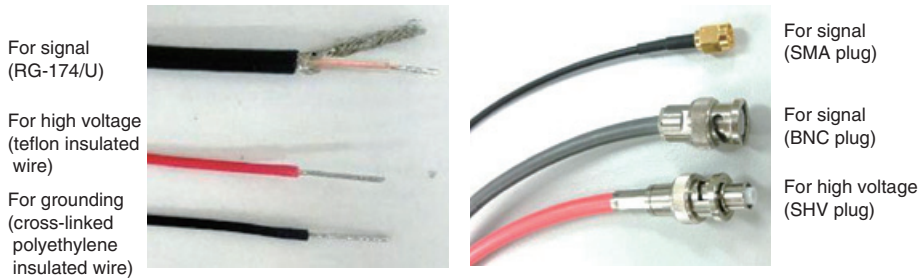


Figure 5-40: Lead wires, signal cables and connectors

Coating materials and potting materials

Coating and potting is sometimes used for voltage-divider circuits that handle high voltages in order to improve insulation and fix components in place. Before attempting coating or potting, confirm in advance that there will be no adverse effects (no corrosion or hardening failures) on mounted components or photomultiplier tubes.

Moreover, materials having a high dielectric strength and large volumetric resistance and surface resistance are required as electrical characteristics. These materials also require a low dielectric constant since they may be used at high frequencies. When sealing the entire voltage-divider circuit or the photomultiplier tube with a potting material, it is also necessary to consider the expansion coefficient and thermal conductivity of the potting material. Silicone resin is a typical material that is frequently used, but urethane resin and epoxy resin are also adopted according to the particular application.

Though a factor in all types of potting material, epoxy resins in particular tend to become extremely hard after curing/hardening, so expansion and shrinkage of the potting material due to fluctuations in ambient temperature may damage the circuit components or photomultiplier tube, so caution is required. The water absorption also varies according to the potting material and may cause the insulation to deteriorate depending on the environment where used, so select the material carefully after checking the material properties in advance. In cases where the potting or coating material also serves as a light shield for a the photomultiplier tube, use a material such as black silicone resin of a certain thickness that besides adding a sealing property also prevents unwanted light from passing through it or reflecting on it.

Potting requires preparing many items such as selecting raw materials, carefully deciding the type of curing, and enhancing the work environment, etc. Many problems may occur due to improper handling, so it is important to acquire sufficient experience in this task.

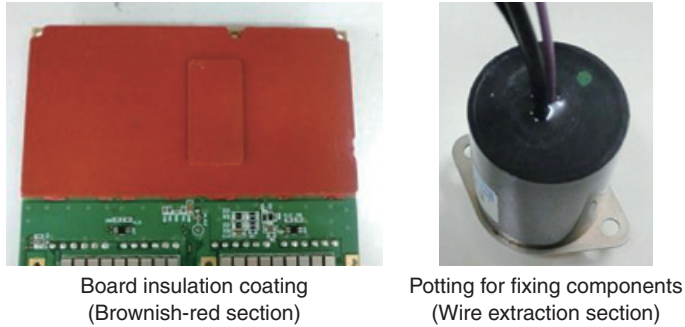


Figure 5-41: Coating and potting

(2) Precautions for mounting components

It is important to know the role of components to be mounted on the voltage-divider circuit. The example shown in Fig. 5-30 will help understand the roles of those components.

General

Components for the voltage-divider circuits handle high voltage, so leakage current may occur and cause a problem if the component surfaces may become dirty or absorb moisture. Always work with clean hands and keep components clean. Degrease and dry them beforehand as needed.

Also, applying heat more than allowable to photomultiplier tubes and sockets during soldering may not only harm the component's external appearance but may also adversely affect its performance characteristics, so caution is required.

Resistor mounting

Voltage-divider resistors have different voltage potentials depending on the dynodes connected and so must not contact each other. Also, consider the heat dissipation of the components by setting an appropriate gap between the resistors. Especially when using resistors having a low resistance value or in the case of very weak light measurement in which an increase in dark current due to a temperature rise becomes a problem, it is necessary to provide a certain gap between the voltage-divider resistors and the pins and socket of the photomultiplier tube to ensure that the Joule heat (mainly heat loss due to resistance) generated in the voltage-divider circuit is not directly transmitted to the photomultiplier. On the other hand, lengthening the distance from the resistors to the photomultiplier tube may increase the lead inductance (L component), which may cause ringing, degrades frequency characteristics, or generates noise, so it is necessary to set an optimal distance.

The longer the wire length the greater the effect exerted on the load resistance and damping resistance, so keeping the wire short is necessary.

Also, when attaching a resistor having leads, care should be taken not to damage it because the mechanical strength at the base portion of the body and lead wire is generally low. Even with chip resistors, the electrode part has a junction point with the ceramic component body, which is mechanically weak and requires care. This is also true for capacitors and other components.

Capacitor mounting

As already described, the lead wires for the decoupling capacitor used for the voltage-divider circuit for high-speed pulse operation must be kept as short as possible because the L component affects the frequency characteristics and ringing. So even when using a chip capacitor having no lead wires, it is essential to keep the pattern wiring on the board as short as possible. Also, when mounting the voltage-divider resistor away from the photomultiplier tube due to heat emission and other problems, only the decoupling capacitor needs to be mounted as close as possible to the photomultiplier tube pins and socket. Doing this does not cause a problem because the heat loss of the decoupling capacitor is minor. When using chip capacitors, an insulation coating is preferably applied after mounting on the board as a countermeasure against the surface leakage current, since the chip surface is not covered with insulation such as found on components with leads.

Mounting on a printed circuit board

When designing patterns for printed circuit boards, the creep distance between required patterns should preferably be set as large as possible to deal with discharges that might occur. There should be at least a distance of 1 millimeter for each difference in potential of 1 kilovolt.

Any unnecessary routing of the pattern wiring increases the L component of the circuit and exerts unwanted effects when a high-speed response is required, so it is important to keep the wiring as short as possible while taking the insulation into account. Besides creep distances, the spatial distance of the actually mounted components must be considered. This is especially true for discrete components whose leads are still exposed after mounting and for components where the terminals are still largely exposed such as chip resistors. It is therefore essential to prevent possible spatial discharge from occurring due to the difference in voltage potential that occurs during actual use.

Before mounting components, remove any moisture contained in the printed circuit board by a baking process and so on. Also be sure to perform degreasing to remove the oxide film on the lands and pads that will be soldered.

Lead wire and connector mounting

Careful attention is required because lead wire work involves tasks such as cutting so there is the risk of damaging components.

When stripping the lead wire coating away to expose the conductor (core wire) portion, the conductor portion might become scratched, or in the case of multi-core wires, damage might decrease the number of core wires and otherwise cause wire breakage disconnection, discharge, and unnecessary heat loss, and so must be avoided. Also in the coaxial cable, damage to the insulator covering the core wire will cause insulation failure to occur between the insulator and shielded wire, causing problems such as short circuits, so caution is required.

Lead wires, especially Teflon-insulated wires and coaxial cables have a structure with a relatively hard finish and so forcibly bending them may cause breakage or a loss in characteristic performance. Therefore, when bending the wiring for use with a measuring system, follow the cable bending radius specifications.

When soldering the lead wires to a printed circuit boards, there is a specific temperature at which the cable covering material and the insulator may soften, melt or deteriorate. Since PVC (polyvinyl chloride) used for example in RG-174/U and other items starts to soften at around 65 °C, applying too much heat should definitely be avoided.

In cases where using a single wire as a signal line, twisting the signal line and signal ground line (twisted pair) may help to reduce common mode noise, so employ this technique if necessary.

When attaching the connector, besides observing the precautions described above, the tools must be compatible with the accurate dimensions based on each of the specifications and process drawings. Assembly and installation might be impossible if the accuracy is wrong or if the wrong tools were used, and even if assuming it was assembled and installed, these problems may cause internal short circuits and conduction failures.

Typical problems from using incompatible tools or the wrong accuracy in the signal connector may cause impedance matching failures, and signal disruptions especially at high frequencies. In terms of use as a high voltage connector, internal discharges may occur and attempting to use with a poor setup, the wrong tools, or wrong accuracy may prove hazardous and so must absolutely be avoided. Problems with the signal output and voltage supply when using the connector may lead to possible malfunctions in the photomultiplier tube and voltage-divider circuit, and there may be errors in wiring locations and internal machining, so it is essential to check that the connector attached to the product has been correctly fabricated and installed.

Signal output system

As mentioned in resistor mounting, signal output systems including load resistors require shortening the wiring length as much as possible. Moreover, the wiring must be placed far away from components that are supplied with high voltage lines and high voltage. When the anode and the high voltage section are near to each other on the circuit board, consideration must be given to avoid the direct flow of leakage current from the high voltage section by using measures such as providing insulation and enclosing the anode at ground potential after securing insulation, or cutting into the substrate.

Especially when handling high-speed pulse signals, ground one point of the signal system and the power supply system as necessary to suppress unnecessary noise generation by the ground loop. Also, when a signal line runs parallel to another signal line or a control pulse line, the signals might become superimposed on the other signal line as induced noise, so avoid routing them in this way. Furthermore, when handling a very small output current, consideration must also be given to shielding of the signal path and prevention of leakage current.

Coating and potting

Be careful not to allow the coating material and potting material to adhere to any parts other than where needed. Foreign matter that penetrates into the coating or potting can cause hardening defects and discharges. In addition, deterioration of the insulation can become a major concern if air pockets remain in the potting area and voids are generated, so defoam the potting material as necessary. Since the temperature, humidity, standing time, and other factors are important curing conditions, these must be carefully checked in advance before starting work. Coating and potting types such as two-liquid mixed types may not cure or harden if their mixing ratio is wrong, or the desired characteristics may not be obtained so caution is required.

5.2 Selecting the high voltage power supply

There are mainly two types of high voltage power supplies available: a module type that can be mounted on printed circuit boards and a general-purpose bench-top type. The module type operates on low voltage power and the bench top type operates on AC power.

Since high voltage power supply characteristics directly affect the photomultiplier tube signal output, the high voltage power supply requires a high degree of stability that gives a good overall combination of characteristics such as for drift, ripple and noise, temperature dependence, input regulation, and load regulation. High voltage power supply schemes and characteristics are described here.

The series regulator type has been widely used for high voltage power supplies because it provides low noise, but on the other hand, it does have problems with power efficiency, heat generation and is not suited for downsizing. Because of these drawbacks, the switching regulator type has recently become the mainstream among high voltage power supplies. Many switching regulator systems providing both a high output voltage and high output current are commercially available even in small sizes and so their use with photomultiplier tubes is increasing. However, depending on the type, switching noise might become superimposed on the high voltage output, or switching noise might be emitted to peripheral equipment. It is essential to carefully select the high voltage power supply especially when measuring very weak light such as in photon counting or when signal processing at a fast response speed is needed. The following table shows a general guideline for performance when selecting a high voltage power supply.

| Parameters | Content and Values |
|---------------------------|--------------------|
| ① Input regulation | ±0.1 % or less |
| ② Load regulation | ±0.2 % or less |
| ③ Ripple noise | 0.01 or less |
| ④ Temperature coefficient | ±0.05 %/°C or less |

Table 5-1: Characteristics required for high voltage power supplies

- ① This is the percentage (%) of change in the output voltage during maximum voltage output relative to a given change in the input voltage, usually defined by changing ±10 % of the input voltage.
- ② This is a measure of the ability of the output voltage to remain constant when the output current is changed by a change in the load. The load regulation is the difference between the output voltage at no load (zero output current) and the output voltage at full load (maximum output current), expressed as a percentage (%) of the output voltage at full load.
- ③ Ripple is the variation (peak) in the output synchronized with the oscillator frequency of the high voltage pulse generator circuit. The characteristic value includes not only the variation (peak value) but also fluctuation components (noise) other than in the oscillator frequency. Some power supplies may show only the ripple component on the product tag or specs and not other fluctuation components, so care is needed when selecting a power supply for actual operation.
- ④ This indicates the output fluctuation rate (%/°C) under output conditions (mostly during maximum output) defined within the ambient operating temperature range.

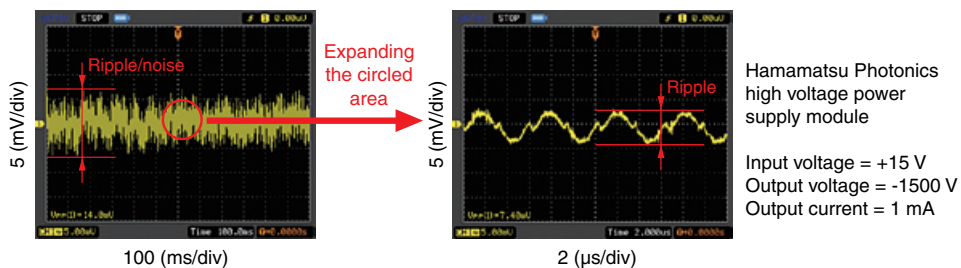


Figure 5-42: Examples of ripple noise

Take the following points into account when selecting and using a high voltage power supply.

- High voltage power supplies generate high voltages, so take full precautions to prevent electrical shock and handle according to instructions in the operating manual.
- Select a high voltage power supply whose electrical characteristics (input regulation, load regulation, temperature coefficient, ripple and noise, etc.) are at least 10 times better than the stability required for the photomultiplier tube. Output changes over time (drift) must also be taken into account. Especially, it is preferable that ripple/noise be 100 mV p-p or less. The stability and noise characteristics of the low-voltage power supply on the input side, which is the base power supply, also affect the high voltage output, so also use low voltage power supplies whose performance characteristics are as good as possible.
- In view of the need for an ample margin of current carrying capacity, select a high voltage power supply whose current carrying capacity allows outputting a current 1.5 times or more than the current flowing through the voltage-divider circuit. The high voltage output might drop if there is no extra margin in the output current. Moreover, when operating multiple photomultiplier tubes from one high voltage power supply, select a high voltage power supply that is a high output type with a large maximum output current, by calculating the necessary current capacity from the combined resistance value of all the voltage-divider circuits. In this case also, the high voltage power supply should have an ample margin of current capacity.
- When using a grounded-cathode (+HV) scheme, the high voltage is biased via the resistor to the anode and further coupled by a coupling capacitor, so noise from the high voltage power supply easily tends propagate to the signal output. This means extra caution is needed regarding ripple and noise characteristics.
- Ripple and noise can be improved by inserting a low-pass filter circuit along the high voltage input line. In this case, select components having excellent surge immunity while taking into account the transient voltage that occurs when the high voltage power supply is turned on. When a low-pass filter circuit is added, the high voltage response is affected by the time constant of the added filter circuit, so the high voltage rise time becomes longer compared to when no filter circuit is added.
- Though the output voltage rise and fall times of the high voltage power supply differ depending on the power supply type, the fall time is generally slower than the rise time. This is because it takes time for the capacitor in the power supply circuit to discharge while lowering the voltage. So special consideration is required for applications where the high voltage is changed sharply.
- High voltage power supplies also have power loss, so it is recommended to select a power supply having the highest possible efficiency relative to the input power. If the efficiency is too low, the ambient temperature might rise in some cases. The ambient temperature of the high voltage power supply might rise drastically if something is covering the periphery of the power supply such as when installed inside the equipment. In such cases, be careful not to exceed the rated operating ambient temperature.
- Some high voltage power supplies have output voltage overshoot (phenomenon in which the output voltage exceeds the setting value) that might possibly damage the photomultiplier tube and the voltage-divider circuit. So it is essential to use a high voltage power supply designed photomultiplier tubes, which will exhibit no overshoot.
- The input side and the high voltage output side of high-voltage power supplies typically share a common ground. So unlike dry cell batteries, high voltage power supplies cannot be connected in series. When power supplies must be connected in series, a floating insulated high voltage power supply is utilized. However, since the base voltage potential of the power supply floats on the high voltage side, care is required during handling and operation.

- Most module type high voltage power supplies are controlled by analog voltage, but some are controlled digitally by a PC via an interface such as the RS-485. This type of power supply is more suited for remote control and automatic control applications.



Model: C10940-03-R2
(with RS-485 interface)

Dimensions (W × H × D): 15 mm × 18 mm × 15 mm
 Input voltage: +5 V
 Maximum output voltage: -1200 V
 Maximum output current: 0.6 mA

Figure 5-43: Miniature high voltage power supply module

- Most bench-top type high voltage power supplies use a high voltage cable with connector. This requires selecting a cable having appropriate rated voltage specifications. Even though the connector may look the same, the cable itself may have different dielectric strength voltage specifications, so use a cable with specifications that match the power supply.



Model: C9525-02

Input voltage: 100 V AC
 Maximum output voltage: -2000 V
 Maximum output current: 1.8 mA

Figure 5-44: Bench-top type high voltage power supply

- When operating multiple photomultiplier tubes by using a single high voltage power supply, select a high voltage power supply with a large current capacity as required after totaling the current that will flow through all of the voltage-dividers to be connected.

When connecting a high voltage power supply to multiple photomultiplier tubes, an important point to note is that some high voltage power supplies have a short-circuit protection function, so that if some connected photomultiplier tubes or voltage-divider circuits fail in short-circuit mode, this protection function will activate to stop the high voltage supply to ensure safety. However, this function might stop high voltage supply even to a normally operating photomultiplier tube. In such cases, it is recommended to turn off the power supply and eliminate the cause of the short circuit. However, if it is not desired to shut down all the photomultiplier tubes, install a breaker shutoff circuit on each one that will shut off just the photomultiplier tube having the electrical short.



Model: C11784-12

Dimensions (W × H × D): 62 mm × 15 mm × 45 mm
 Input voltage: +24 V
 Maximum output voltage: -2000 V
 Maximum output current: 5 mA

Figure 5-45: High output type high voltage power supply module

- In some cases, medical equipment and other equipment must have obtained UL certification as a safety specification for high voltage power supplies.



Model: C10673

Dimensions (W × H × D): 46 mm × 24 mm × 12 mm

Input voltage: +15 V

Maximum output voltage: -1250 V

Maximum output current: 0.6 mA

Figure 5-46: UL-certified high voltage power supply module

- As mentioned in 13.1.2 of Chapter 13, some photomultiplier tubes are used at exceedingly high temperatures compared to typical photomultiplier tubes. Hamamatsu therefore offers high voltage power supplies capable of operating even in high temperature environments.



Model: C12733-01

Dimensions: $\phi 22.2$ mm × 85.4 mm

(excluding terminals and cables)

Input voltage: +15 V

Output voltage: -1000 V to -1800 V

Maximum output current: 0.09 mA

Operating ambient temperature: -40 °C to +175 °C

Figure 5-47: High voltage power supply module for high temperature use

5.3 Connection to the External Circuit

5.3.1 Measuring an output signal

To measure the output signal of a photomultiplier tube, various methods are used depending on the operating conditions as illustrated in Figures 5-48, 5-49 and 5-50.

As described in section 5.1.2 in this chapter, there are two schemes for voltage-divider circuit operation: anode grounded and cathode grounded schemes. The anode grounded scheme allows operation in both DC output and pulse output modes as shown in Figures 5-48 and 5-49. The cathode grounded scheme, on the other hand, requires a coupling capacitor to connect to an ordinary amplifier circuit or measuring device since a high voltage is applied to the anode, and the capacitor blocks the DC signals so that only pulse signals are output. Although there is no DC output is obtained, this scheme has the advantage of minimizing effects from unwanted signals produced by background light containing DC components.

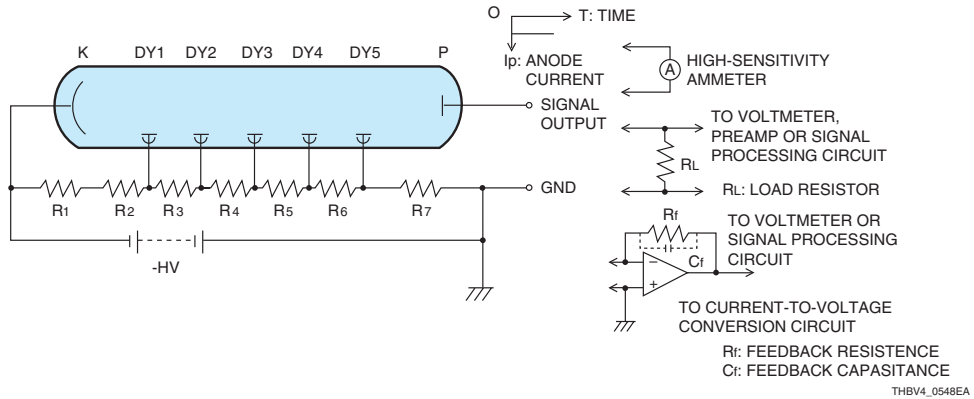


Figure 5-48: Anode grounded scheme in DC output mode

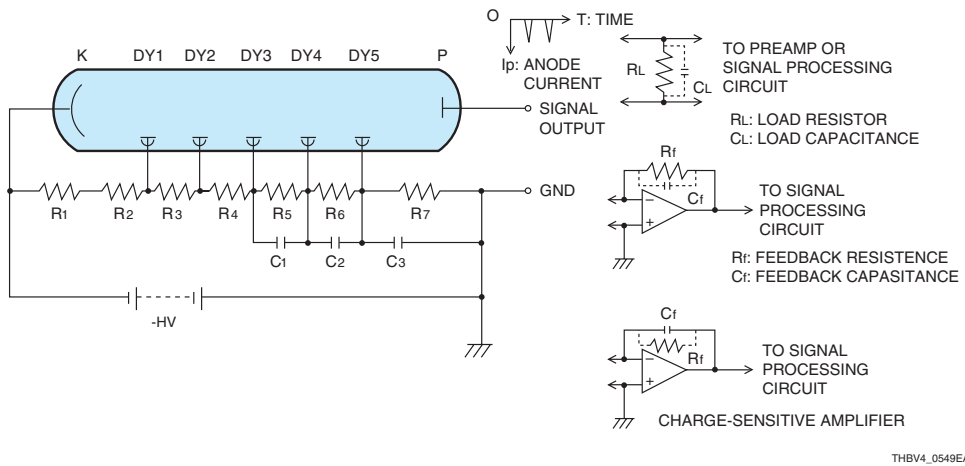


Figure 5-49: Anode grounded scheme in pulse output mode

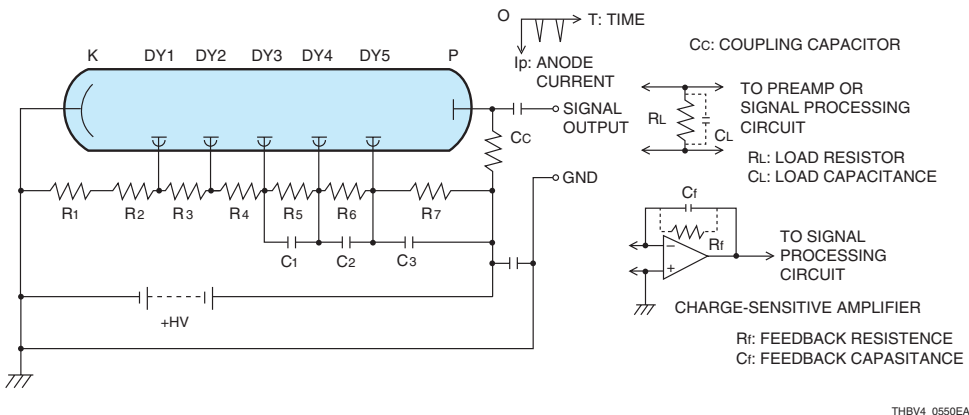


Figure 5-50: Cathode grounded scheme in pulse output mode

When using a photomultiplier tube by connecting it to a downstream signal processing circuit such as an amplifier circuit, the photomultiplier tube must first be connected to the signal processing circuit before turning on the high voltage power supply to start operation. When a high voltage is applied to the voltage-divider circuit, the photomultiplier tube starts operating and, even if no light is incident, a charge produced by dark current is accumulated on the anode. Under this condition, if the voltage-divider circuit is connected to the amplifier circuit, the charge will instantaneously flow into the signal processing circuit, possibly damaging the circuit. Extreme care should be taken when using high-speed circuits since these are more susceptible to this type of damage. To avoid this, use a terminating resistor for the anode output so that unwanted charges will not accumulate.

5.3.2 Effects of a coupling capacitor

As mentioned previously, a coupling capacitor is usually required in cathode grounded schemes. However, a coupling capacitor can also be used in an anode grounded scheme in pulse output mode in order to eliminate the DC components in the anode current. This section describes precautions for using a voltage-divider circuit connected to a coupling capacitor.

Output waveform

In the circuit shown in Figure 5-51, which is connected to the anode of a photomultiplier tube, if the anode output pulse width P_w is sufficiently shorter than the time constant CR (R is parallel resistance of R_a and R_L), the impedance of the coupling capacitor can be ignored so the signal pulse current branches to flow into R_L and R_a . In this case, the input waveform is transmitted to the output waveform without distortion regardless of the capacitance of the coupling capacitor. However, if P_w is close to or longer than CR , the output will have a differential waveform. Since this coupling capacitor is merely used as a coupling element between the voltage-divider circuit and the amplifier circuit, the P_w value must be at least several dozen times shorter than the CR value in order to allow the input waveform to reproduce the output waveform without distortion. When a 50-ohm resistor is used for R_a to optimize fast response operation, the time constant CR becomes small, so care should be taken of this point.

In case of low frequency applications, the impedance of the coupling capacitor cannot be ignored. Since its impedance $Z_C = \frac{1}{2\pi fC}$, the output signal decays by 3 dB (approximately to 7/10ths of the pulse height) at a frequency $f=1/2\pi CR_L$.

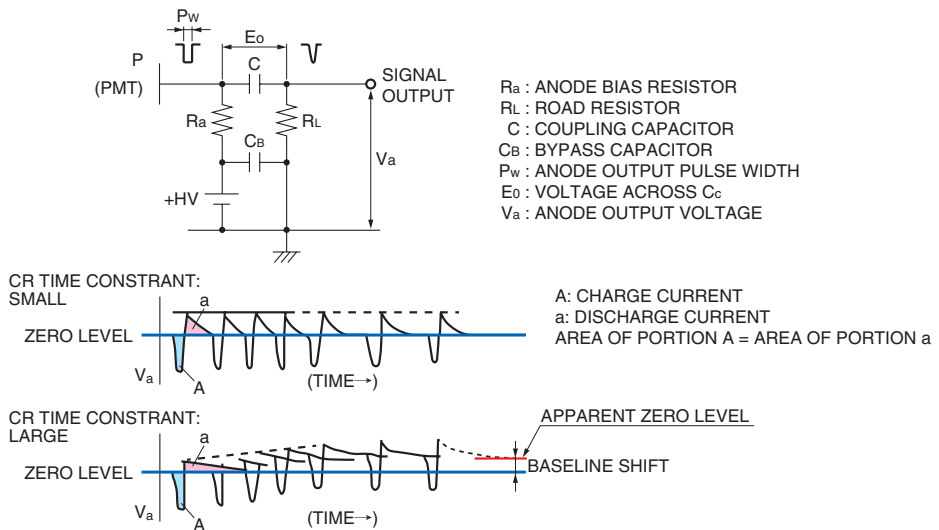


Figure 5-51: Baseline shift

Baseline shift

As mentioned previously, the amount of the signal passing through the coupling capacitor is stored as a corresponding charge on the capacitor. This stored charge Q generates a voltage of $E_0=Q/C$ across both sides of the capacitor in the reverse flow direction of the signal. This voltage E_0 attenuates by the following factor related to the time constant CR which is determined by the capacitance C and the serial resistance R of R_a and R_L .

$$V = E_0 e^{-t/CR}$$

The voltage induced in the capacitor is divided by R_a and R_L , and the output voltage V_a is given by the following equation (Eq. 5-6):

$$V_a = E_0 e^{-t/CR} \times \frac{R_a}{R_a + R_L} \dots\dots\dots (Eq. 5-6)$$

Here, if the signal pulse repetition rate increases, the baseline does not return to the original level and creates an apparent zero level that is shifted from the true zero level as shown in Figure 5-51 (lower graph). This is known as baseline shift and can be minimized by reducing the time constant CR . Here, reducing the capacitance has the advantage of increasing the signal voltage E_0 but shortens the discharge time, and the signal waveform is likely to be differentiated as mentioned above. Generally, the load resistance R_L is increased as needed to make it easier to process the signal voltage. Decreasing the resistance to avoid a baseline shift reduces the signal voltage, which might affect the signal-to-noise ratio. If the R_a value is large and the anode output is high, the voltage generated across R_a lowers the anode potential, which affects the photomultiplier tube gain, so use caution when changing the resistance.

As shown in Figure 5-51, when the amount of signal charge stored on the capacitor (portion A in Figure 5-51) is discharged in a certain time period (portion "a" in Figure 5-51), the area of portion A is equal to the area of portion "a" regardless of the discharge time constant. When the circuit time constant is set larger than the signal pulse width, this discharge time will have less effect on the pulse height. However, when the signal pulse repetition rate is high or accurate information on the output pulse height is needed, the discharge time cannot be ignored. If a baseline shift occurs, the signal is observed at an apparently lower level. So, when designing the circuit, the optimum resistance and capacitance must be selected so that the output pulse height exhibits no fluctuations even if the signal repetition rate is increased.

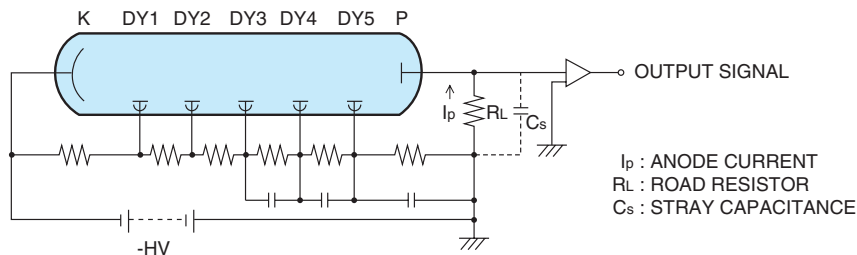
Furthermore, when multiple pulses enter within the resolving time of the measurement system including an amplifier, these pulses are added to cause a large pulse (so-called pile-up) problem to occur. In cases where a pulse height discriminator is used to discern the height of individual pulses, the time resolution of the measurement device must be taken into account.

5.3.3 Current-to-voltage conversion of photomultiplier tube output

The output of a photomultiplier tube is a current (charge), while the externally connected signal processing circuit is usually designed to handle voltage signals. This current output must be converted into a voltage signal by some means, except when measuring the output with a high-sensitivity ammeter. The following describes how to perform the current-to-voltage conversion and the precautions to take.

(1) Current-to-voltage conversion using load resistance

One method for converting the current output of a photomultiplier tube into a voltage output is to use a load resistance. Since the photomultiplier tube may be thought of as an ideal constant-current source in a low output current region, theoretically a load resistance with a considerably large value can be used. The output voltage V_o can therefore be obtained by multiplying the anode current I_p by the load resistance R_L . In practice however, the load resistance value is limited by factors such as the required frequency characteristics and output linearity characteristics as discussed below.



THBV4_0552EA

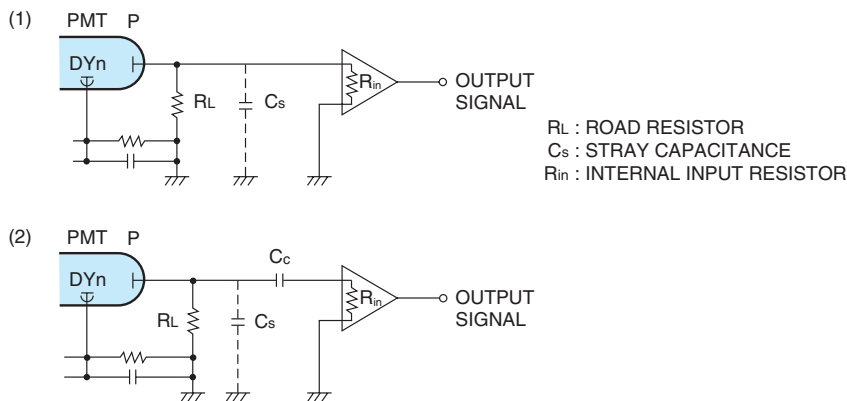
Figure 5-52: Photomultiplier tube and output circuit

In the circuit of Figure 5-52, if the load resistance is R_L and the total electrostatic capacitance of the photomultiplier tube anode to all other electrodes including stray capacitance such as wiring capacitance is C_s , then the high-range cutoff frequency f_c is given by the following equation (Eq. 5-7):

$$f_c = \frac{1}{2\pi C_s R_L} \text{ (Hz)} \dots\dots\dots \text{(Eq. 5-7)}$$

Even if the photomultiplier tube and the connected measuring device such as an oscilloscope have fast response, the high-range cutoff frequency f_c is determined by the signal output circuit of the photomultiplier tube.

If R_L is made unnecessarily large, then the voltage drop by $I_p \times R_L$ at the anode potential becomes large, causing a drop in the final dynode-to-anode voltage. This increases the space charge effect and degrades the output linearity. In most cases, therefore, the output voltage should be less than several percent (about 1 volt or less) of the last-dynode-to-anode voltage.



THBV4_0553EA

Figure 5-53: Amplifier internal input resistance

When selecting the optimum load resistance, it is also necessary to take into account the internal input resistance (input impedance) of the amplifier connected to the photomultiplier tube. Figure 5-53 shows equivalent circuits for the photomultiplier tube output when connected to an amplifier. In this figure, if the load resistance is R_L and the input resistance is R_{in} , the resultant parallel resistance R_0 is calculated from the following relation (Eq. 5-8):

$$R_0 = \frac{R_{in} \cdot R_L}{R_{in} + R_L} \dots\dots\dots \text{(Eq. 5-8)}$$

This value of R_0 , less than the R_L value, is then the effective load resistance of the photomultiplier tube. The relation between the output voltage V_0 at $R_{in} = \infty \Omega$ when the anode current was ideally all consumed in the load resistance R_L and the output voltage V_0 when the output was affected by the actual amplifier R_{in} is expressed by the following equation (Eq. 5-9):

$$V_0' = V_0 \times \frac{R_{in}}{R_{in} + R_L} \dots\dots\dots (Eq. 5-9)$$

With $R_{in} = R_L$, the V_0' value is one-half the value of V_0 . This means that the upper limit of the load resistance is actually the input resistance R_{in} of the amplifier and that making the load resistance greater than this value does not have a significant effect.

Till now our description assumed that the load resistance and internal input resistance of the amplifier are purely resistive. In practice, however, phase terms such as stray capacitance and stray inductance are added, so these must be considered as compound impedances, especially in measurement at high frequencies.

As shown in Figure 5-53 (2), when placing a coupling capacitor C_c between the photomultiplier tube and the amplifier to block DC signals and just extracting the pulse components, be aware of the value of the load resistance R_L , because setting it too large a value may cause bad effects from stray capacitance C_s or cause problems with frequency characteristics or the pulse height of the signals.

(2) Current-to-voltage conversion using an op-amp

A combination of a current-to-voltage conversion circuit using an op-amp and a voltmeter allows accurate measurement of the anode output from a photomultiplier tube without having to use a high-sensitivity ammeter.

This method also ensures good linearity characteristics while avoiding adverse effects on the anode output resulting from a voltage drop between the last dynode and the anode, which occurs when the anode current is converted to a voltage via the load resistance R_L .

A basic current-to-voltage conversion circuit using an op-amp is shown in Figure 5-54.

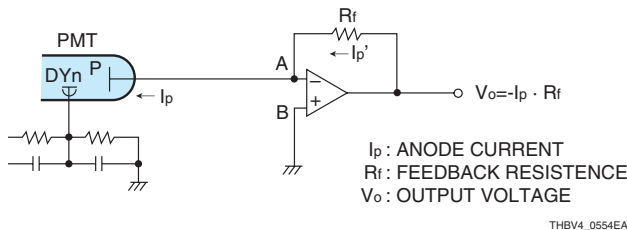


Figure 5-54: Current-to-voltage conversion circuit using an op-amp **Figure 5-55: Amplifier circuit example**

In this circuit, the output voltage V_0 is expressed by the following equation (Eq. 5-10):

$$V_0 = -I_p \cdot R_f \dots\dots\dots (Eq. 5-10)$$

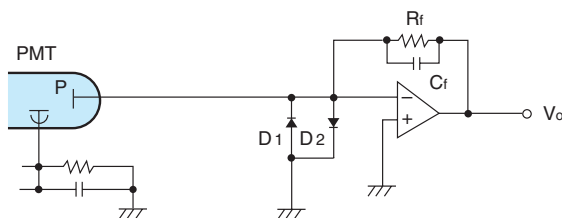
This relation can be understood as follows:

Since the input impedance of the op-amp is extremely high, the output current of the photomultiplier tube is blocked from flowing into point A in Figure 5-54, or in other words the inverting input terminal (-) of the op-amp. Therefore, most of the output current flows through the feedback resistance R_f and a voltage of $I_p' \times R_f$ is developed across R_f (I_p and I_p' can be regarded as being equal). On the other hand, the op-amp gain (open loop gain) is very high and about 10^5 (100 dB), and it always acts so as to maintain the potential of the inverting input terminal at a potential equal to that (ground potential) of the non-inverting input terminal at point B. (This effect is known as an imaginary short or virtual ground.) Because of this, the op-amp outputs voltage V_0 which is equal to the voltage developed across R_f and theoretically, converts the current to a voltage with an accuracy as high as the reciprocal of the open loop gain.

When an op-amp is used, factors that determine the minimum measurable current are the op-amp offset current (I_{OS}), the quality of R_f and insulating materials used, and wiring methods. To accurately measure a very low current on the order of picoamperes (10^{-12} amperes), the following points should be observed in addition to the above factors:

- As the signal output cable, use a low-noise coaxial cable with sufficiently high insulating properties.
- Select a connector with high insulating properties for example, a Teflon-insulated connector. When using a coaxial connector, select one with high frequency characteristics.
- For connecting the photomultiplier tube anode to the input signal pin of the op-amp, do not use a trace on the printed circuit board but use a Teflon-insulated conductive terminal to avoid leakage current.
- Carefully adjust the output offset voltage (V_{OS}) of the op-amp and also provide sufficient phase compensation to avoid oscillation.
- The actual output is $V_o = -(I_p + I_{OS}) \cdot R_f + V_{OS}$. So if the R_f value is large, the offset current (I_{OS}) may cause a problem. To avoid this, use a FET input op-amp with a high input impedance and an offset current of less than 0.1 picoamperes which also exhibits minimum input conversion noise and temperature drift. Moreover, grounding the non-inverting input terminal via a resistor with resistance equal to the feedback resistance provides a balance for the input bias and reduces the offset current between the input terminals.
- Use a metal-film resistor or other resistor with a minimum temperature coefficient and small resistor tolerance in the feedback resistance. Keep the resistor surface free from dirt or foreign material. In addition, when the resistance value is 1 gigaohm (10^9 ohms) or more, use a glass-sealed resistor that ensures low leakage current. Some resistors may emit noise depending on the type, so be aware of this when selecting a resistor.
- Use a printed circuit board made of glass-epoxy or similar materials with better insulating properties (about 10^{14} ohms).
- The maximum output voltage of op-amps is usually 1 to 2 volts lower than the supply voltage, so be aware of the upper limit of the measurement range.

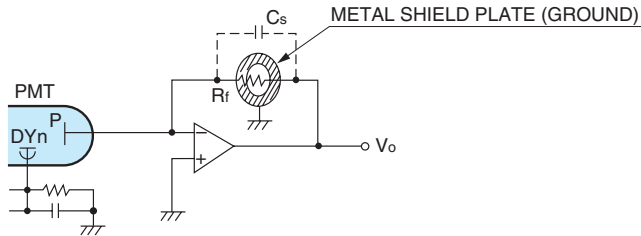
A high voltage is applied during photomultiplier tube operation. If for some reason this high voltage is accidentally output from the anode, a protective circuit consisting of diodes (D_1 and D_2) as shown in Figure 5-56 is effective in protecting the op-amp from being damaged. In this case, these diodes should have minimum leakage current and junction capacitance. The B-E junction of a low-signal-amplification transistor or FET is sometimes used.



THBV4_0556EA

Figure 5-56: Protective circuit for op-amp

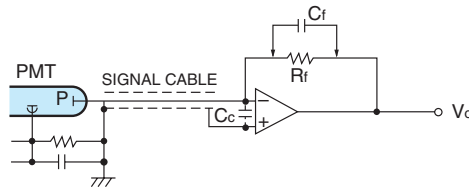
When a high feedback resistance R_f of about 10^9 ohms is used to increase the current-to-voltage conversion factor, if a stray capacitance C_s that is parasitic to R_f exists as shown in Figure 5-57, then the circuit has a time constant of $C_s \times R_f$. This limits the bandwidth and may cause problems depending on the application. As illustrated in the figure, passing R_f through a hole in a metal shield plate at the ground potential can reduce C_s and improve the response speed.



THBV4_0557EA

Figure 5-57: Canceling the stray capacitance on amplifier feedback resistance

On the other hand, as shown in Figure 5-58, when a long coaxial cable having a capacitance is used as the signal output cable for a photomultiplier tube and its equivalent capacitance is C_c , the time constant of $C_c \times R_f$ creates a phase delay in the feedback loop of the op-amp, which may be the cause of oscillation. In this case, placing C_f in parallel with R_f for phase compensation will avoid this oscillation but some degradation in response speed is inevitable.



THBV4_0558EA

Figure 5-58: Canceling the signal cable capacitance

(3) Charge-sensitive amplifier using an op-amp

Figure 5-39 (1) shows the basic circuit of a charge-sensitive amplifier using an op-amp. The output charge Q_p of a photomultiplier tube is stored in C_f , and the output voltage V_o is expressed by the following equation (Eq. 5-11):

$$V_o = Q_p/C_f \dots\dots\dots (Eq. 5-11)$$

Here, if the output current of the photomultiplier tube is I_p , then V_o becomes

$$V_o = -\frac{1}{C_f} \int_0^t I_p dt \dots\dots\dots (Eq. 5-12)$$

When the output charge is continuously accumulated, the V_o finally increases up to a level near the supply voltage for the op-amp as shown in Figure 5-59 (2) and (3).

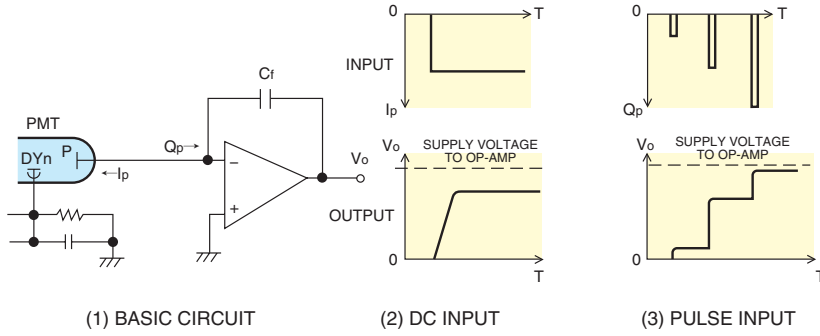


Figure 5-59: Charge-sensitive amplifier circuit and its operation

THBV4_0559EA

In Figure 5-59 (1), if a circuit is added by connecting a FET switch in parallel to C_f so that the charge stored in C_f can be discharged as needed, this circuit acts as an integrator that stores the output charge during the measurement time, regardless of whether the photomultiplier tube output is DC or pulse.

In scintillation counting, the individual output pulses of a photomultiplier tube must be converted into corresponding voltage pulses. Therefore, R_f is connected in parallel with C_f as shown in Figure 5-60 to use a circuit having a discharge time constant $\tau=C_f \cdot R_f$.

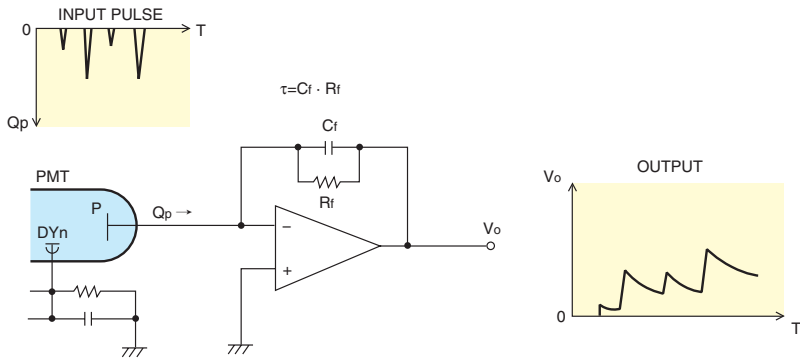


Figure 5-60: Pulse input type charge-sensitive amplifier

THBV4_0560EA

If the time constant τ is reduced, the output V_0 is more dependent on the pulse height of the input current. Conversely, if τ is increased, V_0 will be more dependent on the input pulse charge and eventually approaches the value of $-Q_p/C_f$. In the case of scintillation counting, the output pulse voltage waveform $V(t)$ is given by the following equation³⁾ from the relation between the circuit time constant $\tau=CR$ and the fluorescent decay constant τ_s of the scintillator:

$$V(t) = \frac{Q \cdot \tau}{\tau - \tau_s} (e^{-t/\tau} - e^{-t/\tau_s}) \dots\dots\dots (Eq. 5-13)$$

when $\tau \gg \tau_s$, $V(t)$ becomes

$$V(t) \approx \frac{Q}{C} (e^{-t/\tau} - e^{-t/\tau_s}) \dots\dots\dots (Eq. 5-14)$$

While, when $\tau \ll \tau_s$, $V(t)$ is

$$V(t) \approx \frac{Q}{C} \cdot \frac{\tau}{\tau_s} (e^{-t/\tau_s} - e^{-t/\tau}) \dots\dots\dots (Eq. 5-15)$$

When the circuit time constant τ is larger than the scintillator decay constant τ_s , the rise of the output waveform depends on τ_s , while the fall depends on τ , and the maximum pulse height is given by Q/C . In contrast, when the circuit time constant τ is smaller than τ_s , the rise of the output waveform depends on τ , while the fall depends on τ_s , and the maximum pulse height is given by $Q/C \cdot \tau/\tau_s$. In most cases, the condition of $\tau \gg \tau_s$ is used since it is likely to provide higher energy resolution since the output pulse height of the charge-sensitive amplifier is less affected by fluctuations of the input signal. However, the pulse width becomes longer due to a larger τ and, if the repetition rate is high, a pile-up tends to occur. If measurement requires a high counting rate, then reducing τ is effective in creating an output waveform as fast as the scintillator decay time, but this leads to a sacrifice in the energy resolution.

The time constant τ should therefore be set according to the application as to which is more important, a high counting rate or energy resolution. When changing the time constant, in most cases, reduce the load resistance as long as the operation permits and then determine the resistance value. When a NaI(Tl) scintillator is used, the time constant is usually selected to be from a few microseconds to several dozen microseconds.

In scintillation counting, the noise generated in the charge-sensitive amplifier circuit degrades the energy resolution. Besides the noise resulting from the circuit elements such as the amplifiers, care should also be taken with the cable capacitance C_s indicated in Figure 5-61, because the output charge of the photomultiplier tube is divided and stored in C_f and C_s , which can be a cause of noise. To improve the signal-to-noise ratio, the value of $A \cdot C_f / C_s$ should be large. In actual operation however, since the $A \cdot C_f$ value cannot be made larger than a certain value due to various limiting conditions, the value of C_s is usually made as small as possible to cope with this problem.

In scintillation counting measurements, a common method for reducing the effects of the cable capacitance is to place a preamplifier in the vicinity of the photomultiplier tube.

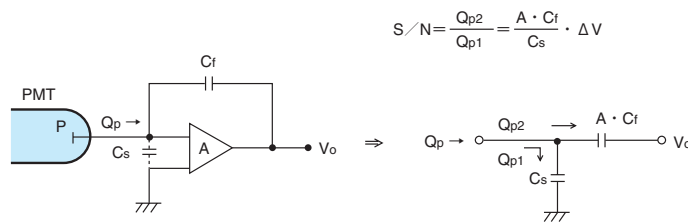


Figure 5-61: Effects of input distribution capacitance

THBV4_0561EA

5.3.4 Output circuit for fast response photomultiplier tubes

In detection of ultra-short light pulses, a coaxial cable with 50-ohm impedance is usually used to connect the photomultiplier tube to the subsequent circuit.

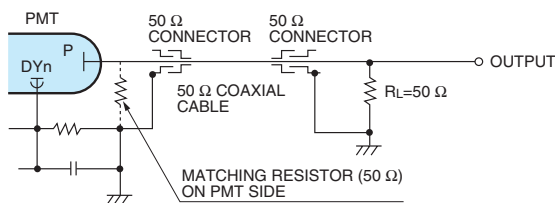
To transmit the signal output waveform with good fidelity, the output end must be terminated in a pure resistance equal to the characteristic impedance of the coaxial cable as shown in Figure 5-62. This allows the impedance seen from the photomultiplier tube to remain constant regardless of the cable length, making it possible to reduce “ringing” which might be observed in the output waveform. However, when using an MCP-PMT for observation of an ultra-fast phenomenon where the signal rise time is less than 1 nanosecond, the signal waveform may be distorted by a loss of signal in the coaxial cable itself if the cable length is unnecessarily long so caution on this point.

Unless a proper impedance match is provided at the output end, the impedance seen from the photomultiplier tube will vary with the frequency, and the impedance value will be further affected by the coaxial cable length, and ringing may appear in the output. Such a mismatch may be caused not only by the coaxial cable and its terminated resistance but also by the connector used or the termination method of the coaxial cable. So, sufficient care must be taken to select a proper connector and also to avoid creating impedance discontinuity when connecting the coaxial cable to the photomultiplier tube or the connector.

If there is an impedance mismatch at the coaxial cable ends, not all of the output signal energy is consumed at the output end, and part of the signal energy is reflected back to the photomultiplier tube. In this case, unless a matching resistor is provided on the photomultiplier tube side, the anode of the photomultiplier tube is viewed as an open end, so the signal will reflect from the anode and returned to the output end again. This reflected signal is measured as a pulse appearing after the main pulse with a time delay equal to the round trip through the coaxial cable. This signal repeats the round trip until its total energy is consumed, and as a result, ringing occurs at the output end. Here, for example, consider how signal reflection occurs when observing a high-speed signal by connecting a 50-ohm impedance coaxial cable between the signal source and the signal receiver where no impedance matching was done. If the coaxial cable has a capacitance 100 nF/km (nanofarads per kilometer) and a length of 1 meter, then by calculation, the reflected signals return to the receiver approximately every 10 nanoseconds while being attenuated.

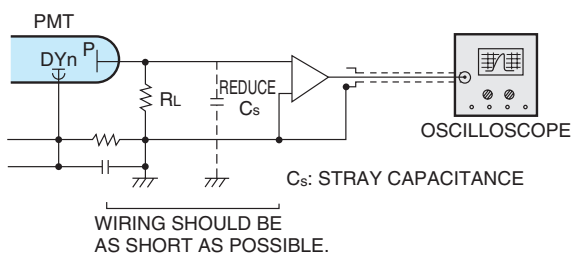
To prevent this, providing an impedance match not only at the output end but also at the photomultiplier tube side is effective to some extent, although the output voltage will be reduced to one-half in comparison with that obtained when there is an impedance match only at the output end. When using a photomultiplier tube in applications where a high-speed response is not required or when using a coaxial cable with a short length, an impedance matching resistor is not necessarily needed on the photomultiplier tube side. Whether or not to connect this resistor to the photomultiplier tube can be determined by doing trial-and-error impedance matching. Among photomultiplier tubes, there are special types having a 50-ohm matched output impedance. These photomultiplier tubes do not require any matching resistor.

Next, let's consider the measurement of fast pulse waveforms using an oscilloscope. A coaxial cable terminated with a matching resistor offers the advantage that the cable length will not greatly affect its characteristics. Since the matching resistance is usually as low as 50 to 100 ohms, the output voltage drops to a very low value, requiring the use of a wide-band amplifier with a high gain in some cases. However, such an amplifier usually has large noise which possibly makes it difficult to measure low-level signals. In this case, to achieve the desired output voltage, it is more advantageous to bring the photomultiplier tube as close as possible to the amplifier to reduce the stray capacitance as shown in Figure 5-63, and also to use a large load resistance R_L as long as it does not affect the frequency characteristics.



THBV4_0562EA

Figure 5-62: Output circuit impedance match



THBV4_0563EA

Figure 5-63: Using an amplifier

It is relatively simple to fabricate a fast amplifier with a wide bandwidth using a video IC or pulse type IC. However, in exchange for such design convenience, these ICs tend to cause various problems such as noise. So when using such an amplifier, it is necessary to know their performance limits and take corrective action. As detailed in section 5.3.2 of this chapter, as the pulse repetition rate increases a phenomenon called “baseline shift” creates another reason for concern. This baseline shift occurs when the DC signal component is blocked due to using a coupling capacitor in the signal circuit. If this occurs, the zero reference level shifts from the original ground level to an apparent zero level equal to the average of the output pulses. Furthermore, when multiple pulses enter within the time resolution of the measuring system including the amplifier, they are integrated so that a large output pulse or a so-called a “pile-up” problem, appears. Care should be taken in cases where a pulse height discriminator is used to find the amplitude of individual pulses.

5.3.5 Selecting an amplifier for measurement using a photomultiplier tube

This section describes how to select an amplifier to connect to a photomultiplier tube and an example of the circuit configuration using the related products available from Hamamatsu Photonics. This section also explains the precautions to take when using amplifiers.

When measuring very-low-level light, the single photon counting technique is advantageous in the signal-to-noise ratio. Analog output measurement is used when the light level is higher than the single photon counting region.

(1) Single photon counting (Also refer to Chapter 6, “Photon Counting”)

For single photon counting, a system like that shown in Figure 5-64 is used and the photomultiplier tube gain is basically set to about 3×10^6 . The C9744 photon counting unit is connected to the signal output from the photomultiplier, and a frequency counter is connected to the C9744 to measure the output.

When transferring the data to a PC (personal computer), a photon counting unit equipped with an interface, for example the C8855-01, is connected in place of the frequency counter. If the photomultiplier tube gain is lower than 3×10^6 , a wide-band amplifier (with high frequency characteristics) is connected between the photomultiplier tube and the C9744.

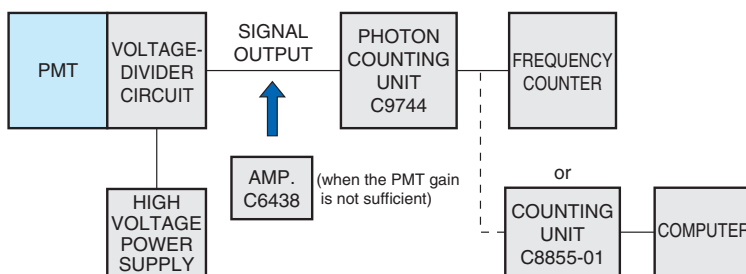


Figure 5-64: System for single photon counting measurement

THBV4_0564EA

(2) Analog output measurement

The appropriate amplifier must be selected by considering the light level to be measured, the required frequency bandwidth (signal speed), output amplitude (output voltage value), and polarity. First select an amplifier with frequency characteristics slightly higher than required, and calculate the voltage value to extract from the amplifier by multiplying the expected anode output current by the current-to-voltage conversion factor of the amplifier. Then set the output voltage range based on the calculated value.

The required frequency bandwidth can be calculated from the rise time of the anode output, as follows:

$$\text{Frequency (MHz)} = 350 / \text{Rise time (ns)} \quad \dots\dots\dots (\text{Eq. 5-16})$$

For example, the amplifier used must have frequency characteristics higher than 100 megahertz to measure signals with a rise time of 3.5 nanoseconds or higher than 10 megahertz to measure signals with a rise time of 35 nanoseconds. The frequency bandwidth calculated here is the frequency at which the amplifier gain decreases by 3 dB, which is a commonly used definition. To keep the amplifier gain from decreasing at up to the maximum frequency, use an amplifier with a frequency bandwidth that is about 1.4 times higher.

If an amplifier with frequency characteristics higher than necessary is used, the noise may increase, so selecting an amplifier with the appropriate frequency range is important. When using an amplifier for A/D (analog-to-digital) conversion in analog measurement, sampling at a frequency at least twice the frequency characteristics of the amplifier is required due to the sampling theorem.

In applications where the timing signal for measuring high-speed signals must be amplified, a high-speed amplifier (such as the C5594) is required. High-speed amplifiers usually eliminate low-frequency components including direct current due to the internal AC coupling. Caution is also needed since, if signal components near the cut-off frequency are input, these are not sufficiently amplified resulting in waveform distortion.

(3) Precautions for using an amplifier

Although some amplifiers contain a protective circuit against excessive input, most ordinary amplifiers may be damaged if transient noise with high peak current is input. An amplifier circuit has signal input and output terminals and also a power input terminal having electrical polarity (positive or negative). Making a wrong connection to these terminals can cause malfunction or breakdown, so take the following precautions when using an amplifier circuit.

- Never attempt to connect or disconnect the anode output (signal line) to or from the amplifier while a high voltage is supplied to the photomultiplier tube. After making sure that all cables for the measurement system are securely connected, turn on the power to the amplifier and then supply the high voltage to the photomultiplier tube. Since a charge might be remaining on the anode output (signal line, especially coaxial cable) which is not terminated, short the anode output to ground to remove the stored charge, and then connect it to the amplifier.
- Before turning on the power to the amplifier, make sure the polarity of the power is correct. Also use a constant voltage power supply to supply the rated voltage.
- Before starting measurement, check the maximum output current of the photomultiplier tube and adjust the input signal level so as not to exceed the amplifier rating. If the rating is likely to be exceeded during operation, adjust the incident light level or reduce the photomultiplier tube gain so that the amplifier output stays within the correct range.
- When finishing the measurement, first slowly reduce the high voltage supplied to the photomultiplier tube and then turn off the power supply. After that, turn off the power to the amplifier.

Hamamatsu Photonics provides various types of amplifiers with different frequency characteristics and current-to-voltage conversion factors that allow the user to select the desired amplifier. Our major products are amplifier units that can be used on a desk or bench, but module types such as the M7279 and M8879, which can be mounted on a printed circuit board are also available.

| Type No. | Frequency bandwidth (-3 dB) | Current-to-voltage conversion factor | Output polarity |
|----------|--|---|---|
| C7319 | DC to 20 kHz DC to 200 kHz (switchable) | 0.1 V/μA, 1 V/μA, 10 V/μA (switchable) | Inverted output |
| C12419 | DC to 1 MHz | 1 V/μA | Inverted output |
| C9999 | DC to 10 MHz | 50 mV/μA | Non-inverted output |
| C9999-01 | | 10 mV/μA | Inverted/non-inverted output (switchable) |
| C6438 | DC to 50 MHz | 0.5 mV/μA | Non-inverted output |
| C6438-01 | | 25 mV/μA | Non-inverted output |
| C6438-02 | | 5 mV/μA | Inverted/non-inverted output (switchable) |
| C9663 | DC to 150 MHz | 4 mV/μA | Non-inverted output |
| C11184 | DC to 300 MHz | 1.25 mV/μA | Non-inverted output |
| C5594 | 50 kHz to 1.5 GHz | 3.15 mV/μA | Non-inverted output |
| M7279 | DC to 10 MHz | 10 mV/μA | Non-inverted output |
| M8879 | DC to 150 MHz | 4 mV/μA | Non-inverted output |

Table 5-2: Amplifiers available from Hamamatsu Photonics



Figure 5-65: Amplifier units available from Hamamatsu Photonics

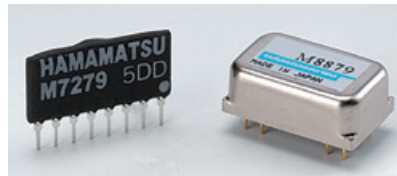


Figure 5-66: Amplifier modules available from Hamamatsu Photonics
Left: M7279, Right: M8879

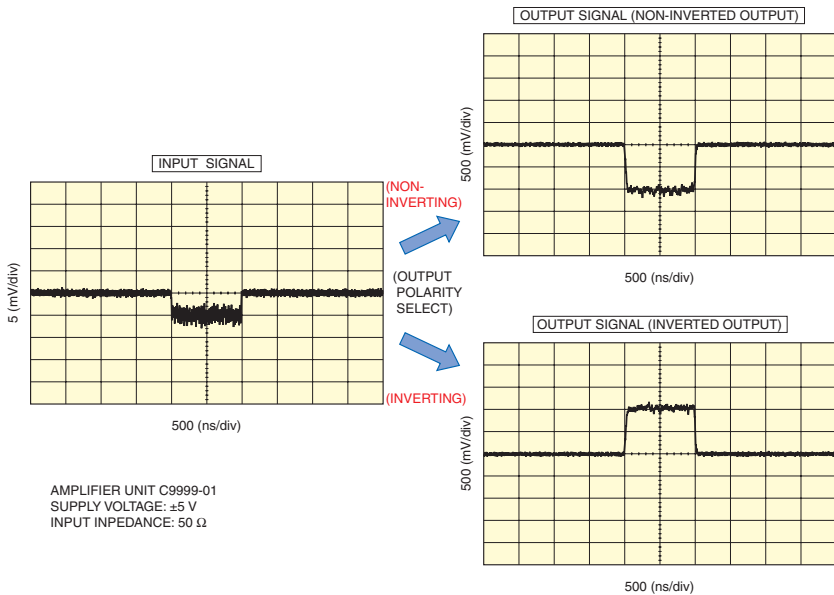


Figure 5-67: Output examples of C9999-01 amplifier unit

5.4 Housing

A photomultiplier tube housing is primarily used to contain and secure a photomultiplier tube, but it also provides the following functions:

1. Shields out extraneous light
2. Eliminates effects from external electrostatic fields
3. Reduces effects from external magnetic fields

The following sections describes each of these functions

5.4.1 Light shield

Since a photomultiplier tube is a highly sensitive photodetector, light leakage can be a source of noise so care must be exercised in shielding out extraneous light. For instance, when a connector is used for signal input/output there is the possibility of light leakage through the connector itself or through its mounting holes and screw holes. Furthermore, light leakage may occur through seams between the components or covers used in the housing.

One corrective action is to use black silicone rubber at any location where light leakage might occur when mounting connectors or other components in the housing. Also, use black soft tape or an O-ring to fill in any gaps around the components attached to the housing, and coat the inside of the housing with black matte paint to prevent reflection of scattered light.

5.4.2 Electrostatic shield

Since most photomultiplier tube housings are made of metal such as aluminum because it is durable and easy to machine, these provide good electrical conduction. Maintaining the housing at ground potential serves as an effective shield against external electrostatic fields. However, in general, the surface of aluminum is usually treated to form an anodic oxide coating known as alumite which makes it difficult to provide electrical conduction from the coating surface, so remove the anodic oxide coating as needed. The inside of the housing is usually coated with black paint to prevent irregular reflection of light, so also remove this paint as needed to prevent causing contact failures at the connection point of the ground line. Any object at ground potential may increase noise if brought close to the bulb of the photomultiplier tube, so the inner side of the housing should be adequately separated from the photomultiplier tube.

5.4.3 Magnetic shield

As will be described in Chapter 13, photomultiplier tubes are very sensitive to magnetic fields. Even the earth's magnetism will adversely affect photomultiplier tube performance.⁴⁾ In precision photometry or in applications where the photomultiplier tube must be used in a highly magnetic field, a magnetic shield case must be used. However, unlike an electrostatic shield, completely shielding out magnetic fields is not possible. One common technique for reducing the effect of an external magnetic field is to wrap a metal shield having high permeability around the photomultiplier tube bulb. However, such a metal shield cannot completely block out the magnetic field. An optimum shielding material and method must also be selected according to both the strength and frequency of the magnetic fields.

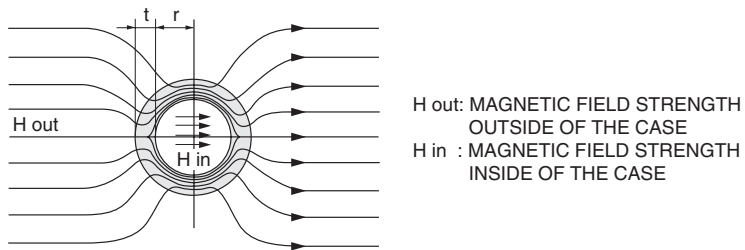
In general applications, placing a photomultiplier tube into a cylindrical shield case made from highly permeable material will prove quite effective. As a magnetic shielding material, permalloy (Iron-nickel soft magnetic material) is best, and among permalloys, PC materials with high permeability and low coercive force are widely used. The effects provided by magnetic shield cases are described below.



Figure 5-68: Magnetic shield cases E989 series

(1) Shielding factor of magnetic shield case and orientation of magnetic field

Photomultiplier tubes and especially the head-on types are very sensitive to external magnetic fields. To eliminate the effect of the earth’s magnetism or to operate a photomultiplier tube in a magnetic field, a magnetic shield case must be used. The desired magnetic shielding effect can be obtained by utilizing the fact that a magnetic field is shunted through an object with high permeability. (Refer to Chapter 13.) The magnetic shielding effect of a shielding material can be calculated as the magnetic shielding factor as given by the equation below using Figure 5-69.



THBV4_0569EA

Figure 5-69: Shielding effect of a magnetic shield case

As mentioned, the magnetic shield case is commonly fabricated from metal with high permeability such as permalloy. The shielding factor S of such a magnetic shield case is expressed as follows:

$$S = \frac{H_{out}}{H_{in}} = \frac{3t\mu}{4r} \dots\dots\dots (Eq. 5-17)$$

where H_{in} and H_{out} are respectively the magnetic field strength inside and outside the shield case, t is the thickness, r is the radius, and μ is the permeability of the magnetic shield case. When two or more magnetic shield cases with different radii are used in combination, the resultant shielding factor S' will be the product of the shielding factor of each shield case as expressed by the following equation:

$$\begin{aligned}
 S' &= S_1 \times S_2 \times S_3 \dots S_n \\
 &= \frac{3t_1\mu_1}{4r_1} \times \frac{3t_2\mu_2}{4r_2} \times \frac{3t_3\mu_3}{4r_3} \times \dots \times \frac{3t_n\mu_n}{4r_n} \dots\dots\dots (Eq. 5-18)
 \end{aligned}$$

When a magnetic shield case is used, the magnetic field strength inside the case H_{in} which is actually imposed on the photomultiplier tube is reduced to a level of H_{out}/S . For example, if a magnetic shield case with a shielding factor of 10 is employed for a photomultiplier tube operated in an external magnetic field of 3 milliteslas, this means that the photomultiplier tube is operated in a magnetic field of 0.3 milliteslas. In practice, the edge effect of the magnetic shield case as will be described later, creates a loss of the shielding effect. But this approach is basically correct.

Figure 5-70 shows the output variations of a photomultiplier tube with and without a magnetic shield case which is made of a PC material (Ni-Fe-Mo-Cu) with a 0.6 millimeter thickness. The graphs clearly show that the shielding is very effective for both X and Y axes. But this effect is slightly better on the Y axis than on the X axis, although the shielding factor of the magnetic shield case is equal for both axes. This is because the Y axis magnetic characteristic is better than the X axis when the magnetic shield case is not used. In the case of the Z axis which is parallel to the tube axis, the photomultiplier tube used with the magnetic shield case shows larger output variations. The direction of the magnetic field is probably bent near the edge of the shield case as described in the section on the edge effect.

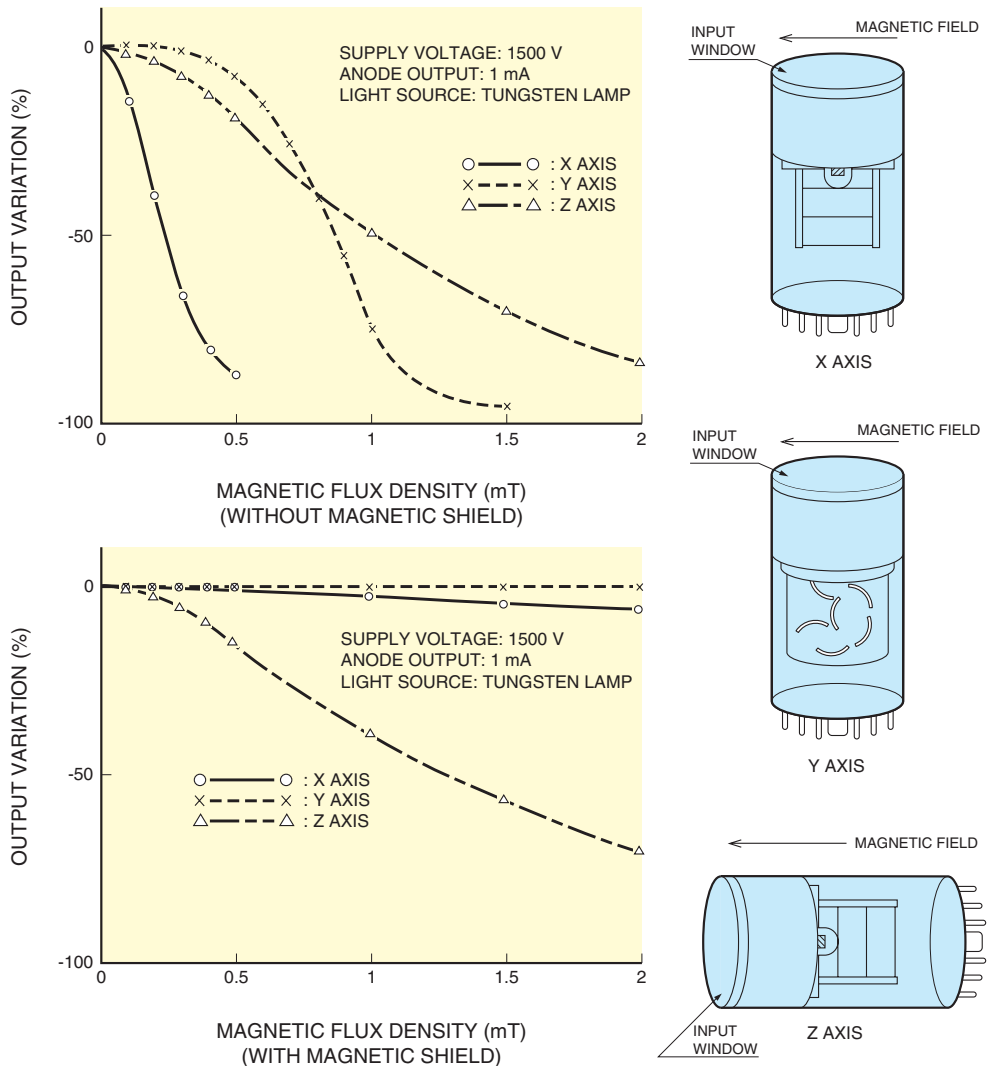
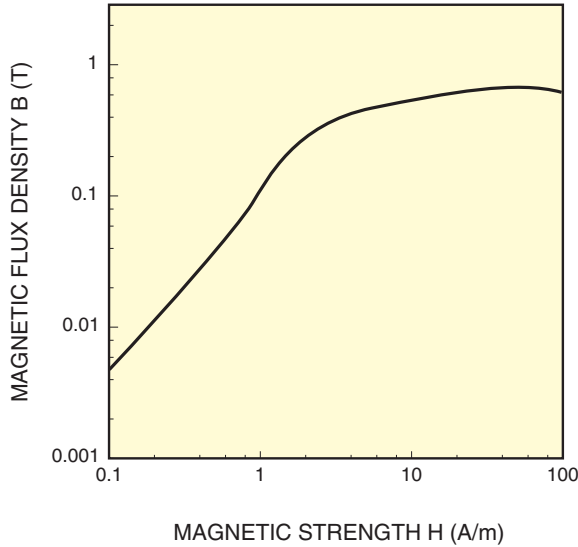


Figure 5-70: Magnetic characteristics of a photomultiplier tube

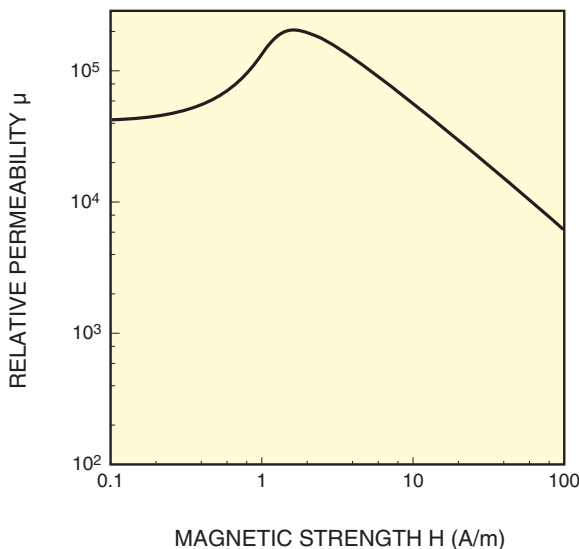
(2) Saturation characteristics

When plotting a B-H curve which represents the relationship between the external magnetic field strength (H) and the magnetic flux density (B) traveling through a magnetic material, a saturation characteristic is seen as shown in Figure 5-71.



THBV4_0571EA

Figure 5-71: DC magnetization curve (B-H curve)

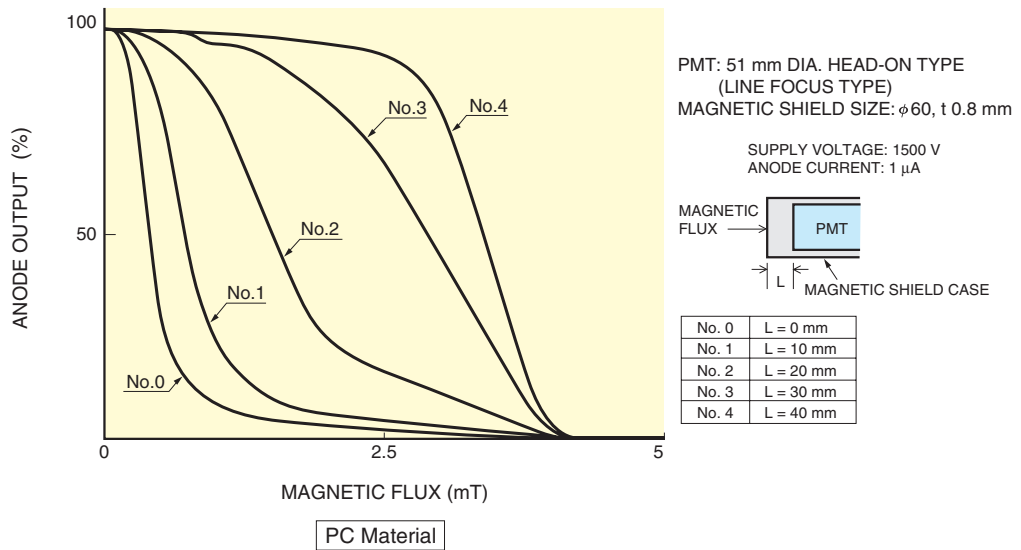


THBV4_0572EA

Figure 5-72: Permeability and external magnetic field strength

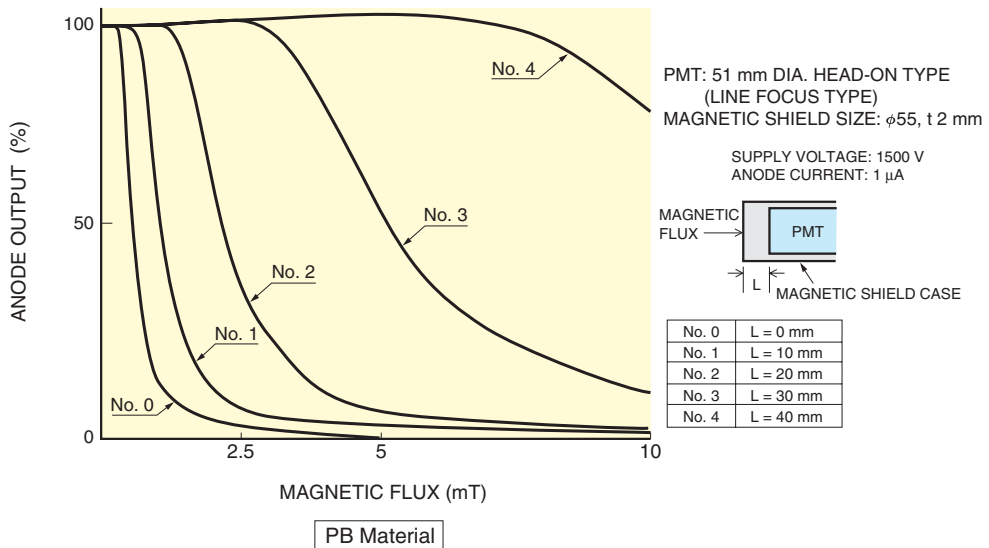
Since the relative permeability μ of a magnetic material is given by the B/H ratio, the B/H curve has a peak at a certain H level as shown in Figure 5-72, and above this level the permeability or shielding factor degrades sharply. Data shown in Figure 5-72 was measured using a magnetic shield case E989 (0.8 millimeter thick) manufactured by Hamamatsu Photonics when a magnetic field is applied in a direction perpendicular to the axis of the shield case.

Magnetic shield cases are made of a PC material which contains large quantities of nickel. This material assures very high permeability but has a rather low saturation level of magnetic flux density. In a weak magnetic field such as from the earth's magnetism, the PC material provides a shielding factor as high as 10^3 and thus proves effective in shielding out the earth's magnetism. In contrast, PB materials (Ni-Fe) which contain small quantities of nickel offer high saturation levels of magnetic flux density, though the permeability is lower than that of the PC material. Figures 5-73 and 74 respectively show the anode output variations of a photomultiplier tube used with a magnetic shield case made of a PC and PB material. As the magnetic flux density increases, the anode output from the photomultiplier tube used with the PC material shield case drops sharply while that used with the PB material shield case drops slowly. In a highly magnetic field, a PC material shield case should be used in conjunction with a shield case made of thick PB material or soft-iron with a thickness of 3 to 10 millimeters, which exhibits a high saturation level of magnetic flux density.



THBV4_0573EA

Figure 5-73: Magnetic characteristics of a photomultiplier tube used with magnetic shield case (PC material)

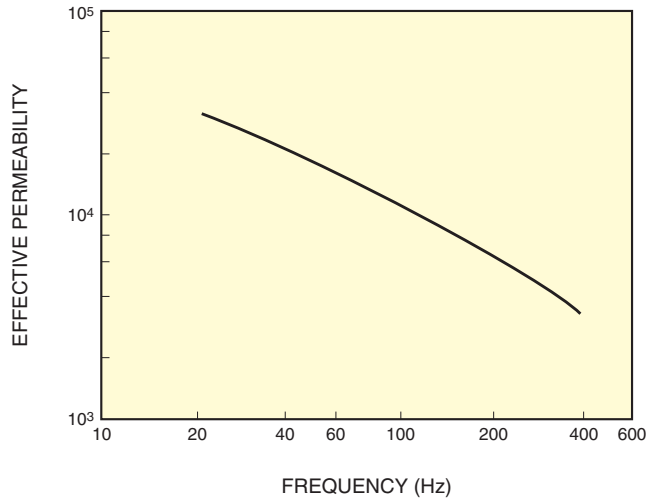


THBV4_0574EA

Figure 5-74: Magnetic characteristics of a photomultiplier tube used with magnetic shield case (PB material)

(3) Frequency characteristics

The above description about the effects of magnetic shield cases refers entirely to DC magnetic fields. In AC magnetic fields, the shielding effect of a magnetic shield case decreases with a higher frequency as shown in Figure 5-75. This is particularly noticeable for thick materials, so it will be preferable to use a thin shield case of 0.05 to 0.1 millimeter thickness when a photomultiplier tube is operated in an RF magnetic field at frequencies from 1 to 10 kilohertz. The thickness of a magnetic shield case must there be carefully determined to find the optimum compromise between the saturation magnetic flux density and frequency characteristics.

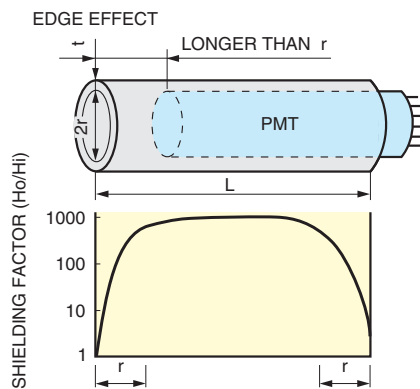


THBV4_0575EA

Figure 5-75: Frequency characteristics of a magnetic shield case

(4) Edge effect

The shielding effect given by $3\mu/4r$ applies to the case where the magnetic shield case is sufficiently long relative to the overall length of the photomultiplier tube. Considering the distance from the measurement light and the connection to the optical system, making the magnetic shield case a few millimeters to a few centimeters longer than the photomultiplier tube is practical, and its shielding effect deteriorates near both ends as shown in Figure 5-76. Since the photocathode to the first dynode region is likely to be affected by a magnetic field, this region must be carefully shielded in applications where the magnetic characteristics are important. For example, in the case of a head-on photomultiplier tube, it should be positioned deep inside the magnetic shield case so that the photocathode surface is hidden from the shield case edge by a length equal to the shield case radius or diameter.



THBV4_0576EA

Figure 5-76: Edge effect of a magnetic shield case

(5) Photomultiplier tube magnetic characteristics and shielding effect

Figure 5-77 below shows magnetic characteristics of typical photomultiplier tubes (anode output variations versus magnetic flux density) and the shielding effects of magnetic shield cases (Hamamatsu E989 series). These graphs prove that use of a shield case can greatly reduce the effect from magnetic flux density of a few milliteslas.

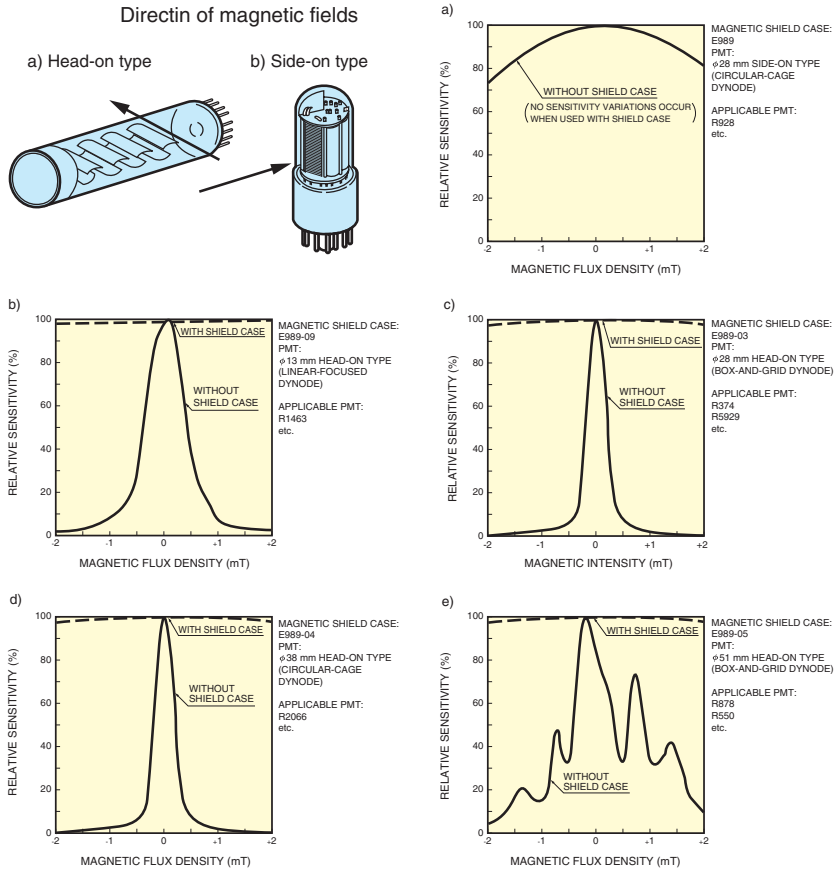


Figure 5-77: Effects of magnetic shield case

(6) Handling the magnetic shield case

Magnetic shield cases are subject to deterioration in performance due to mechanical shock and deformation. Once the performance has deteriorated, a special annealing process is required for recovery. Special skill is also needed to drill and machine shield cases so extreme care should be exercised during handling.

In the case of a photomultiplier tube with a grounded anode, its light input window and glass bulb are maintained at a negative high voltage. If any object at ground potential is brought close to those portions, the photomultiplier tube noise increases significantly. Because of this, a magnetic shield case larger than the diameter of the photomultiplier tube is used and the photomultiplier tube should be properly installed in the center of the shield case to avoid possible electrical problems. To do this, a cushioning material such as soft tape is used to wrap around the photomultiplier tube so that the gap to the magnetic shield case is uniform. In this case, the cushioning material must have high insulation properties since a high voltage is applied to the photomultiplier tube.

Connecting a magnetic shield case to the cathode potential via a resistor of 5 to 10 megohms helps reduce the effects from noise except when using a photomultiplier tube with HA treatment (see 13.8.2 in Chapter 13) or a grounded cathode scheme with a positive high voltage applied to the anode. In this case, sufficient care must be taken with regards to the insulation of the magnetic shield case to prevent electrical shock.

Figures 5-78 and 5-79 show examples of magnetic shield cases assembled with a housing and flange available from Hamamatsu Photonics. These assemblies have a structure that easily integrates a photomultiplier tube, socket assembly (voltage-divider circuit), and magnetic shield case. The flange can be used for connection to other equipment.

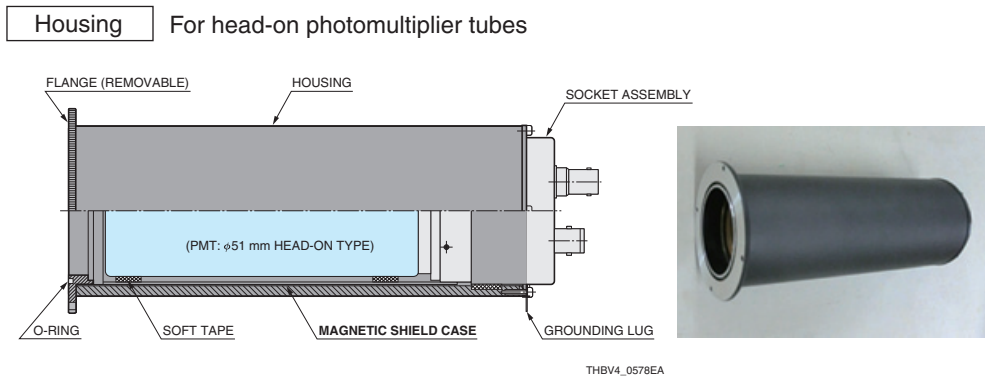


Figure 5-78: Magnetic shield case assembled in E1341-01 housing

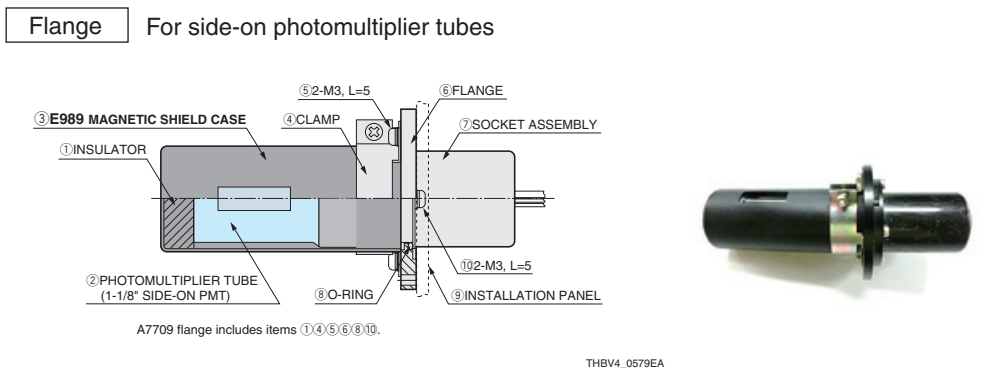


Figure 5-79: Magnetic shield case assembled with A7709 flange

5.5 Cooling

As described in Chapter 4, thermionic emission of electrons is a major cause of dark current in a photomultiplier tube. When the photomultiplier tube is operated in a normal supply voltage range, the thermionic electron emissions from the photocathode are predominant. This means that cooling the photomultiplier tube can effectively reduce the dark current and the resulting noise pulses, improving the signal-to-noise ratio and enhancing the lower detection limit. Although dependent on measurement conditions, one guideline for improving the signal-to-noise ratio of typical photomultiplier tubes by cooling is that the photocathode temperature is kept below 0 °C. Thermionic electron emission will be drastically reduced if further cooled down to around -30 °C.

Commonly used cooling techniques include air cooling, water cooling, and thermoelectric cooling. Air cooling using a heatsink needs only a simple structure and easy to use but the cooling effect is limited by the ambient temperature. In contrast, water cooling and thermoelectric cooling are capable of cooling to a temperature below the ambient temperature and so are more effective than air cooling. However, the design and structure used for water cooling and thermoelectric cooling are usually large and complex.

Hamamatsu Photonics provides cooled type side-on photomultiplier tubes, for example, the R9182-01 is designed so that the photocathode is directly cooled to reduce dark current and improve the signal-to-noise ratio by one order of magnitude compared to room temperature operation. These cooled type photomultiplier tubes have a heat-conductive metal top plate directly connected to the photocathode for efficient cooling. Hamamatsu Photonics also provides a thermoelectrically cooled photosensor module (H7844) which integrates a R9182-01 photomultiplier tube, a thermoelectric cooling element, and a highly efficient high voltage power supply into a compact housing.



Figure 5-80: Cooled type side-on photomultiplier tube R9182-01



Figure 5-81: Thermoelectrically cooled photosensor module H7844

The cooled type photomultiplier tubes described above have a structure that allows direct cooling of the photocathode. But not all photomultiplier tubes have such a structure ideal for direct photocathode cooling and in actual use the entire photomultiplier tube is usually cooled. (The cooling temperature differs depending on the photomultiplier tube.)

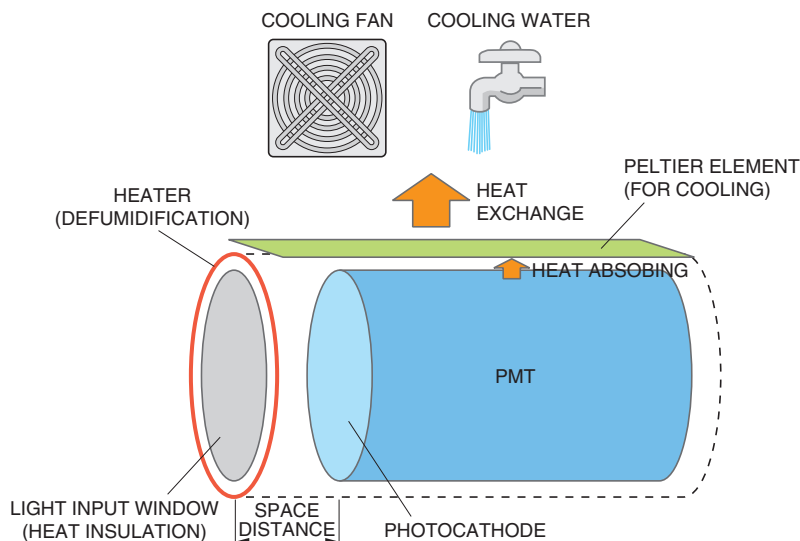
Now we explain coolers that cool the entire photomultiplier tube.

Figure 5-82 is a schematic diagram of a thermoelectric cooler, and Figure 5-83 shows coolers currently available from Hamamatsu Photonics. The C10372 is designed for 51 or 38 millimeter diameter head-on photomultiplier tubes, the C10373 is for MCP-PMT (microchannel plate – photomultiplier tubes), and the C9143 and C9144 are for 28 millimeter diameter photomultiplier tubes. The C9144 is an air-cooled thermoelectric cooler and the others are water-cooled thermoelectric coolers. The thermoelectric cooling element used for these coolers is a Peltier element. The Peltier element is a semiconductor device that freely conducts cooling, heating, and temperature regulation by controlling the current flow. The Peltier element has no parts that mechanically move and generate vibration or sound which means it is highly reliable and ideal for cooling of photomultiplier tubes.

Besides the Peltier element, these coolers include heat exchange devices (heatsink, cooling fan, or water circulator, etc.) that dissipate and exhaust heat generated as a result of cooling. Furthermore, since the cooling temperature in these coolers reaches below 0 °C, their light input window uses an evacuated double-pane made of silica glass to insulate heat from the ambient air. A heater is also installed around the light input window to prevent moisture condensation. The time needed to reach the maximum cooling temperature after cooling starts is about 60 minutes for the C9143 (ambient temperature: 20 °C, cooling temperature: -30 °C).

These coolers are designed for low-light-level measurement requiring high sensitivity. However, as shown by the schematic in Figure 5-82, there is a space between the light input window and the photocathode, and the incident light does not directly strike the photocathode. The light intensity may be affected by distance so when using a cooler, be aware of this distance from the light input window and the photocathode of the photomultiplier tube. A common technique to avoid the light attenuation due to this distance is to use an optical system for focusing the incident light.

Also be aware of environmental conditions, since the cooling capacity depends on the ambient temperature and also on the cooling water temperature for the water-cooled type. Moreover, the cooling capacity may drastically drop if a heat-exchange device such as the fan or the cooling water hose is clogged, so periodic maintenance is necessary as described in the instruction manual.



THBV4_0582EA

Figure 5-82: Schematic diagram of a cooler

Special measures should also be necessary for socket assemblies (including voltage-divider circuit) that are used during cooling. For example, care should be taken to avoid various problems relating to heat insulation, heat dissipation, moisture condensation, and mechanical stress on the photomultiplier tube. Using a socket assembly equipped with no measures against these factors may not only reduce the cooling capacity, but also cause moisture condensation on the photomultiplier tube which may deteriorate the insulation and damage the voltage-divider circuit, etc. We provide socket assemblies⁵⁾ including the necessary measures specifically for use with our coolers.



C10372/C10373 series coolers for head-on photomultiplier tubes



C9143/C9144 series coolers (including accessories) for side-on photomultiplier tubes

Figure 5-83: Coolers (C10372/C10373, C9143/C9144) available from Hamamatsu Photonics

References in Chapter 5

- 1) Hamamatsu Photonics Catalog: Photomultiplier Tubes and Related Products
- 2) S. Uda; Musen Kogaku (Wireless Engineering) I, New Edition, Transmission Section, Maruzen
- 3) Hamamatsu Photonics Technical Information: Photomultiplier Tubes for Use in Scintillation Counting
- 4) H. Igarashi, et al.: Effect of Magnetic Field on Uniformity of Gamma Camera, Nuclear Medicine Vo. 28, No. 2 (1991)
Ref. to "Improvement of 20-inch diameter photomultiplier tubes" published by A. Suzuki (KEK, Tsukuba) and others
- 5) Hamamatsu Photonics Catalog: Photomultiplier Tubes and Related Products

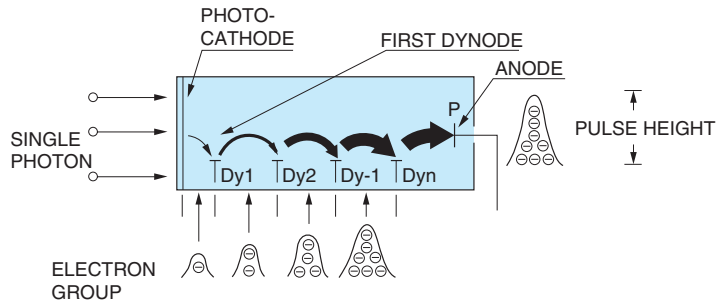
CHAPTER 6

PHOTON COUNTING ^{1) 2) 4) - 12)}

Photon counting is an effective technique used to detect very-low-level-light such as Raman spectroscopy, fluorescence analysis, and chemical or biological luminescence analysis where the absolute magnitude of the light is extremely low. This chapter describes the principles of photon counting, its operating methods, detection capabilities, and advantages as well as typical characteristics of photomultiplier tubes (PMT) designed for photon counting.

6.1 Analog and Digital (Photon Counting) Modes

The methods of processing the output signal of a photomultiplier tube can be broadly divided into analog and digital modes, depending on the incident light intensity and the configuration and bandwidth of the output processing circuit. As Figure 6-1 shows, when light strikes the photocathode of a photomultiplier tube, photoelectrons are emitted. These electrons are multiplied by secondary emission repeated in the electron multiplier (normally 10^6 to 10^7 times) and finally reach the anode connected to an output processing circuit.

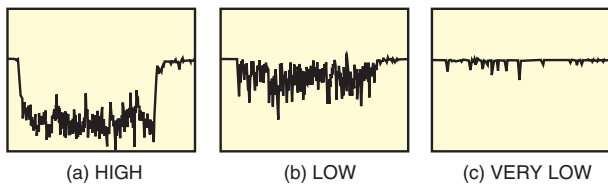


THBV4_0601EA

Figure 6-1: Photomultiplier tube operation in photon counting mode

When observing the output signal of a photomultiplier tube with an oscilloscope while varying the incident light level, output pulses like those shown in Figure 6-2 are seen. At higher light levels, the output pulse intervals are narrow so that they overlap each other, producing an analog waveform (similar to (a) and (b) of Figure 6-2). If the light level becomes very low, the ratio of AC component (fluctuation) in the signal increases, and finally the output signal will be discrete pulses (like (c) of Figure 6-2). By discriminating these discrete pulses at a proper binary level, the number of the signal pulses can be counted in a digital mode. This is commonly known as photon counting.

In analog mode measurements, the output signal is the mean value of the signals including the AC components shown in Figure 6-2 (a). In contrast, the photon counting can detect each pulse shown in Figure 6-2 (c), so the number of counted pulses equals the signal. This photon counting uses a pulse height discriminator that easily separates the signal pulses from the noise components, enabling high-precision measurement with a higher signal-to-noise ratio compared to the analog mode and making photon counting exceptionally effective in detecting low level light.



THBV4_0602EA

Figure 6-2: Photomultiplier tube output waveforms observed at different light levels

6.2 Principle of Photon Counting

When light incident on a photomultiplier tube becomes very low and reaches a state in which no more than two photoelectrons are emitted within the time resolution (pulse width) of the photomultiplier tube, this light level is called the single photoelectron region and photon counting is performed in this region. Quantum efficiency, an important parameter for photon counting, signifies the probability of photoelectron emission when a single photon strikes the photocathode.

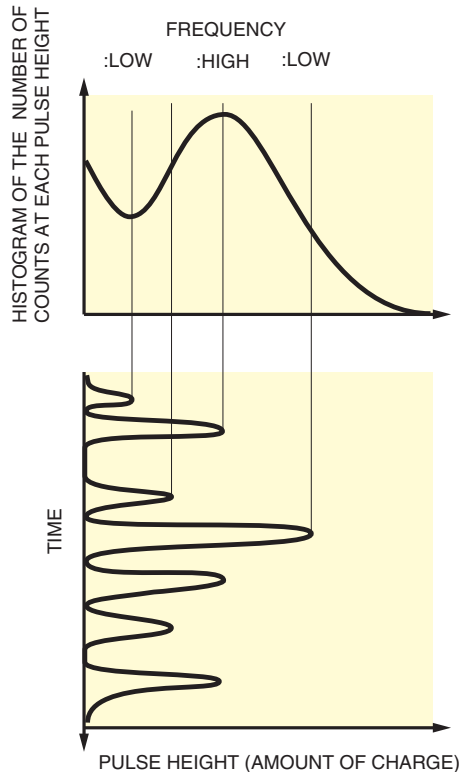
In this single photoelectron region, the number of emitted electrons per photon is one or zero and the quantum efficiency can be viewed as the ratio of the number of photoelectrons emitted from the photocathode to the number of incident photons per unit time. The probability that the photoelectrons emitted from the photocathode (primary electrons) will impinge on the first dynode and contribute to gain is referred to as collection efficiency. Some photoelectrons may not contribute to gain because they deviate from the normal trajectories and are not collected by the first dynode. Additionally, in the photon counting mode, the ratio of the number of counted pulses (output pulses) to the number of incident photons is called detection efficiency or photomultiplier tube counting efficiency and is expressed by the following equation:

$$\text{Detection efficiency (counting efficiency)} = (N_d/N_p) = \eta \times \alpha \quad \text{..... (Eq. 6-1)}$$

in the photon counting region

where N_d is the counted value, N_p is the number of incident photons, η is the quantum efficiency of the photocathode, and α is the collection efficiency of the electron multiplier. The detection efficiency greatly depends on the threshold level used for binary processing.

The number of secondary electrons released from the first-stage dynode is not constant. It is around several secondary electrons per primary electron, with a broad probability roughly seen as a Poisson distribution. The average number of electrons per primary electron δ corresponds to the secondary-electron multiplication factor of the dynode. Similarly, this process is repeated through the second and subsequent dynodes until the final electron bunch reaches the anode. In this way the output multiplied in accordance with the number of photoelectrons from the photocathode appears at the anode. If the photomultiplier tube has n stage dynodes, the photoelectrons emitted from the photocathode are multiplied up to δ^n times and derived as an adequate electron bunch from the anode. In this process, each output pulse obtained at the anode exhibits a certain distribution in pulse height because of fluctuations in the secondary multiplication factor at each dynode (statistical fluctuation due to multiplication), non-uniformity of multiplication depending on the dynode position and electrons deviating from their favorable trajectories. Figure 6-3 illustrates a histogram of photomultiplier tube output pulses. The abscissa indicates the pulse height and the anode output pulses are integrated with time. This graph is known as the pulse height distribution. Figure 6-3 also shows the relation between the pulse height distribution and the actual output pulses obtained with a photomultiplier



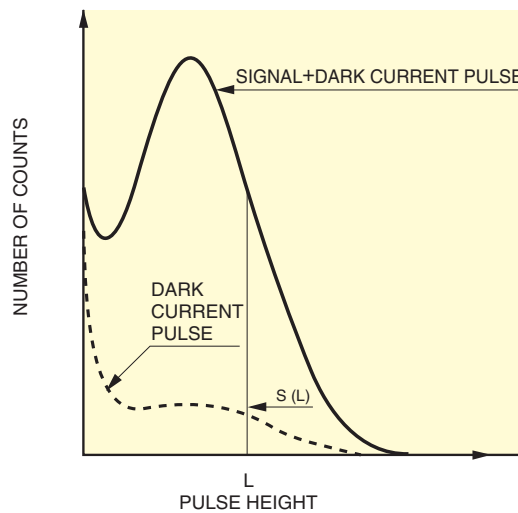
THBV4_0603EA

Figure 6-3: Photomultiplier tube output and its pulse height distribution

tube, as seen in the time series. The pulse height distribution is usually taken with a multichannel analyzer (MCA) frequently used in radiation measurement applications.

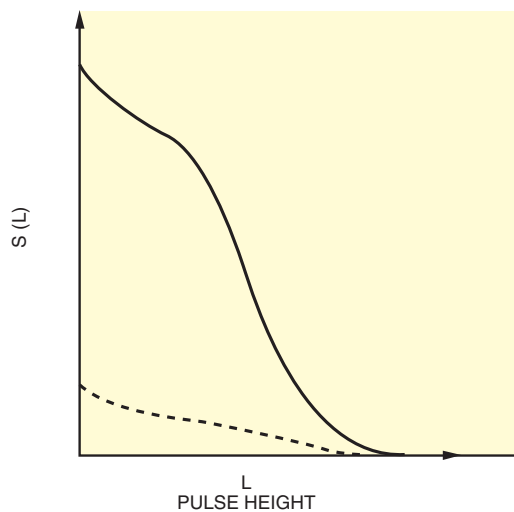
Figure 6-4 (a) shows examples of the pulse height distribution obtained with a photomultiplier tube. There are output pulses present even if no light falls on the photomultiplier tube, and these are called dark current pulses or noise pulses. The broken line indicates the distribution of the dark current pulses, with a tendency to build up somewhat in the lower pulse height region (left side). These dark pulses mainly originate from the thermal electron emission at the photocathode and also at the dynodes. The thermal electrons from the dynodes are multiplied less than those from the photocathode and are therefore distributed in the lower pulse height region.

Figure 6-4 (b) indicates the distribution of the total number of counted pulses $S(L)$ with amplitudes greater than a threshold level L shown in (a). Graphs (a) and (b) have differential and integral relations to each other. Graph (b) is a typical integral curve taken with a photon counting system using a photomultiplier tube.



(a) DIFFERENTIAL SPECTRUM

THBV4_0604EAa



(b) INTEGRAL SPECTRUM

THBV4_0604EAb

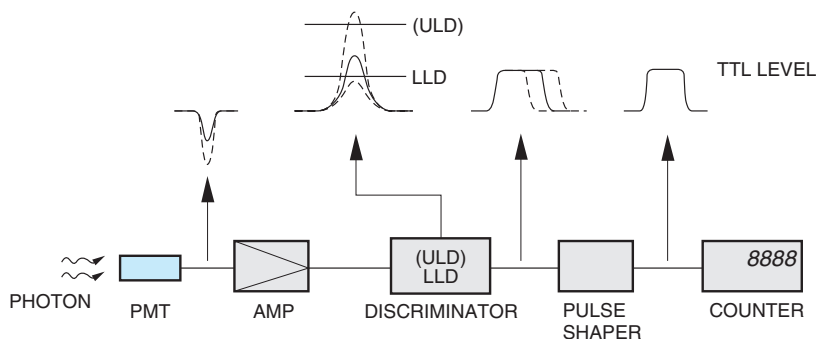
Figure 6-4: Differential and integral representations of pulse height distribution

6.3 Operating Method and Characteristics of Photon Counting

This section discusses specific circuit configurations used to perform photon counting and the basic characteristics involved in photon counting.

(1) Circuit configuration

Figure 6-5 shows a typical circuit configuration for photon counting and a pulse waveform obtained at each circuit.



THBV4_0605EA

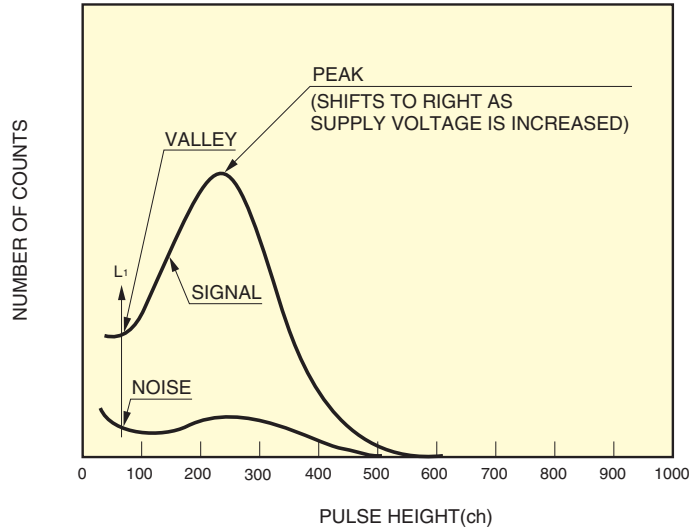
Figure 6-5: Circuit configuration for photon counting

In the above system, current output pulses from a photomultiplier tube are converted to a voltage by a wide-band preamplifier and amplified. These voltage pulses are fed to a pulse height discriminator and then to a pulse shaper. Finally the number of pulses is counted by a counter. The discriminator compares the input voltage pulses with the preset reference voltage (threshold level) and eliminates those pulses with amplitudes lower than this value. In general, the LLD (lower level discrimination) level is set at the lower pulse height side. The ULD (upper level discrimination) level may also be often set at the higher pulse height side to eliminate noise pulses with higher amplitudes. The counter is usually equipped with a gate function, allowing measurement at different timings and intervals.

(2) Basic characteristics of photon counting

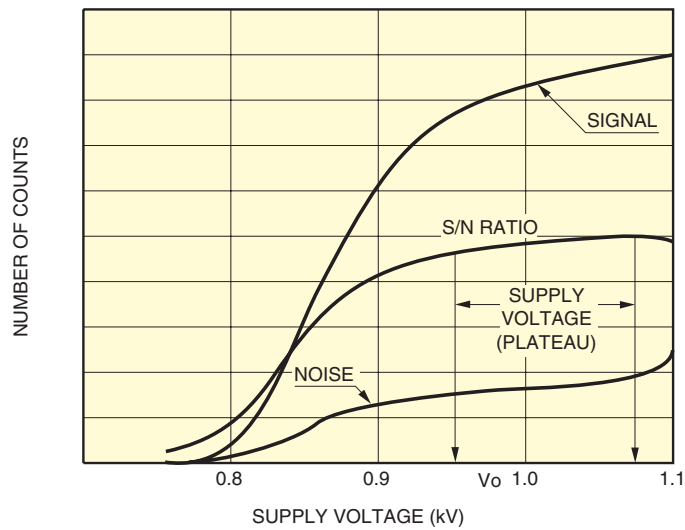
a) Pulse height distribution and plateau characteristics

If a multichannel pulse height analyzer is available, a proper threshold level can be set in the pulse height distribution. Typical pulse height distributions of signal pulses and noise pulses are shown in Figure 6-6. Because the dark current pulses are usually distributed in the lower pulse height region, setting the LLD level in the vicinity of the valley (L_1) of the distribution can effectively eliminate such noise pulses without sacrificing the detection efficiency. In actual operation, however, using a pulse height analyzer is not so popular. Other methods that find plateau characteristics using the circuit of Figure 6-5 are more commonly employed. By counting the total number of pulses with amplitudes higher than the preset threshold level while varying the supply voltage for the photomultiplier tube, plots similar to those shown in Figure 6-7 can be obtained. These plots are called the plateau characteristics. In the plateau range, the change in the number of counts less depends on the supply voltage. This is because only the number of pulses is digitally counted in photon counting, while in the analog mode the gain change of the photomultiplier tube directly affects the change of the output pulse height.



THBV4_0606EA

Figure 6-6: Pulse height distribution characteristics



THBV4_0607EA

Figure 6-7: Plateau characteristics

b) Setting the photomultiplier tube supply voltage

The signal-to-noise ratio is an important factor from the viewpoint of accurate measurements. Here the signal-to-noise ratio is defined as the ratio of the mean value of the signal count rate to the fluctuation of the counted signal and noise pulses (expressed in standard deviation or root mean square). The signal-to-noise ratio curve shown in Figure 6-7 is plotted by varying the supply voltage, the same procedure which is used to obtain the plateau characteristics. This figure implies that the photomultiplier tube should be operated in the range between the voltage (V_0) at which the plateau region begins and the maximum supply voltage.

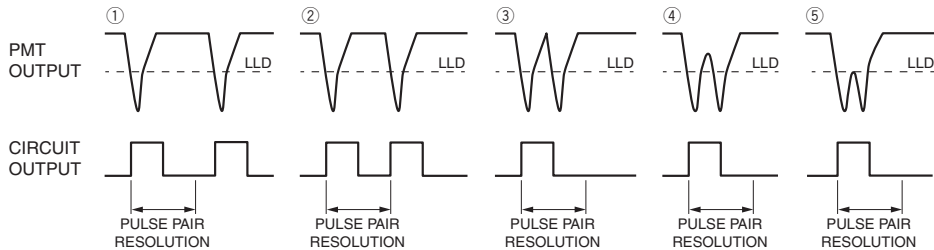
c) Count rate linearity

Pulse pair resolution

The photon counting mode offers excellent linearity over a wide range. The lower limit of the count rate linearity is determined by the number of dark current pulses, and the upper limit by the maximum count rate. The maximum count rate further depends on pulse-pair resolution, which is the minimum time between pulses or namely the minimum time interval at which each pulse can be separated.

The pulse pair resolution is determined by the response speed of the photomultiplier tube itself and also by the signal processing circuit including the amplifier, discriminator, and pulse shaper. Generally, the response speed of the photomultiplier tube itself is faster than the signal processing speed, so the pulse pair resolution during counting is determined by the pulse pair resolution of the signal processing circuit.

Figure 6-8 below shows the relation between the output pulse intervals from a photomultiplier tube and the output pulses from a signal processing circuit.



THBV4_0608EA

Figure 6-8: Linearity of count rate

When the output pulse intervals of the photomultiplier tube are wider than the pulse pair resolution of the circuit (① and ②), the number of pulses output from the circuit is equal to the number of pulses output from the photomultiplier tube. However, when the output pulse intervals from the photomultiplier tube are narrower than the pulse pair resolution of the circuit (③ and ④), the number of pulses output from the circuit is less than the pulses output from the photomultiplier tube even if each output pulse is separated. This difference in output pulses causes a loss of count. When the output pulse interval of the photomultiplier tube shortens further (⑤), the individual photomultiplier tube output pulses can no longer be separated to count.

Linearity

There are two factors that affect the linearity in the photon counting mode: a “paralyzed model” and a “non-paralyzed model.” In the “paralyzed model,” no output is obtained (paralyzed) when the counted pulses continuously overlap. In the “non-paralyzed model,” however, an output can be obtained at pulse pair resolution intervals even if the pulses overlap.

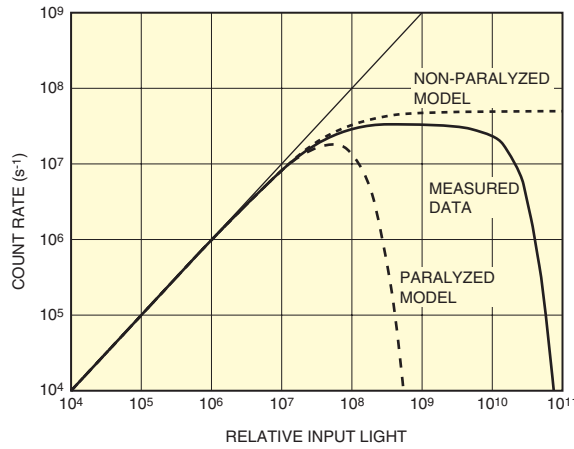
When the output pulses of a photomultiplier tube overlap, individual pulses cannot be separated and the operation is “paralyzed.” Here, if we let the true count rate be N (s^{-1}) and the pulse pair resolution be t (s^{-1}), then the measured count rate M (s^{-1}) in the paralyzed state is expressed by the following equation:

$$M = N \cdot \exp(-N \cdot t) \dots\dots\dots \text{(Eq. 6-2)}$$

In “non-paralyzed” operation, the loss in the count rate $N - M$ can also be expressed as $N \cdot M \cdot t$ using the dead time $M \cdot t$ caused by pulse overlapping. So the measured count rate, from $N - M = N \cdot M \cdot t$, is therefore given as follows:

$$M = \frac{N}{N \cdot t + 1} \dots\dots\dots \text{(Eq. 6-3)}$$

Figure 6-9 shows linearity data for a pulse pair resolution of 20 ns by comparing the result calculated using the above equations with the actually measured count rate from photon counting. In the region where linearity is relatively good, the measured count rate is nearly the same as the calculated result for non-paralyzed operation. When the light level is further increased, the output count rate drastically decreases as in the case of paralyzed operation. This is caused not only by overlapping output pulses from the photomultiplier tube but also by a baseline shift resulting from anode capacitor coupling and a change in DC linearity (change in photomultiplier tube gain) caused by an increase in the average current.



THBV4_0609EA

Figure 6-9: Linearity in photon counting mode

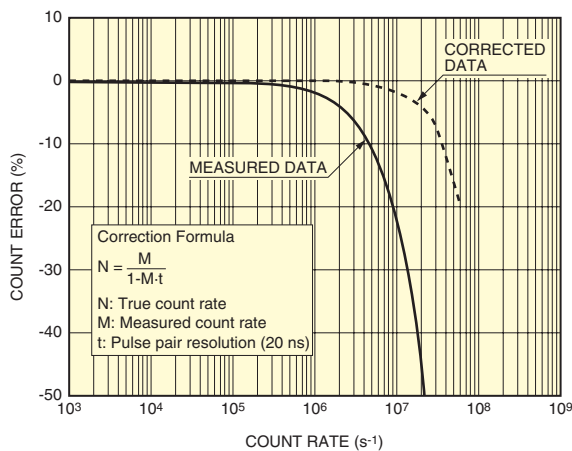
Count rate correction

As described above, in the region where linearity is relatively good, the measured count rate is nearly the same as non-paralyzed operation. The true count rate N can therefore be obtained by using the following equation which is a modified form of the equation for non-paralyzed operation.

$$N = \frac{M}{1-M \cdot t} \dots\dots\dots (Eq. 6-4)$$

The count error can then be corrected by using this equation.

Figure 6-10 shows examples of count rate linearity data before and after correction, measured using a system with a pulse pair resolution of 20 nanoseconds. The count error is corrected to within 2 % even at a count rate exceeding 10^7 s^{-1} .



THBV4_0610EA

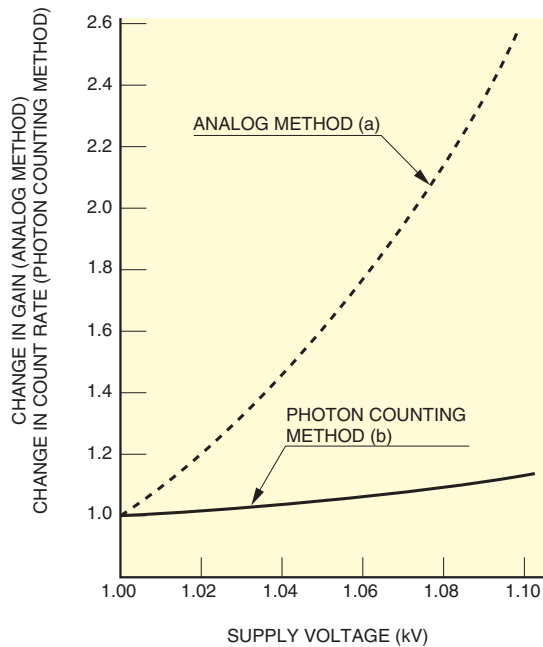
Figure 6-10: Linearity correction of count rate

d) Advantages of photon counting

Photon counting offers several advantages over the analog mode. This section describes stability and signal-to-noise ratio.

(I) Stability

One of the advantages photon counting offers is stability. This means that the photon counting mode is resistant to variations in supply voltage and photomultiplier tube gain. If the supply voltage is set within the plateau region, a change in the voltage has less effect on the output count. In the analog mode, however, this change in voltage has a large effect on the output current. Immunity to variations in the supply voltage means that the photon counting mode also ensures high stability against gain change of in the photomultiplier tube. Normally the photon counting mode offers very high immunity to such variations compared to the analog mode. (See Figure 6-11.)



THBV4_0611EA

Figure 6-11: Stability versus changes in supply voltage

High stability means that the count rate does not decrease much even if the photomultiplier tube output drops after a long period of operation. Figure 6-12 shows examples of output changes over a long period of time. In the photon counting mode, the output current of the photomultiplier tube is low (1 μA or less) so the photomultiplier tube undergoes less change over time. In addition, the output is also stable against gain fluctuations, allowing stable operation over extended periods of time that are much longer than in the analog mode.

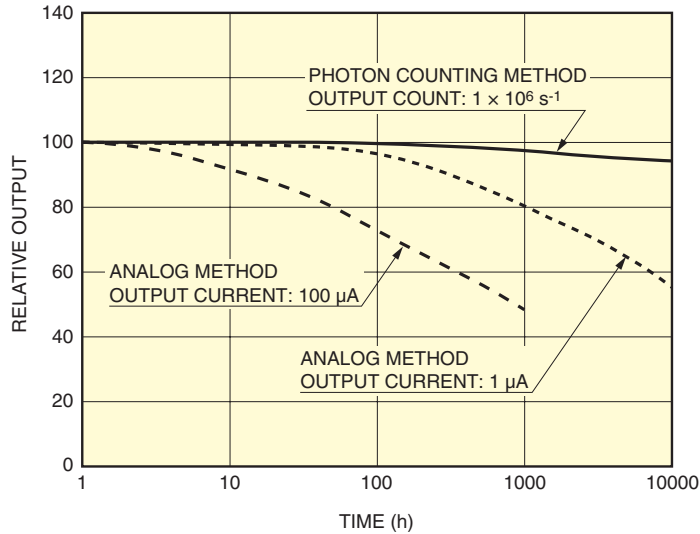


Figure 6-12: Changes in output over time

THBV4_0612EA

(II) Signal-to-noise ratio

When signal light strikes the photocathode of a photomultiplier tube, photoelectrons are emitted and directed to the dynode section where secondary electrons are produced. The number of photoelectrons produced per unit time and also the number of secondary electrons produced show fluctuations (AC components) since they are determined by the statistical probability of events which is represented by Poisson distribution. The signal-to-noise ratio is also described in 4.3.7 in Chapter 4. The AC component noise superimposed on the signal can be categorized by origin as follows:

- (1) Shot noise resulting from signal light
- (2) Shot noise resulting from background light
- (3) Shot noise resulting from dark current

In the analog mode, the signal-to-noise ratio^(2) - 9, 11) of the photomultiplier tube output including these shot noises becomes

$$SN \text{ ratio}(\text{current}) = \frac{I_{ph}}{\sqrt{2eNF B \{I_{ph} + 2(I_b + I_d)\}}} \dots\dots\dots (\text{Eq. 6-5})$$

where

- I_{ph}: signal current produced by incident light (A)
- e: electron charge (c)
- NF: noise figure of the photomultiplier tube
- I_b: cathode current resulting from background light (A)
- I_d: cathode current resulting from dark current (A)
- B: Bandwidth of measurement system (Hz)

Here the true signal current I_{ph} is obtained by subtracting I_b+I_d from the total current. The noise originating from the latter-stage amplifier is considered negligible because the typical gain μ of a photomultiplier tube is sufficiently large. The signal-to-noise ratio in the photon counting mode is given by the following equation:

$$SN \text{ ratio} = \frac{N_s\sqrt{T}}{\sqrt{N_s+2(N_b+N_d)}} \dots\dots\dots (Eq. 6-6)$$

where

- Ns: number of counts/second resulting from incident light per second
- Nb: number of counts/second resulting from background light per second
- Nd: number of counts/second resulting from dark current per second
- T: measurement time (s)

Here the number of counts/second of true signals N_s is obtained by subtracting N_b+N_d from the total number of counts.

By utilizing the common equivalent relation between the time and frequency ($T=1/2B$), if $B=1$ (Hz) and $T=0.5$ (s), the signal-to-noise ratio can be found as follows:

In the analog mode

$$SN \text{ ratio(current)} = \frac{I_{ph}}{\sqrt{2eNF\{I_{ph}+2(I_b+I_d)\}}} \dots\dots\dots (Eq. 6-7)$$

In the photon counting mode

$$SN \text{ ratio} = \frac{N_s}{\sqrt{N_s+2(N_b+N_d)}} \dots\dots\dots (Eq. 6-8)$$

The above analysis shows that the photon counting mode provides a better signal- to-noise ratio by a factor of the noise figure NF. Since the dark current includes thermal electrons emitted from each dynode in addition to those from the photocathode, its pulse height distribution will shift toward the lower pulse height side. The dark current component can therefore be effectively eliminated by use of a pulse height discriminator while maintaining the signal component to ensure further improvement in the signal-to-noise ratio. Moreover, since only the AC pulses are counted, the photon counting mode is not affected by the DC leakage current.

References in Chapter 6

- 1) IEC PUBLICATION 306-4, 1971
- 2) Illes P. Csorba "Image Tubes" Howard W, Sams & Co. (1985)
- 3) F. Robben: Noise in the Measurement of Light with PMs, pp. 776-, Appl. Opt., 10, 4 (1971)
- 4) R. Foord, R. Jones, C. J. Oliver and E. R. Pike: Appl. Opt., 8, 10, (1969)
- 5) R. Foord, R. Jones, C.J. Oliver and E.R. Pike: Appl. Opt. 1975, 8 (1969)
- 6) J.K. Nakamura and S.E. Schmarz: Appl. Opt., 1073, 7, 6 (1968)
- 7) J.K. Nakamura and S. E. Schwarz: Appl. Opt., 7, 6 (1968)
- 8) R.R. Alfano and N. Ockman: Journal of the Optical Society of America, 58, 1 (1968)
- 9) T. Yoshimura, K. Hara and N. Wakabayashi: Appl. Optics, 18, 23 (1979)
- 10) T.S. Durrani and C. A. Greated: Appl. Optics, 14, 3 (1975)
- 11) Hamamatsu Photonics Technical Publication: Photon Counting (2001)
- 12) A. Kamiya, K. Nakamura, M. Niigaki: Journal of the Spectroscopical Society of Japan, 52, 4, 249 (2003)

CHAPTER 7

SCINTILLATION COUNTING

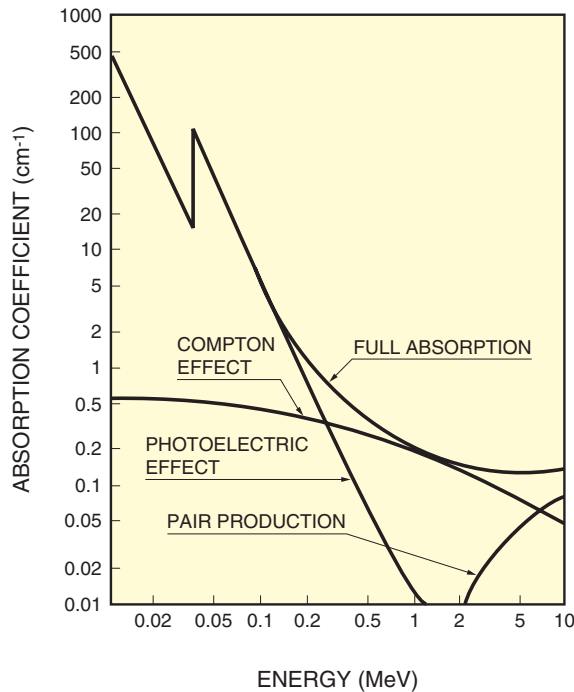
Radiation of various types is widely utilized for non-destructive inspection and diagnosis such as in medical applications, engineering applications, material analysis, and other diverse fields. In such applications, radiation detectors play an important role. There are various methods for detecting radiation.^{1) 2) 3) 4)}

For example, typical detectors include proportional counters and semiconductor detectors that make use of gas and solid ionization respectively and radiation-sensitive films, cloud chambers, and scintillation counters that utilize physicochemical changes.

In scintillation counting, the combination of a scintillator and photomultiplier tube is one of the most commonly used detectors for practical applications.^{5) 6)} Scintillation counting has many advantages over other detection methods, for example, a wide choice of scintillator materials and fast time response, high detection efficiency, and a large detection area that are features of photomultiplier tubes. This section gives definitions of photomultiplier tube characteristics required for scintillation counting and explains their measurement methods and typical data.

7.1 Scintillators and Photomultiplier Tubes

When ionizing radiation enters a scintillator, it produces a fluorescent flash with a short decay time. This is known as scintillation. In the case of gamma rays, this scintillation occurs as a result of excitation of the bound electrons by means of free electrons inside the scintillator. These free electrons are generated by the following three mutual interactions: the photoelectric effect, Compton effect, and pair production. The probability of occurrence of these interactions depends on the type of scintillators and the energy level of the gamma rays. Figure 7-1 shows the extent of these interactions when gamma-ray energy is absorbed by a NaI(Tl) scintillator.



THBV4_0701EA

Figure 7-1: Gamma-ray absorption characteristics of NaI(Tl) scintillator

From Figure 7-1, it is clear that the photoelectric effect predominates at low energy levels of gamma rays, but electron-hole pair production increases at high energy levels. Of the above three interactions, the amount of scintillation produced by the photoelectric effect is proportional to gamma-ray energy because all the energy of the gamma ray is given to the orbital electrons. The photomultiplier tube outputs an electrical charge in proportion to the amount of this scintillation, so the output pulse height from the photomultiplier tube is essentially proportional to the incident radiation energy. Accordingly, a scintillation counter consisting of a scintillator and a photomultiplier tube provides accurate radiation energy distribution and its dose rate by measuring the photomultiplier tube output pulse height and count rate. To carry out energy analysis, the current output from the photomultiplier tube is converted into a voltage output by an integrating preamplifier and fed to a PHA (pulse height analyzer) for analyzing the pulse height.²⁾ A typical block diagram for scintillation counting is shown in Figure 7-2.

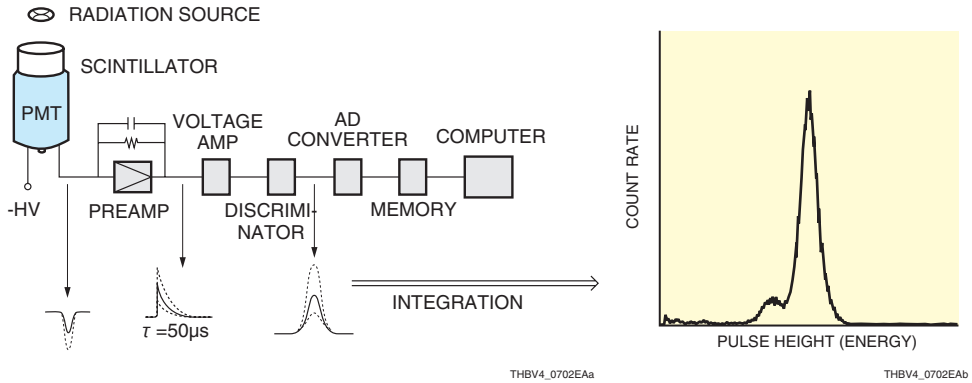


Figure 7-2: Block diagram for scintillation counting and pulse height distribution

Scintillators are divided into inorganic scintillators and organic scintillators. Most inorganic scintillators are made of a halogen compound such as NaI(Tl), BGO, BaF₂, CsI(Tl), and ZnS. Of these, the NaI(Tl) scintillator is most commonly used. These inorganic scintillators offer advantages of excellent energy conversion efficiency, high absorption efficiency and a good probability for the photoelectric effect compared to organic scintillators. Unfortunately, however, they are not easy to handle because of deliquescence and vulnerability to shock and impact. Recently, as an alternative for NaI(Tl) scintillators, YAP:Ce with high density and no deliquescence was developed. Other scintillators with high density such as LSO:Ce and GSO:Ce are used for PET (Positron Emission Tomography) scanners.

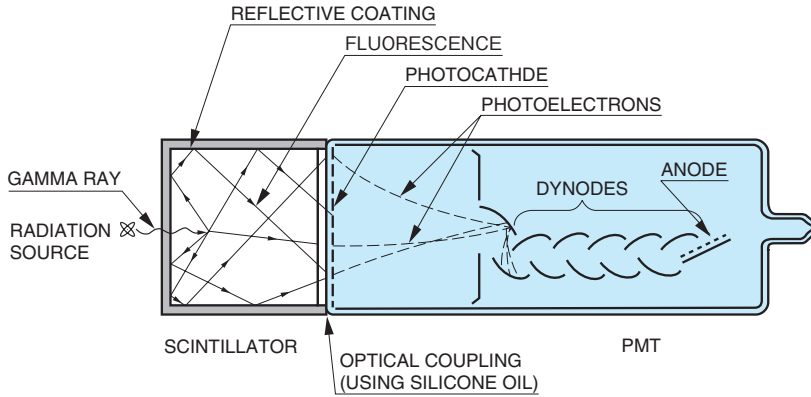
Organic scintillators include plastic scintillators, liquid scintillators, and anthracene of organic crystal. These scintillators display a short decay time and have no deliquescence. Plastic scintillators are easy to cut and shape, so they are available in various shapes including large sizes and special configurations. They are also easy to handle. However, in the detection of gamma rays, these scintillators have a low absorption coefficient and exhibit less probability for the photoelectric effect, making them unsuitable for energy analysis applications. Table 7-1 shows typical characteristics and applications of major scintillators which have been developed up to the present.

Scintillators

| Scintillators | Density (g/cm ³) | Emission Intensity (NaI(Tl) normalized at 100) | Emission Time (ns) | Peak Emission Wavelength (nm) | Applications |
|-----------------------|------------------------------|--|--------------------|-------------------------------|---|
| NaI(Tl) | 3.67 | 100 | 230 | 410 | Surveymeter, area monitor, gamma camera |
| BGO | 7.13 | 15 | 300 | 480 | PET |
| CsI(Tl) | 4.51 | 45 to 50 | 1000 | 530 | Surveymeter, area monitor |
| Pure CsI | 4.51 | <10 | 10 | 310 | High energy physics |
| BaF ₂ | 4.88 | 20 | 0.9/630 | 220/325 | TOF PET, high energy physics |
| GSO:Ce | 6.71 | 20 | 30 | 310/430 | Area monitor, PET |
| Plastic | 1.03 | 25 | 2 | 400 | Area monitor, neutron detection |
| LaBr ₃ :Ce | 5.29 | 130 | 25 | 380 | TOF PET, surveymeter |
| LSO:Ce | 7.35 | 70 | 40 | 420 | PET |
| YAP:Ce | 5.55 | 40 | 30 | 380 | Surveymeter, compact camera |
| LYSO | 7.3 | 85 to 90 | 41 | 420 | TOF PET |
| PWO | 8.28 | 0.7 | 15 | 470 | High energy physics |
| ZnS(Ag) | 4.09 | 130 | 110 | 450 | α-ray detection |

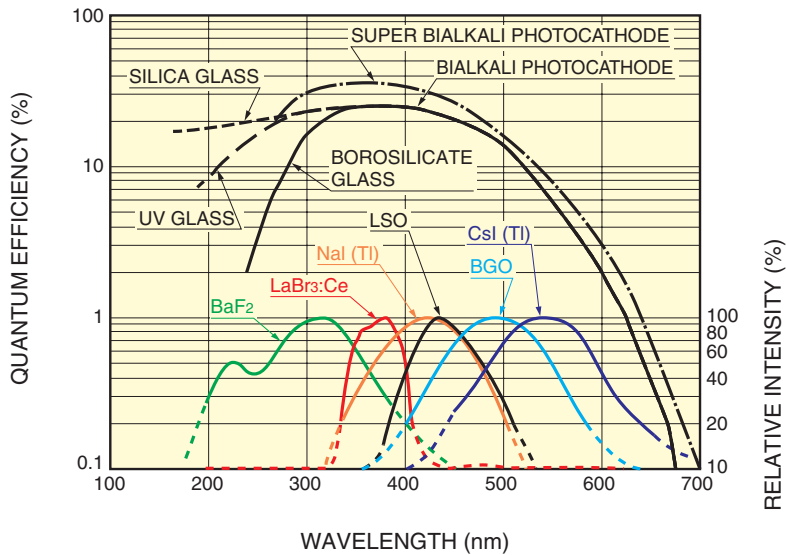
Table 7-1: Typical characteristics and applications of scintillators

A scintillator is made close contact with a photomultiplier tube by using a coupling agent as shown in Figure 7-3. The coupling agent is used in place of an air layer in order to minimize optical loss between the scintillator and the photocathode faceplate. Silicone oil having an index of refraction close to that of the glass faceplate is widely used as a coupling agent. However, selecting the proper material which provides good transmittance over the emission spectrum of the scintillator is necessary. Figure 7-4 indicates typical emission spectra of major scintillators and photocathode spectral responses of photomultiplier tubes.



THBV4_0703EA

Figure 7-3: Gamma-ray detection using a NaI(Tl) scintillator and a photomultiplier tube



THBV4_0704EA

Figure 7-4: Photocathode quantum efficiency and emission spectra of major scintillators

7.2 Characteristics

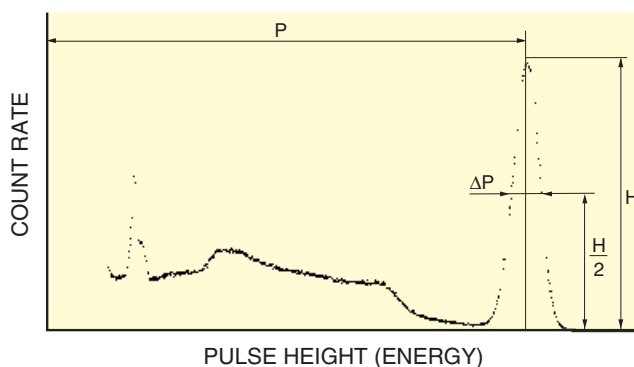
(1) Energy resolution

There are two measurement methods in scintillation counting. One is the spectrum method that uses a pulse height analyzer to measure an energy spectrum. The other is the counting method (described later on) that does not use a pulse height analyzer. In the spectrum method, pulse height discrimination is very important to determine photoelectric peaks produced by various types of radiation. This is evaluated as "energy resolution" which is also called "pulse height resolution (PHR)."

Energy resolution is defined by the following equation using Figure 7-5. It is generally expressed as a percent.

$$R = \frac{\Delta P}{P} \dots\dots\dots (\text{Eq. 7-1})$$

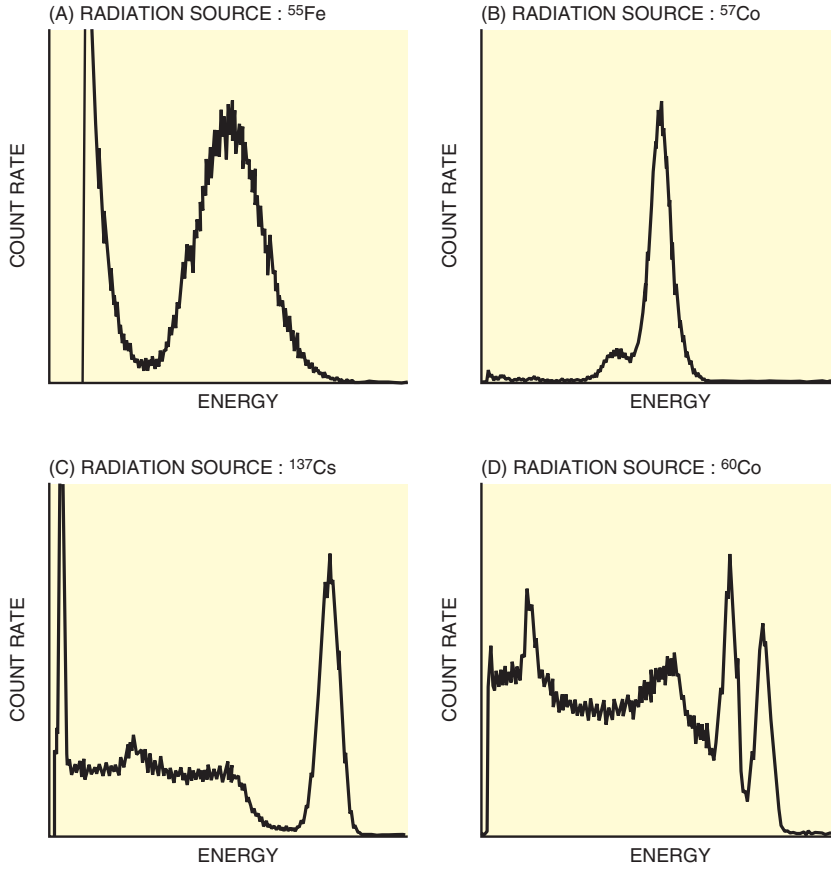
R : energy resolution
 P : peak value
 ΔP : FWHM (Full width at half maximum)



THBV4_0705EA

Figure 7-5: Definition of energy resolution

Figure 7-6 shows typical pulse height distributions for characteristic X-rays of ^{55}Fe and various kinds of gamma rays (^{57}Co , ^{137}Cs , ^{60}Co) detected by a photomultiplier tube coupled to an NaI(Tl) scintillator (measured using the same method as in Figure 7-2).



THBV4_0706EA

Figure 7-6: Typical pulse height distributions

The following factors affect the energy resolution.

- (1) Energy conversion efficiency of the scintillator
- (2) Intrinsic energy resolution of the scintillator
- (3) Light collection efficiency of the photomultiplier tube photocathode
- (4) Quantum efficiency (η) of the photomultiplier tube photocathode
- (5) Collection efficiency (α) at first dynode
- (6) Fluctuations in the gain of photomultiplier tube

Generally, energy resolution is given by

$$R^2(E) = R_s^2(E) + R_p^2(E) \quad \text{..... (Eq. 7-2)}$$

where

$$R_p^2(E) = \frac{5.56}{N\eta\alpha} \left(\frac{\delta}{\delta-1} \right) \quad \text{..... (Eq. 7-3)}$$

in which N is the average number of photons incident on the photocathode per unit disintegration, η is the quantum efficiency, α is the collection efficiency, and σ is the secondary emission yield at each dynode (assumed to be constant here). In the above equations, $R_s(E)$ is the energy resolution of the scintillator and $R_p(E)$ is that of the photomultiplier tube, both of which depend on the energy (E) of the incident gamma ray. $R_p^2(E)$ is inversely proportional to E .

When a 51-mm diameter by 51-mm length NaI(Tl) scintillator and a 51-mm diameter photomultiplier tube (Hamamatsu R6231) are used, R , R_s and R_p will be approximately as follows:

With $E = 122$ keV (^{57}Co), $R = 8.5\%$, $R_s = 6\%$, $R_p = 6\%$

With $E = 662$ keV (^{137}Cs), $R = 6.5\%$, $R_s = 5.5\%$, $R_p = 3.4\%$

To obtain higher energy resolution, the photomultiplier tubes must have high quantum efficiency and collection efficiency. Along with using a scintillator with high conversion efficiency and good inherent energy resolution, good optical coupling between the scintillator and the photomultiplier tube should be provided to reduce optical loss. For this purpose, as mentioned previously it is helpful to couple the scintillator and the photomultiplier tube using silicone oil having an index of refraction close to that of the faceplate of the photomultiplier tube.

When the scintillator is sufficiently thick, the intensity distribution of light entering the photomultiplier tube is always constant over the photocathode regardless of the radiation input position, so the photomultiplier tube uniformity has little effect on the energy resolution. However, if the scintillator is thin, the distribution of light flash from the scintillator varies with the radiation input position. This may affect the energy resolution depending on the photomultiplier tube uniformity characteristics. To avoid this problem, a light-guide is sometimes placed between the scintillator and the photomultiplier tube so that the light flash from the scintillator is diffused and allowed to enter uniformly over the photocathode.

| γ -ray source | Energy (keV) | NaI(Tl) + PMT | BGO + PMT |
|----------------------|--------------|----------------|----------------|
| ^{55}Fe | 5.9 | 40 % to 50 % | — |
| ^{241}Am | 59.5 | 12 % to 15 % | 70 % to 150 % |
| ^{57}Co | 122 | 8.5 % to 10 % | 35 % to 50 % |
| ^{22}Na | 511 | 7.5 % to 9.0 % | 13 % to 25 % |
| ^{137}Cs | 662 | 6.5 % to 8.5 % | 11 % to 20 % |
| ^{60}Co | 1,170 | 5 % to 6.5% | 8.5 % to 11 % |
| | 1,330 | 4.5 % to 5.5 % | 8.0 % to 9.5 % |

Table 7-2: Energy resolution for typical gamma-rays, obtained with NaI(Tl) or BGO scintillator

Energy resolution is one of the most important characteristics for radiation measurement devices such as gamma cameras and spectrometers. Photomultiplier tubes used in these applications are usually tested for energy resolution. Table 7-2 summarizes energy resolution for typical gamma rays measured with a combination of a NaI(Tl) and photomultiplier tube or a BGO and photomultiplier tube. As shown in the table, each data has a certain width in energy resolution. This is due to the non-uniformity of the physical size of the scintillator or photomultiplier tube and also the performance variations between individual photomultiplier tubes. If necessary, it is possible to select only those photomultiplier tubes that meet specific specifications.

(2) Relative pulse height

In scintillation counting, when a photomultiplier tube is operated at a constant supply voltage and the amplification factor of the measuring circuit is fixed, the variation of the pulse height at a photoelectric peak is referred to as the relative pulse height (RPH) and is commonly stated in terms of the channel number. This relative pulse height indicates the variation of the pulse height obtained with a photomultiplier tube in scintillation counting. It usually shows a good correlation with measurement data taken by users (instrument manufacturers) and is therefore used to select the gain range of photomultiplier tubes. When used with a NaI(Tl) scintillator, the relative pulse height provides a close correlation with blue sensitivity because the emission spectrum of the NaI(Tl) resembles the spectral transmittance of the Corning filter CS No.5-58 which is used for the blue sensitivity measurement, so the relative pulse height has a strong correlation with the anode blue sensitivity index. (Refer to (3) in 4.1.4 of Chapter 4.)

(3) Linearity

Linearity of the output pulse height of a photomultiplier tube with respect to the amount of scintillation flash is another important parameter to discuss. Since linearity of general-purpose photomultiplier tubes has already been described earlier, this section explains how to measure linearity related to scintillation counting. Figure 7-7 shows a typical pulse height distribution for the ^{226}Ra taken with a NaI(Tl) and Figure 7-8 indicates the relationship between each peak channel and the gamma-ray energy. Because the ^{226}Ra releases various kinds of radiation ranging in energy from 10.8 keV to 2.2 MeV, it is used for linearity measurements over a wide energy range.

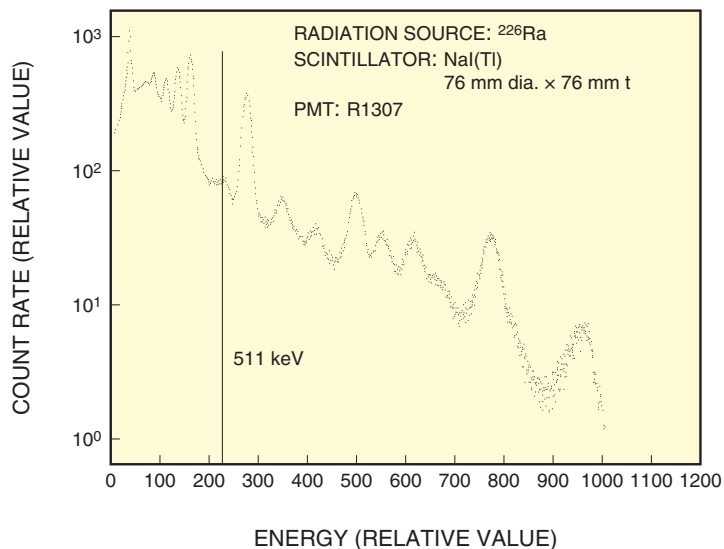
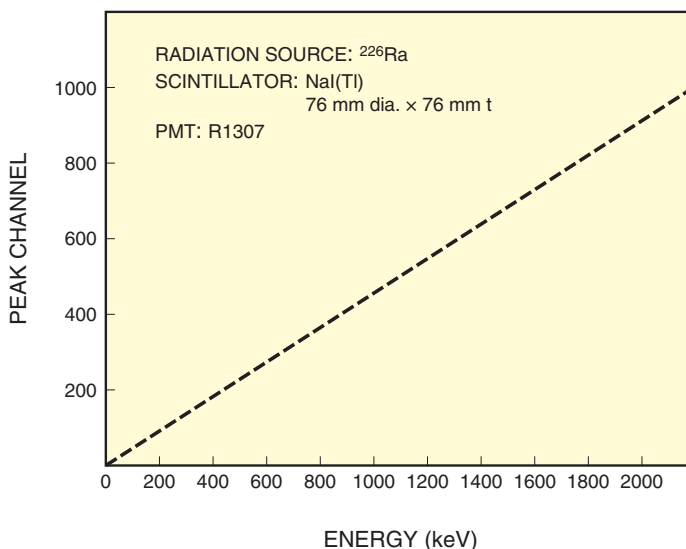


Figure 7-7: Pulse height distribution for ^{226}Ra taken with NaI(Tl)



THBV4_0708EA

Figure 7-8: Relation between peak channel and gamma-ray energy

Amount of emission from a NaI(Tl) scintillator equals about 30 photons per 1 keV of gamma-ray energy. Accordingly, some 20 000 photons ($662 \text{ keV} \times 30$) are generated with ^{137}Cs and some 40 000 photons ($1330 \text{ keV} \times 30$) are generated with ^{60}Co . When ^{60}Co is used for linearity measurements under the conditions that the photomultiplier tube gain is at 10^6 and the decay constant (τ_s) of the NaI(Tl) scintillator is 230 nanoseconds, the photomultiplier tube output current (I_p) is given by

$$\begin{aligned}
 I_p &= \frac{N \times \eta \times \mu \times e}{\tau_s} \dots\dots\dots (\text{Eq. 7-4}) \\
 &= \frac{4 \times 10^4 \times 0.25 \times 10^6 \times 1.6 \times 10^{-19}}{230 \times 10^{-9}} \\
 &= 7 \times 10^{-3} \text{ (A)}
 \end{aligned}$$

N : amount of light flash per event produced from scintillator
 η : quantum efficiency of photocathode (assumed to be 25 %)
 μ : gain of photomultiplier tube
 e : electron charge
 τ_s : decay time of NaI(Tl)

Thus in this measurement the photomultiplier tube must have a pulse linearity over 7 milliamperes. In particular, care should be taken with respect to the linearity range when measuring radiation at higher energy levels as the photomultiplier tube detects a large amount of light flash.

(4) Uniformity

The uniformity characteristics of a photomultiplier tube affect the performance of systems utilizing scintillation counting, especially in such equipment as SPECT (Single Photon Emission Computed Tomography) cameras used to detect the incident position of radiation. Uniformity of a photomultiplier tube is commonly defined as the variation in the output current with respect to the photocathode position on which a light spot is scanned.

(5) Stability

There are two types of stability tests used in scintillation counting: long term stability and short term stability. Both stability tests employ a ¹³⁷Cs radiation source and a NaI(Tl) scintillator. The variation in the photopeak pulse height obtained from a photomultiplier tube is measured with a multi-channel analyzer (MCA). The measurement method of these stability tests differ slightly from general stability tests described earlier (see 4.2.4 in Chapter 4).

a) Long term stability

The long term stability is also referred to as the photopeak drift. In this stability test, the photomultiplier tube is allowed to warm up for one hour with the photopeak count rate maintained at 1000 s⁻¹. After this, the variation rate of the photopeak pulse height (channel number) is measured for a period of 16 hours.

The same measurement setup shown in Figure 7-2 is used and the variation occurring in the peak channel is recorded as the time elapses. This variation rate (D_{LTS}) is calculated by Eq. 7-5 and typical variation data is shown in Figure 7-9 below.

$$D_{LTS} = \frac{\sum_{i=1}^n |P_i - \bar{P}|}{n} \cdot \frac{100}{\bar{P}} \text{ (%) } \dots\dots\dots \text{(Eq. 7-5)}$$

where

- \bar{P} : mean value of photopeak pulse height (channel)
- P_i: peak pulse height at the i-th reading
- n : total number of readings for 16 hours

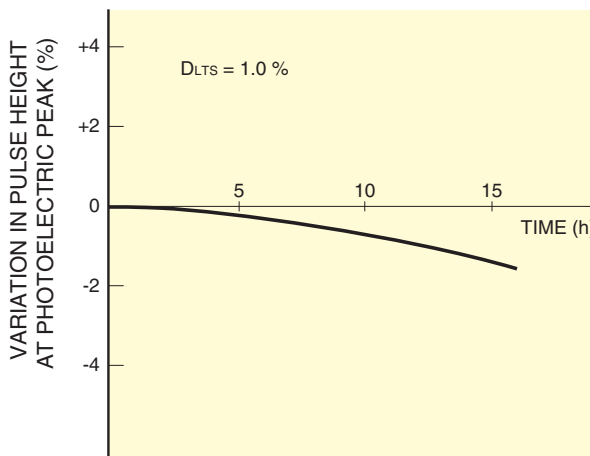


Figure 7-9: Typical long-term stability of photomultiplier tube

There are a few photomultiplier tube types that exhibit somewhat of a tendency to increase variation in photopeak pulse height during the period of 16 hours. However, most photomultiplier tubes tend to show decreasing values, with a variation rate within plus or minus several percent. This tendency is analogous to the drift characteristic explained earlier, but this test method is more practical for scintillation applications. Numerically, as shown in Eq. 7-5, the long term stability is defined as the mean deviation of the peak pulse height (or mean gain deviation) with respect to the mean pulse height. It usually has a value of 1 or 2 percent. A major cause of this output variation is that the secondary electron multiplication factor of the dynodes (particularly at the latter stages) changes over time.

b) Short term stability

The short term stability is also referred to as the count rate stability or count rate dependence. To evaluate this stability, the variation in the photopeak pulse height is measured by changing the photopeak count rate from $10\,000\text{ s}^{-1}$ to 1000 s^{-1} . If the photopeak pulse height at a count rate of $10\,000\text{ s}^{-1}$ is given by A and that at 1000 s^{-1} by B, the variation rate (D_{STS}) is given by the following equation. This value is about ± 1 percent in most cases.

$$D_{\text{STS}} = \left(1 - \frac{B}{A}\right) \times 100 (\%) \quad \dots\dots\dots (\text{Eq. 7-6})$$

It is thought that this output instability is caused mainly by a change of the electron trajectories occurring in the electron multiplier section of a photomultiplier tube. This instability is also caused by a change in the voltage applied to the latter-stage dynodes, which may occur when operated at a high count rate and the output current increases to near the voltage-divider current. (Refer to 5.1.3 in Chapter 5.) In this case, photomultiplier tubes whose gain is less dependent on voltage (the slope of gain-voltage curve is not sharp) are less affected by the dynode voltage change. Short term stability is also closely related to the hysteresis effect in photomultiplier tubes. (Refer to 4.3.5 in Chapter 4.)

(6) Noise

In scintillation counting, a signal pulse is usually produced by multiple photoelectrons simultaneously emitted from the photocathode, which create a higher pulse height than most dark current pulses do. Using a discriminator effectively eliminates most dark current pulses with lower amplitudes. Accordingly, only noise pulses with higher amplitudes may be a problem in scintillation counting.

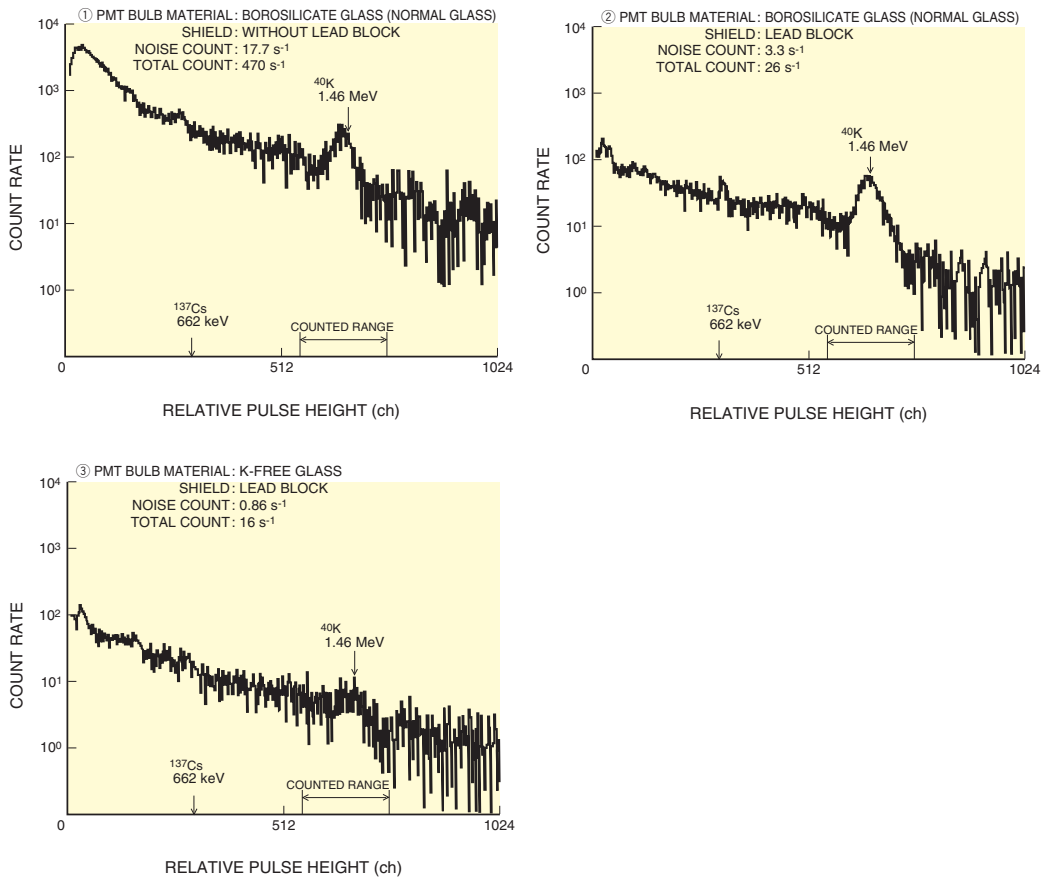
Noise pulses with higher amplitudes may be caused by radiation released from natural radioactive elements contained in a reinforced concrete building or in the atmosphere. These noise pulses may be a problem, particularly in low-level-radiation measurements. Concrete used to construct a building usually contains Rn, Th, and ^{40}Fe , and steel contains U, Th, and ^{60}Co . Radioactive floating dust and Rn or Th gases may be present in the atmosphere, and a scintillator may also contain minute amounts of ^{40}K and ^{208}Tl . Furthermore, borosilicate glass used to fabricate the faceplate of photomultiplier tubes contains potassium of which ^{40}K comprises 0.118 percent. The ^{40}K releases gamma rays of 1.46 MeV which can also be a cause of high-amplitude noise pulses.

Figure 7-10 shows background noise data measured with a Hamamatsu 127mm diameter photomultiplier tube (127 mm diameter, borosilicate glass, bialkali photocathode) coupled to a NaI(Tl) scintillator (127 mm diameter \times 51 mm length). ① in Figure 7-10 was measured without taking any countermeasures, while ② was measured by shielding the tube with two lead blocks of 100 millimeter and 50 millimeter thickness, each being placed respectively in the lower, side section and upper section. ③ is data taken with the same type of photomultiplier tube but employs a so-called K-free glass containing a very minute amount of potassium for its faceplate and side bulb envelope. Since these measurements were made using the setup in which the peak of ^{137}Cs (662 keV) becomes 300 channels, the energy range measured covers from several keV to 2.2 MeV. In this energy range, the background noise, which is as high as 470

s^{-1} during normal measurement, can be drastically reduced to $26 s^{-1}$ (about 1/20) by shielding the tube with lead blocks. This means that most background noise originate from environmental radiation. In addition, use of the 127 mm diameter photomultiplier tube with K-free glass (refer to 4.1.2 in Chapter 4) further reduces the total noise counts down to about $16 s^{-1}$. Particularly, in the energy range from 1.2 MeV to 1.6 MeV where noise count mainly results from the ^{40}K (1.46 MeV), the noise count of $3.3 s^{-1}$ measured with the 127 mm diameter photomultiplier tube (normal borosilicate glass) is reduced to $0.9 s^{-1}$ (below 1/3) with the 127 mm diameter photomultiplier tube (K-free glass).

Recently in high energy physics experiments, there is a demand for photomultiplier tubes using materials that contain extremely low levels of radioactive impurities. Such experiments are often performed deep underground where natural radioactive impurities are eliminated and therefore impose heavy demands on the photomultiplier tubes to be used there. Glass materials used for these photomultiplier tubes must be investigated to make sure the content of radioactive impurities, not only ^{40}K but also uranium and thorium series, is sufficiently low.

Since the external parts of a photomultiplier tube and the scintillator are usually maintained at ground potential, a cathode ground scheme with the high voltage applied to the anode is often used in scintillation counting. (Refer to 5.1.2 in Chapter 5.)

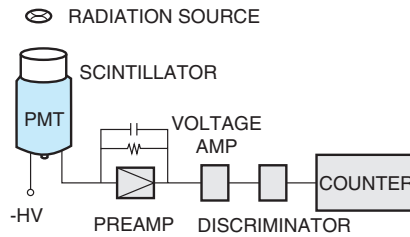


THB4_0710EA

Figure 7-10: Background noise of 127 mm diameter photomultiplier tube + NaI(Tl)

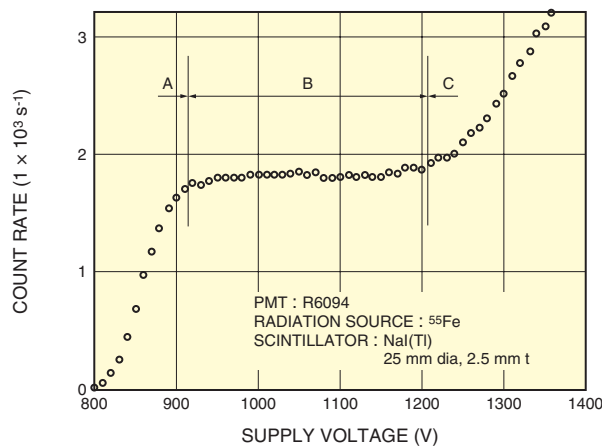
(7) Plateau characteristic

As stated, there are two measurement methods in scintillation counting. One method called the spectrum method using a pulse height analyzer has already been explained. This section will describe the other method called the counting method that does not use a pulse height analyzer. In the counting method, plateau characteristics are very important. Plateau characteristics are measured by setting a discrimination level and counting all pulses with amplitudes greater than that level. This operation is done while changing the supply voltage for the photomultiplier tube. Figure 7-11 (a) shows a block diagram for plateau characteristic measurement. Figures 7-11 (b) and (c) show typical plateau characteristics and pulse height distribution when a NaI(Tl) scintillator and ^{55}Fe radiation source are used.



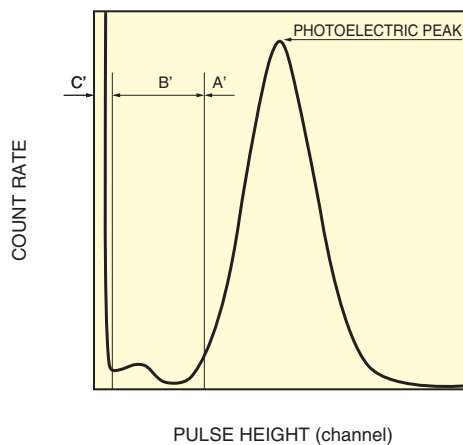
THBV4_0711EAa

Figure 7-11 (a): Block diagram for plateau characteristic measurement



THBV4_0711EAb

Figure 7-11 (b): Example of plateau characteristics

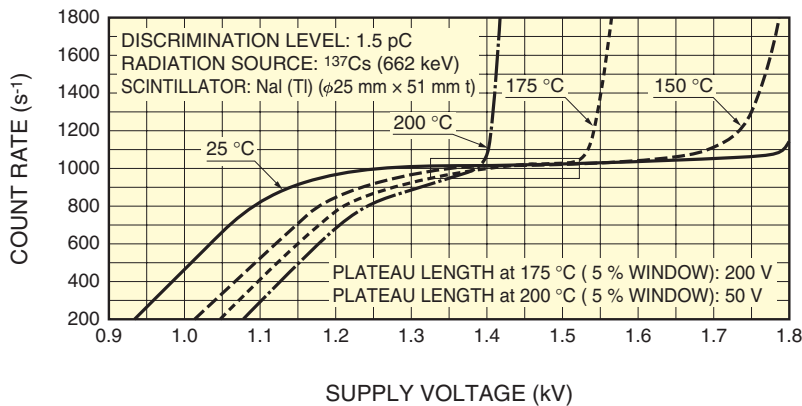


THBV4_0711EAc

Figure 7-11 (c): Pulse height (^{55}Fe and NaI(Tl) combination)

Plotting the count rate versus the photomultiplier tube supply voltage gives a curve like that shown in Figure 7-11 (b). This data can be divided into three regions (A, B and C). Region B is referred to as the plateau. In Figure 7-11 (c), region B corresponds to region B' that is the valley of the pulse height distribution. In most cases, the supply voltage should be set within this region. The count rate will not vary significantly even if the supply voltage is changed within this region. In the analog measurement method, a change in the gain of the photomultiplier tube directly affects the change in the pulse height amplitude. However, the counting method does not cause such a problem, since only the number of the binarized pulses is counted.

As an application example using the counting method, photomultiplier tubes are used for oil well logging (refer to 14.7 in Chapter 14). In this application, geological strata type and density are measured by detecting and analyzing the number of scattered radiations or natural radiations from strata. Photomultiplier tubes used for oil well logging (often called "high-temperature photomultiplier tubes") are usually tested in combination with a ^{137}Cs radiation source and a NaI(Tl) scintillator. Typical plateau characteristics obtained by this test are shown in Figure 7-12.



THBV4_0712EA

Figure 7-12: Typical plateau characteristics of a high-temperature photomultiplier tube

This measurement example shows plateau characteristic taken at 25 °C along with those obtained at 150 °C, 175 °C, and 200 °C. Because the gain of the photomultiplier tube decreases as the temperature increases, the supply voltage at which the signal appears (corresponding to region A in Figure 7-11 (b)) shifts to the higher voltage side. The dark current on the other hand increases with temperature, so its count rate sharply increases (corresponding to region C in Figure 7-11 (b)) at a low supply voltage. Consequently, the plateau width (supply voltage range) measured at higher temperatures (150 °C, 175 °C, and 200 °C) becomes narrower than that obtained at room temperatures (25 °C).

References in Chapter 7

- 1) Glenn. F. Knoll: "RADIATION DETECTION and MEASUREMENT (Third Edition)" John Wiley & Sons, Inc. (1999)
- 2) Fumio Yamazaki: "Radiation" Kyoritsu Shuppan Co., Ltd (1981) (Published in Japanese)
- 3) E. Kawada: "Radiation measurement technology" University of Tokyo Press (1978) (Published in Japanese)
- 4) M. Okamura: "Radiation measurement circuits and systems" Nikkan Kogyo Shimbun, Ltd. (1978) (Published in Japanese)
- 5) H. Kume, T. Watanabe, M. Iida, T. Matsushita and S. Suzuki: IEEE Trans. Nucl. Sci, NS-33[1], 364 (1986)
- 6) H. Kume: "Radiation" 16.11 (1989) (Published in Japanese)

MEMO

CHAPTER 8

PHOTOMULTIPLIER TUBE MODULES

This chapter describes the structure, usage, and characteristics of photomultiplier tube (PMT) modules. These PMT modules consist of a photomultiplier tube, a voltage-divider circuit, and a high voltage power supply circuit all carefully assembled into the same case.

8.1 What Are Photomultiplier Tube Modules?

Photomultiplier tube (PMT) modules basically consist of a photomultiplier tube, high voltage power supply circuit, and voltage-divider circuit to distribute a voltage to each electrode, all integrated into a compact case. In addition to this basic configuration, some PMT modules further include a current-to-voltage conversion circuit (amplifier circuit), photon counting circuit, PC interface, and cooling device. PMT modules are easy to handle and use since they eliminate the need for troublesome wiring for high voltages and operate from a low external voltage.

Hamamatsu PMT modules are broadly classified into 3 types: current output type, voltage output type, and photon counting head. Figure 8-1 shows the functions of PMT modules.

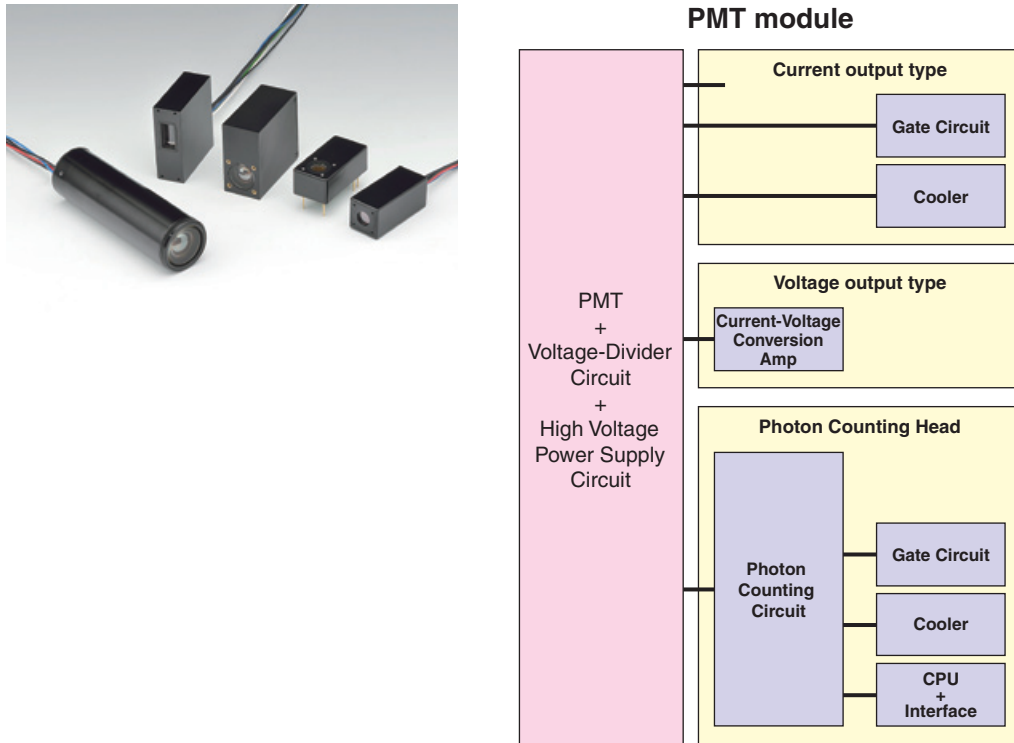


Figure 8-1: PMT module functions

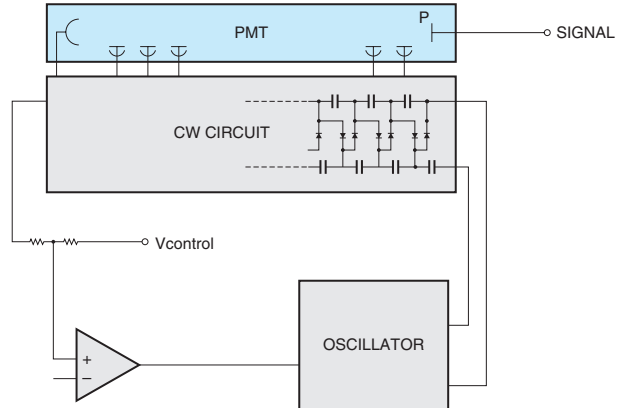
THBV4_0801EA

8.2 Power Supply Circuits

(1) High voltage power supply circuit

There are mainly two types of high voltage power supply circuits used in PMT modules. One is a Cockcroft-Walton (CW) circuit (see (1)-④ in 5.1.3 of Chapter 5) and the other is a combination of Cockcroft-Walton circuit and active divider circuit (see (1)-② in 5.1.3 of Chapter 5).

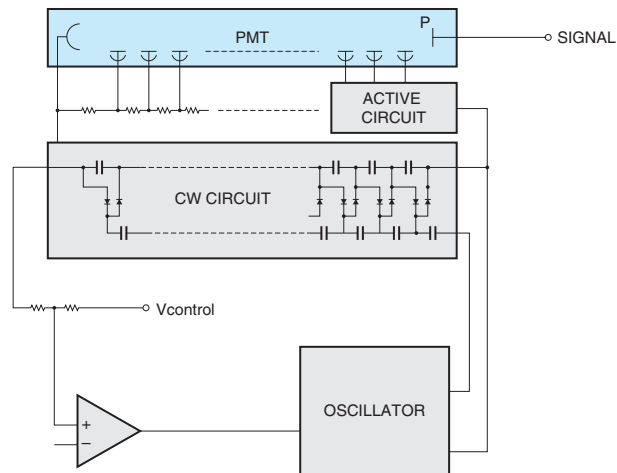
The Cockcroft-Walton circuit is a voltage multiplier circuit using capacitors and diodes. As shown in Figure 8-2, capacitors are arranged along each side of alternate connection points of serially connected diodes. The reference voltage supplied to this circuit is raised in integer multiples such as 1 times, 2 times, 3 times... and that boosted voltage then applied to each electrode. This circuit features low power consumption and good linearity for both DC and pulsed currents and has a compact design.



THBV4_0802EA

Figure 8-2: Cockcroft-Walton (CW) power supply circuit

In a power supply circuit using a Cockcroft-Walton circuit combined with active divider circuit, the voltage supplied to the entire photomultiplier tube is generated by the Cockcroft-Walton circuit, and the voltage supplied to each electrode is generated by the active divider circuit. In the active divider circuit, several voltage-divider resistors near the last dynode stages are replaced with transistors. This eliminates the effect of photomultiplier tube signal current on the interdynode voltage, achieving good linearity up to 60 or 70 % of the divider circuit current. This circuit features a shorter settling time compared to power supply circuits using only a Cockcroft-Walton circuit.



THBV4_0803EA

Figure 8-3: Power supply circuit using a Cockcroft-Walton (CW) circuit combined with active divider circuit

(2) Input voltage

Since PMT modules contain an internal high voltage power supply circuit and voltage-divider circuit inside the case, there is no need to supply a high voltage from an external power supply. In general, current-output type and voltage-output type PMT modules can be operated by simply inputting a low voltage and control voltage, and photon counting heads operated by just inputting a low voltage. When the low voltage input is within the range specified in our catalog, the high voltage supplied to the photomultiplier tube from the power supply circuit in the PMT module is kept stable. This holds true even if the output of the low voltage power supply fluctuates somewhat. However, fluctuations in the control voltage input greatly affect the output, so a low voltage power supply with high stability is required.

(3) Output current and input current

The output of a photomultiplier tube changes in proportion to the incident light intensity. As the output increases, the input current increases. An example of this relation is shown in Figure 8-4 below.

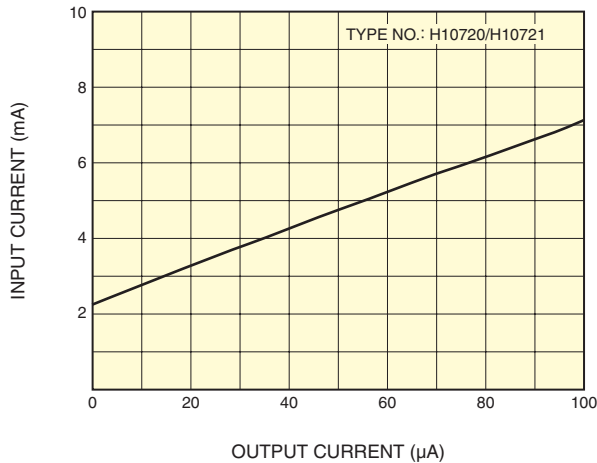


Figure 8-4: Output current vs. input current

THEV4_0804EA

8.3 Current Output Type and Voltage Output Type

(1) Gain adjustment

The PMT module gain can be adjusted by changing the control voltage. There are two methods for adjusting the control voltage as shown in Figures 8-5 and 8-6.

When directly inputting the control voltage as in Figure 8-5, supply a control voltage that does not exceed the maximum rating. The reference voltage output terminal must be left unconnected. Be careful not to let it make contact with ground.

Figure 8-6 shows a gain adjustment method using a trimmer potentiometer which is connected between the control voltage and reference voltage outputs. Adjust the trimmer potentiometer while monitoring the control voltage and be careful not to exceed the maximum rating.

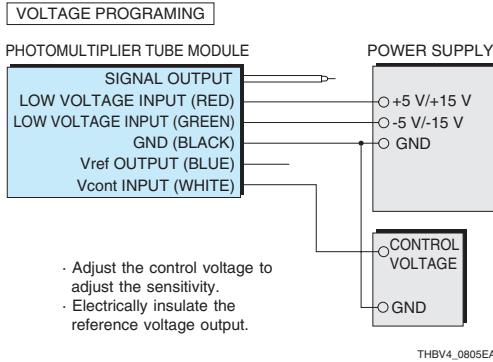


Figure 8-5: Gain adjustment by changing control voltage

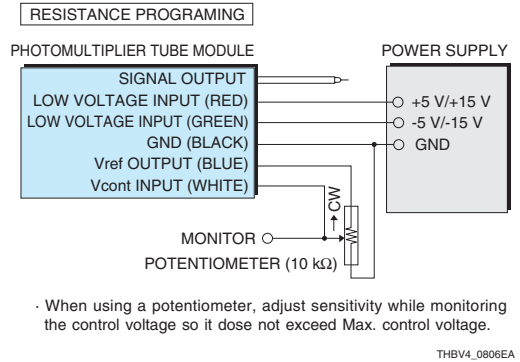


Figure 8-6: Gain adjustment using trimmer potentiometer

(2) Ripple noise

Since the high voltage power supplies in PMT modules use an oscillator circuit, unwanted oscillation noise is often coupled into the signal output by induction. This induction noise is called "ripple noise." This ripple can be observed on an oscilloscope by connecting the signal cable from a PMT module to the oscilloscope while no light is incident on the PMT module. For example, under the conditions that the load resistance is 1 megohm, load capacitance is 22 picofarads, and coaxial cable length is 45 centimeters, an output is seen along the baseline in the low voltage range. This signal output has an amplitude from about 0.1 to 1 millivolts and a frequency bandwidth of about 200 to 300 kilohertz.

Figure 8-7 shows an example of this ripple noise.

Hamamatsu PMT modules are designed to minimize this ripple noise. However, it is not possible to completely eliminate this noise. Use the following methods to further reduce ripple noise.

- ① Place a low-pass filter downstream from the PMT module signal output.
- ② Raise the control voltage to increase the photomultiplier tube gain and lower the amplifier gain.

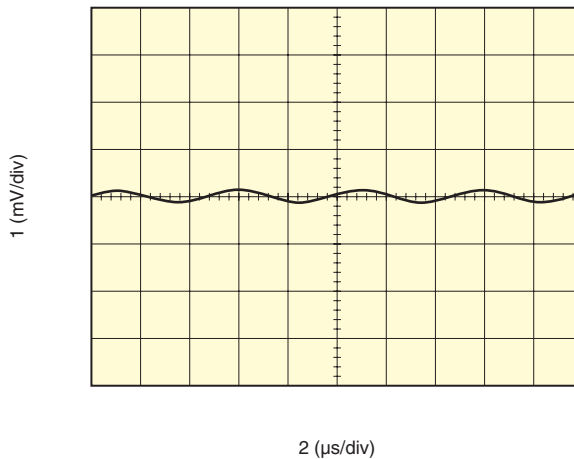


Figure 8-7: Ripple noise

THBV4_0807EA

(3) Settling time

The high voltage supplied to the photomultiplier tube changes along with a change in the input voltage for the PMT module control voltage. However, this response has a slight delay versus changes in the control voltage. The time required for the high voltage to reach the target voltage is called the "settling time." The settling time for Hamamatsu PMT modules is defined as the time required to reach the target high voltage when the control voltage is changed from +1.0 to +0.5 volts. Power supply circuits using a Cockcroft-Walton (CW) circuit combined with an active divider circuit have a fast settling time. Figure 8-8 shows a change in the high voltage supplied to the cathode.

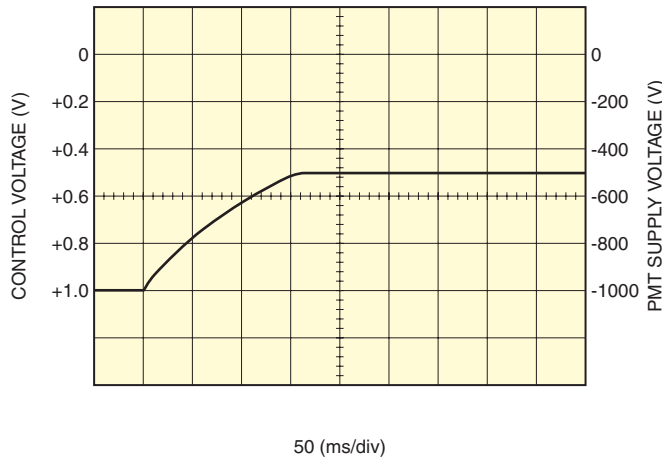


Figure 8-8: Settling time of a PMT module containing a power supply using a Cockcroft-Walton (CW) circuit combined with active divider circuit

THBV4_0808EA

8.3.1 Current output type modules

In current output type PMT modules, the anode current of the photomultiplier tube is directly available as the output (current) from the module. The output voltage changes according to the connected device load. Since the signal processing unit that connects to a photomultiplier tube usually handles voltage signals, the output current must be converted into voltage signals by some means except in cases where an ammeter is connected. An optimal current-to-voltage conversion method should be selected according to the application and measurement purpose.

(1) Output linearity (DC output mode)

PMT modules use a Cockcroft-Walton circuit and an active divider circuit with excellent output linearity, so when operated at higher control voltages, the output linearity is maintained up to the maximum average output current of the internal photomultiplier tube.

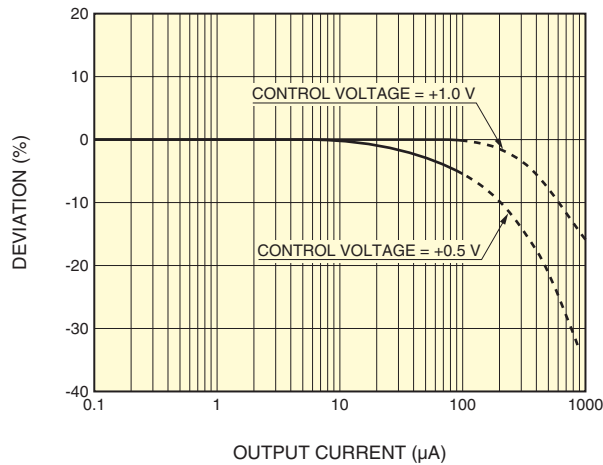


Figure 8-9: Output linearity (DC output mode)

THBV4_0809EA

8.3.2 Voltage output type modules

In voltage output type PMT modules, an op-amp is connected near the photomultiplier tube anode to convert the current to a voltage. This is more resistant to external noise than when extracting the current output of a photomultiplier tube by using a signal cable. The internal amplifier is especially effective in a measurement frequency range from a few dozen kilohertz to several megahertz where external noise effects start to become noticeable. However, amplifier power consumption tends to increase at frequency ranges higher than 10 megahertz. So in that case it is better to use a current output type PMT module by externally connecting an amplifier.

Voltage output type PMT modules incorporate an op-amp for current-to-voltage conversion. The amp's feedback resistor and capacitor also function as a charge amplifier making it possible to perform pulse measurements such as scintillation counting.

(1) Frequency characteristics

When the amplifier circuits used in PMT modules have different frequency characteristics, their output waveforms seen on an oscilloscope also differ even when the same optical phenomenon is measured. So, if a high-speed optical phenomenon is measured with a PMT module that uses a low-frequency amplifier circuit, the change in the optical phenomenon over time will not be captured correctly. Frequency characteristics must be selected by taking into account the optical phenomena to be measured.

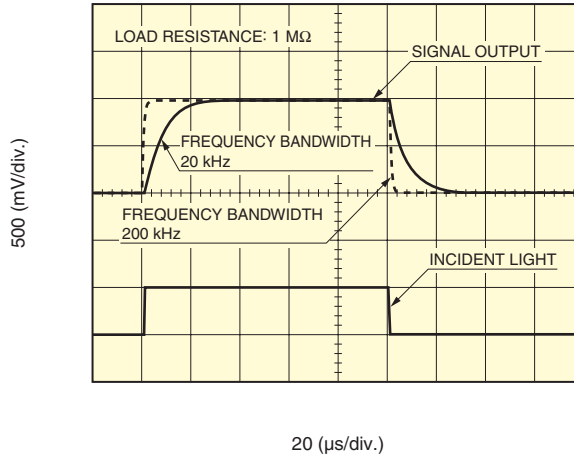


Figure 8-10: Frequency characteristics

THBV4_0810EA

(2) Offset voltage

Voltage output type PMT modules produce a small output even when the control voltage is 0 volts and the internal photomultiplier tube is not operating. This output is called the offset voltage. The offset voltage is generated by variations in the internal op-amp characteristics and appears as a positive voltage or negative voltage even when using the same type of PMT modules.

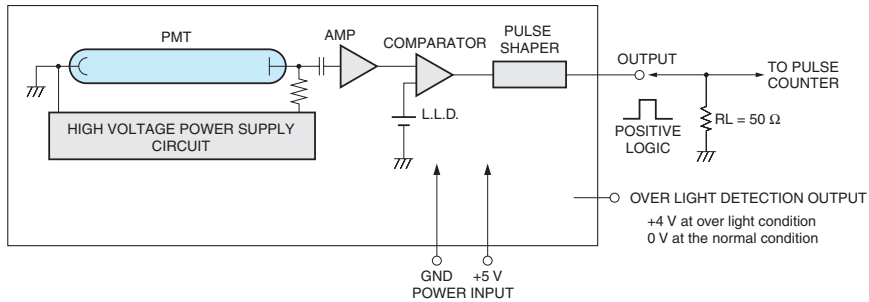
When operating a voltage output type PMT module in a dark state, an output appears that is the sum of the voltage outputs resulting from the photomultiplier tube dark current and this offset voltage.

(3) Output signal voltage

The output voltage of voltage output type PMT modules is limited by the input voltage. The output voltage is available up to a level slightly lower than the input voltage. When using a PMT module with a large current-to-voltage conversion factor, the output voltage may become saturated and result in an inaccurate output even if the output current of the photomultiplier tube is small, so use caution. In such cases, reduce the incident light level or lower the gain so that the output voltage will not saturate during measurement.

8.4 Photon Counting Heads

Photon counting heads are PMT modules that contain a photomultiplier tube, high voltage power supply, and photon counting circuit all integrated into a compact case. In a photon counting head, the current pulses from the photomultiplier tube are amplified by the amplifier, and then only those pulses higher than the set threshold level are allowed to pass through the pulse shaper for pulse output. Photon counting heads are preadjusted so that a high voltage within the plateau range is supplied to the photomultiplier tube. Supplying a low voltage from an external power supply is all that is needed to operate a photon counting head.



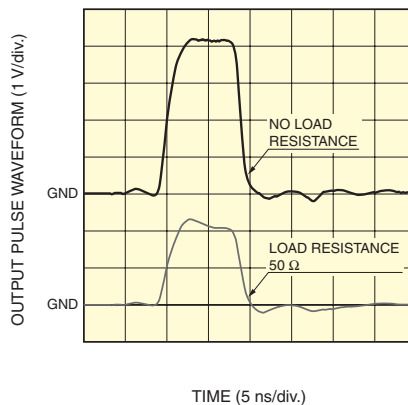
THBV4_0811EA

Figure 8-11: Block diagram of a photon counting head

(1) Output characteristics

The design of the photon counting circuit in each photon counting head differs according to the time characteristics and pulse waveforms of the internal photomultiplier tube. Because of this, the pulse voltage and pulse width differ depending on the individual photon counting head, though their output is a positive logic signal.

The output impedance of photon counting heads is designed to be approximately 50 ohms in order to handle high-speed signals. When connecting a photon counting head to a measurement device with a cable, a 50-ohm impedance cable should preferably be used and the input impedance of the measurement device should be set to 50 ohms. If the input impedance of the external circuit is not around 50 ohms and an impedance mismatch occurs, the pulses reflected from the input end of the external circuit return to the photon counting head and then reflect back from there. This might result in erroneous counts.



THBV4_0812EA

Figure 8-12: Output characteristics

(2) Count sensitivity

The counting sensitivity of a photon counting head indicates the number of output counts per second obtained when an incident light of 1 picowatt at a certain wavelength enters the photon counting head and is expressed in units of $\text{s}^{-1} \cdot \text{pW}^{-1}$. The count sensitivity is directly related to the quantum efficiency and collection efficiency of the photomultiplier tube.

(3) Dark count

Photomultiplier tubes generate a small number of dark current pulses even when operated in a dark state with no incident light. These dark current pulses are amplified by the internal amplifier and those pulses higher than the set threshold level are allowed to pass through the pulse shaper for pulse output. The dark count is the number of these output pulses per second, expressed in units of s^{-1} . The output of a photon counting head is the sum of the signal count and the dark count, so the dark count can serve as a general guide for the signal detection limit level.

(4) Pulse pair resolution

Pulse-pair resolution is the minimum time interval at which two consecutive pulses are separated and counted. Photons entering a photon counting head within this time interval are counted as only one pulse, even if two or more photons have entered. See (2)-C. in section 6.3 of Chapter 6.)

(5) Count linearity

When individual photons cyclically enter a photon counting head at a time interval equal to the pulse-pair resolution of the photon counting head, it is theoretically possible to measure the photons up to the reciprocal of the pulse-pair resolution. Photon counting is usually used in low-light-level measurements of chemiluminescence and bioluminescence, and the light input is a random phenomenon. In such cases, as the light level increases and then exceeds a certain light level, the count value becomes no longer proportional to the light level. Count linearity is a measure that indicates the loss in the counted value compared to the theoretical value. This is defined as the count value at 10 % loss. The count linearity characteristics of a photon counting head are determined by the pulse-pair resolution of the internal circuit. At a higher count rate, however, the time characteristics of the photomultiplier tube also become an important factor. Figure 8-13 shows typical count linearity characteristics of a photon counting head with a pulse pair resolution of 20 nanoseconds. The count value at 10 % loss is $5 \times 10^6 \text{ s}^{-1}$.

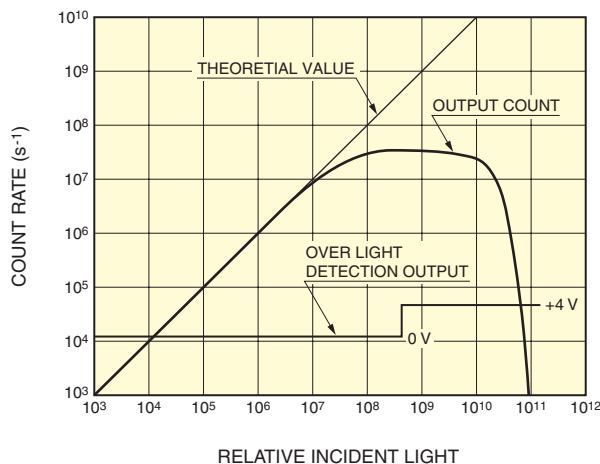


Figure 8-13: Count linearity characteristics

(6) Improving the count linearity

When the number of counts measured during photon counting exceeds 10^6 s^{-1} , the pulses begin to overlap causing counting errors. To increase the count linearity:

- ① Increase the pulse-pair resolution of the circuit.
- ② Use a prescaler to divide the frequency.
- ③ Approximate the output by using a correction formula.

The figure below shows the improvement in count linearity when the output is approximated by a correction formula.

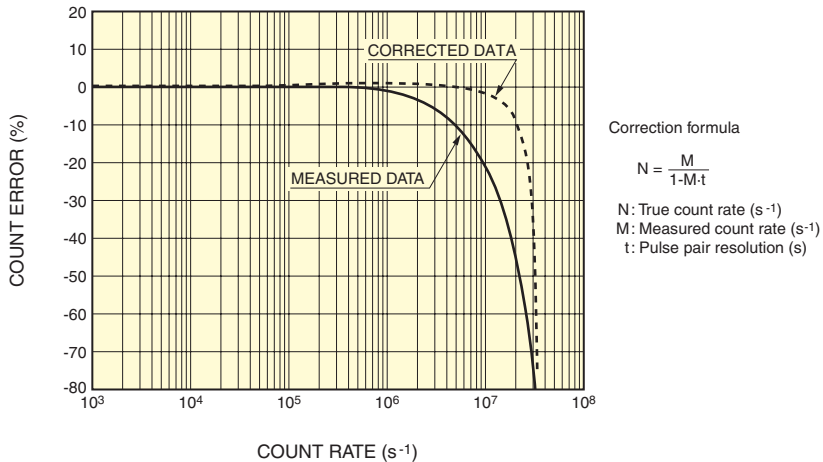


Figure 8-14: Count linearity before and after correction

THBV4_0814EA

(7) Over-light detection

As the pulses overlapping with each other increase, the output pulse count gradually plateaus and then begins to decrease, finally becoming 0 (see Figure 8-13). This means, for example, that an output pulse count of $1 \times 10^6 \text{ (s}^{-1}\text{)}$ appears at two light levels: one where the count linearity is maintained and the other where not maintained due to the input of excessive light. Some photon counting heads have an over-light detection function that outputs a voltage when excessive light enters the photomultiplier tube. Monitoring this output allows determining whether the incident light level is within the count linearity range or not. This output can also be used to control an optical shutter to reduce the incident light level and also set the photon counting head input voltage to 0 volts to stop its operation.

To check the incident light level condition for a photon counting head that does not have an over-light detection function, install for example a neutral density filter having 10 % transmittance in front of the light input surface. If the output pulse count is reduced to 1/10th, the light level is within the count linearity range. If not reduced to 1/10th, the light level is too high.

8.5 Gate Function

When excitation light such as from a laser or xenon flash lamp enters a photomultiplier tube, the signal processing circuit may become saturated causing adverse effects on the measurement. There is a method to block such excessive light by using a mechanical shutter but this method has problems such a limited mechanical shutter speed and service life. On the other hand, an electronic shutter (gate), which is controlled by changing the potential of an electrode in the photomultiplier tube, offers much higher speed and a higher extinction ratio.

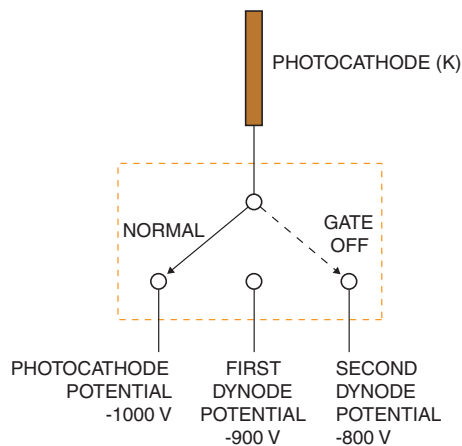
Gated PMT modules include a gate circuit that controls the potential on an electrode.

8.5.1 Gate operation

(1) Operating principle

In gate operation of a photomultiplier tube, the potential on an electrode is controlled to allow or not allow the generated photoelectrons or secondary electrons from reaching the next stage electrode. To obtain a signal output, a voltage gradient must be set up from the input toward the output at a higher potential. To set the gate operation to OFF, the potential of an electrode is set higher than the next stage electrode. As a result, photoelectrons and secondary electrons with a negative charge cannot reach the next stage electrode since it is at a lower potential, causing an interruption of the signal flow that stops the output.

Figure 8-15 shows a gate circuit example for controlling the photocathode potential. Gate OFF operation is performed by setting the photocathode potential to the same potential as the second dynode potential which is higher than the first dynode potential. Gate operation is maintained as long as this condition is maintained.



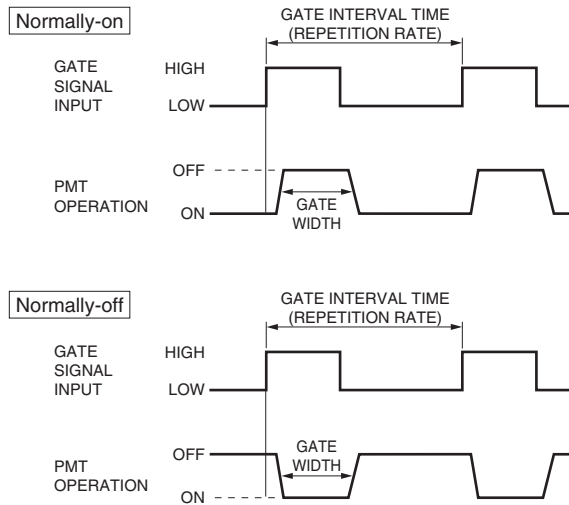
THBV4_0815EA

Figure 8-15: Gate circuit principle

Gate operation can be performed by changing the potential of only one electrode; however, controlling the potentials of two or more electrodes delivers a higher extinction ratio.

(2) Operation mode

There are two modes of gate operation: normally-on and normally-off. In normally-on mode, the photomultiplier tube is normally operated and its operation stops when a gate signal is input. In normally-off mode, the photomultiplier tube is normally not operated and operates when a gate signal is input. Select the operation mode according to the type of light to block out and the application or in other words depending on whether you want to turn the photomultiplier tube operation on or off within the gate time.



THBV4_0816EA

Figure 8-16: Operation mode

(3) Operation method

A voltage from a few dozen to 200 volts is applied between each electrode in a photomultiplier tube. It is not easy to directly change the potentials of those electrodes at high-speeds from an external source. Gated PMT modules contain a gate circuit capable of controlling the electrode potentials at high-speeds. Just supplying a low-voltage pulse signal will change the electrode potential to allow gating operation.

8.5.2 Gate characteristics

(1) Time characteristics

Time characteristics of gated PMT modules include gate time and repetition frequency, rise and fall times, and delay time. Select a gated PMT module having an optimal gate time and repetition frequency according to the application.

(2) Switching noise

Performing high-speed gate operation requires high-speed gate signals. When a gate signal is input, induction noise is induced in the anode signal through the electrostatic capacitance present across the electrodes of the photomultiplier tube as shown in Figure 8-17. This is referred to as "switching noise." This noise can be reduced by reducing the gate signal voltage or by using a noise-canceling technique. However, completely eliminating this noise is difficult.

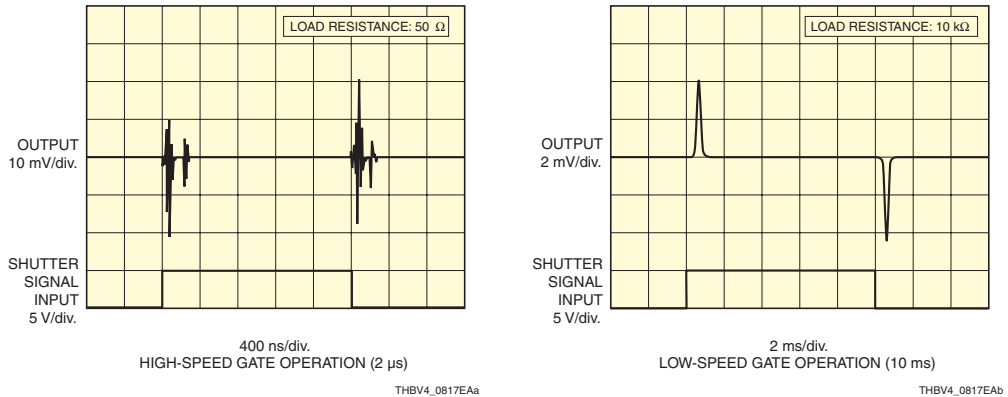


Figure 8-17: Switching noise

(3) Extinction ratio

Gate operation allows suppressing the anode current of a photomultiplier tube even if the anode current exceeds the maximum rating or a strong light causing the external circuit to be saturated is input to the photomultiplier tube. The extinction ratio is the ratio of the output when the gate is "on" to the output when the gate is "off" while a constant light level is incident on the photomultiplier tube. For example, if the output at "gate-off" is 1 nanoampere and the output at "gate-on" is 10 microamperes, then the extinction ratio is expressed in $1 \text{ nanoampere} : 10 \text{ microamperes} = 1 : 10^4$.

Even if the current is being controlled by gate operation, a small amount of current equal to the percentage of the extinction ratio flows to the anode. The anode current must be kept below the maximum rating of the photomultiplier tube even during gate operation. If high energy light such as a laser beam enters the photomultiplier tube, the photocathode structure itself might be damaged even if gate operation is performed. Some measures must be taken to prevent strong light from entering the photomultiplier tube.

8.6 Built-in CPU and Interface Type

The output current of a photomultiplier tube is usually converted into a voltage signal by a current-to-voltage conversion amplifier. The voltage signal is then converted to digital data: or in photon counting the output pulses are counted within a certain time. Digital data can be easily transferred to an external processing unit while the photomultiplier tube is controlled by commands from the external unit. To make such external control easier, built-in CPU and interface type PMT modules are available that include a signal processing circuit, a control CPU, and an interface for data transfer all housed within a single case. Figure 8-18 shows the block diagram of a built-in CPU and interface type PMT module intended for photon counting. The 32-bit counter following the photon counting circuit counts the voltage pulses and the count data is transferred to a PC through the USB interface.

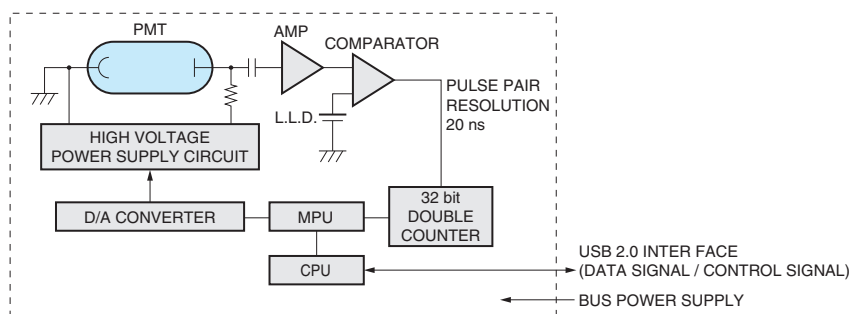


Figure 8-18: Block diagram of a built-in CPU and Interface type

THBV4_0818EA

8.7 Failure and Malfunction

This section describes the causes of failure and malfunctions that may occur with PMT modules, as well as precautions to take when handling or using PMT modules. First-time photomultiplier tube users should read this section before use to ensure correct and long-lasting operation of PMT modules.

8.7.1 Causes of failure and malfunction

The photomultiplier tube envelope is made of glass. Dropping it may cause the glass envelope to crack or rupture. In the case of PMT modules, a photomultiplier tube is contained in the case or housing. Even if you drop a PMT module and the impact causes the photomultiplier tube envelope to crack, you might not notice it from the external appearance. Even a tiny crack will degrade photomultiplier tube performance and lead to a serious damage. Moreover, the drop impact might damage the internal circuit and, if a magnetic shield case is used as the housing, its magnetic shielding affect might change.

The following are the basic precautions to be taken for handling PMT modules and the trouble that may arise from failing to follow the instructions.

- Do not expose the photocathode to strong light such as sunlight even when not in operation.
 - Noise increase, sensitivity deterioration
- Do not touch the light input window with bare hands. Keep it clean.
 - Drop in light transmittance
- Do not drop the PMT module or do not subject it to strong vibrations or shocks.
 - Performance degradation, breakage
- Do not use in locations exposed to wet, high temperature, or high humidity
 - Performance degradation, breakage
- Do not supply a voltage higher than the rating → Damage to circuit
- When using a current output type PMT module, do not disconnect or reconnect the signal cable during operation
 - Damage to subsequent circuits

8.7.2 Troubleshooting

The following are the troubles we are frequently asked about and their possible solutions.

(1) No signal is output.

No signal is output when the specified input voltage is not supplied or the control voltage is 0 volts. Check to see if the connections are correct and the specified voltage is input. Also check the input load of the connected device. For example, if a current signal of 1 microampere is input to the 50-ohm input of an oscilloscope, the output signal will be a maximum of 50 microvolts, which might not be recognized. In this case, increase the input load or use an amplifier for signal amplification.

(2) Cannot control the gain.

If the output signal cannot be changed by the gain control even when the PMT module is correctly connected and operated with the specified input voltage and control voltage supplied, the output might be saturated by excessive light input. Try reducing the incident light level by using a neutral density filter and check if the output signal changes accordingly.

(3) Output signal waveform differs from the actual phenomenon.

When measuring a high-speed phenomenon, the frequency range of the connected amplifier and PMT module's internal amplifier might affect the output signal waveform. When the current signal is directly input to an oscilloscope, use the appropriate value of input load resistance so that the high-speed phenomenon can be captured.

(4) Number of output pulses from a photon counting head is 0 (zero).

As the light level incident on a photon counting head is increased, the output pulse count gradually plateaus and then begins to decrease, finally becoming 0. The output might be zero due to excessive light input. Try reducing the incident light level by using a neutral density filter and check if the pulse count increases.

(5) Dark current fluctuates.

Possible causes are deterioration in the internal photomultiplier tube or the effect from excessive light input. If the dark current fluctuation results from excessive light input, storing the PMT module in a dark state for about one hour may relieve it.

8.8 Related optical products

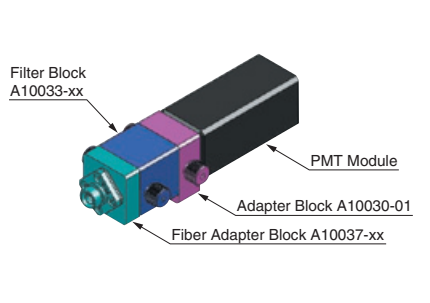
To actually use a PMT module, an input optical system and output signal processing system are also required. Input optical systems often need to be custom-designed which usually takes time and effort so the customer may wish a ready-to-use optical system. To make it easier to use PMT modules, Hamamatsu provides a line-up of optical blocks that can be combined to configure various types of input optical systems.

Optical blocks can incorporate optical components such as bandpass filters and dichroic mirrors and are designed while taking low-light-level measurement into account. Optical blocks ensure highly precise arrangement of optical components and provide light-blocking capability. Each optical block can be easily and freely connected or disconnected by hand to change the combination and setup. Optical blocks can also be used in conjunction with a light source such as a laser or with a microscope objective lens in order to assemble a confocal optical system or fluorescence microscope system.



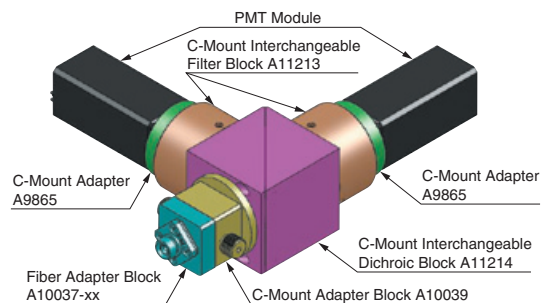
Figure 8-19: Optical blocks

Figure 8-20 shows an example of optical block combination for single wavelength detection using a bandpass filter, and Figure 8-21 shows an example of optical block combination for fiber-input dual wavelength detection using a bandpass filter and a dichroic mirror.



THBV4_0820EA

Figure 8-20: Example of combination for single wavelength detection



THBV4_0821EA

Figure 8-21: Example of combination for dual wavelength detection

MEMO

CHAPTER 9

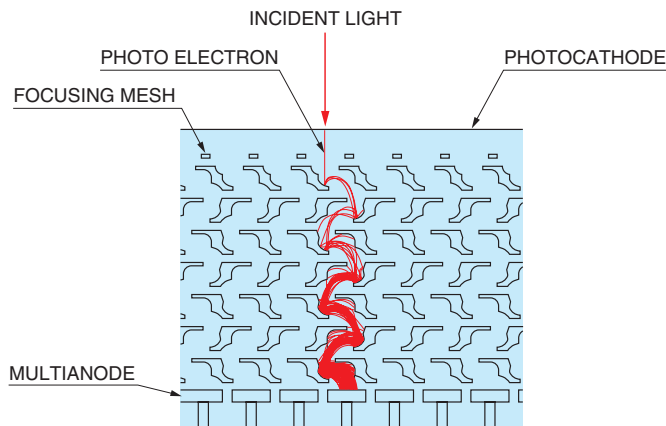
MULTIANODE TYPE AND POSITION-SENSITIVE PHOTOMULTIPLIER TUBES

This chapter introduces position-sensitive photomultiplier tubes such as those with multiple anodes. These position-sensitive photomultiplier tubes use metal channel dynodes in their electron multiplier.

Position-sensitive photomultiplier tubes can be divided into two types depending on the method for reading out a cluster of secondary electrons from the electron multiplier. One type uses independent multiple anodes each of which reads out electric charges and so is called the multianode photomultiplier tube. The other type uses a cross-plate anode that detects the center-of-gravity position of a secondary electron distribution and is called the cross-plate anode photomultiplier tube.

9.1 Multianode Photomultiplier Tubes

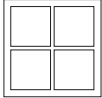
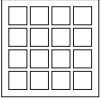
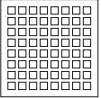
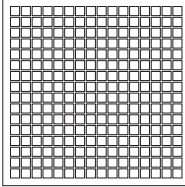
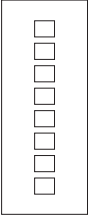
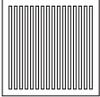
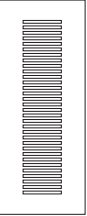
Figure 9-1 shows the electrode structure for metal channel dynodes and the electron trajectories. The electron multiplier made up of metal channel dynodes has a structure consisting of large number of fine dynode channels (paths along which photoelectrons and secondary electrons flow). A photoelectron emitted from the photocathode is directed onto a first dynode by the focusing mesh to produce secondary electrons which then flow to the second dynode, third dynode, . . . and last dynode while being multiplied, and finally reach the anode. In this process, there is little spatial spread of secondary electrons to the adjacent dynode channels. Combining this electron multiplier having a minimum spatial spread of secondary electrons with multiple independent anodes (multianode) allows detecting the incident light position with high accuracy. The electron multiplier of metal channel dynodes has a low height profile and is also designed so that the gap between each dynode stage is very narrow. This makes the overall length short and the size compact.



THBV4_0901EA

Figure 9-1: Electrode structure and electron trajectories

Multianode photomultiplier tubes can be roughly classified into two types or namely a matrix type and a linear type.

| Type | Multianode photomultiplier tubes | | | | | | |
|------------------|---|---|---|---|---|--|---|
| | Matrix | | | | Linear | | |
| | M4 | M16 | M64 | M256 | L8 | L16 | L32 |
| Anode shape |  |  |  |  |  |  |  |
| Number of anodes | 4 | 16 | 64 | 256 | 8 | 16 | 32 |

THBV4_0902EA

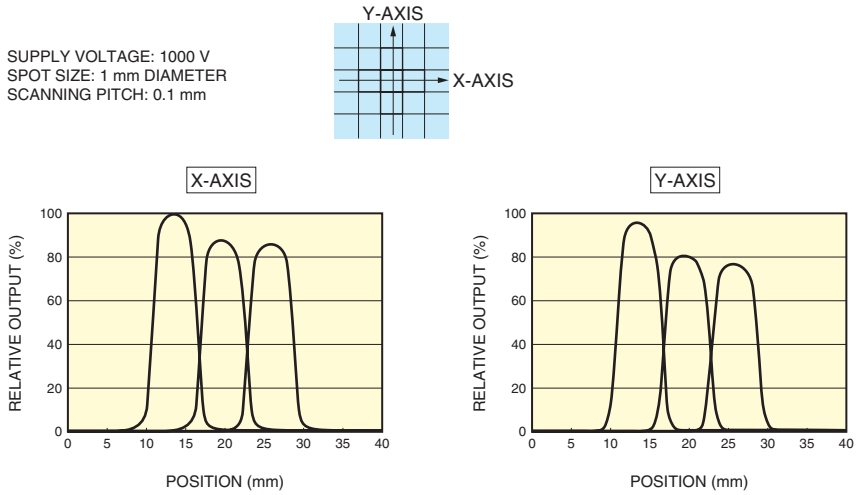
Figure 9-2: Anode patterns for multianode photomultiplier tubes

9.1.1 Matrix multianode photomultiplier tubes

Matrix multianode photomultiplier tubes are available in a metal package measuring 26 millimeters square and a flat panel measuring 51 millimeters square. The number of anode channels is available from 4 (2 × 2) to 256 (16 × 16) with different channel sizes and so can be selected according to the application and purpose of use.

Taking up the basic characteristics of matrix multianode photomultiplier tubes, let’s discuss “spatial resolution,” “crosstalk,” “magnetic immunity,” and “uniformity” using a 64-channel flat panel type multianode photomultiplier tube as an example.

Figure 9-3 shows spatial resolution data measured using light emitted from a tungsten lamp and passed through a blue filter. The light is collimated to a 1 millimeter diameter spot and is scanned near the center of the photocathode to measure the spatial resolution (output distribution characteristics of each anode) of the photomultiplier tube.

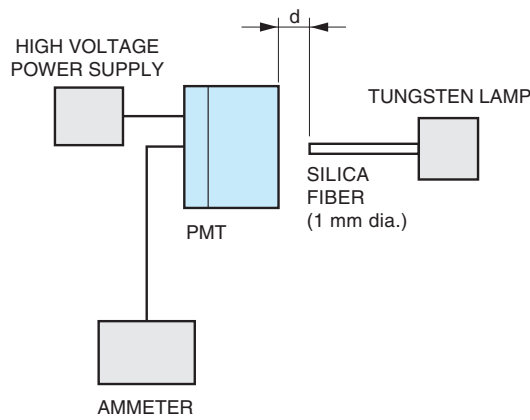


THBV4_0903EA

Figure 9-3: Spatial resolution of center anodes

Crosstalk is a phenomenon in which the light incident on only one channel causes the neighboring channels to respond to that light. Crosstalk is mainly caused by the broadening of photoelectrons, which occurs when they flow from the photocathode to the first dynode. Moreover, the incident light spread within the faceplate is another probable cause of crosstalk.

A typical setup for measuring crosstalk is shown in Figure 9-4 and an example of measurement data in Figure 9-5.



THBV4_0904EA

Figure 9-4: Crosstalk measurement method

| | P1 | P2 | P3 | P4 | P5 | P6 | P7 | P8 | |
|-----|-----|-----|-----|-----|-----|-----|-----|-----|-----|
| P1 | 100 | 2.0 | — | — | — | — | — | — | P8 |
| P9 | 0.9 | 0.1 | — | — | — | — | — | — | P16 |
| P17 | — | — | 0.0 | 0.5 | 0.1 | — | — | — | P24 |
| P25 | — | — | 0.5 | 100 | 0.6 | — | 0.1 | 0.7 | P32 |
| P33 | — | — | 0.1 | 0.7 | 0.1 | — | 0.5 | 100 | P40 |
| P41 | — | — | — | — | — | — | 0.1 | 0.6 | P48 |
| P49 | — | — | 0.2 | 1.0 | 0.2 | — | — | — | P56 |
| P57 | — | — | 2.1 | 100 | 1.9 | — | — | — | P64 |
| | P57 | P58 | P59 | P60 | P61 | P62 | P63 | P64 | |

THBV4_0905EA

Figure 9-5: Crosstalk data measured by using a 1 mm diameter optical fiber (d= 0 mm)

Figure 9-5 shows the anode outputs of some adjacent channels measured by irradiating a light spot on the photomultiplier tube faceplate. The anode output of each channel is expressed as a relative value with 100% being equal to the anode output of the channel with a corresponding light spot.

This data was measured by using a 1 millimeter diameter optical fiber positioned in tight contact with the photomultiplier tube faceplate (d=0 mm) and shows crosstalk that ranges from 0.1% to 2.1% depending on the incident light position. The crosstalk of the vertically or horizontally adjacent channels is smaller than that of the diagonally adjacent channels. As this measurement shows, when an optical fiber is used to guide the light to the photomultiplier tube faceplate, the crosstalk becomes worse when the optical fiber separates away from the faceplate, so be aware of this point. This effect is due to the light spread from the optical fiber. When making measurements using scintillating fibers of optical fibers, bringing the optical fiber into tight contact with the photomultiplier tube faceplate is recommended.

Figure 9-6 shows the crosstalk measured by illuminating a light spot of 5 millimeters square onto a channel near the center of the photocathode. (The channel to channel spacing is 6 millimeters.) The crosstalk ranges between 2 % to 3 %.

| | | | | | | |
|--|---|-----|-----|-----|---|--|
| | — | — | — | — | — | |
| | — | 0.2 | 1.8 | 0.2 | — | |
| | — | 1.5 | 100 | 2.7 | — | |
| | — | 0.2 | 2.6 | 0.3 | — | |
| | — | — | — | — | — | |

SUPPLY VOLTAGE: 1000 V
 LIGHT SOURCE: TUNGSTEN LAMP
 SPOT SIZE: 5 mm square

THBV4_0906EA

Figure 9-6: Crosstalk data of the center channel in response to a 5 mm square light

In order to widen the effective photocathode area of flat panel type multianode photomultiplier tubes, photoelectrons released from the peripheral area of the photocathode are focused and directed onto the first dynode. Because of this, the channels in the corners of the photocathode in particular tend to have a larger crosstalk (3 % to 6 %) as shown in Figure 9-7.

| | | | |
|-----|-----|---|--|
| 100 | 5.5 | — | |
| 3.5 | 0.5 | — | |
| — | — | — | |
| | | | |

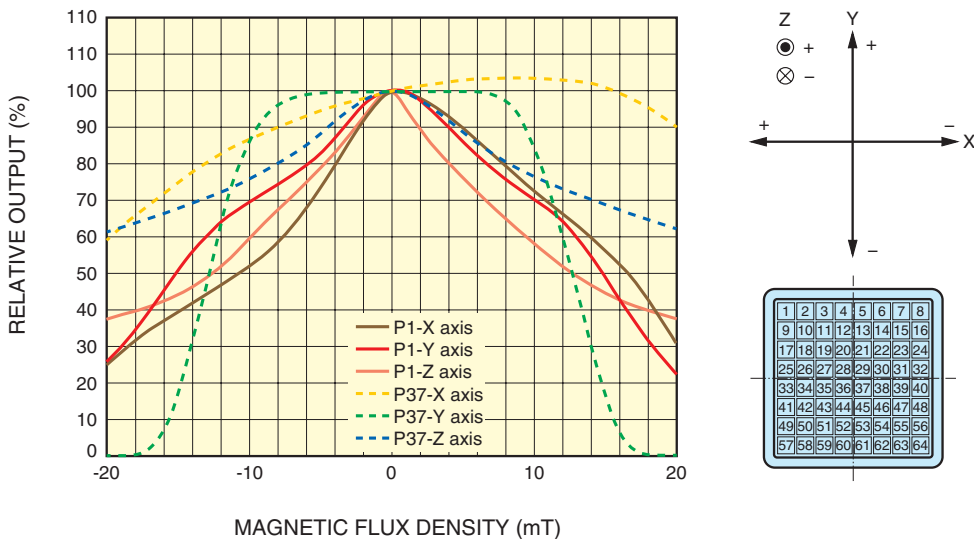
SUPPLY VOLTAGE: 1000 V
 LIGHT SOURCE: TUNGSTEN LAMP
 SPOT SIZE: 5 mm square

THBV4_0907EA

Figure 9-7: Crosstalk data of the corner channels in response to a 5 mm square light

Next, let's discuss magnetic characteristics. Matrix multianode photomultiplier tubes are comparatively less affected by magnetic fields. This is mainly because all parts except the light input window are housed in a metal package and also because the distance between the photocathode and the first dynode is very short. Magnetic characteristics of a 64-channel flat panel type multianode photomultiplier tube are explained below.

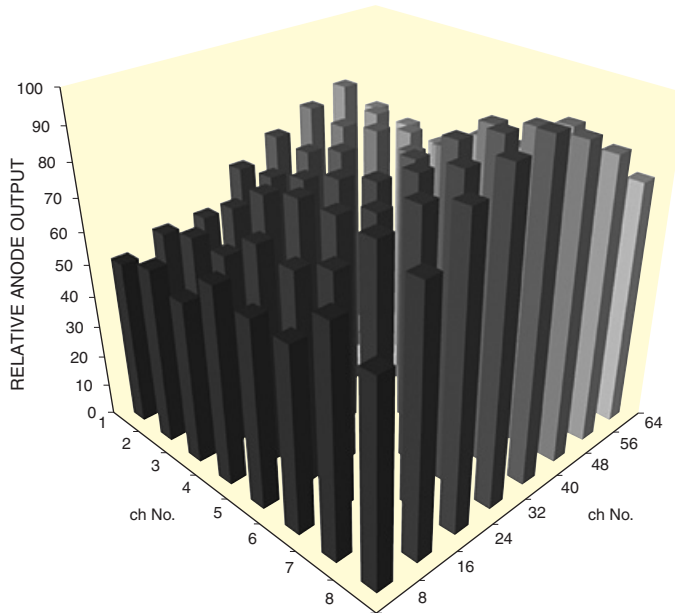
Figure 9-8 shows how the anode outputs of channel No. 1 (corner of photocathode) and channel No. 37 (center of photocathode) are affected by external magnetic fields applied along the three axes (X, Y, Z). Each data is plotted as a relative output value with 100 % corresponding to an output with no magnetic field applied. Magnetic characteristics differ depending on the channel position.



THBV4_0908EA

Figure 9-8: Effects of external magnetic fields on anode output (channel No. 1 and No. 37)

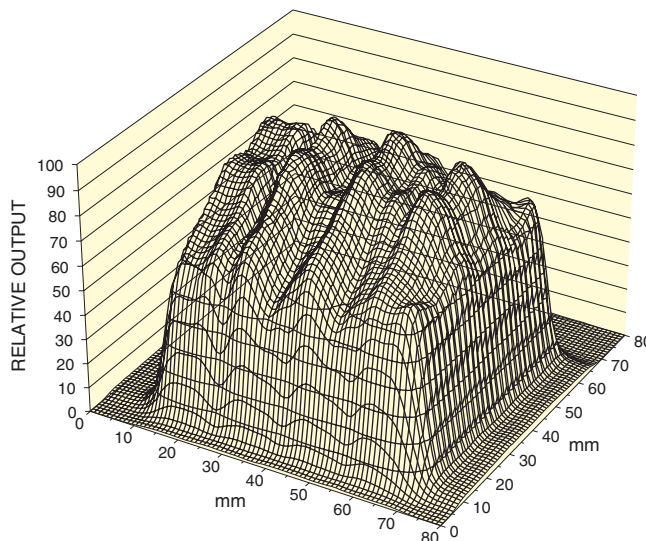
Now let's check out the uniformity characteristics (output sensitivity uniformity). Figure 9-9 shows typical uniformity data obtained by measuring the anode outputs when a 6 millimeter square light is incident on each channel of a multianode photomultiplier tube. The non-uniformity observed here probably originates from gain variations in the electron multiplier because the photocathode itself has good uniformity. Non-uniformity between each anode output is about "1:2" in Figure 9-9.



THBV4_0909EA

Figure 9-9: Anode output uniformity (typical example)

Figure 9-10 shows a typical example of the anode output uniformity within one channel. This data was measured by irradiating a light spot with a 50 micrometer diameter onto a channel of 6 millimeters square while scanning the light spot every 0.1 millimeters.



THBV4_0910EA

Figure 9-10: Anode output uniformity within one channel (typical example)

When optically coupled to a scintillator, matrix multianode photomultiplier tubes can be used for two-dimensional imaging and measurement of radiation such as gamma rays. Figure 9-11 shows a wiring example of a 64-channel multianode photomultiplier tube for two-dimensional radiation imaging, and Figure 9-12 shows an example of scintillation imaging of gamma rays obtained with a 64-channel flat panel type multianode photomultiplier tube coupled to a mosaic scintillator. As seen in Figure 9-11, each anode channel is wired by way of a resistive chain circuit and the outputs from 64 channels are collected and read out by 4 output terminals. These outputs are then calculated by the Anger method (Eq. 9-1) to obtain the center-of-gravity position in the XY directions of secondary electrons produced by scintillation. This position can also be calculated by separately reading the outputs of the 64 channels.

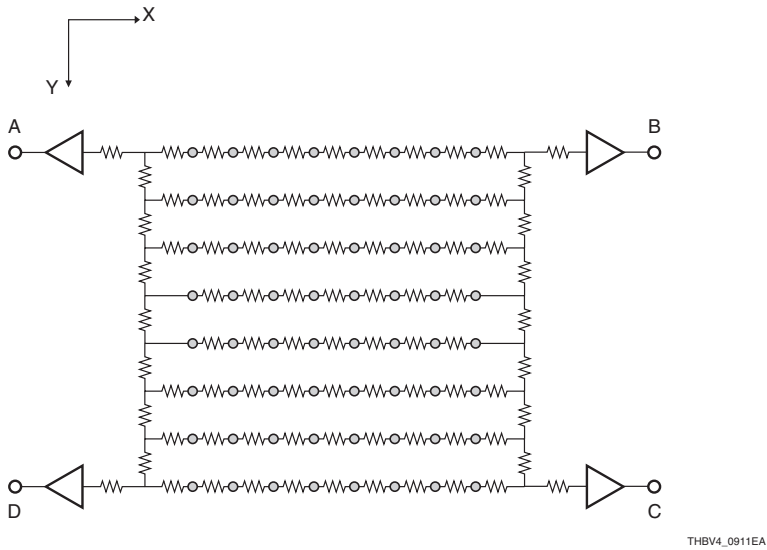


Figure 9-11: Wiring example showing resistive chain circuit for 64 channels

$$X = (B+C)/(A+B+C+D)$$

$$Y = (C+D)/(A+B+C+D) \dots\dots\dots (Eq. 9-1)$$

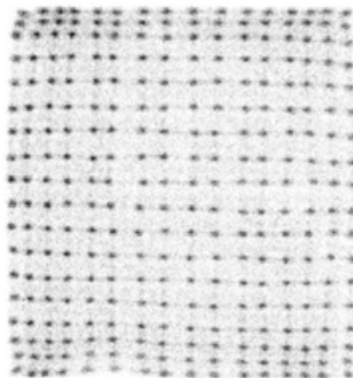
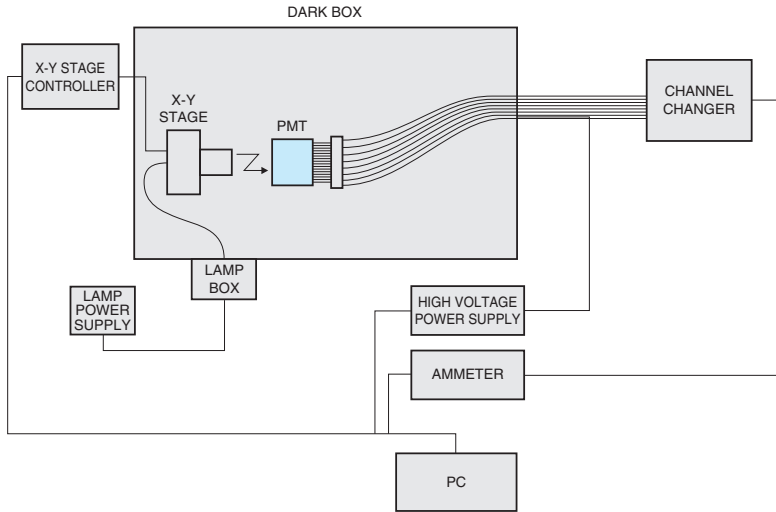


Figure 9-12: Example of scintillation imaging of gamma rays irradiated onto a mosaic scintillator (Scintillator: LYSO, array format: 16 (H) × 18 (V), element size: 2.9 mm × 2.9 mm × 20 mm, gamma ray source: ²²Na at 511 keV)

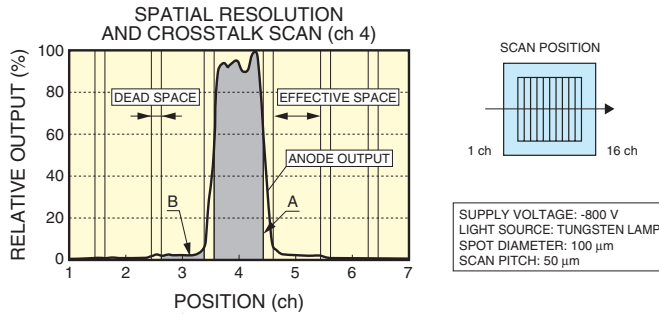
9.1.2 Linear multianode photomultiplier tubes

We next describe basic "crosstalk" and "uniformity" characteristics of linear multianode photomultiplier tubes. A typical setup for measuring crosstalk of a 16-channel linear multianode photomultiplier tube is shown in Figure 9-13 and typical measurement data is shown in Figure 9-14. In this measurement, a light spot emitted through the 100 micrometer diameter aperture in the X-Y stage was scanned along the photocathode. Typical crosstalk obtained from this 16-channel linear multianode is approximately 3 %.



THBV4_0913EA

Figure 9-13: Crosstalk measurement method



| CROSS-TALK RATIO (%) | | | | | | | | | | | | | | | | |
|----------------------|-----|-----|-----|-----|-----|-----|-----|-----|-----|-----|-----|-----|-----|-----|-----|-----|
| ch | 1 | 2 | 3 | 4 | 5 | 6 | 7 | 8 | 9 | 10 | 11 | 12 | 13 | 14 | 15 | 16 |
| 1 | 100 | 2.9 | 0.6 | 0.2 | 0.1 | — | — | — | — | — | — | — | — | — | — | — |
| 2 | 2.9 | 100 | 3.1 | 0.5 | 0.2 | 0.1 | — | — | — | — | — | — | — | — | — | — |
| 3 | 0.8 | 2.8 | 100 | 2.8 | 0.6 | 0.2 | 0.1 | — | — | — | — | — | — | — | — | — |
| 4 | 0.3 | 0.8 | 2.7 | 100 | 3.2 | 0.6 | 0.2 | 0.1 | — | — | — | — | — | — | — | — |
| 5 | 0.1 | 0.3 | 0.8 | 2.9 | 100 | 3.1 | 0.6 | 0.2 | 0.1 | — | — | — | — | — | — | — |
| 6 | — | 0.1 | 0.3 | 0.8 | 2.7 | 100 | 3.0 | 0.6 | 0.2 | 0.1 | — | — | — | — | — | — |
| 7 | — | — | 0.1 | 0.3 | 0.8 | 2.7 | 100 | 3.0 | 0.6 | 0.2 | 0.1 | — | — | — | — | — |
| 8 | — | — | — | 0.1 | 0.3 | 0.8 | 2.9 | 100 | 2.9 | 0.6 | 0.2 | 0.1 | — | — | — | — |
| 9 | — | — | — | — | 0.1 | 0.3 | 0.8 | 2.9 | 100 | 2.9 | 0.6 | 0.2 | 0.1 | — | — | — |
| 10 | — | — | — | — | — | 0.1 | 0.3 | 0.8 | 3.1 | 100 | 2.7 | 0.6 | 0.2 | 0.1 | — | — |
| 11 | — | — | — | — | — | — | 0.1 | 0.4 | 0.8 | 3.3 | 100 | 3.8 | 0.6 | 0.2 | 0.1 | — |
| 12 | — | — | — | — | — | — | — | 0.1 | 0.4 | 0.9 | 3.2 | 100 | 2.8 | 0.6 | 0.2 | 0.1 |
| 13 | — | — | — | — | — | — | — | — | 0.1 | 0.4 | 0.8 | 3.1 | 100 | 2.8 | 0.6 | 0.3 |
| 14 | — | — | — | — | — | — | — | — | — | 0.1 | 0.4 | 0.8 | 3.1 | 100 | 2.7 | 0.6 |
| 15 | — | — | — | — | — | — | — | — | — | — | 0.1 | 0.4 | 0.9 | 3.2 | 100 | 2.9 |
| 16 | — | — | — | — | — | — | — | — | — | — | — | 0.1 | 0.4 | 0.9 | 3.1 | 100 |

CROSSTALK (%):
AREA B / AREA A × 100

THBV4_0914EA

Figure 9-14: Example of crosstalk in the 16-channel linear type

Some 16-channel and 32-channel linear multianode photomultiplier tubes are low crosstalk types. Some use a special faceplate containing black glass partitions or an electrode structure having shielding walls between the anodes of each channel. Typical crosstalk values measured with a low crosstalk type are shown in Figure 9-1.

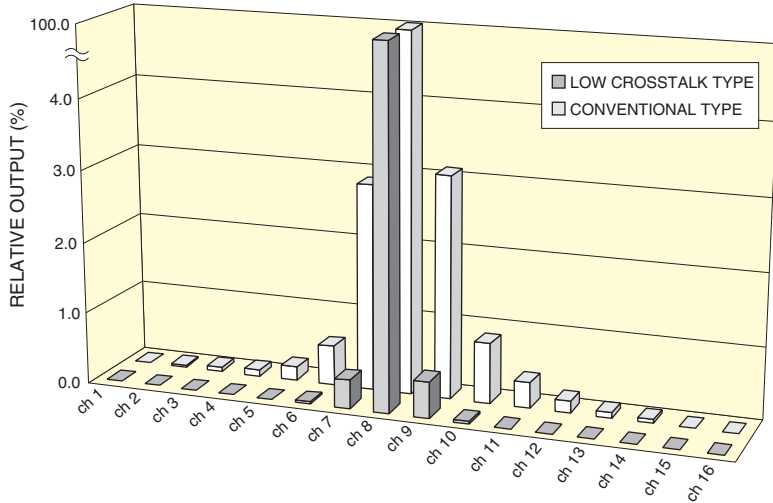


Figure 9-15: Crosstalk data examples of 16-channel linear multianode types

THBV4_0915EA

Figure 9-16 shows typical uniformity data of a linear multianode photomultiplier tube. This data was obtained by measuring the anode outputs when uniform light was illuminated over the entire photocathode of a 32-channel linear multianode photomultiplier tube. Just as with the matrix type, non-uniformity mainly originates from gain variations in the electron multiplier. Non-uniformity between each anode output is about "1:1.7" on average.

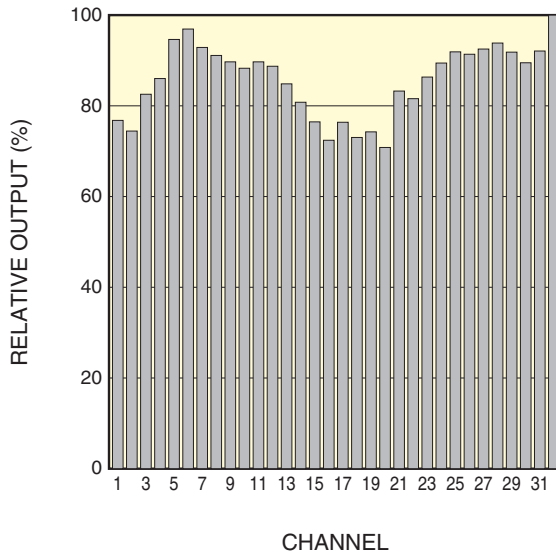


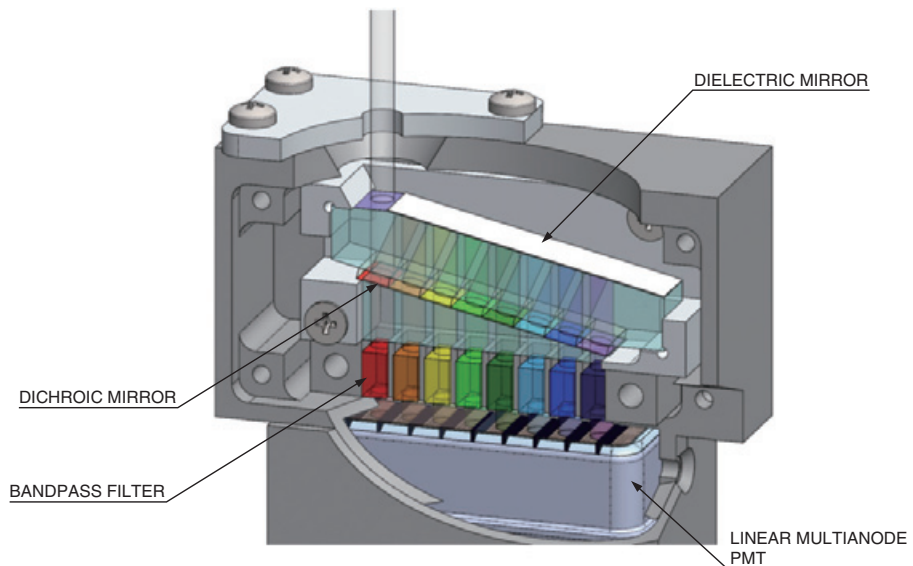
Figure 9-16: Anode uniformity data example of a 32-channel linear multianode type

THBV4_0916EA

9.1.2.1 Linear multianode type for multichannel spectrometry

Since linear multianode photomultiplier tubes are one-dimensional arrays, they are mainly used as detectors for multichannel spectrometry. To detect a light spectrum, multiple wavelength signals must be acquired at the same time. Using multiple single-channel photomultiplier tubes to detect a spectrum requires a large optical system. However, a linear multianode photomultiplier tube only requires a compact optical system to serve as a spectrum detector. In particular, due to its shape, 32-channel linear multianode photomultiplier tubes are often used in combination with a grating or prism and recent applications include laser scanning microscopes.

Another means for dispersing light into a spectrum is a spectrum filtering method that uses dichroic mirrors and bandpass filters. An example of this method is illustrated in Figure 9-17. In this spectrum filtering method, the incident light is dispersed into a spectrum while it causes multiple reflections between the dielectric mirrors and the multiple dichroic mirrors with different characteristics from each other. This allows detecting light just in the wavelength range of interest and also ensures highly efficient detection due to little loss of light.

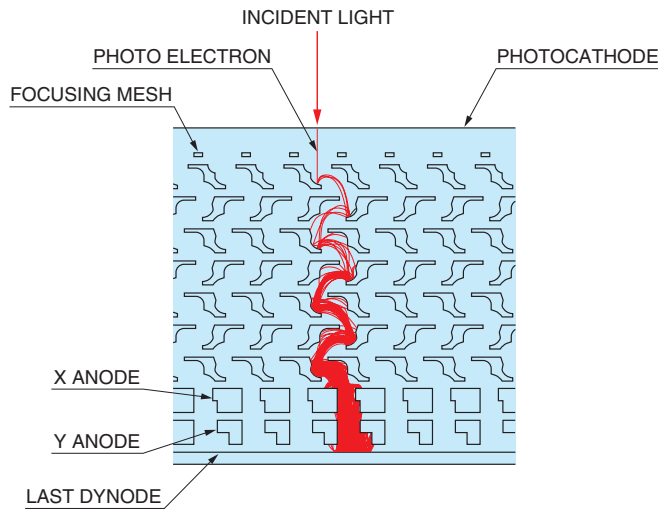


THBV4_0917EA

Figure 9-17: Schematic diagram of a mini-spectrometer using a linear multianode photomultiplier tube

9.2 Center-of-Gravity Position Sensitive Photomultiplier Tubes

Figure 9-18 shows the electrode structure of a metal channel dynode type position sensitive photomultiplier tube using cross-plate anodes, along with the electron trajectories. In this photomultiplier tube, photoelectrons emitted from the photocathode are multiplied by the electron multiplier and the multiplied secondary electrons are then reflected back from the last dynode and read out from the plate type anodes (cross-plate anodes) arranged in two layers intersecting with each other.

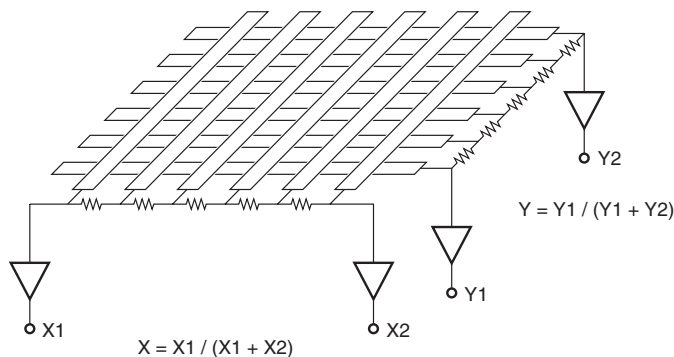


THBV4_0918EA

Figure 9-18: Electrode structure

Figure 9-19 illustrates the center-of-gravity detection method for reading out the output signal from a position-sensitive photomultiplier tube using cross-plate anodes. The electron bunch released from the last dynode is collected by anodes linearly arranged in the X and Y directions. Since each anode in the same direction is connected by a resistor string, the collected electrons are divided into four signal components X1, X2, Y1 and Y2 corresponding to the anode position at which the secondary electrons arrive. By summing and dividing these signals, the center of gravity of the secondary electrons in the X and Y directions can be obtained from Eq. 9-2.

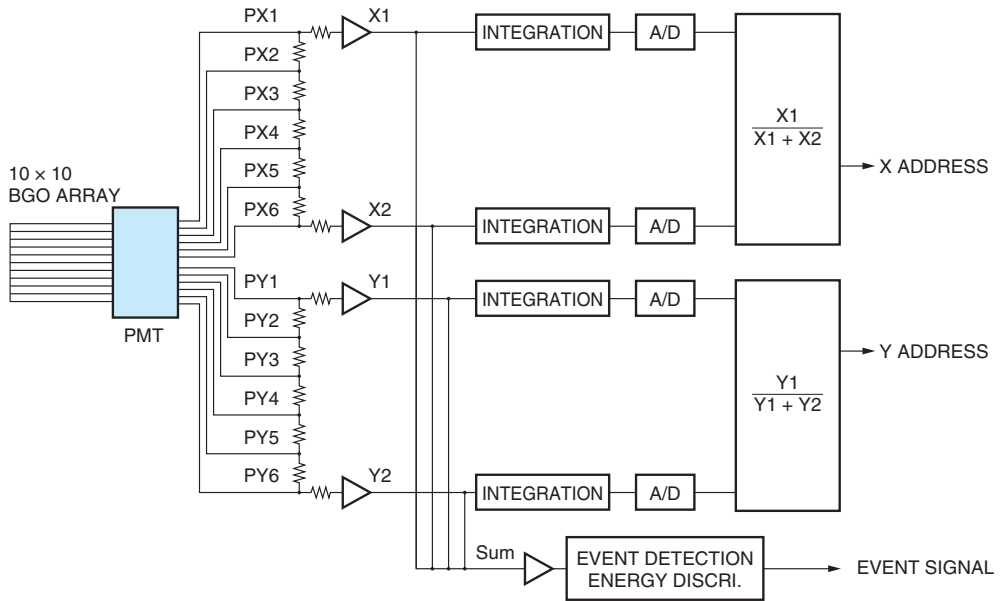
$$\begin{aligned}
 X &= X1 / (X1 + X2) \\
 Y &= Y1 / (Y1 + Y2)
 \end{aligned}
 \quad \dots\dots\dots \text{(Eq. 9-2)}$$



THBV4_0919EA

Figure 9-19: Center-of-gravity measurement method using resistive chains

Figure 9-20 shows a measurement diagram for scintillation imaging using a mosaic array of scintillators coupled to a 6 (X) + 6 (Y) cross-plate anode photomultiplier tube. The mosaic array of scintillators consists of BGO scintillators arranged in the format of 10×10 (total of 100 pieces), each of which measures $2.2 \times 2.2 \times 15$ millimeters. An example of a scintillation image is shown in Figure 9-21 which was obtained by irradiating the scintillators with gamma rays at an energy of 662 keV.



THBV4_0920EA

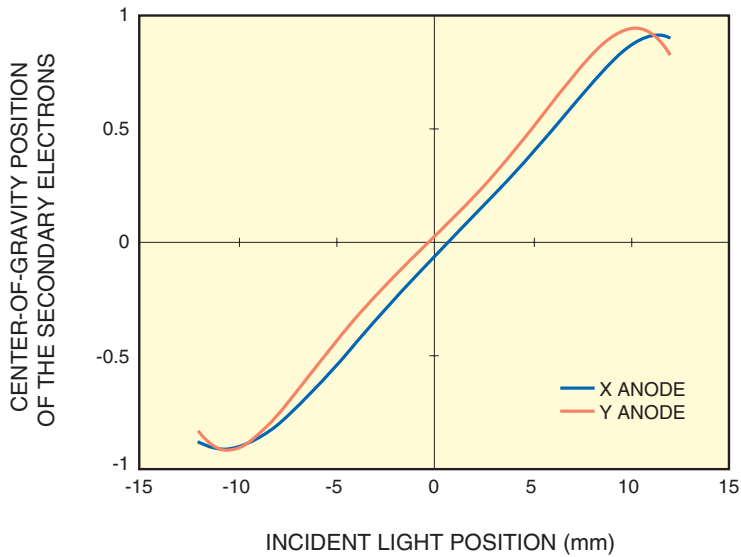
Figure 9-20: Measurement diagram for scintillation imaging of gamma ray irradiation on a mosaic array of scintillators (BGO)



Figure 9-21: Example of scintillation image obtained by using the setup in Figure 9-20 (Scintillators: BGO, array format: 10 (H) \times 10 (V), scintillator size: 2.2 mm \times 2.2 mm \times 15 mm, gamma ray source: ^{137}Cs at 662 keV)

Figure 9-21 proves that the cross-plate anode photomultiplier tube clearly detects and discriminates the scintillation light emitted from each of the 100 scintillators.

In the peripheral area of the photocathode, the center-of-gravity position of the secondary electrons includes a slight distortion due to the limited number of anodes. Figure 9-22 shows the relation between the incident light position (horizontal axis) and the center-of-gravity position of the secondary electrons (vertical axis). In other words, these are spatial linearity characteristics, measured by scanning a light spot of 1 millimeter diameter over the photocathode surface. In the peripheral area of the photocathode, there are non-linear regions where a linear relation is not maintained between the incident light position and the center-of-gravity position of the secondary electrons. This causes distortion in the peripheral area of the photocathode however this distortion can be corrected by a lookup table or similar techniques.



THBV4_0922EA

Figure 9-22: Spatial linearity of a center-of-gravity detection type photomultiplier tube

CHAPTER 10

Micro PMT

A micro PMT is the world's smallest and lightest photomultiplier tube. A micro PMT is developed by utilizing MEMS which is a semiconductor manufacturing technology.

A micro PMT is small enough to fit on a fingertip yet still having the high performance of photomultiplier tubes, which has been made possible by merging MEMS semiconductor manufacturing technologies with advanced technologies for electron trajectory design, vacuum sealed packaging, and vacuum processing accumulated over long years of experience in photomultiplier tube manufacture.

10.1 Micro PMT overview

A micro PMT has a three-layer structure where a silicon substrate is sandwiched between two glass plates. The electron multiplier section of micro PMT is fabricated by a deep etching process (900 μm) using MEMS (Micro Electro Mechanical Systems) semiconductor manufacturing technology¹⁾ for micromachining silicon substrates. Anodic bonding in MEMS technology is utilized to securely join the silicon substrate to the glass plates. Finally, the substrate (see Figure 10-1) is cut into chips measuring only 10 mm square and 2 mm thick, and weighing only 0.5 grams. These are so tiny that each can even fit on a fingertip (see Figure 10-2). Micromachining such a substrate to fabricate electron multiplier sections allows high volume production of photomultiplier tubes with a simple structure that is also highly resistant to mechanical shocks compared to conventional photomultiplier tubes.

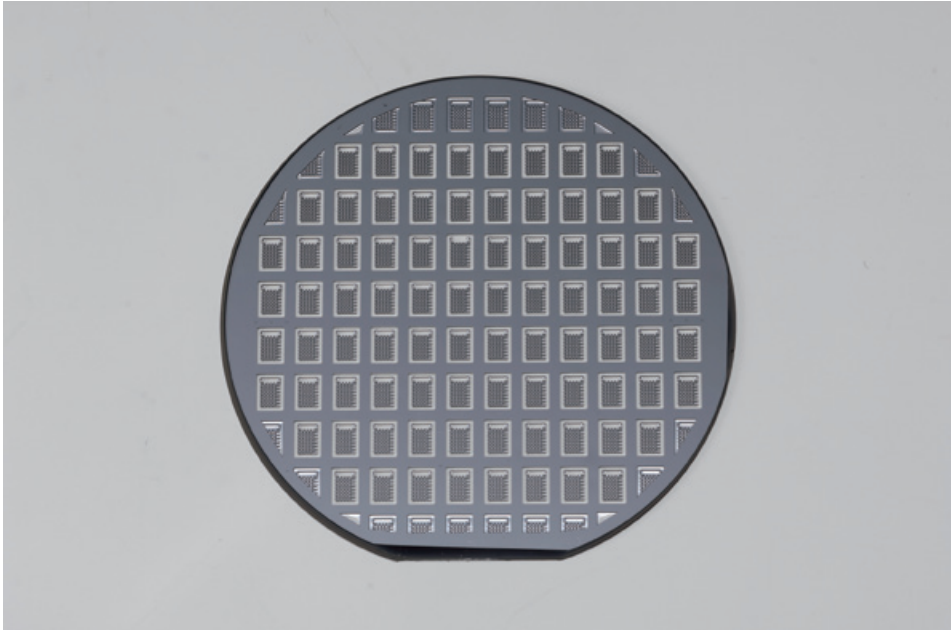


Figure 10-1: Micro PMT fabricated on a 150 mm (6 inch) diameter substrate

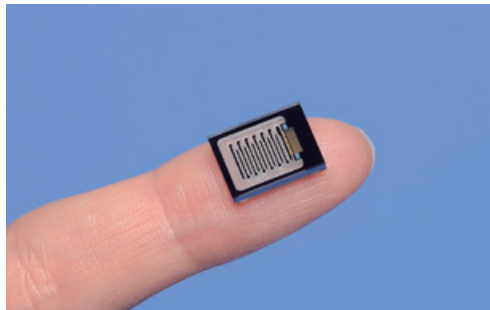
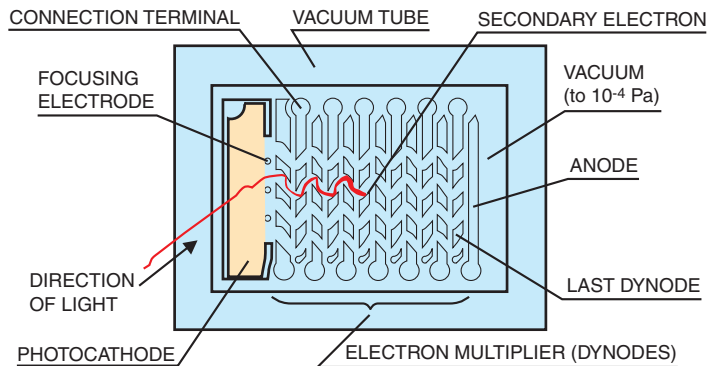


Figure 10-2: Micro PMT on a fingertip

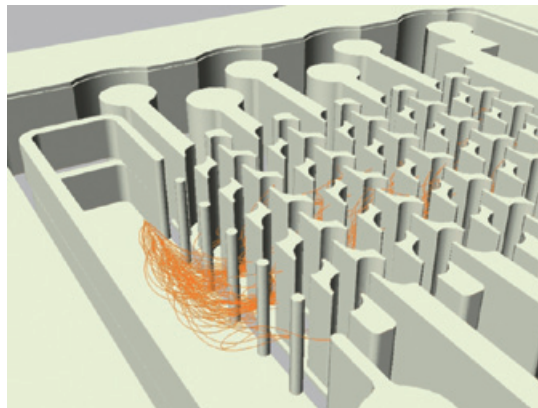
10.2 Micro PMT operating principle

The basic operating principle of micro PMT is the same as that of conventional photomultiplier tubes. Light entering through the input window is converted into photoelectrons at the photocathode. The trajectories of the photoelectrons are then bent 90 degrees by an electric field perpendicular to the photocathode surface so the electrons are guided to the electron multiplier section. The electrons accelerated by the electric field impinge on the secondary emissive surface formed on each stage of the electron multiplier to produce secondary electrons according to the accelerating voltage. This process is repeated by the number of electron multiplier stages and finally the electrons are multiplied about one million times and output from the anode as electrical current (Figures 10-3, 10-4 and 10-5).



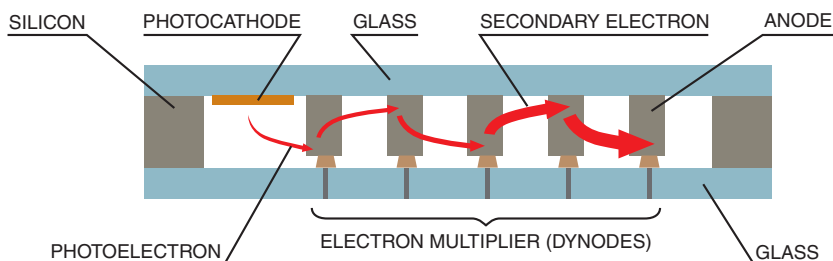
THBV4_1003EA

Figure 10-3: Structure of micro PMT



1004

Figure 10-4: Electron trajectories (orange lines) in micro PMT



THBV4_1005EA

Figure 10-5: Cross section of micro PMT and electron multiplication process

10.3 Key features

1. Easy to mass-produce and customize

Mass-producing photomultiplier tubes has proven extremely difficult up to now. However, micro PMTs can be produced in high volume by techniques from semiconductor manufacturing technology and can also be easily customized to match customer's operating conditions and environments.

2. Tiny and resistant to mechanical impacts

Micro PMTs are tiny and highly resistant to mechanical impacts, making them an ideal start for designing and developing high-performance portable analytical devices small enough to fit into one's pocket.

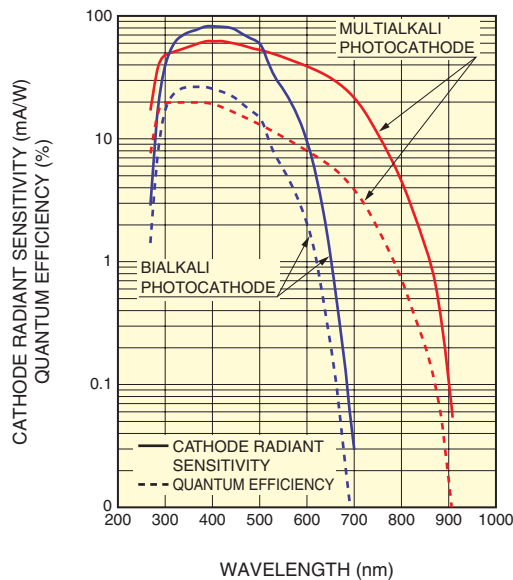
3. Available in various configurations such as an assembly type easily mountable into equipment and a module type with built-in high voltage power supply

Micro PMTs are available in various configurations for ease of use. The assembly type includes a micro PMT and voltage-divider circuit, and the module type contains a high voltage power supply along with a micro PMT and voltage-divider circuit. A photon counting head is also available that includes a photon counting circuit.

10.4 Characteristics

(1) Spectral response characteristics

The spectral response range of the bialkali photocathode type is from 300 nm to 650 nm with a typical quantum efficiency of 26 % at 350 nm. The spectral response of the multialkali photocathode type covers a wide range from 300 nm to 850 nm. (See Figure 10-6.)

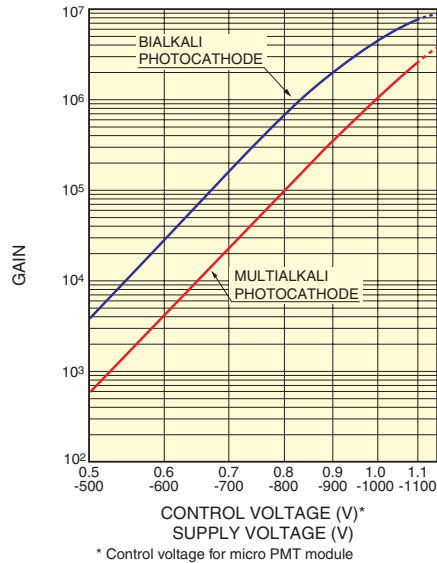


THBV4_1006EA

Figure 10-6: Spectral response characteristics

(2) Gain characteristics

Gain characteristics differ slightly depending on the photocathode type. The bialkali photocathode type produces a gain of about two million times at a supply voltage of -900 V (Figure 10-7). The gain of the module type can be adjusted by controlling a supply voltage that is easily varied with a control voltage in a range from +0.5 V to +1.0 V.

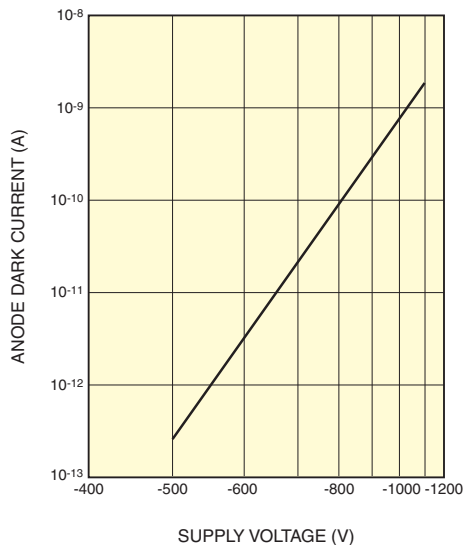


THBV4_1007EA

Figure 10-7: Typical gain characteristics

(3) Dark current characteristics

A small amount of current is output from a micro PMT even when operated in a completely dark state. Figure 10-8 shows a typical dark current versus the supply voltage. Increasing the supply voltage boosts the gain but also causes an increase in dark current. Dark current of a micro PMT is usually lower than other photomultiplier tubes. For example, the typical dark current of a micro PMT is 0.3 nA at a rated voltage of 900 V and a gain of 2×10^6 , while that of a TO-8 type PMT is 1.0 nA at a rated voltage of 1000 V and a gain of 2×10^6 . This is due to the difference in the photocathode size.

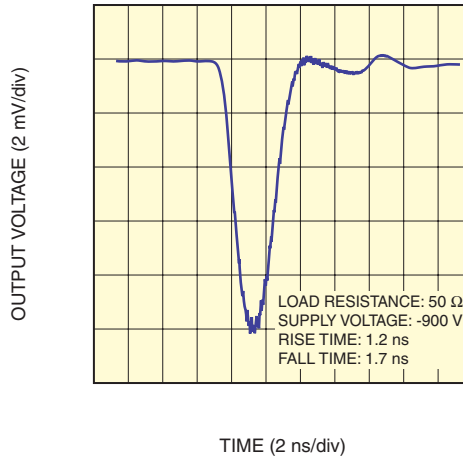


THBV4_1008EA

Figure 10-8: Typical anode dark current

(4) Time characteristics

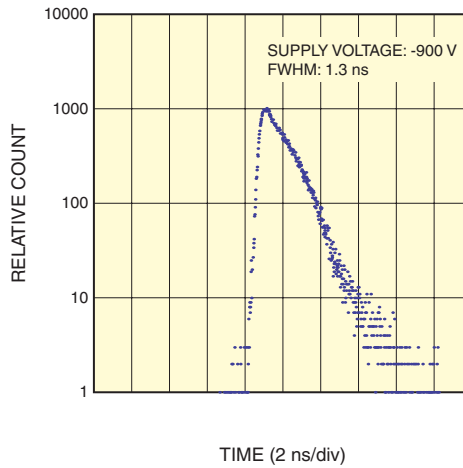
Figure 10-9 shows an output waveform of a micro PMT when pulsed light (pulse width: 70 ps) is input. The rise time is 1.2 ns and the fall time is 1.7 ns at a supply voltage of -900 V.



THBV4_1009EA

Figure 10-9: Output waveform

A typical T.T.S. (transit time spread) of a micro PMT is 1.3 ns (Figure 10-10).



THBV4_1010EA

Figure 10-10: T.T.S. waveform

(5) Uniformity characteristics

Figure 10-11 shows an example of anode output measured by scanning a light spot of 1 mm diameter at a wavelength of 400 nm over the photocathode surface of a micro PMT at a pitch of 0.1 mm in the X and Y axis directions. This figure shows that a nearly uniform output is obtained.

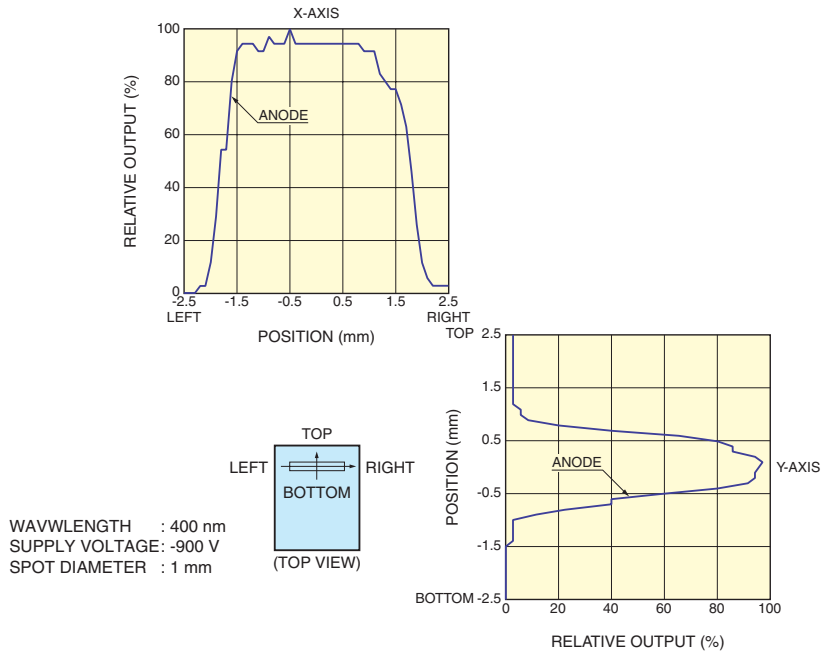


Figure 10-11: Uniformity characteristics

THBV4_1011EA

(6) Magnetic characteristics

Magnetic fields change the output of a micro PMT. The extent of change depends on the strength and direction of magnetic fields. The magnetic field in the Z direction has the strongest effect on output (see Figure 10-12). Terrestrial magnetism (earth's magnetic field) which is less than 0.1 mT has almost no effect on the micro PMT output. However, the output might be affected when used near a device such as a motor that generates magnetic fields. A magnetic shield is needed in such cases to reduce the effects from magnetic fields.

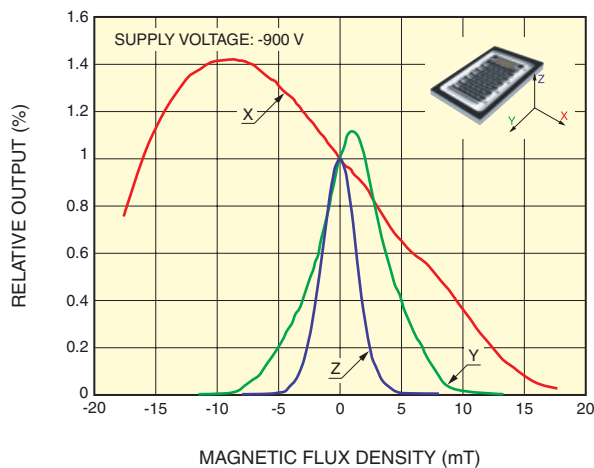


Figure 10-12: Effect of magnetic fields

THBV4_1012EA

References in Chapter 10

- 1) Technical Information Institute Co., Ltd.: MEMS device processing, installation and evaluation technology

CHAPTER 11

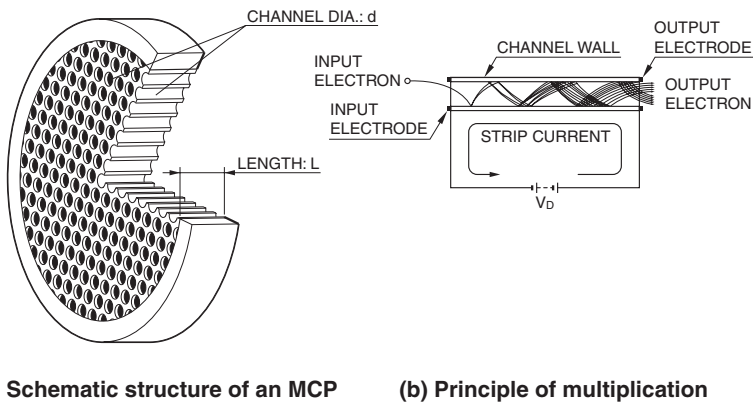
Microchannel Plate- Photomultiplier Tube

Using microchannel plates¹⁾ (abbreviated as MCP hereafter) as an electron multiplier, photomultiplier tubes have evolved into more versatile devices capable of wide-bandwidth measurements down to the picosecond level as well as low-light-level detection at the photon counting level. This chapter describes ultra-fast and high-sensitivity microchannel plate-photomultiplier tube (abbreviated as MCP-PMT²⁾ hereafter).

11.1 Structure

11.1.1 Structure of MCP

Figure 11-1 (a) shows the schematic structure of an MCP. The MCP consists of a two-dimensional array of a great number of glass capillaries (channels) bundled in parallel and formed into the shape of a thin disk. Each channel has an internal diameter ranging from 6 to 25 microns with the inner wall processed to have the proper electrical resistance and secondary emissive properties. Accordingly, each channel acts as an independent electron multiplier. The cross section of a channel and its principle of multiplication are illustrated in Figure 11-1 (b). When a primary electron impinges on the inner wall of a channel, secondary electrons are emitted. Being accelerated by the electric field created by the voltage V_D applied across both ends of the MCP, these secondary electrons bombard the channel wall again to produce additional secondary electrons. This process is repeated many times along the channel and as a result, a large number of electrons are released from the output end.



(a) Schematic structure of an MCP **(b) Principle of multiplication**

THBV4_1101EA

Figure 11-1: Schematic structure of an MCP and its principle of multiplication

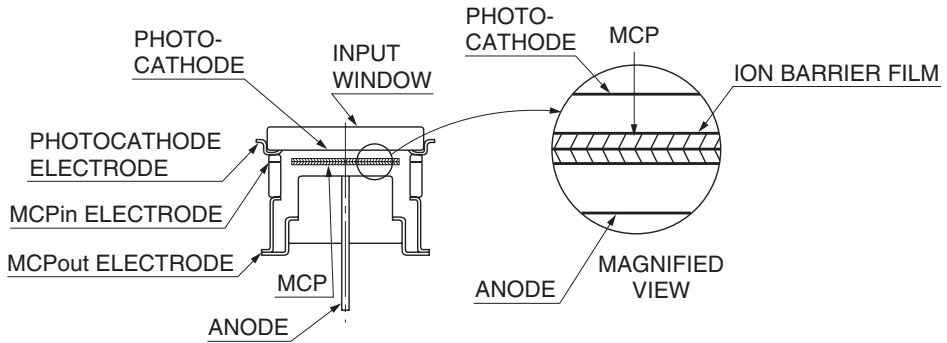
MCPs are quite different in structure and operation from conventional discrete dynodes and therefore offer the following outstanding features:

- 1) Compact and lightweight
- 2) Fast time response
- 3) Two-dimensional detection with high spatial resolution
- 4) Stable operation even in high magnetic fields
- 5) Sensitive to charged particles, ultraviolet radiation, X rays, gamma rays, and neutrons
- 6) Low power consumption

There are various types of detectors that utilize the advantages offered by MCP, for example fast time response photomultiplier tubes that incorporate an MCP (MCP-PMT), image intensifiers for low-light-level imaging, and streak tubes for ultra-fast photometry.

11.1.2 Structure of MCP-PMT

Figure 11-2 shows the cross section of a typical MCP-PMT. This MCP-PMT consists of an input window, photocathode, MCP, and anode. The photoelectrons emitted from the photocathode enter the channels of the MCP and impinge on the inner wall where they are multiplied by means of secondary emission. This process is repeated along the channels, and finally a large number of electrons are collected by the anode as an output signal. The photocathode to MCP distance is approximately 2 millimeters, forming a close-proximity structure. Two or more MCPs can be stacked to obtain sufficient gain. A thin film called "ion barrier film" is usually formed on the photoelectron input side of the MCP in order to prevent ions generated inside the MCP from returning to the photocathode. Figure 11-3 shows MCP-PMTs complete with a housing case.



THBV4_1102EA

Figure 11-2: Cross section of a typical MCP-PMT



R3809U series



R5916U series (gateable tube)

Figure 11-3: External view of MCP-PMTs

11.1.3 Voltage-divider circuit and housing structure

To operate an MCP-PMT, proper voltage must be supplied to each part, just as with a photomultiplier tube, and so a voltage-divider resistor circuit is usually used. Figure 11-4 shows a basic voltage-divider circuit used to operate an MCP-PMT (with a two-stage MCP) and the configuration of the housing that contains the MCP-PMT with the voltage-divider circuit.

As shown in the figure, a negative high voltage is applied to the photocathode, and the voltage-divider circuit gives a voltage gradient between the photocathode, MCP-in, MCP-out, and the anode by dividing the high voltage with properly selected resistors. The housing and circuit are designed for detection of ultra-fast signal waveforms, with careful consideration given to prevent "ringing" so that the output waveform distortion is suppressed to a minimum level.

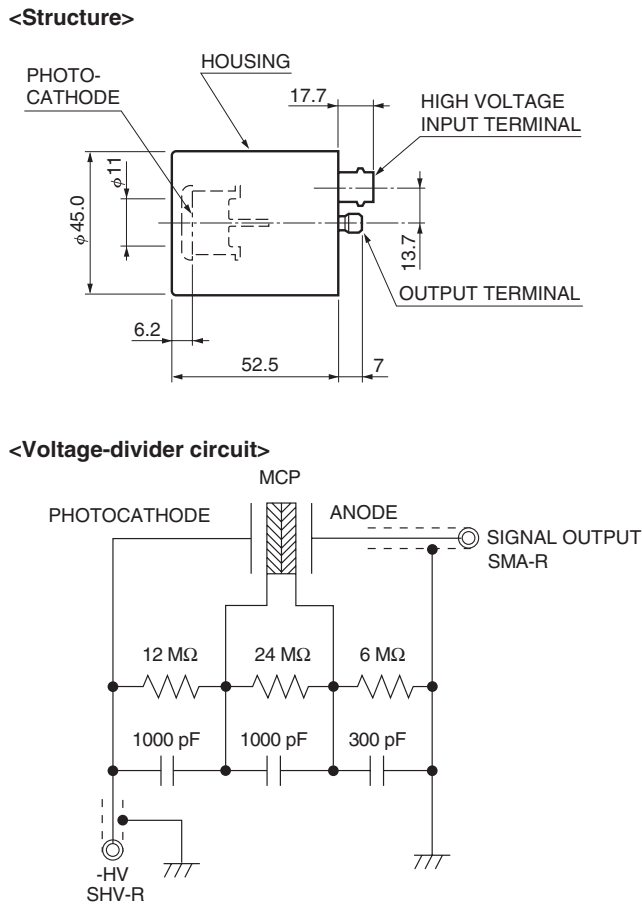


Figure 11-4: Housing configuration and operating circuit for MCP-PMT

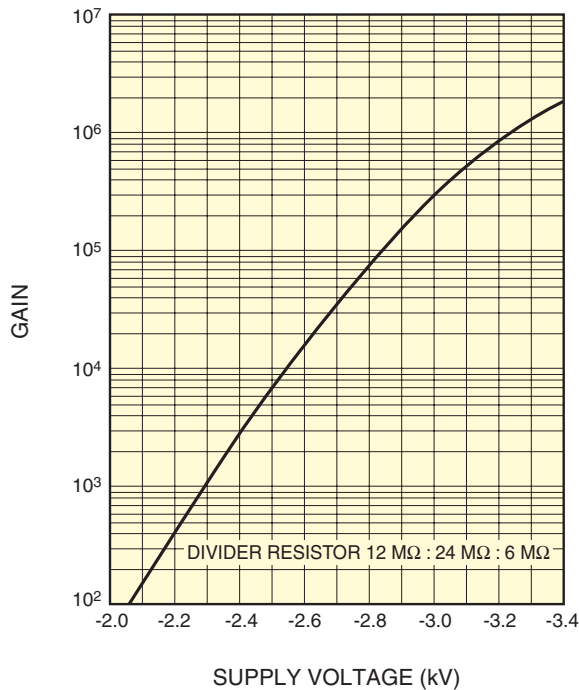
11.2 Basic Characteristics of MCP-PMT

11.2.1 Gain characteristics¹⁾

The gain of an MCP-PMT depends on the number of MCPs incorporated in the tube. Figure 11-5 shows the typical gain versus supply voltage characteristics of an MCP-PMT. The gain¹⁾ (μ) of an MCP is determined by the length-to-diameter ratio α ($=L/d$) of a channel, and approximated as follows:

$$\mu = \exp(G \cdot \alpha)$$

where G is the secondary emission characteristics called the gain factor. This gain factor G is an inherent characteristic of the channel wall material and is a function of the electric field intensity inside the channel.



THBV4_1105EA

Figure 11-5: Typical gain of an MCP-PMT (using a two-stage MCP of 6 μ m channel diameter)

In general, a higher gain can be obtained as α is made greater, though the gain rising point moves to the higher supply voltage side. However, if the gain becomes higher than 10⁴, noise begins to increase significantly due to ion feedback effects, which causes a serious problem. To avoid this, α is usually selected to be around 40 so that a single MCP provides a gain of about 10⁴ at 1 kV supply voltage. As shown in Figure 11-5 above, a higher gain can be obtained from a two-stage MCP-PMT. This gain level enables photon counting measurements.

11.2.2 Time characteristics²⁾

In ordinary photomultiplier tubes, the signal pulse can broaden during the multiplication process from the photocathode to the anode. This is due to the emission angle distribution and initial-velocity distribution of photoelectrons and secondary electrons, as well as the effects of the focusing lens. In an MCP-PMT, a strong electric field is applied in nearly parallel from the photocathode to MCP-in and the MCP-out to anode, so that the emission-angle distribution and initial-velocity distribution of photoelectrons can be almost ignored. Furthermore, since MCPs are used in place of conventional dynodes, the electron transit time in the secondary electron multiplication process is very short, allowing a dramatic improvement in the transit time spread. Due to these features, the MCP-PMTs offer time response characteristics that are the best among currently available photomultiplier tubes.

(1) Rise time, fall time

The rise and fall times of an MCP-PMT are evaluated from the output waveform when the MCP-PMT detects a light pulse whose width is sufficiently short compared to the time response of the MCP-PMT. These parameters are especially important when observing the waveform of ultra-short pulsed light. For the measurement method, refer to 4.3.1 in Chapter 4. Figure 11-6 shows an actual waveform obtained with an MCP-PMT.

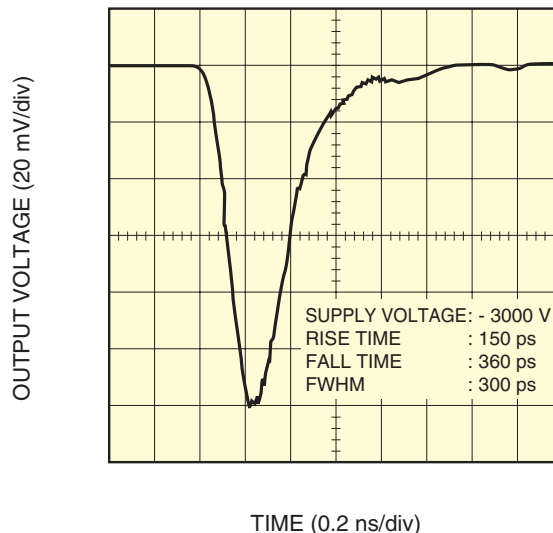


Figure 11-6: Pulse response waveform of MCP-PMT (R3809U-50)

THBV4_1106EA

(2) Transit time

The transit time is the time delay between the input of a light pulse at the photomultiplier tube and the appearance of the output pulse from the photomultiplier tube. For the measurement method, refer to 4.3.1 in Chapter 4.

(3) T.T.S. (Transit Time Spread), I.R.F. (Instrument Response Function)

When one photon enters an MCP-PMT, the photocathode converts it into an electron which travels to the anode while being multiplied. The transit time of an electron bunch slightly differs depending on each input photon. The fluctuation of this transit time is referred to as the transit time spread or T.T.S.. This T.T.S. is an important parameter, especially in the time-correlated single photon counting technique³⁾ where the measurement of timing is of prime consideration. For the measurement method, refer to 4.3.1 in Chapter 4.

At Hamamatsu Photonics, T.T.S. is evaluated with the measurement system shown in Figure 11-7. In this system, the I.R.F. (instrument response function) value is measured as the time characteristic for the entire system including the MCP-PMT. This is because the measurement system uses a laser pulse with approximately 35 picosecond pulse width, which acts as a time jitter nearly equal to the T.T.S. of the MCP-PMT. The relation between the T.T.S. and I.R.F. is given by the following equation:

$$(I.R.F.)^2 = (T.T.S.)^2 + T_w^2 + T_j^2$$

T_w : laser pulse width

T_j : other time jitter in the measurement system

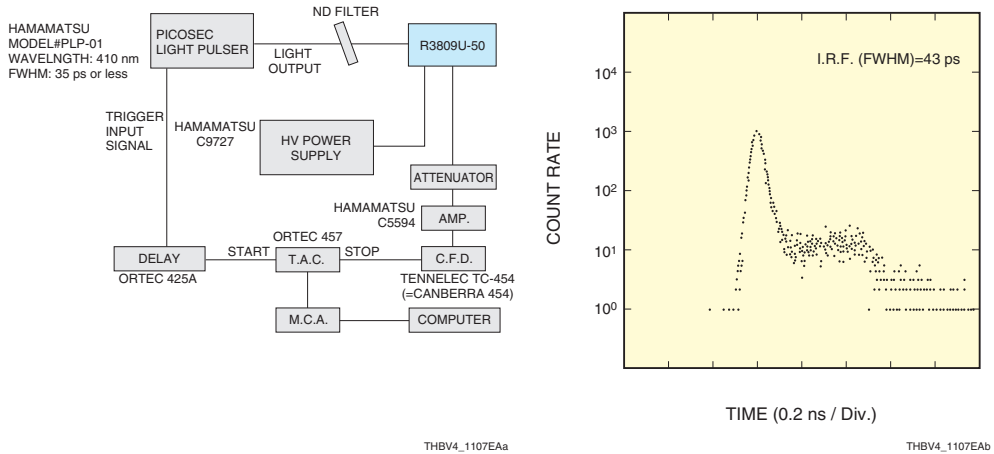


Figure 11-7: I.R.F. measurement using MCP-PMT (R3809U-50)

To evaluate the T.T.S. of an MCP-PMT more accurately, the measurement system shown in Figure 11-8 was used and data of 25.0 picoseconds has been obtained. This system uses a laser pulse with a 5 picosecond pulse width which is shorter than the T.T.S. of the MCP-PMT, therefore enabling accurate measurements.

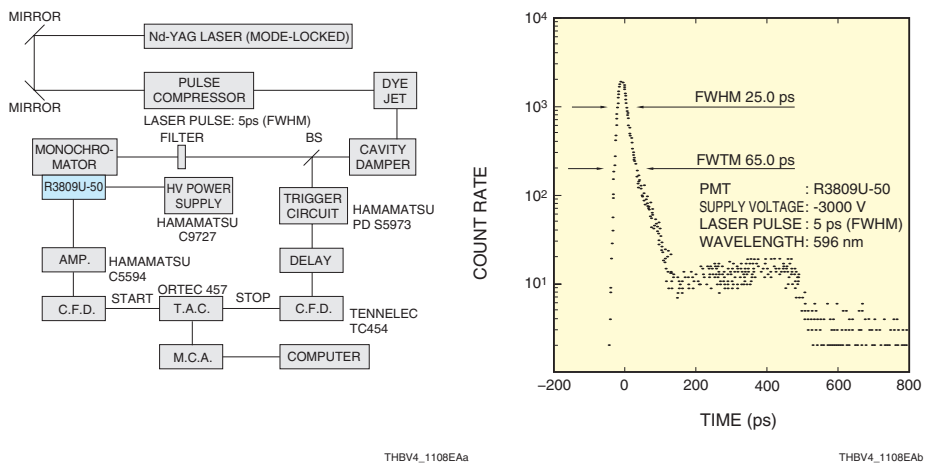


Figure 11-8: T.T.S. measurement of MCP-PMT (R3809U-50)

(4) Time characteristics of MCP-PMT

Time characteristics of various MCP-PMTs are summarized in Table 11-1 below. MCP-PMTs using a crystalline photocathode (GaAs, GaAsP) show a larger T.T.S. due to time spread in the photocathode. The gated MCP-PMT is slightly inferior in time characteristics compared to other types. This is because the electric field between the cathode and the gate mesh electrode is weak so that the photoelectron emission angle and initial velocity distribution tend to affect the time characteristics adversely to some extent.

| MCP-PMT Type No. | Photocathode | No. of MCPs | Rise time | Fall time | Transit time | I.R.F. (FWHM) |
|------------------|-------------------------|-------------|-----------|-----------|--------------|---------------|
| R3809U-50 | Multialkali | 2 | 160 ps | 360 ps | 550 ps | 45 ps |
| R3809U-61 | GaAs | 2 | 200 ps | 500 ps | 550 ps | 150 ps |
| R3809U-63 | Infrared extended GaAsP | 2 | 180 ps | 400 ps | 550 ps | 80 ps |
| R3809U-64 | GaAsP | 2 | 180 ps | 400 ps | 550 ps | 80 ps |
| R5916U-50 | Multialkali | 2 | 180 ps | 700 ps | 1 ns | 95 ps |

Note: Bialkali photocathode is also available.

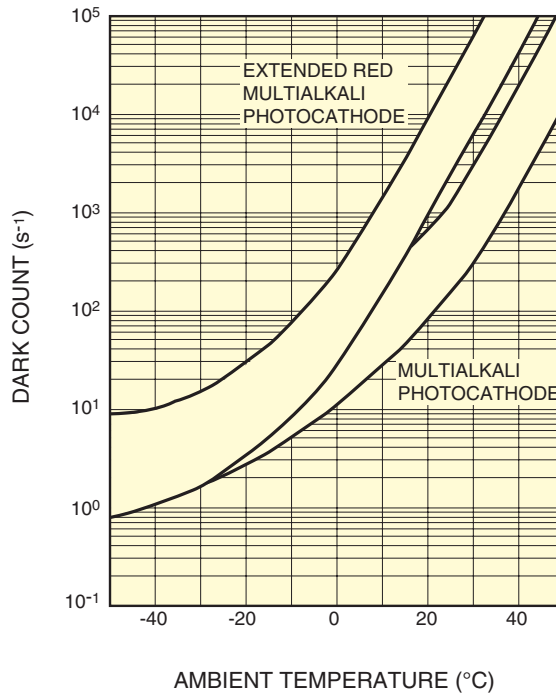
Note: Data in the above table shows typical values including the light source and circuit jitters.

A picosecond laser with a pulse width (FWHM) of less than 35 picoseconds is used for I.R.F. measurement. The R5916U-50 is a gated MCP-PMT.

Table 11-1: Comparison of MCP-PMT time characteristics

11.2.3 Temperature characteristics and cooling

As with normal photomultiplier tubes, the dark current and dark count of MCP-PMTs greatly depend on the photocathode type and operating temperature. In particular, the dark current and dark count of a multialkali photocathode with enhanced red sensitivity are relatively high at room temperatures, so MCP-PMTs using such a photocathode may need to be cooled during use.



THBV4_1109EA

Figure 11-9: Dark count vs. ambient temperature

Hamamatsu Photonics provides an optional thermoelectric cooler and holder specifically designed for MCP-PMTs. Using this cooler and the holder allows easy cooling of an MCP-PMT (at a temperature of approximately -30 °C).

11.2.4 Saturation characteristics

In general, the saturation of a photodetector is defined as the phenomenon in which the amount of output signal is no longer proportional to the incident light intensity. In the case of MCP-PMTs, the causes of this saturation are different from those of normal photomultiplier tubes using multiple stages of discrete dynodes. The saturation is caused by the dead time during which the MCP output current is limited and also by space charge effects inside the MCP. Precautions must be taken so that saturation by the dead time will not occur. Saturation characteristics of MCP-PMTs are described in detail below.

(1) Dead time¹⁾

When an MCP is irradiated by a pulsed electron current, a positive charge is generated at the MCP output end in accordance with the released electron current. This phenomenon deforms the potential distribution and weakens the electric fields so that the subsequent electron multiplication is suppressed. This charge is neutralized by the strip current flowing through the channel wall. However, a certain amount of time is required for neutralization because the strip current is small due to the high resistance of the MCP. The gain of signals entering within this period is usually low. The time required for neutralization is referred to as the dead time or recovery time. If the output charge per channel is given by Q_{out} and the strip current per channel by I_s , then the dead time τ_d is given by the following relation:

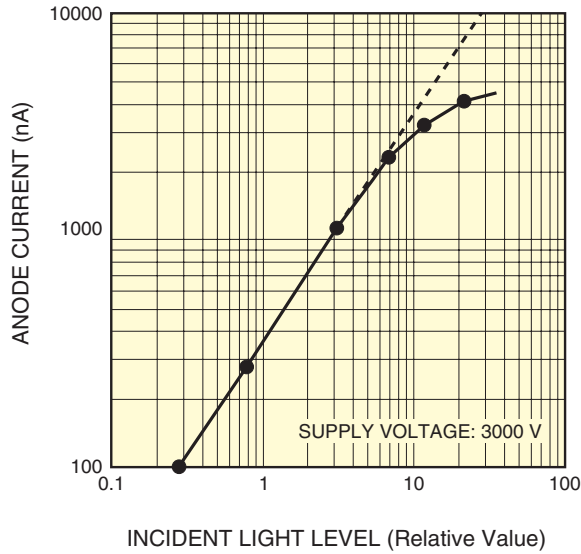
$$\tau_d = Q_{out} / I_s$$

When an MCP-PMT is operated in such a way that the next electron enters the MCP within this dead time, various types of output saturation occur as described below. If the MCP-PMT is operated at saturated levels, it cannot exhibit adequate performance, and also degrades the photocathode sensitivity and MCP gain.

(2) Saturation by DC light

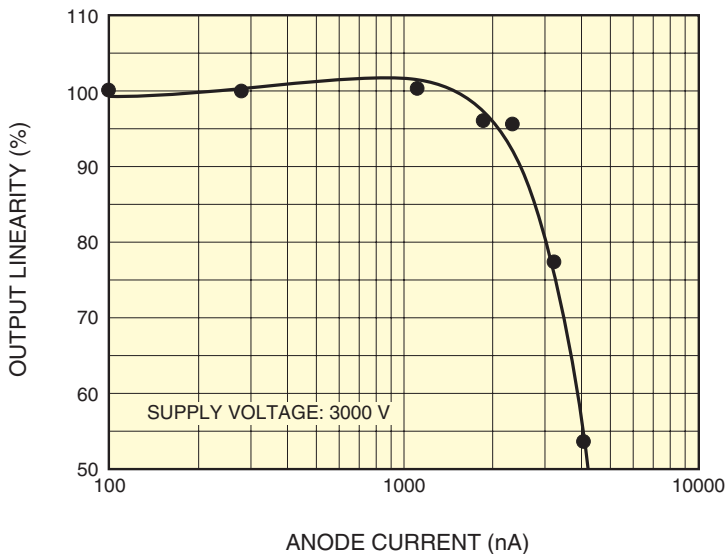
An MCP has a high resistance ranging from tens to hundreds of megohms, which limits the output current that can be extracted. Because of this, output current saturation occurs as the input current increases, as shown in Figures 11-10 (a) and (b). This is mainly caused by a decrease in the electric field intensity due to variations in the potential distribution at the output end of the MCP which results from large amounts of secondary electrons extracted from the MCP.

The decrease in the electric field intensity is recovered by the strip current flowing through the channel wall. Saturation in DC operation usually begins to occur when the output current becomes approximately 7 percent or more of the strip current, so use caution.



THBV4_1110EAa

Figure 11-10 (a): Saturation characteristics of MCP-PMT (11 mm effective diameter, 6 μm channel diameter) in DC operation (1)

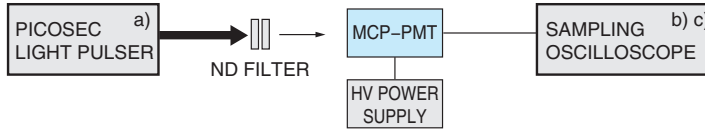


THBV4_1110EAb

Figure 11-10 (b): Saturation characteristics of MCP-PMT (11 mm effective diameter, 6 μm channel diameter) in DC operation (2)

(3) Saturation by pulsed light

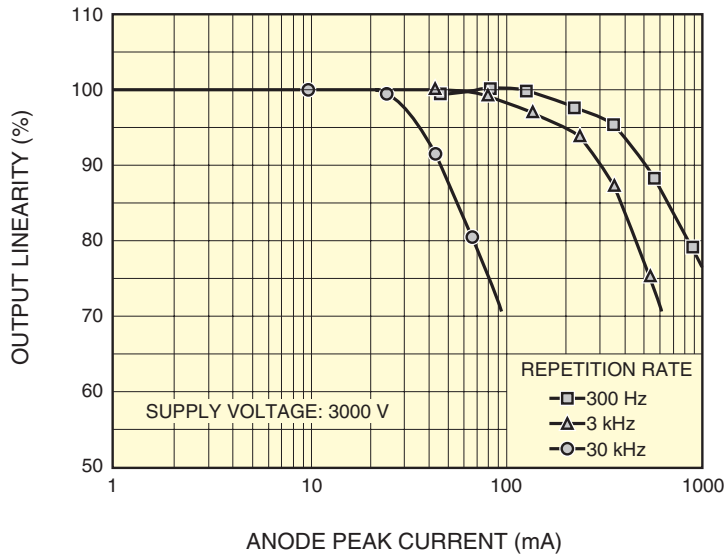
When pulsed light enters the MCP-PMT at a time interval that is longer than the dead time, the output linearity can be maintained to some extent. Figure 11-13 shows the linearity data of an MCP-PMT when detecting pulsed light.



- a) PICOSEC LIGHT PULSER: PLP-01 (HAMAMATSU)
 WAVELENGTH: 780 nm FWHM: 50 ps
 b) SAMPLING OSCILLOSCOPE: 11802 (TEKTRONIX)
 FREQUENCY BAND: 20 GHz
 c) SAMPLING HEAD: SD-26

THBV4_1111EAa

Figure 11-11 (a): Block diagram for MCP-PMT pulse linearity measurement



THBV4_1111EAb

Figure 11-11 (b): Pulse linearity of an MCP-PMT (11 mm effective diameter, 6 mm channel diameter)

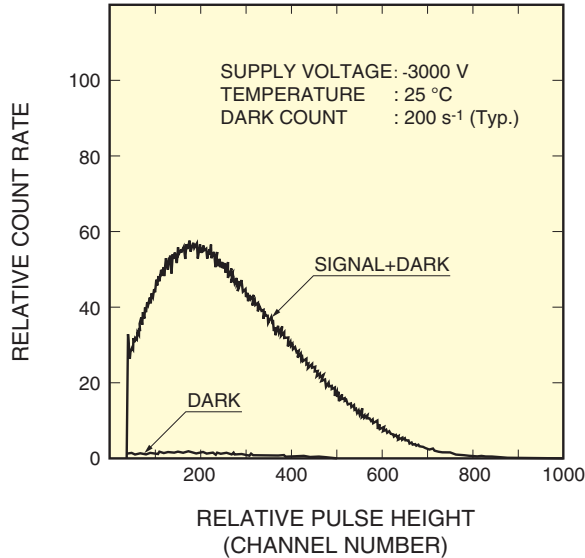
Figure 11-11 (a) shows a block diagram for measuring pulse linearity. A picosecond light pulser is used as the light source. The intensity of the pulsed light (FWHM 50 ps) is adjusted by ND (neutral density) filters and input to the MCP-PMT. Figure 11-11 (b) shows a typical pulse linearity plot for a MCP-PMT measured at a pulse repetition rate of 300 Hz to 30 kHz. Pulse currents up to a peak of 350 milliamperes can be extracted at a repetition rate of 300 Hz or less.

The maximum pulse current at a low repetition rate is determined by the product of the number of electrons released from one channel governed by space charge effects and the number of MCP channels. On the other hand, the maximum pulse current at a high repetition rate is determined by the ratio of the strip current to the total amount of charge which is determined by the product of the charge per pulse and the repetition rate.

When the repetition rate is too high, the MCP gain begins to drop because the next pulse enters within the dead time (see (1) in 11.2.4), causing output saturation.

(4) Saturation gain characteristics (pulse height distribution) in photon counting mode

Figure 11-12 shows pulse height distributions of photoelectron signals and dark current pulses taken with an MCP-PMT in the photon counting mode. Unlike single-photon pulse height distributions obtained with normal photomultiplier tubes, a distinct peak is formed in the pulse height distribution obtained with the MCP-PMT. This is due to the saturation occurring in the MCP channel by the space charge effect caused by a single photon.

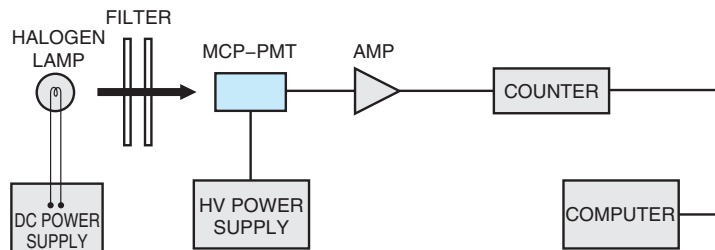


THBV4_1112EA

Figure 11-12: Typical pulse height distribution in single photon counting

(5) Count rate linearity in photon counting mode

Figure 11-13 illustrates a block diagram for measuring the count-rate pulse linearity in photon counting. Light intensity is reduced by neutral density filters down to the single photoelectron level. The number of single photoelectron pulses is counted by the counter connected to the MCP-PMT, and the count rate is measured and plotted while changing the number of incident photons.



THBV4_1113EA

Figure 11-13: Block diagram for measuring count-rate linearity in photon counting mode

Figure 11-14 shows count-rate linearity data measured in photon counting mode. A good linearity is maintained up to 10^7 s^{-1} .

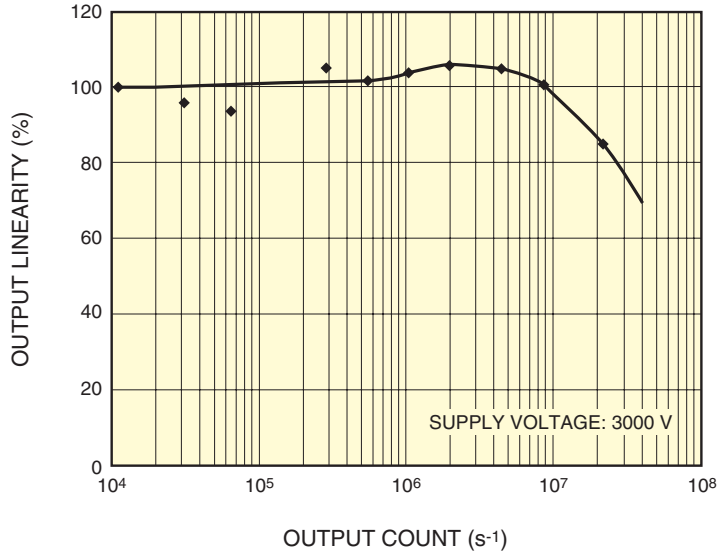


Figure 11-14: Count-rate linearity of an MCP-PMT (11 mm effective diameter, 6 mm channel diameter) in photon counting mode

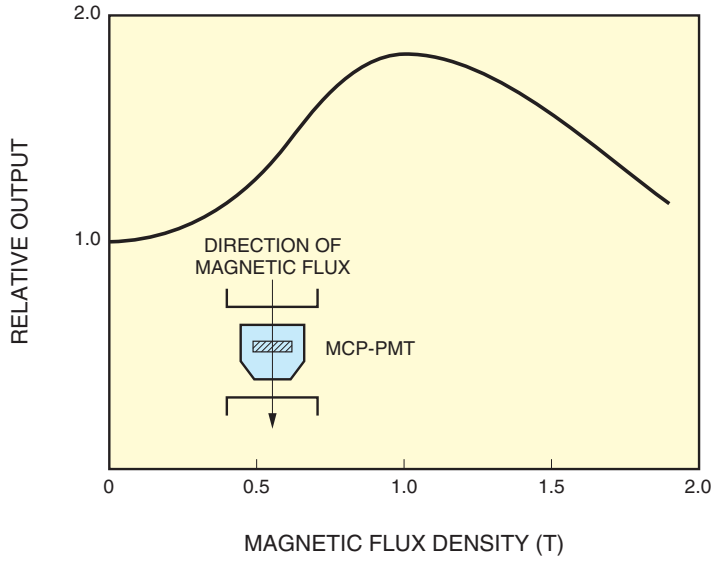
THBV4_1114EA

11.2.5 Magnetic characteristics²⁾

The following points are essential to improve magnetic characteristics.

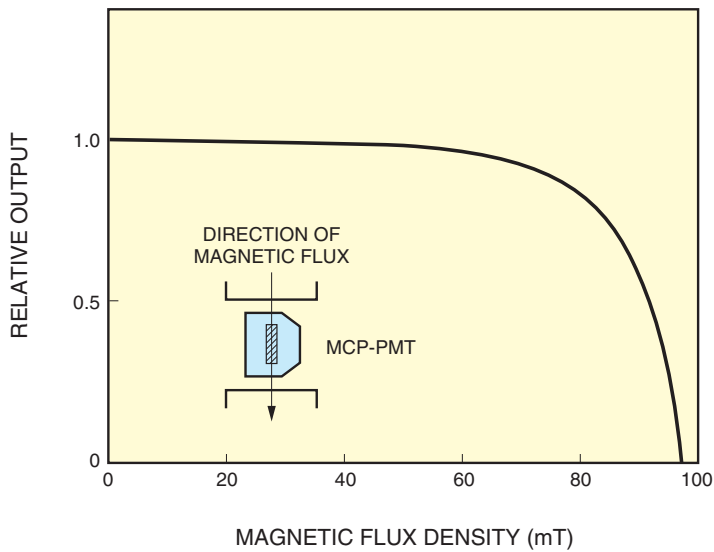
- (1) The distance between the photocathode, dynodes and anode should be shortened to minimize the electron transit distance.
- (2) The electrodes should be designed to apply a parallel electric field from the photocathode to the anode so that the secondary electrons do not converge but travel in parallel to the tube axis.
- (3) A high electric field intensity should be applied.

The MCP-PMT meets all the above requirements and provides superior magnetic characteristics. Figure 11-15 shows typical magnetic characteristics of an MCP-PMT. The extent of the effect of a magnetic field on the output depends on the direction of the magnetic field with respect to the MCP axis. In magnetic fields parallel to the tube axis, the MCP-PMT can operate at up to 2.0 tesla (T), but in magnetic fields perpendicular to the tube axis, the output drops drastically if fields exceed 70 millitesla (mT).



THBV4_1115EAa

(a) When in magnetic fields parallel to tube axis



THBV4_1115EAb

(b) When in magnetic fields perpendicular to tube axis

Figure 11-15: Typical magnetic characteristics of an MCP-PMT

11.3 Gated MCP-PMT²⁾

In applications in fields such as fluorescence lifetime measurement, laser Raman spectroscopy, and laser radar, photodetectors with a gate function are often required for more precise measurements. The gate function should have the following performance characteristics:

- (1) Shortest possible gate rising and falling times
- (2) Large switching ratio (gate on/off ratio)
- (3) Low switching noise

Figure 11-16 shows the structure of a gated MCP-PMT (R5916U-50). This tube basically consists of a photocathode, gate mesh, MCP, and anode. The gating function is performed by controlling the gate mesh which is positioned in close proximity to the photocathode as shown in Figure 11-16. Applying a reverse potential with respect to the photocathode potential to the gate mesh sets the "OFF" mode, while applying a forward potential sets the gate operation "ON" mode.

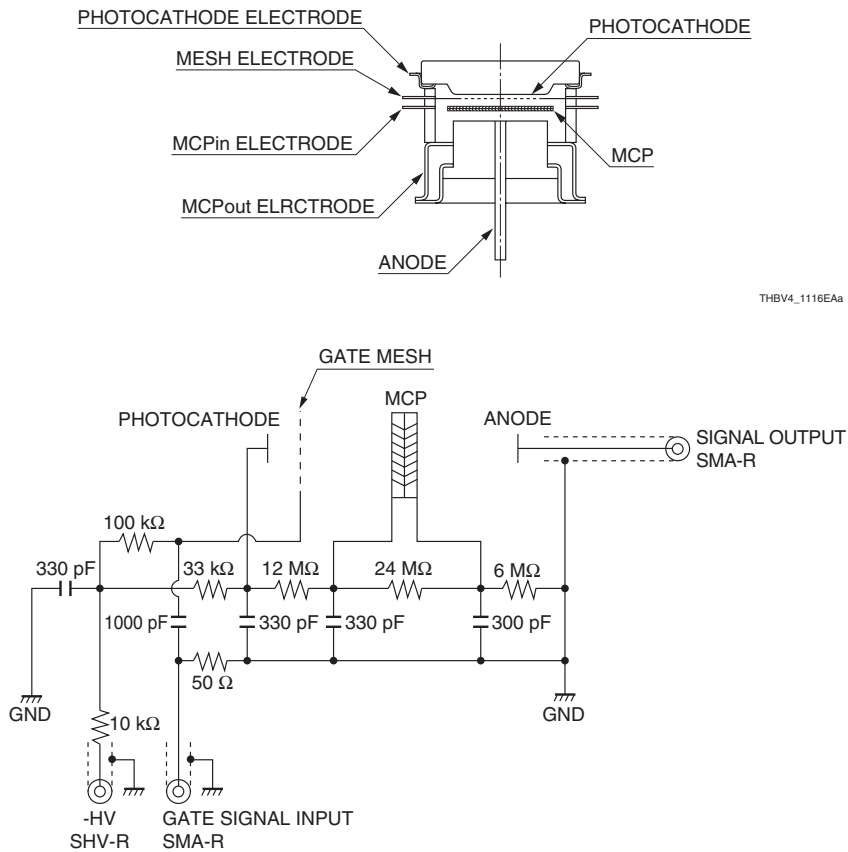
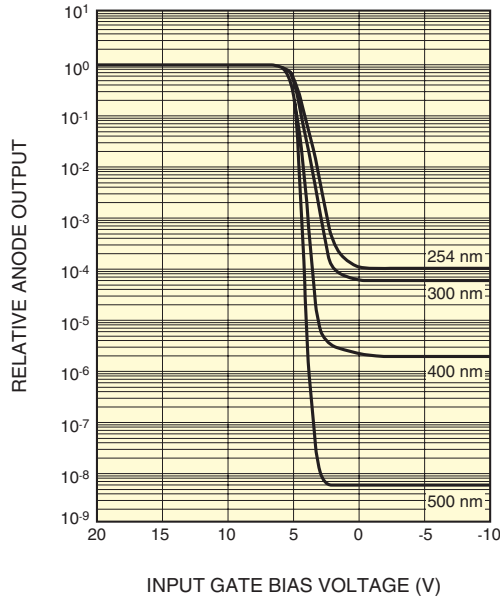


Figure 11-16: Structure of an MCP-PMT with gate mesh and its operating circuit (The typical example of gate off mode)

THBV4_1116EAb

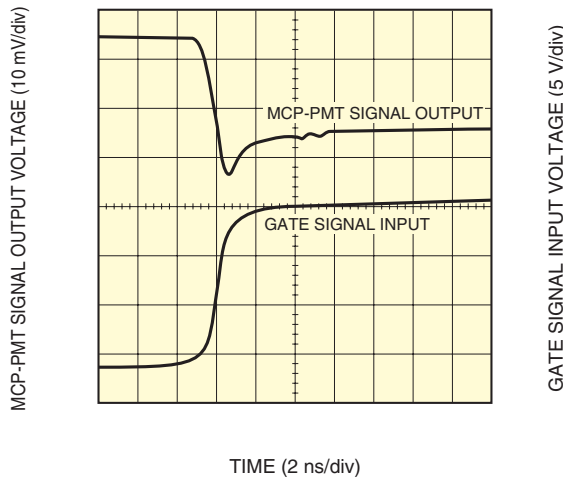
Figure 11-17 shows the basic characteristic of the gate function for a typical switching ratio taken with a gated MCP-PMT operating under static conditions. This data is the relation between the anode output and the voltage applied to the gate mesh (input gate bias voltage) when the photocathode potential is maintained at 0 volts and proves that the switching ratio is better than 10^8 (incident light wavelength: 500 nanometers).



THBV4_1117EA

Figure 11-17: Switching ratio characteristic under static operating conditions

Figure 11-18 shows the dynamic gate performance obtained with a gated MCP-PMT when a gate pulse is applied while continuous light is allowed to enter it. The MCP-PMT signal starts rising in approximately 1 nanosecond.



THBV4_1118EA

Figure 11-18: Dynamic gate characteristic

As explained above, the gated MCP-PMT offers significant improvement in gate speed and switching ratio in comparison with ordinary photomultiplier tubes.

References in Chapter 11

- 1) Hamamatsu Photonics Technical Information: MCP assembly, No. TMCP9001E01
- 2) Hamamatsu Photonics Catalog: Ultrafast MCP-PMT R3809U (Feb. 1992)
Hamamatsu Photonics Catalog: Microchannel Plate - Photomultiplier Tubes (MCP-PMTs), No. T-112-02 (Feb. 1990)
H. Kume et al.: Ultrafast Microchannel Plate - Photomultiplier Tubes, *Applied Optics*, Vol. No. 27 (Mar. 15, 1988)
- 3) Hamamatsu Photonics Technical Information: Applications of MCP-PMTs to Time Correlated Single Photon Counting and Related Procedures. No. ET-03 (Feb. 1991)
Desmond V. O'Connor, David Phillips: *Time-Correlated Single Photon Counting*, Academic Press (Harcourt Brace Jovanovich, Publishers), The Royal Institution, London, UK

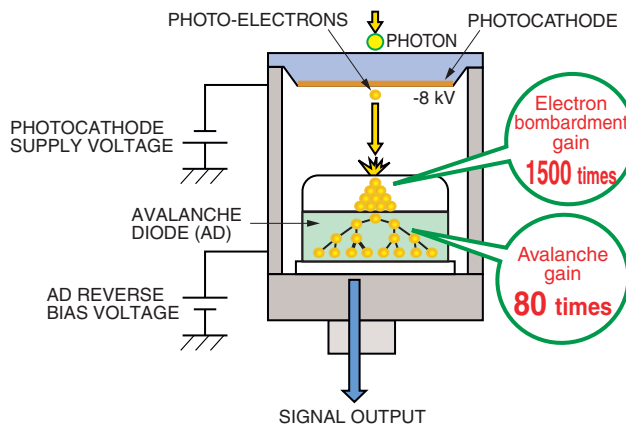
CHAPTER 12

HPD (Hybrid Photo-Detector)

HPD (Hybrid Photo-Detector)¹⁾²⁾³⁾ incorporates a semiconductor device (avalanche diode or AD) into an electron tube. In HPD operation, photoelectrons released from the photocathode are accelerated by a high voltage to directly strike the semiconductor device where secondary electrons are multiplied by the process of secondary emission. Features offered by HPD include extremely little fluctuation during the multiplication, single photoelectron resolution, high stability, and excellent time characteristics. These features make the HPD useful for a wide range of advanced applications such as laser microscopy, fluorescence lifetime imaging microscopy (FLIM), fluorescence correlation spectroscopy (FCS), LIDAR (Light Detection and Ranging), and high-energy physics experiments.⁴⁾⁵⁾⁶⁾

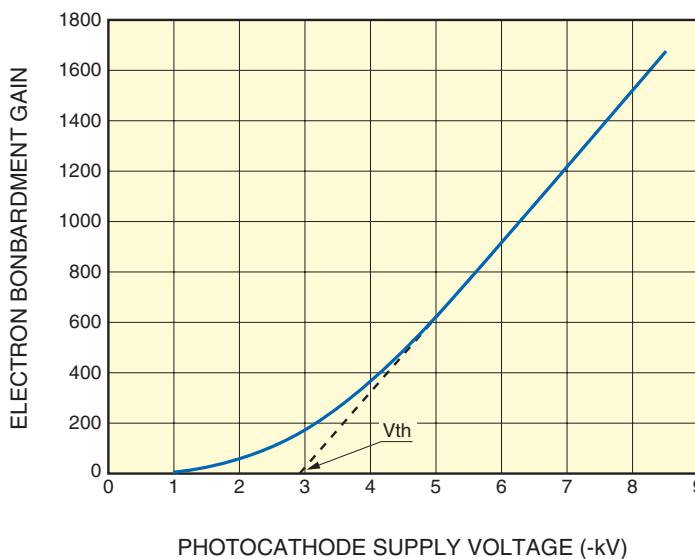
12.1 Operating Principle of HPD

Figure 12-1 shows the operating principle of an HPD. The HPD consists of a photocathode that converts light into electrons and a semiconductor device (avalanche diode or AD) designed for electron bombardment, sealed into a vacuum tube. When light enters the photocathode, photoelectrons are emitted from the photocathode according to the amount of light. These photoelectrons are accelerated by a high negative voltage ranging from a few to about 10 kilovolts supplied to the photocathode and are then bombarded onto the avalanche diode where electron-hole pairs are generated according to the incident energy of the photoelectrons. This is called "electron bombardment gain." A typical relation between this electron bombardment gain and the photocathode supply voltage is plotted in Figure 12-2. This electron bombardment gain is in principle proportional to the photocathode supply voltage. However, there is actually a loss of energy during electron bombardment due to the insensitive surface layer of the avalanche diode, so their proportional relation does not hold at a low voltage. In Figure 12-2, the voltage at a point on the voltage axis (horizontal axis) where the dotted line intersects is called the threshold voltage [V_{th}].



THBV4_1201EA

Figure 12-1: Schematic principle of an HPD



THBV4_1202EA

Figure 12-2: Electron bombardment gain characteristics

The internal avalanche diode of an HPD generates an electron and hole pair per an incident energy of approximately 3.6 eV. The electron bombardment gain G_b can be expressed by Eq. 12-1 using the electrical potential difference V_{pc} [V] between the photocathode and the avalanche diode (a difference equal to the photocathode supply voltage) and the threshold voltage [V_{th}] that is determined by the avalanche diode. In Figure 12-2, V_{th} is approximately 3 kilovolts.

$$G_b = (V_{pc} - V_{th}) / 3.6 \quad \text{..... (Eq. 12-1)}$$

The cluster of secondary electrons acquired by electron bombardment is further multiplied by the avalanche gain in the avalanche diode. The avalanche gain increases or decreases according to the reverse bias voltage applied to the avalanche diode. Here, if the gain of the avalanche diode is G_t , then the HPD total gain G is given by Eq. 12-2.

$$G = G_b \times G_t \quad \text{..... (Eq. 12-2)}$$

In the case of an HPD made by Hamamatsu Photonics, the electron bombardment gain G_b is approximately 1500 when the photocathode supply voltage is -8 kilovolts. Moreover, an avalanche gain G_t of approximately 80 can be attained by applying a reverse voltage of about 400 volts to the avalanche diode. The total gain G will therefore be approximately 120000.

12.2 Features of HPD

In low-level-light measurement, detectors such as photomultiplier tubes and SPAD⁷⁾ (single photon avalanche diode) are widely used. HPDs have the following advantages over those detectors.

The electron bombardment gain of an HPD corresponds to the gain obtained by the first dynode of an ordinary photomultiplier tube. As already mentioned, HPDs deliver an electron bombardment gain of about 1500 at a photocathode supply voltage of -8 kilovolts, which is much higher than the first dynode gain of an ordinary photomultiplier tube. This means that gain fluctuation is significantly reduced.

When measuring pulsed light using an ordinary low-light detector, spurious pulses (afterpulses) appear following the output pulse that corresponds to the input signal. HPDs feature very few afterpulses.⁸⁾ (See 12.3.6 in Chapter 12.)

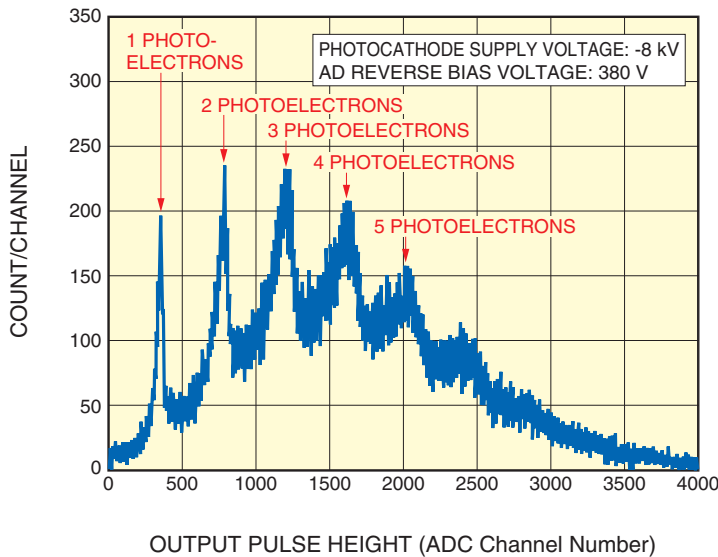
The electron trajectories in an HPD are designed so that all electrons released from the photocathode enter the avalanche diode. This contributes to high collection efficiency and good uniformity characteristics.

Just as with ordinary photomultiplier tubes, various photocathodes are available to allow selecting the desired type that has the highest quantum efficiency at the incident light wavelengths. Compared to semiconductor detectors such as SPAD having an effective area of 100 square micrometers, HPDs offer a large effective area of more than several square millimeters. Even larger diameter types and position-sensitive types⁹⁾¹⁰⁾¹¹⁾¹²⁾¹³⁾ are also available.

12.3 Various Characteristics of HPD

12.3.1 Pulse height resolution

Since the electron bombardment gain that corresponds to the gain of the first dynode of an ordinary photo-multiplier tube is very high, HPDs ensure ideal signal amplification with very little fluctuation in the electron multiplication. For example, when pulsed light adjusted to a light level that causes the photocathode to emit 3 photoelectrons on average is repeatedly input to an HPD, multiple signal peaks corresponding to 1 to 5 photoelectrons can be detected by plotting the output pulse height distribution as shown in Figure 12-3. The reason why these multiple signal peaks are detectable is that the electron multiplication fluctuation is extremely small. This is a significant feature of HPD.

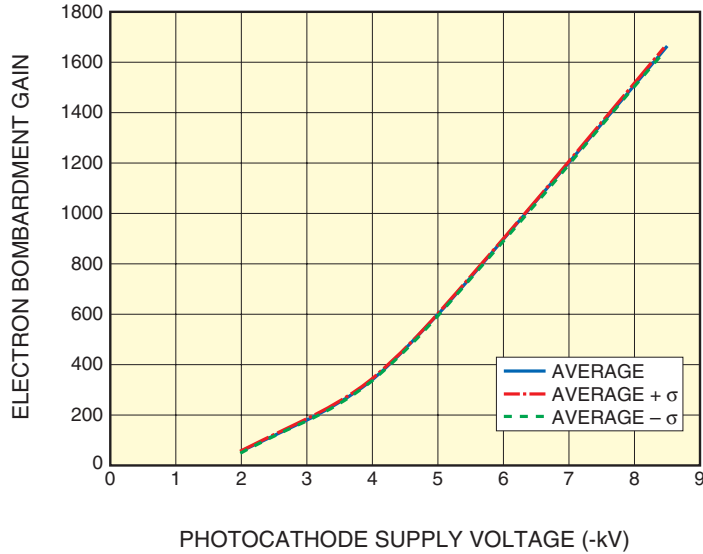


THBV4_1203EA

Figure 12-3: Output pulse height distribution in a multi-photoelectron event

12.3.2 Gain characteristics and electron bombardment gain uniformity

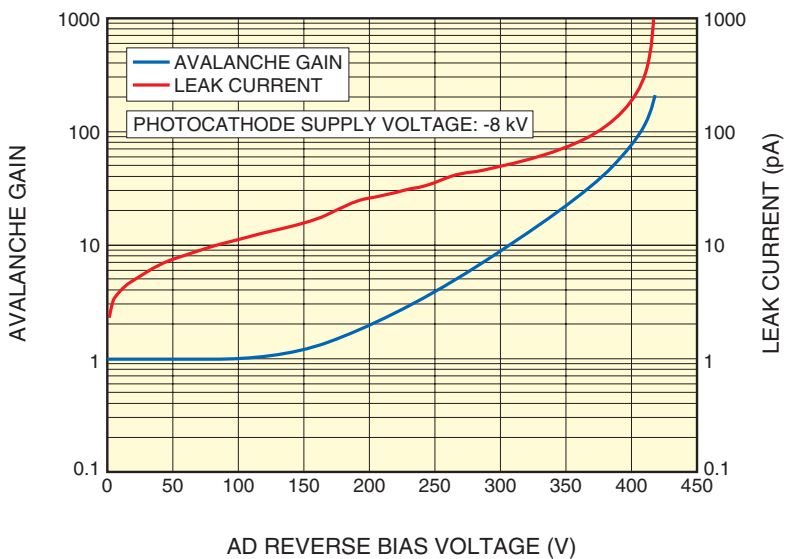
As described in the operating principle section, HPD gain is expressed by the product of the electron bombardment gain G_b and the avalanche gain G_t (see Eq. 12-2). As shown in Figure 12-2, when a certain threshold voltage is exceeded, the electron bombardment gain increases in proportion to the photocathode supply voltage according to Eq. 12-1. The electron bombardment gain depends on the electron accelerating voltage and the electron input surface structure of the avalanche diode. However, because the electron input surface of the avalanche diode is homogeneous, the individual difference in electron bombardment gain between individual HPDs is very small. This difference in the electron bombardment gain between individual HPDs is plotted in Figure 12-4.



THBV4_1204EA

Figure 12-4: Difference in electron bombardment gain between individual HPDs

Figure 12-5 shows the gain and leak current characteristics of the avalanche diode. The avalanche gain gradually increases from a point where the voltage supplied to the avalanche diode (AD reverse bias voltage) exceeds a certain value and then sharply increases at a point near the breakdown voltage. The breakdown voltage for Hamamatsu HPDs is defined as the voltage at which the leak current reaches 1 microampere. If an HPD is used near the breakdown voltage, it is difficult to maintain stable operation since the gain varies sharply. The maximum AD reverse bias voltage is therefore specified as a voltage that is 10 volts lower than the breakdown voltage. The avalanche gain differs slightly depending on the production lot of the avalanche diode. The avalanche gain is also temperature dependent. See 12.3.5 "Temperature characteristics" for details on temperature characteristics.



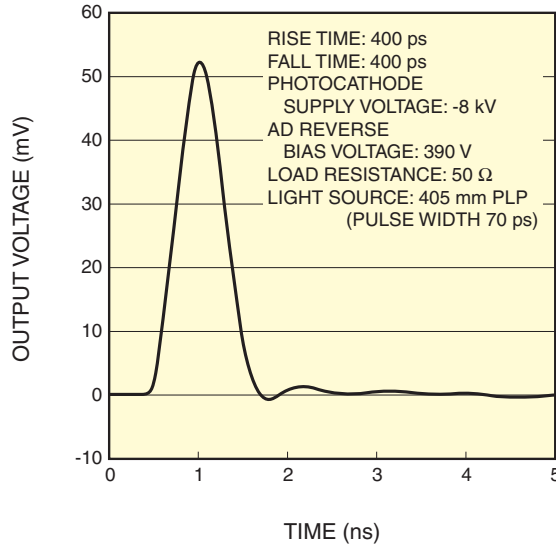
THBV4_1205EA

Figure 12-5: Avalanche gain and leak current characteristics

12.3.3 Time response characteristics

(1) Rise time, fall time, and electron transit time

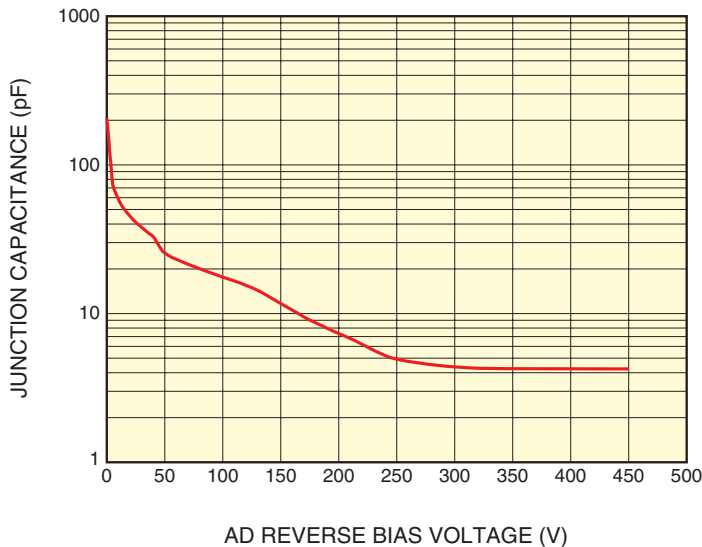
Figure 12-6 shows a typical output waveform of a Hamamatsu high-speed HPD. This output waveform was obtained by using a semiconductor pulsed laser (FWHM: approximately 70 picoseconds, wavelength: 405 nanometers). Time response characteristics of the HPD are determined by the junction capacitance of the internal avalanche diode. The rise time and fall time are nearly constant even when the AD reverse bias voltage is changed within the voltage range where the avalanche diode is fully depleted.



THBV4_1206EA

Figure 12-6: Time response waveform

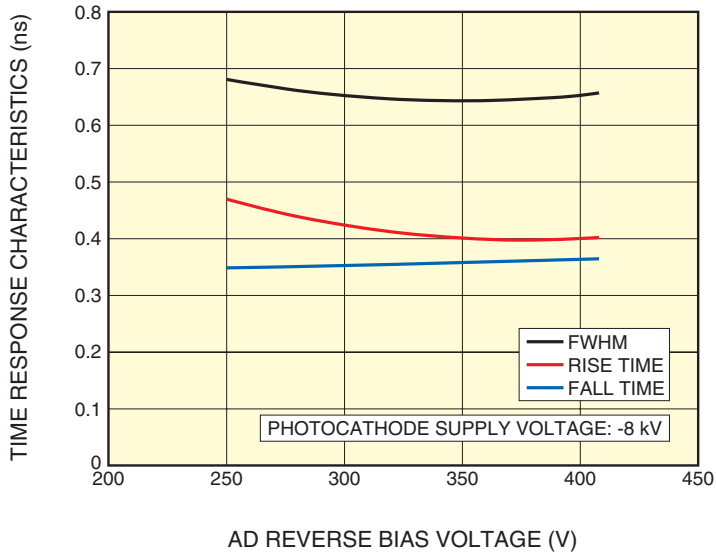
Figure 12-7 shows the junction capacitance of a high-speed HPD versus the AD reverse bias voltage. The graph clearly shows that the avalanche diode is fully depleted when the AD reverse bias voltage higher than 300 volts is applied.



THBV4_1207EA

Figure 12-7: Junction capacitance vs. AD reverse bias voltage

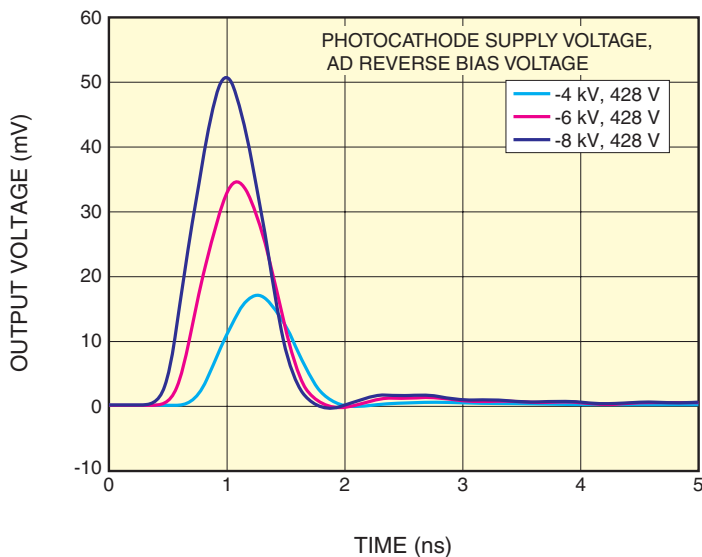
Figure 12-8 shows the time response characteristics when the AD reverse bias voltage is changed while the photocathode supply voltage is kept constant. As seen in the graph, the rise time and fall time are nearly constant at an AD reverse bias voltage of 300 volts or higher that cause full depletion of the avalanche diode.



THBV4_1208EA

Figure 12-8: Time response characteristics vs. AD reverse bias voltage

On the other hand, when the photocathode supply voltage is changed while the AD reverse bias voltage is kept constant, the rise time and fall time do not vary but the electron transit time does fluctuate. This is because the time taken for the photoelectrons released from the photocathode to move to the surface of the avalanche diode varies with the photocathode supply voltage. Figure 12-9 shows the difference in the electron transit time when the photocathode supply voltage is changed. As the graph shows, the higher the photocathode supply voltage, the shorter the electron transit time.



THBV4_1209EA

Figure 12-9: Difference in electron transit time when photocathode supply voltage is changed

(2) T.T.S. (Transit Time Spread)

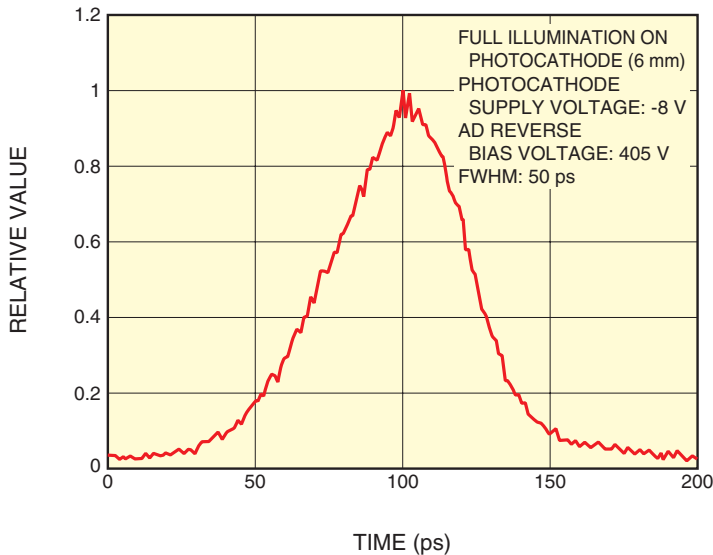
When a photocathode is fully illuminated with light, the transit time of each single photoelectron pulse fluctuates. This fluctuation is called T.T.S. (see (2) in 4.3.1 of Chapter 4). The following three factors are mainly related to the T.T.S. in HPDs.

The first factor is the transit time within the photocathode. Light is converted into photoelectrons in the photocathode, and those photoelectrons move within the photocathode toward the vacuum. When the photocathode layer is thick, the position (depth) at which the input light is converted into photoelectrons varies, increasing the fluctuation in transit time within the photocathode. Generally, the photocathode layer of crystalline photocathodes made from GaAsP(Cs) and GaAs(Cs) is thick compared to photocathodes made from alkali metals, so there is a large fluctuation in the transit time.

The second factor is the variation in the time taken for the photoelectrons to move in the vacuum from the photocathode to the avalanche diode. Since the distance to the avalanche diode differs depending on the light incident position on the photocathode, the transit time fluctuates. Some Hamamatsu high-speed HPDs with an alkali metal photocathode use a light input window having a certain curvature which keeps the distance from the light incident positions on the photocathode to the avalanche diode constant.

The third factor is the electron transit time within the avalanche diode. Since large amounts of electrons are produced in the avalanche diode by electron bombardment gain, the difference in their transit time within the avalanche diode can be ignored.

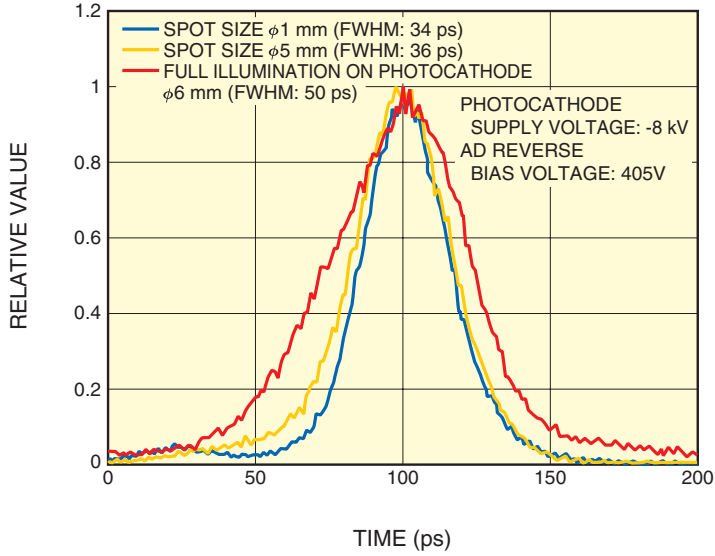
Figure 12-10 shows a typical T.T.S. of a high-speed HPD measured when its alkali photocathode is fully illuminated. A T.T.S. of 50 picoseconds was achieved including the fluctuations in the measurement system.



THBV4_1210EA

Figure 12-10: T.T.S. of a high-speed HPD

As described earlier, the T.T.S. varies since the transit time will vary depending on the light incident position on the photocathode. Figure 12-11 shows T.T.S. measured when the size of the incident light spot was changed.



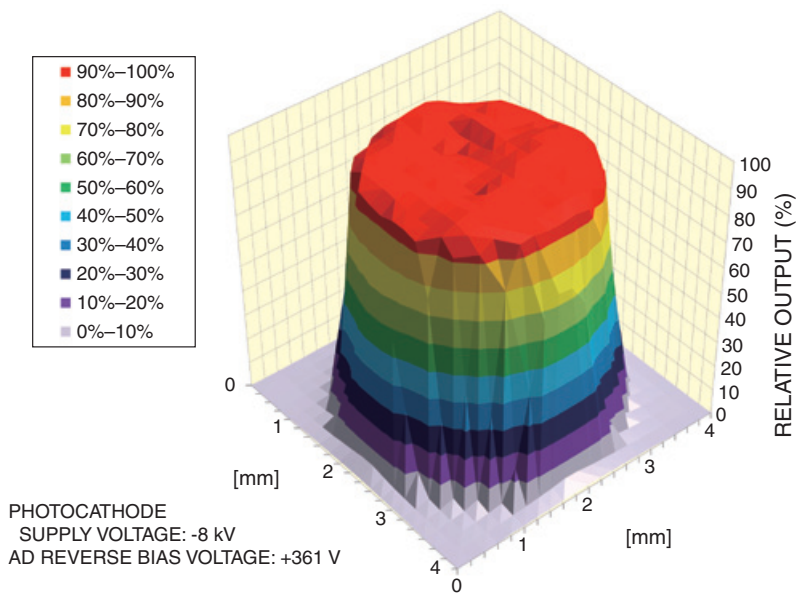
THBV4_1211EA

Figure 12-11: T.T.S. measured with different incident light spot sizes

Using a smaller incident light spot size limits the positions on the photocathode from which photoelectrons are released. This smaller light spot acts to suppress variations in transit time, so adjusting the light spot size will improve the T.T.S. of the same HPD.

12.3.4 Uniformity

Uniformity is the variation of output sensitivity versus the photocathode position. Anode uniformity of an HPD is determined by the photocathode and avalanche diode. Typical anode uniformity characteristics are shown in Figure 12-12. HPDs have extremely uniform sensitivity since the electron trajectories in HPDs are designed so that all electrons emitted from the photocathode enter the avalanche diode.



THBV4_1212EA

Figure 12-12: Typical anode uniformity characteristics of an HPD

12.3.5 Temperature characteristics

An HPD incorporates an avalanche diode as the electron multiplier and so is temperature dependent the same as with commonly used avalanche photodiodes. HPD temperature dependence can be broadly divided into two categories.

(1) Temperature dependence of leak current and breakdown voltage

As mentioned earlier, as the AD reverse bias voltage increases, the leak current also sharply increases from a certain point. The breakdown voltage for Hamamatsu HPDs is defined as the voltage at which the leak current reaches 1 microampere. The leak current and breakdown voltage tend to decrease as the ambient temperature decreases. Figure 12-13 shows the temperature dependence of the leak current, and Figure 12-14 shows the temperature dependence of the breakdown voltage.

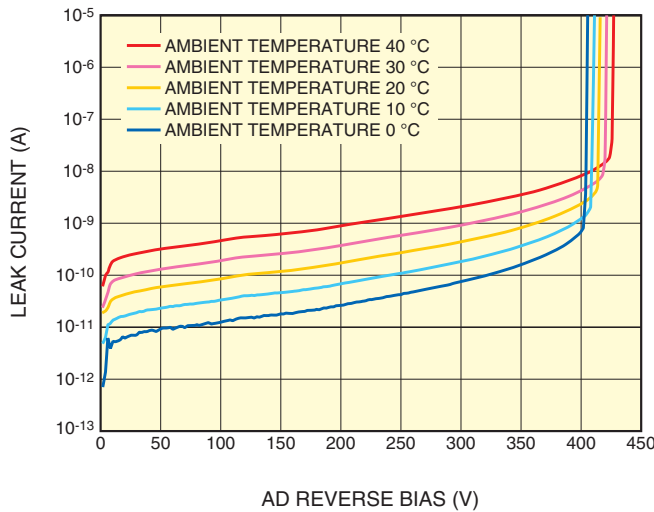


Figure 12-13: Temperature dependence of leak current

THBV4_1213EA

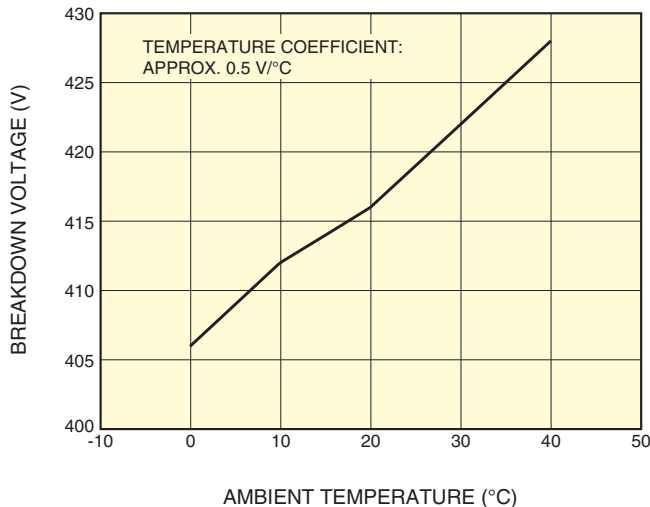


Figure 12-14: Temperature dependence of breakdown voltage

THBV4_1214EA

(2) Temperature dependence of avalanche gain

The avalanche gain tends to decrease as the ambient temperature increases. Figure 12-15 shows the temperature dependence of the avalanche gain.

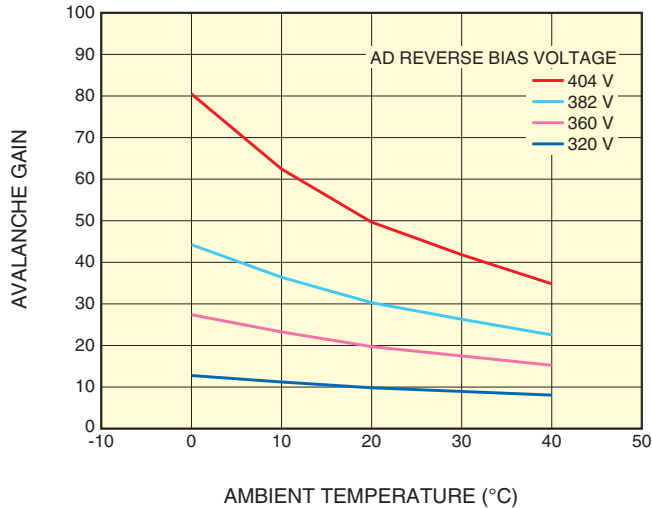


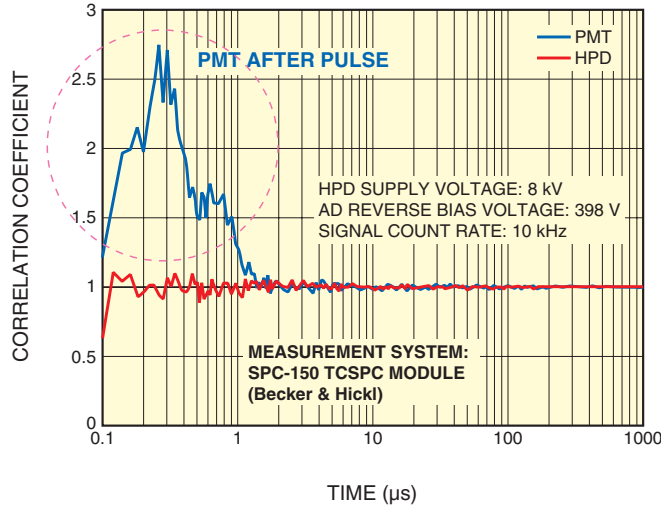
Figure 12-15: Temperature dependence of avalanche gain

THBV4_1215EA

The avalanche gain also varies depending on the AD reverse bias voltage. As the graph in Figure 12-15 shows, the avalanche gain varies sharply when the AD reverse bias voltage is high, but varies mildly when the AD reverse bias voltage is low. This means that when operating an HPD at a higher AD reverse bias voltage, the ambient temperature should be controlled to ensure stable operation. During operation at a higher AD reverse bias voltage, the HPD gain drastically increases as the ambient temperature decreases, so caution must be taken to avoid damaging the avalanche diode. In general, cooling the photocathode reduces the dark current. However, it also causes the gain and breakdown voltage to vary, so these factors should also be taken into account when cooling an HPD.

12.3.6 Afterpulsing

When measuring pulsed light, spurious pulses may appear following the output pulse that corresponds to the input signal. These pulses are called afterpulses (see section 4.3.8 in Chapter 4). There are several types of afterpulses. Afterpulses with a long delay are caused by the positive ions generated by the ionization of residual gases in a detector, which occurs when the residual gases collide with electrons. The positive ions generated by the ionization return to the photocathode (ion feedback) and produce many photoelectrons which result in afterpulses. However, in the case of HPDs, this ion feedback is very unlikely to occur compared to photomultiplier tubes, because HPDs have a simple internal structure compared to photomultiplier tubes and so maintain a high vacuum with few residual gases. Afterpulses measured with an HPD and photomultiplier tube are plotted in Figure 12-13. This data shows the probability at which afterpulses may occur when a single photoelectron is input. The data was measured from a point 100 nanoseconds after the signal pulse was generated. The photomultiplier tube used for comparison generated multiple afterpulses in a time range from 100 nanoseconds to 1 microsecond, while the HPD generated few afterpulses. This makes HPD useful in application fields where high-speed phenomena are measured such as in fluorescence lifetime measurement, fluorescence correlation spectroscopy (FCS), and laser radar (LIDAR).



THBV4_1216EA

Figure 12-16: Afterpulses of HPD and photomultiplier tube (PMT)

12.3.7 Effects of X-ray feedback

When the accelerated photoelectrons strike the avalanche diode, X-rays are emitted at a certain probability from the avalanche diode. These generated X-rays are Bremsstrahlung X-rays and characteristic X-rays. If these X-rays enter the photocathode, a large amount of photoelectrons are released from the photocathode. This phenomenon is called X-ray feedback. In a Hamamatsu high-speed HPD, this X-ray feedback occurs approximately 500 nanoseconds after the true signal is output, making it difficult to discriminate the X-ray feedback from the true signal. The number of photoelectrons and the probability that photoelectrons might be produced by X-ray feedback differ depending on the photocathode. In general, there is a tendency towards fewer such photoelectrons being generated in alkali metal photocathodes with thin photocathode layers than in crystalline photocathodes. The probability of generating noise pulses of Hamamatsu high-speed HPDs with a crystalline photocathode is an extremely small level that is one ten-thousandth per single photoelectron. However, when the incident light intensity increases, the number of photoelectrons also increases, which then increases the probability that X-rays might be generated. This X-ray feedback might therefore causes problems when measuring high intensity incident light, so caution is required. X-ray feedback on the other hand is unlikely to occur in photon counting measurement that detects single photoelectrons and so rarely causes problems.

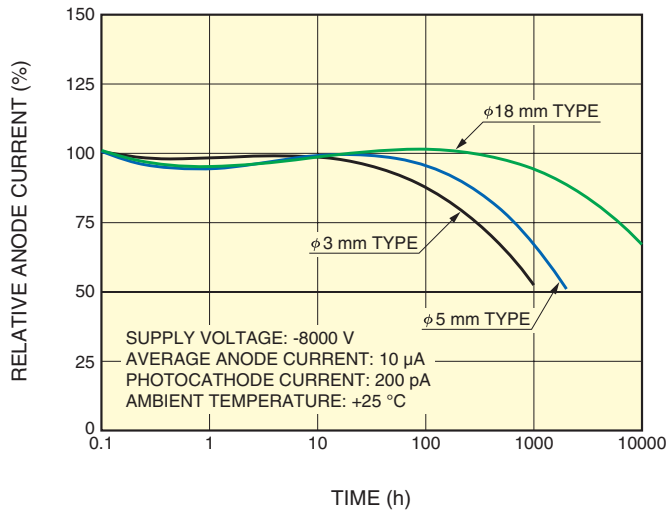
12.3.8 Drift characteristics

Variation (instability) over a short time period of several hours is mainly referred to as drift. In ordinary photomultiplier tubes, the drift is mainly caused by variations in the secondary emission ratio of each dynode. However, HPDs have no dynodes and so exhibit good drift characteristics.

12.3.9 Life characteristics

There are two main factors that determine the lifetime of an HPD. One is the degradation of the electron bombardment gain. The other is the deterioration of the photocathode which greatly differs depending on the photocathode material and size.

Generally, when the photocathode material is the same, an HPD with a larger photocathode size has a longer lifetime if operated at the same photocurrent level. Figure 12-17 shows the life characteristics of HPDs with different photocathode sizes. Three types of lifetime data are plotted by measuring the anode output current of HPDs having the same photocathode (GaAsP(Cs)) but different effective areas (3, 5 and 8 millimeters in diameter). Each HPD was fully illuminated and the incident light was adjusted so that the maximum value of the photocathode average current is 200 picoamperes. This graph clearly shows that the larger the effective area, the longer the lifetime will be. This is because the amount of the incident light per unit area is reduced by using a larger area while keeping the average photocathode current constant, and so there is less damage to the photocathode. In contrast, when HPDs with different photocathode sizes are illuminated with the same size light spot, they exhibit similar life characteristics since the amount of the incident light per unit is the same. We therefore recommend making the size of the incident light as large as possible.



THBV4_1217EA

Figure 12-17: Life characteristics of HPDs with different photocathode sizes

Life characteristics also differ depending on the photocathode material. The lifetime of alkali metal photocathodes is longer than that of crystalline photocathodes made from GaAsP(Cs) and GaAs (Cs). For example, bialkali photocathodes of 6 millimeters in diameter will have hardly any deterioration. One cause of deterioration in crystalline photocathodes is ion feedback in which positive ions damage the photocathode.

12.4 Precautions when using an HPD

To use an HPD safely and correctly, take the following precautions:

- When a voltage is supplied to the HPD, be careful not to touch the HPD and power cable. Touching them may cause electrical shock.
- Before supplying a voltage to the HPD, make sure that all circuits are securely connected and grounding is properly done. Also make sure there is no light incident on the HPD.
- When supplying a voltage to the HPD, first supply an AD reverse bias voltage to the avalanche diode, and then supply the voltage to the photocathode.
- Before connecting or disconnecting the HPD to a subsequent circuit, make sure that all power supplies are turned off and the HPD is not charged up. Ignoring this instruction may cause electrical shock or damage to the subsequent circuit.
- To prevent leak current and discharge problems with the HPD which might occur due to supplying a high voltage, avoid using the HPD in locations exposed to high humidity.
- The maximum value of the average photocathode current is specified for each type of HPD. Do not allow excessive light to enter the HPD, since this might cause a current higher than that rated value to flow.
- Use an AD reverse bias voltage that does not exceed its maximum rating. The breakdown voltage (AD reverse bias voltage at which the leak current reaches 1 microampere) differs depending on the ambient temperature. Always set the AD reverse bias voltage to a level that is at least 10 volts lower than the breakdown voltage.

References in Chapter 12

- 1) M. Suyama et al.: A Compact Hybrid Photodetector, *IEEE Trans. Nucl. Sci.* NS-44, No.3, pp.985-989, 1997
- 2) A. Fukasawa et al.: High Speed HPD for Photon Counting, *IEEE Trans. Nucl. Sci.*, vol. 55, No.2, April 2008 pp.758-762
- 3) Atsuhito Fukasawa (Editor: Krzysztof Iniewski): *Semiconductor Radiation Detection Systems Chapter 7 Hybrid Photodetectors (HPDs) for Single-Photon Detection*, CRC Press(2010)
- 4) M. Hayashida et al.: Development of HPDs with an 18-mm-diameter GaAsP photo cathode for the MAGIC-II, *Nuclear Instruments and Methods in Physics Research A* 567 (2006) 180-183
- 5) A. Fukasawa, K. Arisaka, H. Wang, M. Suyama: QUPID, a single photon sensor for extremely low radioactivity, *Nuclear Instruments and Methods in Physics Research A* 623 (2010) 270-272, Proceedings of the 1st International Conference on Technology and Instrumentation in Particle Physics, Tsukuba, Japan, March 12-17, 2009
- 6) H. Nakayama et al.: Development of a 13-in Hybrid Photo-Detector (HAPD) for a next generation water Cherenkov detector, *Nuclear Instruments and Methods in Physics Research A* 567 (2006) 172-175
- 7) S. Cova et al., "Avalanche photodiodes and quenching circuits for single-photon detection," *APPLIED OPTICS* Vol.35 No.12 (1996) 1956-1976
- 8) X. Michalet et al.: *Proc. SPIE* 6862, in press, 2008
- 9) S. Nishida et al.: Development of an HAPD with 144 channels for the aerogel RICH of the Belle upgrade, *Nucl. Instrum. Meth. A*595, pp.150-153, 2008
- 10) M. Suyama et al.: Development of a multi-pixel photon sensor with single-photon sensitivity, "Nuclear Instruments and Methods in Physics Research A 523 (2004) 147-157
- 11) M. Suyama et al.: Development of a Multipixel Hybrid Photodetector with High Quantum Efficiency and Gain, *IEEE Trans. Nucl. Sci.*, vol. 51, No.3, pp. 1056-1059, June 2004
- 12) A. Fukasawa et al.: "Multichannel HPD for high-speed single photon counting," *Nuclear Instruments and Methods in Physics Research Section A: Accelerators, Spectrometers, Detectors and Associated Equipment*, Volume 812, 11 March 2016, Pages 81–85
- 13) A. Fukasawa: Dissertation theses for The Graduation School for the Creation of New Photonics Industries, "Development and promotion of hybrid photodetectors (HPDs) used in biological fluorescence microscopes" May, 2016

MEMO

CHAPTER 13

ENVIRONMENTAL RESISTANCE AND RELIABILITY

Photomultiplier tube characteristics, for example, sensitivity and dark current, are susceptible to environmental conditions such as ambient temperature, humidity, and magnetic fields. To obtain the fullest capabilities from a photomultiplier tube, it is necessary to know how environmental conditions affect the photomultiplier tube and to take corrective action. This chapter discusses these points and also describes operating stability over time and reliability.

13.1 Effects of Ambient Temperature

13.1.1 Temperature characteristics

Photomultiplier tubes are more susceptible to ambient temperature than ordinary electronic components (such as resistors and capacitors). Therefore in precision measurement, they must be operated with temperature control so that the effects of ambient temperature are minimized. When performing temperature control, note that the interior of a photomultiplier tube is a vacuum and that heat conducts through it very slowly. The photomultiplier tube should be left for one hour or longer until the internal temperature reaches the same level as the ambient temperature and the characteristics become stable.

(1) Sensitivity

Temperature characteristics of anode sensitivity can be divided into those for cathode sensitivity (photocathode) and gain (dynode).

Temperature characteristics for cathode sensitivity depend on the wavelength. In general, the temperature coefficient of cathode sensitivity varies significantly from a negative value to a positive value near the long wavelength limit.

Unlike cathode sensitivity (photocathode), the temperature coefficient of gain tends to vary to a negative value and has virtually no dependence on wavelength and supply voltage. Figure 13-1 shows temperature coefficients versus wavelength for photomultiplier tubes using typical photocathodes.

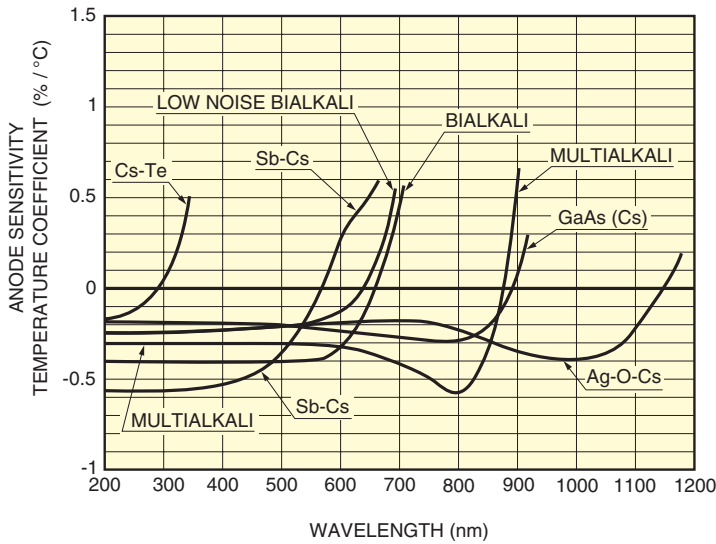
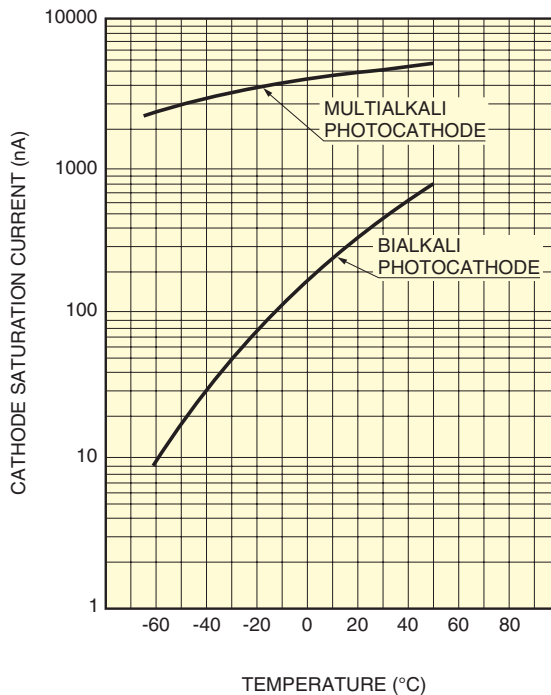


Figure 13-1: Temperature coefficients of photocathode

THBV4_1301EA

When a photomultiplier tube with a transmission mode photocathode is used at very low temperatures, the subsequent increase in the photocathode surface resistance may cause a cathode current saturation effect, resulting in a loss of output linearity with respect to the incident light level. This effect appears drastically with certain types of bialkali photocathodes, so care is required when using such photomultiplier tubes. (Refer to 4.3.2 in Chapter 4.)

Figure 13-2 shows typical cathode saturation current versus temperature for transmission type bialkali and multialkali photocathodes.

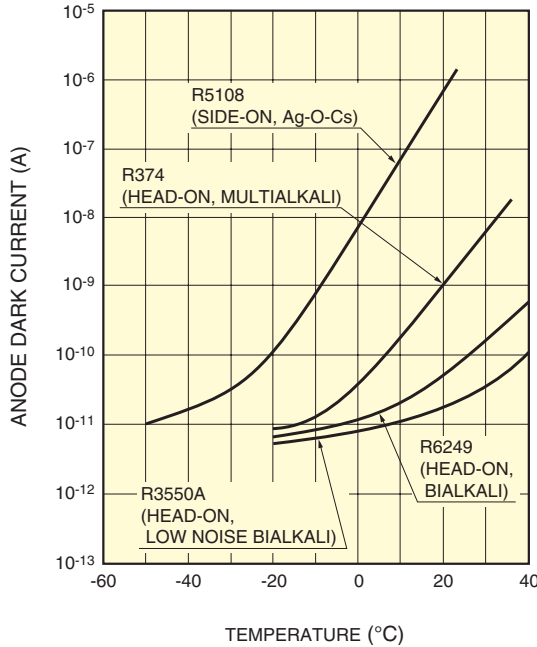


THBV4_1302EA

Figure 13-2: Measurement example of cathode saturation current vs. temperature for transmission type photocathodes

(2) Dark current

A photocathode consists of materials having small energy gap and electron affinity so that photoelectrons can be released efficiently. This means that dark current is very sensitive to the ambient temperature. In low-light-level detection, this effect of the ambient temperature on the dark current is an important factor to consider. For example, cooling a photomultiplier tube is most effective in reducing the dark current and improving the signal-to-noise ratio, especially for photomultiplier tubes with high sensitivity in the red to near infrared region. Conversely, using a photomultiplier tube at a high temperature reduces the signal-to-noise ratio, so use of a low noise bialkali photocathode (Sb-Na-K) may be necessary. Figure 13-3 shows dark current versus temperature characteristics of typical photocathodes. For details on dark current, refer to 4.3.6 in Chapter 4.



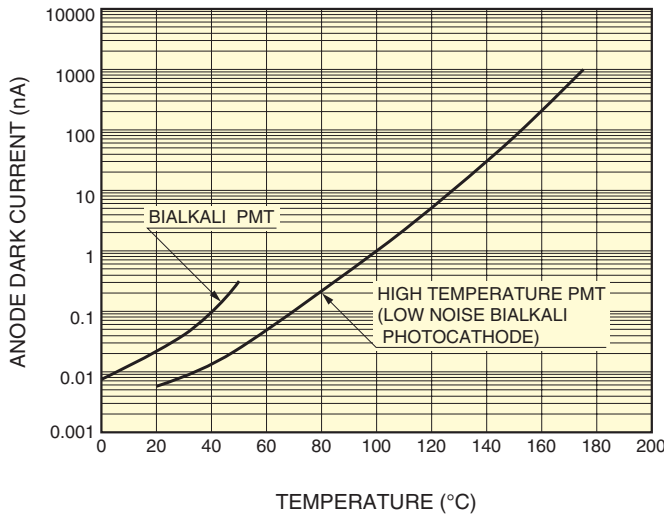
THBV4_1303EA

Figure 13-3: Dark current of various photocathodes versus temperature

13.1.2 High temperature photomultiplier tubes

Although the guaranteed operating temperature range for general photomultiplier tubes is up to 50 °C, high temperature photomultiplier tubes can operate at high temperatures up to 200 °C. These tubes use a low-dark-current bialkali photocathode and an electron multiplier employing copper-beryllium (CuBe) dynodes designed and optimized for use at high temperatures.

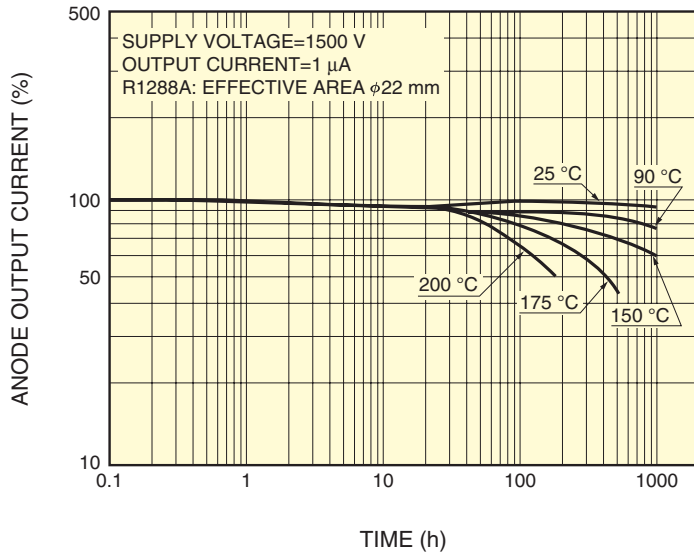
Typical characteristics for high temperature photomultiplier tubes are shown below. Dark current versus temperature characteristics are plotted in Figure 13-4, anode output current and relative pulse height change over time at different temperatures in Figure 13-5, relative pulse height and energy resolution (pulse height resolution or PHR) versus temperature in Figure 13-6, and plateau characteristics at different temperatures in Figure 13-7.



THBV4_1304EA

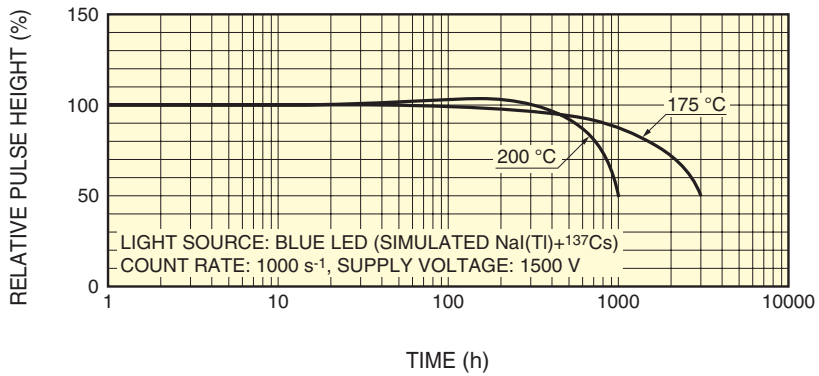
Figure 13-4: Dark current vs. temperature

Typical high temperature photomultiplier tube



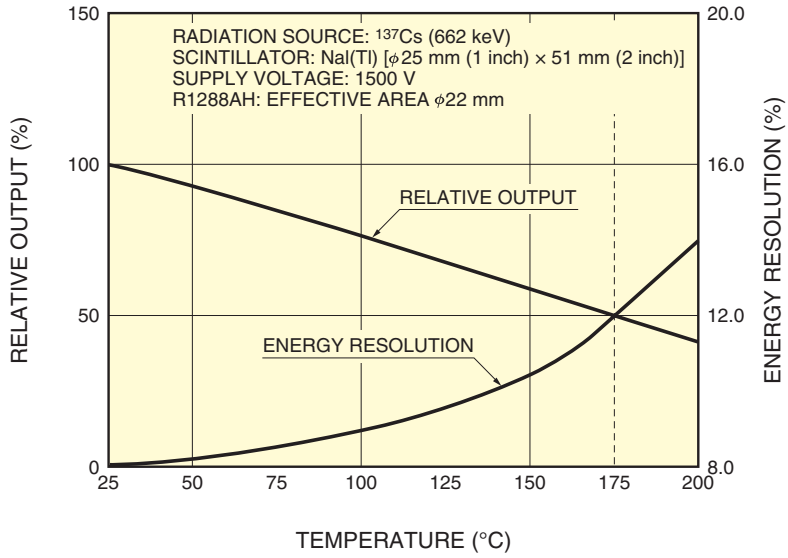
THBV4_1305EAa

High temperature photomultiplier tube capable of operation at 200 °C



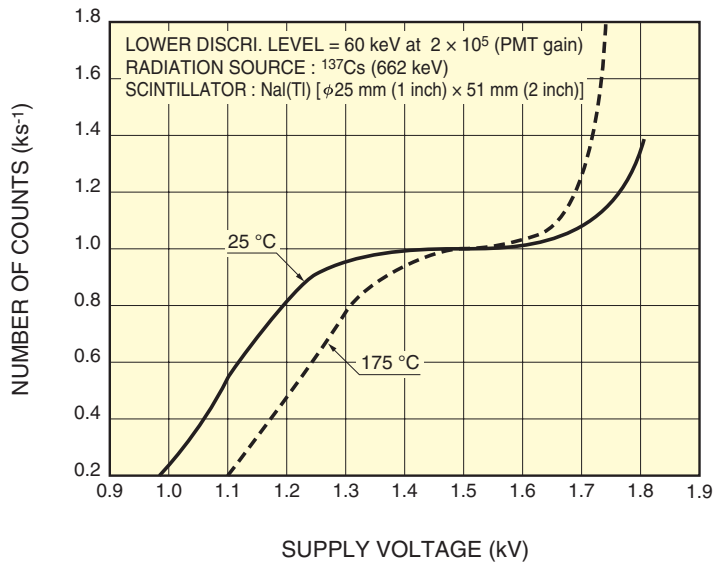
THBV4_1305EAb

Figure 13-5: Anode current change over time at different temperatures



THBV4_1306EA

Figure 13-6: Relative pulse height and energy resolution vs. temperature



THBV4_1307EA

Figure 13-7: Plateau characteristics at different temperatures

13.1.3 Storage temperature and cooling precautions

Photomultiplier tube sensitivity varies somewhat during storage, even at room temperatures. This is probably due to the movement of alkali metals activating the photocathode and dynode surfaces. If a photomultiplier tube is left at a high temperature, this sensitivity variation will be accelerated. It is therefore recommended that the photomultiplier tube be stored in locations where the temperature is kept low.

As explained in “(2) Dark current” in section 13.1.1, photomultiplier tubes using a photocathode with high red-to-white sensitivity such as multialkali, GaAs(Cs), InGaAs, and Ag-O-Cs are often cooled during operation to reduce the dark current. In this case, the following precautions should be observed, otherwise the difference in thermal expansion coefficient between the photomultiplier tube glass bulb, base, and adhesive (epoxy resin) may cause the glass to crack.

- Avoid using a photomultiplier tube with a plastic base when cooling to $-30\text{ }^{\circ}\text{C}$ or below.
- Assemble a voltage-divider circuit on a PC board and connect it to the socket using thin, soft wires, so that excessive force is not applied to the lead pins of a photomultiplier tube.
- Avoid subjecting a photomultiplier tube to drastic temperature changes.

13.2 Effects of Humidity

13.2.1 Operating humidity

Since the photomultiplier tube is operated at high voltages and handles very low current in the order of picoamperes to micro-amperes, leakage current between the lead pins may create a significant problem. This leakage current sometimes increases by several orders of magnitude due to a rise in the ambient humidity. It is recommended that the photomultiplier tube be operated at a humidity below 60 percent or so.

13.2.2 Storage humidity

If a photomultiplier tube is left at a high humidity for a long period of time, the following problems may occur: an increase in the leakage current on the bulb stem surface, contact failure due to rust formed on the lead pin surface and, for UV-transmitting glass, a loss of transmittance. Photomultiplier tubes must therefore be stored in locations of low humidity. Since dirt on the photomultiplier tube surface may be a cause of increased leakage current and rust formation on the leads, avoid touching the bulb stem, lead pins, and especially around the anode pin of a plastic base with bare hands. These portions must be kept clean but, if they become contaminated, use anhydrous alcohol for cleaning. In general, it is recommended to store photomultiplier tubes at a humidity below 85 percent (no condensation should occur).

13.3 Effects of External Magnetic Fields

13.3.1 Magnetic characteristics

In photomultiplier tube operation, because electrons travel along a long path in a vacuum, their trajectories are affected by even a slight magnetic field such as terrestrial magnetism, possibly causing an anode sensitivity variation. A prime reason for this sensitivity variation is that the electron trajectories are affected by the magnetic fields. Particularly, photomultiplier tubes having a long distance between the photocathode and the first dynode or a small first-dynode opening in comparison with the photocathode area are more vulnerable to effects of a magnetic field. For most head-on photomultiplier tubes, the anode sensitivity will be reduced by as much as 50 percent by a magnetic flux density of below 0.1 to several milliteslas. The sensitivity is most vulnerable to a magnetic flux in the direction parallel to the photocathode surface (X axis). Side-on photomultiplier tubes are less affected by magnetic fields since the distance from the photocathode to the first dynode is short. The magnetic flux density at which the anode sensitivity reduces 50 percent is approximately 3.5 milliteslas for 28 mm (1-1/8 inch) side-on types. Metal-package type photomultiplier tubes (R9880 series) offer excellent immunity to magnetic fields because they have a short distance from the photocathode to the first dynode and the metal case has magnetic shield effects. Figure 13-8 shows the effects of magnetic fields on typical photomultiplier tubes. Also note that the higher the supply voltage to a photomultiplier tube, the less the effects of magnetic fields.

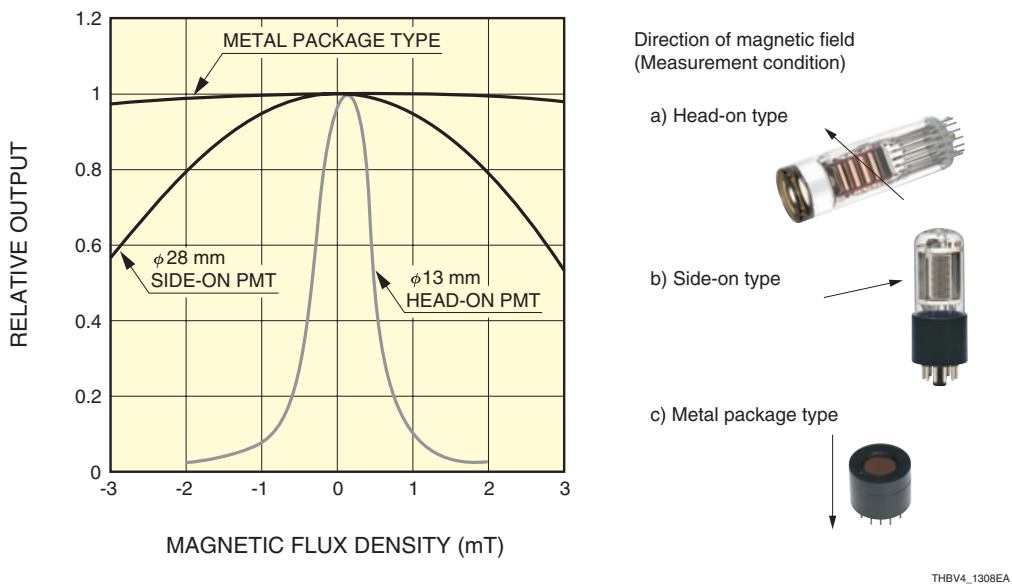
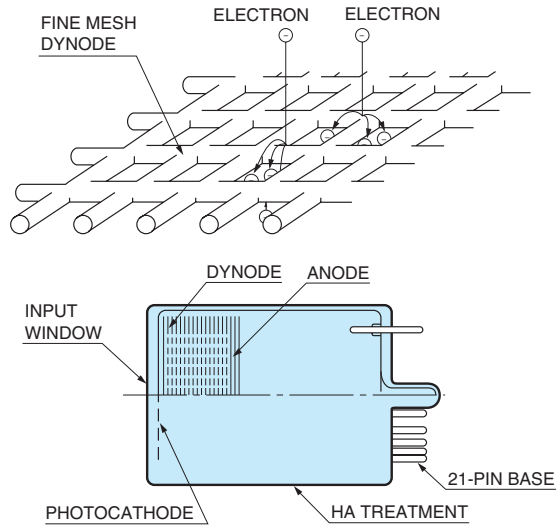


Figure 13-8: Magnetic characteristics of typical photomultiplier tubes

It is preferable that the photomultiplier tube be used in locations where no magnetic source is present. In particular, avoid using the photomultiplier tube near such devices as transformers and magnets. If the photomultiplier tube must be operated in a magnetic field, be sure to use a magnetic shield case. Refer to section 5.4 of Chapter 5 for more details and specific usage of magnetic shield cases.

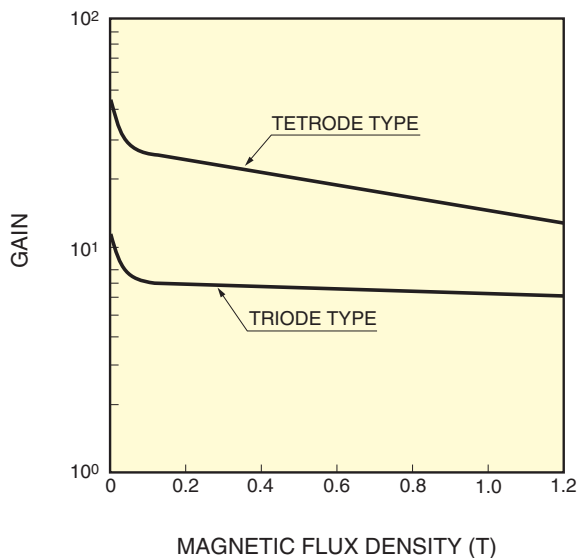
13.3.2 Photomultiplier tubes for use in highly magnetic fields

As stated previously, normal photomultiplier tubes exhibit a large variation in a magnetic field, for example, sensitivity reduces at least one order of magnitude in a magnetic field of 10 milliteslas. In high-energy physics applications, however, photomultiplier tubes capable of operating in a magnetic field of more than one tesla are demanded. To meet these demands, special photomultiplier tubes with fine-mesh dynodes have been developed and put into use. These photomultiplier tubes include a "triode" type using a single stage dynode, a "tetrode" type using a two-stage dynode and a high-gain type using multiple dynode stages.¹⁾ The structure of this photomultiplier tube is illustrated in Figure 13-9. Figure 13-10 shows gain versus magnetic field perpendicular to the photocathode (tube axis) for a tetrode and triode types, and relative gain of a 19-stage photomultiplier tube versus magnetic field at different angles.



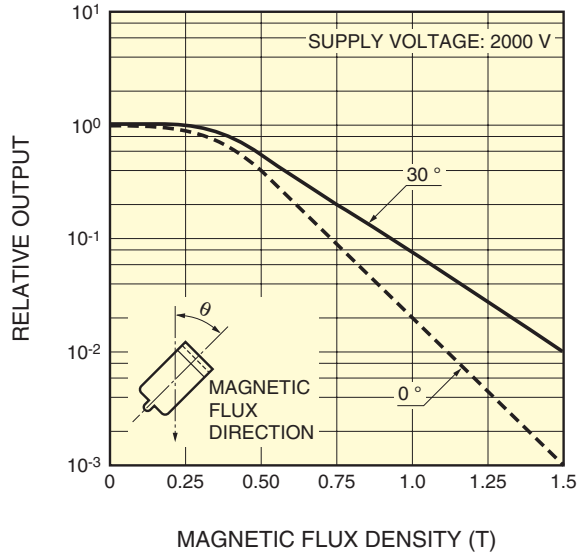
THBV4_1309EA

Figure 13-9: Structure of a photomultiplier tube designed for use in highly magnetic fields



THBV4_1310EAa

Figure 13-10: Magnetic characteristics of photomultiplier tubes for highly magnetic fields (1)



THBV4_1310EAd

Figure 13-10: Magnetic characteristics of photomultiplier tubes for highly magnetic fields (2)

13.3.3 Magnetization

Some dynode substrates are made from nickel with magnetic properties, and the photomultiplier tube leads and electrodes are also made from metals which can be magnetized. There will be no problem as long as the photomultiplier tube is operated in a weak magnetic field such as from terrestrial magnetism. If the magnetic field strength increases and exceeds the initial permeability of the dynode substrate and electrode materials, they will remain magnetized even after the magnetic field has been removed (residual magnetism). The gain after the magnetic field has once been applied will differ from that before the magnetic field is applied. If magnetized, they can be demagnetized by applying an AC magnetic field to the photomultiplier tube and gradually attenuating it.

In applications where a photomultiplier tube must be used in a highly magnetic field or magnetization of the tube is unwanted, photomultiplier tubes made of nonmagnetic materials are required. Photomultiplier tubes for highly magnetic fields use nonmagnetic materials for the dynode substrate, and so is capable of stable operation in highly magnetic fields and also minimal magnetization.

13.4 Vibration and Shock

Resistance to vibration and shock can be categorized into two conditions: one is under non-operating conditions, for example, during transportation and the other is under conditions when photomultiplier tubes are actually installed and operated in equipment.

13.4.1 Resistance to vibration and shock during non-operation

Photomultiplier tubes are usually designed to withstand tens of m/s^2 of vibration and 750 to 1000 m/s^2 of shock. However, if excessive vibration and shock are applied to a photomultiplier tube, its characteristics may vary and the glass envelope may break.

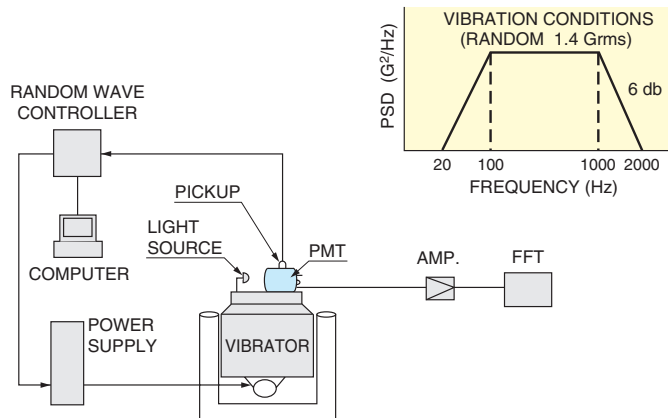
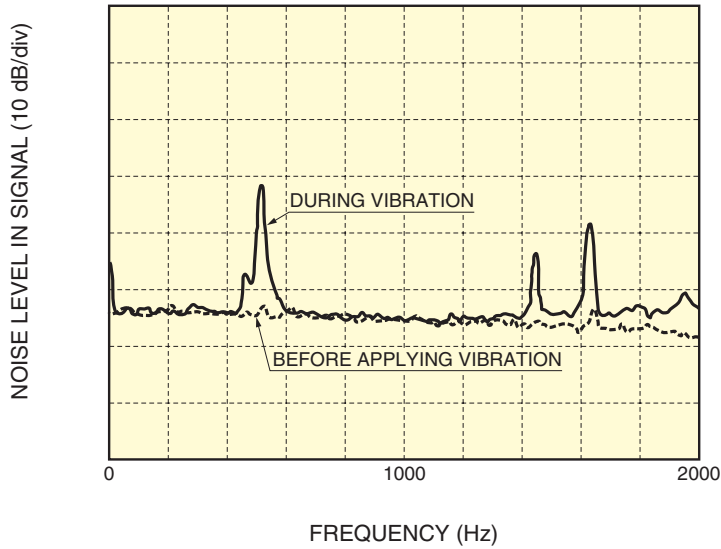
In general, photomultiplier tubes with a smaller size, lighter weight, and shorter overall length exhibit better resistance to vibration and shock. Even so, sufficient care must be exercised when handling. The following table shows the maximum vibration and shock values which ordinary photomultiplier tubes can withstand when not in operation.

| PMT type | | Maximum vibration (m/s^2) | Maximum shock (m/s^2) |
|--------------|-----------------------------|-------------------------------|---------------------------|
| Side-on type | 13 mm (1/2 inch) diameter | 100 (10 Hz to 2000 Hz) | 1000 (6 ms) |
| | 28 mm (1-1/8 inch) diameter | 100 (10 Hz to 500 Hz) | 1000 (11 ms) |
| Head-on type | Metal package TO-8 | 100 (10 Hz to 500 Hz) | 1000 (11 ms) |
| | 13 mm (1/2 inch) diameter | 100 (10 Hz to 500 Hz) | 1000 (11 ms) |
| | 28 mm (1-1/8 inch) diameter | 50 (10 Hz to 500 Hz) | 1000 (11 ms) |
| | 51 mm (2 inch) diameter | 50 (10 Hz to 500 Hz) | 750 (11 ms) |
| | 76 mm (3 inch) diameter | 50 (10 Hz to 500 Hz) | 750 (11 ms) |

The photomultiplier tube envelope is made of glass, so it is vulnerable to direct mechanical shock. Envelopes with silica windows are especially vulnerable to shock on the bulb side because of a graded glass seal. Sufficient care must be taken in handling this type of tube. Furthermore, photomultiplier tubes designed for liquid scintillation counting use a very thin faceplate that is 0.5 millimeters thick. Some of them may be broken even by a slight shock. If the glass envelope is broken, implosion may cause it to fly apart in fragments. Precautions are required, especially in handling a large diameter tube of more than 204 millimeters (8 inches).

13.4.2 Resistance to vibration and shock during operation (resonance)

Photomultiplier tubes are not normally designed to receive vibration and shocks during operation, except for specially-designed ruggedized types. If a photomultiplier tube suffers vibration or shocks during operation, problems such as variations of the signal level and an increase in the microphonic noise may occur. Attention should be given to the mounting method and arrangement of the photomultiplier tube. Moreover, the photomultiplier tube may have a resonance at a certain frequency, but this resonant frequency differs from tube to tube. If vibration is increased at this resonance point, the above problems will be more noticeable, being likely to damage the envelope. Figure 13-11 shows the variations in the frequency spectrum of photomultiplier tube output subjected to vibration, along with the measurement block diagram.



THBV4_1311EA

Figure 13-11: Resonance noise in the output signal of a photomultiplier tube subjected to vibration

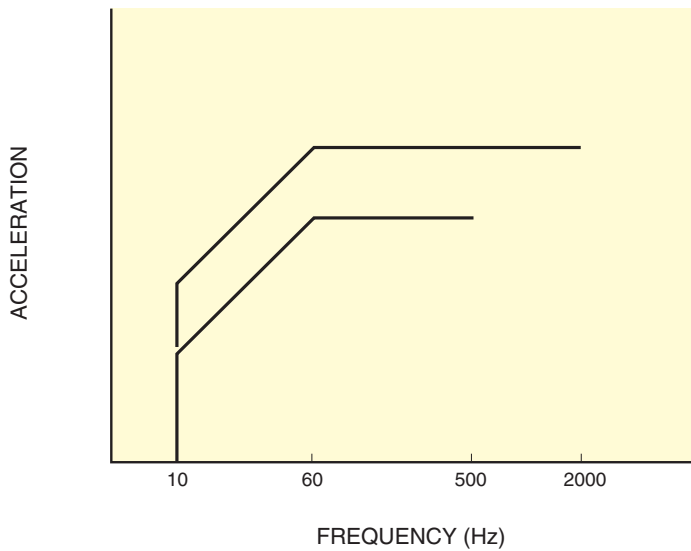
In this experiment, the photomultiplier tube is subjected to random vibration (1.4 Grms) from 20 Hz to 2 kHz and its output signal is frequency-analyzed using a FFT (Fast Fourier Transform). It is obvious from Figure 13-11 that the noise sharply increases at frequencies near 0.5 kHz, 1.45 kHz and 1.6 kHz.

When measurement is made at extremely low light levels, even a slight vibration caused by the table on which the equipment is placed may be a source of noise. Precautions should be taken to ensure the equipment is installed securely and also the cable length to the preamplifier and the cable mounting method should be checked.

13.4.3 Testing methods and conditions

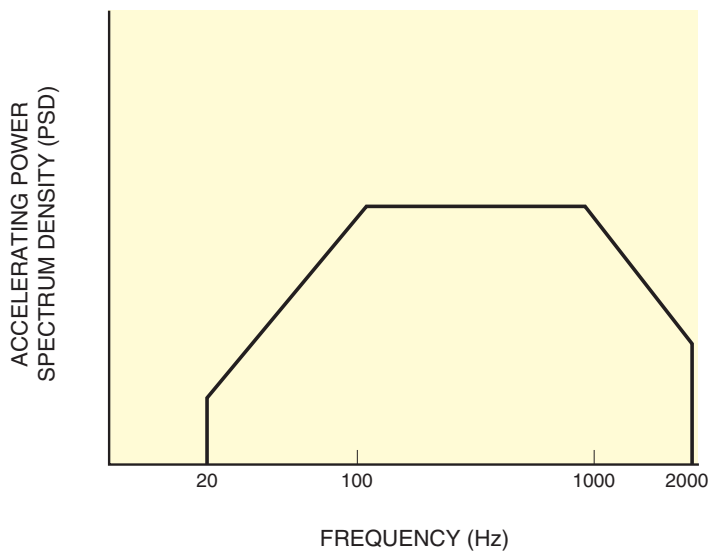
There are two vibration test methods²⁾: sinusoidal-wave and random-wave application tests. In the first method, the sinusoidal wave used for vibration tests is determined by the frequency range, displacement (amplitude), acceleration, vibration duration, and sweep time. The frequency sweep method commonly employed is a logarithmic sweep method. In the second method, the random wave is determined by the acceleration power spectrum density (G^2/Hz) of vibration and the vibration duration, and is expressed in terms of the root mean square (RMS) value. This method allows tests to be performed under conditions close to the actual use. Figures 13-12 (A) and (B) show vibration pattern examples created by sinusoidal wave and random wave.

(A) Sinusoidal wave vibration pattern example



THBV4_1312EAa

(B) Random vibration pattern example



THBV4_1312EAb

Figure 13-12: Vibration pattern curves

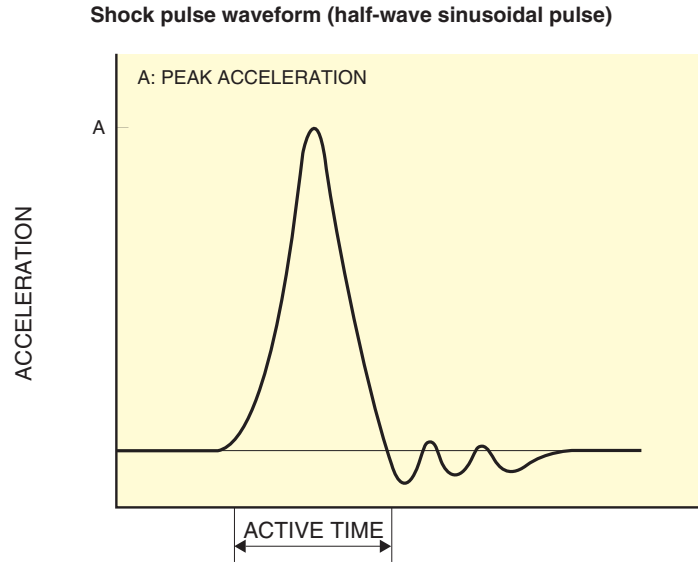


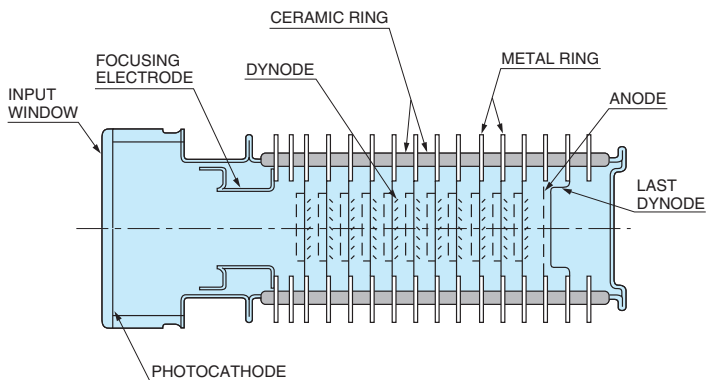
Figure 13-13: Shock pulse

Various methods are used in shock tests such as half-wave sinusoidal pulses, sawtooth wave pulses, and trapezoidal wave pulses. Hamamatsu Photonics performs shock tests using half-wave sinusoidal pulses. The test conditions are determined by the peak acceleration, shock duration, and the number of shocks applied. A typical shock pulse waveform is shown in Figure 13-13.

Official standards for vibration and shock test methods include IEC 60068, JIS C60068-2-6 (vibration), JIS C60068-2-27 (shock), MIL STD-810G and MIL STD-202G.³⁾ Hamamatsu Photonics performs the vibration and shock tests in conformance to these official standards. The above data for vibration and shock tests were measured under these official conditions. For instance, the shock tests were carried out along three orthogonal axes for a shock duration period of 11 milliseconds, three times each in the plus and minus directions, so that shocks were applied a total of 18 times. Accordingly, even if the test proves that a photomultiplier tube withstands a shock of 1000 m/s^2 , this does not mean that it will survive such shocks dozens or hundreds of times.

13.4.4 Ruggedized photomultiplier tubes⁴⁾

In geological surveys such as oil well logging or in space research in which photomultiplier tubes are launched in a rocket, extremely high resistance to vibration and shock is required.⁵⁾ To meet these applications, ruggedized photomultiplier tubes have been developed, which can operate reliably during periods of 200 m/s^2 to 500 m/s^2 vibration and 1000 m/s^2 to 10000 m/s^2 shock. A variety of ruggedized types are available ranging in diameter from 13 to 51 millimeters ($1/2$ to 2 inches) and are also available with different dynode structures. Most ruggedized photomultiplier tubes are based on conventional glass-envelope photomultiplier tubes, but feature improvements to their electrode supports, lead pins, and dynode structure so that they will withstand severe shock and vibration. These ruggedized photomultiplier tubes have a diameter of 51 millimeters (2 inches) or less, and can withstand vibrations of 200 m/s^2 up to 300 m/s^2 . If even higher performance is required, specially-designed ruggedized photomultiplier tubes having a stacked ceramic bulb are used instead of the glass envelope. Figure 13-14 shows the cross section of this type of ruggedized photomultiplier tube.



THBV4_1314EA

Figure 13-14: Cross section of a ruggedized photomultiplier tube using a stacked ceramic bulb

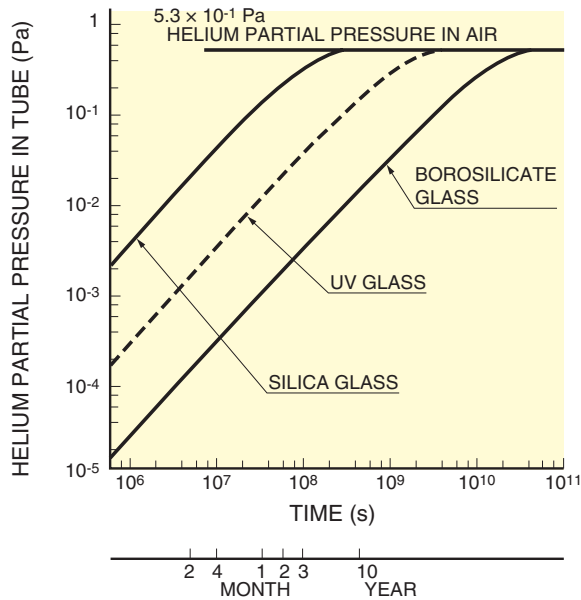
As illustrated in the figure, each dynode electrode of this ruggedized photomultiplier tube is securely welded to a ceramic ring. This structure resists electrical discontinuity, contact failure, and envelope rupture even under severe vibration and shock. This is because the dynodes resist deformation and peeling. No lead wires, ceramic spacers or cathode contacts are required, and few fragile glass parts need to be used. The voltage-divider resistors can be soldered on the outside of the metal rings which are fused to the ceramic rings, assuring high ruggedness even after the voltage-divider circuit has been assembled on the tube. The typical maximum vibration and shock for a 34 mm (1-3/8 inch) stacked-ceramic photomultiplier tube using a low noise bialkali photocathode and a 12-stage dynode multiplier is as follows:

| | |
|-------------------------|---|
| Resistance to vibration | 500 m/s ² (50 Hz to 2000 Hz) |
| Resistance to shock | 10000 m/s ² (0.5 ms) |

13.5 Effects of Helium Gas

It is well known that helium gas permeates through glass.⁶⁾ The extent of helium permeation through glass depends on the glass materials, their composition, and ambient temperature. Photomultiplier tubes designed for UV light detection usually employ silica glass for the input window. Helium gas may cause a problem since it is more like to permeate through silica glass than through other window materials. So if such a photomultiplier tube is stored or operated in environments where helium gas is present, a gas increase occurs inside the tube, leading to an increase in dark current and promoting a degradation of the breakdown voltage level. This eventually causes a discharge in the photomultiplier tube, making it unusable. For example, if a photomultiplier tube using silica glass is placed in helium gas at one atmosphere, a drastic increase of afterpulse due to helium gas will be seen in about 30 minutes. This will cause an unrecoverable damage to the tube and must be avoided. To reduce the effects of helium gas, it is best to store the photomultiplier tube in helium-free gases such as argon gas and nitrogen gas.

Helium gas exists on the earth at a partial pressure of about 0.5 Pa. As stated above, the permeability of helium through silica glass is extremely high, as much as 10^{-19} cm²/s (at a pressure difference of 1.013×10^5 Pa) at room temperatures. Because of this, the helium partial pressure inside the photomultiplier tube gradually increases and finally reaches a level close to the helium partial-pressure in the atmosphere. The time needed to reach that level depends on the surface area and thickness of the silica glass. For example, if a side-on photomultiplier tube (28 mm diameter type) using silica glass is left in the atmosphere, the helium partial pressure inside the tube will increase to 9×10^{-2} Pa after one year. (Refer to Figure 13-15.)



THBV4_1315EA

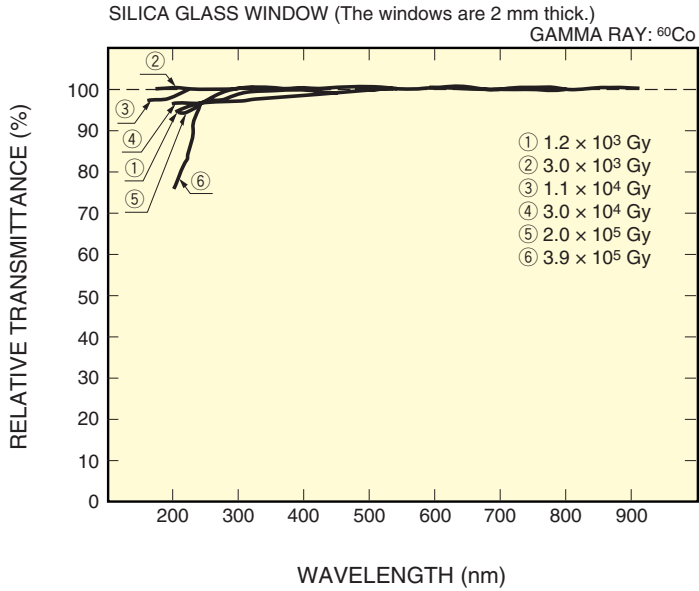
Figure 13-15: Bulb materials and variations in helium partial-pressure inside photomultiplier tubes

13.6 Effects of Radiation

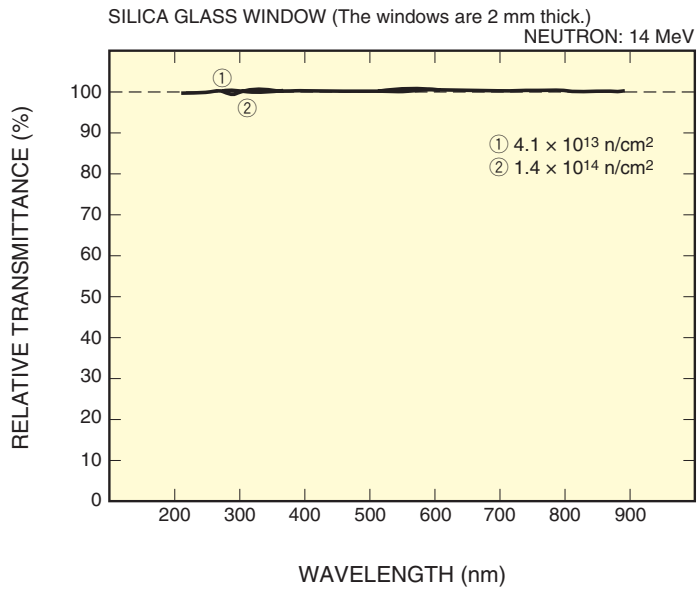
Photomultiplier tubes are used in a wide range of applications including high energy physics, nuclear medicine, X-ray instrumentation, and space research. In these applications, photomultiplier tubes are usually exposed to radiation (X-rays, alpha rays, beta rays, gamma rays, neutrons, etc.) which somewhat affect the performance characteristics of photomultiplier tubes.⁷⁾ For example, radiation can be a cause of background noise of photomultiplier tubes and may deteriorate the glass materials used for photomultiplier tubes.

13.6.1 Deterioration of window transmittance

Even when a photomultiplier tube is exposed to radiation, the cathode sensitivity and secondary electron multiplication exhibit very little variation. However, a loss of transmittance through the window occurs due to coloring of the glass.⁸⁾ Figures 13-16 to 13-18 show variations in the window transmittance when photomultiplier tubes are irradiated by gamma rays from a ^{60}Co radiation source and also by neutrons (4 MeV). (The windows are 2 mm thick.)

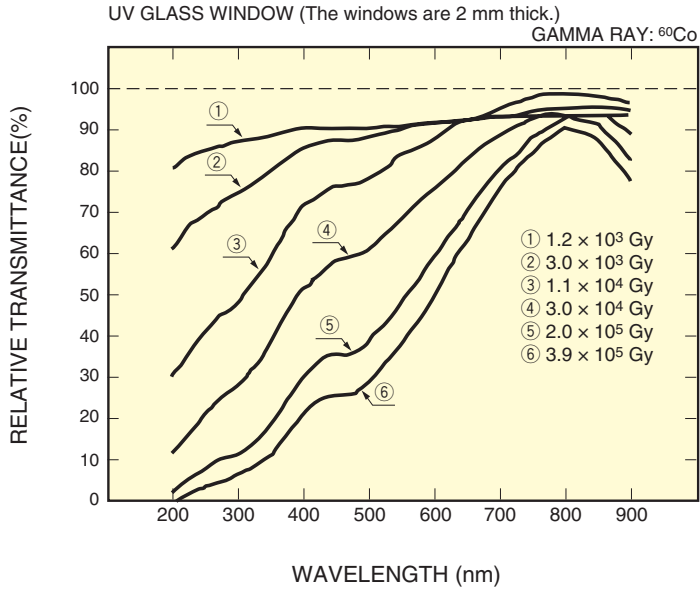


THBV4_1316EAa

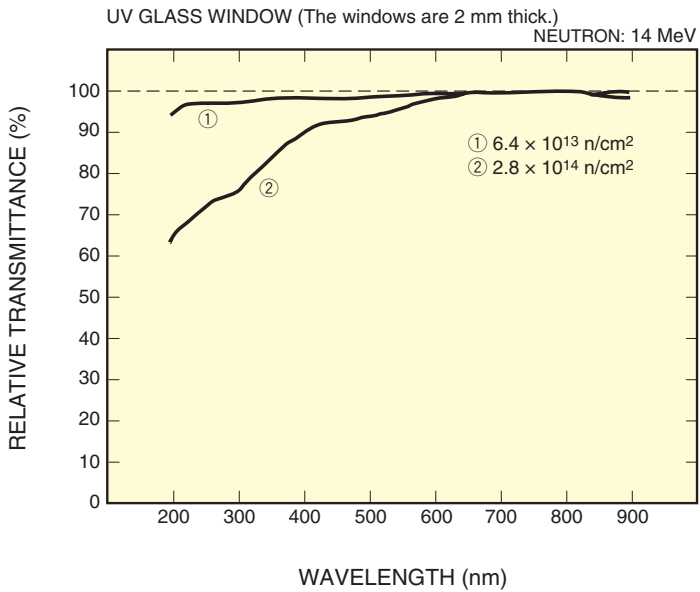


THBV4_1316EAb

Figure 13-16: Transmittance change of silica glass window irradiated by gamma rays/neutrons



THBV4_1317EAa



THBV4_1317EAb

Figure 13-17: Transmittance change of UV glass window irradiated by gamma rays/neutrons

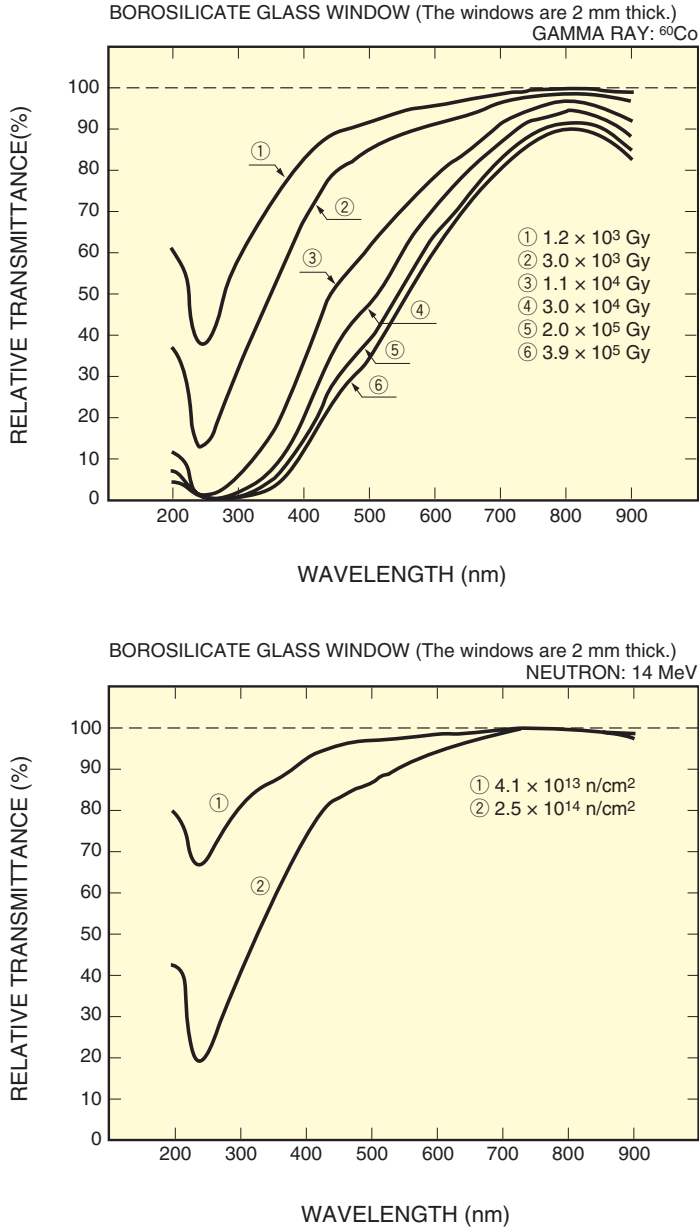


Figure 13-18: Transmittance change of borosilicate glass window irradiated by gamma rays/neutrons

As can be seen from these figures, a decrease in transmittance caused by exposure to radiation occurs more noticeably in the UV region. The silica glass is least affected by radiation and virtually no variation is seen after irradiation of gamma rays of 2.0×10^5 Gy and neutrons of 1.4×10^{14} n/cm². In contrast to this, a decrease in transmittance occurs for the borosilicate glass even at exposure to 1.2×10^3 Gy. But the extent of this decrease is smaller for the UV glass which is a kind of borosilicate glass. Please note that this tendency is not constant even for the same type of glass, because the composition differs depending on the fabrication method. The transmittance that has dropped due to exposure to radiation will recover to some extent after storage, and this is more effective when stored at higher temperatures.

13.6.2 Glass scintillation

Photomultiplier tubes are slightly sensitive to radiation and produce a resultant noise. This is primarily due to unwanted scintillation of the glass window caused by beta and alpha rays, or scintillation of the glass window and electron emission from the photocathode and electron multiplier caused by gamma rays and neutrons.⁹⁾ Of these, the scintillation of the glass window most likely affects noise, but it is thought that the amount of scintillation differs depending on the type of glass. Glass scintillation further causes a continual fluorescence or phosphorescence to occur even after radiation has been removed, resulting in yet another source of noise. Figure 13-19 shows a variation in the dark current after a photomultiplier tube is irradiated by gamma rays, indicating that it takes 40 to 60 minutes to reach a steady level. In the case of neutron irradiation, it has been confirmed that the electron multiplier materials are made radioactive.

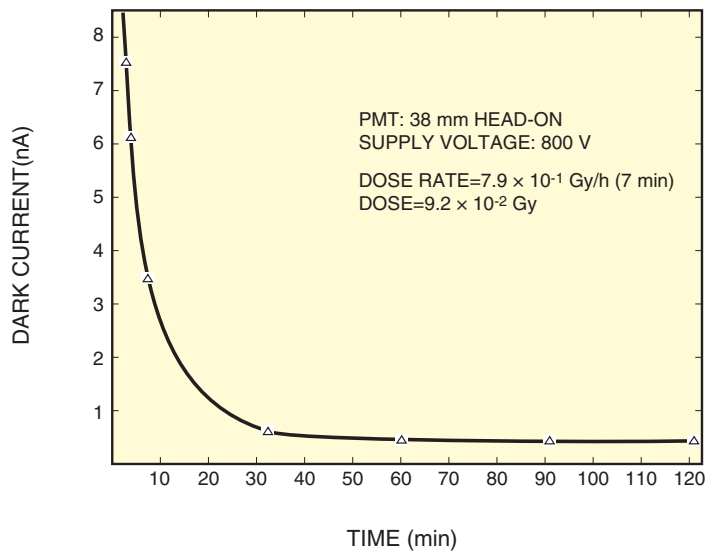


Figure 13-19: Dark current variation after exposure to gamma ray

THBV4_1319EA

13.7 Effects of Atmosphere

Photomultiplier tubes may be used in environments not only at one atmosphere (1×10^5 Pa) but also at very low pressures or in depressurized areas such as in aircraft or an artificial satellite.

A pressure change from the atmospheric pressure down to a near vacuum in outer space may cause a discharge occurring between the leads in the photomultiplier tube base. This phenomenon is known as Paschen's Law. This law states that the minimum sparking potential between two electrodes in a gas is a function of the product of the distance between the electrodes and the gas pressure, if the electric field is uniform and the ambient temperature is constant.

The distance between the leads on the outside base and on the socket is set to an interval that does not cause a discharge in environments at one atmosphere or in a vacuum. However, these structures tend to discharge most frequently at pressures from 100 Pa to 1000 Pa*. If the photomultiplier tube is to be operated in this pressure range, sufficient precautions must be taken in the design and wiring of the parts where a high voltage is supplied. (* 133 Pa = 1 torr)

Take the following precautions when using photomultiplier tubes in a vacuum.

- (1) After making sure that a sufficient vacuum level is obtained, apply high voltage to the tube (gradually from low to high voltage).
- (2) When the photomultiplier tube has a plastic base, it will take a long time until the inside of the base is evacuated to a specified vacuum. Drilling a small hole in the base is needed.
- (3) A change from 0.1 to 1 Pa may increase the dark current and cause fluctuations in the signal output.

Precaution must be taken to maintain the optimal installation conditions.

In high-energy physics applications such as neutrino detection experiments, photomultiplier tubes are sometimes operated while underwater or in the sea. In this case, a pressure higher than the atmospheric pressure is applied to the photomultiplier tube. The breaking pressure depends on the configuration, size and bulb material of the photomultiplier tube. In most cases, smaller tubes can withstand higher pressure. However, 204 mm (8 inch) and 508 mm (20 inch) diameter photomultiplier tubes, specifically developed for high energy physics experiments, have a hemispherical shape capable of withstanding a high pressure. For example, 204 mm (8 inch) diameter tubes can withstand up to 7×10^5 Pa and 508 mm (20 inch) diameter tubes up to 8×10^5 Pa.

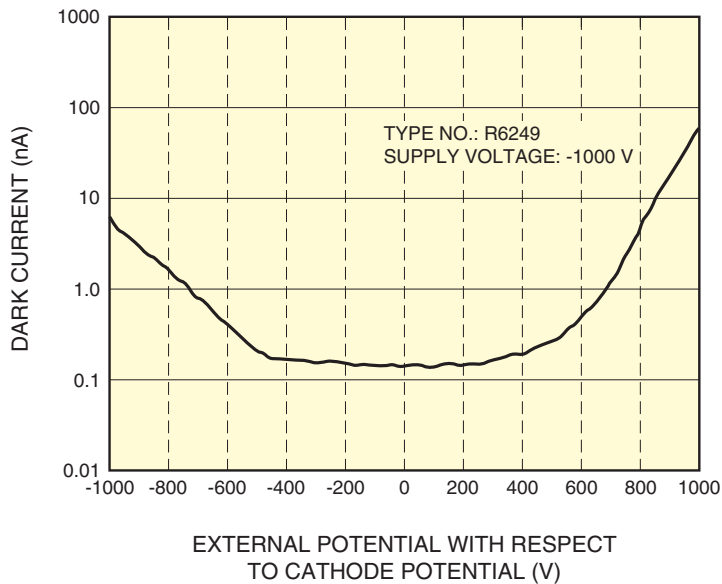
As for the bulb materials, photomultiplier tubes using a silica glass provide lower pressure-resistance due to the graded seal. There are various shapes of input windows used for head-on photomultiplier tubes, including a plano-plano type (both the faceplate and photocathode are flat), a plano-concave type (the faceplate is flat but the photocathode is concave) and a convex-concave type (the faceplate is convex but the photocathode is concave). Compared to the plano-plano type, the plano-concave and convex-concave types offer higher pressure-resistance.

13.8 Effects of External Electric Potential

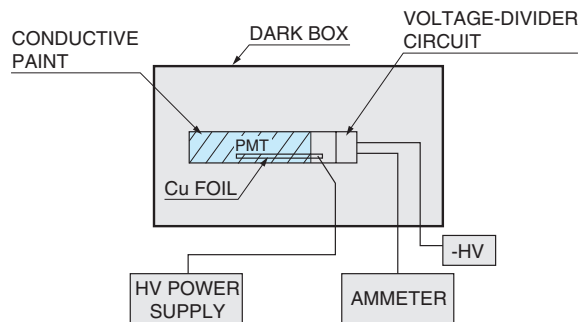
Glass scintillation occurs by exposure to radioactive rays or UV light as explained in section 13.6.2 of this chapter. It also occurs when a strong electric field is applied to the glass. These types of glass scintillations will cause the dark current to increase.

13.8.1 Experiment

Figure 13-20 shows the dark current variations of a photomultiplier tube whose side bulb is coated with conductive paint and anode is grounded, measured while changing the electric potential of this conductive coating with respect to the cathode potential.



THBV4_1320EAa

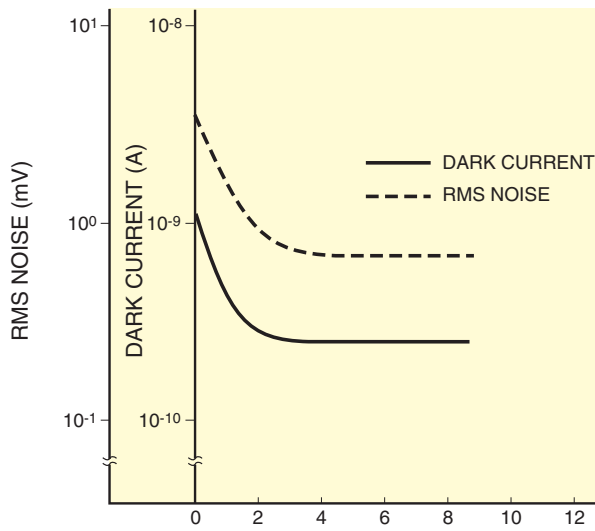
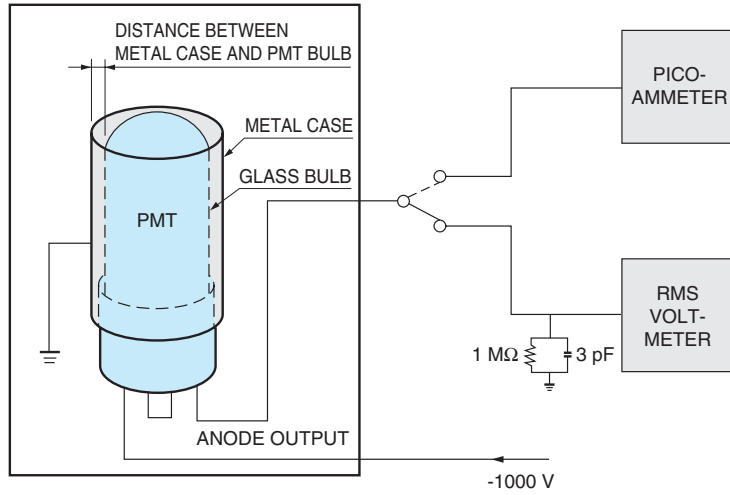


THBV4_1320EAb

Figure 13-20: Dark current vs. potential difference between cathode and conductive coating

It can be seen that the larger the potential difference between the cathode and the conductive coating, the higher the dark current. The reason for this effect is that the inner surface of the bulb near the cathode of head-on photomultiplier tubes is aluminum-coated and maintained at the cathode potential, and if the outside of the bulb has a large potential difference with respect to the cathode, scintillation will occur in the glass between the two surfaces. This scintillation light will reflect into the photocathode, causing an increase in the dark current.

The housing for photomultiplier tubes is usually made of metal and is grounded. This means that a grounded conductive material is around the photomultiplier tube and may cause the dark current to increase. This problem can be solved by allowing an adequate distance between the photomultiplier tube and the grounded conductive material. Figure 13-21 shows the dark current variations of a side-on photomultiplier tube while the distance to the grounded case is changed, proving that there is no increase in the dark current when the separation is 4 millimeters or more.



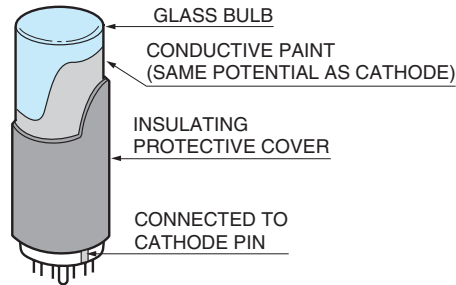
DISTANCE BETWEEN METAL CASE AND GLASS BULB (mm)

Figure 13-21: Dark current vs. distance to grounded case

THBV4_1321EA

13.8.2 Taking corrective action

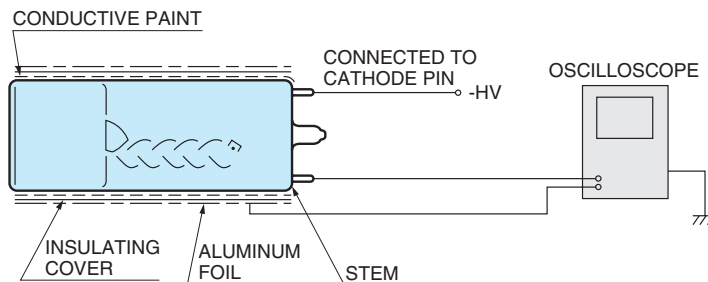
The above effects of external electric potential can be eliminated by use of the cathode grounding scheme with the anode at a positive high voltage, but photomultiplier tubes are frequently operated in the anode grounding scheme with the cathode at a negative high voltage. In this case, a technique of applying a conductive paint around the outside of the bulb and connecting it to the cathode potential can be used, as illustrated in Figure 13-22.



THBV4_1322EA

Figure 13-22: HA treatment

This technique is called "HA treatment" by Hamamatsu Photonics and, since a negative high voltage is applied to the outside of the bulb, the whole bulb is covered with an insulating cover (heat-shrinkable tube) for safety. The HA treatment is effective in reducing a noise increase caused by the surrounding electric potential. Even so, in cases where a metal foil at ground potential is wrapped around the HA treatment as shown in Figure 13-23, minute amounts of noise may still occur. This noise is probably caused by a small discharge which tends to occur due to dielectric breakdown in the insulating cover and produces a glass scintillation reaching the photocathode. Therefore, when using the photomultiplier tube in the anode grounding scheme, do not allow the metal case or housing to make direct contact with the photomultiplier tube even if it is an HA treatment type.



THBV4_1323EA

Figure 13-23: Observing the effect of external electric potential on HA treatment

As mentioned above, the HA treatment can be effectively used to eliminate the effects of external potential on the side of the bulb. However, if a grounded conductive object is located on the photocathode faceplate, there are no effective countermeasures, so any grounded object, even insulating materials, should not make contact with the faceplate. If such an object must make contact with the faceplate, use teflon or similar materials with high insulating properties. Another point to be observed is that a grounded object located on the faceplate can cause not only a noise increase but also deterioration of the photocathode sensitivity. Once deteriorated, the sensitivity will never recover to the original level. Take precautions for the mounting method of the photomultiplier tube, so that no object makes contact with the photocathode faceplate and peripheral portions.

13.9 Reliability

13.9.1 Stability over time (life characteristic)

Stability over time of photomultiplier tubes exhibits a somewhat specific pattern according to the type of photocathode and the electron multiplier materials, but usually depends on the operating conditions (especially on the output current) and the fabrication process. Also, stability varies from product to product. In normal operation, the cathode current flowing through the photocathode is on the order of picoamperes, and the photocathode fatigue can virtually be ignored, so the operating stability of the electron multiplier is an important factor that largely affects the stability over time of the photomultiplier tube. Figure 13-24 shows typical stability data over time when photomultiplier tubes are operated at an anode current of 100 microamperes which is the maximum rating for most photomultiplier tubes.

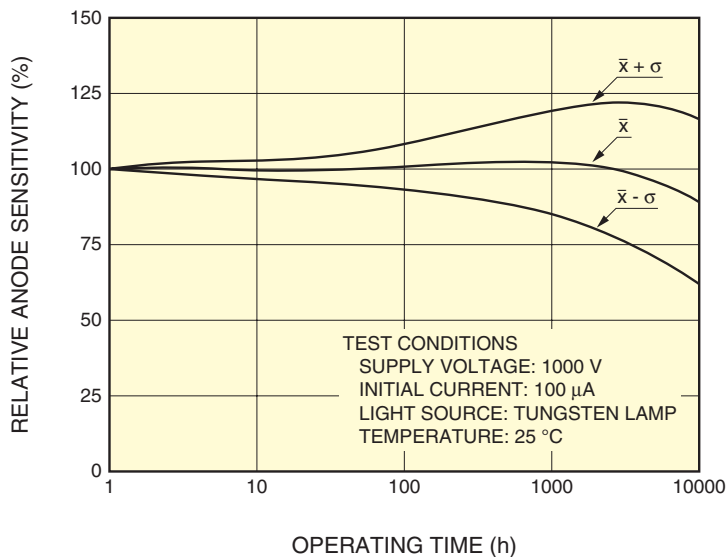


Figure 13-24: Stability over time of a photomultiplier tube

THBV4_1324EA

13.9.2 Current stress and stability

As mentioned in the preceding section, time stability of photomultiplier tubes differs depending on the operating conditions. In general, the larger the anode current, the earlier and more significant the variation that occurs (high-stress condition). Figure 13-25 shows typical stress on a photomultiplier tube versus the anode current.

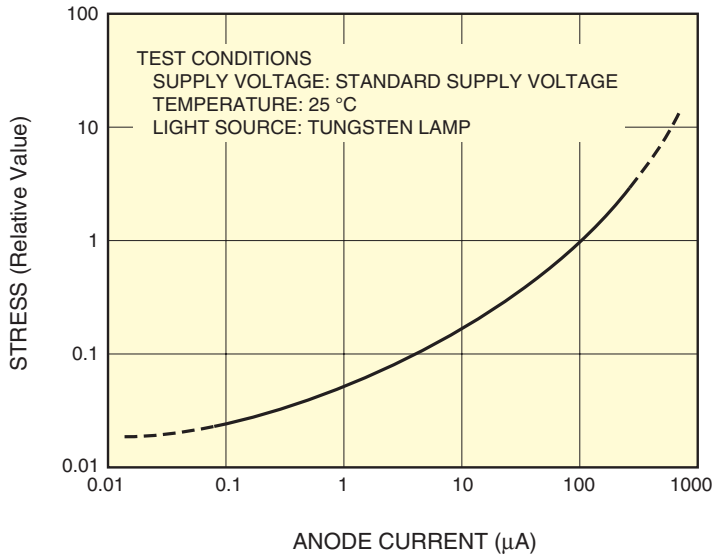
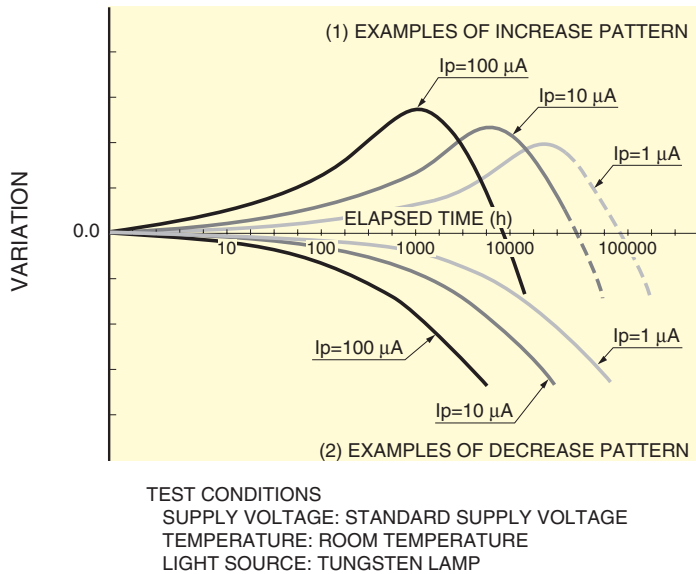


Figure 13-25: Changes in stress on a photomultiplier tube (at different anode currents)

THBV4_1325EA

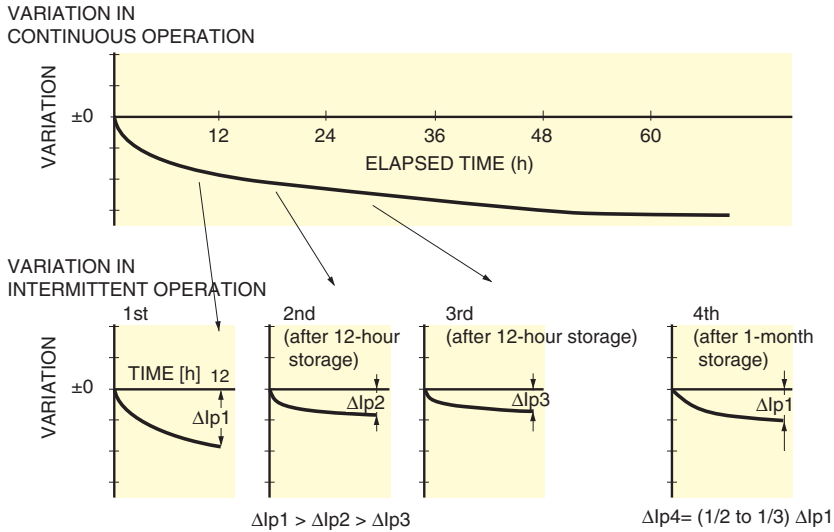
Figure 13-26 shows typical time stability of photomultiplier tubes when their operating anode currents I_p are set to 1, 10 and 100 microamperes, indicating both increasing and decreasing patterns.



THBV4_1326EA

Figure 13-26: Typical time stability of photomultiplier tubes (at different anode currents)

Stability over time can be improved by aging the tube (see (2) in section 4.3.2 of Chapter 4) while allowing light to enter the tube. Figure 13-27 shows the initial output variations when a photomultiplier tube is intermittently operated. It is obvious from the figure that a large variation during the initial operation can be reduced to nearly half during the second or later operations. When the photomultiplier tube is left unused for long periods of time, stability will return to its original values. In applications where high stability is prerequisite, we recommend the photomultiplier tube be aged before use.

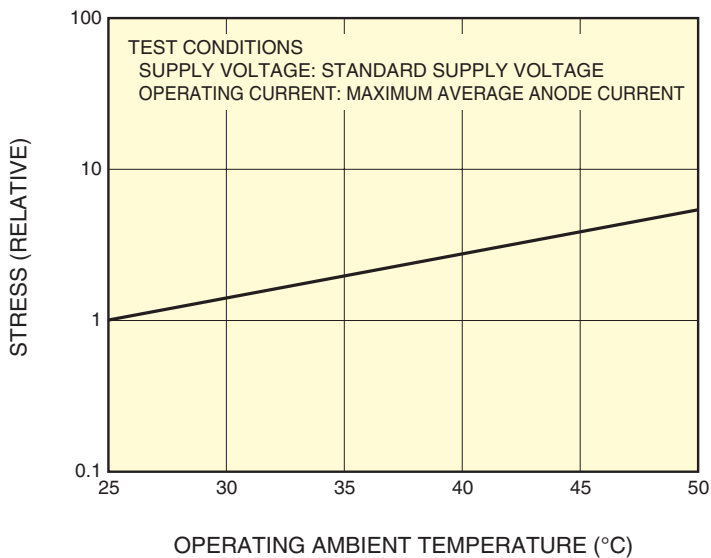


THBV4_1327EA

Figure 13-27: Effects of intermittent photomultiplier tube operation (aging effect)

13.9.3 Temperature stress and stability

When the ambient temperature is changed during operation, time stability of photomultiplier tubes also depends on the operating conditions. In general, the higher the operating ambient temperature, the earlier and more significant the variation that occurs. Figure 13-28 shows typical stress on a photomultiplier tube versus the operating ambient temperature.



THBV4_1328EA

Figure 13-28: Temperature stress

13.9.4 Reliability

In applications where a large number of photomultiplier tubes (sometimes hundreds or occasionally even thousands of tubes) are used in one instrument. In these applications, predicting and verifying the photomultiplier tube reliability are very important.

(1) Failure mode

Failure mode for photomultiplier tubes is roughly classified into gradual failure and breakdown failure. The main failure mode is gradual failure, which includes cathode sensitivity degradation, a loss of gain, an increase in dark current, and a decrease in dielectric resistance. Gradual failure is accelerated by excessive light input during operation and the resulting lower voltage operation and also by the storage or operation in high-temperature and high-humidity environments. Breakdown failure includes cracks in the glass faceplate, bulb envelope and stem portion, and also air leakage through microscopic cracks. Those glass cracks and damage may be caused by use in harsh environments such as at low temperatures and by improper handling such as dropping, exposing to strong impact or vibration, or applying excessive stress to the stem pins. Breakdown failure fatally damages the photomultiplier tube, making it permanently unusable.

Most causes of the failure mode lie in an increase in dark current and a loss (or variation) of gain. This does not mean the photomultiplier tube can no longer be used immediately from that point. The loss of gain will usually recover by adjusting the operating voltage.

(2) Failure rate

Failure rate⁽¹⁰⁾⁽¹¹⁾ is defined as the probability of failure per unit time. Failure rate is estimated by using the following two kinds of data in most cases:

1. In-house reliability test data
2. Field data

Actual results obtained from field data prove that the photomultiplier tube failure rate is at a level of 2×10^{-6} to 2×10^{-7} failures/hour with operating conditions at room temperatures, a rated supply voltage, and an anode output current of 100 nanoamperes. In particular, it is predicted that those tubes which have undergone screening provide a failure rate as small as 5×10^{-7} failures/hour.

(3) Mean life

There is a measure of reliability which is commonly referred to as MTBF⁽¹⁰⁾⁽¹¹⁾ (mean time between failure) or MTTF (mean time to failure). This is the average hours of time until any failure occurs or, in other words, mean failure life.

Since the definitions and fundamental calculations of these terms are described in detail in various papers, this section only briefly explains these terms. The relation between the failure rate (λ) and the mean failure life (θ) can be expressed on the assumption that it has failure distribution in accordance with exponential distribution, as follows:⁽¹⁰⁾⁽¹¹⁾

$$\theta = 1 / \lambda$$

Therefore, the reciprocal of the failure rate is the mean failure life.

As an example, when a photomultiplier tube is operated in room environments with an anode output current of about 100 nanoamperes, a mean failure life of 5×10^5 to 5×10^6 hours can be predicted based on the failure rate explained above. For those tubes which have passed screening, the mean life would be more than 2×10^6 hours.

(4) Reliability

Based on the fundamental calculation for stability data, reliability R is defined as follows.^{10) 11)}

$$R(t) = e^{-\lambda t}$$

t: operating time in hours

λ : failure rate

Therefore, using a typical failure rate λ of photomultiplier tubes of 2×10^{-6} to 2×10^{-7} failures/hours, reliability R becomes as follows:

| Elapsed time in operation | Reliability R(t) | |
|---------------------------|---------------------------------|---------------------------------|
| | at $\lambda = 2 \times 10^{-6}$ | at $\lambda = 2 \times 10^{-7}$ |
| One year (8760 hours) | 98.3 % | 99.8 % |
| 2 years (17520 hours) | 96.6 % | 99.7 % |
| 3 years (26280 hours) | 94.9 % | 99.5 % |
| 4 years (35040 hours) | 93.2 % | 99.3 % |
| 5 years (43800 hours) | 91.6 % | 99.1 % |

The above results can be used as a reference in determining approximate reliability levels of photomultiplier tubes, and prove that the photomultiplier tube provides considerably high reliability levels when operated under favorable conditions.

13.9.4 Reliability tests and criteria used by Hamamatsu Photonics

Hamamatsu Photonics performs in-house reliability tests by setting the following test conditions and failure criteria to obtain the failure rate.

Reliability test conditions

- 1) Environmental stress conditions
Room temperature (25 °C) and high temperature (55 °C) (5 °C above the maximum rating)
- 2) Test procedures
Storage and operating life
- 3) Operating conditions (photomultiplier tubes)
Supply voltage: catalog-listed standard operating voltage, 1000 to 3000 V
Anode output current: catalog-listed maximum rating, 10 to 100 μ A

Failure criteria

- 1) Anode sensitivity judged as the end of life: ± 50 % variation
- 2) Anode sensitivity during non-operation (storage): ± 25 % variation
- 3) Cathode sensitivity: ± 10 % variation during storage, ± 25 % variation during operation
- 4) Anode dark current (DC): more than 10 times increase, faulty dielectric withstanding voltage
- 5) Other failure: discharge, crack, anode leakage current, etc.

Notice that the above criteria are specified by Hamamatsu Photonics for evaluation and do not necessarily indicate that a tube outside these standards is unusable.

Hamamatsu Photonics has continually performed reliability tests under the above conditions over extended periods of time and has collected large amounts of data. Our evaluation results show that the failure rate of photomultiplier tubes ranges from 1×10^{-3} to 1×10^{-4} failures/hour and the mean time is from 1000 up to 10 000 hours. Based on these results, the ratio of the failure rate at room temperatures and an anode output current of 100 nanoamperes, to the failure rate under operating conditions at a maximum rating temperature and current (50 °C, 10 to 100 microamperes) will be approximately 200 times. This means that our in-house test conditions have an acceleration factor approximately 200 times that of the field data.

References in Chapter 13

- 1) Hamamatsu Photonics Technical Data Sheet: T-101
- 2) Special Committee for Measurement and Research into Vibration and Shock, Society of Electricity: Electric/Electronic Equipment and Vibration/Shock, Corona Publication Co., Ltd
- 3) IEC Publication 68-2: Basic Environmental Testing Procedures
JIS C 60068-2-6: Environmental testing procedures (electrical and electronic items), Sinusoidal vibration test method
JIS C 60068-2-27: Environmental testing procedures (electrical and electronic items), Impact test method
MIL-STD-810G: Environmental test methods and engineering Guidelines
MIL-STD-202G: Test methods for electronic and electrical component parts
- 4) Hamamatsu Photonics Catalog: Ruggedized High-Temperature Photomultiplier Tubes TPMH0001EA
- 5) Bicron Corp.: Ruggedized High-Temperature Detector Technology
- 6) J.R. Incandela, S.P. Ahlen, J. Beatty, A. Ciocio, M. Felcini, D. Levin, D. Ficenech, E. Hazen, A. Marin, J.L. Stone,
L.R. Sulac, W. Worstell: Nucl. Instrum. & Methods, Phys. Res. A269, 237-245 (1988)
- 7) L.W. Howell, H.F. Kennel: Optical Engineering, 25, 4, 545 (1986)
M.M. Brinbaum, R.L. Bunker, J. Roderick, K. Stephenson: AIAA Guidance and Control Conference (1984)
- 8) S. Sakubana, T. Kyono, K. Takahashi: Glass Handbook, 825, Asakura Shoten
- 9) W. Viehamann, A.G. Eubanks, G.F. Pieper, J.H. Bredekamp: Applied Optics, 14,9, 2104 (1975)
- 10) Shinkabe: Introduction to Reliability Engineering, Japanese Standards Association
- 11) K. Kitagawa: Principles of Reliability and Its Technology, Corona Publication Co., Ltd

CHAPTER 14

APPLICATIONS

Photomultiplier tubes are widely used as photodetectors in various applications including industrial and scientific measurements and academic research. This chapter introduces major applications of photomultiplier tubes in the measurement and research fields and describes their principles and detection methods for each application.

14.1 Spectrophotometry

14.1.1 Overview

Spectrophotometry is a technique used primarily for analyzing various substances using light. Photometric instruments used in this field are broadly divided into two methods. One utilizes light absorption, reflection, or polarization at specific wavelengths, and the other uses external energy to excite a sample and measure the subsequent light emission or absorption. This field has a long history and photomultiplier tubes have been most widely used as the photodetectors.

Photometric instruments used in this field are:

- 1) UV-visible spectrophotometers
 - 2) Infrared spectrophotometers
 - 3) Atomic emission spectrophotometers
 - 4) Fluorescence spectrophotometers
 - 5) Atomic absorption spectrophotometers
 - 6) Optical rotation and circular dichroism measurement devices
 - 7) Raman spectrophotometers
 - 8) Densitometers, colorimeters, and color meters
- etc.

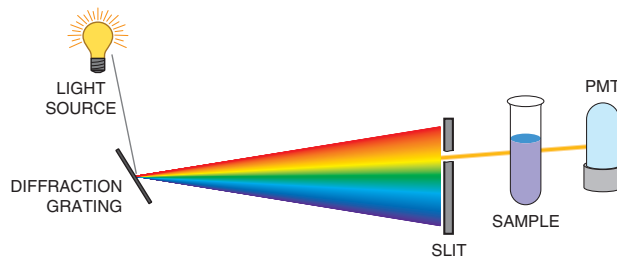
14.1.2 Application examples

The following describes typical photometric instruments that use photomultiplier tubes to measure light absorption or emission.

(1) UV-visible spectrophotometers

UV-visible spectrophotometers are used for quantitative analysis and absorption spectrum measurement of solution samples by utilizing their light absorption to plot the absorbance at each light wavelength. These can also be used to measure a spectrum of light transmitted through or reflected from solid-state samples. The measurement wavelength range covers the UV (200 nanometers to 380 nanometers) to visible (380 nanometers to 780 nanometers) region.

In a spectrophotometer, a beam of light from a light source is dispersed into a spectrum by a prism or diffraction grating to extract monochromatic light of the wavelengths used for measurement, which then enters the sample. Photomultiplier tubes are used to detect the light transmitted through or reflected from the sample. The transmittance or reflectance can be calculated from the ratio of the transmitted or reflected light level to the incident light level.

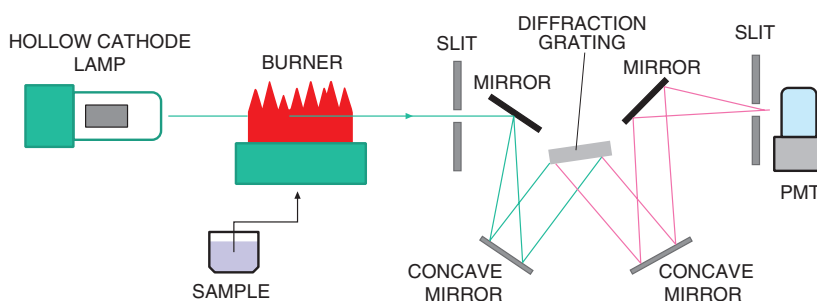


THEV4_1401EA

Figure 14-1: Principle of a spectrophotometer using a diffraction grating¹⁾

(2) Atomic absorption spectrophotometers

In an atomic absorption spectrophotometer, a sample solution is sprayed into a high temperature flame of 1700 °C to 2700 °C where molecules are vaporized and thermally decomposed into their constituent atoms. The vaporized atoms are then irradiated with light from a hollow cathode lamp whose cathode is made up of the element to be measured. If the sample contains the same element as the cathode, the light of the wavelength specific to that element is absorbed. By measuring this absorbance with a photomultiplier tube, the concentration of the element in the sample solution can be determined. Basically, one hollow cathode lamp emits line spectra produced by one element, so a different hollow cathode lamp is needed for each element to be analyzed. Since the light of the specific wavelength is absorbed in proportion to the concentration of the element in the sample, this method can determine the element's concentration in the sample by comparing the extent of absorption between the sample and a premeasured standard sample.

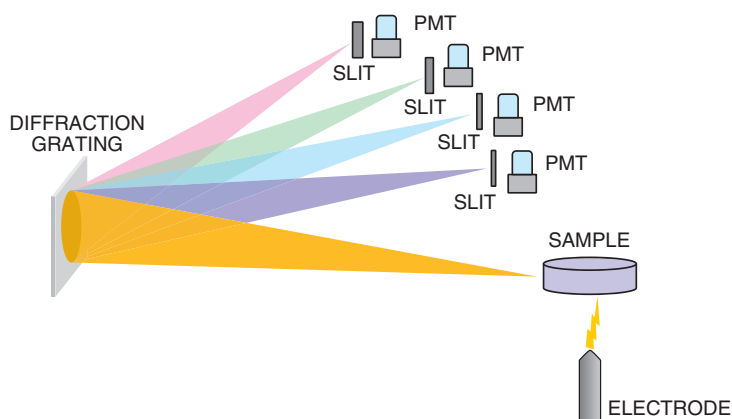


THBV4_1402EA

Figure 14-2: Optical systems used in an atomic absorption spectrometer

(3) Atomic emission spectrophotometers

In an atomic emission spectrophotometer, when external electrical energy is applied to a metal sample, the atoms and ions are excited to emit line spectra that are specific to the elements contained in the sample. These line spectra are separated by a monochromator according to wavelength, and are then measured with photomultiplier tubes to perform qualitative and quantitative analysis of the elements. The excitation sources include spark discharge, arc discharge, and glow discharge. They also include what could be called inductively coupled plasma (ICP).



THBV4_1403EA

Figure 14-3: Optical systems used in an atomic emission spectrophotometer

(4) Fluorescence spectrophotometers

Fluorescence spectrophotometers are used for research in biology and chemistry, and widely used especially in molecular biology. When a molecule is irradiated with light of a specific wavelength, it emits light at a wavelength longer than the irradiation light. This light emission is known as fluorescence. Measuring this light intensity and spectra allows quantitative and qualitative analysis of the sample. When measuring a low-concentration sample, fluorescence photometry is more frequently used than absorption photometry since it has higher sensitivity.

A fluorescence spectrophotometer consists of a light source, monochromators on the excitation light side and fluorescence side, and a photodetector. The light source usually has a xenon lamp that emits a wide continuous spectrum with high intensity. The monochromators on the excitation light side and fluorescence side use a diffraction grating or prism. The photodetector uses a photomultiplier tube.

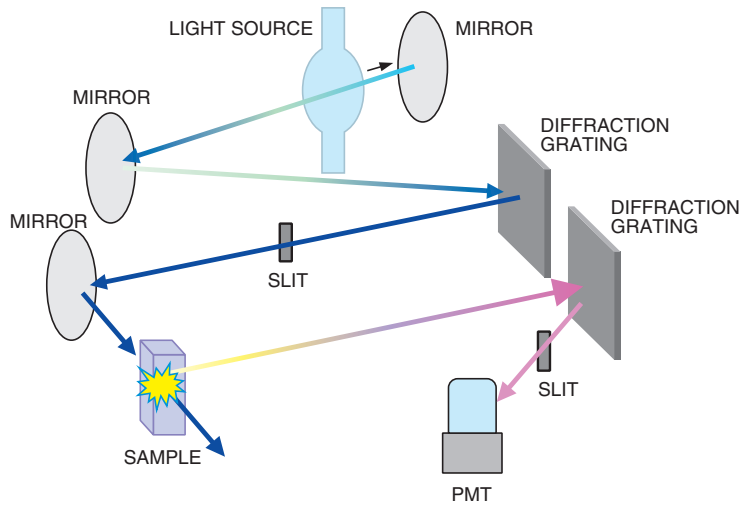


Figure 14-4: Schematic of a fluorescence spectrophotometer

THBV4_1404EA

14.2 Environmental Measurement

14.2.1 Overview

Photomultiplier tubes are also used as detectors in environmental measurement equipment such as dust counters for measuring dust contained in air or liquids and for radiation survey monitors used in nuclear power plants. This section describes some of these applications.

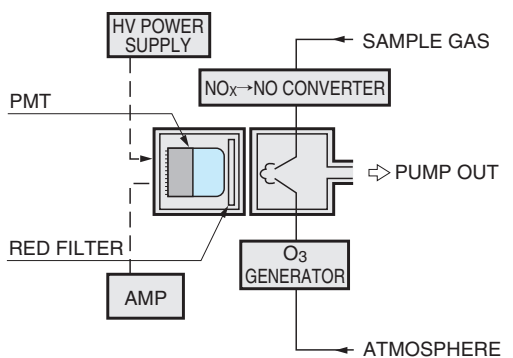
14.2.2 Application examples

(1) NO_x analyzers

These instruments are used to measure nitrogen oxide (NO_x) which is an air-polluting gas contained in exhaust gases from automobiles and other internal combustion engines. Nitrogen oxide in the air is directly harmful to humans (primary pollutant) and also generates secondary pollutants that are the cause of photochemical smog. It is therefore essential to monitor nitrogen oxide. NO_x is a general term indicating nitrogen monoxide (NO) and nitrogen dioxide (NO₂) and in many countries the concentration of NO_x is limited by air pollution regulations so that it shall not exceed a certain level.

Figure 14-5 shows the configuration of a gas-phase chemiluminescence-based NO_x analyzer.²⁾ NO_x is converted into NO gas by a converter. The NO gas then reacts with ozone (O₃) gas to generate NO₂ in an excited state. When it returns to the ground state, chemiluminescence is released. Measuring the intensity of this chemiluminescence allows determining the concentration of NO gas since the chemiluminescence intensity is proportional to the concentration of NO gas. When a red filter is used, only chemiluminescence of NO and O₃ in the long wavelength region (590 nanometers to 2500 nanometers) can be selectively measured.

Photomultiplier tubes suited for NO_x analyzers usually have a multialkali photocathode with sensitivity extending to the near infrared region where the target chemiluminescence occurs. A cooler is usually used to cool the photomultiplier tube, because chemiluminescence is very weak when the concentration of NO gas is low, the reaction chamber becomes hot at around 50 °C, and the dark current of the detector directly affects the performance of NO_x analyzer. Taking these points into account, Hamamatsu provides a line-up of compact photomultiplier tubes that can be directly cooled.



THBV4_1405EA

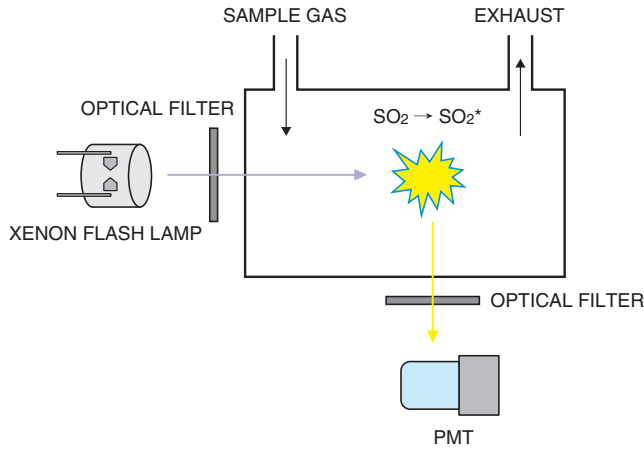
Figure 14-5: Schematic of a chemiluminescence-based NO_x analyzer



Figure 14-6: Photomultiplier tube for chemiluminescence measurement

(2) SO_x analyzers

Sulfur oxide analyzers measure sulfur dioxide concentrations in the atmosphere mostly by using a UV fluorescence method. This method irradiates sulfur dioxide (SO₂) in the atmosphere with UV light to produce SO₂ in an excited state. The intensity of fluorescence emitted from SO₂ is then measured to determine the sulfur dioxide concentrations in the atmosphere. A typical setup for a UV fluorescence-based SO₂ analyzer is shown in Figure 14-7.

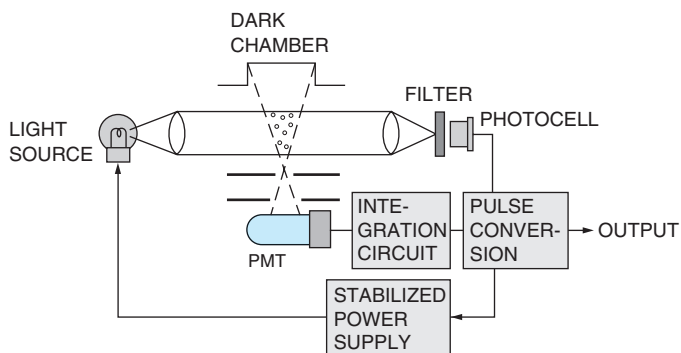


THBV4_1407EA

Figure 14-7: Schematic of a UV fluorescence-based SO₂ analyzer

(3) Dust counters

Dust counters measure the concentration of suspended particles in the atmosphere or inside a room by making use of light scattering or absorption of beta rays.³⁾ In the case of dust counters using light scattering, if suspended particles are present in the light path, light strikes them and is then scattered. The quantity of this scattered light is proportional to the quantity of the suspended particles. A photomultiplier tube is used to detect the scattered light, and the output signal is integrated and then converted into a pulse signal which is processed to correspond to the particle concentration. This method offers the advantage that the output signal can immediately follow up on changes in the concentration making it ideal for continuous monitoring over time.



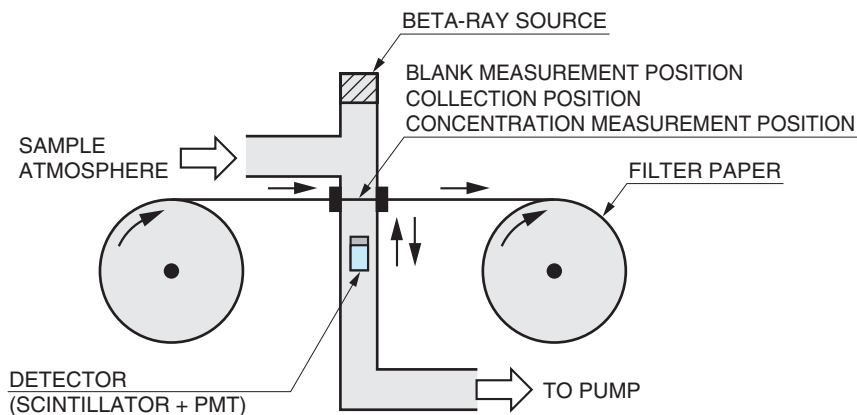
THBV4_1408EA

Figure 14-8: Schematic of a dust counter using light scattering

Dust counters utilizing light scattering have the drawback that the amount of scattered light varies depending on the size and refractive index of particles even if the particle concentrations are constant. Another type of dust counters make use of beta ray absorption which is proportional to the mass of a substance through which the beta rays are transmitted. Filter paper is used to collect the suspended particles, and the mass of the suspended particles are determined by detecting the extent of gamma-ray absorption. A photomultiplier tube coupled to a scintillator is used as the detector.

This determination method using beta-ray absorption is also used in part for the measurement of particulate matter 2.5 (PM_{2.5}) which serves as an air quality index marker.

* For more details on the measurement principle, see Chapter 7, "Scintillation counting."



Blank measurement position → Suction → Concentration measurement → Filter paper take-up

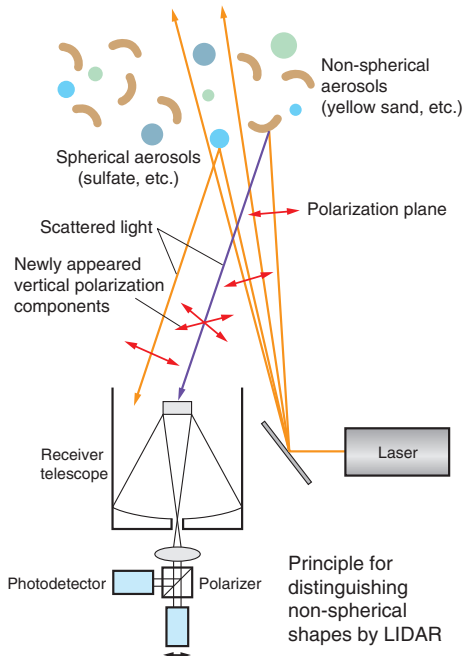
THBV4_1409EA

Figure 14-9: Schematic of a dust counter using beta-ray absorption⁴⁾

(4) Laser radar (LIDAR)⁵⁾

Laser radar, often called LIDAR (Light detection and ranging) is a principle and system that transmits pulsed laser light into atmospheric space and receives the light backscattered from scatterers such as suspended matter in the atmosphere (atmospheric molecules, aerosols, clouds, etc.) and flying objects in order to obtain information such as the distance to the scatterers and their concentrations, shapes, and speeds. The laser transmitter and detector are installed in the same place and the laser beam is scanned across the target area to obtain a three-dimensional spatial distribution. Optical signals are converted by the detector into electrical signals which are then converted into digital signals and processed by a computer.

In this application the detector response speed is important in improving the spatial resolution so high-speed detectors such as MCP-PMT are sometimes used when high-speed is particularly essential.



THBV4_1410EA



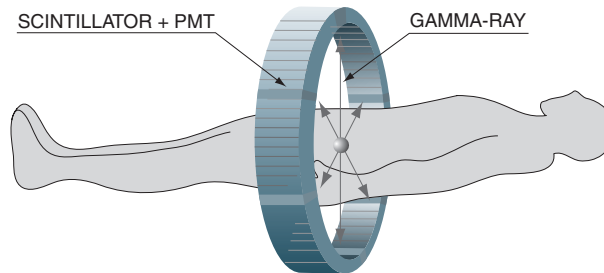
Photo of LIDAR observation⁷⁾

Figure 14-10: Schematic of a LIDAR for atmospheric observation⁶⁾

14.3 Medical Diagnosis

14.3.1 PET (Positron Emission Tomography) / CT (Computed Tomography)

Photomultiplier tubes are used for nuclear medicine diagnostic equipment such as PET (positron emission tomography) scanners as well as the gamma cameras and SPECT described later. This section describes specific examples of PET. The schematic diagram of a PET scanner is shown in Figure 14-11 and the external view in Figure 14-12.



THBV4_1411EA

Figure 14-11: Concept view of a PET scanner



Figure 14-12: External view of Hamamatsu Photonics SHR-74000 PET scanner (Reference example)

When a positron released from a positron-emitting RI (radioactive isotope) combines and annihilates with an electron, two gamma-ray photons of 511 keV are emitted in opposite directions. PET scanners are designed to detect and measure these two photons at the same time. PET provides tomographic images of a living body in the active state and allows early diagnosis of lesions and tumors by injecting pharmaceuticals labeled with positron-emitting radioisotope into the body and measuring their concentrations. Typical positron-emitting radioisotopes used for PET measurement are ^{11}C , ^{13}N , ^{15}O and ^{18}F .

Positrons released within the body combine with the electrons in the neighboring tissues, emitting a pair of gamma rays at 180 degrees opposite each other. A ring-shaped array of detectors surrounding the subject detects and measures these gamma rays by the coincidence counting technique. After arranging the acquired data at each angle, the PET scanner creates a tomographic image by image reconstruction in the same way as used for X-ray CT.

A prime feature of PET is that it allows quantitative measurement of physiological or biochemical information such as the metabolism, blood flow, and neural transmission within the body. PET is therefore used in clinical facilities, proving effective in diagnosing and detecting cancer at an early stage as well as in diagnosing brain disease such as dementia. Currently, PET is being put to active use in medical diagnosis. In addition, PET/CT which combines PET and X-ray CT is becoming widely used in order to accurately pinpoint the location of abnormalities such as cancer and also to correct gamma-ray absorption within the body of a patient.

Detectors used for PET are photomultiplier tubes in combination with scintillators. To efficiently detect high-energy gamma rays (511 keV) released from inside the body, scintillators with high gamma-ray stopping power such as BGO and LSO crystals are commonly used.

Recently, TOF-PET is being put to use in practical applications. TOF-PET utilizes the annihilation position information obtained by measuring the TOF (time-of-flight) of gamma-ray pairs generated by positron annihilation. TOF-PET utilizes high-speed photomultiplier tubes and scintillators (LSO or LYSO) with a short fluorescence decay. Use of TOF information helps improve PET image quality. It also allows reducing the concentration of radioactivity administered to a subject, making it effective in lowering the subject's radioactive exposure and shortening the examination time.

PET scanners for animals are used in applications such as animal experiments for research that cannot be easily done with humans, as well as for developing new medicines and evaluating the pharmacological effects of general medicines. Small laboratory animals such as mice and rats and large animals such as monkeys or baboons are commonly used.

Generally, since the animals' organs are relatively small, PET scanners must provide high resolution. In one example for this purpose, the Hamamatsu Photonics model SHR-38000 PET scanner uses a large number of scintillation detectors each consisting of a position sensitive photomultiplier tube combined with 648 LGSO scintillators. One PET scanner utilizes a total of 60 photomultiplier tubes and 38 880 BGO scintillators.

The SHR-38000 offers an effective field of view of 330×108 millimeters and a center resolution of 2.3 millimeters. Figure 14-13 shows the gantry unit and detector module for the SHR-38000.

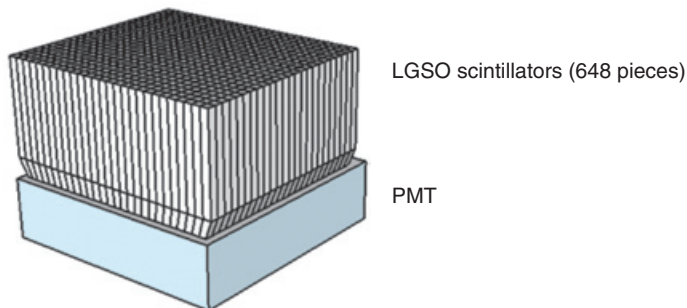


Figure 14-13: External view of gantry unit and detector module of Hamamatsu Photonics SHR-38000 PET scanner for animals

Figure 14-14 shows images of sugar metabolic activity in a monkey brain observed by using the SHR-38000.

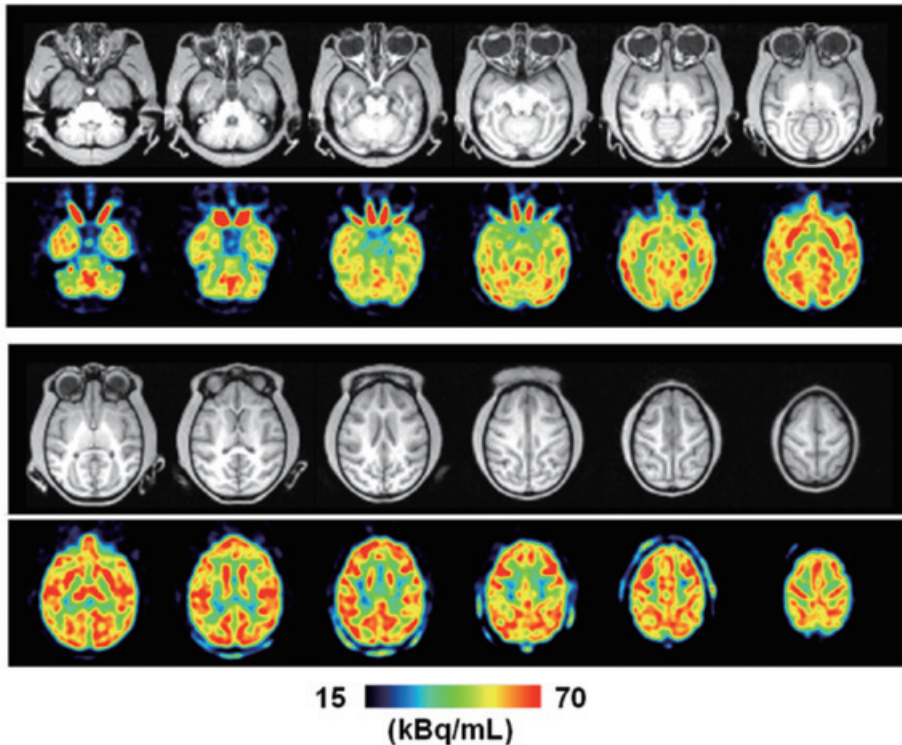


Figure 14-14: PET images (upper row) and MRI images (lower row) of sugar metabolic activity in a monkey brain

14.3.2 Planar imaging devices

Planar imaging devices have a pair of radiation position detectors that use a position-sensitive photomultiplier tube coupled to a scintillator array and are arranged opposite each other. These are designed to capture two-dimensional images of a positron-emitting nuclide tracer injected into the subject and to measure changes in those images over time. When a living plant or small living animal is placed between the two detector units, the activity of substances within its body can be measured as two-dimensional images in nearly real-time.

Positron-emitting nuclides such as ^{11}C , ^{13}N and ^{15}O are major elements that constitute living bodies and are also the basic substances used for organic synthesis, so many kinds of pharmaceutical compounds labeled with positron-emitting nuclides can be used. (Example: $^{11}\text{CO}_2$, ^{11}C -methionine, ^{15}O -water, etc.) When a positron-emitting nuclide with a short half-life period is used for example, ^{11}C (20 minutes), ^{13}N (10 minutes) or ^{15}O (2 minutes), then measurements can be repeated using the same individual. This allows measurement of changes over a day or measurement under two or more different conditions while eliminating errors that might be caused by individual differences. Since annihilation gamma rays (511 keV) are used for imaging, self-absorption within the object being measured can almost be ignored, allowing accurate measurement of the distribution of substances in a plant or small animal. Compared to medical PET scanners, the planar imaging device can obtain images with a higher signal-to-noise ratio and spatial resolution because the image generation technique is simple. Unlike tomographic PET images, when the object being measured is relatively thin, it is easier to visually recognize the image since the image obtained is a (pseudo) projected image. The block diagram and external view of a planar imaging device are shown in Figure 14-15.

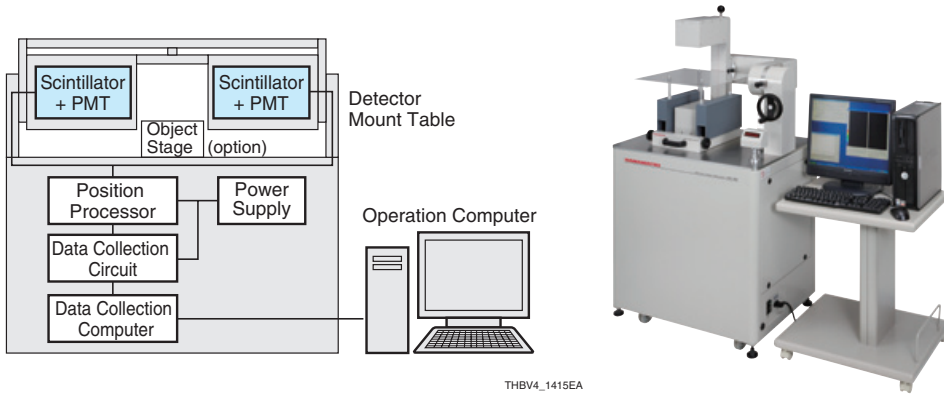


Figure 14-15: Block diagram and external view of Hamamatsu Photonics PPIS-4800 planar imaging device

14.3.3 Gamma cameras

Imaging equipment utilizing a radioactive isotope (RI) first appeared as a scintillation scanner and underwent successive improvements leading to the gamma camera developed by Anger (USA). Then, more sophisticated equipment called SPECT (single photon emission computed tomography) was developed that is capable of tomographic imaging. More recently, SPECT/CT that combines SPECT and X-ray CT is coming into use. An external view of a SPECT camera is shown in Figure 14-16. The detection unit is rotated around the patient and the acquired image data is processed to reconstruct a tomographic image.

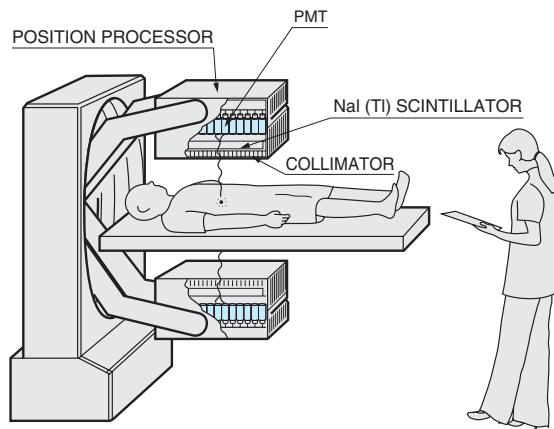
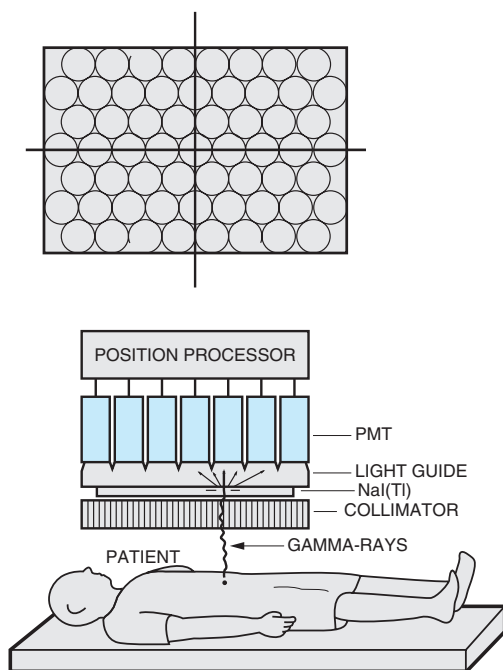


Figure 14-16: External view of a SPECT camera

Figure 14-17 shows the sectional views of a detector used in gamma cameras. Photomultiplier tubes are installed in combination with a large-diameter thallium-activated sodium-iodide (NaI(Tl)) scintillator serving as a gamma-ray detector.



THBV4_1417EA

Figure 14-17: Sectional views of a detector used in gamma cameras

To make gamma cameras more effective for medical diagnosis, a variety of gamma-ray nuclide drugs have been developed. Improvements in the position processing circuit have also achieved higher resolution, making gamma cameras more popular in medical diagnosis. Major nuclides used for nuclear medical imaging are listed in Table 14-1.

| Nuclide | Gamma-ray energy (keV) | Half-life |
|-------------------|---------------------------------------|-----------|
| ^{99m}Tc | 141 (no β) | 6.01 h |
| ^{133}Xe | 81 (β : 346) | 5.243 d |
| ^{67}Ga | 93 (37 %), 185 (20 %), 300 (17 %) | 78.3 h |
| ^{201}Tl | 70.8 (Hg-X), 16.7 (11 %), 135 (2.8 %) | 72.91 h |
| ^{131}I | 364 (81 %) (β : 606) | 8.04 d |
| ^{123}I | 159 (83 %) | 13.2 h |
| ^{81m}Kr | 190 (67 %) | 13 s |
| ^{111}In | 245 (94 %), 171 (90 %) | 2.83 d |

Values in parentheses () indicate the stripping efficiency.

Table 14-1: Major nuclides used for nuclear medical imaging

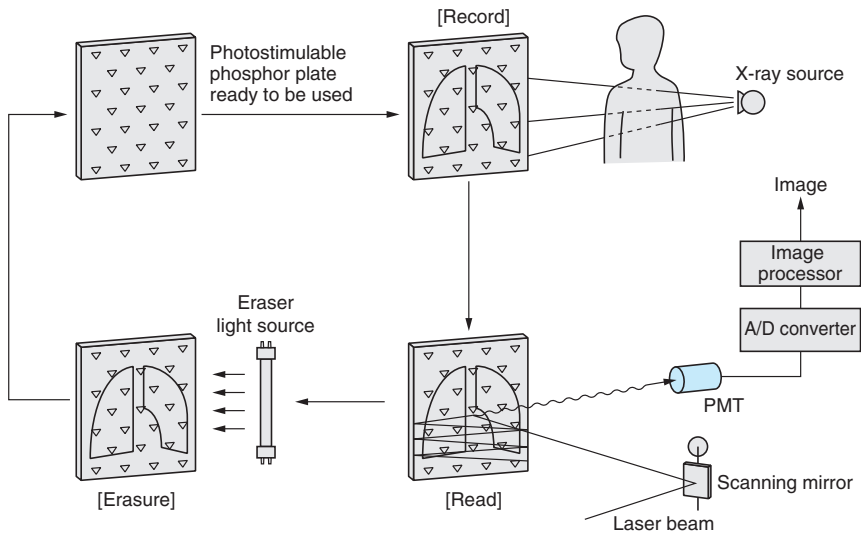
14.3.4 X-ray image diagnostic equipment

The X-ray image diagnostic equipment seen at many medical clinics and facilities has been using film for years. With the recent trend toward filmless X-ray imaging, computed radiography (CR) that uses an imaging plate (photostimulable phosphor), and digital radiography (DR) using a flat panel detector that combines a scintillator and a TFT sensor are now becoming the mainstream.

(1) Computed radiography (CR)

X-ray image diagnosis equipment includes computed radiography equipment that uses a special photostimulable phosphor plate. In this equipment, an X-ray image is temporarily accumulated on the phosphor plate and a laser beam then scans (excites) the image formed on the phosphor plate, causing it to give off light according to the amount of accumulated X-rays. A photomultiplier tube is used to convert this weak visible light into electrical signals which are then digitally processed to reconstruct an image. Compared to conventional X-ray film imaging, computed radiography has several advantages such as short imaging time, fewer imaging errors, and digital image processing and data analysis that permit high density storage and simple retrieval of image data. These useful features have led to its widespread use around the world.

Besides general medical imaging, computed radiography is also used for dental examination and industrial non-destructive inspection.



THBV3_1418EA

Figure 14-18: X-ray image acquisition using photostimulable phosphor plates

14.3.5 Laboratory testing

The analysis and inspection of blood and urine samples collected from a living body is referred to as laboratory testing. It is used for physical checkups, diagnosis of disease, investigation of the disease cause, and evaluation of drug potency. Laboratory testing can be classified as shown in Table 14-2. Among these, the concentrations of most tumor markers, hormones, drugs and viruses that are viewed as immunological testing items are extremely low. So, detecting these items requires high-sensitivity inspection equipment that mostly utilizes photomultiplier tubes.

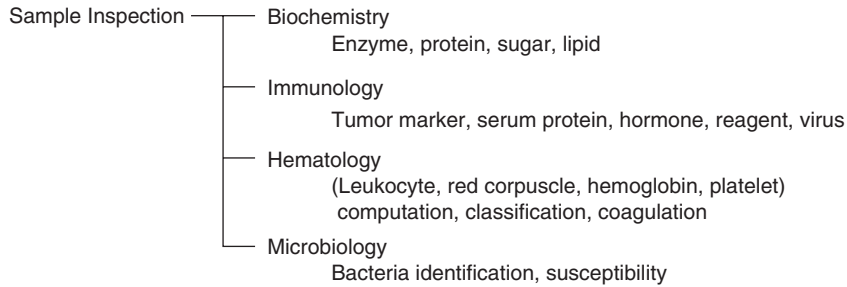


Table 14-2: Classification of laboratory testing items

In immunological testing, a measurement technique called immunoassay is widely used that relies on the specificity of the antigen-antibody reaction. The principles of immunoassay⁸⁾ are illustrated in Figure 14-19.

(a) Sandwich Method

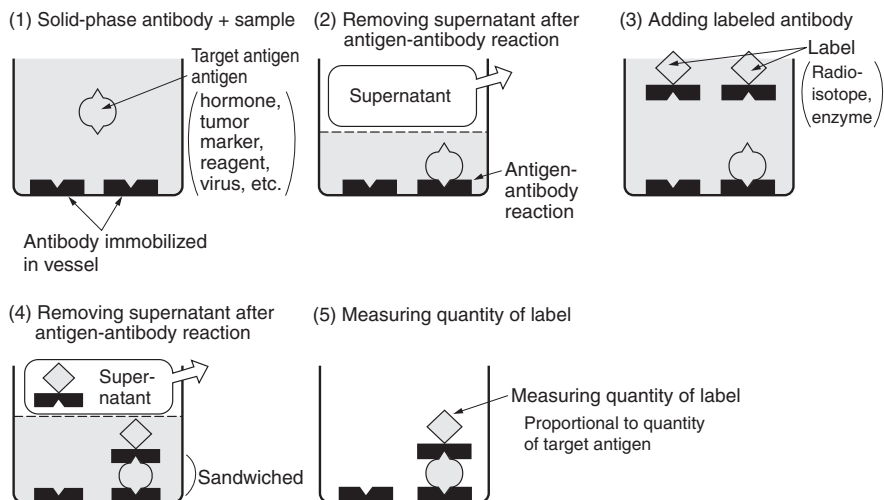
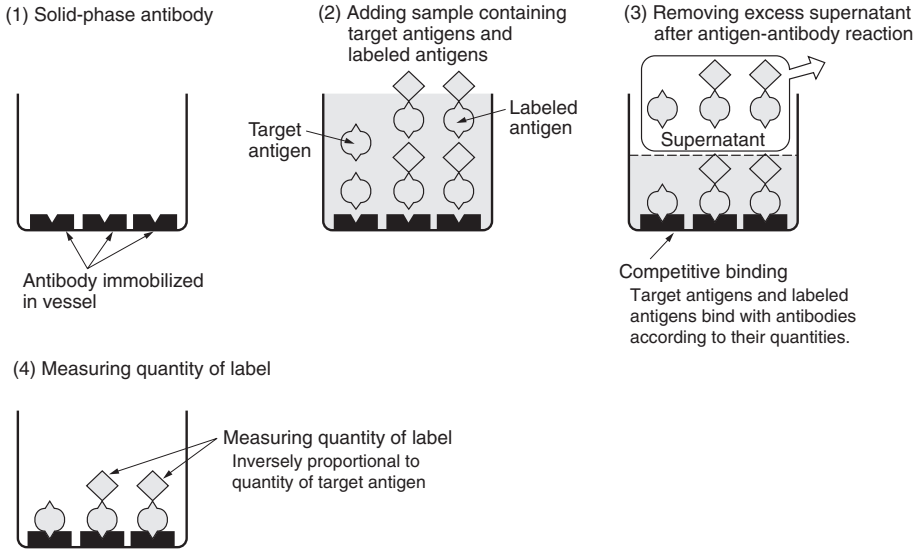


Figure 14-19(a): Principles of immunoassay

(b) Competitive Method

THBV4_1419EA

Figure 14-19(b): Principles of immunoassay

Figure 14-19 (a) is a technique known as the sandwich method. It includes the following steps:

- (1) A sample containing target antigens (hormones, tumor markers, etc.) is introduced into the vessel in which antibodies reactive with target antigens are immobilized (solid-phase antibodies).
- (2) Antigen-antibody reaction occurs and each target antigen binds with a solid-phase antibody. This reaction has an extremely high specificity and hardly ever occurs with a different antigen. After the antigen-antibody reaction, excess supernatant is removed, leaving antigen/antibody complexes.
- (3) Labeled antibodies reactive with target antigens are added.
- (4) Antigen-antibody reaction occurs again so that a target antigen is sandwiched between antibodies. The excess supernatant is then removed.
- (5) The quantity of label is measured by a photometric technique (fluorescence measurement) using a photomultiplier tube.

Figure 14-19 (b) shows another technique called the competitive method.

It includes the following steps:

- (1) Antibodies reactive with target antigens are immobilized in a vessel.
- (2) A sample containing target antigens is added along with labeled target antigens (labeled antigens).
- (3) Competitive reaction occurs in which target antigens and labeled antigens bind with antibodies according to their quantities in the sample and reach a state of equilibrium. After the antigen-antibody reaction, excess supernatant is then removed.
- (4) The quantity of label is measured by a photometric technique utilizing a photomultiplier tube.

In the sandwich method, the larger the quantity of target antigen, the greater the quantity of label that remains. In the competitive method, on the other hand, the larger the quantity of target antigen, the smaller the quantity of label that remains.

Immunoassay can be further categorized according to the material used for labeling as follows:

- (1) Using radioactive isotopes for labeling R.I.A. (Radioimmunoassay)
- (2) Using enzymes for labeling E.I.A. (Enzymeimmunoassay)
- (3) Using light-emitting reagent for labeling C.I.A. (Chemiluminescence immunoassay)

(1) R.I.A. (Radioimmunoassay)

Radioactive isotopes (RI) are used for labeling as explained above, and radiation (gamma rays or beta rays) from the RI labels remaining on the sample is detected by the combination of a scintillator and a photomultiplier tube, so that the target antigen can be quantified. Radioactive isotopes most frequently used for labeling are ^3H , ^{14}C , ^{57}Co , ^{75}Se , ^{125}I , and ^{131}I . (See Table 14-3.)⁹⁾ Among these, ^{125}I offers useful characteristics for labeling and is very widely used. Because radioactive isotopes other than ^3H and ^{14}C also emit gamma rays, a scintillator of sodium iodide crystals having a high gamma-ray to light conversion efficiency is used. On the other hand, ^3H and ^{14}C emit beta rays which are in very low quantities and so are measured with a liquid scintillation counter.

| Radioisotope | Half-life | Energy | Detection Method |
|------------------|-------------|-----------------|-----------------------|
| ^3H | 12.26 years | β | Liquid scintillation |
| ^{14}C | 5730 years | β | Liquid scintillation |
| ^{57}Co | 270 days | γ | Scintillation crystal |
| ^{75}Se | 120.4 days | γ | Scintillation crystal |
| ^{125}I | 60 days | γ | Scintillation crystal |
| ^{137}I | 8 days | β, γ | Scintillation crystal |

Table 14-3: Radioactive isotopes used for labeling in radioimmunoassay

Automated radioimmunoassay systems also make full use of automatic well scintillation counters. These systems incorporate sodium iodide scintillators having a well-like hole to enhance efficiency for converting the radiation emitted from radioisotopes into light. Measurements are made by automatically inserting test tubes which contain antigen/antibody complexes including labels into the hole in each scintillator. (See Figure 14-20.) Each detector section including a scintillator is covered by a lead shield to block extraneous radiation. This method has high specificity and high sensitivity but is generally being replaced by other detection methods due to the restrictions on the handling of radioisotopes.

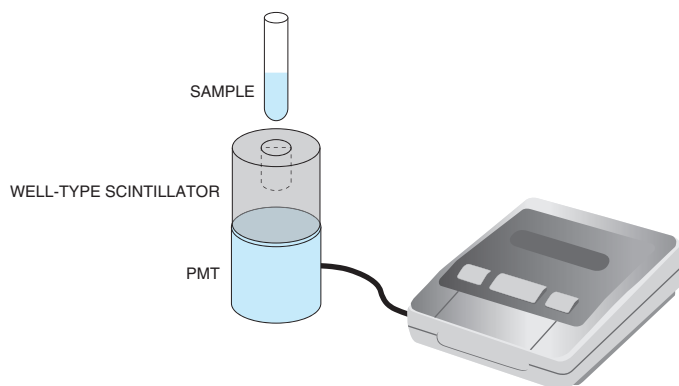
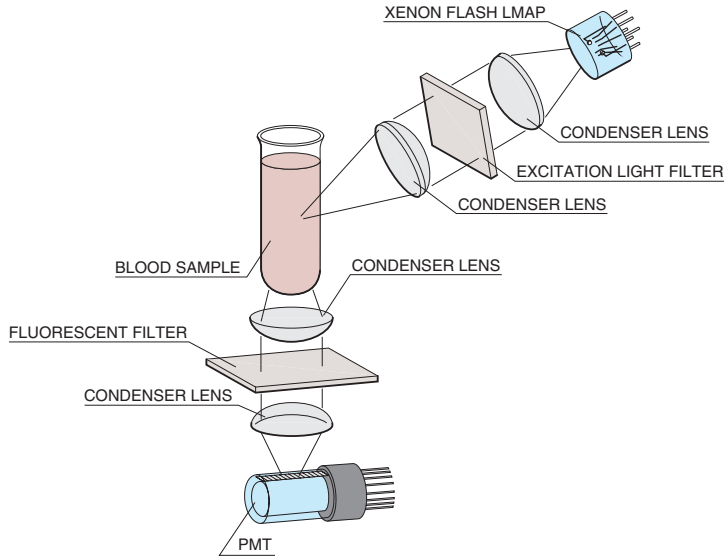


Figure 14-20: Schematic of a well scintillation counter

THBV4_1420EA

(2) Fluorescence immunoassay

One of these is fluorescence immunoassay or in which a fluorescent substance is used for labeling. The final remaining antigen/antibody complexes are irradiated by an excitation light and the resulting fluorescence is measured with regard to the intensity, wavelength shift, and polarization to determine the label amount. Figure 14-21 shows the schematic drawing of an immunoreaction measurement system for fluorescence immunoassay.



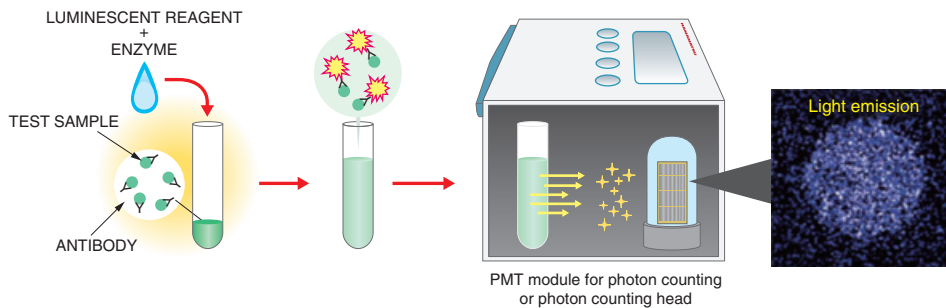
THBV4_1421EA

Figure 14-21: Schematic layout of a fluorescent immunoreaction measurement system

(3) Chemiluminescence immunoassay

Chemiluminescence immunoassay has several benefits such as high sensitivity, wide dynamic range, simple measurement without using detection antigens, and needs no special facilities unlike radioimmunoassay. Chemiluminescent immunoassay is applied to detect certain infectious diseases in biochemical testing (blood test).

When enzymes are added to antibodies or antigens labeled with a luminescent reagent, a chemical reaction occurs. Light emission accompanying the reaction is detected with a photomultiplier tube module for photon counting or with a photon counting head.



THBV4_1422EA

Figure 14-22: Schematic of chemiluminescence measurement

14.4 Microscopy

14.4.1 Overview

In the field of microscopy, photomultiplier tubes are mainly used to detect fluorescence and scattered light. Major applications include confocal laser microscopy and two-photon excitation microscopy.

14.4.2 Application examples

(1) Confocal laser scanning microscopy

In confocal laser scanning microscopy, the laser beam emitted from a laser light source is focused on a sample through an objective lens and the fluorescence from the excited sample is collected by the same objective lens. The collected light which contains both reflected laser light and fluorescence, is passed through a dichroic mirror and fluorescent filter so that only the fluorescence component is extracted and then detected by a photomultiplier through a pinhole. The pinhole eliminates extraneous components such as background light and fluorescence from locations other than the focal point. This optical setup and combination allow acquiring a high resolution images with less noise.

The laser beam scans the sample in two dimensions by using a galvano scanner or similar device. A three-dimensional image can also be constructed when a piezo scanner is used to change the height position.

Since the gain of the photomultiplier tube can be continuously varied by several orders of magnitude, it is easy to adjust the brightness and contrast of the image. Until recently, high-sensitivity side-on photomultiplier tubes have generally been used. However, photomultiplier modules and HPD (hybrid photodetectors) using a GaAsP photocathode having photoelectric conversion efficiency especially in the visible region are becoming more widespread.

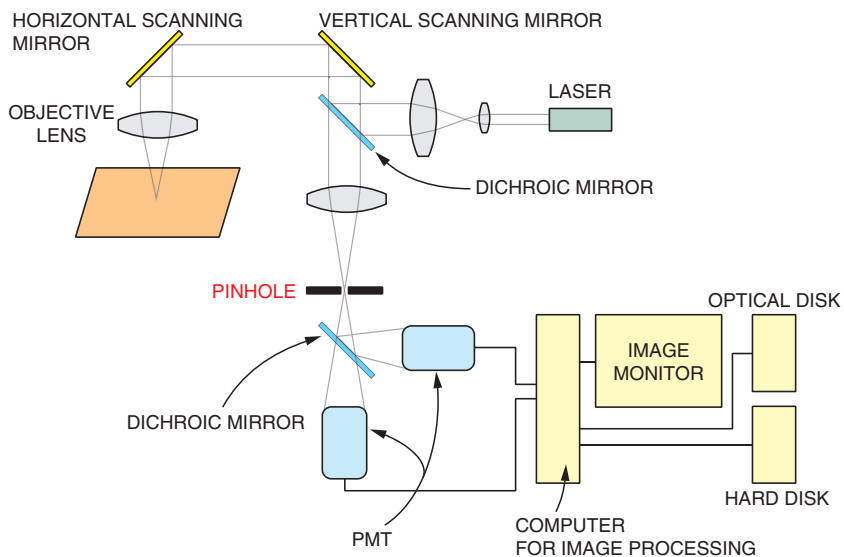
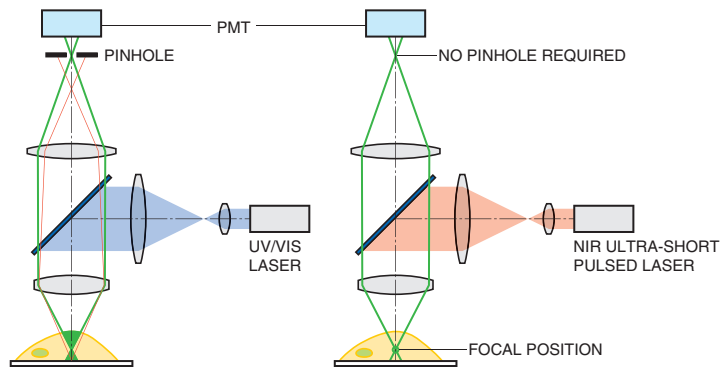


Figure 14-23: Schematic of a confocal laser microscope system¹⁰⁾

(2) Two-photon microscopy

Two-photon microscopy utilizes the fact that when two photons are absorbed by a fluorescent molecule within a sample nearly simultaneously in space and time, that sample is excited by energy that is one-half the energy of each photon or twice the wavelength (near infrared light). The two-photon excitation light is generated by focusing the light from a high-power femtosecond laser onto one small point through a high NA objective lens and increasing the photon density. Fluorescence emitted from the focus point is detected by a photomultiplier tube and an image of the fluorescence intensity distribution is acquired by scanning the focus point.

Two-photon microscopy uses near infrared light that is less scattered in a living body and allows observing deep into a sample. Because only the focal region with a high photon density is excited, confocal optics are not required, allowing the photomultiplier tube to be placed very close to the objective lens. This also ensures a high spatial resolution in the depth direction and so a three-dimensional image can be acquired. Due to these features, two-photon microscopy is used to observe deep regions of living tissues such as the brain and myocardial tissues.



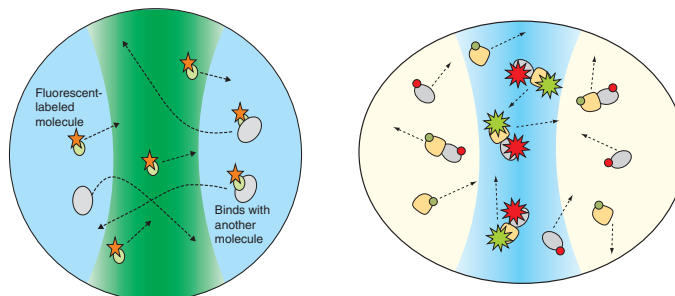
THBV4_1424EA

Figure 14-24: Comparison of one-photon excitation (left) and two-photon excitation microscope (right)¹¹⁾

(3) Fluorescence correlation spectroscopy¹²⁾

Fluorescence correlation spectroscopy (FCS) uses a confocal laser scanning microscope or two-photon microscope to analyze the motion of molecules passing through a very small region of a sample. When fluorescent-labeled molecules pass through the focal region of the laser beam, these are excited and emit fluorescence. Since this fluorescence from the molecules is very weak, a photomultiplier tube is used to detect it in photon counting mode. The fluorescence intensity fluctuates depending on the size and number of the molecules passing through the focal region of the laser beam. The fluctuations in the fluorescence intensity are obtained as the count data over time and then analyzed by the autocorrelation method to find the “molecular diffusion rate,” “number of molecules,” and “fluorescence intensity per molecule.”

In addition, fluorescence cross-correlation spectroscopy (FCCS) is also in use today. This method uses two different fluorescent dyes for labeling the molecules to utilize the cross-correlation between two fluorescence channels. The cross-correlation method allows a direct analysis of the “simultaneity” of two fluorescence signals, or in other words, intermolecular interactions, while the autocorrelation method measures the differences in the translational diffusion time of molecules.



THBV4_1425EA

Figure 14-25: Principle of fluorescence cross-correlation spectroscopy

14.5 Life Science

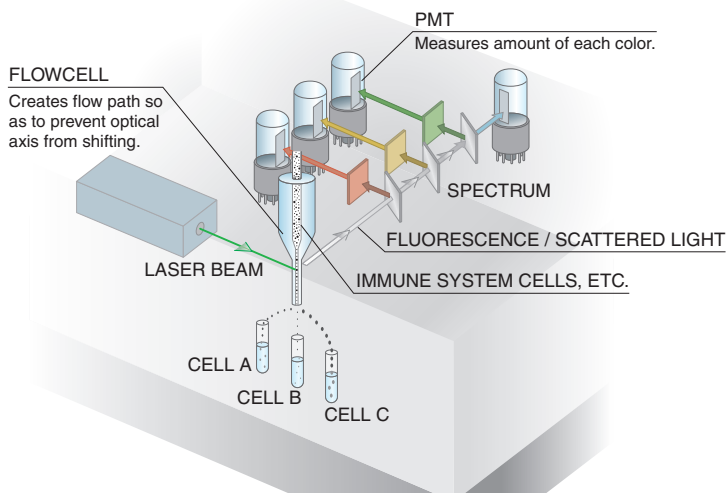
14.5.1 Overview

In the field of life science, photomultiplier tubes are mainly used for detecting fluorescence and scattered light. Major applications include flow cytometry, real-time PCR, and digital PCR.

14.5.2 Application examples

(1) Flow cytometer

When light is irradiated onto a rapidly flowing solution that contains cells or chromosomes, fluorescence and scattered light is released from the cells or chromosomes. Analyzing this fluorescence and scattered light helps unravel the cell properties and their structures. This field of study is known as flow cytometry. Flow cytometers are typical instruments used in this field for example, for research in cytology, immunology, and hematology, and also in part for laboratory testing (medical front) including blood analysis. Flow cytometers include a cell sorter equipped with a function for selecting and collecting only specific cells labeled with a fluorescent substance from a mixture of cells in a solution. (Figure 14-26)



THBV4_1426EA

Figure 14-26: Major components of a flow cytometer (cell sorter)

In a cell sorter, a fluorescent substance matching the particular purpose and called a fluorescent probe, is first attached to the cells which are then randomly mixed to a suspension and made to flow into a thin tube. The cells move through the thin tube at certain intervals. When each cell passes through a small area irradiated with intense laser light, it emits fluorescence and the intensity of this fluorescence is detected by a photomultiplier tube. The photomultiplier tube outputs an electrical signal in proportion to the number of fluorescent molecules attached to each cell. At the same time, the laser light scattered forward by the moving cells is detected to obtain information on the cell volume. By processing these two signals, the cell sorter creates an electrical pulse that causes the liquid flow to become charged at a point when only the portion of the liquid containing the desired cells is formed into a droplet, so that the droplet is charged. The dropping direction of this charged droplet is shifted by the deflection electrodes when it passes through between them and is sorted into the corresponding container.

To make the cell sorters more versatile, a detector with a wider dynamic range is needed and so photomultiplier tubes with a wide variable gain range are used.

(2) Real-time PCR / digital PCR

DNA measurement (quantification) applications are spreading widely to various areas including research in molecular genetics and physiology as well as medical diagnosis and food inspection. PCR is used as a DNA quantification technique.

Particular DNAs are amplified by polymerase chain reaction (PCR) and the amplification by-products are detected and quantified by making use of fluorescence. The PCR technique includes three steps: (1) denaturation, (2) annealing, and (3) elongation, and this cycle is repeated a number of times. The initial amount of DNA can be determined by comparing the quantity of replicated DNA and the cycle count with a calibration curve that is prepared in advance.

The real-time PCR technique has improved the quantification accuracy and other problems such as errors caused by contamination while the digital PCR technique allows statistical analysis.

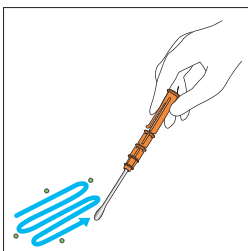
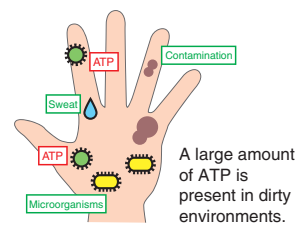
In both PCR techniques, fluorescent label probes that combine a fluorescent substance and a fluorescence-inhibiting substance are used at both ends of a DNA with a short specific sequence. The probes are coupled to the sample DNA to be amplified, and when the probes come off the sample DNA in the DNA elongation process, fluorescence is emitted or not emitted depending on the change in the distance between the fluorescent substance and the fluorescence-inhibiting substance.

The wavelength of fluorescence differs according to the reagent, so the detector uses a photomultiplier tube with a wide spectral response range that covers the range of fluorescence wavelengths.

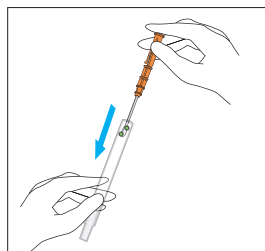
Luminometer for hygiene monitoring

Luminescence measurements are also applied to detect the presence of invisible organic contaminations and microorganisms. Adenosine triphosphate (ATP), which is a chemical substance present in and around all living organisms including animals, plants, and microorganisms has the property of emitting light that reacts with luciferase and enzyme. This is known as bioluminescence. By utilizing this principle, the hygiene monitoring luminometer checks the degree of contamination on food processing lines and machines, kitchen equipment and people's hands. To allow rapid measurements in work sites, the luminometer should be portable and easy to carry, so its detector uses a compact photomultiplier tube module capable of photon counting with low power consumption.

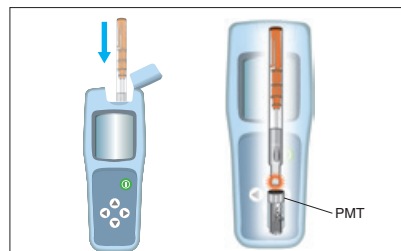
ATP test is an effective technique for monitoring cleanliness since it allows rapid determination of biological contamination levels.



(1) Wipe the location to be tested to collect ATP



(2) Let ATP react with reagent



(3) Measure luminescence by reaction

THBV4_1427EA

Figure 14-27: Luminometer for hygiene monitoring

14.6 High Energy Experiments

14.6.1 Overview

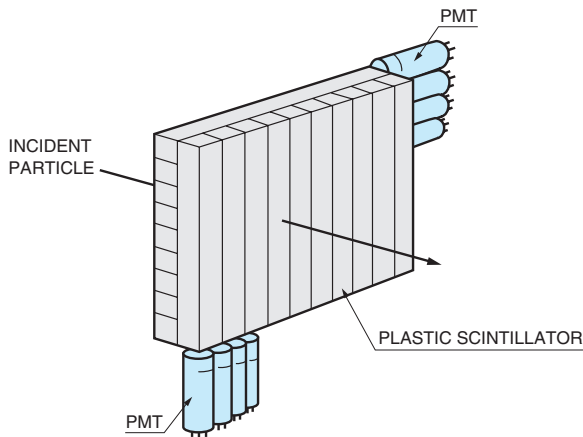
Photomultiplier tubes are also extensively used as detectors in high-energy physics experiments. For example, when a charged particle passes through a scintillator, a light flash is given off according to extent of the particle energy. Detecting this light flash makes it possible to measure the energy, speed, and direction of the charged particle. This technique is absolutely essential in high-energy physics research which is constantly aiming at new scientific discoveries.

14.6.2 Collision experiments

In collision experiments, primary particles such as electrons and protons are accelerated to high energy by an accelerator so that they will collide with each other to produce secondary particles. The energy, speed, and kinetic momentum of these secondary particles are observed and measured. There are several particle detection methods that use photomultiplier tubes including, for example, hodoscopes, TOF counters, calorimeters, and Cherenkov counters.

(1) Hodoscopes

Figure 14-28 shows a schematic¹³⁾ of a hodoscope. Plastic scintillators are arrayed in two orthogonal layers followed by photomultiplier tubes. The position and time at which a charged particle passes through certain scintillators are detected by the corresponding photomultiplier tubes.

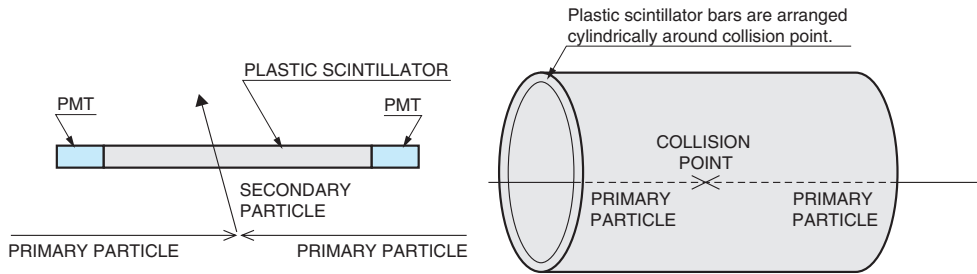


THBV4_1428EA

Figure 14-28: Schematic of a hodoscope

(2) TOF counters

TOF counters measure the time of flight (TOF) of particles to identify the type of particle. A schematic of a TOF counter is shown in Figure 14-29. When primary particles collide with each other, secondary electrons are generated. The time of flight of these secondary particles from the collision point to the TOF counter is measured to find the velocity of the particles. A typical detector consists of a long plastic scintillator bar with both ends coupled to a photomultiplier tube. A large number of plastic scintillator bars are arranged cylindrically around the collision point.

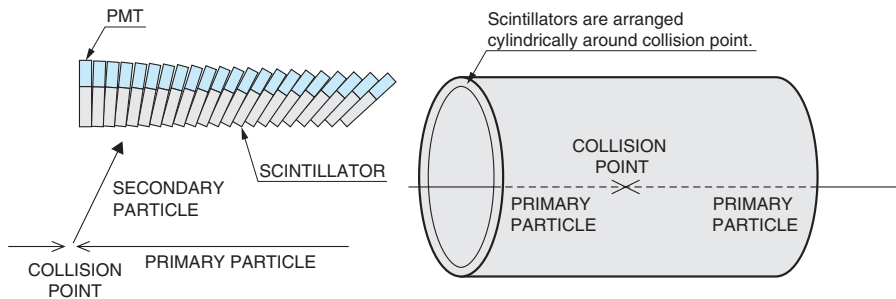


THBV4_1429EA

Figure 14-29: Detector and overall schematic of a TOF counter

(3) Calorimeters

Calorimeters measure the energy of secondary particles such as electrons, photons, and hadrons. A schematic of a calorimeter is shown in Figure 14-30. The collision point is surrounded by detectors such as a TOF counter. In the case of calorimeters, the energy of particles is released into matter and converted into light or an electric charge. This is usually measured with detectors consisting of an inorganic scintillator or lead glass combined with a photomultiplier tube. Recently, sampling calorimeters are also in use employing a multilayer structure of plastic scintillators and heavy metals such as iron and lead, instead of using inorganic scintillators.



THBV4_1430EA

Figure 14-30: Detectors and overall schematic of a calorimeter

(4) Cherenkov counters

Cherenkov light is emitted when a charged particle with a velocity or energy greater than a certain level passes through matter called a "radiator" (transparent medium). This Cherenkov light is a kind of shock wave and is emitted in a cone around the direction of the charged particle, forming a ring pattern. The energy and type of the particle can be identified on the basis of the size and brightness of this ring.

Figure 14-31 shows a schematic example of a Cherenkov counter called "RICH" (Ring Imaging Cherenkov counter).¹⁴⁾ This example uses aerogel as the radiator. When pi mesons or K mesons pass through the radiator, Cherenkov light is emitted in a cone pattern. This light is detected by photodetector arrays and the type of the particles is identified from the ring image information.

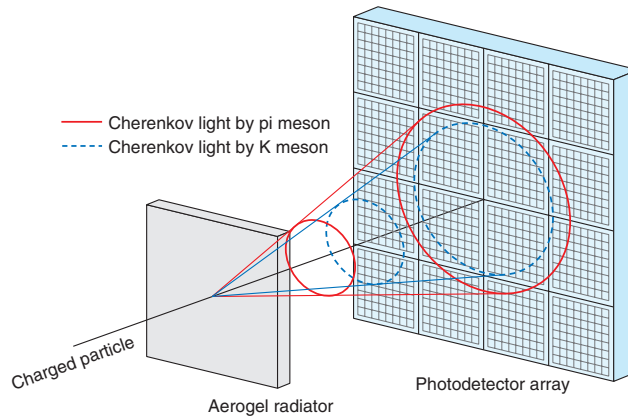


Figure 14-31: Schematic of RICH

THBV4_1431EA

14.6.3 Proton decay and neutrino observation experiments

Kamiokande / Super-Kamiokande

Kamiokande (KAMIOKA Nucleon Decay Experiment) is an experimental facility built in an underground mine in Hida City (formerly Kamioka Town) in Gifu Prefecture in Japan. Under the guidance of the Institute for Cosmic Ray Research (ICRR) and the High Energy Physics Research Laboratory, Faculty of Science, University of Tokyo, the Kamiokande detector was installed with a huge tank filled with pure water and equipped with 1050 pieces of the world's largest 50-centimeter (20-inch) diameter photomultiplier tubes. The experiments at Kamiokande started in 1983 for the purpose of observing proton decay. The Kamiokande detector was then modified to observe not only proton decay but also solar neutrinos and in 1987 for the first time in the world, the Kamiokande detector succeeded in observing neutrinos travelling from the supernova 1987A that appeared in a corner of the Large Magellanic Cloud.

After that, to keep pace with the recent mainstream prediction in the Grand Unified Theory or namely that proton lifetime may extend to 10^{34} years, a new plan for "Super-Kamiokande" experiments with 10 times to 100 times the performance of Kamiokande was unveiled. Another huge water tank of 39.2 meters in diameter and 41.4 meters in height was constructed and filled with 50 000 tons of ultrapure water. This is about 16 times the size of the Kamiokande tank, and 11 200 pieces of 50-centimeter (20-inch) diameter photomultiplier tubes with improved performance were installed on all inner walls of the water tank. Observation began in 1996 at Super-Kamiokande. In 1998, Super-Kamiokande discovered atmospheric neutrino oscillation which indicates that neutrinos have mass. Precision verification was made by using artificial neutrinos and that observation currently continues.

The 20-inch diameter photomultiplier tube we developed for Kamiokande was awarded an IEEE milestone in October, 2014. This photomultiplier tube was developed at the request of Masatoshi Koshiba who is currently a special honor professor of the University of Tokyo and received the Nobel Prize in Physics 2002 for his observation of neutrinos in 1987. In addition, Takaaki Kajita, the director of the Institute for Cosmic Ray Research, University of Tokyo, was also awarded the Nobel Prize in Physics 2015 for the discovery of neutrino oscillations that indicate a neutrino has a mass.



Figure 14-32: IEEE Milestone award plaque

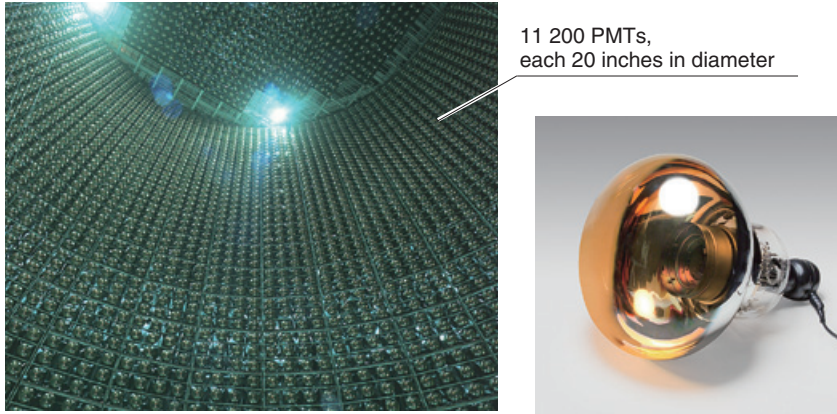


Figure 14-33: Interior of Super-Kamiokande detector tank and 20-inch photomultiplier tube

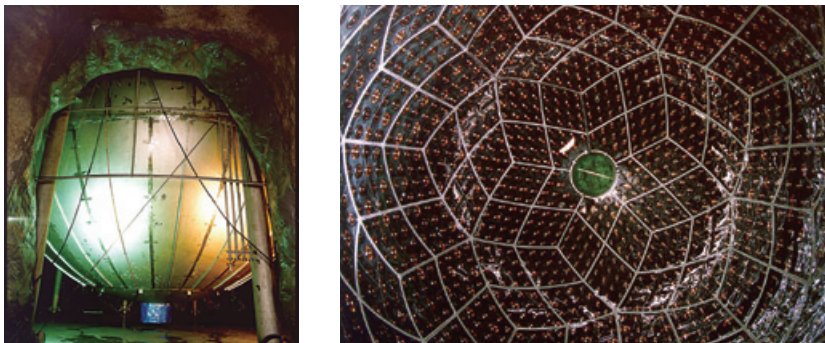
KamLAND (Kamioka Liquid-scintillator Anti-Neutrino Detector)

In January 2002, experiments commenced with the "KamLAND" operated by the Research Center for Neutrino Science at Tohoku University.

The KamLAND detector was constructed utilizing the former Kamiokande site yet functions as an even more sophisticated neutrino detector. Instead of pure water, KamLAND makes use of 1000 tons of liquid scintillator to capture neutrinos. The intensity of the light emitted from the neutrinos reacting with the liquid scintillator is on a much larger scale than the Cherenkov light trapped at Kamiokande, and allows detecting neutrinos at even lower energy levels. This liquid scintillator is held in a round balloon of about 13 meters in diameter made from special transparent film. The balloon itself is contained within a spherical tank of stainless steel 18 meters in diameter and has a volume of 3000 cubic meters.

The inner wall of the tank is lined with approximately 1900 pieces of 50-centimeter (20-inch) diameter photomultiplier tubes (effective area: 43 centimeters in diameter) that are improved versions of the Super-Kamiokande tubes. The outer wall of this spherical tank is further enclosed by a tank filled with pure water and this section is also lined with 50-centimeter (20-inch) diameter photomultiplier tubes. At KamLAND, the time difference between two light emissions occurring from reaction with the neutrinos and the time delay from the emission of light until the light reaches the photomultiplier tubes are measured. This allows finding the location within the balloon where the neutrino reaction occurred.

In 2002, it was announced that there was oscillation present in neutrinos coming from nuclear power plants and the mystery of solar neutrinos was determined to be due to this neutrino oscillation. Japan is a leader in the field of neutrino research and these superb experimental devices are certainly one of the main reasons it retains this lead.



Spherical stainless steel tank

Photomultiplier tubes installed on the inner wall
PMTs spherical tank

Figure 14-34: KamLAND¹⁵⁾

14.6.4 Gamma-ray telescopes

Gamma-ray telescopes are used for observing the energy and direction of high-energy gamma rays coming from celestial bodies with high energy such as supernovas, neutron stars, and black holes.

Gamma-ray telescopes are carried on an artificial satellite to make direct observations of gamma rays or are installed on Earth to observe atmospheric Cherenkov light generated from the interaction of gamma rays with the Earth's atmosphere.

The CTA (Cherenkov Telescope Array)¹⁶⁾ is a gamma-ray telescope developed for the observation of atmospheric Cherenkov light. It uses a special camera installed on Earth, which contains an array of 7 photomultiplier tube modules per cluster.

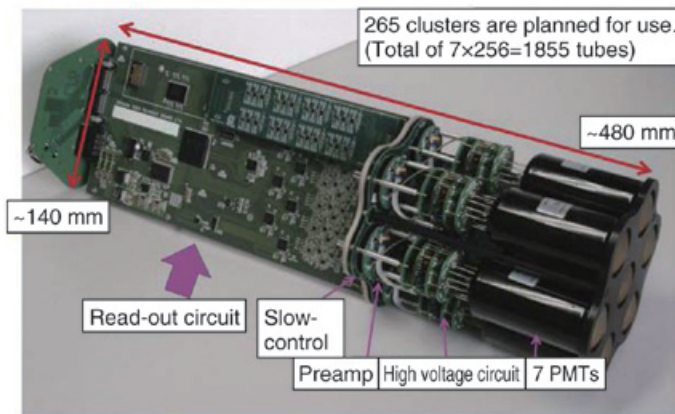
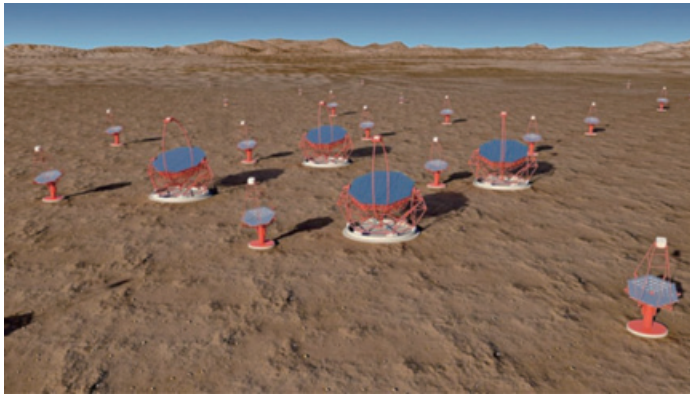


Figure 14-35: CTA (Cherenkov Telescope Array)

14.6.5 Dark matter experiments

Recently, an unidentified, invisible substance that constitutes part of our universe and called dark matter is the focus of much attention in high energy physics.

In dark matter experiments, ultraviolet scintillation light is emitted when in rare cases dark matter collides with an atom in liquid xenon (at $-108\text{ }^{\circ}\text{C}$) or liquid argon (at $-186\text{ }^{\circ}\text{C}$). This light is very weak and is detected by a photomultiplier tube. Since dark matter very rarely interacts with ordinary matter, the radiation level contained in the photomultiplier tube must be reduced to an extreme limit to minimize the background radiation to allow measurement. In addition, when the photomultiplier tube is installed under low temperature conditions, the photocathode resistance increases and causes the photocathode current to become saturated. This requires a special photocathode with low resistance that will not cause photocathode current saturation even at low temperatures.

In Kamioka Town, Gifu Prefecture, Japan, the XMASS detector filled with one ton of liquid xenon is installed for dark matter observation. It uses photomultiplier tubes with low radiation levels and low photocathode resistance developed specifically for XMASS experiments.

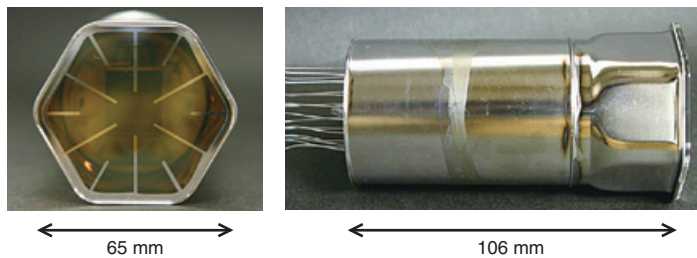


Figure 14-36: Photomultiplier tube for XMASS experiments¹⁷⁾

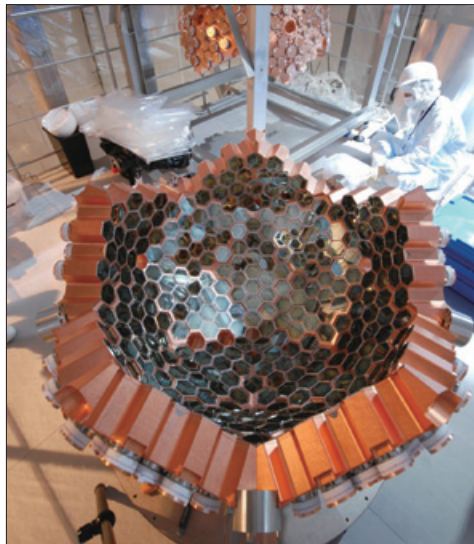
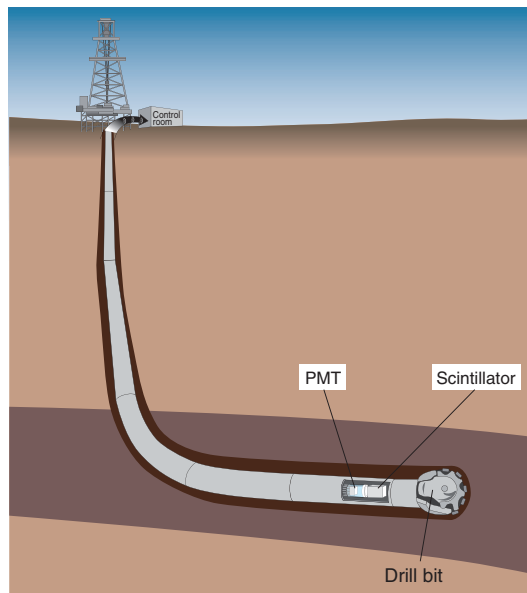


Figure 14-37: XMASS detector¹⁷⁾

14.7 Oil Well Logging

Special ruggedized, high-temperature photomultiplier tubes have been developed that ensure reliable operation even in harsh environments exposed to high temperatures and severe vibrations and shocks. This section explains oil well exploration (oil well logging) as an application of these photomultiplier tubes.

Oil well logging is conducted to locate an oil deposit and get information on its size. Photomultiplier tubes are used as detectors for density well logging using radiation, neutron well logging, and natural gamma-ray-spectrum well logging. In these oil well loggings, a probe containing a radiation source and scintillation counter is lowered into an exploratory well to detect and analyze the scattered radiation or natural radioactivity from the geological formations to estimate their type and density. This technique is called wireline logging and has been widely used. However, more advanced systems are needed to explore more complex geological formations and to identify unconventional oil wells and gas wells. A technique called MWD (measuring while drilling) was developed. MWD uses various types of sensors installed near the drill bit to allow real-time measurements of geophysical parameters such as geological orientation and inclination. In addition, a technique called LWD (logging while drilling) was also developed and is being put into use. LWD allows drilling a well and identifying geological formations by using sensors including photomultiplier tubes while measuring and analyzing the information on the geological formations. Figure 14-37 shows the measurement method for oil well logging using radiation and the cross sectional view of the geological formations.



THBV4_1438EA

Figure 14-38: Oil well logging

Generally, the depth of an exploratory drilled well may be as deep as several thousand meters where the ambient temperature reaches 150 °C to 200 °C. Furthermore, shocks and vibrations are also applied during drilling that impose extremely harsh environmental conditions on the photomultiplier tubes. To meet these requirements, various types of ruggedized, high-temperature photomultiplier tubes have been developed, which ensure satisfactory performance even in these harsh environments. These photomultiplier tubes have a special photocathode that exhibits a minimal increase in dark current even at high temperatures and their electron multiplier uses materials capable of withstanding high temperatures. Their electrode structures are also carefully designed by taking the thermal expansion and vibration into account.

Hamamatsu Photonics also provides high voltage power supplies to operate these photomultiplier tubes that are subject to high temperatures and vibrations.

14.8 Radiation Monitoring

14.8.1 Overview

Radiation monitors have long been used at nuclear power plants and nuclear research facilities. In recent years however, the loss or theft of nuclear materials has become a serious concern so that inspection and detection of nuclear materials has become a high priority at national borders such as harbors and airports. Photomultiplier tubes are used for various types of radiation inspection devices and monitors in combination with a scintillator that matches the radiation emitted from the nuclear materials.

14.8.2 Application examples

(1) Handheld radiation monitors (radiation pager)

Handheld radiation monitors are designed to help customs, border guards, and others keep watch for smuggled radioactive materials. A detector consisting of a photomultiplier tube coupled to a scintillator is used to detect radiation. Compact, metal package photomultiplier tubes are mostly used for handheld applications. Figure 14-38 shows a schematic diagram and photo¹⁸⁾ of a handheld radiation monitor.

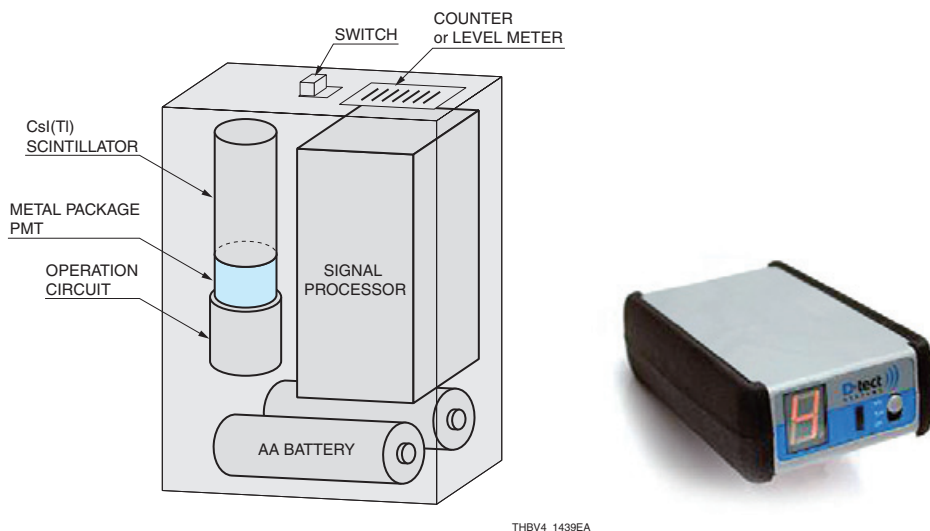
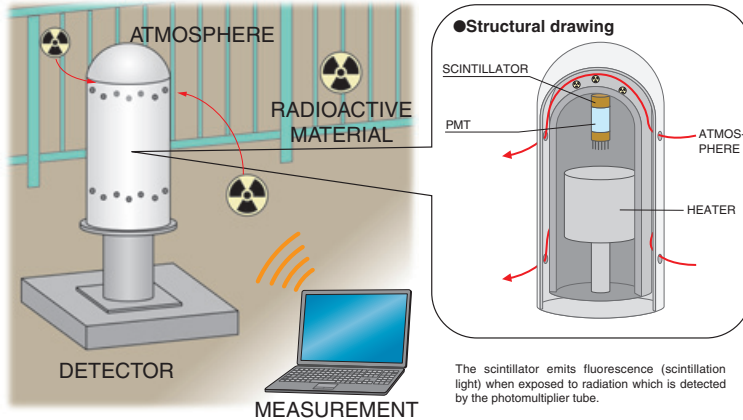


Figure 14-39: Schematic of a handheld radiation monitor

(2) Radiation monitoring posts

Radiation monitoring posts are installed in or around the site of a nuclear plant to constantly measure and monitor the radiation levels in the air.

Photomultiplier tubes combined with a scintillator or ionization chambers are used as detectors. Routine monitoring of the radiation levels helps provide residents with information about evacuation measures in cases where a radiation leakage or nuclear accident occurs in a nuclear power plant.



THBV4_1440EA

Figure 14-40: Schematic of a radiation monitoring post

(3) OSL (optically stimulated luminescence) dosimeters

In nuclear medical facilities, nuclear power plants, particle accelerator laboratories, and other facilities using radiation, the personnel and workers wear a small OSL dosimeter for monitoring individual exposure dose. The OSL dosimeter contains a sensor element that stores energy in proportion to the amount of radiation exposure. This sensor element is usually made of lithium fluoride, calcium sulfate, and aluminum oxide by a molding process.

When radiation enters and interacts with the sensor element, ionization occurs within a crystal in the sensor element and the resulting free electrons and holes are trapped by impurities in the crystal. Under this condition, when the sensor element is stimulated by light from a LED or laser, the trapped free electrons and holes return to the ground level while emitting light that is proportional to the amount of radiation stored in the sensor element. By reading the intensity of this light with a photomultiplier tube, the exposure dose can be monitored.

Until recent years, thermoluminescent dosimeters, or TLD, have commonly been used that emit light proportional to the radiation exposure when the sensor element is heated. However, OSL dosimeters are becoming more widely used, because they have advantages over TLD dosimeters in that the exposure dose can be reread several times, no heating process is required, and the device durability is good.

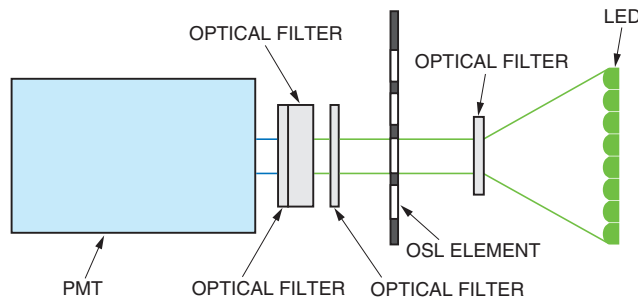


Figure 14-41: Schematic of an OSL dosimeter reader¹⁹⁾

THBV4_1441EA

14.9 Industrial Measurements

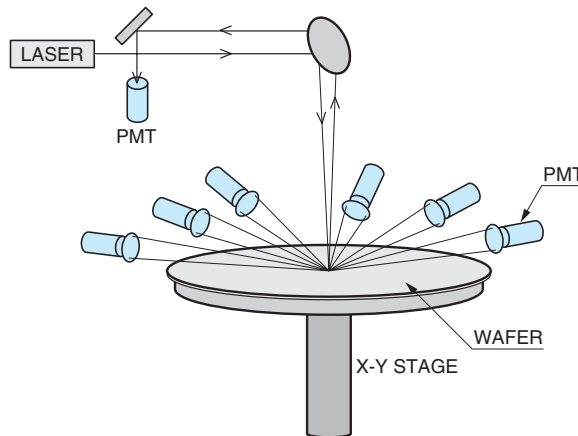
14.9.1 Overview

In non-contact measurement on a production line and other industrial applications where rapid measurement with high accuracy and high quality is essential, various measuring devices using light such as optical thickness gauges and laser scanners are widely used. These devices employ photomultiplier tubes as their photodetectors.

14.9.2 Application examples

(1) Semiconductor wafer inspection equipment

In semiconductor wafer inspection, a laser beam is scanned over the wafer surface or the wafer itself is scanned while a laser beam is focused onto a fixed point. In either case, photomultiplier tubes are used to detect the scattered light caused by dirt, stains or defects on the wafer surface. (Figure 14-41)

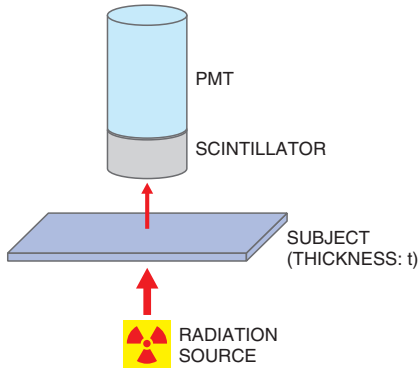


THBV4_1442EA

Figure 14-42: Optical system for semiconductor wafer inspection equipment

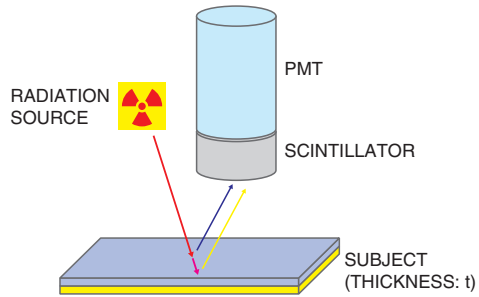
(2) Thickness gauges

To measure the thickness of paper, plastics, and steel plates on a production line, non-contact measurement techniques that use radiation such as beta rays, X rays or gamma rays are favored. These techniques can be roughly divided into two methods: one method measures the amount of beta or gamma rays transmitted through an object (Figure 14-42) and the other method measures the amount of fluorescent Xrays (Figure 14-43).



THBV4_1443EA

Figure 14-43: Principle of a transmission-mode thickness gauge



THBV4_1444EA

Figure 14-44: Principle of a fluorescent X-ray thickness gauge

When the intensity of radiation incident on a material is I_0 , the transmitted radiation intensity I can be expressed by the following relation:

$$I = I_0 e^{-\mu \rho t}$$

t : thickness (m)
 ρ : density (g/m^3)
 μ : mass absorption coefficient (m^2/g)

Since the transmitted radiation intensity is proportional to the count rate, the thickness of the material can be determined by calculating the count rate. In most cases, beta rays are used to measure rubber, plastics, and paper which have a small surface density (thickness \times density), while gamma rays are used to measure materials with a large surface density such as steel plates. In addition, infrared light is also used for measuring the thickness of films, plastics and other similar materials.

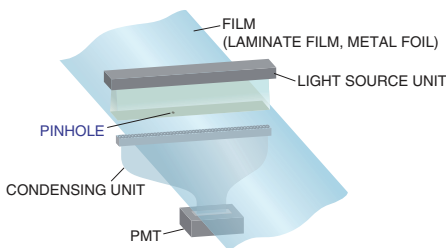
Fluorescent X-rays are used to measure the film thickness of plating and deposition layers. Fluorescent X-rays are secondary X-rays generated when a material is excited by radiation and have characteristic energy that is unique to the material. By detecting and discriminating this energy, the object material can be quantitatively measured.

There are a variety of detectors used for thickness gauges such as proportional counter tubes, photomultiplier tubes, and semiconductor radiation detectors. Photomultiplier tubes are used in conjunction with scintillators mainly for detection of gamma rays and X-rays.

(3) Pinhole inspections

Pinhole inspection of production materials used in industrial applications is performed by visible checks, camera sensing, air leakage, or electric current detection. Optical pinhole inspection utilizes the light transmitting through pinholes in workpieces and is mainly used for high-value-added materials such as aluminum laminated films used as the outer package of batteries and those products requiring rigorous quality control such as beverage cans. When inspecting pinholes in films, solid-state sensors such as photodiodes are used if the pinhole size is around a few dozen micrometers, while photomultiplier tubes are used to detect even smaller pinholes that are only a few micrometers in size.

Figure 14-44 shows a schematic drawing and external view of an optical pinhole inspection unit that uses a photomultiplier tube.



THBV4_1445EA

Figure 14-45: Schematic of an optical pinhole inspection unit



14.10 Solid Surface Analysis

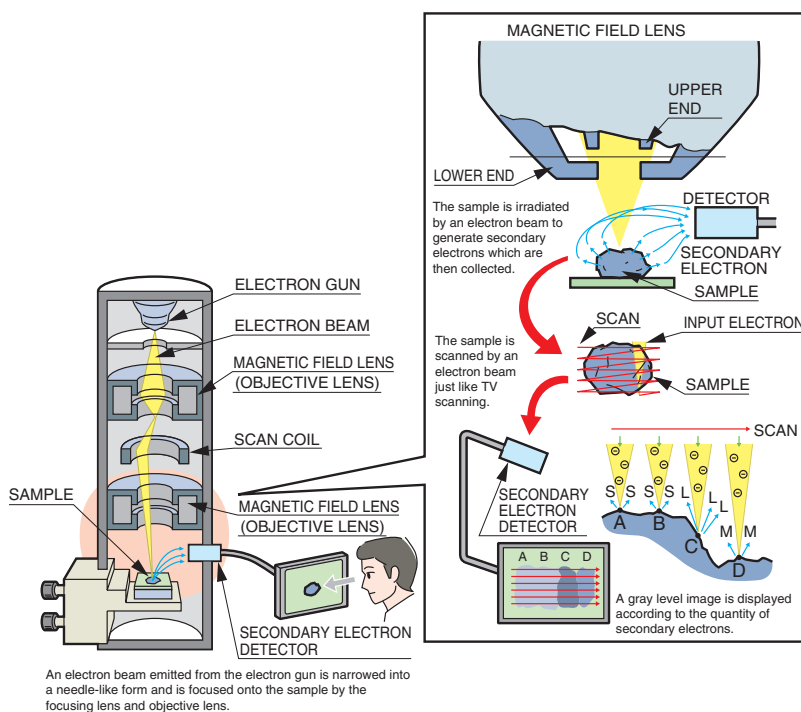
Solid surface analysis is a technique for examining the surface state of a sample based on the photoelectrons, secondary electrons, reflected electrons, transmitting electrons, Auger electrons, or X-rays generated as a result of interactions of incident electrons with atoms composing the sample, which take place when an electron beam or X-ray irradiates the sample. Photomultiplier tubes and microchannel plates are used as detectors in this application.

14.10.1 Solid surface analyzers²⁰⁾

Solid surface analyzers are broadly divided into two groups: one group uses electron beams to irradiate a sample and the other uses X-rays. Major solid surface analyzers currently used are as follows.

- Scanning electron microscope (SEM) based analyzers with element analysis function
- Auger electron spectrometer (AES)
- X-ray photoelectron spectrometer (XPS)
- X-ray fluorescence analyzer (XRF)

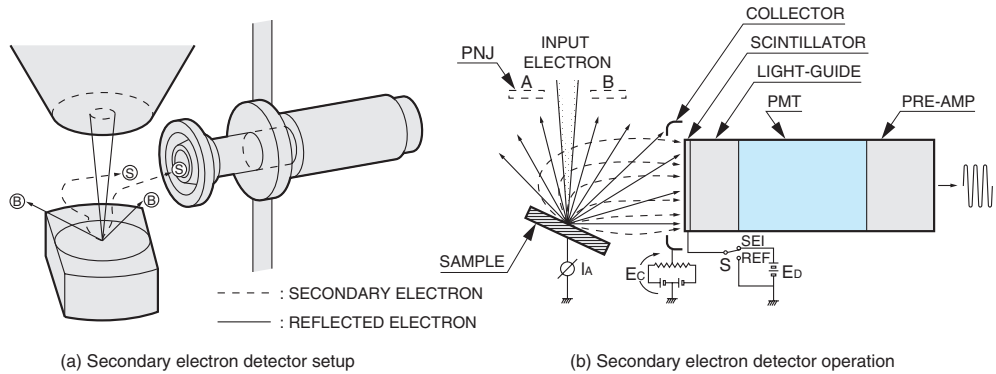
Among these 4 types of solid surface analyzers, the scanning electron microscope (SEM) is the most widely used. Its structure and principle are illustrated in Figure 14-45.²¹⁾



THBV4_1446EA

Figure 14-46: Structure and principle of a scanning electron microscope

An electron beam emitted from the electron gun is accelerated at a voltage of 0.1 kilovolts to 30 kilovolts. This accelerated electron beam is then condensed by the electromagnetic lens action of the focusing lens and objective lens and finally formed into a very narrow beam of 3 nanometers to 100 nanometers in diameter, irradiating on the surface of a sample. Secondary electrons are then produced from the surface of the sample where the electron beam landed, and are detected with a secondary electron detector. The electron beam can be scanned in the XY directions across a predetermined area on the surface of the sample by scanning the electromagnetic lens. A magnified secondary electron image can be displayed on the screen in synchronization with the signals of the secondary electron detector. Figure 14-46 shows the setup and operation of the secondary electron detector.



THBV4_1447EA

Figure 14-47: Setup and operation of a secondary electron detector

A typical secondary electron detector consists of a collector electrode, scintillator, light-guide, photomultiplier tube, and preamplifier. A voltage is applied to the collector electrode and scintillator to accelerate the electrons so that the scintillator emits light efficiently. Most of the secondary electrons produced from the sample enter the scintillator and are converted into visible light. This converted visible light then passes through the light-guide and is detected with the photomultiplier tube.

References in Chapter 14

- 1) Japan Analytical Instruments Manufacturers' Association (JAIMA): Principle of Analysis, 01 The world seen by electromagnetic waves (Published in Japanese)
- 2) Japan Analytical Instruments Manufacturers' Association (JAIMA): Guide to Analytical Instruments, Third Edition, 179 (1986) (Published in Japanese)
- 3) Japan Analytical Instruments Manufacturers' Association (JAIMA): Guide to Analytical Instruments, Third Edition, 228 (1986) (Published in Japanese)
- 4) Japan Analytical Instruments Manufacturers' Association (JAIMA): Guide to Analytical Instruments, 22nd Edition, 180 (2016) (Published in Japanese)
- 5) Nobuo Takeuchi, et al.: Laser Radar, Laser Handbook, Chapter 27, Ohmsha (Published in Japanese)
- 6) MOEJ (Ministry of the Environment of Japan): Dust and sandstorm information
- 7) Y. Endo and K. Miyai: Protein, Nucleic Acid and Enzyme, Separate Volume 31, Enzyme Immunoassay, 13, Kyoritsu Publishing Corp. (1987) (Published in Japanese)
- 8) G. Kawashima: Introduction to Immunoassay, 29, Nanzando Publishing Co., Ltd. (1987) (Published in Japanese)
- 9) Japan Analytical Instruments Manufacturers' Association (JAIMA): Guide to Analytical Instruments, Third Edition, 228 (1986) (Published in Japanese)
- 10) Toho University: High-speed imaging of calcium ions in myocardial cells
- 11) Japan Microscope Manufacturer's Association: Knowledge of a microscope
- 12) Akira Sasaki and Masataka Kinjo: Fluorescence cross-correlation spectroscopy for molecular dynamics in the living cells, Biochemistry Vol. 84, No.12 (2012)
- 13) T. Hayashi: Photomultiplier Tubes For Use In High Energy Physics (1992)
- 14) High Energy Accelerator Research Organization, Institute of Particle and Nuclear Studies: Particle identification device "Aerogel-based RICH Counter"
- 15) Tohoku University: KamLAND (Kamioka Liquid-scintillator Anti-Neutrino Detector)
- 16) Institute for Cosmic Ray Research, University of Tokyo: Cherenkov Telescope Array (CTA) project
- 17) Kamioka Observatory, Institute for Cosmic Ray Research, University of Tokyo: XMASS experiment - Operating principle
- 18) D-tect Systems, a division of ATK-mission Research
- 19) Nagase Landauer, Ltd.
- 20) Japan Analytical Instruments Manufacturers' Association (JAIMA): Guide to Analytical Instruments, Third Edition, 143 (1986) (Published in Japanese)
- 21) Japan Analytical Instruments Manufacturers' Association (JAIMA): Guide to Analytical Instruments, Third Edition, 143 (1986) (Published in Japanese)
- 22) JEOL Ltd.: Introduction to the World of SEM (Published in Japanese)
- 23) The Nikkan Kogyo Shimbun: Structure of Machine/Wonder of Technology, No.3, 42, 1996 (Published in Japanese)

MEMO

Index

A

Afterpulsing 79
Ag-O-Cs 33
Aging 66
Al₂O₃ crystal; window material 38
Analog mode 144
Angular response 64
Anode 20
Anode grounding and cathode grounding 87
Anode linearity 56
Anode luminous sensitivity 42
Applications 277
Atmosphere, Effect of 266
Atomic absorption spectrophotometers 279
Atomic emission spectrophotometer 279

B

Base-line shift 119
Basic operating method 23
Beryllium oxide (BeO), Dynode material 19
BGO 157, 286
Bialkali 32
Blue sensitivity 43
Borosilicate glass 38
Box-and-grid type, Dynode structure 46

C

Calorimeter 300
Cathode linearity 56
Cathode luminous sensitivity 41
Cell sorter 297
Center-of-Gravity Position 200
C.F.D. (constant fraction discriminator) 53
Charge-sensitive amplifier 124
Circular-cage type, Dynode structure 10, 17, 46
Cockcroft-Walton circuit 94, 172
Collection efficiency 17, 47
Confocal laser microscope 295
Connection to the external circuit 117
Cooling 139
Cooling precautions 251
Count rate linearity, Photon counting 149
Countermeasures for fast response circuits 101
Coupling capacitor 108, 119
CPU 185
C.R.T. (coincident resolving time) 55
Cs-I, Photocathode material 32
Cs-Te, Photocathode material 32

C.T.T.D. (cathode transit time difference) 54
Current output type module 176
Current-to-voltage conversion 120
 Using an op-amp 122
 Using load resistance 120

D

Dark current 69
 Temperature characteristics 71
Dead time, MCP-PMT 220
Digital mode 144
DNA 298
Drift (time stability) 65, 240
Dust counter 283
Dynode 14, 19
Dynode types 45
 Box-and-grid type 46
 Circular-cage type 46
 Linear-focused type 46
 MCP (Microchannel plate) 46
 Mesh type 46
 Metal channel dynode 46
 Venetian blind type 46
 Electron bombardment type 46
 Box-and-line type 46
 Circular and linear-focused type 47

E

EADCI (equivalent anode dark current input) 73
Edge effect, Shield case 136
Electron affinity (EA) 16
Electron multiplier 19
Electron trajectory 17
 Circular-cage type 17
 Linear-focused type 17
 Metal channel type 18
Electron transit time 51
Electrostatic shield 131
Energy resolution, Scintillation counting 159
ENI (equivalent noise input) 74
Environmental conditions 245
Environmental measurement 281
External electric potential, Effect of 267

F

Failure mode, Reliability test 273
Failure rate, Reliability test 273
Fall time 51
Field emission 72
Flat panel type multianode photomultiplier tubes 191
Fluorescence spectrophotometer 280
Frequency characteristics, Shield case 136

G

GaAs (Cs), Photocathode material 33
GaAsP (Cs), Photocathode material 33
Gain 48
Gain, MCP-PMT 215
Gain, Micro PMT 207
Gain, HPD 232
Gamma camera 288
Gate circuit 104
Gate function 182
Gated MCP-PMT 218
Glass scintillation 265
Glass-epoxy PCB 109

H

HA treatment 269
Helium gas, Effect of 261
High temperature photomultiplier tube 248
High-energy physics 299
High-voltage power supply 27, 114
Hodoscope 299
Housing 27, 131
HPD (Hybrid Photo-Detector) 229
Humidity 251
 Operating humidity 251
 Storage humidity 251
Hysteresis 67
 Light hysteresis 67
 Voltage hysteresis 68

I

IEC 60068 258
III-V compound semiconductor photocathode 15
Immunoassay 291
Industrial Measurement 309
InGaAs (Cs) 33
InP/InGaAs(Cs) 33
Ion feedback 72
Irradiance 7

J

JIS-C60068-2-6 (vibration) 258
JIS-C60068-2-27 (shock) 258

K

K-free glass 38
K⁴⁰ 38
Kamiokande 302
KamLAND 303
Kovar glass 38

L

Laser radar 284
Laser scanner 309
Leakage current (ohmic leakage) 70
LIDAR 284
Life characteristics 65
Light hysteresis 67
Light intensity 5
Light shield 131
Linear-focused type 46
Linearity 56
Linearity measurement 58
Linearity, Scintillation counting 162
Long term stability, Scintillation counting 164
Long wavelength limit 40
Low-pass filter 175
Luminous sensitivity 40
LWD (Logging While Drilling) 306

M

Magnesium oxide (MgO), Dynode material 19
Magnetic characteristics 252
Magnetic characteristics, MCP-PMT 224
Magnetic characteristics, Micro PMT 209
Magnetic shield 131
Magnetic shielding effect 137
Magnetization 254
M.C.A. (multichannel analyzer) 53
MCP (microchannel plate) 46, 212
MCP-PMT 211
 Dead time 220
 Gain 215
 Gated MCP-PMT 226
 Magnetic characteristics 224
 Saturation characteristics 220
 Structure 213
 Time characteristics 216
 Voltage-divider circuit 214
Mean life, Reliability test 273
Mesh type dynode 46
Metal channel dynode 46, 190, 200
MgF₂ crystal 38
MIL STD-202G 258
MIL STD-810G 258
Multianode Photomultiplier Tubes 190
MWD (Measuring While Drilling) 306

N

NaI(Tl) scintillator 30
NEA (negative electron affinity) 16
Neutrino observation 302
Noise, Scintillation counting 165

NOx analyzer 281
NF (Noise Figure) 152

O

Oil well logging 306
Output circuit
 For fast response photomultiplier tube 126
Output linearity 88
 DC output mode 91
 Pulse output mode 96

P

Permalloy 132
PET (Positron Emission Tomography) 285
Photocathode 15
 III-V compound semiconductor 15
Photocathode band model 15
Photocathode materials 32
 Ag-O-Cs 33
 Bialkali 32
 Cs-I 32
 Cs-Te 32
 GaAs (Cs) 33
 Low noise bialkali 32
 III-V compound semiconductor 10
 InGaAs (Cs) 33
 InP/InGaAs(Cs) 33
 Multialkali 33
 Sb-Cs 32
 Sb-K-Cs 32
 Sb-Na-K 32
 Sb-Na-K-Cs 33
 Sb-Rb-Cs 32
Photocathodes, History of 10
Photoelectron emission 15
Photometric units 4
Photomultiplier tubes for use highly magnetic field 253
Photomultiplier tubes, History of 10
Photon counting 143
 Circuit configuration 147
 Operating method 147
 Principle of photon counting 145
 Signal-to-noise ratio 152
 Stability 151
Photon counting head 179
Planar imaging device 287
Plateau characteristic, Scintillation counting 167
Plateau characteristics, Photon counting 147
PMT module 171
Polarized-light dependence 80
Position-sensitive photomultiplier tubes 189
Positron emission tomography (PET) 285
Power supply circuit 172

Proton decay 302
Pulse height distribution, Photon counting 147

Q

Quantum efficiency 39

R

Radiance 9
Radiant emittance 8
Radiant energy 7
Radiant flux 6
Radiant intensity 8
Radiant sensitivity 39
Radiation monitor 307
Radiation, Effect of 261
Radioimmunoassay 292
Red-to-white ratio 43
Reflection mode photocathodes 36
Relative pulse height, Scintillation counting 162
Reliability 270
Reliability tests and criteria 275
Ripple noise 175
Rise time 51
Rise time, MCP-PMT 216
Ruggedized photomultiplier tubes 258

S

S number 16
Sapphire 38
Saturation characteristics, MCP-PMT 220
Saturation characteristics, Shield case 134
Sb-Cs, Photocathode material 32
Sb-K-Cs, Photocathode material 32
Sb-Na-K, Photocathode material 32
Sb-Na-K-Cs, Photocathode material 33
Sb-Rb-Cs, Photocathode material 32
Scintillation counting 155
 Energy resolution 159
 Linearity 162
 Long term stability 164
 Noise 165
 Plateau characteristic 167
 Relative pulse height 162
 Short term stability 165
 Stability 165
 Uniformity 164
Scintillators
 BaF₂ 157
 BGO 157
 CsI(Tl) 157
 ZnS(Ag) 157

Secondary emission ratio 19
Secondary emissive materials 19
Settling time 176
Shielding factor of magnetic shield case 132
Short term stability, Scintillation counting 165
Short wavelength limit 40
Shot noise 75
Signal-to-noise ratio 75
Signal-to-noise ratio, Photon counting 151
Silica glass 38
Socket assemblies 27
Solid surface analysis 311
Solid surface analyzer 311
SOx analyzer 282
Spatial uniformity 62
Spectral regions 4
Spectral response characteristics 34, 35
Spectral response range 40
Spectral transmittance 39
Spectrophotometers 278
Spectrophotometry 278
Stability 65
Stability over time 270
Stability, Photon counting 151
Stability, Scintillation counting 164
Storage temperature 251
Stress and stability 271
Super bialkali 37
Super-Kamiokande 302

T

T.A.C. (time-to-amplitude converter) 53
Temperature characteristics 238
Thermionic emission 69
Thermoelectric cooler 140
Thickness gauge 309
Time characteristics 50
Time characteristics, MCP-PMT 216
Time characteristics, Micro PMT 208
TOF counter 300
Transit time, MCP-PMT 216
Transmission mode photocathode 37
T.T.S. (transit time spread) 52
T.T.S. (transit time spread), MCP-PMT 216

U

Ultra bialkali 37
Uniformity 61
 Angular response 64
 Spatial uniformity 62
Uniformity, Scintillation counting 164
UV-transmitting glass (UV glass) 38

V

Venetian blind type, Dynode structure 46
Vibration and Shock 255
Voltage hysteresis 68
Voltage output type module 174
Voltage-divider circuit 27, 86
 Fast response circuit 101
 Selecting the parts 107
 Precautions for mounting components 111
Voltage-divider circuit, MCP-PMT 214

W

Warm-up 66
Well scintillation counter 293
Window materials 38
 Borosilicate glass 38
 MgF₂ crystal 38
 Sapphire 38
 Spectral transmittance characteristics 37
 Silica glass 38
 UV-transmitting glass 38
Window transmittance
 Deterioration 261

X

X-ray image diagnostic equipment 298
XMASS 305

Z

Zener diode 93

"PHOTOMULTIPLIER TUBES" Editorial Committee

| | |
|------------------|------------------|
| Editorial Chief | Nobuya Matsunaga |
| Editorial Staff | Akifumi Kamiya |
| | Mikihito Goto |
| | Tsuyoshi Kodama |
| | Hisaaki Saito |
| | Tsutomu Ozawa |
| | Hiromi Ohishi |
| | Tsuyoshi Ema |
| | Takanori Nakaya |
| | Masatoshi Suzuki |
| | Kenichi Nagaoka |
| | Shota Nagai |
| | Keisuke Akiyama |
| | Kengo Watase |
| | Harutoshi Tahara |
| | Masayuki Sato |
| | Hisayuki Matsui |
| | Masaki Nakamura |
| Editorial Office | Hideto Hakamata |

PHOTOMULTIPLIER TUBES
– Basics and Applications –

March 1994 First Edition
April 1999 Second Edition
February 2006 Third Edition
August 2007 Third Edition (Edition 3a with minor revisions)
April 2017 Fourth Edition

| | |
|-----------|--|
| Authors | Hamamatsu Photonics K.K. Editorial Committee |
| Editing | Inproject, Inc. |
| Publisher | Hamamatsu Photonics K.K. Electron Tube Division |

© 2017 HAMAMATSU PHOTONICS K.K., Electron Tube Division
No part of this publication may be reproduced in any form without permission
of Hamamatsu Photonics K.K. TOTH9001E04